BEFORE-AFTER CONTROL-IMPACT (BACI) STUDIES IN THE OCEAN

EDITED BY: Edward Urban, Kerri D. Seger, Juan J. Schmitter-Soto and Renata Sousa-Lima

PUBLISHED IN: Frontiers in Marine Science

frontiers Research Topics

Frontiers eBook Copyright Statement

The copyright in the text of individual articles in this eBook is the property of their respective authors or their respective institutions or funders. The copyright in graphics and images within each article may be subject to copyright of other parties. In both cases this is subject to a license granted to Frontiers.

The compilation of articles constituting this eBook is the property of Frontiers.

Each article within this eBook, and the eBook itself, are published under the most recent version of the Creative Commons CC-BY licence. The version current at the date of publication of this eBook is CC-BY 4.0. If the CC-BY licence is updated, the licence granted by Frontiers is automatically updated to the new version.

When exercising any right under the CC-BY licence, Frontiers must be attributed as the original publisher of the article or eBook, as applicable.

Authors have the responsibility of ensuring that any graphics or other materials which are the property of others may be included in the CC-BY licence, but this should be checked before relying on the CC-BY licence to reproduce those materials. Any copyright notices relating to those materials must be complied with.

Copyright and source acknowledgement notices may not be removed and must be displayed in any copy, derivative work or partial copy which includes the elements in question.

All copyright, and all rights therein, are protected by national and international copyright laws. The above represents a summary only. For further information please read Frontiers' Conditions for Website Use and Copyright Statement, and the applicable CC-BY licence.

ISSN 1664-8714
ISBN 978-2-88971-948-8
DOI 10.3389/978-2-88971-948-8

About Frontiers

Frontiers is more than just an open-access publisher of scholarly articles: it is a pioneering approach to the world of academia, radically improving the way scholarly research is managed. The grand vision of Frontiers is a world where all people have an equal opportunity to seek, share and generate knowledge. Frontiers provides immediate and permanent online open access to all its publications, but this alone is not enough to realize our grand goals.

Frontiers Journal Series

The Frontiers Journal Series is a multi-tier and interdisciplinary set of open-access, online journals, promising a paradigm shift from the current review, selection and dissemination processes in academic publishing. All Frontiers journals are driven by researchers for researchers; therefore, they constitute a service to the scholarly community. At the same time, the Frontiers Journal Series operates on a revolutionary invention, the tiered publishing system, initially addressing specific communities of scholars, and gradually climbing up to broader public understanding, thus serving the interests of the lay society, too.

Dedication to Quality

Each Frontiers article is a landmark of the highest quality, thanks to genuinely collaborative interactions between authors and review editors, who include some of the world's best academicians. Research must be certified by peers before entering a stream of knowledge that may eventually reach the public - and shape society; therefore, Frontiers only applies the most rigorous and unbiased reviews.
Frontiers revolutionizes research publishing by freely delivering the most outstanding research, evaluated with no bias from both the academic and social point of view. By applying the most advanced information technologies, Frontiers is catapulting scholarly publishing into a new generation.

What are Frontiers Research Topics?

Frontiers Research Topics are very popular trademarks of the Frontiers Journals Series: they are collections of at least ten articles, all centered on a particular subject. With their unique mix of varied contributions from Original Research to Review Articles, Frontiers Research Topics unify the most influential researchers, the latest key findings and historical advances in a hot research area! Find out more on how to host your own Frontiers Research Topic or contribute to one as an author by contacting the Frontiers Editorial Office: frontiersin.org/about/contact

BEFORE-AFTER CONTROL-IMPACT (BACI) STUDIES IN THE OCEAN

Topic Editors:
Edward Urban, Scientific Committee On Oceanic Research, United States
Kerri D. Seger, Applied Ocean Sciences, United States
Juan J. Schmitter-Soto, The South Border College (ECOSUR), Mexico
Renata Sousa-Lima, Federal University of Rio Grande do Norte, Brazil

Citation: Urban, E., Seger, K. D., Schmitter-Soto, J. J., Sousa-Lima, R., eds. (2021). Before-After Control-Impact (BACI) Studies in the Ocean. Lausanne: Frontiers Media SA. doi: 10.3389/978-2-88971-948-8

Table of Contents

05 ***Editorial: Before-After Control-Impact (BACI) Studies in the Ocean***
Kerri D. Seger, Renata Sousa-Lima, Juan J. Schmitter-Soto and Edward R. Urban Jr.

08 ***Reduction of Low-Frequency Vessel Noise in Monterey Bay National Marine Sanctuary During the COVID-19 Pandemic***
John P. Ryan, John E. Joseph, Tetyana Margolina, Leila T. Hatch, Alyson Azzara, Alexis Reyes, Brandon L. Southall, Andrew DeVogelaere, Lindsey E. Peavey Reeves, Yanwu Zhang, Danelle E. Cline, Brent Jones, Paul McGill, Simone Baumann-Pickering and Alison K. Stimpert

21 ***Measuring Sound at a Cold-Water Coral Reef to Assess the Impact of COVID-19 on Noise Pollution***
Laurence H. De Clippele and Denise Risch

33 ***Underwater Sound Levels in Glacier Bay During Reduced Vessel Traffic Due to the COVID-19 Pandemic***
Christine M. Gabriele, Dimitri W. Ponirakis and Holger Klinck

47 ***Changes in Underwater Noise and Vessel Traffic in the Approaches to Halifax Harbor, Nova Scotia, Canada***
Heather Breeze, Shihan Li, Emmaline C. Marotte, James A. Theriault, Jessica Wingfield and Jinshan Xu

60 ***Soundscapes in the German Baltic Sea Before and During the Covid-19 Pandemic***
Fritjof Basan, Jens-Georg Fischer and Dennis Kühnel

73 ***Broad-Scale Responses of Harbor Porpoises to Pile-Driving and Vessel Activities During Offshore Windfarm Construction***
Aude Benhemma-Le Gall, Isla M. Graham, Nathan D. Merchant and Paul M. Thompson

91 ***Restoration of Abundance and Dynamics of Coastal Fish and Lobster Within Northern Marine Protected Areas Across Two Decades***
Even Moland, Albert Fernández-Chacón, Tonje Knutsen Sørdalen, David Villegas-Ríos, Susanna Huneide Thorbjørnsen, Kim Tallaksen Halvorsen, Mats Huserbråten, Esben Moland Olsen, Portia Joy Nillos Kleiven, Alf Ring Kleiven, Halvor Knutsen, Sigurd Heiberg Espeland, Carla Freitas and Jan Atle Knutsen

103 ***Changes in the Movement and Calling Behavior of Minke Whales* (Balaenoptera acutorostrata) *in Response to Navy Training***
Ian N. Durbach, Catriona M. Harris, Cameron Martin, Tyler A. Helble, E. Elizabeth Henderson, Glenn Ierley, Len Thomas and Stephen W. Martin

117 ***Far-Field Effects of Impulsive Noise on Coastal Bottlenose Dolphins***
Oihane Fernandez-Betelu, Isla M. Graham, Kate L. Brookes, Barbara J. Cheney, Tim R. Barton and Paul M. Thompson

129 ***Slower Ship Speed in the Bahamas Due to COVID-19 Produces a Dramatic Reduction in Ocean Sound Levels***
Charlotte Dunn, James Theriault, Leigh Hickmott and Diane Claridge

141 ***The Efficacy of Management Measures to Reduce Vessel Noise in Critical Habitat of Southern Resident Killer Whales in the Salish Sea***
Rianna E. Burnham, Svein Vagle, Caitlin O'Neill and Krista Trounce

159 ***Distance-Based Sampling Methods for Assessing the Ecological Effects of Offshore Wind Farms: Synthesis and Application to Fisheries Resource Studies***
Elizabeth T. Methratta

177 ***The Behavioural Impacts of Commercial Swimming With Whale Tours on Humpback Whales*** **(Megaptera novaeangliae)** ***in Hervey Bay, Australia***
Stephanie H. Stack, Kate R. Sprogis, Grace L. Olson, Florence A. Sullivan, Abigail F. Machernis and Jens J. Currie

193 ***Spatial Analysis of Beaked Whale Foraging During Two 12 kHz Multibeam Echosounder Surveys***
Hilary Kates Varghese, Kim Lowell, Jennifer Miksis-Olds, Nancy DiMarzio, David Moretti and Larry Mayer

207 ***Contextualizing Thermal Effluent Impacts in Narragansett Bay Using Landsat-Derived Surface Temperature***
Jonathan Benoit and Baylor Fox-Kemper

222 ***Assessing the Role of Sampling Uncertainty When Predicting Behavioral Responses of Tagged Cetaceans Exposed to Naval Sonar***
Phil J. Bouchet, Catriona M. Harris and Len Thomas

frontiers in Marine Science

EDITORIAL
published: 05 November 2021
doi: 10.3389/fmars.2021.787959

Editorial: Before-After Control-Impact (BACI) Studies in the Ocean

Kerri D. Seger[1], Renata Sousa-Lima[2], Juan J. Schmitter-Soto[3] and Edward R. Urban Jr.[4]*

[1] Applied Ocean Sciences (AOS), Fairfax Station, VA, United States, [2] Laboratory of Bioacoustics (LaB), Federal University do Rio Grande do Norte, Natal, Brazil, [3] El Colegio de la Frontera Sur (ECOSUR), Chetumal, Mexico, [4] Scientific Committee on Oceanic Research, Newark, NJ, United States

Keywords: BACI, ocean, sound, impacts, acoustics

Editorial on the Research Topic

Before-After Control-Impact (BACI) Studies in the Ocean

INTRODUCTION TO BEFORE-AFTER CONTROL-IMPACT METHODOLOGIES

The responses of marine organisms to changes in their environments can be studied using a variety of methods. Captive studies are highly controlled approaches that measure one or more parameters of interest in an enclosed area. Sample sizes are usually small, but experimental design and measurement methods are more controllable than in natural environments. However, captive experiments are not good models for the natural environment and cannot study the effects of large-scale disturbances, human-driven or otherwise, on large marine organisms, populations of marine organisms, or ecosystems.

The Before-After Control-Impact (BACI) methodology (Green, 1979; Stewart-Oaten and Bence, 2001) is commonly used in terrestrial and limnological ecology studies; they are non-randomized methods that can employ a variety of statistical tests. BACI approaches include time and impact factors, with a control site and a comparably impacted site, both represented by data before and after the impact. The BACI approach makes it possible to account for any natural or preexisting differences between the sites, and thus to estimate the "true" effect of an impact variable between the control and the impacted site. "Before" can be either a "true" baseline for both sites, or just a comparatively unimpacted situation; likewise, "control" can refer to a group either fully or partially sheltered from the impact. Other approaches, such as studying only the present (post-impact) situation, or even comparing the past and present situation in a single site or group, are less powerful. These approaches cannot capture the variability due to differences in time elapsed or location vs. the variability caused by the impact (Christie et al., 2020).

BACI methods have been applied in a variety of ocean studies (e.g., Francini-Filho and Moura, 2008; Schmitter-Soto et al., 2018), but is not a well-known approach in the oceanography community. BACI is not a perfect methodology, as site choice and sampling rate need to be determined strategically (Smokorowki and Randall, 2017), but baseline studies before expected large-scale impacts lend themselves to the "before" or "control" portions of BACI experiments. Therefore, learning how to best implement BACI methodologies from other ecological fields and applying them to the ocean could provide a common language for understanding human impacts. The rationale for this Research Topic was to encourage wider use and standardization of BACI in the ocean environment. It provides examples of BACI and related approaches used to study acoustical and other impacts in the ocean, including six papers on the impacts of the COVID-19 pandemic on ocean sound, six other acoustical papers, and four papers on non-acoustical topics.

OPEN ACCESS

Edited and reviewed by:
Angel Borja, Technological Center Expert in Marine and Food Innovation (AZTI), Spain

****Correspondence:***
Kerri D. Seger
kerri.seger.d@gmail.com; kerri.seger@appliedoceansciences.com

Specialty section:
This article was submitted to Marine Ecosystem Ecology, a section of the journal Frontiers in Marine Science

Received: *01 October 2021*
Accepted: *18 October 2021*
Published: *05 November 2021*

Citation:
Seger KD, Sousa-Lima R, Schmitter-Soto JJ and Urban ER Jr (2021) Editorial: Before-After Control-Impact (BACI) Studies in the Ocean. Front. Mar. Sci. 8:787959. doi: 10.3389/fmars.2021.787959

SUMMARY OF COVID-19 PAPERS

The six papers that examined the impacts of the COVID-19 pandemic on ocean sound levels do not all strictly meet the criteria to be considered BACI studies as laid out in Smokorowki and Randall (2017), but they do provide important information for managers of sound-producing activities. Specifically, the COVID-19 pandemic provided more of a "reverse BACI," or "ICAB" (impact-control after-before) scenario with decreases in sound from shipping and other human activities during the early stages of the pandemic, relieving acoustical disturbance on ecosystems for a short time. In each of these articles, some reductions in ocean sound were observed, showing the magnitude of sound reductions possible from management measures to reduce ship traffic. The articles show that sound was significantly reduced during the early months of the pandemic (1) at a cold-water coral reef under a passenger ferry route between Norway and Sweden (De Clippele and Risch), (2) in a high-traffic area for cruise ships in Glacier Bay National Park in Alaska (Gabriele et al.), (3) in a sperm whale habitat in the Bahamas (Dunn et al.), (4) at two sites in the Baltic Sea (Basan et al.), (5) in the Monterey Bay National Marine Sanctuary (Ryan et al.), and (6) in the Halifax Harbor of Nova Scotia (Breeze et al.). Each paper used different methods to analyze changes, so the results are not directly comparable. Ambient sound in the ocean is thought to have increased 3 dB per decade (Hildebrand, 2009): the same magnitude as the sound *decrease* reported in some of these articles over a few months' time. Studies published in other journals have also found reductions in sound levels due to the pandemic (Thomson and Barclay, 2020; León-López et al., 2021; Pine et al., 2021).

SUMMARY OF NON-COVID ACOUSTICAL PAPERS

Six papers took a more straightforward BACI approach of measuring effects from an acoustical disturbance after a relatively less disturbed state. Varghese et al. found that multibeam echosounders in a beaked whale feeding area did not significantly alter their preferred foraging location. Durbach et al. found that minke whales altered their movement patterns and ceased calling during naval sonar training. Bouchet et al. performed a modeling study of the effects of naval sonar on tagged cetaceans to measure their responses and is the sole paper in this Research Topic to tackle the statistical implications of predicting sampling uncertainty in behavioral responses. Fernandez-Betelu et al. found that far-field impulsive sounds from pile driving do not force coastal bottlenose dolphins to vacate their habitat, but do affect their behavior, whereas Benhemma-Le Gall et al. determined that harbor porpoises were displaced during pile-driving activities and from associated construction vessel activity for offshore wind farms. Burnham et al. found that vessel management efforts put in place to reduce stress on Southern Resident Killer Whales in the U.S. Pacific Northwest region decreased sound levels in frequency bands important to killer whale communication.

SUMMARY OF NON-ACOUSTICAL PAPERS

Four papers dealt with non-acoustical topics. Moland et al. examined the successful recovery of the structure and function of fish and lobster populations after 20 years of protection in the North Sea. Methratta reviewed methods to study the impact of offshore wind farms on various marine organisms by comparing BACI to alternative designs such as distance-stratified control-impact, before-after-gradient, and after-gradient (see also Benedetti-Cecchi, 2001 for a discussion of "beyond BACI methods"). Methratta is particularly useful for determining which impact study style may be more pertinent than others for oceanic research. Benoit and Fox-Kemper analyzed the impact of thermal effluents in Narragansett Bay, Rhode Island, demonstrating the effect of global warming over four decades. Finally, Stack et al. used a "before-after" scale of hours in a tropical environment in Australia, to show potentially detrimental behavioral changes in humpback whales due to ecotourism activities.

CONCLUSION

Currently, a standard set of guidelines does not exist for BACI studies in oceanography. Learning lessons from the ocean and other environments where BACI methodology has been applied (Underwood, 1994) will hopefully expedite formation of an accepted set of protocols in ocean science to accurately quantify disturbances and an ocean ecosystem's subsequent reaction. As climate change increases the rate of Arctic ice recession, warms the upper ocean, acidifies large regions of water, and expands oxygen minimum zones (IPCC, 2021), many of these impacts could be studied using BACI methods. We hope this Research Topic will lead to further development of BACI methods for ocean research to gain a more holistic understanding of anthropogenic effects on our planet. An important highlight of these studies is the importance of baseline measurements of important parameters before expected (e.g., windfarm construction) or unexpected (e.g., global pandemics and other natural disasters) environmental changes occur. Baseline studies are often the responsibility of governments because the results may not fit the usual requirements of experimental science. Such studies also should be funded by the industries that create environmental disturbances, and carried out by unbiased institutions and academia.

AUTHOR CONTRIBUTIONS

KS and EU developed the idea for the Research Focus, served as editors for some of the articles, and co-wrote this editorial. JS-S and RS-L served as editors for some of the articles and co-wrote this editorial. All authors contributed to the article and approved the submitted version.

REFERENCES

Benedetti-Cecchi, L. (2001). Beyond BACI: optimization of environmental sampling designs through monitoring and simulation. *Ecol. Appl.* 11, 783–799. doi: 10.1890/1051-0761(2001)0110783:BBOOES2.0.CO;2

Christie, A. P., Abecasis, D., Adjeroud, M., Alonso, J. C., Amano, T., Anton, A., et al. (2020). Quantifying and addressing the prevalence and bias of study designs in the environmental and social sciences. *Nat. Commun.* 11:6377. doi: 10.1038/s41467-020-20142-y

Francini-Filho, R. B., and Moura, R. L. (2008). Evidence for spillover of reef fishes from a no-take marine reserve: an evaluation using the before-after control-impact (BACI) approach. *Fish. Res.* 93, 346–356. doi: 10.1016/j.fishres.2008.06.011

Green, R. H. (1979). *Sampling Design and Statistical Methods for Environmental Biologists*. New York, NY: John Wiley & Sons.

Hildebrand, J. A. (2009). Anthropogenic and natural sources of ambient noise in the ocean. *Mar. Ecol. Prog. Ser.* 395, 5–20. doi: 10.3354/meps08353

IPCC (2021). "Summary for policymakers," in *Climate Change 2021: The Physical Science Basis. Contribution of Working Group I to the Sixth Assessment Report of the Intergovernmental Panel on Climate Change*, eds V. Masson-Delmotte, P. Zhai, A. Pirani, S. L. Connors, C. Péan, S. Berger, N. Caud, Y. Chen, L. Goldfarb, M. I. Gomis, M. Huang, K. Leitzell, E. Lonnoy, J. B. R. Matthews, T. K. Maycock, T. Waterfield, O. Yelekçi, R. Yu, and B. Zhou (Cambridge University Press), 41.

León-López, B., Romero-Vivas, E., and Viloria-Gomora, L. (2021). Reduction of roadway noise in a coastal city underwater soundscape during COVID-19 confinement. *J. Acoust. Soc. Am.* 149, 652–659. doi: 10.1121/10.0003354

Pine, M. K., Wilson, L., Jeffs, A. G., McWhinnie, L., Juanes, F., Scuderi, A., et al. (2021). A Gulf in lockdown: how an enforced ban on recreational vessels increased dolphin and fish communication ranges. *Glob. Change Biol.* 27, 4839–4848. doi: 10.1111/gcb.15798

Schmitter-Soto, J. J., Aguilar-Perera, A., Cruz-Martínez, A., Herrera-Pavón, R. L., Morales-Aranda, A. A., and Cobián-Rojas, D. (2018). Interdecadal trends in composition, density, size, and mean trophic level of fish species and guilds before and after coastal development in the Mexican Caribbean. *Biodiv. Conserv.* 27, 459–474. doi: 10.1007/s10531-017-1446-1

Smokorowki, K. E., and Randall, R. G. (2017). Cautions on using the Before-After-Control-Impact design in environmental effects monitoring programs. *Facets* 2, 212–232. doi: 10.1139/facets-2016-0058

Stewart-Oaten, A., and Bence, J. R. (2001). Temporal and spatial variation in environmental impact assessment. *Ecol. Monogr.* 71, 305–339. doi: 10.1890/0012-9615(2001)0710305:TASVIE2.0.CO;2

Thomson, D. J. M., and Barclay, D. R. (2020). Real-time observations of the impact of COVID-19 on underwater noise. *J. Acoust. Soc. Am.* 147, 3390–3396. doi: 10.1121/10.0001271

Underwood, A. J. (1994). On beyond BACI: sampling designs that might reliably detect environmental disturbances. *Ecol. Appl.* 4, 3–15. doi: 10.2307/1942110

Conflict of Interest: The authors declare that the research was conducted in the absence of any commercial or financial relationships that could be construed as a potential conflict of interest.

Publisher's Note: All claims expressed in this article are solely those of the authors and do not necessarily represent those of their affiliated organizations, or those of the publisher, the editors and the reviewers. Any product that may be evaluated in this article, or claim that may be made by its manufacturer, is not guaranteed or endorsed by the publisher.

Copyright © 2021 Seger, Sousa-Lima, Schmitter-Soto and Urban. This is an open-access article distributed under the terms of the Creative Commons Attribution License (CC BY). The use, distribution or reproduction in other forums is permitted, provided the original author(s) and the copyright owner(s) are credited and that the original publication in this journal is cited, in accordance with accepted academic practice. No use, distribution or reproduction is permitted which does not comply with these terms.

frontiers in Marine Science

ORIGINAL RESEARCH
published: 02 June 2021
doi: 10.3389/fmars.2021.656566

Reduction of Low-Frequency Vessel Noise in Monterey Bay National Marine Sanctuary During the COVID-19 Pandemic

John P. Ryan[1], John E. Joseph[2], Tetyana Margolina[2], Leila T. Hatch[3], Alyson Azzara[4], Alexis Reyes[4], Brandon L. Southall[5], Andrew DeVogelaere[6], Lindsey E. Peavey Reeves[7], Yanwu Zhang[1], Danelle E. Cline[1], Brent Jones[1], Paul McGill[1], Simone Baumann-Pickering[8] and Alison K. Stimpert[9]*

[1] Monterey Bay Aquarium Research Institute, Moss Landing, CA, United States, [2] Department of Oceanography, Naval Postgraduate School, Monterey, CA, United States, [3] Stellwagen Bank National Marine Sanctuary, NOS-NOAA, Scituate, MA, United States, [4] Maritime Administration, US Department of Transportation, Washington, DC, United States, [5] Southall Environmental Associates, Soquel, CA, United States, [6] Monterey Bay National Marine Sanctuary, NOS-NOAA, Monterey, CA, United States, [7] Office of National Marine Sanctuaries, NOS-NOAA, Silver Spring, MD, United States, [8] Scripps Institution of Oceanography, University of California, San Diego, La Jolla, CA, United States, [9] Moss Landing Marine Laboratories, Moss Landing, CA, United States

OPEN ACCESS

Edited by:
Edward Urban,
Scientific Committee On Oceanic Research, United States

Reviewed by:
William Halliday,
Wildlife Conservation Society, Canada
Nathan D. Merchant,
Centre for Environment, Fisheries, and Aquaculture Science (CEFAS), United Kingdom
Olaf Boebel,
Alfred Wegener Institute, Germany

***Correspondence:**
John P. Ryan
ryjo@mbari.org

Specialty section:
This article was submitted to Marine Ecosystem Ecology, a section of the journal Frontiers in Marine Science

Received: 21 January 2021
Accepted: 27 April 2021
Published: 02 June 2021

Citation:
Ryan JP, Joseph JE, Margolina T, Hatch LT, Azzara A, Reyes A, Southall BL, DeVogelaere A, Peavey Reeves LE, Zhang Y, Cline DE, Jones B, McGill P, Baumann-Pickering S and Stimpert AK (2021) Reduction of Low-Frequency Vessel Noise in Monterey Bay National Marine Sanctuary During the COVID-19 Pandemic. Front. Mar. Sci. 8:656566. doi: 10.3389/fmars.2021.656566

Low-frequency sound from large vessels is a major, global source of ocean noise that can interfere with acoustic communication for a variety of marine animals. Changes in vessel activity provide opportunities to quantify relationships between vessel traffic levels and soundscape conditions in biologically important habitats. Using continuous deep-sea (890 m) recordings acquired ∼20 km (closest point of approach) from offshore shipping lanes, we observed reduction of low-frequency noise within Monterey Bay National Marine Sanctuary (California, United States) associated with changes in vessel traffic during the onset of the COVID-19 pandemic. Acoustic modeling shows that the recording site receives low-frequency vessel noise primarily from the regional shipping lanes rather than via the Sound Fixing and Ranging (SOFAR) channel. Monthly geometric means and percentiles of spectrum levels in the one-third octave band centered at 63 Hz during 2020 were compared with those from the same months of 2018–2019. Spectrum levels were persistently and significantly lower during February through July 2020, although a partial rebound in ambient noise levels was indicated by July. Mean spectrum levels during 2020 were more than 1 dB re 1 μPa^2 Hz^{-1} below those of a previous year during 4 months. The lowest spectrum levels, in June 2020, were as much as 1.9 (mean) and 2.4 (25% exceedance level) dB re 1 μPa^2 Hz^{-1} below levels of previous years. Spectrum levels during 2020 were significantly correlated with large-vessel total gross tonnage derived from economic data, summed across all California ports ($r = 0.81$, $p < 0.05$; adjusted $r^2 = 0.58$). They were more highly correlated with regional presence of large vessels, quantified from Automatic Identification System (AIS) vessel tracking data weighted according to vessel speed and modeled acoustic transmission loss ($r = 0.92$, $p < 0.01$; adjusted $r^2 = 0.81$). Within the 3-year study period, February–June 2020 exhibited persistently quiet low-frequency noise and anomalously low statewide

port activity and regional large-vessel presence. The results illustrate the ephemeral nature of noise pollution by documenting how it responds rapidly to changes in offshore large-vessel traffic, and how this anthropogenic imprint reaches habitat remote from major ports and shipping lanes.

Keywords: ocean acoustics, shipping noise, COVID-19 pandemic, marine mammals, national marine sanctuaries

INTRODUCTION

Shipping is a dominant source of low-frequency anthropogenic noise in the ocean (Wenz, 1962; Hildebrand, 2009; Southall et al., 2017). Research using passive acoustic monitoring off California has identified increasing trends in low-frequency ocean noise of ∼3 dB per decade over ∼40 years, attributed to increases in commercial ship traffic (Andrew et al., 2002; McDonald et al., 2006), though trends may have changed differently in different areas since the 1990s (Andrew et al., 2011). Reduction of shipping noise off California has been observed over shorter time scales (<1 year) as a result of economic recession and associated reduction of maritime shipping activity, as well as regulatory changes that affected routing (McKenna et al., 2012).

Among the many human activities curtailed by the COVID-19 pandemic during 2020 was maritime shipping, resulting in reduced low-frequency ocean noise levels documented in some areas (Thomson and Barclay, 2020). This major change in global economic activity enables a rare opportunity to quantify the relationship between vessel activity and soundscape conditions in biologically important marine habitats. The habitat that is the focus of this study is centered within Monterey Bay National Marine Sanctuary (MBNMS), which extends ∼ 300 km along the central California coast and includes a wide variety of rich habitats, including an offshore biodiversity hotspot–Davidson Seamount (**Figure 1**). Years of continuous sound recording within MBNMS (Ryan et al., 2016), enabled by the Monterey Accelerated Research System (MARS) cabled observatory (**Figure 1**), support examination of 2020 ambient noise levels relative to those existing in previous years.

Located within the highly productive California Current Large Marine Ecosystem (Ekstrom, 2009), and centered over the largest submarine canyon off the North American west coast, MBNMS is an important habitat for abundant and diverse marine life, including at least 34 mammal species (NOAA, 2017). MBNMS is considered to be a biologically important area (BIA) for multiple species of baleen whales (Calambokidis et al., 2015), whose use of low-frequency sound for communication makes them relatively susceptible to interference from low-frequency anthropogenic noise. Particularly soniferous species of baleen whales that inhabit MBNMS include blue, fin, and humpback (**Figure 2**). The region is also an important habitat for gray whales that migrate along the eastern margin of the North Pacific, moving through MBNMS where their calves are susceptible to predation by orcas (Goley and Straley, 1994). In their NE Pacific breeding habitat, gray whales have exhibited increased vocalization rates and source levels in response to vessel noise (Dahlheim and Castellote, 2016), a response that could influence acoustic detection by orcas and associated predation risk in MBNMS if exhibited during northward migration.

Protection of acoustic habitat in the ocean is an ongoing and rising priority (Southall et al., 2009; Hatch et al., 2016; Chou et al., 2021; Duarte et al., 2021), and passive acoustic monitoring has become integral to the management of marine protected areas (Gottesman et al., 2020; Kline et al., 2020). The ways that anthropogenic noise can affect marine mammals include interference with communication (masking), behavioral disturbance such as avoidance of key habitat areas essential to fitness and survival, induction of chronic or acute stress, and in severe cases physiological damage (Hatch et al., 2008, 2012; Rolland et al., 2012; Gedamke et al., 2016; Erbe et al., 2019; Simonis et al., 2020a). Within MBNMS, the threat posed by fishery explosions to acoustically sensitive harbor porpoise has been considered (Simonis et al., 2020b). In this contribution, we examine changes in ocean noise within MBNMS resulting from pandemic-induced reductions in maritime shipping activity. We consider how this unanticipated change provides a window into noise as a pollutant that can be managed within a multi-use ocean environment to better protect biologically important habitats and the species that inhabit them.

MATERIALS AND METHODS

Acoustic Data and Analyses

Acoustic recordings were acquired through the Monterey Accelerated Research System (MARS) cabled observatory, located in the center of MBNMS (**Figure 1**). Since 28 July 2015, MARS has supported nearly continuous recording at a sample rate of 256 kHz using an Ocean Sonics icListen HF—an omnidirectional hydrophone with a bandwidth of 10 Hz–200 kHz. Data stream directly to the Ocean Sonics *Lucy* software for shore-side recording. Because the potential impacts of the COVID-19 pandemic on U.S. shipping traffic began during the first few months of 2020, we examine January through July recordings from 2020 in relation to the same months of the preceding 2 years. During this study period, recording temporal coverage was 96.4%. This entire period was recorded by one continuously deployed hydrophone that exhibited no long-term trends in low-frequency noise, thus supporting effective comparison across years.

The shipping noise metric computed was mean-square sound pressure spectral density, ISO 18405 3.1.3.13 (ISO, 2017), for the

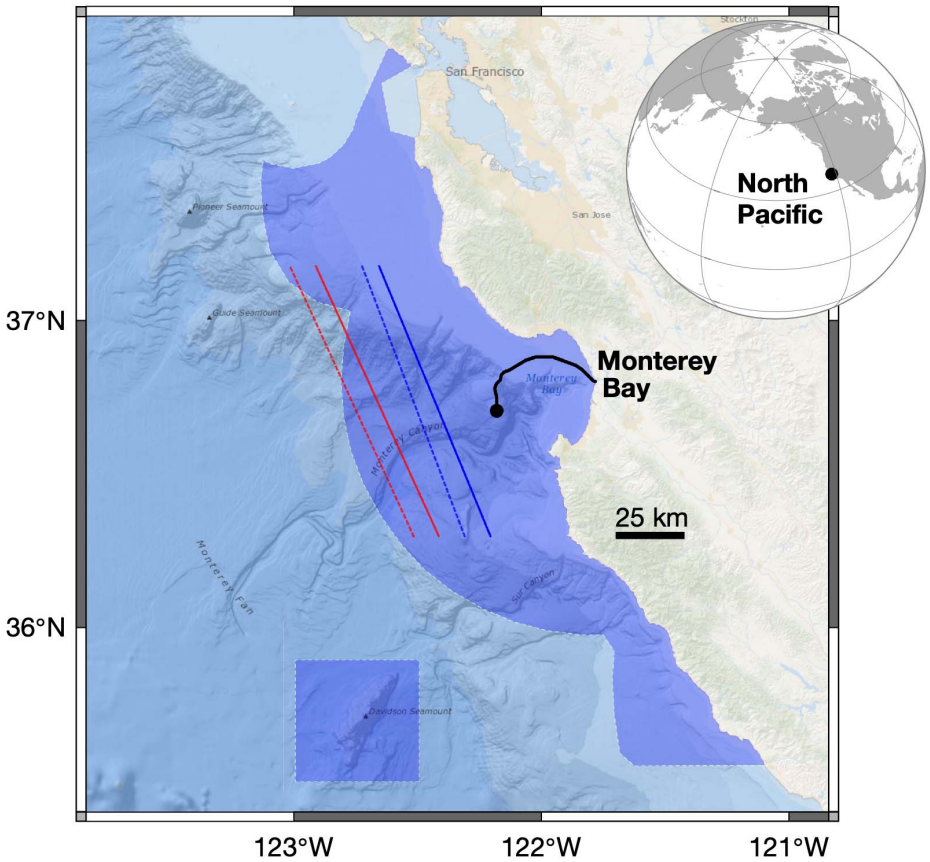

FIGURE 1 | The study region along the eastern margin of the North Pacific. Blue shaded regions define the Monterey Bay National Marine Sanctuary, which includes a region adjacent to the California coast centered on Monterey Bay and an offshore region around Davidson Seamount. The hydrophone is connected to the Monterey Accelerated Research System (MARS) cabled observatory (black line and circle; main node at 36.713°N, 122.186°W, 891 m depth). Blue and red lines define recommended tracks for northbound (solid) and southbound (dashed) shipping traffic for vessels 300 gross tons and above; red lines are for vessels carrying hazardous cargo in bulk or crude oil.

one-third octave band centered at 63 Hz (Band 18, Dekeling et al., 2014). Power spectral density (PSD) was computed from 2 kHz data at resolutions of 1 s and 1 Hz using Welch's method in MATLAB (pwelch, FFT length = 2,000 points, Hanning window length = 2,000 points). PSD was averaged for the 63 Hz one-third octave band, and median (L50) values were extracted for the temporal observation window (IQOE, 2019) of 1 min. Calibrated spectrum levels were computed by subtracting the manufacturer-measured hydrophone sensitivity for the low-frequency range (−177.9 dB re 1 V/μPa at 250 Hz). The icListen is a digital hydrophone in which there is no separation between the sensor element, filters, amplifier, and analog-to-digital converter. The internal amplifier gain is included in the reported sensitivity. Although independent calibration in the focal frequency band is ideal, this is not a concern for this analysis, which applies relative comparison of monthly ambient noise statistics. Monthly statistics, including geometric mean and exceedance levels at 10, 25, 50, 75, and 90%, were examined to quantify changes during 2020 and to compare 2020 with the preceding 2 years. For the year-to-year comparisons of monthly data, we applied analysis of variance and Tukey Honest Significant Differences (HSD) multiple comparison tests using the stats package in R (Version 3.6).

The acoustic data processing methods described above effectively removed two signals that would otherwise confuse analysis of shipping noise. The first signal is biophony from blue whales, specifically the fourth harmonic of the song-associated B call. The strong signal of this source in the 63 Hz one-third octave band is effectively eliminated by the 1-min L50 (**Figure 3A**). During fall months when blue whale song rises to peak occurrence (Oestreich et al., 2020), chorusing of blue whales is more probable, and this method may be less effective. However, it is reliable for the winter, spring, and summer months of our study. The second signal is not part of the soundscape, but instead caused by mechanical disturbance of the hydrophone. These extreme, transient broadband signals sound like direct contact between animals and the hydrophone (bio-abrasion). Because these transient signals do not occupy a large percentage of the time windows within which they occur, the 1-min L50 effectively eliminates this signal from monthly statistical descriptions (**Figure 3B**).

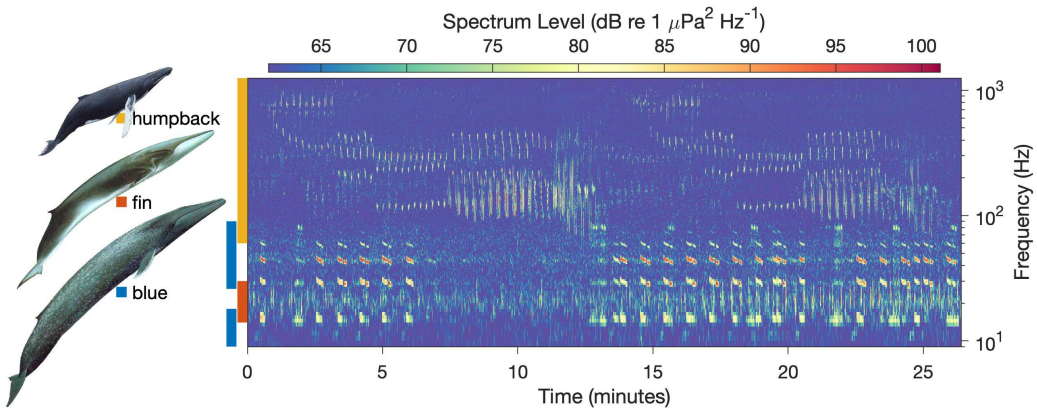

FIGURE 2 | Simultaneous song from three baleen whale species recorded in Monterey Bay National Marine Sanctuary. Spectrogram calculation used 12.8 kHz data (decimated from 256 kHz), 12,800 pt. FFT, Hanning window, 50% overlap; start time is 10-Jan-2017 13:33 UTC. Colored bars along the vertical axis define the approximate frequency ranges used by each species. Humpback song spans the greatest frequency range and is the most complex, with two full songs represented (beginning at ∼1 and 15 min). Blue whale song includes three call types: A calls—pulse-trains centered near 80 Hz, B calls—the loudest calls produced with fundamental frequency centered near 14.5 Hz and harmonics centered near 29, 43.5, and 58 Hz, and C calls—the subtlest of the three, centered near 11 Hz. Fin whale song is the simplest, consisting of brief (∼ 1 s) pulses that are modulated in frequency and variably paired in singlets, doublets, and triplets (Helble et al., 2020). Baleen whale song occurrence within the foraging habitat of MBNMS spans 7–9 months of the year, depending on the species (Ryan et al., 2019; Oestreich et al., 2020). Whale artist: Larry Foster.

Economic Data and Analyses

Data on marine vessels entering and leaving U.S. ports are collected by Customs and Border Protection and provided as a weekly dataset to the Maritime Administration. Each record includes the date and time of entry or clearance, the name of the port, and information of the vessel such as its tonnage and type. For the period of the acoustic data analyses, January through July of 2018–2020, the Maritime Administration aggregated the data on vessel entries into ports in California and calculated monthly summary statistics including the total number of port calls and the total gross tonnage by port. Most of the reported gross tonnage (91%) was for cargo vessel types (container, tanker, roll-on/roll-off, dry bulk, general cargo, barge) while the remaining 9% comprised passenger vessels.

Automatic Identification System Vessel Tracking Data and Analyses

Automatic Identification System (AIS) data for Monterey Bay and the surrounding region were acquired from the U.S. Coast Guard, covering the time period of the acoustic data analyses, January through July of 2018–2020. The data are summaries of average positions every 5 min for every vessel recorded, and ancillary data for each vessel. AIS data covering a large domain (35–38.5°N, 124.5–120.5°W) were acquired, including the intensive shipping traffic associated with ports in San Francisco Bay. Two categories of AIS records were removed prior to analysis. Records having positions over land or within San Francisco Bay were removed using the *inpolygon* function of the *pracma* package for R (Version 3.6.3) with a land polygon mask defined by full-resolution GSHHS coastline data. Redundant records were removed by requiring that a vessel, identified by its Maritime Mobile Service Identity (MMSI) number, be represented only once in each 5-min data summary. Vessel length was computed by adding the AIS data fields that quantify the distances between the AIS transmitter and the vessel's bow and stern. This length was used to confirm that records in the category of *other types of ship* represented large vessels of interest in this study (USCG, 2021; ship and cargo type beginning with 9).

A proxy for potential low-frequency noise from large vessels was derived from a vessel noise model and AIS vessel presence records weighted by two scaling factors. The first was vessel speed. A statistical model developed using nearly 600 examples of recorded container vessel transits showed that vessel speed had the greatest predictive power for noise across the full frequency range examined, 20–1,000 Hz (McKenna et al., 2013). According to this model, vessel noise source level (SL) is a quasi-exponential function of vessel speed. In the present study, the duration of each record of vessel presence (5 min) was weighted based on vessel speed using the published model function for the octave band centered at 63 Hz. Records having unreasonably high vessel speeds (>25 knots, 0.04% of records) were excluded. The second factor used modeled acoustic transmission loss (TL) at 63 Hz (section "Acoustic Modeling"). Specifically, the weighting factor = $10^{[-(TL\ -TLmin)/10]}$, scaled such that the minimum TL within the model domain (near the hydrophone) was assigned a weighting value of 1 and all other TL values were assigned weighting values below 1. Specification of this weighting factor is based on the definition TL = $10\log_{10}$(linear-scale transmission loss).

Relationships Between Vessel Activity and Low-Frequency Noise

Because monthly geometric means of ambient noise levels consistently track monthly changes quantified by exceedance levels, unlike arithmetic means, we use monthly geometric means

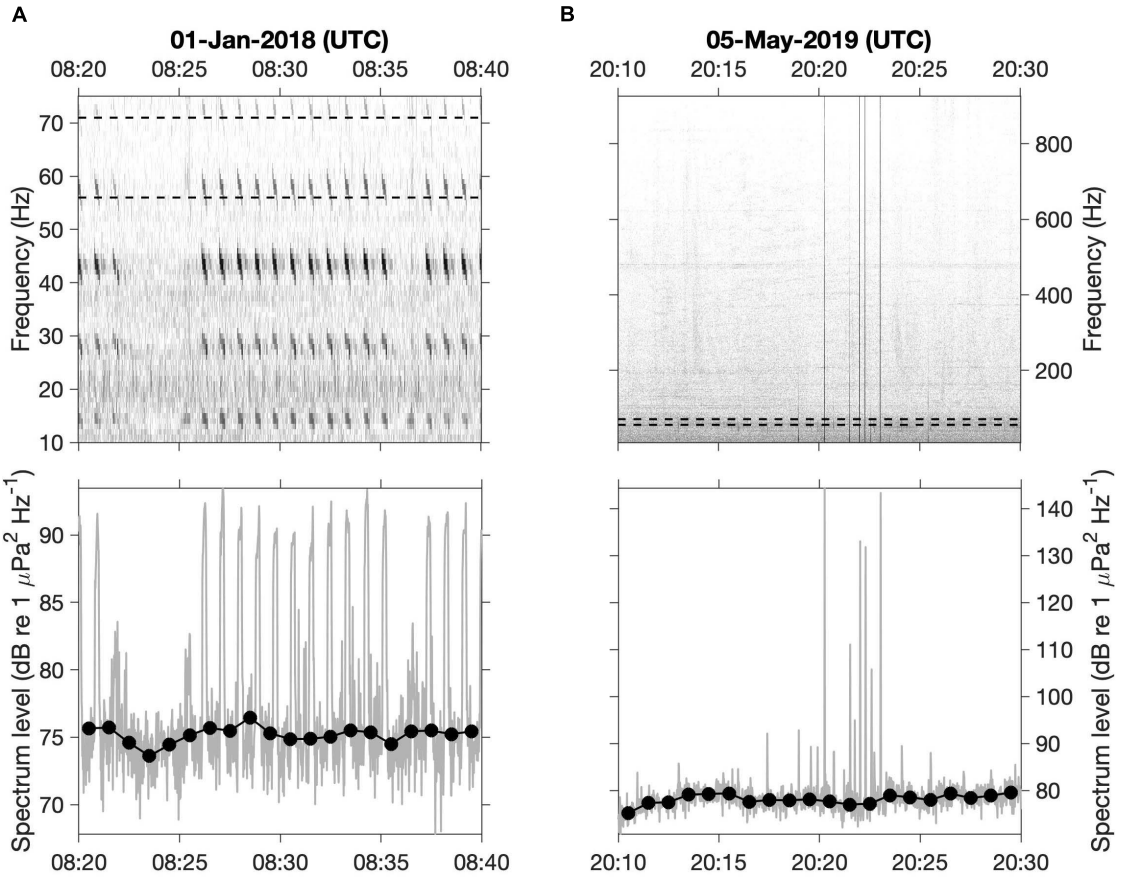

FIGURE 3 | Non-shipping signals in the focal frequency band. Focal signals are **(A)** the fourth harmonic of the blue whale B call, and **(B)** bio-abrasion (mechanical disturbance of the recorder by an animal). Spectrograms (top) were computed using 2 kHz data (decimated from 256 kHz), 2,000 pt. FFT, Hanning window, no overlap; the 63-Hz one-third octave band is represented by dashed lines. Spectrum levels within the focal frequency band (bottom) are represented for 1-s resolution (gray) and 1-min L50 (black).

in examining relationships between ambient noise and vessel activity. Relationships were examined for: (1) 2020 only, to consider causality of variation during the year that exhibited reduced noise, and (2) 2018–2020, to consider the strength of relationships within the full data set. These analyses were applied to examining relationships between the ambient noise metric and each shipping activity metric separately (derived from statewide port data and regional AIS data), as well as both shipping activity metrics together. Linear regression was conducted on the noise spectrum level (in dB) as a function of the logarithm of shipping activity, so that both the abscissa and the ordinate were on logarithmic scales. All statistical analyses were conducted in R, version 3.6. Correlations and their significance were examined using cor.test from the stats package. Linear models were fitted using lm from the stats package. Generalized additive models (GAMs) were fitted using gam from the mgcv (Mixed GAM Computation Vehicle with Automatic Smoothness Estimation) package. GAM modeling could be applied only to the full time series because input of 2020 data only would produce a smoothing term having fewer unique covariate combinations than the specified maximum degrees of freedom. Therefore, adjusted r^2-values are from lm for 2020 data only, and from gam for 2018–2020 data. For GAM results we report the smoothing parameter estimation method (REML) and the effective degrees of freedom (EDF) (Zuur and Ieno, 2016), as well as the significance of the smoothing term.

Acoustic Modeling

Acoustic modeling was applied for two purposes. The first was to provide context for the recording site on the continental slope, surrounded by complex bathymetry, thereby explaining the typical pattern of noise received from large vessels transiting in the offshore shipping lanes. Using the BELLHOP model (Porter, 2011) we produced eigenray plots showing the rays that connect the receiver to vessels transiting in the shipping lanes. Eigenrays were examined for a series of bearing angles relative to the receiver, covering the full directional range spanned by the spatial relationship between the receiver and the shipping lanes. The nature and number of boundary interactions for each bearing were evaluated to characterize the directional range from which shipping noise can effectively reach the receiver. To consider the potential for distant shipping noise to reach

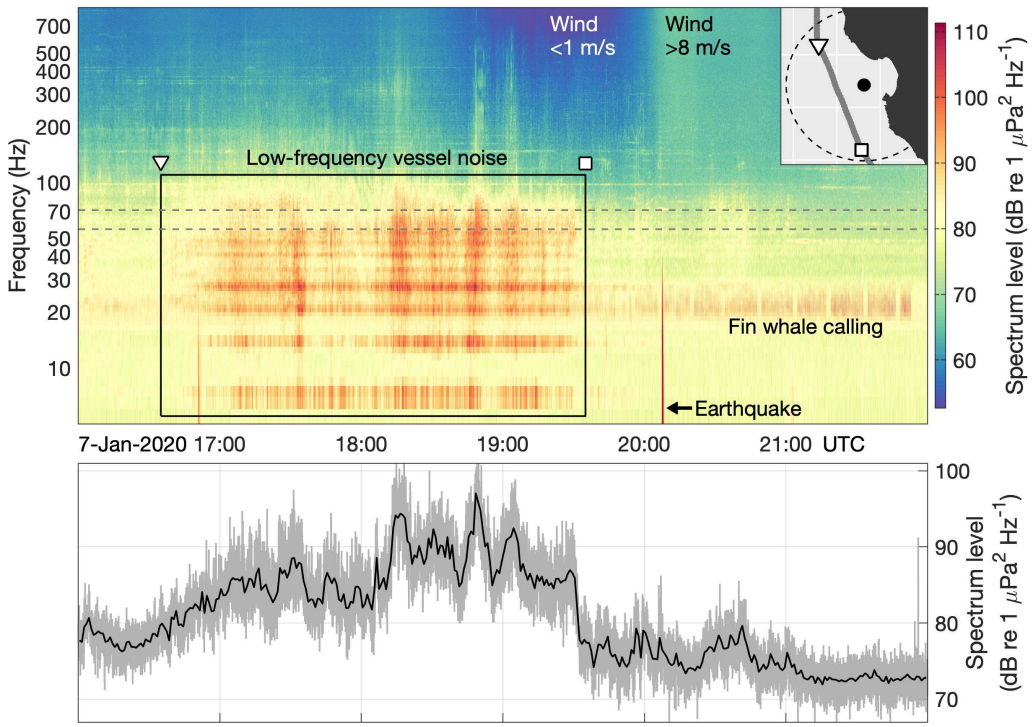

FIGURE 4 | Low-frequency vessel noise within the greater soundscape at MARS. Spectrogram calculation used 2 kHz data (decimated from 256 kHz), 2,000 pt. FFT, Hanning window, no overlap. The box bounds temporal and frequency limits of the strongest signal from a southbound transit of the container vessel *MSC SILVANA* (IMO: 9309459; length overall 332 m). A portion of the vessel track is shown in the inset map, with time markers corresponding to those in the spectrogram (triangle, square); vessel speed was steady at 21.4 ± 0.16 knots during this portion of the transit. The black dashed line in the inset map defines an 80 km radius from MARS for scale reference. Other identifiable sounds include biological (fin whale calling) and geophysical (wind, earthquake). The fin whale calls are series of ∼ 1 s pulses with peak energy near 20 Hz. The increase in spectrum levels above ∼150 Hz beginning near hour 20 followed a rapid increase in wind speeds from < 1 m/s to > 8 m/s (measured at NDBC Station 46042, located 20.6 km NW of MARS). The dashed gray lines define the frequency band used to quantify shipping noise from the recording time series, the one-third octave band centered at 63 Hz. The lower panel represents spectrum levels for this focal frequency band at 1-s resolution (gray) and 1-min L50 (black).

the receiver via the SOFAR channel, ray tracing was modeled for the bearing of 242°, near the closest point of approach (CPA) within historical shipping lanes. Ray tracing shows the general pattern that sound energy originating from anywhere in the water column will arrive at the MARS receiver. Interaction with the surface and bottom boundaries results in significant energy loss from scattering and absorption, particularly at the ocean bottom.

The second purpose was to quantify acoustic transmission loss, as a basis for weighting AIS vessel records. This application used a wave-theory parabolic equation model that accounts for absorption in both the water column and the bottom, scattering in the water column and at the surface and bottom, geometric spreading (spherical and cylindrical), refraction, and diffraction (Collins, 1993). Source depth was specified as 6 m, and source frequency was specified as 63 Hz to be consistent with the shipping noise metric. The model domain extended 165 km from the receiver. Specification of regional ocean temperature and salinity was based on the January climatology from the US Navy Generalized Digital Environmental Model (GDEM). Bathymetry was specified at 250 m resolution.

RESULTS

Acoustical Site Description

Typical attributes of low-frequency vessel noise received at the recording site are represented by a southbound transit of a large (332 m LOA) container vessel traveling at high speed (∼21 knots) in the lane second nearest to the recording site (**Figures 1**, **4**). The first typical attribute is strong signal up to ∼100 Hz. The 63 Hz one-third octave band (overlaid in **Figure 4**) is effective for quantifying shipping noise at this location. The second typical attribute is indicated by the triangle and square markers within the spectrogram and inset reference map (**Figure 4**), which identify the steep rise and fall of received noise at specific points along the track. Results from the acoustic ray tracing model explain how the complex bathymetry of the continental shelf and slope surrounding the recording site (**Figure 1**) cause this attribute (**Figure 5**). Steep rise of noise for this southbound transit occurred when the ship crossed the continental shelf break, moving from shallow to deep water (triangles in **Figures 4**, **5A**). North of this location, strong transmission loss results from many bottom reflections, particularly over the shelf (**Figures 5B,C**, 330°). The number of reflections and associated levels of

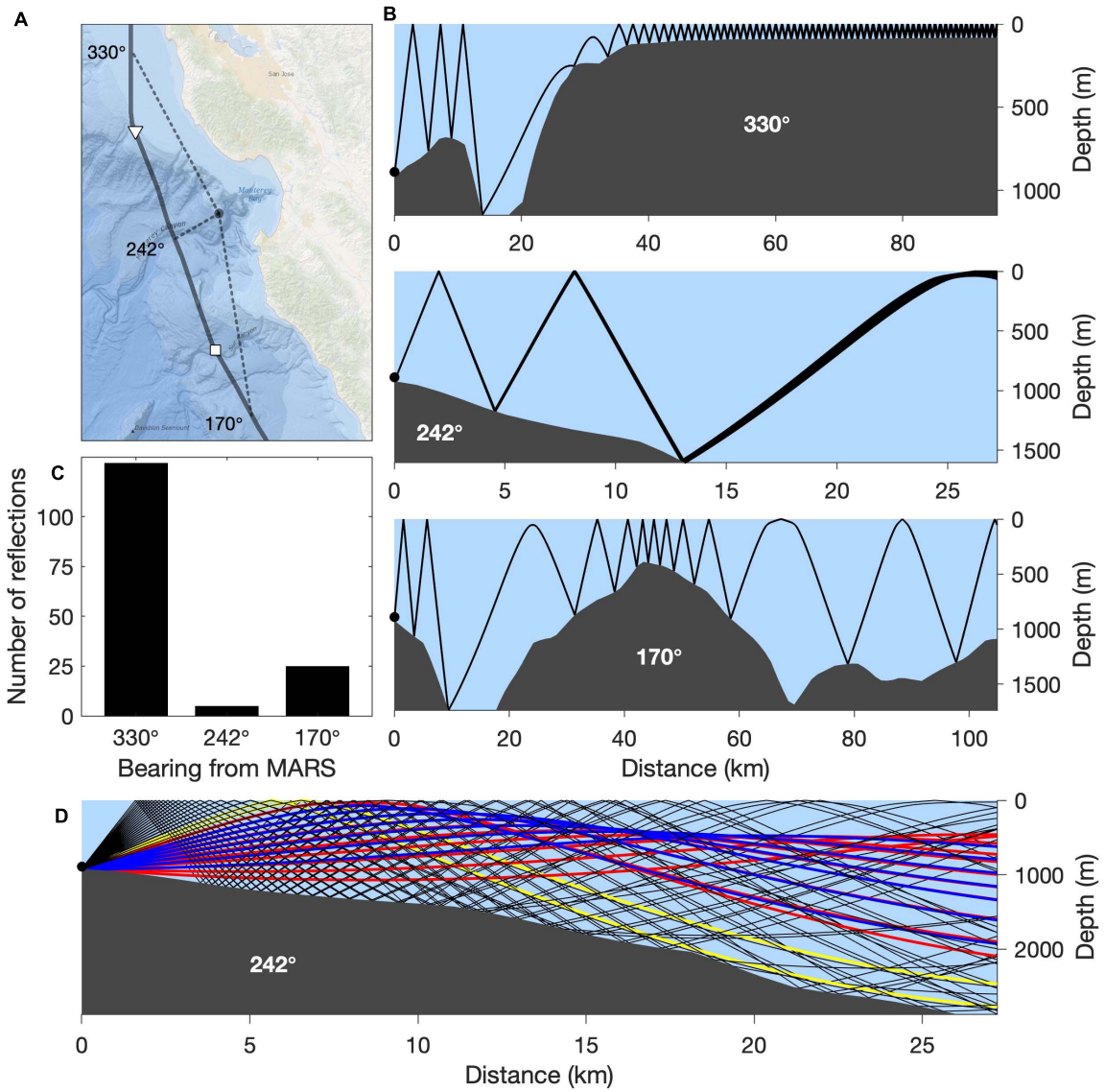

FIGURE 5 | Acoustical characterization of the recording site. **(A)** Map showing the track of the *MSC SILVANA* (as in **Figure 4**). **(B)** Eigenrays between vessel source and MARS receiver computed using the BELLHOP model for the bearings identified in **(A)**. **(C)** Total number of bottom and surface reflections for paths represented in **(B)**. **(D)** Ray trace results for the 242° bearing. Black lines represent ray paths with multiple boundary interactions (high loss). Yellow lines represent paths that have only one surface reflection (small loss, particularly on calm days). Blue lines represent paths with only one bottom bounce, very near the receiver. Red lines represent paths with no boundary interaction over the range shown. The blue and red paths are in the SOFAR channel.

transmission loss decrease as the ship moves over deeper water, to a minimum at CPA (**Figures 5B,C**, 242°). After moving south of CPA, the increased received levels (after ∼ 18:10 in **Figure 4**) are presumably due to the stern-facing attitude of the vessel relative to the receiver. As the ship passed Sur Ridge on the continental slope, received levels dropped steeply (squares in **Figures 4**, **5A**). This was also caused by an increased number of bottom reflections due to the influence of the ridge on the ray paths (**Figures 5B,C**, 170°).

Because the recording site is within the depth range of the SOFAR channel, it is also important to consider the potential for distant shipping noise to reach the recorder via transmission within the SOFAR channel. Here again, bathymetry of the region surrounding the recording site is a primary determinant. Because ocean margin shipping lanes north and south of the recording site are bathymetrically blocked, the only directional range over which shipping noise could originate to reach the recording site via the SOFAR channel is offshore (∼ 180–300°). Results of the ray tracing model show that direct path sound energy from the SOFAR channel (red and blue eigenrays in **Figure 5D**) would have to originate from ∼ 500 m, well below the depth of vessel noise sources near the surface. Further, this directional range opens to low levels of vessel traffic beyond the shipping lanes (section "*Relationship Between Low-Frequency Noise and*

Large-Vessel Activity") and the full expanse of the North Pacific between the recorder and shipping activity of the western Pacific. Therefore, we conclude that our vessel noise metric effectively represents regional shipping activity, and that it is representative of what animals would be exposed to if located near our recording site (**Figure 4**).

Low-Frequency Noise

Measured at the same site with the same calibrated instrument, low-frequency noise levels during February through July 2020 were significantly lower ($p < 0.01$) than they were during the same months of both 2018 and 2019 (**Table 1**). During 4 months, geometric mean spectrum levels during 2020 were more than 1 dB re 1 μPa^2 Hz^{-1} below those of a previous year. The differences in means and exceedance levels across years indicate that reduced noise during 2020 was persistent during February through June, with January and July being more similar across years (**Figures 6A,B**). The lowest spectrum levels, in June 2020, were as much as 1.9 (mean) and 2.4 (25% exceedance level) dB re 1 μPa^2 Hz^{-1} below levels of previous years. These changes in central tendency and distribution paralleled reductions in the percent of time during which relatively loud ambient noise (>3 dB above the overall mean) was recorded (**Figure 6C**).

Relationship Between Low-Frequency Noise and Large-Vessel Activity

Shipping total gross tonnage data cover four ports to the north of Monterey Bay and four ports to the south (**Figure 7A**). During the study period, total gross tonnage across the most- to least-active ports spanned more than three orders of magnitude (**Figure 7B**). AIS vessel tracking data (**Figure 8A**), weighted by modeled acoustic transmission loss (**Figure 8B**) and vessel speed, enable examination of the relationship between shipping and ambient noise within a more regional context.

Variations in low-frequency ambient noise were significantly correlated with both total gross tonnage across all California ports and weighted regional AIS vessel presence (**Figure 9** and **Table 2**). For the AIS metric, the highest adjusted r^2-values resulted from inclusion of only the vessel categories having the largest average vessel length: cargo, tanker, other large (USCG ship and cargo types beginning with 9), and enforcement; these comprised 66% of all records within the 165 km radius of MARS. The lowest values of both large-vessel activity and ambient noise occurred during 2020, with the three lowest values during March, May, and June (**Figures 6** and **9**). Using both port and AIS data across all years, the generalized additive model for the relationship between large-vessel activity and ambient low-frequency noise had an adjusted r^2 of 0.61. Considered independently, the more regional metric of large-vessel activity (AIS) was the better predictor (**Table 2**). The relationships between large-vessel activity metrics and ambient noise considering only 2020 were stronger than the overall relationships, with the AIS-based linear model having an adjusted r^2 of 0.81 (**Table 2**).

TABLE 1 | Results from Tukey Honest Significant Differences (HSD) multiple comparison applied to ANOVA models fit to data from each month across 2018–2020.

	2020 vs.	Difference	Lower	Upper
January	2018	0.74	0.67	0.80
	2019	−0.11	−0.17	−0.04
February*	2018	−0.51	−0.57	−0.45
	2019	−1.30	−1.36	−1.24
March*	2018	−0.87	−0.93	−0.81
	2019	−1.12	−1.17	−1.06
April	2018	−0.77	−0.83	−0.72
	2019	−0.53	−0.59	−0.47
May*	2018	−1.47	−1.52	−1.41
	2019	−1.38	−1.44	−1.33
June*	2018	−1.86	−1.93	−1.80
	2019	−1.94	−2.00	−1.88
July	2018	−0.52	−0.59	−0.46
	2019	−0.16	−0.22	−0.10

*For each month the estimate of the mean difference between 2020 and the same month of the two preceding years is presented together with lower and upper bounds of the confidence interval on the difference estimate. All results are significant ($p < 0.001$). Negative values indicate lower spectrum levels during 2020 in the 63-Hz one-third octave band (representing shipping noise, in dB re 1 μPa^2/Hz). Asterisks indicate months during which spectrum levels were lower during 2020 by at least 1 dB re 1 μPa^2/Hz relative to at least one of the two preceding years (**Figure 6**).*

TABLE 2 | Summary of statistical relationships between monthly mean spectrum levels in the 63 Hz one-third octave band and shipping activity metrics (**Figure 9**).

	Correlation (*p*-value)	Adjusted r^2	EDF (*p*-value)
January–July of 2020			
Port activity	0.81 ($p < 0.05$)	0.58	–
AIS activity	0.92 ($p < 0.01$)	0.81	–
Both	–	0.79	–
January–July of 2018–2020			
Port activity	0.64 ($p < 0.01$)	0.43	2.73 ($p < 0.01$)
AIS activity	0.77 ($p < 0.01$)	0.58	2.36 ($p < 0.01$)
Both	–	0.61	3.97 ($p < 0.01$)

*Port activity represents monthly total gross tonnage summed across all California ports. AIS activity represents monthly sums of vessel presence, weighted according to vessel speed and modeled acoustic transmission loss (**Figure 8**). EDF is the estimated degrees of freedom of the Gaussian smoothing term in the generalized additive model.*

DISCUSSION

COVID-related changes in maritime transportation were directly linked with low-frequency ambient noise within the protected marine habitat of MBNMS. Independent measures of variation in large-vessel activity, based on statewide economic data and regional AIS vessel tracking, were significantly correlated with variation in ambient noise at the MARS recording site. Considering only variations within 2020, the year during which pandemic impacts on shipping activity began to emerge along the U.S. west coast, reduction of low-frequency noise was clearly caused by reduced vessel traffic. Considering variations across 2018–2020, this causal relationship also explains why 2020 ambient noise levels

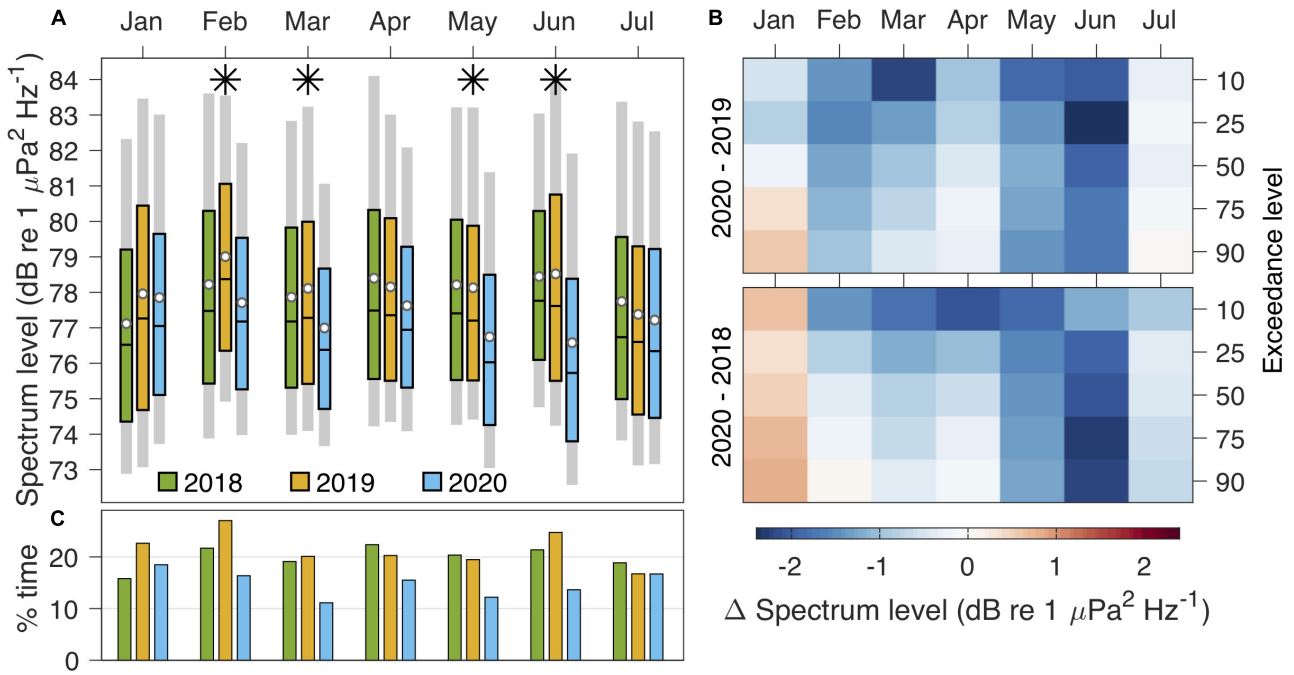

FIGURE 6 | Reduction of low-frequency noise during 2020. **(A)** Monthly statistics for spectrum levels computed from MARS recordings (location in **Figure 1**) for a frequency band that is representative of low-frequency vessel noise (one-third octave band centered at 63 Hz, **Figure 4**). Shown are the range of the 10th–90th exceedance levels (light gray bars), the median and interquartile range (colored boxes), and the geometric mean (white circles). Asterisks indicate months during which spectrum levels were lower during 2020 by at least 1 dB re 1 μPa^2 Hz^{-1} relative to at least one of the two preceding years. **(B)** Percentile-dependent differences between 2020 and the prior 2 years. **(C)** Monthly percent of time during which 1-min L50 values were more than 3 dB re 1 μPa^2 Hz^{-1} above the overall time-series mean.

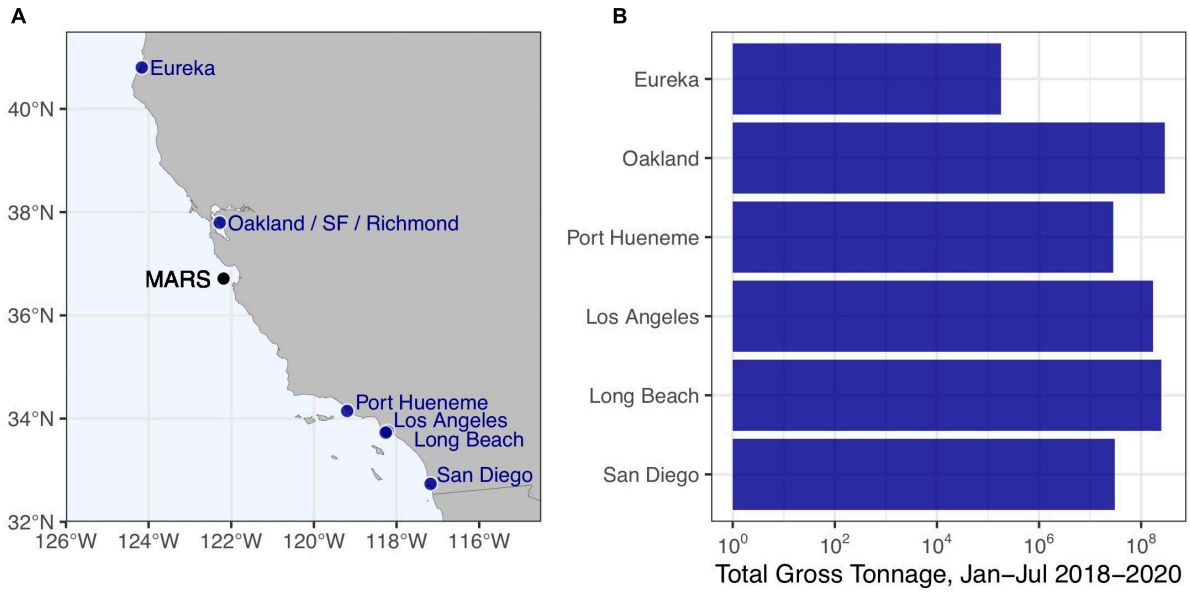

FIGURE 7 | Statewide port activity. **(A)** Locations of California ports relative to MARS, and **(B)** total gross tonnage for January through July, 2018 through 2020, the time period for which acoustic data were analyzed (**Figure 6**). Records for the ports of San Francisco and Richmond are grouped with Oakland; Los Angeles and Long Beach port entry locations nearly coincide.

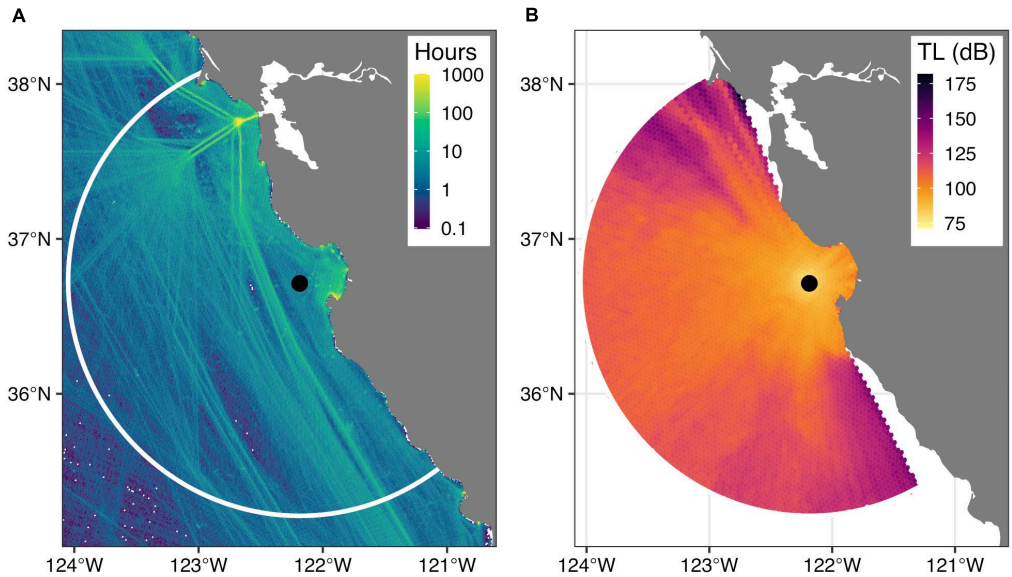

FIGURE 8 | Regional vessel traffic and its weighting. **(A)** Map of total hours of vessel presence during January through July of 2018–2020, derived from AIS records. Data from within San Francisco Bay were excluded as they would not be relevant to sound recordings at MARS (black circle). **(B)** Modeled acoustic transmission loss (TL) for a 63 Hz source at 6 m depth (section "Acoustic Modeling"), used as one of two weighting factors for AIS records (section "Automatic Identification System Vessel Tracking Data and Analyses"). The white arc in (**A**) represents a 165-km radius around MARS, corresponding to the domain of TL modeling in (**B**).

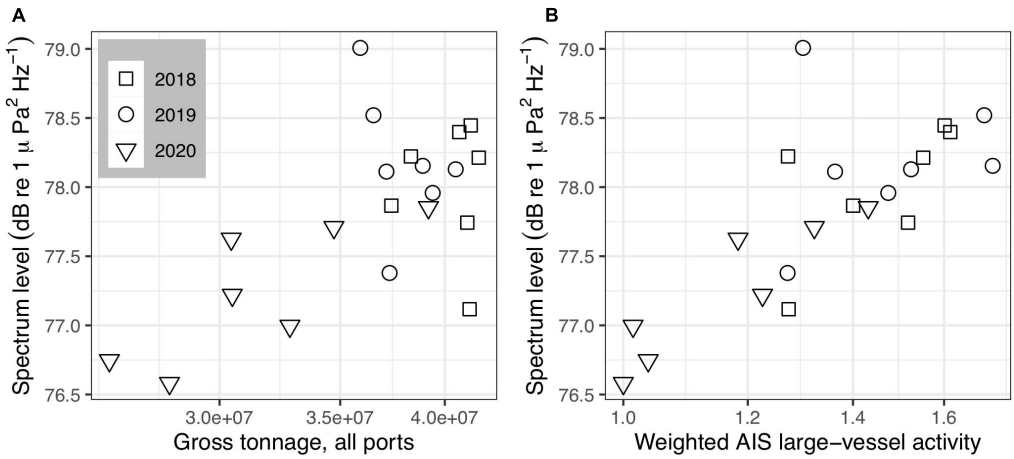

FIGURE 9 | Relationships between metrics of regional large-vessel activity and low-frequency noise at MARS. The low-frequency noise metric is the monthly geometric mean spectrum level for the 63 Hz one-third octave band (**Figure 6**); both vessel activity metrics are plotted on a logarithmic scale. Metrics of regional large-vessel activity are **(A)** monthly sums of gross tonnage for California ports (**Figure 7**), and **(B)** monthly sums of vessel presence derived from AIS records that were weighted according to modeled acoustic transmission loss (**Figure 8**) and vessel speed. Monthly sums in **(B)** are normalized to the minimum to facilitate interpretation. The maximum is ∼ 72% greater than the minimum.

were anomalously low. Acoustic modeling supported the conclusions that the ambient noise measurements represent regional changes in shipping traffic, and that the changes are representative of what animal populations near the recording site would experience.

A previous study off southern California revealed a clear relationship between economic recession, reduced shipping activity, and reduced ambient noise (McKenna et al., 2012). Examining 1 Hz bands centered at 40 and 90 Hz, this earlier study found decreases of 5.1 and 3.1 dB, respectively, between July 2008 and May 2009. Our methods differ from those of this study in a number of ways, including proximity of the recorder to the shipping lanes (distance ∼4X greater in our study), frequency bands used to characterize vessel noise, minimizing error from transient signals, and quantifying change (trend from a continuous data series less than 1 year in length vs. year-to-year comparison of same months across 3 years). Therefore, it is difficult to directly compare results from these

studies quantitatively. However, the cause of quieting, traced to economic drivers of maritime shipping, is consistent.

The reduced noise during 2020 relative to preceding years (2018 and 2019) was evident in not only the statistics of central tendency and distribution (mean, percentiles), but also the percentage of time during which relatively loud noise (>3 dB above the mean for the entire study period) was recorded. The consistency of these measures illustrates the cause and effect relationship: less frequent presence of shipping noise caused a decrease in the mean and percentiles for the band that represents this noise source. The nature of this relationship, in turn, frames consideration of consequences. From the perspective of animals that use low-frequency sound to communicate, individual vessel transits would not be quieter, but there would be less time during which vessel noise could mask communication, reduce communication range, or induce stress (Hatch et al., 2012; Erbe et al., 2016, 2019). Evaluation of the consequences of variations in noise exposure requires consideration of both source attributes (spatial, temporal, frequency) and receiver attributes (hearing responses of different species (Southall et al., 2019) and proximity of their populations to noise sources). While direct hearing measurements are lacking for baleen whales for whom changes in low-frequency noise may be most relevant among marine mammals, previous auditory studies have demonstrated that other marine mammal species are able to distinguish between certain sounds with relative differences on the order of 2–3 dB (Moore and Schusterman, 1976; Johnson, 1986).

The ambient noise reduction during 2020 approached the magnitude of decadal increase in low-frequency noise caused by growth in eastern North Pacific shipping activity between the 1950's and 1990's (Andrew et al., 2002, 2011; McDonald et al., 2006). Occurring over 5 months (between January and June), this represents a rapid rate of change compared to the decadal trends associated with increased shipping activity in the region. These relative measures of change illustrate the ephemeral nature of noise as an energetic pollutant (Boebel et al., 2018). Noise does not have the degree of persistence that other forms of energetic (heat) or substantial (chemical, plastic, greenhouse gas) pollution have, which offers immediate response to the application of solutions. Collaborations across industry, academia, non-profit, and governmental sectors have great potential to rapidly enhance habitat quality and protection by engineering transitions to a quieter ocean through measures ranging from ship design to speed regulation (McKenna et al., 2013; Southall et al., 2017; Erbe et al., 2019; Chou et al., 2021). This remains an important area of evolving effort in ocean stewardship[1].

Impacts of this global pandemic on ocean soundscapes will vary greatly from region to region, depending on local environmental factors and the type and amount of anthropogenic noise that was typically present before pandemic impacts occurred. Located somewhat near offshore shipping lanes and within MBNMS, the MARS observatory was effective for examining changes in low-frequency noise from large vessels and associated impacts on protected habitat. In considering impacts on marine animals, this study examined frequencies important to baleen whale communication having a high degree of overlap with shipping noise (e.g., Erbe et al., 2019). While these baleen whale species, two of which remain endangered (blue and fin whales), are central to considering impacts of low-frequency noise, it is also important to consider the impacts of this type of noise on other mammals (mysticetes, odontocetes, pinnipeds) that inhabit the sanctuary, as well as fish species that use low-frequency communication (Erbe et al., 2019; Bolgan and Parmentier, 2020; Duarte et al., 2021). Moored recorders have been deployed in other parts of MBNMS, including sites closer to vessel activities of fishing and tourism, and these recordings may enable different insights into the relationships between changes in human activity and acoustic habitat in this marine sanctuary. Soundscape monitoring across U.S. National Marine Sanctuaries (NOAA, 2021) can expand perspective on the acoustic consequences of the pandemic within marine protected areas at the national scale. Global efforts to comprehensively examine changes in ocean soundscapes resulting from the COVID-19 pandemic are ongoing, such as through the International Quiet Ocean Experiment project (Tyack et al., 2021). Advancing our understanding of ocean soundscapes is an essential element of both holistic ecosystem assessment and promotion of ocean health.

DATA AVAILABILITY STATEMENT

The datasets generated and analyzed in this study are available online: https://doi.org/10.6084/m9.figshare.c.5356514.v1. For reproducibility and extensibility of results, original audio recordings for the entire study period, decimated to a sample rate of 2 kHz, are accessible through the AWS Open Data registry: arn:aws:s3:::pacific-sound-2khz.

AUTHOR CONTRIBUTIONS

JR, JJ, LH, BS, AD, LP, TM, SB-P, and AS contributed to conception and design of the study. JR, JJ, TM, LH, AA, AR, DC, BJ, YZ, and PM contributed to data acquisition, processing, and analysis. JR wrote the first draft of the manuscript. All authors contributed to revision of the original and post-review manuscripts and read and approved the submitted versions.

FUNDING

The NSF funded installation and maintenance of the MARS cabled observatory through awards 0739828 and 1114794. The SanctSound project, co-led by the US Navy and NOAA, supported collaboration by JR, JJ, LH,

[1]https://green-marine.org/certification/scope-and-criteria/underwater-noise-ship-owners/
https://www.portvancouver.com/environmental-protection-at-the-port-of-vancouver/maintaining-healthy-ecosystems-throughout-our-jurisdiction/echo-program/

AD, TM, BS, LP, SB-P, and AS on this project. Sound recording through the MARS cabled observatory was supported by the Monterey Bay Aquarium Research Institute, with funding from the David and Lucile Packard Foundation.

ACKNOWLEDGMENTS

We thank C. Dawe, D. French, and the crew of the R/V *Rachel Carson* for design, deployment, and maintenance of the MARS hydrophone system.

REFERENCES

Andrew, R. K., Howe, B. M., and Mercer, J. A. (2011). Long-time trends in ship traffic noise for four sites off the North American West Coast. *J. Acoust. Soc. Am.* 129:642. doi: 10.1121/1.3518770

Andrew, R. K., Howe, B. M., Mercer, J. A., and Dzieciuch, M. A. (2002). Ocean ambient sound: comparing the 1960s with the 1990s for a receiver off the California coast. *ARLO* 3, 65–70. doi: 10.1121/1.1461915

Boebel, O., Burkhardt, E., and van Opzeeland, I. (2018). "Input of energy/underwater noise," in *Handbook on Marine Environment Protection*, eds M. Salomon, and T. Markus, (Berlin: Springer), 1024. doi: 10.1007/978-3-319-60156-4 .

Bolgan, M., and Parmentier, E. (2020). The unexploited potential of listening to deep-sea fish. *Fish Fish.* 21, 1238–1252. doi: 10.1111/faf.12493

Calambokidis, J., Steiger, G. H., Curtice, C., Harrison, J., Ferguson, M. C., Becker, E. A., et al. (2015). Biologically important areas for selected cetaceans within U.S. waters – West Coast region. *Aquat. Mamm.* 41, 39–53. doi: 10.1578/AM.41.1.2015.39

Chou, E., Southall, B. L., Robards, M., and Rosenbaum, H. C. (2021). International policy, recommendations, actions and mitigation efforts of anthropogenic underwater noise. *Ocean Coast. Manag.* 202:105427. doi: 10.1016/j.ocecoaman.2020.105427

Collins, M. D. (1993). A split-step Padé solution for the parabolic equation method. *J. Acoust. Soc. Am.* 93, 1736–1742. doi: 10.1121/1.406739

Dahlheim, M., and Castellote, M. (2016). Changes in the acoustic behavior of gray whales *Eschrichtius robustus* in response to noise. *Endanger. Species Res.* 31, 227–242. doi: 10.3354/esr00759

Dekeling, R. P. A., Tasker, M. L., Van der Graaf, A. J., Ainslie, M. A., Andersson, M. H., Andrei, M., et al. (2014). *Monitoring Guidance for Underwater Noise in European Seas, Part II: Monitoring Guidance Specifications, JRC Scientific and Policy Report EUR 26555 EN*. Luxembourg: Publications Office of the European Union.

Duarte, C. M., Chapuis, L., Collin, S. P., Costa, D. P., Devassy, R. P., Eguiluz, V. M., et al. (2021). The soundscape of the Anthropocene ocean. *Science* 371:eaba4658. doi: 10.1126/science.aba4658

Ekstrom, J. A. (2009). California current large marine ecosystem: publicly available dataset of state and federal laws and regulations. *Mar. Policy* 33, 528–531. doi: 10.1016/j.marpol.2008.11.002

Erbe, C., Marley, S. A., Schoeman, R. P., Smith, J. N., Trigg, L. E., and Embling, C. B. (2019). The effects of ship noise on marine mammals—a review. *Front. Mar. Sci.* 6:606. doi: 10.3389/fmars.2019.00606

Erbe, C., Reichmuth, C., Cunningham, K., Lucke, K., and Dooling, R. (2016). Communication masking in marine mammals: a review and research strategy. *Mar. Poll. Bull.* 103, 15–38. doi: 10.1016/j.marpolbul.2015.12.007

Gedamke, J., Harrison, J., Hatch, L., Angliss, R., Barlow, J., Berchok, C., et al. (2016). *NOAA Ocean Noise Strategy Roadmap*. Washington, DC: NOAA, 138.

Goley, P. D., and Straley, J. M. (1994). Attack on gray whales (Eschrichtius robustus) in Monterey Bay, California, by killer whales (*Orcinus orca*) previously identified in Glacier Bay, Alaska. *Can. J. Zool.* 72, 1528–1530. doi: 10.1139/z94-202

Gottesman, B. L., Sprague, J., Kushner, D. J., Bellisario, K., Savage, D., McKenna, M. F., et al. (2020). Soundscapes indicate kelp forest condition. *Mar. Ecol. Prog. Ser.* 654, 35–52. doi: 10.3354/meps13512

Hatch, L., Clark, C., Merrick, R., Van Parijs, S., Ponirakis, D., Schwehr, K., et al. (2008). Characterizing the relative contributions of large vessels to total ocean noise fields: a case study using the Gerry E. Studds Stellwagen Bank National Marine Sanctuary. *Environ. Manage.* 42, 735–752. doi: 10.1007/s00267-008-9169-4

Hatch, L. T., Clark, C. W., Van Parijs, S. M., Frankel, A. S., and Ponirakis, D. W. (2012). Quantifying loss of acoustic communication space for right whales in and around a U.S. National Marine Sanctuary. *Conserv. Biol.* 26, 983–994. doi: 10.1111/j.1523-1739.2012.01908.x

Hatch, L. T., Wahle, C. M., Gedamke, J., Harrison, J., Laws, B., Moore, S. E., et al. (2016). Can you hear me here? Managing acoustic habitat in US waters. *Endang. Species Res.* 30, 171–186. doi: 10.3354/esr00722

Helble, T. A., Guazzo, R. A., Alongi, G. C., Martin, C. R., Martin, S. W., and Henderson, E. E. (2020). Fin whale song patterns shift over time in the Central North Pacific. *Front. Mar. Sci.* 7:907. doi: 10.3389/fmars.2020.587110

Hildebrand, J. A. (2009). Anthropogenic and natural sources of ambient noise in the ocean. *Mar. Ecol. Prog. Ser.* 395, 5–20. doi: 10.3354/meps08353

IQOE, (2019). *IQOE Workshop Report: Guidelines for Observation of Ocean Sound*. St. Petersburg, FL: IQOE.

ISO, (2017). *International Standard ISO 18405:2017(E), Underwater Acoustics – Terminology*. Geneva: ISO.

Johnson, C. S. (1986). "*Dolphin audition and echolocation capacities*," in *Dolphin Cognition and Behavior: A Comparative Approach*, eds R. J. Schusterman, J. A. Thomas, F. G. Wood, and R. Schusterman, (Boca Raton, FL: CRC Press), 115–136.

Kline, L. R., DeAngelis, A. I., McBride, C., Rodgers, G. G., Rowell, T. J., Smith, J., et al. (2020). Sleuthing with sound: understanding vessel activity in marine protected areas using passive acoustic monitoring. *Mar. Policy* 120:104138. doi: 10.1016/j.marpol.2020.104138

McDonald, M. A., Hildebrand, J. A., and Wiggins, S. M. (2006). Increases in deep ocean ambient noise in the Northeast Pacific west of San Nicolas Island, California. *J. Acoust. Soc. Am.* 120:711. doi: 10.1121/1.2216565

McKenna, M. F., Katz, S. L., Wiggins, S. M., Ross, D., and Hildebrand, J. A. (2012). A quieting ocean: unintended consequence of a fluctuating economy. *J. Acoust. Soc. Am.* 132, EL169–EL175. doi: 10.1121/1.4740225

McKenna, M. F., Wiggins, S. M., and Hildebrand, J. A. (2013). Relationship between container ship underwater noise levels and ship design, operational and oceanographic conditions. *Sci. Rep.* 3:1760. doi: 10.1038/srep01760

Moore, P. W., and Schusterman, R. J. (1976). Discrimination of pure-tone intensities by the California sea lion. *J. Acoust. Soc. Am.* 60, 1405–1407. doi: 10.1121/1.381234

NOAA, (2017). *Marine Mammals: MBNMS*. Washington, DC: NOAA.

NOAA, (2021). *Sound Monitoring*. Washington, DC: NOAA.

Oestreich, W. K., Fahlbusch, J. A., Cade, D. E., Calambokidis, J., Margolina, T., Joseph, J., et al. (2020). Animal-borne metrics enable acoustic detection of blue whale migration. *Curr. Biol.* 30, 4773–4779. doi: 10.1016/j.cub.2020.08.105

Porter, M. B. (2011). *The BELLHOP Manual and User's Guide: PRELIMINARY DRAFT*. La Jolla, CA: Heat Light and Sound Research Inc.

Rolland, R. M., Parks, S. E., Hunt, K. E., Castellote, M., Corkeron, P. J., Nowacek, D. P., et al. (2012). Evidence that ship noise increases stress in right whales. *Proc. Biol. Sci.* 279, 2363–2368. doi: 10.1098/rspb.2011.2429

Ryan, J., Cline, D., Dawe, C., McGill, P., Zhang, Y., Joseph, J., et al. (2016). "New passive acoustic monitoring in Monterey Bay National Marine Sanctuary," in *Proceedings of the OCEANS 2016 MTS/IEEE Monterey* (Monterey, CA: IEEE), 1–8 doi: 10.1016/s0025-3227(01)00258-4

Ryan, J. P., Cline, D. E., Joseph, J. E., Margolina, T., Santora, J. A., Kudela, R. M., et al. (2019). Humpback whale song occurrence reflects ecosystem variability in feeding and migratory habitat of the northeast Pacific. *PLoS One* 14:e0222456. doi: 10.1371/journal.pone.0222456

Simonis, A. E., Brownell, R. L., Thayre, B. J., Trickey, J. S., Oleson, E. M., Huntington, R., et al. (2020a). Co-occurrence of beaked whale strandings and naval sonar in the Mariana Islands, Western Pacific. *Proc. Biol. Sci.* 287:20200070. doi: 10.1098/rspb.2020.0070

Simonis, A. E., Forney, K. A., Rankin, S., Ryan, J., Zhang, Y., DeVogelaere, A., et al. (2020b). Seal bomb noise as a potential threat to Monterey Bay Harbor porpoise. *Front. Mar. Sci.* 7:142. doi: 10.3389/fmars.2020.00142

Southall, B., Berkson, J., Bowen, D., Brake, R., Eckman, J., Field, J., et al. (2009). *Addressing the Effects of Human-Generated Sound on Marine Life: An Integrated Research Plan for U.S. Federal Agencies, Interagency Task Force on Anthropogenic Sound and the Marine Environment of the Joint Subcommittee on Ocean Science and Technology*. Washington, DC: Marine Mammal Commission.

Southall, B. L., Finneran, J. J., Reichmuth, C., Nachtigall, P. E., Ketten, D. R., Bowles, A. E., et al. (2019). Marine mammal noise exposure criteria: updated scientific recommendations for residual hearing effects. *Aquat. Mamm.* 45, 125–232. doi: 10.1578/AM.45.2.2019.125

Southall, B. L., Scholik-Schlomer, A. R., Hatch, L., Bergmann, T., Jasny, M., Metcalf, K., et al. (2017). *Underwater Noise from Large Commercial Ships—International Collaboration for Noise Reduction. Encyclopedia of Maritime and Offshore Engineering*. Hoboken, NJ: John Wiley & Sons, Ltd. doi: 10.1002/9781118476406.emoe056

Thomson, D. J. M., and Barclay, D. R. (2020). Real-time observations of the impact of COVID-19 on underwater noise. *J. Acoust. Soc. Am.* 147:3390. doi: 10.1121/10.0001271

Tyack, P. L., Miksis-Olds, J., Ausubel, J., and Urban, E. R. Jr. (2021). *Measuring Ambient Ocean Sound During the COVID-19 Pandemic*. Livonia, MI: EOS, 102

USCG, (2021). *Navigation Center, United States Coast Guard*. Available online at: https://www.navcen.uscg.gov/?pageName=AISMessagesAStatic#TypeOfShip (accessed November 1, 2020).

Wenz, G. M. (1962). Acoustic ambient noise in the ocean: spectra and sources. *J. Acoust. Soc. Am.* 34, 1936–1956. doi: 10.1121/1.1909155

Zuur, A. F., and Ieno, E. N. (2016). A protocol for conducting and presenting results of regression-type analyses. *Methods Ecol. Evol.* 7, 636–645. doi: 10.1111/2041-210X.12577

Conflict of Interest: The authors declare that the research was conducted in the absence of any commercial or financial relationships that could be construed as a potential conflict of interest.

Copyright © 2021 Ryan, Joseph, Margolina, Hatch, Azzara, Reyes, Southall, DeVogelaere, Peavey Reeves, Zhang, Cline, Jones, McGill, Baumann-Pickering and Stimpert. This is an open-access article distributed under the terms of the Creative Commons Attribution License (CC BY). The use, distribution or reproduction in other forums is permitted, provided the original author(s) and the copyright owner(s) are credited and that the original publication in this journal is cited, in accordance with accepted academic practice. No use, distribution or reproduction is permitted which does not comply with these terms.

frontiers in Marine Science

ORIGINAL RESEARCH
published: 24 June 2021
doi: 10.3389/fmars.2021.674702

Measuring Sound at a Cold-Water Coral Reef to Assess the Impact of COVID-19 on Noise Pollution

Laurence H. De Clippele[1] and Denise Risch[2]*

[1] *Changing Oceans Research Group, School of GeoSciences, University of Edinburgh, Edinburgh, United Kingdom,*
[2] *Scottish Association for Marine Science (SAMS), Oban, United Kingdom*

This study compares the noise levels at the cold-water coral Tisler reef, before and after the closure of the border between Norway and Sweden, which occurred as a direct result of the COVID-19 pandemic. The Tisler reef is a marine protected area located under a ferry "highway" that connects Norway and Sweden. Cold-water coral reefs are recognised as being important hotspots of both biodiversity and biomass, they function as breeding and nursing grounds for commercially important fish and are essential in providing ecosystem functions. Whilst studies have shown that fishery, ocean warming, and acidification threaten them, the effects of noise pollution on cold-water coral reefs remains unstudied. To study the severity of noise pollution at the Tisler reef, a long-term acoustic recorder was deployed from 29 January 2020 until 26 May 2020. From 15 March COVID-19 lockdown measures stopped passenger vessel traffic between Norway and Sweden. This study found that the overall noise levels were significantly lower after border closure, due to reduced ferry traffic, wind speeds, and sea level height. When comparing the median hourly noise levels of before vs. after border closure, this study measured a significant reduction in the 63–125 Hz 1/3 octave band noise levels of 8.94 ± 0.88 (MAD) dB during the day (07:00:00–19:59:59) and 1.94 ± 0.11 (MAD) dB during the night (20:00:00–06:59:59). Since there was no ferry traffic during the night, the drop in noise levels at night was likely driven by seasonal changes, i.e., the reduction in wind speed and sea level height when transitioning from winter to spring. Taking into account this seasonal effect, it can be deduced that the COVID-19 border closure reduced the noise levels in the 63–125 Hz 1/3 octave bands at the Tisler reef by 7.0 ± 0.99 (MAD) dB during the day. While the contribution of, and changes in biological, weather-related and geophysical sound sources remain to be assessed in more detail, understanding the extent of anthropogenic noise pollution at the Tisler cold-water coral reef is critical to guide effective management to ensure the long-term health and conservation of its ecosystem functions.

Keywords: COVID-19, cold-water coral reef, passive acoustic monitoring, noise pollution, soundscape, passenger vessels, marine ecosystem

OPEN ACCESS

Edited by:
Edward Urban,
Scientific Committee on Oceanic Research, United States

Reviewed by:
Mike Van Der Schaar,
Universitat Politecnica de Catalunya, Spain
Matthew Wale,
Edinburgh Napier University, United Kingdom

****Correspondence:***
Laurence H. De Clippele
laurence.de.clippele@gmail.com

Specialty section:
This article was submitted to Marine Ecosystem Ecology, a section of the journal Frontiers in Marine Science

Received: *01 March 2021*
Accepted: *20 May 2021*
Published: *24 June 2021*

Citation:
De Clippele LH and Risch D (2021) Measuring Sound at a Cold-Water Coral Reef to Assess the Impact of COVID-19 on Noise Pollution. Front. Mar. Sci. 8:674702. doi: 10.3389/fmars.2021.674702

INTRODUCTION

Coral reefs are not restricted to the shallow tropics, they also thrive in the cold aphotic waters at depths of 40–2,000 m (Davies et al., 2008; Morato et al., 2020; Sundahl et al., 2020), with some cold-water corals being able to grow as deep as 6,000 m (Roberts et al., 2009). Cold-water corals occur throughout the world's oceans and form complex reef ecosystems that can be 10–100s m in height, constructed by only a handful of scleractinian coral species [*Lophelia pertusa* (Recently synonymised to *Desmophyllum pertusum* (Addamo et al., 2016)), *Madrepora Ocolata*, *Solenosmilia variabilis*, *Oculina varicose*] (Roberts et al., 2009). The extensive reef structures they build can be of considerable age, with nearshore reefs in Norway dating back to 8,600 years before present (Wisshak et al., 2005) and deeper off-shore cold-water coral carbonate mounds likely being thousands to millions of years old, with some continuously growing for at least the last circa 11,000 years (Roberts et al., 2006; Wheeler et al., 2007; Mienis et al., 2009; Van der Land et al., 2014).

In contrast to tropical corals, cold-water corals lack the presence of symbiotic zooxanthellae algae, giving them white to orange coloured polyps (Hennige et al., 2014; De Clippele et al., 2019; **Figure 1**). They opportunistically feed on dissolved organic matter, bacteria, algae, and zooplankton (Mueller et al., 2014). They are ecologically important as hotspots of biomass (De Clippele et al., 2021) and biodiversity (Buhl-Mortensen et al., 2010; Henry et al., 2010; Kazanidis et al., 2016), function as breeding and nursing grounds for fish (Baillon et al., 2012), sharks and skates (Henry et al., 2013, 2016), are paleoclimatic archives (Douarin et al., 2014) and are essential in providing ecosystem functions such as carbon and nitrogen recycling (van Oevelen et al., 2009; Cathalot et al., 2015; Rovelli et al., 2015; de Froe et al., 2019; Maier et al., 2020; De Clippele et al., 2021).

Due to recent advances in technology, there has been a dramatic increase in our understanding of these diverse ecosystems, as well as growing evidence that many cold-water coral habitats have been degraded by bottom trawling and are threatened by ocean warming and acidification (Wheeler et al., 2005; Clark et al., 2006; Roberts et al., 2009; Hennige et al., 2015; Sweetman et al., 2017; Morato et al., 2020).

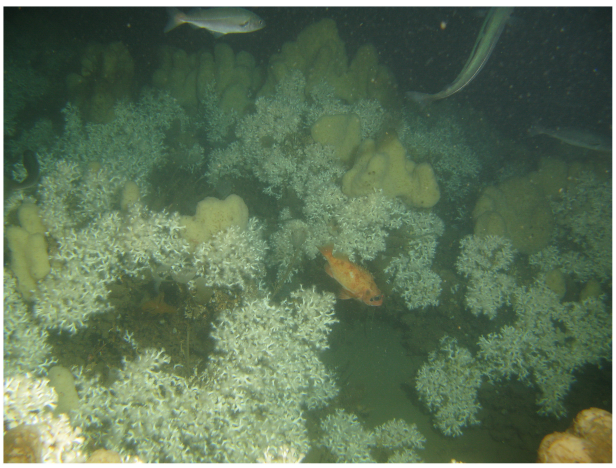

FIGURE 1 | Dense coverage of the cold-water scleractinian coral *Lophelia pertusa* at the Tisler reef with the sponge *Mycale lingua* growing within its framework, the fish *Sebastes* sp. and the fish *Pollachius* sp. (Saithe).

Since the industrial revolution, the number of powered vessels has grown rapidly, bringing with them a new type of pollution, noise pollution (Andrew et al., 2002, 2011; Frisk, 2012; Simmonds et al., 2014; Duarte et al., 2021). A recent review summarises the current knowledge on how the prevalence and intensity of anthropogenic noise pollution can affect the behaviour, physiology and ecology of tropical coral reef organisms (Ferrier-pages et al., 2021). For example, noise pollution can cause sensory confusion, or mask communication among reef animals (Simpson et al., 2011; Carroll et al., 2017; Stanley et al., 2017), which can produce sounds during reproductive behaviour, territorial defence and predator deterrence (Myrberg and Fuiman, 2002). However, due to their often remote and inaccessible nature, the prevalence, noise levels, and effects of noise pollution have not been studied yet for cold-water coral reefs.

Acoustic landscapes, or soundscapes, are composed of biological, geophysical, and anthropogenic sounds. In healthy tropical coral reefs, the soundscape is typically dominated by biological sounds produced by, for example, grunting fish and snapping shrimps (Piercy et al., 2014). In the last two decades advances in technology have allowed us to study cold-water coral reefs, and simultaneously noise pollution from ships have increasingly affected marine soundscapes. While the effects of noise pollution on terrestrial ecosystems have been recognised, the effects on marine ecosystems are still widely understudied (Duarte et al., 2021). Anthropogenic noise, including vessel noise, can affect all frequencies (Duarte et al., 2021), but the 1/3–octave bands centred at 63, 100 and 125 Hz have often been used as indicators of low-frequency vessel noise (Tasker et al., 2010; Peng et al., 2015; Merchant et al., 2016; Thomson and Barclay, 2020). These frequency bands were selected as they are generally less influenced by pseudo flow noise and wind noise (Wenz, 1962; Strasberg, 1979; Bassett et al., 2014; Peng et al., 2015; Merchant et al., 2016).

A global slowdown in private and commercial shipping traffic as a measure to mitigate the threat of COVID-19 to human life and welfare has inadvertently resulted in a natural "before and after impact" experiment offering unanticipated insight into how human behaviour affects ocean noise levels. Already in the first quarter of 2020, large negative trends of 2.3–7.1 dB at 100 Hz have been observed near the port of Vancouver, Canada, coinciding with a 21.5% reduction in Automatic Identification System (AIS) ship-tracking transmissions (Thomson and Barclay, 2020). In terrestrial rural and urban environments, drops of 3.6–7.4 dB in the ambient noise levels led to positive changes in the communication distance and salience of the performance of the songs of birds (Derryberry et al., 2020). These drastic changes shown for these two habitats raise the question of what the extent and effect is of the reduction of anthropogenic noise pollution

due to COVID-19 in other ecological systems, including cold-water coral reefs, which are currently understudied in terms of their soundscape.

This study quantified the prevalence and the noise levels at the Tisler cold-water coral reef in Norway before and after the international border between Sweden and Norway closed on 15 March 2020 as a result of the COVID-19 pandemic.

MATERIALS AND METHODS

Study Area

The Tisler cold-water coral reef lies in the north-eastern part of the Skagerrak in the Hvaler area in Norway (Lavaleye et al., 2009; **Figure 2**). North of Tisler Island, the reef grows in a NW–SE direction in the Ytre Hvaler, a 48-km-long ocean channel through which Atlantic water of around 8°C flows (Wagner et al., 2011; Guihen et al., 2013; De Clippele et al., 2018). The reef is approximately 8,600–8,700 year old (Wisshak et al., 2005), 1.2 km long, 200 m wide and has live coral growing between 70 and 160 m depth (Lavaleye et al., 2009; De Clippele et al., 2018). The Tisler Reef has been protected against bottom-impacting fishing techniques by Norwegian fishery regulations since 2003 (Fosså et al., 2010).

Acoustic Data Analysis

We established a recording station at 120 m depth on the southeast side of the Tisler reef (Longitude: 10.970683, Latitude: 58.9947) to collect long-term passive acoustic underwater recordings from 12:00:00 (CET) 29 January 2020 to 00:45:01 (CEST) 26 May 2020. The local time switched from CET to CEST on 29 March 2020. The SoundTrap ST500 long-term recorder (Ocean Instruments, Auckland, New Zealand) used for this study, sampled at 96,000 Hz, providing an effective analysis bandwidth of 20–60,000 Hz. The sensitivity of the whole system chain (recorder, hydrophone and applied gain) was -175.5 dB re 1 V/μPa at 250 Hz. Recordings were saved in the lossless X3 compressed file format (Johnson et al., 2013). The recorder was fixed at approximately 3.5 m above the seafloor using submersible floats attached to a deep-sea acoustic release canister (ARC) (RS Aqua, United Kingdom). The ARC allowed for a quick recovery without leaving the anchor behind in the Tisler reef, a marine protected area. The acoustic recorder collected data continuously for 118 days. After the recorder was retrieved, waveform audio files were generated using the SoundTrap Host for further analysis. Visual inspections with a remotely operated vehicle (ROV) indicated the ST500 was surrounded by rubble, dead coral framework, and live coral colonies.

The sound pressure levels were further quantified by 1/3–octave bands (TOB) from 20 to 20,000 Hz using the "TOL" (Third Octave Levels) function in PAMGuide to describe distributions and trends in noise levels. For the statistical analyses, hourly medians of the TOBs were calculated in R using the openair package (Carslaw and Ropkins, 2012).

Spectrograms (Window type: Hanning, 50%, hop size: 256, DFT size: 512 samples, grid spacing: 188 Hz) generated using Raven Pro 1.6.1 (K. Lisa Yang Center for Conservation Bioacoustics, 2019) were used to visually pinpoint the closest point of approach (CPA) of the ferries to the acoustic recordings.

Passenger Vessel Traffic

The Tisler reef is located under a ferry "highway" between Sandefjord (Norway) and Strömstad (Sweden). The recorder was located approximately 91 m from this ferry "highway." Three types of ferries are used by two companies. The company ColorLine uses the M/S Colour Viking (capacity: 1,720 passengers, 370 cars) and, their second vessel, the world's largest plug-in hybrid, runs on batteries to reduce its noise level (capacity: 2,000 passengers). The third vessel is run by Fjordline and is slightly smaller (capacity: 1,350 passengers). Unless there is a cancellation due to bad weather or docking periods, the ferries will sail up to 12 times a day above the reef (**Figure 2** and **Table 1**).

Due to the closure of borders between Norway and Sweden, as a result of the COVID-19 pandemic, there were no sailings

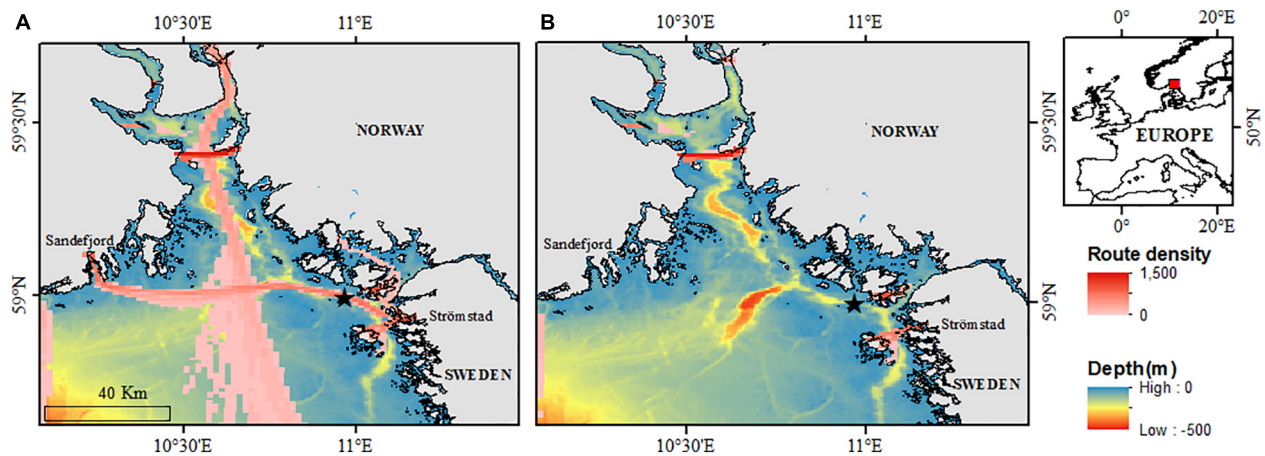

FIGURE 2 | Map indicating the location of the Tisler cold-water coral reef (black star and red square) and the passenger routes density (Source: EMODnet Human Activities: EMSA Route Density Map) in **(A)** February 2020 (before COVID-19 border closure) and **(B)** April 2020 (after COVID-19 border closure).

TABLE 1 | Departure times of the two ferry companies that sail between Sandefjord and Strömstad, 2020.

	Colorline	Fjordline
From Sandefjord to Strömstad	07:00, 10:00, 13:30, 17:00	08:30, 15:20
From Strömstad to Sandefjord	10:00, 13:40, 17:00, 20:00	12:00, 18:30

from March 15, 2020 to the present (May 2021) (**Figure 2A** vs. **Figure 2B**). In the period between 29 January and 15 March, consistent strong signals from the passing ferries, lasting for ∼30 min, had an approximate CPA, as determined by visual inspection of the sound files, at 07:50, 09:25, 09:30, 11:03, 11:29, 13:09, 14:25, 16:17, 16:30, 17:52, 17:57, and 19:27 on each day of the week.

Route Density

The total and average monthly route density of marine vessels (i.e., passenger, fishing, cargo, tanking, and all other types) were calculated using the open source EMODnet Human Activities EMSA Route Density Maps. Route density maps were downloaded as .TIF format for February, March, April and May 2020 and imported in the ArcGIS 10.1, ESRI Software. The "Extract by mask" ArcGIS tool was used to clip these route density maps to an area of 100 km^2 around the Tisler reef. The ArcGIS "raster to point" tool was then used to create an attribute table from which the total and average monthly route density of marine vessels could be extracted and calculated.

Shipping Noise Indicators

While all the TOB can be affected by vessel noise (Hildebrand, 2009; McKenna et al., 2012), the ones centred at 63, 79, 100, and 125 Hz were used, as these are the current noise indicators of low-frequency vessel noise in an European management context (Dekeling et al., 2016; Garrett et al., 2016), and are less influenced by flow and wind noise (Wenz, 1962; Tasker et al., 2010; Peng et al., 2015; Merchant et al., 2016; Thomson and Barclay, 2020).

Environmental Variables

Hourly data on the wind speed (m/s) and sea level height (cm) were downloaded from the Nordkoster and Kungsvik SMHI meteorological stations[1]. A categorical variable "ferry" was created, representing the hours at which the ferry would have their CPA to the recorder on the reef and were labelled as "ferry passage" vs. "no ferry passage" [i.e., 07:00, 09:00, 11:00, 13:00, 14:00, 16:00, 17:00, and 19:00 (CET)]. The latter was determined by checking repeated patterns of vessel passage over the reef in Raven Pro 1.6.1 (see section *Acoustic data analyses*).

Statistical Analyses

The 25th percentile, median, mean absolute deviation (MAD), and 75th percentile of the median hourly TOB sound pressure levels, were used to assess the change in noise levels before (29 January–14 March 2020) and during (15 March–26 May 2020) border closure in the statistical software R (R Development Core Team, 2010; Wickham, 2011).

[1]smhi.se

The distribution of the response variables (TOB) did not follow a Gaussian distribution. Therefore the more flexible Generalised Linear Modelling (GLM) approach was used. The probability distributions of the noise levels analysed here belong to the exponential quasi-Poisson family (McCullagh and Nelder, 1989; Dobson and Barnett, 2008). The software R was used to perform the GLM. The GLM models were run four times for all TOB (25–15,849 Hz). Once for daytime recordings (07:00:00–19:59:59) before (593 samples) and after closure (936 samples) and once for nighttime recordings (20:00:00–06:59:59) before (499 samples) and after border closure (795 samples). The model performance of the quasi-Poission GLM regressions were indicated by the quasi-Akaike information criterion (QAIC) (Bolker, 2020). A lower QAIC indicates a better goodness of fit. Correlation between variables was tested using the cor.test() function in R. No variables were correlated and since no ferries run at night this variable was excluded from the nighttime models.

Data Visualisation

The ggplot2 package in R was used to plot the seasonal variables against the shipping noise indicators and the higher frequency TOB that according to the Wenz curve should be heavily influenced by wind (100–10,000 Hz) (Wenz, 1962). A LOESS curve was fitted with a span of 0.05 to make the comparison of the trends more intuitive.

To assess daily and weekly noise level changes, the hourly median 63–125 Hz TOB were plotted using the timeVariation function from the openair package in R (Carslaw and Ropkins, 2012). Diurnal and weekly changes were assessed separately for the data collected before (29 January–14 March 2020) and during (15 March–26 May 2020) border closure. This function plots the 95% confidence intervals and the median, which were calculated through bootstrap simulation, providing the diurnal variation of the noise levels. These plots were used to identify any diurnal or weekly patterns in elevated noise levels in the before and after periods.

RESULTS

Route Density

In February and March 2020, passenger route density (RD) is the highest, while in April and May fishing RD is the highest compared to the other vessel types (**Figure 3** and **Table 2**). The route density of cargo vessels remain relatively similar from February to May 2020. From February to May 2020, the total marine vessel RD increased 15%, passenger RD decreased 47%, cargo RD increased 8%, fishing RD increased 46%, tanker RD decreased 2%, and all other types of vessel RD increased 76% within the 100 km^2 area around the Tisler reef (**Figure 3** and **Table 2**).

Statistical Analysis

When comparing the noise levels before vs. after the borders closed and ferry traffic ceased, the difference between hourly median TOB (25–15,849 Hz) ranged from 0.6 to 6.9 dB at

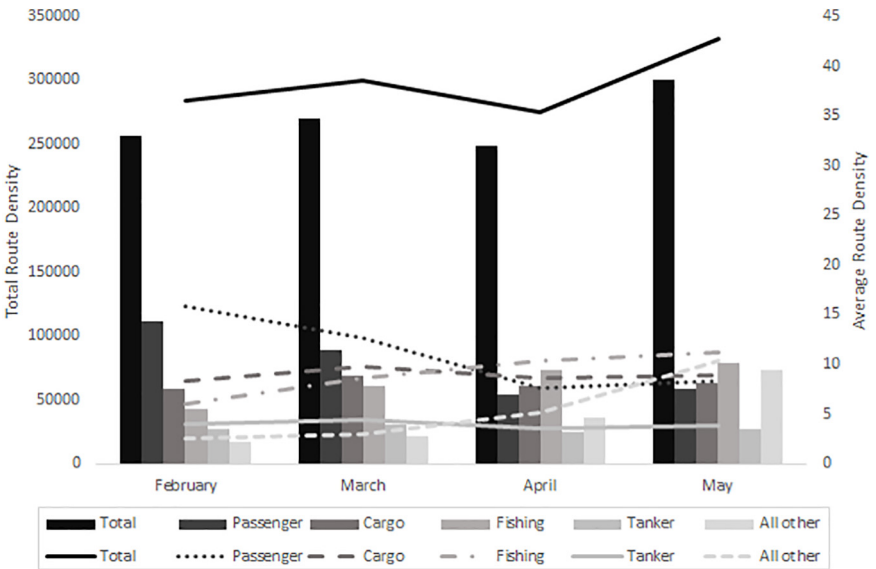

FIGURE 3 | Bar and line diagram showing the total (primary axis) and average (secondary axis) route density (routes per km^2) of the total, passenger, cargo, fishing, tanker, and all other types of ships within the 100 km^2 area around the Tisler reef.

night and from 0.8 to 9.8 dB during the day. The shipping noise indicators (63–125 Hz), had a reduction of 8.9 ± 0.9 (MAD) dB during the day and 1.9 ± 0.1 (MAD) dB during the night (**Table 3**). Before lockdown, the median noise levels were 3.5 ± 2.19 (MAD) dB higher during the day vs. the night. After lockdown, the noise levels were 0.9 ± 0.52 (MAD) dB higher during the day vs. the night (**Table 3**).

During the day, the variable "ferry" and "wind speed" significantly affected the variability in shipping noise indicator levels before border closure, while "wind speed" and "sea level" affected the variability in the noise levels after border closure (**Table 4**). During the night, "wind speed" and "sea level" affected the variability in the noise levels, although this is not or less significant at the 63 and 79 Hz TOB after border closure (**Table 4**). However, wind speed had a strong effect on almost all TOB throughout this time series (**Figure 4** and **Table 4**). Before border closure, sea level affected noise levels the least during the day and the most during the night. After border closure, sea level mostly affected the TOB above and below the 251–3981 Hz TOB. The seasonal changes in the wind speed and sea level are given in **Table 5**.

TABLE 2 | Total and average route density (routes per km^2) of the total, passenger, cargo, fishing, tanker, and all other types of vessels within the 100 km^2 area around the Tisler reef (Source: EMODnet Human Activities: EMSA Route Density Map).

Vessel type	February		March		April		May	
	Total	Av.	Total	Av.	Total	Av.	Total	Av.
Total	256,452	36.57	270,384	38.56	248,565	35.5	300,288	42.82
Passenger	110,959	15.82	89,166	12.72	53,736	7.66	58,855	8.39
Cargo	58,106	8.29	68,946	9.83	60,603	8.64	62,923	8.97
Fishing	42,398	6.05	60,431	8.61	72,694	10.4	78,666	11.21
Tanker	27,634	3.94	30,583	4.36	25,169	3.59	27,152	3.87
All other	17,355	2.47	21,258	3.03	36,363	5.18	72,692	10.36

Diurnal, Weekly, and Monthly Variation

Events with high sound pressure levels at 09:00, 16:00, and 17:00 are visible as high peaks in the diurnal "before border closure" plot (**Figure 5A**). Lower but still distinct peaks are observed at 07:00, 11:00, 13:00, 14:00, and 19:00. These peaks coincide with the ferry CPA timings. The strong shipping noise-driven diurnal pattern disappears after border closure and manifests itself as a flatter, quieter, curve in the diurnal plot (**Figure 5B**). The pattern observed during border closure appears more similar to what can be observed during nighttime before border closure.

Before border closure, weekly changes in the noise levels indicate higher sound pressure levels on Wednesdays and at the weekends (**Figure 5C**). A reverse pattern with a slight decrease in the sound levels on Wednesdays and Sundays is observed after border closure, together with a slight increase on Saturdays (**Figure 5D**).

DISCUSSION

This study shows that the noise levels at the Tisler reef significantly reduced after the international border closed between Norway and Sweden as a consequence of the COVID-19 pandemic. While a seasonal reduction in wind speed and sea level accounted for a decrease in the noise levels at the Tisler reef, the ceasing of ferry traffic greatly reduced the levels of noise pollution at the reef during the day.

TABLE 3 | Median noise levels (dB re 1 μPa) of the 1/3 octave bands.

	NIGHT (20:00:00–06:59:59)									DAY (07:00:00–19:59:59)								
	Before border closure				After border closure					Before border closure				After border closure				
	25th Perc.	Median	± MAD	75th Perc.	25th Perc.	Median	± MAD	75th Perc.	≠	25th Perc.	Median	± MAD	75th Perc.	25th Perc.	Median	± MAD	75th Perc.	≠
25 Hz	72.3	82.9	16.9	100.4	70.9	75.9	8.6	90.9	−6.9	73.6	83.6	16.9	104.3	71.3	75.3	7.2	87.9	−8.3
32 Hz	71.9	77.2	9.3	91.1	71.2	75.1	6.6	87.5	−2.1	74.6	83.7	14.8	97.0	71.5	74.8	5.7	84.9	−8.9
40 Hz	72.2	75.5	6.8	86.4	71.7	73.5	3.3	80.9	−2.0	74.4	80.8	11.1	92.3	72.0	73.8	3.3	80.4	−7.1
50 Hz	72.0	75.4	6.9	84.6	72.1	73.7	2.9	78.9	−1.7	74.9	81.9	11.4	91.1	72.5	74.3	3.4	79.7	−7.6
63 Hz	71.1	75.2	7.2	82.7	71.7	73.4	3.2	78.3	−1.7	75.6	83.5	11.2	90.8	72.1	74.0	3.5	79.5	−9.5
79 Hz	70.9	75.5	8.0	82.3	71.8	73.6	3.2	77.8	−1.9	76.8	84.5	10.7	91.2	72.4	74.7	4.2	79.6	−9.8
100 Hz	70.3	76.2	8.3	80.9	71.6	74.1	4.5	78.4	−2.0	77.7	84.0	9.9	90.8	72.4	75.6	5.3	80.3	−8.4
125 Hz	70.2	76.7	8.7	81.8	71.5	74.7	5.5	79.1	−2.0	78.2	84.1	9.0	90.1	72.8	76.7	6.0	80.9	−7.4
158 Hz	70.6	77.5	8.6	82.4	71.6	75.6	6.6	80.6	−1.9	78.6	84.1	8.1	89.4	73.5	77.6	6.5	82.4	−6.4
200 Hz	70.7	77.8	9.8	84.2	72.0	76.8	7.1	81.6	−1.0	79.2	85.0	8.4	90.5	74.6	78.9	6.6	83.4	−6.2
251 Hz	71.1	78.8	10.9	85.9	72.9	78.2	7.4	82.9	−0.6	80.2	86.0	7.4	90.6	75.6	80.1	6.5	84.4	−5.9
316 Hz	71.5	80.2	10.9	86.7	73.7	79.5	7.4	84.0	−0.7	81.2	86.6	6.9	90.7	76.5	80.9	6.3	85.0	−5.6
398 Hz	72.9	81.7	10.4	87.8	74.9	80.6	7.1	84.6	−1.1	81.6	86.7	6.7	90.7	77.5	81.9	6.0	85.6	−4.8
501 Hz	73.4	85.6	10.8	89.0	75.7	82.0	7.1	85.7	−3.7	82.4	87.5	6.7	91.6	78.4	82.8	5.8	86.3	−4.6
631 Hz	73.7	83.0	10.4	89.0	75.6	81.9	7.2	85.7	−1.0	82.5	87.2	6.5	91.2	78.6	82.9	5.6	86.1	−4.3
794 Hz	73.8	83.0	10.6	89.1	75.4	81.9	7.1	85.7	−1.2	81.7	87.0	6.8	91.1	78.5	82.6	5.7	86.2	−4.4
1,000 Hz	74.3	83.2	10.4	89.2	75.3	81.7	7.3	85.8	−1.5	81.3	86.7	7.1	91.1	78.5	82.7	5.6	86.1	−4.0
1,259 Hz	74.0	83.2	10.4	89.2	75.2	81.7	7.1	85.7	−1.5	80.9	86.2	7.3	90.7	78.2	85.4	5.8	86.0	−0.8
1,585 Hz	73.6	82.9	10.5	88.9	74.3	81.1	7.6	85.4	−1.9	80.2	85.7	7.5	90.2	77.5	82.0	6.0	85.7	−3.7
1,995 Hz	73.3	82.7	10.6	88.8	73.8	80.8	7.7	85.2	−2.0	79.3	85.4	7.8	90.1	77.0	81.5	6.1	85.4	−3.8
2,512 Hz	73.3	82.2	10.4	88.1	73.1	79.8	7.9	84.4	−2.3	78.8	84.6	7.8	89.3	76.2	80.7	6.0	84.6	−3.9
3,162 Hz	73.4	82.7	10.5	88.7	73.6	80.4	7.9	85.0	−2.3	79.2	85.1	7.9	89.8	76.8	81.3	6.0	85.1	−3.8
3,981 Hz	73.0	82.1	10.4	87.9	73.0	80.0	7.9	84.4	−2.1	78.3	84.5	7.9	89.0	76.5	80.9	5.9	84.6	−3.6
5,012 Hz	72.5	81.2	10.0	86.8	72.2	78.9	7.7	83.4	−2.3	77.2	83.5	7.7	87.9	75.8	79.9	5.6	83.5	−3.6
6,310 Hz	72.5	80.9	9.7	86.2	72.0	78.6	7.5	83.0	−2.3	76.6	83.0	7.4	87.2	75.5	79.6	5.5	83.1	−3.4
7,943 Hz	72.6	80.3	9.2	85.6	71.8	78.2	7.3	82.6	−2.1	76.0	82.3	7.3	86.5	75.0	79.1	5.5	82.6	−3.2
10,000 Hz	72.6	79.7	8.9	84.8	71.9	77.7	7.1	82.0	−2.0	75.4	81.6	6.9	85.6	74.5	78.5	5.4	82.0	−3.1
12,589 Hz	72.8	79.5	8.1	84.2	72.3	77.3	6.6	81.6	−2.2	75.3	81.0	6.2	84.6	74.2	78.1	5.4	81.5	−2.9
15,849 Hz	73.1	79.2	6.6	83.0	72.5	76.8	6.1	80.8	−2.3	75.1	80.4	5.0	83.1	74.0	77.4	5.0	80.7	−3.0

Comparing day and night before (29 January–14 March 2020) and after border closure (15 March –26 May 2020). The 25th and 75th percentile as well as the mean absolute deviation (MAD) are given. The difference (≠) indicates how much the noise levels (dB) have reduced after the border closure between Norway and Sweden because of the COVID-19 pandemic.

TABLE 4 | Table showing goodness of fit (QAIC) and the statistical significance (*p*-values) of the GLM regression *analyses* of day and nighttime noise levels before (29 January–14 March 2020) and after border closure (15 March–26 May 2020), accounting for the predictor variables ferry, wind speed (m/s), and sea level height (cm).

	NIGHT (20:00:00–06:59:59)						DAY (07:00:00–19:59:59)							
	Before border closure			After border closure			Before border closure				After border closure			
	QAIC	Wind speed	Sea level	QAIC	Wind speed	Sea level	QAIC	Ferry	Wind speed	Sea level	QAIC	Ferry	Wind speed	Sea level
25 Hz	2.58	0.202	0.878	1.92	0.065	< 0.05	2.76	0.276	0.268	0.056	1.83	0.992	< 0.05	< 0.001
32 Hz	1.72	0.473	0.693	1.51	< 0.05	< 0.05	1.72	< 0.001	0.106	< 0.05	1.41	0.95	< 0.05	< 0.05
40 Hz	1.17	0.209	0.409	0.82	< 0.01	< 0.01	1.18	< 0.001	< 0.01	< 0.05	0.76	0.96	< 0.001	< 0.001
50 Hz	0.89	< 0.01	0.168	0.6	0.053	< 0.05	0.89	< 0.001	< 0.001	< 0.05	0.57	0.938	< 0.001	< 0.001
63 Hz	0.74	< 0.001	0.056	0.55	0.06	< 0.01	0.78	< 0.001	< 0.001	0.097	0.53	0.64	< 0.001	< 0.001
79 Hz	0.54	< 0.001	< 0.05	0.45	0.219	0.09	0.71	< 0.001	< 0.001	0.162	0.46	0.792	< 0.001	< 0.001
100 Hz	0.35	< 0.001	< 0.001	0.41	< 0.001	< 0.05	0.63	< 0.001	< 0.001	0.261	0.44	0.755	< 0.001	< 0.001
125 Hz	0.28	< 0.001	< 0.001	0.4	< 0.001	< 0.05	0.56	< 0.001	< 0.001	0.432	0.46	0.833	< 0.001	< 0.001
158 Hz	0.24	< 0.001	< 0.001	0.42	< 0.001	< 0.05	0.49	< 0.001	< 0.001	0.586	0.45	0.737	< 0.001	< 0.001
200 Hz	0.23	< 0.001	< 0.001	0.4	< 0.001	< 0.05	0.47	< 0.001	< 0.001	0.486	0.42	0.538	< 0.001	< 0.001
251 Hz	0.23	< 0.001	< 0.001	0.41	< 0.001	0.112	0.42	< 0.001	< 0.001	0.697	0.39	0.691	< 0.001	< 0.01
316 Hz	0.23	< 0.001	< 0.001	0.39	< 0.001	0.376	0.37	< 0.001	< 0.001	0.665	0.34	0.74	< 0.001	< 0.01
398 Hz	0.25	< 0.001	< 0.01	0.38	< 0.001	0.351	0.35	< 0.001	< 0.001	0.731	0.32	0.712	< 0.001	< 0.05
501 Hz	0.24	< 0.001	< 0.01	0.38	< 0.001	0.602	0.33	< 0.001	< 0.001	0.73	0.29	0.884	< 0.001	0.084
631 Hz	0.23	< 0.001	< 0.01	0.37	< 0.001	0.884	0.31	< 0.001	< 0.001	0.708	0.27	0.922	< 0.001	0.195
794 Hz	0.24	< 0.001	< 0.01	0.36	< 0.001	0.783	0.29	< 0.001	< 0.001	0.835	0.28	0.742	< 0.001	0.668
1,000 Hz	0.22	< 0.001	< 0.01	0.35	< 0.001	0.496	0.27	< 0.001	< 0.001	0.788	0.26	0.692	< 0.001	0.861
1,259 Hz	0.22	< 0.001	< 0.01	0.36	< 0.001	0.508	0.24	< 0.001	< 0.001	0.829	0.25	0.693	< 0.001	0.861
1,585 Hz	0.22	< 0.001	< 0.01	0.34	< 0.001	0.118	0.24	< 0.001	< 0.001	0.829	0.25	0.678	< 0.001	0.283
1,995 Hz	0.2	< 0.001	< 0.01	0.33	< 0.001	0.066	0.22	< 0.001	< 0.001	0.764	0.23	0.718	< 0.001	0.237
2,512 Hz	0.17	< 0.001	< 0.01	0.3	< 0.001	< 0.05	0.2	< 0.001	< 0.001	0.636	0.22	0.77	< 0.001	0.221
3,162 Hz	0.19	< 0.001	< 0.01	0.3	< 0.001	< 0.05	0.2	< 0.001	< 0.001	0.693	0.22	0.76	< 0.001	0.15
3,981 Hz	0.16	< 0.001	< 0.01	0.27	< 0.001	< 0.01	0.19	< 0.001	< 0.001	0.735	0.2	0.811	< 0.001	0.086
5,012 Hz	0.14	< 0.001	< 0.01	0.23	< 0.001	< 0.01	0.18	< 0.001	< 0.001	0.814	0.18	0.823	< 0.001	< 0.05
6,310 Hz	0.12	< 0.001	< 0.01	0.21	< 0.001	< 0.001	0.16	< 0.001	< 0.001	0.926	0.16	0.821	< 0.001	< 0.05
7,943 Hz	0.1	< 0.001	< 0.01	0.18	< 0.001	< 0.001	0.15	< 0.001	< 0.001	0.696	0.15	0.814	< 0.001	< 0.01
10,000 Hz	0.09	< 0.001	< 0.01	0.15	< 0.001	< 0.001	0.14	< 0.001	< 0.001	0.47	0.13	0.844	< 0.001	< 0.001
12,589 Hz	0.09	< 0.001	< 0.05	0.12	< 0.001	< 0.01	0.13	< 0.001	< 0.001	0.265	0.11	0.908	< 0.001	< 0.001

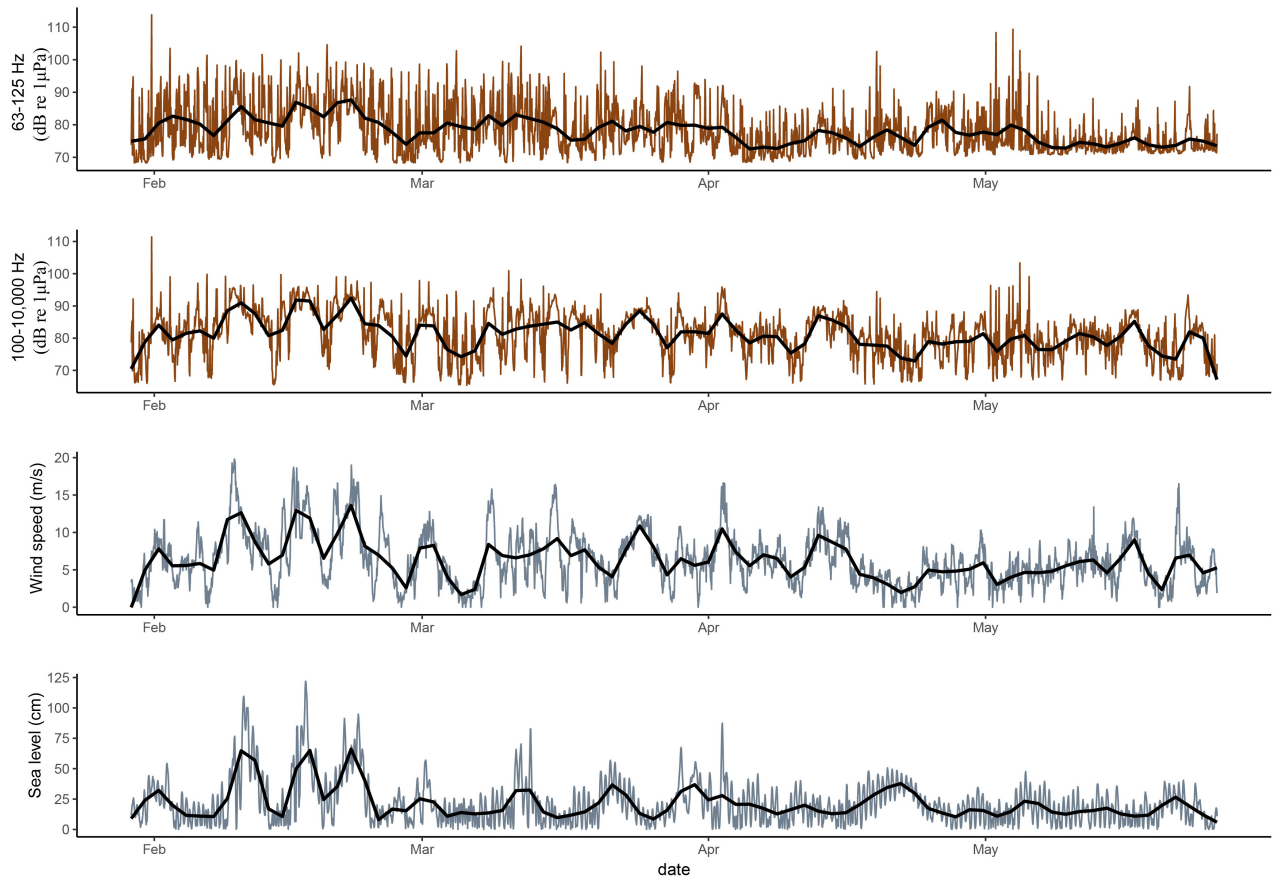

FIGURE 4 | Plots showing the variability in the shipping noise indicators [63–125 Hz TOB sound pressure levels (dB re 1 μPa)], the 100–10,000 Hz TOB sound pressure levels that are more impacted by wind speed (dB re 1 μPa) (Wenz, 1962), wind speed (m/s), and sea level height (cm) between 29 January and 26 May 2020 at the Tisler cold-water coral reef. The brown and grey lines shows the actual data. The black line is a LOESS fitted curve to make the comparison of the trends more intuitive.

TABLE 5 | The median and the mean absolute deviation (MAD) of the wind speed and sea level height at the Tisler reef downloaded from SMHI(smhi.se).

	NIGHT (20:00:00–06:59:59)					DAY (07:00:00–19:59:59)				
	Before border closure		After border closure		≠	Before border closure		After border closure		≠
	Median	± MAD	Median	± MAD		Median	± MAD	Median	± MAD	
Wind speed (m/s)	6.1	4.7	5.0	2.9	−1.1	6.2	4.5	5.3	2.5	−0.9
Sea level height (cm)	18.3	16.9	17.1	10.0	−1.25	19.2	18.6	16.8	10.6	−2.4

The ≠ symbol indicates the difference in the wind speed and sea level after border closure.

Compared to February 2020, the overall vessel route density increased by 15% in May 2020, but passenger vessel route density (i.e., ferry traffic) decreased 20% in March, 52% in April, and 47% in May. The COVID-19 border closure coincides with this reduction in passenger vessel route density. The overall increase in vessel route density from winter to spring can be explained by improved weather conditions making sea-going safer and more appealing for fishing and other vessel types, e.g., recreational vessels such as cruise ships (Robards et al., 2016). Between 1950 and 2007 researchers found that ambient noise levels in the world's oceans increased as much as 3.3 dB per decade due to an increase in vessel traffic (Andrew et al., 2002). The observed drop in noise levels at the Tisler reef could therefore translate to travelling back more than two decades in time. Ferries have been travelling between Sandefjord (Norway) and Strömstad (Sweden) since (at least) 1964[2]. Even though the larger surrounding area's overall vessel route density increased over the time period of this study, the drop in the noise levels at the Tisler reef indicates that the soundscape is heavily impacted by shipping noise, which directly over the reef is dominated by the ferries.

[2]https://www.lardex.net/gruppe/519

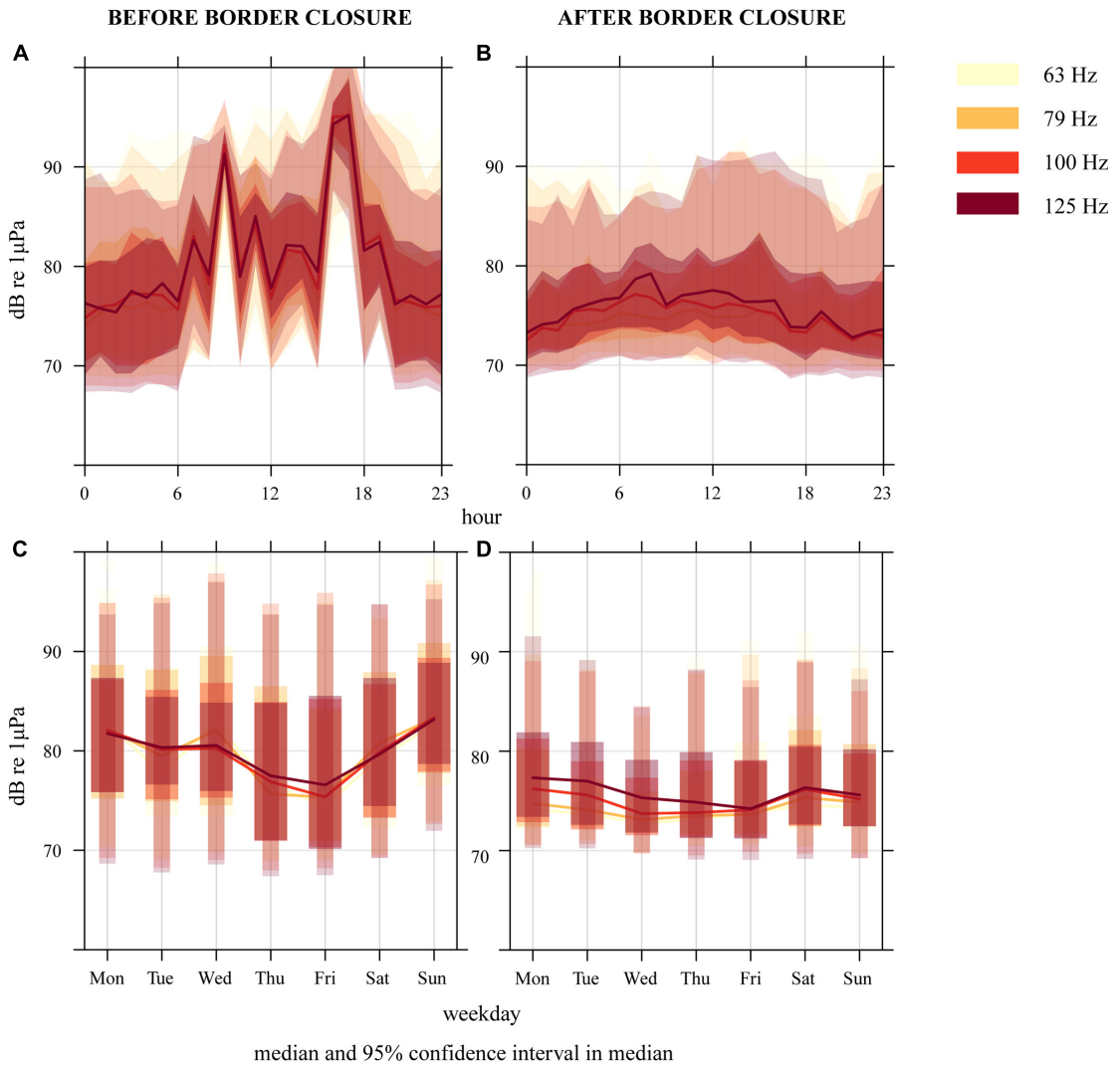

FIGURE 5 | Sound pressure levels in the hourly median 63–125 Hz 1/3 octave frequency bands at the Tisler reef from **(A,C)** 29 January–14 March 2020 and **(B,D)** 15 March–26 May 2020. The plot shows the 95% confidence intervals and the median (line), which are calculated through bootstrap simulation, providing the **(A,B)** diurnal and **(C,D)** weekly variation of noise levels.

Since the ferries do not travel at night, the nighttime noise levels which varied between 73.4 and 85.6 dB re 1 µPa across all the TOB are likely to be more representative of the Tisler reefs' natural soundscape. The reduction of 1.9 ± 0.11 (MAD) dB in the noise levels during the night after border closure were driven by a seasonal change coupled with a reduction of both the wind speed and sea level height (**Figure 4** and **Table 5**). A decrease in wind speed is typically found in temporal regions when transitioning from winter to spring (Wenz, 1962; Haver et al., 2019). Changes in sea level height can be attributed to short-term variations in waves and tides or flood events associated with winter snow melts or severe storms. At Tisler Reef, there is no strong tidal influence, instead, the water flow is channelled over a sill through the Ytre Hvaler sound, which has a NW–SE orientation (De Clippele et al., 2018). Acoustic Doppler Current Profile (ADCP) measurements from 2006 to 2010 indicated that 43% of the time, the currents flow in a north-west direction and 57% in a south-east direction (De Clippele et al., 2018), which could attribute to the observed changes in the sea level height.

During the day, a much larger reduction of 8.9 ± 0.88 (MAD) dB in the 63–125 Hz TOB was observed after the border closed and ferry traffic ceased. If the nighttime reduction of 1.9 ± 0.11 (MAD) dB, which was driven by seasonal changes, is subtracted from the daytime reduction, we can deduce that the anthropogenic acoustic footprint at the Tisler reef was reduced by 7.0 ± 0.99 (MAD) dB as a consequence of the COVID-19 border closure.

Before border closure, the diurnal pattern was strongly driven by anthropogenic activity, i.e., the ferry traffic over the reef. Anthropogenic diurnal patterns have also, for example, been observed near the shore of North Carolina (Haviland-Howell et al., 2007) and in marine protected areas such as Glacier Bay

(Haver et al., 2019). The strong diurnal pattern disappeared during border closure and revealed more subtle changes in noise levels across the frequency bands. Weekly patterns were also observed, particularly during the weekend and on Wednesdays. These were likely linked to variation in the time schedule of vessel traffic further off-shore (**Figure 2**; Haviland-Howell et al., 2007). In addition, the difference in the noise levels between night and day, were much smaller after border closure (before: 3.5 ± 2.19 dB vs. after: 0.9 ± 0.52 dB). This indicates that the noise levels after border closure will reflect that of a much more natural and "unpolluted" soundscape. However, AIS, current speed, and biological data are needed to fully understand and quantify the changes observed in the Tisler reef's soundscape.

Although not yet studied in detail, during "business as usual" the increased noise levels at the Tisler Reef caused by the ferry traffic could cause auditory masking (Simpson et al., 2011; Carroll et al., 2017; Stanley et al., 2017), affect individual and social behaviour (Myrberg and Fuiman, 2002), cause physical damage (Le Prell et al., 2012) and negatively affect the physiological functioning of the reef organisms (Nedelec et al., 2016; Simpson et al., 2016). While some studies indicate that fish might be able to habituate to continuous noise exposure (Nedelec et al., 2016; Holmes et al., 2017; Staaterman et al., 2020), this has not been shown for sporadic exposure (e.g., by ferry traffic), which can impact escape and swimming behaviour (Holmes et al., 2017). Regardless of the type of exposure, some reef fish and invertebrates are less mobile or sessile and are less likely to show clear behavioural changes when exposed to noise pollution (Ferrier-pages et al., 2021). While evidence of the effects of noise pollution on tropical coral reef organisms is growing (Ferrier-pages et al., 2021), none is currently available for cold-water coral reef organisms.

Since growing evidence shows that shipping noise can act as a chronic habitat-level stressor, which harms individual animals and ecosystem linkages (e.g. via disrupting predator-prey interactions) (Ferrier-pages et al., 2021), marine protected areas (MPAs), such as the Tisler reef MPA, should include measures for monitoring and mitigating anthropogenic noise (Haren, 2007; Williams et al., 2015). With or without an MPA to protect vulnerable marine ecosystems such as cold-water coral reefs, diverting shipping lanes or using time and area exclusions can help regulate anthropogenic noise threats (Weilgart, 2006). Studies, such as this one, that quantify the extent of the noise generated by individual components of the anthropogenic soundscape, such as shipping, can inform policymakers and stakeholders in developing legal frameworks and highlight the need for better management and technological solutions to mitigate noise pollution impacts on these sensitive marine environments.

CONCLUSION

A literature search for "cold-water coral" and "deep-sea coral" returned only 15 publications in the year 2000, while in 2020 it returned 253. While advances in technology have enabled us to increase our knowledge on these remote and inaccessible reefs over the last two decades, simultaneously shipping, seismic surveys, oil and gas developments seismic airguns, and military sonar have increased the level of anthropogenic noise in the marine environment (Duarte et al., 2021). The COVID-19 shutdown has significantly reduced anthropogenic noise levels and provided us with the unique opportunity to study relatively unpolluted soundscapes (Derryberry et al., 2020). This study is the first to assess the extent of noise pollution at a cold-water coral reef and provides a baseline to guide us toward more effective management of these ecosystems. Results from "COVID-19 before and after noise pollution experiments" provide valuable insights to understand the extent to which noise pollution affects the functioning of marine ecosystems, especially nearshore, where passenger, fishing, and recreational shipping traffic is denser.

DATA AVAILABILITY STATEMENT

The datasets presented in this article are not readily available because the data is part of an ongoing project. Requests to access the datasets should be directed to corresponding author.

AUTHOR CONTRIBUTIONS

LDC: Conceptualization, fieldwork, writing, methodology. DR: Review and editing of the manuscript and methodology. Both authors contributed to the article and approved the submitted version.

FUNDING

The research leading to the results in this manuscript received funding from the European Union's Horizon 2020 research and innovation programme ASSEMBLE Plus AmpLOPHELIA project (Grant Agreement No. 730984) conducted in 2020 at Tjärnö marine laboratory (University of Gothenburg, Sweden), the Horizon 2020 ATLAS (Grant Agreement No. 678760) and the Horizon 2020 iAtlantic project (Grant Agreement No. 818123). This manuscript reflects the authors' view alone, and the European Union cannot be held responsible for any use that may be made of the information contained herein.

ACKNOWLEDGMENTS

We thank the crew onboard the RV Nereus and all personnel at Tjärnö who helped us during our stay, the deployment and recovery of the sound recorders. We thank Ann Larsson, Susanna Strömberg, and Tomas Lundälv for their support in the AmpLOPHELIA project. We also thank Ewan Edwards and Jack Gillespie for assisting with the logistics and transportation of the equipment. We would also like to thank the two reviewers whose comments allowed us to greatly improve this manuscript.

REFERENCES

Addamo, A. M., Vertino, A., Stolarski, J., García-Jiménez, R., Taviani, M., and Machordom, A. (2016). Merging scleractinian genera: the overwhelming genetic similarity between solitary *Desmophyllum* and colonial *Lophelia*. *BMC Evol. Biol.* 16:108. doi: 10.1186/s12862-016-0654-8

Andrew, R. K., Howe, B. M., and Mercer, J. A. (2011). Long-time trends in ship traffic noise for four sites off the North American West Coast. *J. Acoust. Soc. Am.* 129, 642–651. doi: 10.1121/1.3518770

Andrew, R. K., Howe, B. M., Mercer, J. A., and Dzieciuch, M. A. (2002). Ocean ambient sound: comparing the 1960s with the 1990s for a receiver off the California coast. *Acoust. Res. Lett. Online* 3, 65–70. doi: 10.1121/1.1461915

Baillon, S., Hamel, J. F., Wareham, V. E., and Mercier, A. (2012). Deep cold-water corals as nurseries for fish larvae. *Front. Ecol. Environ.* 10:351–356. doi: 10.1890/120022

Bassett, C., Thomson, J., Dahl, P. H., and Polagye, B. (2014). Flow-noise and turbulence in two tidal channels. *J. Acoust. Soc. Am.* 135, 1764–1774. doi: 10.1121/1.4867360

Bolker, B. (2020). Dealing with quasi-models in R. *Compare* 1, 5–452.

Buhl-Mortensen, L. L., Vanreusel, A., Gooday, A. J., Levin, L. A., Priede, I. G., Buhl-Mortensen, P., et al. (2010). Biological structures as a source of habitat heterogeneity and biodiversity on the deep ocean margins. *Mar. Ecol. Evol. Perspect.* 31, 21–50. doi: 10.1111/j.1439-0485.2010.00359.x

Carroll, A. G., Przeslawski, R., Duncan, A., Gunning, M., and Bruce, B. (2017). A critical review of the potential impacts of marine seismic surveys on fish & invertebrates. *Mar. Pollut. Bull.* 114, 9–24. doi: 10.1016/j.marpolbul.2016.11.038

Carslaw, D. C., and Ropkins, K. (2012). Openair - an r package for air quality data analysis. *Environ. Model. Softw.* 2, 52–61. doi: 10.1016/j.envsoft.2011.09.008

Cathalot, C., Van Oevelen, D., Cox, T. J. S., Kutti, T., Lavaleye, M., Duineveld, G., et al. (2015). Cold-water coral reefs and adjacent sponge grounds: hotspots of benthic respiration and organic carbon cycling in the deep sea. *Front. Mar. Sci.* 2:1–12. doi: 10.3389/fmars.2015.00037

Clark, M. R., Tittensor, D., Rogers, A. D., Brewin, P., Schlacher, T., Rowden, A., et al. (2006). *Seamounts, Deep-Sea Corals and Fisheries: Vulnerability of Deep-Sea Corals to Fishing on Seamounts Beyond Areas of National Jurisdiction*. Cambridge: UNEP-WCMC.

Davies, A. J., Wisshak, M., Orr, J. C., and Murray Roberts, J. (2008). Predicting suitable habitat for the cold-water coral *Lophelia pertusa* (Scleractinia). *Deep. Res. Part I Oceanogr. Res. Pap.* 55, 1048–1062. doi: 10.1016/j.dsr.2008.04.010

De Clippele, L. H., Huvenne, V. A. I., Molodtsova, T. N., and Roberts, J. M. (2019). The diversity and ecological role of non-scleractinian corals (Antipatharia and Alcyonacea) on scleractinian cold-water coral mounds. *Front. Mar. Sci.* 6:184. doi: 10.3389/fmars.2019.00184

De Clippele, L. H., Huvenne, V. A. I., Orejas, C., Lundälv, T., Fox, A., Hennige, S. J., et al. (2018). The effect of local hydrodynamics on the spatial extent and morphology of cold-water coral habitats at Tisler Reef, Norway. *Coral Reefs* 37, 253–266. doi: 10.1007/s00338-017-1653-y

De Clippele, L. H., Rovelli, L., Ramiro-Sánchez, B., Kazanidis, G., Vad, J., Turner, S., et al. (2021). Mapping cold-water coral biomass: an approach to derive ecosystem functions. *Coral Reefs* 40, 215–231. doi: 10.1007/s00338-020-02030-5

de Froe, E., Rovelli, L., Glud, R. N., Maier, S. R., Duineveld, G., Mienis, F., et al. (2019). Benthic oxygen and nitrogen exchange on a cold-water coral reef in the North-East Atlantic Ocean. *Front. Mar. Sci.* 6:665. doi: 10.3389/fmars.2019.00665

Dekeling, R., Tasker, M., Ainslie, M., Andersson, M., André, M., Borsani, F., et al. (2016). "The European marine strategy: noise monitoring in European marine waters from 2014," in *The Effects of Noise on Aquatic Life II*, eds A. N. Popper, and A. Hawkins (New York, NY: Springer), 205–215.

Derryberry, E. P., Phillips, J. N., Derryberry, G. E., Blum, M. J., and Luther, D. (2020). Singing in a silent spring: birds respond to a half-century soundscape reversion during the COVID-19 shutdown. *Science* 370, 575–579. doi: 10.1126/SCIENCE.ABD5777

Dobson, A. J., and Barnett, A. G. (2008). *Introduction to Generalized Linear Models*, 3rd Edn. Boca Raton, FL: Chapman and Hall.

Douarin, M., Sinclair, D. J., Elliot, M., Henry, L. A., Long, D., Mitchison, F., et al. (2014). Changes in fossil assemblage in sediment cores from Mingulay Reef Complex (NE Atlantic): implications for coral reef build-up. *Deep. Res. II Top. Stud. Oceanogr.* 99, 286–296. doi: 10.1016/j.dsr2.2013.07.022

Duarte, C. M., Chapuis, L., Collin, S. P., Costa, D. P., Devassy, R. P., Eguiluz, V. M., et al. (2021). The soundscape of the Anthropocene ocean. *Science* 371:eaba4658. doi: 10.1126/science.aba4658

Ferrier-pages, C., Leal, M. C., Calado, R., Schmid, D. W., Lecchini, D., and Allemand, D. (2021). Noise pollution on coral reefs? — A yet underestimated threat to coral reef communities. *Mar. Pollut. Bull.* 165:112129. doi: 10.1016/j.marpolbul.2021.112129

Fosså, J. H., Skjoldal, H. R., Grafton, R. Q., Hilborn, R., Squires, D., and Tait, M. (2010). *Handbook of Marine Fisheries Conservation and Management*. Oxford: Oxford University Press.

Frisk, G. V. (2012). Noiseonomics: the relationship between ambient noise levels in the sea and global economic trends. *Sci. Rep.* 2:437. doi: 10.1038/srep00437

Garrett, J. K., Blondel, P., Godley, B. J., Pikesley, S. K., Witt, M. J., and Johanning, L. (2016). Long-term underwater sound measurements in the shipping noise indicator bands 63 Hz and 125 Hz from the port of Falmouth Bay, UK. *Mar. Pollut. Bull.* 110, 438–448. doi: 10.1016/j.marpolbul.2016.06.021

Guihen, D., White, M., and Lundälv, T. (2013). Boundary layer flow dynamics at a cold-water coral reef. *J. Sea Res.* 78, 36–44. doi: 10.1016/j.seares.2012.12.007

Haren, A. M. (2007). Reducing noise pollution from commercial shipping in the channel islands national marine sanctuary: a case study in marine protected area management of underwater noise. *J. Int. Wildl. Law Policy* 10, 153–173. doi: 10.1080/13880290701347432

Haver, S. M., Fournet, M. E., Dziak, R. P., Gabriele, C., Gedamke, J., Hatch, L. T., et al. (2019). Comparing the underwater soundscapes of four U.S. National Parks and marine sanctuaries. *Front. Mar. Sci.* 6:500. doi: 10.3389/fmars.2019.00500

Haviland-Howell, G., Frankel, A. S., Powell, C. M., Bocconcelli, A., Herman, R. L., and Sayigh, L. S. (2007). Recreational boating traffic: a chronic source of anthropogenic noise in the Wilmington, North Carolina Intracoastal Waterway. *J. Acoust. Soc. Am.* 122, 151–160. doi: 10.1121/1.2717766

Hennige, S. J., Morrison, C. L., Form, U., Büscher, J., Kamenos, N., and Roberts, J. M. (2014). Self-recognition in corals facilitates deep-sea habitat engineering. *Sci. Rep.* 4:6782. doi: 10.1038/srep06782

Hennige, S. J., Wicks, L. C., Kamenos, N. A., Perna, G., Findlay, H. S., and Roberts, J. M. (2015). Hidden impacts of ocean acidification to live and dead coral framework. *Proc. Biol. Sci.* 282:20150990. doi: 10.1098/rspb.2015.0990

Henry, L. A., Davies, A. J., and Roberts, J. M. (2010). Beta diversity of cold-water coral reef communities off western Scotland. *Coral Reefs* 29, 427–436. doi: 10.1007/s00338-009-0577-6

Henry, L. A., Navas, J. M., Hennige, S. J., Wicks, L. C., Vad, J., and Roberts, J. M. (2013). Cold-water coral reef habitats benefit recreationally valuable sharks. *Biol. Conserv.* 161, 67–70. doi: 10.1016/j.biocon.2013.03.002

Henry, L. A., Stehmann, M. F. W., De Clippele, L., Findlay, H. S., Golding, N., and Roberts, J. M. (2016). Seamount egg-laying grounds of the deep-water skate *Bathyraja richardsoni*. *J. Fish Biol.* 89, 1473–1481. doi: 10.1111/jfb.13041

Hildebrand, J. A. (2009). Anthropogenic and natural sources of ambient noise in the ocean. *Mar. Ecol. Prog. Ser.* 395, 5–20. doi: 10.3354/meps08353

Holmes, L. J., McWilliam, J., Ferrari, M. C. O., and McCormick, M. I. (2017). Juvenile damselfish are affected but desensitize to small motor boat noise. *J. Exp. Mar. Bio. Ecol.* 494, 63–68. doi: 10.1016/j.jembe.2017.05.009

Johnson, M., Partan, J., and Hurst, T. (2013). Low complexity lossless compression of underwater sound recordings. *J. Acoust. Soc. Am.* 133, 1387–1398. doi: 10.1121/1.4776206

Kazanidis, G., Henry, L. A., Roberts, J. M., and Witte, U. F. M. (2016). Biodiversity of *Spongosorites coralliophaga* (Stephens, 1915) on coral rubble at two contrasting cold-water coral reef settings. *Coral Reefs* 35, 193–208. doi: 10.1007/s00338-015-1355-2

K. Lisa Yang Center for Conservation Bioacoustics (2019). *Raven Pro: Interactive Sound Analysis Software (Version 1.6.1) [Computer Software]*. Ithaca, NY: The Cornell Lab of Ornithology. Available online at: http://ravensoundsoftware.com/

Lavaleye, M., Duineveld, G., Lundälv, T., White, M., Guihen, D., Kiriakoulakis, K., et al. (2009). Cold-water corals on the Tisler reef preliminary observations on the dynamic reef environment. *Oceanography* 22, 76–84.

Le Prell, C. G., Henderson, D., and Fay, R. R. (2012). *Noise-Induced Hearing Loss*. Berlin: Springer.

Maier, S. R., Kutti, T., Bannister, R. J., Fang, J. K. H., van Breugel, P., van Rijswijk, P., et al. (2020). Recycling pathways in cold-water coral reefs: use of dissolved organic matter and bacteria by key suspension feeding taxa. *Sci. Rep.* 10:9942. doi: 10.1038/s41598-020-66463-2

McCullagh, P., and Nelder, J. (1989). *Generalised Linear Models*, 2nd Edn. Boca Raton, FL: Chapman and Hall.

McKenna, M. F., Ross, D., Wiggins, S. M., and Hildebrand, J. A. (2012). Underwater radiated noise from modern commercial ships. *J. Acoust. Soc. Am.* 131, 92–103. doi: 10.1121/1.3664100

Merchant, N. D., Brookes, K. L., Faulkner, R. C., Bicknell, A. W. J., Godley, B. J., and Witt, M. J. (2016). Underwater noise levels in UK waters. *Sci. Rep.* 6:36942. doi: 10.1038/srep36942

Mienis, F., van der Land, C., de Stigter, H. C., van de Vorstenbosch, M., de Haas, H., Richter, T., et al. (2009). Sediment accumulation on a cold-water carbonate mound at the Southwest Rockall Trough margin. *Mar. Geol.* 265, 40–50. doi: 10.1016/j.margeo.2009.06.014

Mueller, C. E., Larsson, A. I., Veuger, B., Middelburg, J. J. and Van Oevelen, D., (2014). Opportunistic feeding on various organic food sources by the cold-water coral *Lophelia pertusa*. *Biogeosciences* 11, 123–133. doi: 10.5194/bg-11-123-2014

Morato, T., González-Irusta, J. M., Dominguez-Carrió, C., Wei, C. L., Davies, A., Sweetman, A. K., et al. (2020). Climate-induced changes in the suitable habitat of cold-water corals and commercially important deep-sea fishes in the North Atlantic. *Glob. Chang. Biol.* 26, 2181–2202. doi: 10.1111/gcb.14996

Myrberg, A. A., and Fuiman, L. A. (2002). *The Sensory World of Coral Reef Fishes*. Amsterdam: Elsevier.

Nedelec, S. L., Mills, S. C., Lecchini, D., Nedelec, B., Simpson, S. D., and Radford, A. N. (2016). Repeated exposure to noise increases tolerance in a coral reef fish. *Environ. Pollut.* 216, 428–436. doi: 10.1016/j.envpol.2016.05.058

Peng, C., Zhao, X., and Liu, G. (2015). Noise in the sea and its impacts on marine organisms. *Int. J. Environ. Res. Public Health* 12, 12304–12323. doi: 10.3390/ijerph121012304

Piercy, J. J. B., Codling, E. A., Hill, A. J., Smith, D. J., and Simpson, S. D. (2014). Habitat quality affects sound production and likely distance of detection on coral reefs. *Mar. Ecol. Prog. Ser.* 516, 35–47.

R Development Core Team, (2010). *R: A Language and Environment for Statistical Computing*. Vienna: R Foundation for Statistical Computing.

Robards, M. D., Silber, G. K., Adams, J. D., Arroyo, J., Lorenzini, D., Schwehr, K., et al. (2016). Conservation science and policy applications of the marine vessel Automatic Identification System (AIS)-A review. *Bull. Mar. Sci.* 92, 75–103. doi: 10.5343/bms.2015.1034

Roberts, J. M., Wheeler, A. J., and Freiwald, A. (2006). Reefs of the deep: the biology and geology of cold-water coral ecosystems. *Science* 312, 543–547. doi: 10.1126/science.1119861

Roberts, J. M., Wheeler, A. J., Freiwald, A., and Cairns, S. D. (2009). *Cold-Water Corals: The Biology and Geology of Deep-Sea coral Habitats*. Cambridge: Cambridge University Press.

Rovelli, L., Attard, K. M., Bryant, L. D., Flögel, S., Stahl, H., Roberts, J. M., et al. (2015). Benthic O_2 uptake of two cold-water coral communities estimated with the non-invasive eddy correlation technique. *Mar. Ecol. Prog. Ser.* 525, 97–104. doi: 10.3354/meps11211

Simmonds, M. P., Dolman, S. J., Jasny, M., Parsons, E. C. M., Weilgart, L., Wright, A. J., et al. (2014). Marine noise pollution - increasing recognition but need for more practical action. *J. Ocean Technol.* 9, 71–90.

Simpson, S. D., Radford, A. N., Holles, S., Ferarri, M. C., Chivers, D. P., McCormick, M. I., et al. (2016). "Small-boat noise impacts natural settlement behavior of coral reef fish larvae," in *The Effects of Noise on Aquatic Life II*, eds A. Popper, and A. Hawkins (Berlin: Springer), 1041–1048.

Simpson, S. D., Radford, A. N., Tickle, E. J., Meekan, M. G., and Jeffs, A. G. (2011). Adaptive avoidance of reef noise. *PLoS One* 6:e16625. doi: 10.1371/journal.pone.0016625

Staaterman, E., Gallagher, A. J., Holder, P. E., Reid, C. H., Altieri, A. H., Ogburn, M. B., et al. (2020). Exposure to boat noise in the field yields minimal stress response in wild reef fish. *Aquat. Biol.* 29, 93–103. doi: 10.3354/ab00728

Stanley, J. A., Van Parijs, S. M., and Hatch, L. T. (2017). Underwater sound from vessel traffic reduces the effective communication range in Atlantic cod and haddock. *Sci. Rep.* 7:14633. doi: 10.1038/s41598-017-14743-9

Strasberg, M. (1979). Nonacoustic noise interference in measurements of infrasonic ambient noise. *J. Acoust. Soc. Am.* 66:1487.

Sundahl, H., Buhl-Mortensen, P., and Buhl-Mortensen, L. (2020). Distribution and suitable habitat of the cold-water corals *Lophelia pertusa*, *Paragorgia arborea,* and *Primnoa resedaeformis* on the Norwegian continental shelf. *Front. Mar. Sci.* 7:213. doi: 10.3389/fmars.2020.00213

Sweetman, A. K., Thurber, A. R., Smith, C. R., Levin, L. A., Mora, C., Wei, C.-L., et al. (2017). Major impacts of climate change on deep-sea benthic ecosystems. *Elem. Sci. Anth.* 5:4. doi: 10.1525/elementa.203

Tasker, M. L., Amundin, M., Andre, M., Hawkins, A., Lang, W., Merck, T., et al. (2010). *MSFD Task Group 11 Report: Underwater Noise and Other Forms of Energy*. European Commission Joint Research Centre/ICES Report EUR 24341. Luxembourg: Joint Research Centre.

Thomson, D. J. M., and Barclay, D. R. (2020). Real-time observations of the impact of COVID-19 on underwater noise. *J. Acoust. Soc. Am.* 147, 3390–3396. doi: 10.1121/10.0001271

Van der Land, C., Eisele, M., Mienis, F., de Haas, H., Hebbeln, D., Reijmer, J. J. G., et al. (2014). Carbonate mound development in contrasting settings on the Irish margin. *Deep. Res. II Top. Stud. Oceanogr.* 99, 297–306. doi: 10.1016/j.dsr2.2013.10.004

van Oevelen, D., Duineveld, G., Lavaleye, M., Mienis, F., Soetaert, K., and Heip, C. H. R. (2009). The cold-water coral community as hotspot of carbon cycling on continental margins: a food-web analysis from Rockall Bank (northeast Atlantic). *Limnol. Oceanogr.* 54, 1829–1844. doi: 10.4319/lo.2009.54.6.1829

Wagner, H., Purser, A., Thomsen, L., Jesus, C. C., and Lundälv, T. (2011). Particulate organic matter fluxes and hydrodynamics at the Tisler cold-water coral reef. *J. Mar. Syst.* 85, 19–29. doi: 10.1016/j.jmarsys.2010.11.003

Weilgart, L. S. (2006). "Managing noise through marine protected areas around global hot spots," in *Paper Presented at the 58th Annual Meeting of the International Whaling Commission Scientific Committee 12* (New York, NY: IWC).

Wenz, G. M. (1962). Acoustic ambient noise in the ocean: spectra and sources. *J. Acoust. Soc. Am.* 34, 1936–1956. doi: 10.1121/1.1909155

Wheeler, A. J., Bett, B. J., Billett, D. S. M., Masson, D., and Mayor, D. (2005). The impact of demersal trawling on northeast Atlantic deepwater coral habitats: the case of the Darwin Mounds, United Kingdom. *Am. Fish. Soc. Symp.* 41, 807–817.

Wheeler, A. J., Beyer, A., Freiwald, A., de Haas, H., Huvenne, V. A. I., Kozachenko, M., et al. (2007). Morphology and environment of cold-water coral carbonate mounds on the NW European margin. *Int. J. Earth Sci.* 96, 37–56. doi: 10.1007/s00531-006-0130-6

Wickham, H. (2011). Ggplot2. *Wiley Interdiscip. Rev. Comput. Stat.* 3, 180–185. doi: 10.1002/wics.147

Williams, R., Erbe, C., Ashe, E., and Clark, C. W. (2015). Quiet(er) marine protected areas. *Mar. Pollut. Bull.* 100, 154–161. doi: 10.1016/j.marpolbul.2015.09.012

Wisshak, M., Freiwald, A., Lundälv, T., and Gektidis, M. (2005). "The physical niche of the bathyal *Lophelia pertusa* in a non-bathyal setting: Environmental controls and palaeoecological implications," in *Cold-Water Corals and Ecosystems*, eds A. Freiwald, and J. M. Roberts (Berlin: Springer), 979–1001.

Conflict of Interest: The authors declare that the research was conducted in the absence of any commercial or financial relationships that could be construed as a potential conflict of interest.

Copyright © 2021 De Clippele and Risch. This is an open-access article distributed under the terms of the Creative Commons Attribution License (CC BY). The use, distribution or reproduction in other forums is permitted, provided the original author(s) and the copyright owner(s) are credited and that the original publication in this journal is cited, in accordance with accepted academic practice. No use, distribution or reproduction is permitted which does not comply with these terms.

frontiers in Marine Science

ORIGINAL RESEARCH
published: 25 June 2021
doi: 10.3389/fmars.2021.674787

Underwater Sound Levels in Glacier Bay During Reduced Vessel Traffic Due to the COVID-19 Pandemic

Christine M. Gabriele[1], Dimitri W. Ponirakis[2] and Holger Klinck[2,3]*

[1] Glacier Bay National Park and Preserve, Gustavus, AK, United States, [2] Center for Conservation Bioacoustics, Cornell Lab of Ornithology, Ithaca, NY, United States, [3] Department of Fisheries, Wildlife, and Conservation Science, Marine Mammal Institute, Oregon State University, Newport, OR, United States

The global COVID-19 pandemic caused a sharp decline in vessel traffic in many areas around the world, including vessel-based tourism throughout Alaska, USA in 2020. Marine vessel traffic has long been known to affect the underwater acoustic environment with direct and indirect effects on marine ecological processes. Glacier Bay National Park in southeastern Alaska has monitored underwater sound since 2000. We used continuous, calibrated hydrophone recordings to examine 2020 ambient sound levels compared with previous years: 2018, the most recent year with data available, and 2016 for historical perspective. Park tourism occurs mainly in May–September. Overall, the number of vessel entries in Glacier Bay was 44–49% lower in 2020 (2020: n = 1,831; 2018: n = 3,599; 2016: n = 3,212) affecting all vessel classes, including the complete absence of cruise ships and only three tour vessel trips. In all years, we found clear seasonal and diurnal patterns in vessel generated noise, focused from 06:00 to 20:00 local time (LT) in the summer months. Broadband (17.8–8,910 Hz) sound levels in the 2020 Visitor Season were 2.7 dB lower than 2018 and 2.5 dB lower than 2016. Focusing on morning (06:00–09:00 LT) and afternoon (15:00–18:00 LT) time-blocks when tour vessels and cruise ships enter and exit Glacier Bay, median broadband sound levels were 3.3–5.1 dB lower in 2020 than prior years. At the 95th percentile levels, morning and afternoon peak times in 2020 were 6.3–9.0 dB quieter than previous years. A 3 dB decline in median sound level in the 125 Hz one-third octave band in 2020 reflects a change in medium and large vessel noise energy and/or harbor seal vocalizations. Our results suggest that all types of vessels had a role in the quieter underwater sound environment in 2020, with the combined acoustic footprint of tour vessels and cruise ships most evident in the decrease in the 95th percentile loudest sounds. This and other descriptions of the pandemic-induced quiet, and the gradual return to increased activity, can help inform efforts to improve existing methods to mitigate vessel noise impacts and maintain the ecological integrity of marine protected areas.

Keywords: Alaska, Glacier Bay National Park, marine protected area, soundscape, marine mammal, harbor seal (*Phoca vitulina*), underwater sound

OPEN ACCESS

Edited by:
Renata Sousa-Lima, Federal University of Rio Grande do Norte, Brazil

Reviewed by:
Nathan D. Merchant, Centre for Environment, Fisheries and Aquaculture Science (CEFAS), United Kingdom
Douglas Wartzok, Florida International University, United States

****Correspondence:***
Christine M. Gabriele
chris_gabriele@nps.gov

Specialty section:
This article was submitted to Marine Pollution, a section of the journal Frontiers in Marine Science

Received: *02 March 2021*
Accepted: *25 May 2021*
Published: *25 June 2021*

Citation:
Gabriele CM, Ponirakis DW and Klinck H (2021) Underwater Sound Levels in Glacier Bay During Reduced Vessel Traffic Due to the COVID-19 Pandemic. Front. Mar. Sci. 8:674787. doi: 10.3389/fmars.2021.674787

INTRODUCTION

In 2020, the global COVID-19 pandemic presented a unique opportunity to understand the effects of vessel noise on the underwater acoustic environment in many places around the world. Marine vessel traffic is essential to modern commerce and passenger vessel tourism but produces underwater noise that overlaps in frequency, space and time with marine mammal sounds (Richardson et al., 1995) that are integral to vital life functions such as feeding, navigation, communication, breeding, and rearing young (Brumm and Slabbekoorn, 2005; Tyack, 2008; Barber et al., 2011). Increasing ocean noise and its effects on marine mammal communication have been documented in various studies (Payne and Webb, 1971; Malme et al., 1981; Andrew et al., 2002, McKenna et al., 2012; Miksis-Olds et al., 2013; Houghton et al., 2015). In the North Pacific, ambient sound levels increased by over 3 dB per decade from 1950 to 2007 (Andrew et al., 2002; McDonald et al., 2006; Chapman and Price, 2011) primarily due to increased commercial shipping but also attributable to other human activities. Noise trends are stable or decreasing in some part of the world, such as the Equatorial Pacific and South Atlantic and the North Pacific (Andrew et al., 2011; Miksis-Olds and Nichols, 2016). The shipping industry is affected by global crises (Notteboom et al., 2021) and noise levels have been documented to respond to decreased shipping activity (McKenna et al., 2012).

In Alaskan waters, marine tourism was strongly affected by the COVID-19 pandemic. No-sail orders from the U.S. Centers for Disease Control and Prevention (CDC) canceled all cruise ship visits to Alaska to prevent spreading the virus onboard ships and in ports-of-call (Federal Register, 2020; Ito et al., 2020). The Canadian government announced a series of port closures to cruise ships that began in March 2020 (Transport Canada, 2020) that prevented cruise ship visits to Alaska during the 2020 tourism season because under the United States Jones Act (Section 27 of Pub. L. 66-261), foreign-flag vessels must visit a foreign port between stops at U.S. ports. Although U.S.-flag tour vessels carrying fewer than 250 passengers were exempt from the CDC no-sail order, these tour vessel trips also canceled Alaska sailings in 2020 (KTOO News August 2020). Here, we characterize the underwater acoustic environment in Glacier Bay National Park (GBNP) during 2020's absence of cruise ships and almost all tour vessels to increase our understanding of the acoustic contribution of these vessel classes to the underwater soundscape.

Since 2000, the National Park Service (NPS) has worked with the U.S. Navy to monitor underwater sound in Glacier Bay National Park to inform management of vessel-based visitation. Previous work has resulted in detailed descriptions of the underwater soundscape in the area (Kipple and Gabriele, 2004a; McKenna et al., 2017) and modeling to predict how management actions such as vessel speed limits and scheduling may affect the underwater acoustic environment and communication ability of iconic marine mammals in the park (Frankel and Gabriele, 2017; Gabriele et al., 2018). For example, reduced ship speed is associated with a decrease in individual vessel noise output (Kipple, 2002; Kipple and Gabriele, 2004a) and daily sound exposure levels (Frankel and Gabriele, 2017). Studies in this vast (2,400 km^2) marine protected area have also advanced scientific knowledge of humpback whale (*Megaptera novaeangliae*) and harbor seal (*Phoca vitulina richardsii*) communication in Glacier Bay (Wild and Gabriele, 2014; Matthews et al., 2017a,b, 2020; Fournet et al., 2018a,b; Gabriele et al., 2018). Prior work allows us both a basis of comparison to assess the changes that occurred in 2020, and an understanding of the vocal behavior of these two species to provide biological context on the effects of changes to the underwater sound environment.

MATERIALS AND METHODS

Study Area

Glacier Bay National Park (GBNP) is a tidewater glacier fjord system with over 2,400 km^2 of marine waters (**Figure 1**). The Park experiences tourism-related vessel traffic mainly in May through September. The NPS has jurisdiction over the marine waters of the Park and controls private and commercial vessel traffic during the spring, summer, and fall using a quota system (Code of Federal Regulations 13.65). All types of commercial and private vessels entering Glacier Bay are subject to daily and seasonal limits during the Visitor Season (Code of Federal Regulations Title 36, Part 13, Subpart N). During the May–September Visitor Season, NPS data indicate the date/time that each commercial, private, fishing, or government vessel enters and exits GBNP. Park regulations currently allow up to two cruise ships, three tour vessels, and thirty-one smaller charter and private vessels to enter Glacier Bay daily during the June through August summer season. Glacier Bay is acoustically isolated from most distant shipping noise because it is bounded by land on all sides except its mouth. Freight-carrying vessels crossing the Gulf of Alaska pass the mouth of Glacier Bay but do not enter because it is not a thoroughfare.

Acoustic Data Collection

A cabled calibrated hydrophone system to monitor the underwater acoustic environment has been in place in lower Glacier Bay (58.43501 N, 135.92297 W; **Figure 1**) since May 2000. The seafloor is a remnant of a glacial moraine and is fairly flat at a depth of 40–60 m. In this study, we used continuous acoustic recordings from 2016, 2018, to 2020. The hydrophone system was not operational in 2019. The system consisted of a calibrated ITC type 8215A broadband omnidirectional hydrophone with a nominal sensitivity −174 dB re 1 V/μPa (Gavial ITC Inc., Santa Barbara, CA, United States) mounted on an anchoring tripod 1 m above the seafloor (30.2 m depth). A submerged 5-mile cable connects the hydrophone to a control unit at park headquarters, where continuous recordings were made 24 h a day, archived as 5 min sound files (National Instruments 4451 Digital Signal Analyzer, 22.05 kHz sampling rate, 24-bit resolution, 50 dB gain, ± 10 V ADC clipping level). We established the calibration of the Glacier Bay system with a broadband source by comparison to a calibrated reference hydrophone at the Fox Island Acoustic Laboratory. Those measurements were performed as an end-to-end calibration

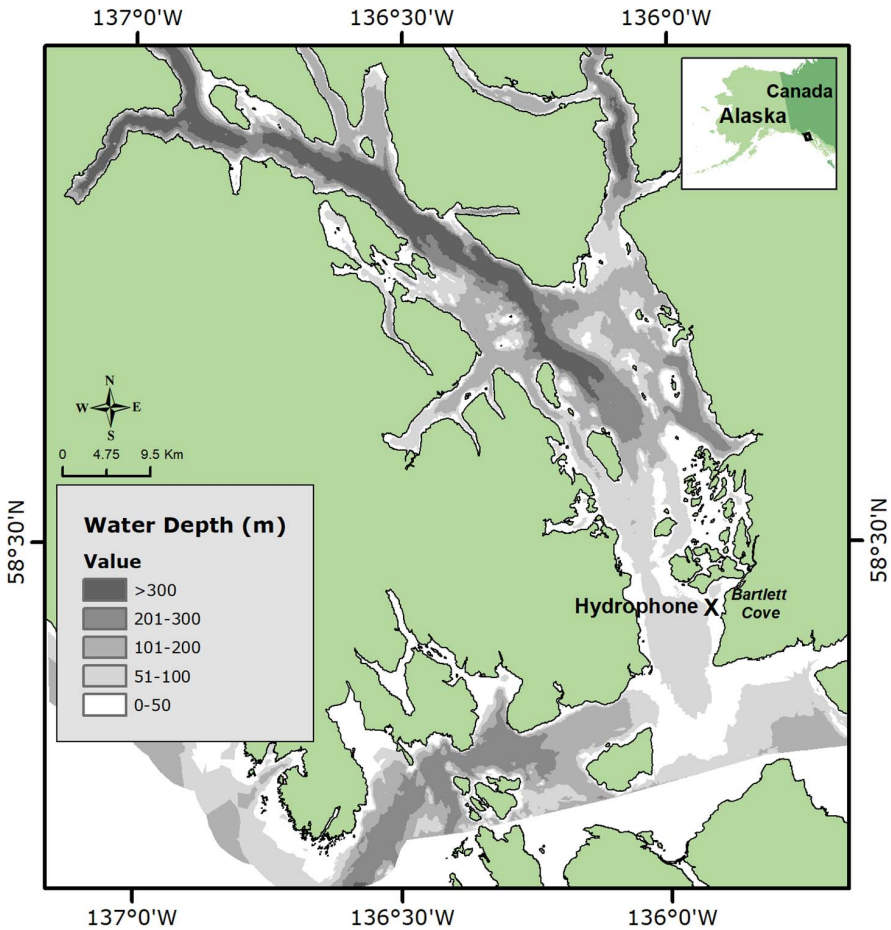

FIGURE 1 | Study area map showing hydrophone location and the bathymetry of Glacier Bay. The geographic location of Glacier Bay is indicated with a black box in the inset Alaska map.

through the full length of cable, in-water, as a function of frequency. We verified calibration of the lab measurement system at each major cable replacement or computer system update and also inspected and periodically removed biofouling from the hydrophone sensor. The recording system had a flat frequency response from 20 to 20 kHz (±2 dB). Received levels in this study are reported as broadband, and one-third octave band sound pressure levels ($L_{eq,10\ min}$) in dB re 1 μPa as measured at the hydrophone.

Ambient Noise Data Processing

Noise levels from the hydrophone data were calculated for consecutive 10 min periods for the entire 2016, 2018, and 2020 data sets. Sound level metrics were computed using Raven-X (Dugan et al., 2011) in a two-stage process. First, the 5 min AIF audio files were processed to calculate spectrum levels. To achieve frequency resolution of 1 Hz and a temporal resolution of 1 s for the spectral data, we calculated spectrum levels with the following parameters: 22,050 FFT, Hann window, and 0% overlap. In the second stage, the Raven-X analyzer then generated broadband (17.8–8,910 Hz) and 1/3-Octave band metrics that were averaged into 10 min sound level values. Ten-minute sound levels for each frequency band were statistically analyzed to quantify the percentile sound level distributions at hourly and monthly resolutions.

Environmental Data

Wind has long been recognized as a primary source of underwater noise (Knudsen et al., 1948; Wenz, 1962). Wind disturbs the ocean surface and results in the wave, turbulence, droplet and bubble activity that comprise wind noise. To account for the role of wind in Glacier Bay's underwater sound environment, we summarized wind speed data from the NOAA National Data Buoy Center station BLTA2 in Bartlett Cove for 2020 and 2018, while the 2016, data were downloaded from Dark Sky API due to lack of available data from BLTA2 (**Supplementary Figures 4**, **5**).

Rain is another prevalent source of ocean ambient noise in the 1–50 kHz frequency range (Amitai and Nystuen, 2008). Prior work in our study area indicated that the acoustic signature of rain characteristically peaks at 16 kHz (Kipple and Gabriele, 2003). However, the contribution of rain to noise levels at lower

frequencies below 1 kHz is less significant in the study area and typically masked by other sources (e.g., vessel noise). To assess the contribution of artifact from tidal current over the hydrophone sensor, we summarized tidal current data for all three years, that were downloaded from NOAA Tides and Currents site station 9452534 Bartlett Cove, Alaska (**Supplementary Figure 6**).

Vessel Traffic Data

Manmade underwater noise in Glacier Bay is primarily associated with motorized vessel activities. Vessel noise is typically due to engine, propulsion system, and propeller-related noise (Ross, 2005). Small craft with high-speed engines and propellers generally produce higher frequency noise while large vessels tend to generate low frequency noise because of their size and their large, slow speed engines and propellers (Barlett and Wilson, 2002; Kipple and Gabriele, 2004a,b; McKenna et al., 2012). All vessels can produce broadband propeller cavitation noise, which occurs at higher frequencies (Erbe, 2002; Kipple, 2002; Kipple and Gabriele, 2004a,b; Erbe et al., 2016; Veirs et al., 2016).

We summarized each vessel entry according to regulatory categories used by the NPS to manage vessel traffic. Currently, GBNP regulations allow up to 2 cruise ships, 3 tour vessels and 6 smaller charter and 25 private vessels per day in June-August (Code of Federal Regulations 13.65). The large *cruise ships* visiting Glacier Bay in 2016 and 2018 were 237–290 m (60,000–114,000 gross ton) vessels carrying 1,000–3,000 passengers, powered by diesel electric or gas turbines with various propeller or azipod propulsion configurations. These ships enter and exit Glacier Bay on a pre-determined schedule (**Supplementary Figures 7**, **8**). The radiated noise signatures of several cruise ships has been characterized (Kipple, 2002, NPS unpublished data). *Tour vessels* during the study were 46–73 m long, carried up to 149 passengers, and operate on a variety of schedules. A daily tour vessel, the 55 m catamaran *Baranof Wind* departed Bartlett Cove daily at 07:30 and returned around 15:30 daily; its source level has been estimated in previous work (Frankel and Gabriele, 2017; Gabriele et al., 2018). *Charter vessels* during the study years ranged from 7 to 29 m and generally carried fewer than 12 passengers for day-trips or overnight excursions. The *private vessel* category encompasses a wide variety of craft, ranging from 6 m outboard engine-powered skiffs, to 12–20 m cabin cruisers and 82 m mega-yachts. *NPS administrative vessel traffic* includes a variety of 5–6 m outboard powered skiffs, several 7–8 m inboard-powered patrol and research vessels, occasional visits from NOAA or U.S. Coast Guard vessels (> 61 m), as well as the 10 m pilot boat *Serac* that embarks Park Ranger naturalists on each entering cruise ship and disembarks the rangers before the ship exits Glacier Bay in late afternoon or early evening. We defined as Operating Hours of 06:00–20:00 LT and Off Hours of 20:00–06:00 LT, based on known patterns of vessel use of Glacier Bay (Kipple and Gabriele, 2004a).

RESULTS

Environmental Variation

We examined the distribution of wind speeds in the study area in 2016, 2018, and 2020 (**Supplementary Figure 3**). The

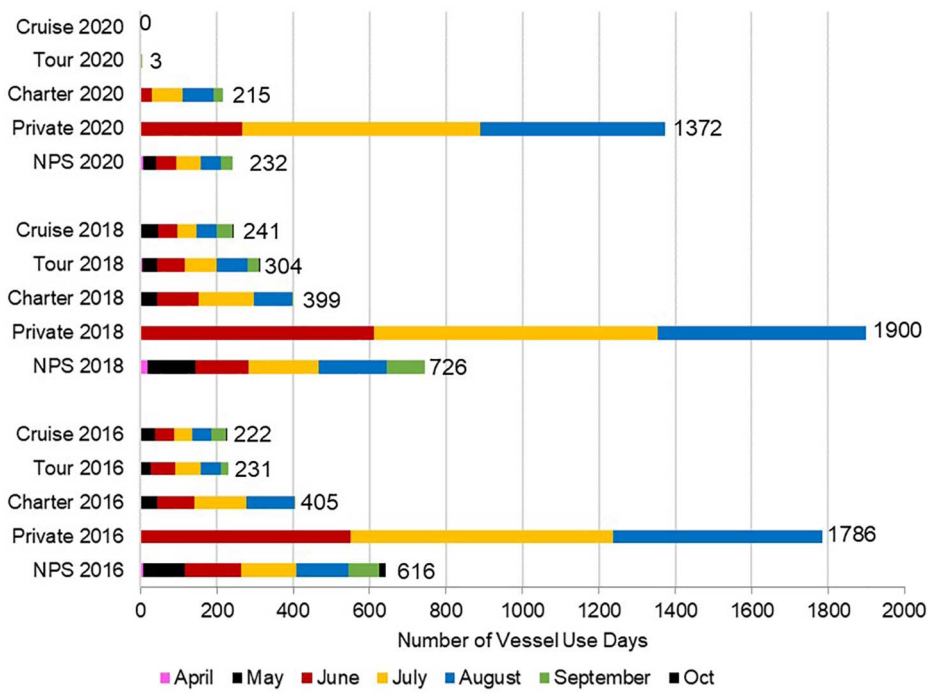

FIGURE 2 | Vessel traffic records for Glacier Bay 2016, 2018, and 2020, showing the numbers of the various categories of vessels in each year. Data values at the end of each bar show the total number of vessels in May–September only.

predominant summer wind pattern of increasing afternoon westerly or south-westerly winds is also evident. Median noise levels increased with increasing wind speed (**Supplementary Figure 4**). We plotted wind speed in May–September 2016, 2018, and 2020 (**Supplementary Figure 5**) demonstrates that all three years are similar up to the 70th percentile, when 2016 becomes distinct with lower sound levels up through the 99th percentile. While wind and rain noise both contributed to the underwater sound environment, there is little or no indication that variation in natural sounds was the primary driver of inter-year differences in noise levels.

Vessel Traffic

Vessel traffic varied among the years studied here (**Figure 2**) with the overall number of recorded vessel entries highest in 2018 (n = 3,599), followed by 2016 (n = 3,288) in contrast to only 1,831 entries in 2020, a 44–49% decline. Tour vessels and cruise ships represented 14–15% of May–September vessel entries in 2016 and 2018 but less than 1% in 2020. In May–September, NPS vessel use declined by 384–494 entries, and fishing/sightseeing charters declined by 184–190 entries. Private vessels were the most numerous class in all years but decreased in 2020 (n = 1,372) compared to other years by 414–528 entries. Small vessels in the charter, private and NPS classes represented a much larger proportion of total vessel traffic in 2020. In 2020, as a COVID-19 safety precaution, private vessels entering Glacier Bay were required to complete an online boater orientation and proceed into Glacier Bay rather than reporting to Bartlett Cove in person prior to starting their visit.

Annual and Seasonal Variability in Ambient Noise

Full-year diel plots of broadband (17.8–8,910 Hz) levels illustrate the primary drivers of Glacier Bay's underwater soundscape (**Figure 3**). These plots revealed variation within years due to vessel traffic patterns and biological and environmental sound sources. We observed two pronounced noise peaks: one in the morning as cruise ships and the daily catamaran tour vessel enter the bay and one during their afternoon/evening departure (**Supplementary Figures 7**, **8**). While vessel noise was still evident in 2020, the lack of tightly scheduled cruise ships and tour vessels resulted in the absence of a visible morning and evening entry and exit peak, particularly in the 63 and 125 Hz one-third octave bands that characterize large vessel noise (**Figure 4** and **Supplementary Figure 1**; Dekeling et al., 2014). Lower sound levels in 2020 are likely in part attributable to private vessels entering Glacier Bay without reporting to Bartlett Cove for an in-person boater orientation. Many private vessels in 2020 traveled directly into the bay at a greater distance from the hydrophone rather than traveling in and out of Bartlett Cove

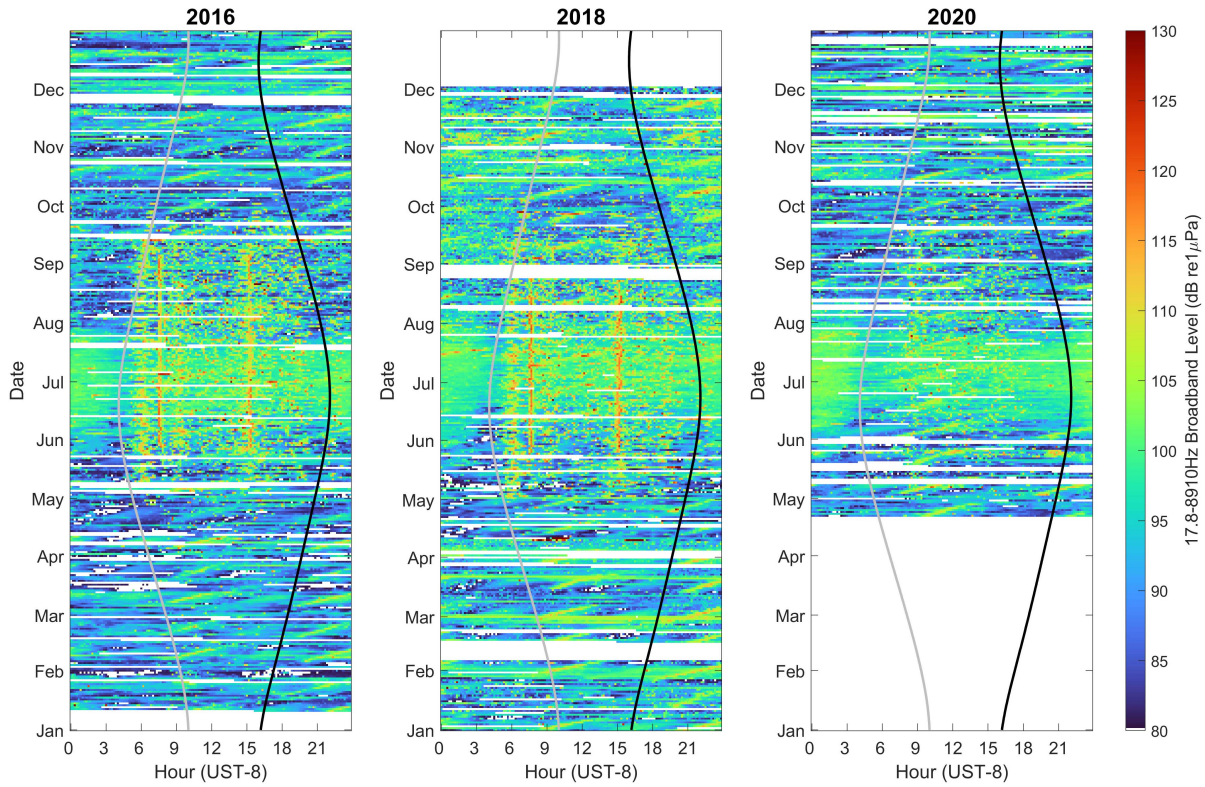

FIGURE 3 | Full Year diel broadband (17.8–8,910 Hz) levels at 10 min resolution for 2016, 2018, and 2020. Band level in dB re 1 μPa is indicated by the color scale at right. White sections indicate missing data. Variation within and between years is due to vessel traffic patterns, harbor seal vocalizations, weather, and the artifact of tidal flow over the hydrophone sensor (regularly spaced, upward-slanted lines). The light gray line indicates sunrise time and the black line indicates sunset time.

at close proximity to the hydrophone at the start of their visit. Harbor seal roars are a dominant noise source during their mating season in May–July (see Matthews et al., 2017a) especially evident in the 125 Hz one-third octave bands (range: 79–200 Hz, **Figure 4** and **Supplementary Figures 1**, **2**). Humpback and killer whale vocalizations occur frequently in Glacier Bay (McKenna et al., 2017), but do not follow a specific temporal pattern that would make them visible at the annual scale. Harbor porpoise also commonly occur but vocalize at frequencies (Mohl and Andersen, 1973) too high for our hydrophone system to detect. Wind-generated noise occurs throughout the year, with storms evident in fall and winter (see also **Supplementary Figure 3**). Also shown as "noise" in **Figure 3** is the artifact of tidal flow over the hydrophone sensor, which appears in the lower frequencies (<200 Hz; **Supplementary Figure 1**) as regularly spaced lines slanted upward as the hour of peak tidal flow advances by one hour each day (see also **Supplementary Figure 6**).

To further quantify the frequencies most affected by the seasonal variability in these acoustic sources, we contrasted the median one-third octave levels (TOL) in 2016, 2018, and 2020

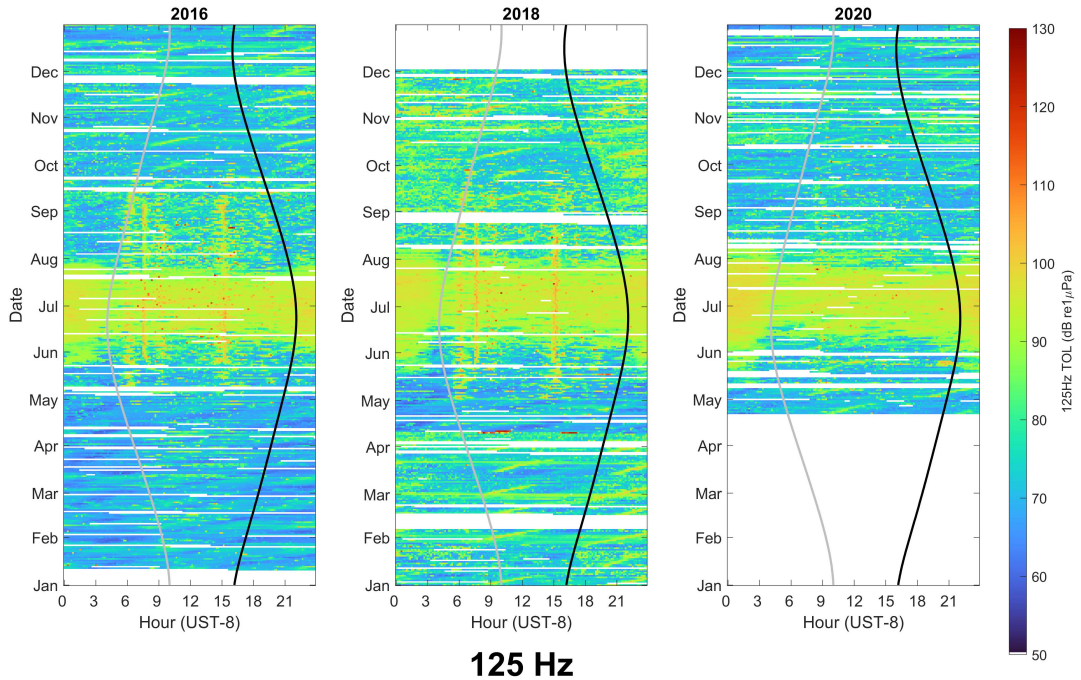

FIGURE 4 | Full year diel levels for the 125 Hz one-third octave at 10 min resolution for 2016, 2018, and 2020. Band level in dB re 1 μPa is indicated by the color scale at right. White sections indicate missing data. Variation within and between years is due to vessel traffic patterns, harbor seal vocalizations, weather, and the artifact of tidal flow over the hydrophone sensor (regularly spaced, upward-slanted lines). The light gray line indicates sunrise time and the black line indicates sunset time.

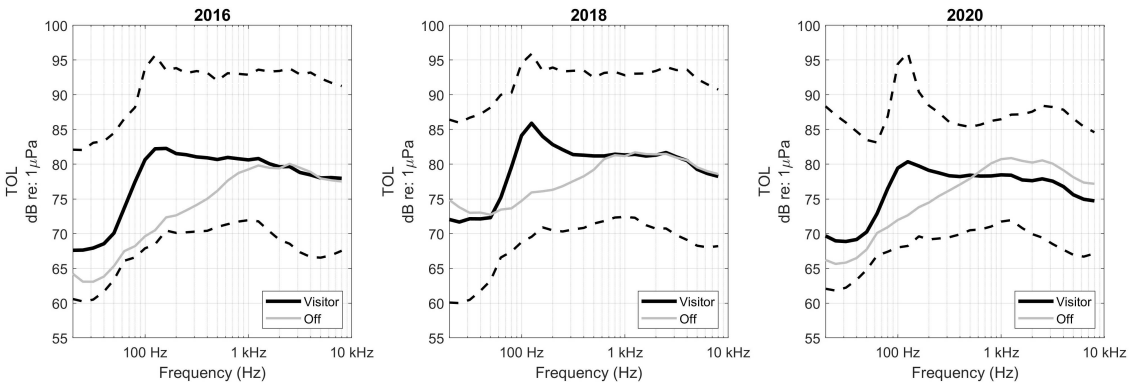

FIGURE 5 | Median sound pressure levels for one-third octave bands (TOL) in the Visitor Season (May–September, black line) and Off Season (October–April, gray line) in lower Glacier Bay. 10th percentile and 90th percentile levels are shown as dotted lines. Peak at 125 Hz in Visitor Season curve corresponds with harbor seal vocalizations in May–July each year.

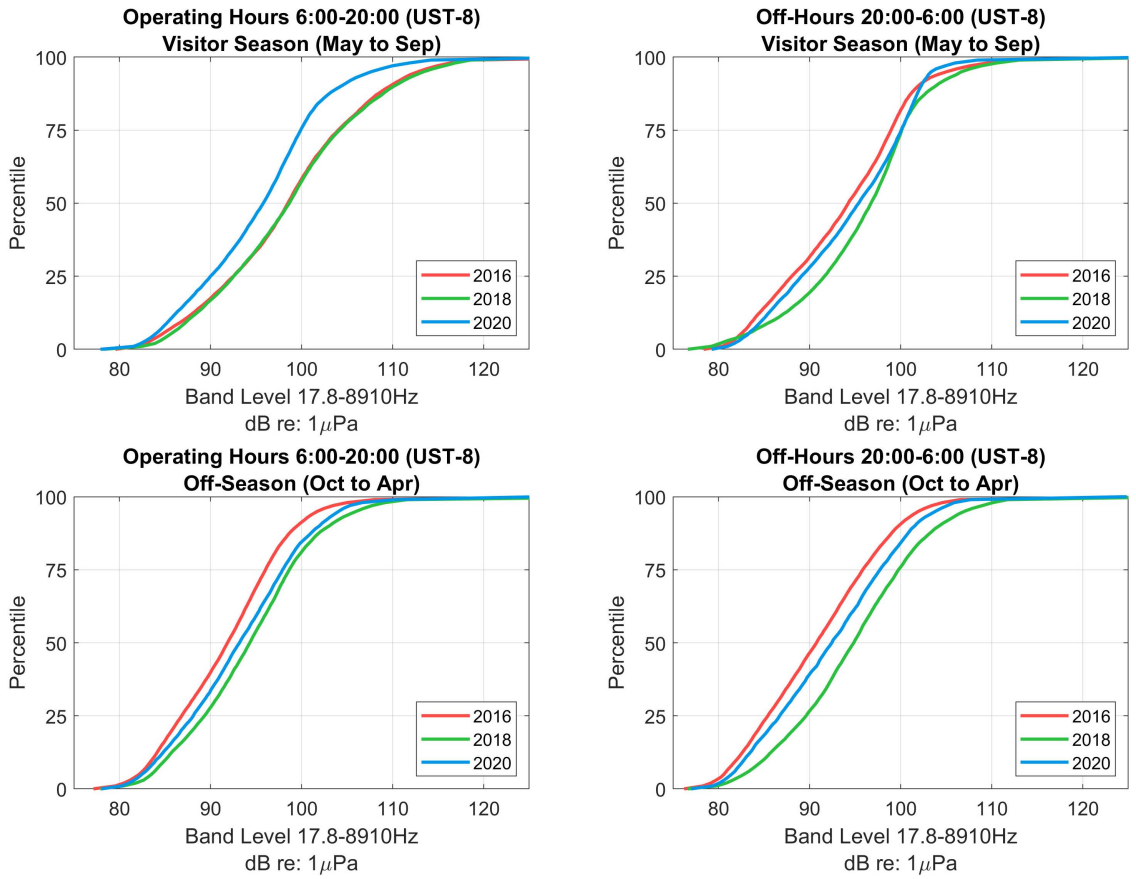

FIGURE 6 | Cumulative Distribution of 10 min resolution Broadband noise levels (17.8–8,910 Hz) for Glacier Bay's Visitor Season and Off Season during 6 a.m.–8 p.m. LT operating hours and 8 p.m.–6 a.m. LT Off Hours.

during the Visitor Season and Off Season (**Figure 5**). Median sound levels in all one-third octave bands were substantially lower in 2020 than in previous years. During the Visitor Season in 2020, the median level in all but one one-third octave band remained below 80 dB, whereas in 2016 and 2018 the noise levels in many bands exceeded 80 dB. Statistically, this results in median broadband levels in Visitor Season Operating Hours 2020 that are 2.5–2.7 dB lower than 2016 and 2018, respectively (**Supplementary Table 1**). At the 95th percentile level, 2020 median broadband levels in Visitor Season Operating Hours were 4.0–4.1 dB quieter than prior years. The harbor seal acoustic signal in the 125 Hz band remained visible in all years, but the median level in 2020 was 3 dB lower than in 2016 or 2018 (**Figure 5**). 2020 was markedly quieter during the daytime in the Visitor Season as a whole (**Figure 6**), particularly in the 125 Hz band although differences between years were not as apparent in the Off Season or at Off Hours (**Figures 5**, **6**).

Monthly Variability in Ambient Noise

Within the Visitor Season, June, July, and August are the months with peak vessel-generated noise (**Figure 7**), with broadband noise levels (17.8–8,910 Hz) peaking in July each year during what we defined as Operating Hours of (06:00–20:00 LT; after Kipple and Gabriele, 2004a) which is not surprising in that vessel numbers peak in July as well (**Figure 2**). In the Off-Hours (20:00–06:00 LT), the years are somewhat similar, including 2020, suggesting that the soundscape did not systematically vary among the years of the study.

Hourly Variability in Ambient Noise

We calculated L_{eq}10 min broadband (17.8–8,910 Hz) noise levels for 2016, 2018, and 2020 and summarized them by hour of day (**Figure 8**). In the 2020 Visitor Season, median hourly sound levels appeared to be less variable than in 2016 and 2018, which showed peaks in the early morning and late afternoon, and the lowest sound levels at 03:00 and 04:00 LT (**Figure 8**). In the Off Season, there was less hourly variation than the Visitor Season (**Figure 8**). These visible peaks in sound energy (**Figures 3**, **4**, 8) led us to quantify and contrast the difference in noise levels between years during time blocks comprising the peak hours of vessel entry and exit of Glacier Bay. We calculated noise levels at 10 min resolution within 3 h time-blocks (00:00–03:00 LT, 06:00–09:00 LT, 09:00–12:00 LT etc.) each day during the Visitor Season (**Figure 9**). Overall, in the morning (06:00–09:00 LT)

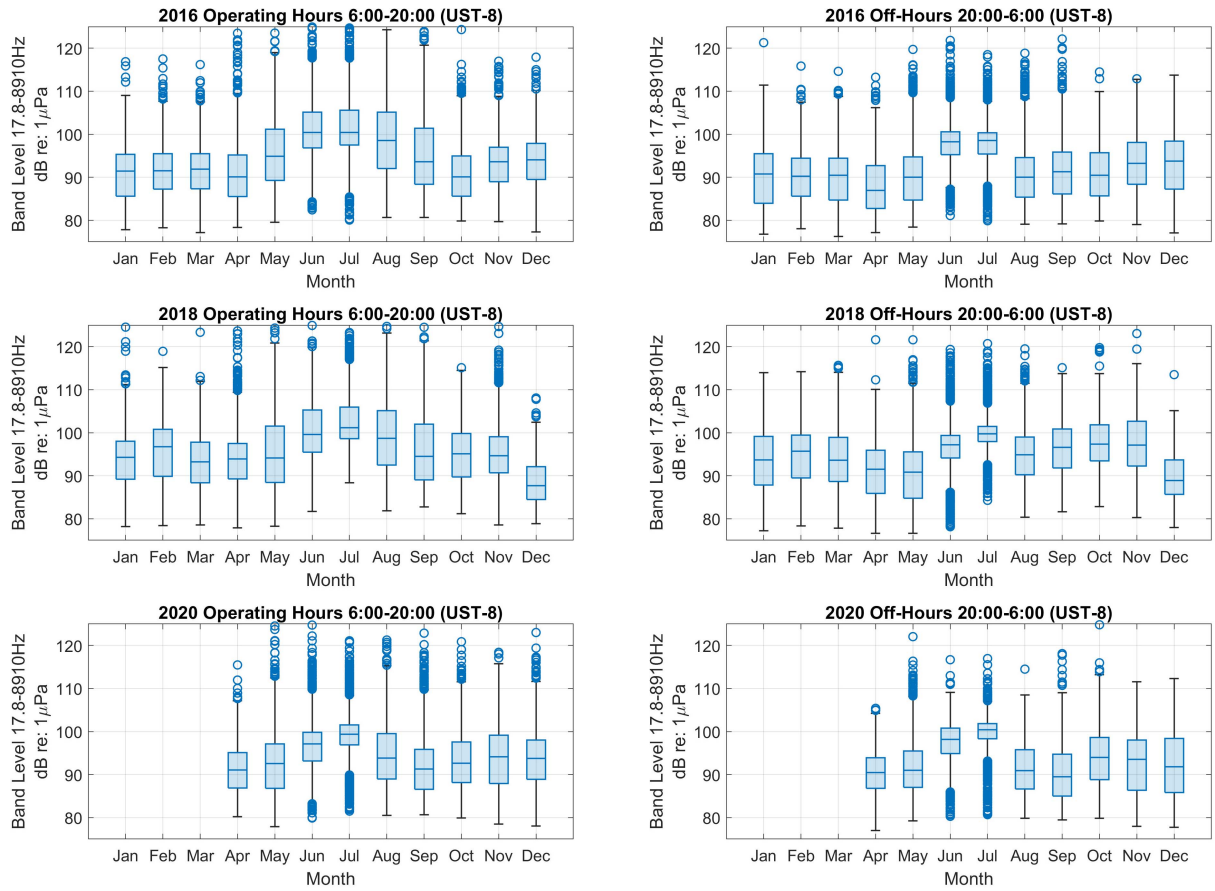

FIGURE 7 | Box-plot showing monthly distributions of 10 min resolution broadband (17.8–8,910 Hz) noise levels for 2016, 2018, and 2020. On each box, the central mark indicates the median, and the bottom and top edges of the box indicate the 25th and 75th percentiles, respectively. The whiskers extend to the most extreme data points not considered outliers, and the outliers are plotted individually using the "o" symbol.

and afternoon (15:00–18:00 LT) time blocks, median broadband sound levels were 3.3–5.1 dB lower in 2020 than prior years. At the 95th percentile level, the loudest sounds at the hydrophone in 2020 were 107.3 dB whereas they were 113.6 and 115.0 dB in 2016 and 2018. In contrast, late at night when vessel traffic is uncommon (00:00–03:00), all three years had median broadband levels between 94.1 and 97.4 dB, and 2020 was similar at 96.7 dB. All the median values for 2020 regardless of time block fell within the night-time range of noise values, whereas all the daytime median values for years 2016 and 2018 exceeded the night-time range of median values. During the morning time-block (06:00–09:00) when cruise ships, the daily catamaran tour and other vessel enter Glacier Bay, 2016 and 2018 median broadband levels were around 100 dB, in contrast to 2020 with its median level of 95 dB (**Table 1**). At the 95th percentile level, the difference was even more pronounced, with morning and afternoon peak times in 2020 were 6.3–9.0 dB quieter than previous years. The loudest sounds at the hydrophone in 2020 were 107.2 dB whereas they were 114.4–116.2 dB in 2016 and 2018, respectively. Similarly, in the afternoon/evening time-block (15:00–18:00) when vessels exit Glacier Bay, median broadband levels in 2020 were 95.8 dB, compared to 99.1 and 99.5 dB in 2016 and 2018 (**Table 1**).

DISCUSSION

Attributing underwater noise to specific vessel types is vital to efforts to reduce noise and preserve natural soundscapes. After estimating the acoustic contributions of cruise ships and tour vessels to Glacier Bay's underwater sound environment (Frankel and Gabriele, 2017), the COVID-19 pandemic created an unintentional experiment which allowed us to directly measure underwater sound levels in the complete absence of cruise ships and assess their relative contribution directly for the first time, albeit complicated by simultaneous reductions in other vessel classes. The overall number of vessel entries in 2020 showed a 44–49% decline compared to 2016 and 2018, respectively. Traffic in 2020 was comprised mainly of private vessels, sport-fishing and sightseeing, and NPS vessels, although these vessel classes too were greatly reduced compared to 2016 and 2018 levels (**Figure 2**). By all measures, Glacier Bay's underwater acoustic environment in 2020 was markedly quieter than 2016 and 2018 during the daytime Operating Hours during the May–September Visitor Season. Prior to 2020, there was a pronounced noise peak in the morning as the daily catamaran tour (NPS, unpublished data) and cruise ships (**Supplementary Figures 7**, **8**) enter the bay

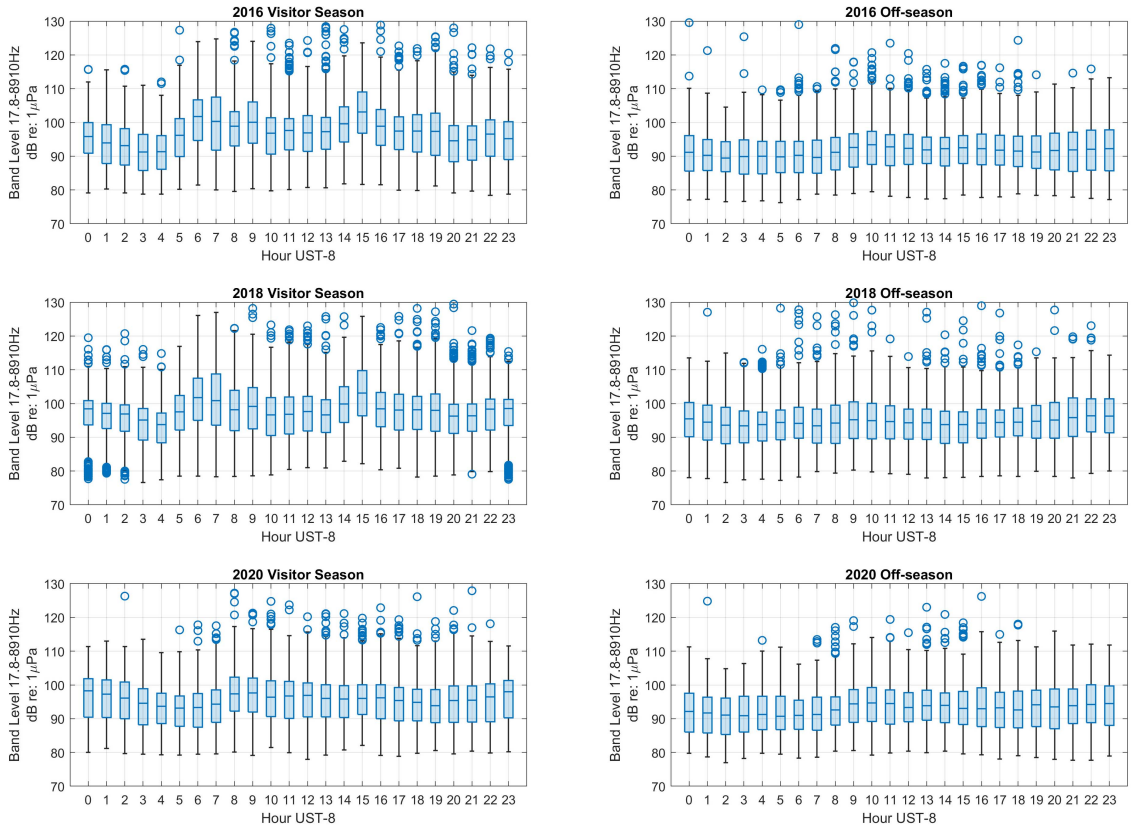

FIGURE 8 | Box-plot showing hourly 10 min resolution broadband (17.8–8,910 Hz) noise levels for 2016, 2018, and 2020. On each box, the central mark indicates the median, and the bottom and top edges of the box indicate the 25th and 75th percentiles, respectively. The whiskers extend to the most extreme data points not considered outliers, and the outliers are plotted individually using the "o" symbol.

and at their afternoon/evening departure. All classes of vessels had a role in the quieter underwater sound environment in 2020 but the acoustic contribution of tour vessels and cruise ships to the underwater soundscape is substantial, especially in terms of the loudest sounds (**Table 1** and **Supplementary Figure 1**). The gradual return of tourism to Glacier Bay in the coming years will provide additional opportunity to explore the contributions of different vessel classes.

Scientific reports of changes in underwater sound levels during the COVID-19 pandemic are just starting to emerge. While it is not unexpected that the underwater acoustic environment would be characterized by lower sound levels when there are fewer vessels, the acoustic effects depend upon the circumstances. Near Vancouver, Canada, the pandemic-induced reduction in commercial shipping traffic resulted in 1.5–2.7 dB reductions in underwater noise in the 100 Hz band at three out of four hydrophone stations in the first 3 months of 2020, whereas the fourth hydrophone showed no difference in sound levels (Thomson and Barclay, 2020). Not all human activities or sectors of the maritime industry were equally affected during the pandemic (Ito et al., 2020; Millefiori et al., 2020; Yazir et al., 2020; Notteboom et al., 2021). In the Mediterranean, for example, decreases in shipping occurred more in coastal areas and lasted longer in sectors other than cargo and tanker shipping (March et al., 2020). Due to the pandemic's sharp and lasting effects on Alaska tourism, the change in Glacier Bay's acoustic environment may be one of the most distinct, because the area lacks other types of traffic that would occur in absence of tourism.

Human behavior appears to drive a clear diurnal pattern of vessel noise in Glacier Bay (**Figure 3**). Human use of Glacier Bay concentrates in the daytime, and in the summer months when the days are long and the weather is often favorable. Most cruise ships as well as the day-tour catamaran enter Glacier Bay early enough to take advantage of prime daylight hours to view the spectacular scenery of the park and exit the bay by late afternoon or early evening (**Supplementary Figures 7**, **8**, NPS unpublished data). Although vessel noise was still evident in 2020, it began later in the morning and did not display a distinct peak, with vessels apparently entering and exiting the bay at various times of day (**Figures 3**, **8**). The contrast in underwater sound levels between 2020 and prior years was much less distinct during Off Hours and Off Season. Previous noise characterization work using over 10,000 audio samples in 2000–2008 demonstrates that vessel noise was less common in the hours between 9:00 p.m and 5:00 a.m LT (Kipple and Gabriele, 2003; McKenna et al., 2017), suggesting that natural sounds such as wind, rain, and harbor seal vocalizations (in May–July) are the more prominent components

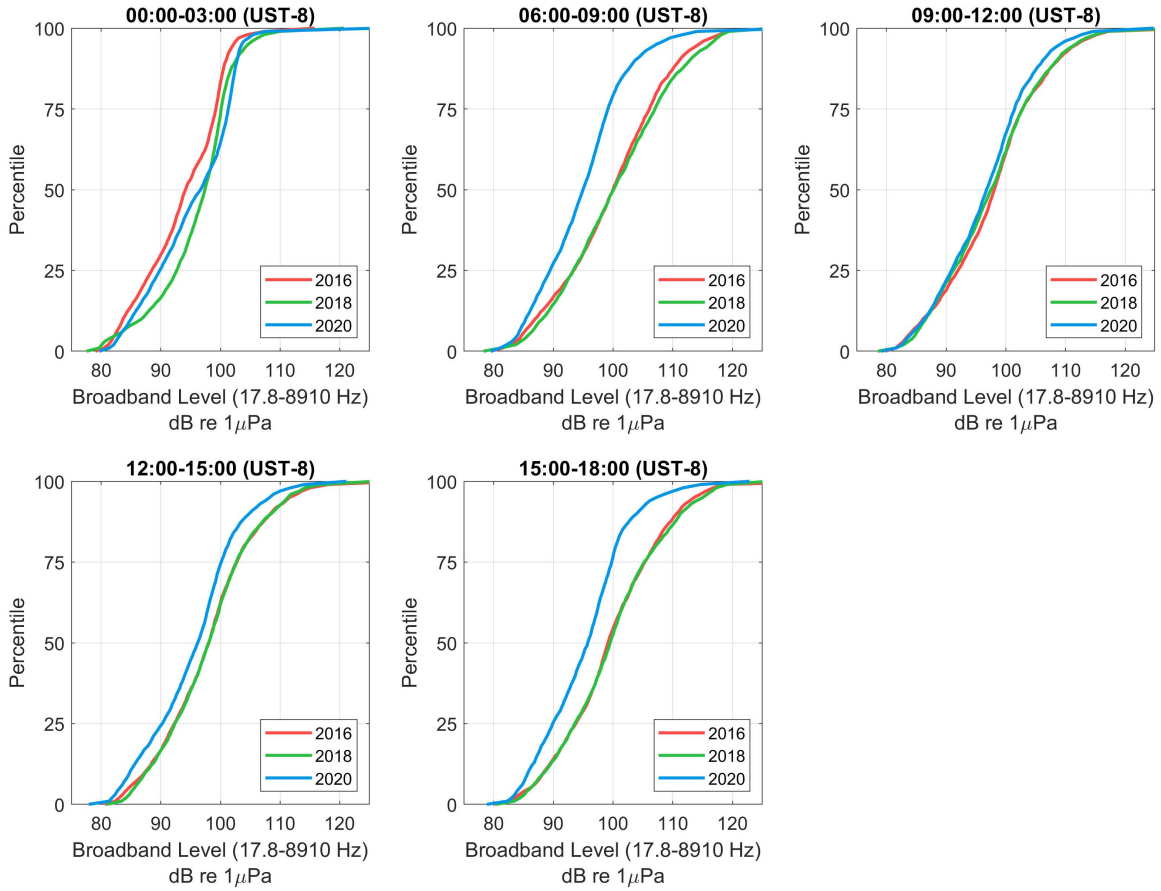

FIGURE 9 | Cumulative distribution of broadband noise levels (17.8–8,910 Hz) in lower Glacier Bay in 2016, 2018, and 2020 for time blocks during daylight hours when vessel traffic is most common and late at night when vessel traffic is uncommon. 2020 is quietest in all time blocks except the midnight to 03:00 LT time block, when all years are equivalent.

of the underwater sound environment in late evening through early morning hours.

To understand the received levels in different frequency bands (**Figure 5**), it is important to note that the hydrophone is located in outer Bartlett Cove, in a location where all small craft and medium-sized tour vessels pass near or even directly over the hydrophone sensor. Thus, in 2020 when visitor traffic was composed predominantly of small vessels, most Glacier Bay vessel traffic was composed of the types of vessels that tend to pass close to the hydrophone. The individual noise events that comprise small vessel passages are a good representation of their influence on the soundscape wherever they travel in Glacier Bay. Cruise ships, in contrast, pass at a much greater distance from the hydrophone (for example vessel tracks see Gende et al., 2011; Frankel and Gabriele, 2017) and reduce their speed to embark and disembark NPS interpretive rangers outside Bartlett Cove. As such, measurements from the Bartlett Cove hydrophone are a minimal estimate of the contributions of cruise ships to Glacier Bay's underwater soundscape, as they are farther from the hydrophone and are often likely to be louder when traveling at their full transiting speed (Kipple, 2002).

During the daytime in the Visitor Season as a whole, 2020 was markedly quieter, particularly in the 63.1–200 Hz bands (**Figure 5** and **Supplementary Table 1**). For the Off Season, 2020 was not quietest, but note that the lack of data in January–mid-April likely missed the period of least vessel traffic (both because it was early in the COVID-19 pandemic and the Off Season). Focusing on the morning and afternoon time blocks when vessel traffic peaks occur (**Figure 3** and **Supplementary Figures 7**, **8**, McKenna et al., 2017), we found that 2020 median broadband levels were 3.5–5.0 dB quieter than in typical recent years, and that the 95th percentile levels were 7–8 dB quieter (**Table 1** and **Figure 9**).

In the Off Season, the distribution of the acoustic energy among one-third octave bands (**Figure 5**) is similar in all years, particularly 2016 and 2020, with 2018 displaying the highest sound levels. Spring and fall wind events (**Supplementary Figure 3**) likely contribute to the increased median noise levels, which increase with increasing wind speed (**Supplementary Figure 4**). It is difficult to interpret the role of vessel noise in Glacier Bay's Off Season in the absence of vessel traffic records for these time periods. During Visitor Season, there is pronounced difference between 2020 and prior years (**Figure 5**), notably

TABLE 1 | Distribution of broadband sound levels (17.8–8,910 Hz dB re 1 μPa) at 10 min resolution in specified time-blocks (LT) in Glacier Bay during the May–September visitor season.

		Percentile						
Year	**Time block**	**1**	**5**	**25**	**50**	**75**	**95**	**99**
2016	0:00–03:00	80.5	82.3	88.5	94.1	99.2	102.2	107.4
2018	0:00–03:00	79.7	82.5	92.7	97.4	100.1	104.6	110
2020	0:00–03:00	81.4	83.2	89.8	96.7	101.3	103.6	107.5
2016	06:00–09:00	81.5	84.7	93.4	100	106.1	114.4	118.9
2018	06:00–09:00	81.2	85.8	93.3	100.1	107	116.2	119.4
2020	06:00–09:00	81.1	84	89.4	95	99.1	107.2	114.1
2016	09:00–12:00	81.6	83.7	92	98	102.8	111.9	117.1
2018	09:00–12:00	81.5	84.8	91.2	97.5	102.8	111.6	116.7
2020	09:00–12:00	81.6	84	90.9	96.7	101.5	109.1	114.6
2016	12:00–15:00	82.4	84.6	92.3	98.1	102.8	111.6	118.1
2018	12:00–15:00	83.4	85.5	92.4	98	102.7	111.3	116.8
2020	12:00–15:00	81.3	83.1	90.2	96.2	100.1	108.3	114
2016	15:00–18:00	82.6	86	93.7	99.1	105.3	113.6	118.2
2018	15:00–18:00	83.4	86.2	93.6	99.5	105.2	115	119.1
2020	15:00–18:00	82.3	84.3	89.9	95.8	99.8	107.3	114.6

The color shading denotes relative sound levels.

between 100–200 Hz, that appears to be attributable to both vessel noise and biological sounds. In previous work, the distinct peak in the 125 Hz one-third octave band was attributed to harbor seal vocalizations (McKenna et al., 2017), but substantial sound energy for cruise ships also falls in the 63 and 125 Hz one-third octave bands (Kipple, 2002) which have been identified as important to quantifying and mitigating ship noise (Dekeling et al., 2014). The median 125 Hz peak is similar between 2016 and 2018 but 3 dB quieter in 2020. However, at the 95th percentile level (**Figure 5**) the 125 Hz peak is more pronounced, perhaps because noise from large vessels is absent.

Harbor seals have been documented to vocalize slightly louder in the presence of vessel noise in the context of typical Glacier Bay vessel traffic in 2015 (Matthews et al., 2020) but the anomalous quiet in 2020 may have created an acoustic environment where quieter (Derryberry et al., 2020) or less frequent vocalizations would suffice. Given the variability in the source levels of individual harbor seal roars (139–159 dBRMS re 1 μPa @ 1 m, 40–500 Hz, Matthews et al., 2017b), it could be that different males were defending territory near the hydrophone in each year. It is also possible that roaring males were farther away in 2020; reduced vessel traffic may have made available preferred habitat farther away from the hydrophone. Glacier Bay's major harbor seal haul-outs are not near the hydrophone location, and the NPS standardized aerial haul-out surveys in 2020 were canceled due to COVID-19 safety concerns, but NPS opportunistic marine mammal sightings during humpback whale surveys documented the highest number of harbor seals since 1997 (NPS, unpublished data). While the current single-hydrophone system cannot determine differences in source levels, future work to discern the contribution of harbor seal roars to the observed acoustic differences could look for systematic differences in diurnal patterns, duration of calls, call rate, and received levels between years. White-crowned sparrows (*Zonotrichia leucophrys*) were documented to sing more quietly and their vocalizations traveled farther in newly quieted neighborhoods during COVID-19 (Derryberry et al., 2020). The pandemic-driven quiet period provides an important opportunity to observe changes in behavior in the context of restored acoustic habitats.

Previous work suggested that aggregate vessel noise on a typical day during Glacier Bay's Visitor Season substantially masks humpback whale and harbor seal vocalizations and reduces their available communication space (Gabriele et al., 2018). That work also estimated that closely spaced cruise ship entries increased the estimated daily amount of communication space available to vocalizing whales and seals (Gabriele et al., 2018). Humpback whales have been found to increase the loudness of their calls in the presence of natural and manmade noise (the Lombard Effect), but were also less likely to vocalize when vessel noise was present (Fournet et al., 2018a) suggesting that they may wait for a quiet time to communicate. Although morning and afternoon concentrations of vessel noise markedly compromised the acoustic environment, we speculate that synchronized traffic with short, louder periods of time, to create quiet periods between vessel noise events, may be beneficial to marine mammal acoustic ecology, as opposed to prolonged time periods of noise without quiet periods (Heise et al., 2017; Merchant, 2019). Work in progress to examine humpback whale calling patterns in 2020 vs. previous years may further elucidate this question.

Our work and future studies will help inform efforts to maintain the integrity of marine protected areas while providing opportunities to visit and enjoy iconic places like Glacier Bay. Globally, there is growing recognition of human impacts on the underwater soundscape, efforts toward mitigation

(e.g., European Commission, 2008; International Maritime Organization, 2014) and a slow but steady increase in knowledge of the direct and indirect effects that underwater noise has on a vast number of marine organisms and ecological processes (Duarte et al., 2021). To decrease vessel noise, vessel speed limits are particularly effective (Frankel and Gabriele, 2017; McKenna et al., 2017) and several other methods have been recommended, including reducing vessel traffic, routing vessel traffic away from sensitive marine resources, designing quieter vessels, and providing incentives for quieter vessels (International Maritime Organization, 2014; Heise et al., 2017; Merchant, 2019). Future work could examine the underwater noise budgets of Glacier Bay and other marine tourism destinations as a function of vessel size and the number of visitors carried. Continuing to characterize the acoustic environment and updating that knowledge as the fleet characteristics and/or vessel management strategies change should be considered a management and conservation priority.

While scientific knowledge of the mechanisms of biological effects often lags behind, it remains clear that global biological diversity is at risk from noise and myriad other sensory pollutants (Dominoni et al., 2020). Noise pollution in otherwise undeveloped environments degrades habitat for marine species whose vital life functions rely upon the underwater sound environment. Marine mammals and other taxa have methods of compensating for noise (Parks et al., 2009; Tennessen and Parks, 2016; Fournet et al., 2018a; Matthews et al., 2020) but the effectiveness of compensatory behavior and the ultimate effects of noise on reproductive success are unknown. In marine protected areas and elsewhere, underwater noise is just one of many stressors that affect marine wildlife (Hatch et al., 2012; Williams et al., 2015; Blair et al., 2016; Haver et al., 2019), for example, the recent catastrophic effects of changing climate and unpredictable conditions on Alaska's marine ecosystems (Oliver et al., 2018; von Biela et al., 2019; Piatt et al., 2020; Arimitsu et al., 2021; Suryan et al., 2021). As maritime activities gradually resume in Glacier Bay and other areas, and marine protected area managers must rise to the challenge to use what has been learned in the pandemic-induced quiet to improve methods to mitigate vessel noise and foster healthy marine ecosystems in these vulnerable and important public resources.

DATA AVAILABILITY STATEMENT

The data analyzed in this study is subject to the following licenses/restrictions: By February 2022, the datasets analyzed for this study will be available in the National Oceanic and Atmospheric Administration's National Center for Environmental Information (NCEI) (https://www.ncei.noaa.gov). Requests to access these datasets should be directed to CG, Chris_Gabriele@nps.gov.

AUTHOR CONTRIBUTIONS

CG, DP, and HK conceived and designed the data analytical approach. CG collected and curated the acoustic and vessel traffic data. DP wrote the data analysis routines and created graphics. CG wrote the manuscript with contributions to drafting, critical review, and editorial input from DP and HK. All authors contributed to the article and approved the submitted version.

FUNDING

The data collection, system maintenance, and manuscript preparation was funded by the U.S. National Park Service commercial user fees. Data processing and analysis were funded by the Center for Conservation Bioacoustics, Cornell Lab of Ornithology, Cornell University.

ACKNOWLEDGMENTS

This hydrophone system design and maintenance that underlies Glacier Bay's unique long time-series of underwater ambient noise data would not have been possible without the skill, dedication and good humor of Blair Kipple, Russ Dukek, Larry Arndt, Kyle Gustafson, and others at the U.S. Naval Surface Warfare Center's Carderock Detachment. Many GBNP staff and volunteers helped with the underwater sound monitoring program over the years. Thanks to Jessica Chen at NAVFAC Pacific for helping jumpstart the 2020 data collection effort.

SUPPLEMENTARY MATERIAL

The Supplementary Material for this article can be found online at: https://www.frontiersin.org/articles/10.3389/fmars.2021.674787/full#supplementary-material

REFERENCES

Amitai, E., and Nystuen, J. A. (2008). "Underwater acoustic measurements of rainfall," in *Precipitation: Advances in Measurement, Estimation and Prediction*, ed. S. Michaelides (Berlin: Springer), 343–363. doi: 10.1007/978-3-540-77655-0_13

Andrew, R. K., Howe, B. M., and Mercer, J. A. (2011). Long-time trends in ship traffic noise for four sites off the North American West Coast. *J. Acoust. Soc. Am.* 129, 642–651. doi: 10.1121/1.3518770

Andrew, R. K., Howe, B. M., Mercer, J. A., and Dzieciuch, M. A. (2002). Ocean ambient sound: comparing the 1960s with the 1990s for a receiver off the California coast. *Acoust. Res. Lett. Online* 3, 65–70. doi: 10.1121/1.1461915

Arimitsu, M., Piatt, J., Hatch, S., Suryan, R. M., Batten, S., Bishop, M. A., et al. (2021). Heatwave-induced synchrony within forage fish portfolio disrupts energy flow to top pelagic predators. *Glob. Chang. Biol.* 27, 1859–1878. doi: 10.1111/gcb.15556

Barber, J. R., Burdett, C. L., Reed, S. E., Warner, K. A., Formichella, C., Crooks, K. R., et al. (2011). Anthropogenic noise exposure in protected natural areas: estimating the scale of ecological consequences. *Landsc. Ecol.* 26, 1281–1295. doi: 10.1007/s10980-011-9646-7

Barlett, M. L., and Wilson, G. R. (2002). Characteristics of small boat signatures. *J. Acoust. Soc. Am.* 112:2221. doi: 10.1121/1.4778778

Blair, H. B., Merchant, N. D., Friedlaender, A. S., Wiley, D. N., and Parks, S. E. (2016). Evidence for ship noise impacts on humpback whale foraging behaviour. *Biol. Lett.* 12:20160005. doi: 10.1098/rsbl.2016.0005

Brumm, H., and Slabbekoorn, H. (2005). Acoustic communication in noise. *Adv. Study Behav.* 35, 151–209.

Chapman, N. R., and Price, A. (2011). Low frequency deep ocean ambient noise trend in the Northeast Pacific Ocean. *J. Acoust. Soc. Am.* 129, EL161–EL165.

Dekeling, R. P. A., Tasker, M. L., Van der Graaf, A. J., Ainslie, M. A., Andersson, M. H., André, M., et al. (2014). *Monitoring Guidance for Underwater Noise in European Seas, Part I: Executive Summary. A Guidance Document within the Common Implementation Strategy for the Marine Strategy Framework Directive by MSFD Technical Subgroup on Underwater Noise*. Luxembourg: Publications Office of the European Union.

Derryberry, E. P., Phillips, J. N., Derryberry, G. E., Blum, M. J., and Luther, D. (2020). Singing in a silent spring: birds respond to a half-century soundscape reversion during the COVID-19 shutdown. *Science* 370, 575–579. doi: 10.1126/science.abd5777

Dominoni, D. M., Halfwerk, W., Baird, E., Buxton, R. T., Fernández-Juricic, E., Fristrup, K. M., et al. (2020). Why conservation biology can benefit from sensory ecology. *Nat. Ecol. Evol.* 4, 502–511. doi: 10.1038/s41559-020-1135-4

Duarte, C. M., Chapuis, L., Collin, S. P., Costa, D. P., Devassy, R. P., Eguiluz, V. M., et al. (2021). The soundscape of the Anthropocene ocean. *Science* 371:eaba4658. doi: 10.1126/science.aba4658

Dugan, P. J., Ponirakis, D. W., Zollweg, J. A., Pitzrick, M. S., Morano, J. L., Warde, A. M., et al. (2011). "SEDNA – bioacoustic analysis toolbox: matlab platform to support high performance computing, noise analysis, event detection and event modeling," in *Proceedings of the IEEE OCEANS 2011*, (Kona, HI).

Erbe, C. (2002). Underwater noise of whale-watching boats and potential effects on killer whales (*Orcinus orca*), based on an acoustic impact model. *Mar. Mamm. Sci.* 18, 394–418. doi: 10.1111/j.1748-7692.2002.tb01045.x

Erbe, C., Liong, S., Koessler, M. W., Duncan, A. J., and Gourlay, T. (2016). Underwater sound of rigid-hulled inflatable boats. *J. Acoust. Soc. Am.* 139, EL223–EL227.

European Commission (2008). *Directive 2017/845 of the European Parliament and of the Council as of 17 June 2008 Establishing a Framework for Community Action in the Field of Marine Environmental Policy (Marine Strategy Framework Directive) OJ L 164.25.6.2008*. Brussels: European Commission, 19.

Federal Register (2020). No Sail Order and Suspension of Further Embarkation; Notice of Modification and Extension and Other Measures Related to Operations. Available online at: (https://www.federalregister.gov/documents/2020/04/15/2020-07930/no-sail-order-and-suspension-of-further-embarkation-notice-of-modification-and-extension-and-other) (accessed June 3, 2021).

Fournet, M. E., Matthews, L. P., Gabriele, C. M., Haver, S., Mellinger, D. K., and Klinck, H. (2018a). Humpback whales Megaptera novaeangliae alter calling behavior in response to natural sounds and vessel noise. *Mar. Ecol. Prog. Ser.* 607, 251–268. doi: 10.3354/meps12784

Fournet, M. E., Matthews, L. P., Gabriele, C. M., Mellinger, D. K., and Klinck, H. (2018b). Source levels of foraging humpback whale calls. *J. Acoust. Soc. Am.* 143, EL105–EL111.

Frankel, A. S., and Gabriele, C. M. (2017). Predicting the acoustic exposure of humpback whales from cruise and tour vessel noise in Glacier Bay, Alaska, under different management strategies. *Endanger. Species Res.* 34, 397–415. doi: 10.3354/esr00857

Gabriele, C. M., Ponirakis, D. W., Clark, C. W., Womble, J. N., and Vanselow, P. (2018). Underwater acoustic ecology metrics in an Alaska marine protected area reveal marine mammal communication masking and management alternatives. *Front. Mar. Sci.* 5:270. doi: 10.3389/fmars.2018.00270

Gende, S. M., Hendrix, A. N., Harris, K. R., Eichenlaub, B., Nielsen, J., and Pyare, S. (2011). A Bayesian approach for understanding the role of ship speed in whale–ship encounters. *Ecol. Appl.* 21, 2232–2240. doi: 10.1890/10-1965.1

Hatch, L. T., Clark, C. W., Van Parijs, S. M., Frankel, A. S., and Ponirakis, D. W. (2012). Quantifying loss of acoustic communication space for right whales in and around a U.S. national marine sanctuary. *Conserv. Biol.* 26, 983–994. doi: 10.1111/j.1523-1739.2012.01908.x

Haver, S. M., Fournet, M. E., Dziak, R. P., Gabriele, C., Gedamke, J., Hatch, L. T., et al. (2019). Comparing the underwater soundscapes of four US National Parks and Marine Sanctuaries. *Front. Mar. Sci.* 6:500. doi: 10.3389/fmars.2019.00500

Heise, K., Barrett-Lennard, L., Chapman, R., Dakin, T., Erbe, C., Hannay, D. E., et al. (2017). Proposed metrics for the management of underwater noise for southern resident killer whales. *Tech. Rep.* 31. doi: 10.25317/CORI20172

Houghton, J., Holt, M. M., Giles, D. A., Hanson, M. B., Emmons, C. K., Hogan, J. T., et al. (2015). The relationship between vessel traffic and noise levels received by killer whales (*Orcinus orca*). *PloS one* 10:e0140119. doi: 10.1371/journal.pone.0140119

International Maritime Organization (2014). *Guidelines for the Reduction of Underwater Noise from Commercial Shipping to Address Adverse Impacts on Marine Life*. MEPC.1/Circ.833. London: International Maritime Organization.

Ito, H., Hanaoka, S., and Kawasaki, T. (2020). The cruise industry and the COVID-19 outbreak. *Transp. Res. Interdiscip. Perspect.* 5:100136. doi: 10.1016/j.trip.2020.100136

Kipple, B. M. (2002). *Southeast Alaska Cruise ship Underwater Acoustic Noise*. Naval Surface Warfare Center report NSWCCD-71-TR-2002/574. Bremerton, WA: Naval Surface Warfare Center, 84.

Kipple, B., and Gabriele, C. (2003). *Glacier Bay Watercraft Noise: Underwater Acoustic Noise Levels of Watercraft Operated by Glacier Bay National Park and Preserve as measured in 2000 and 2002*. Bremerton, WA: Naval Surface Warfare Center – Carderock Division, 54.

Kipple, B. M., and Gabriele, C. M. (2004a). *Glacier Bay Underwater Noise – August 2000-August 2002*. report NSWCCD-71-TR-2004/521. Bremerton, WA: Naval Surface Warfare Center, 70.

Kipple, B. M., and Gabriele, C. M. (2004b). *Glacier Bay Watercraft Noise - Noise Characterization for Tour, Charter, Private and Government Vessels*. Bremerton, WA: Naval Surface Warfare Center.

Knudsen, V. O., Alford, R. S., and Emling, J. W. (1948). Digital communications. *J. Mar. Res.* 7:410.

Malme, C. I., Miles, P. R., and McElroy, P. T. (1981). Acoustic environment of humpback whales in Glacier Bay and Frederick Sound, Alaska. *J. Acoust. Soc. Am.* 70:S85.

March, D., Metcalfe, K., Tintoré, J., and Godley, B. (2020). Tracking the global reduction of marine traffic during the COVID-19 pandemic. *Nat. Commun.* 12, 1–12.

Matthews, L. P., Fournet, M. E., Gabriele, C., Klinck, H., and Parks, S. E. (2020). Acoustically advertising male harbour seals in southeast Alaska do not make biologically relevant acoustic adjustments in the presence of vessel noise. *Biol. Lett.* 16:20190795. doi: 10.1098/rsbl.2019.0795

Matthews, L. P., Gabriele, C. M., and Parks, S. E. (2017a). The role of season, tide, and diel period in the presence of harbor seal (*Phoca vitulina*) breeding vocalizations in glacier bay national park and preserve, Alaska. *Aquat. Mamm.* 43, 537–546.

Matthews, L. P., Parks, S. E., Fournet, M. E., Gabriele, C. M., Womble, J. N., and Klinck, H. (2017b). Source levels and call parameters of harbor seal breeding vocalizations near a terrestrial haulout site in Glacier Bay National Park and Preserve. *J. Acoust. Soc. Am.* 141, EL274–EL280.

McDonald, M. A., Hildebrand, J. A., and Wiggins, S. M. (2006). Increases in deep ocean ambient noise in the Northwest Pacific west of San Nicolas Island, California. *J. Acoust. Soc. Am.* 120, 711–717.

McKenna, M. F., Gabriele, C. M., and Kipple, B. (2017). Effects of marine vessel management on the underwater acoustic environment of Glacier Bay National Park, AK. *Ocean Coast. Manag.* 139, 102–112.

McKenna, M. F., Ross, D., Wiggins, S. M., and Hildebrand, J. A. (2012). Underwater radiated noise from modern commercial ships. *J. Acoust. Soc. Am.* 131:92e103.

Merchant, N. D. (2019). Underwater noise abatement: economic factors and policy options. *Environ. Sci. Policy* 92, 116–123.

Miksis-Olds, J. L., and Nichols, S. M. (2016). Is low frequency ocean sound increasing globally? *J. Acoust. Soc. Am.* 139, 501–511.

Miksis-Olds, J. L., Bradley, D. L., and Maggie Niu, X. (2013). Decadal trends in Indian Ocean ambient sound. *J. Acoust. Soc. Am.* 134, 3464–3475.

Millefiori, L. M., Braca, P., Zissis, D., Spiliopoulos, G., Marano, S., Willett, P. K., et al. (2020). *Covid-19 Impact on Global Maritime Mobility. arXiv [Preprint]*. Available online at: https://arxiv.org/abs/2009.06960 (accessed June 3, 2021).

Mohl, B., and Andersen, S. (1973). Echolocation: high frequency component in the click of the harbor porpoise (*Phocoena phocoena*). *J. Acoust. Soc. Am.* 54, 1368–1372.

Notteboom, T., Pallis, T., and Rodrigue, J. P. (2021). Disruptions and resilience in global container shipping and ports: the COVID-19 pandemic versus the 2008–2009 financial crisis. *Marit. Econ. Logist.* 23, 179–210. doi: 10.1057/s41278-020-00180-5

Oliver, E. C., Donat, M. G., Burrows, M. T., Moore, P. J., Smale, D. A., Alexander, L. V., et al. (2018). Longer and more frequent marine heatwaves over the past century. *Nat. Commun.* 9:1324.

Parks, S. E., Urazghildiiev, I., and Clark, C. W. (2009). Variability in ambient noise levels and call parameters of North Atlantic right whales in three habitat areas. *J. Acoust. Soc. Am.* 125, 1230–1239.

Payne, R. S., and Webb, D. (1971). Orientation by means of long range acoustic signaling in baleen whales. *Ann. N.Y. Acad. Sci.* 188, 110–141.

Piatt, J. F., Parrish, J. K., Renner, H. M., Schoen, S. K., Jones, T. T., Arimitsu, M. L., et al. (2020). Extreme mortality and reproductive failure of common murres resulting from the northeast Pacific marine heatwave of 2014-2016. *PLoS One* 15:e0226087. doi: 10.1371/journal.pone.0226087

Richardson, W. J., Greene, C. R., Malme, C. I., and Thomson, D. H. (1995). *Marine Mammals and Noise*. San Diego, CA: Academic Press.

Ross, D. (2005). Ship sources of ambient noise. *IEEE J. Ocean. Eng.* 30, 257–261.

Suryan, R. M., Arimitsu, M. L., Coletti, H. A., Hopcroft, R. R., Lindeberg, M. R., Barbeaux, S. J., et al. (2021). Ecosystem response persists after a prolonged marine heatwave. *Sci. Rep.* 11:115.

Tennessen, J. B., and Parks, S. E. (2016). Acoustic propagation modeling indicates vocal compensation in noise improves communication range for North Atlantic right whales. *Endanger. Species Res.* 30, 225–237.

Thomson, D. J., and Barclay, D. R. (2020). Real-time observations of the impact of COVID-19 on underwater noise. *J. Acoust. Soc. Am.* 147, 3390–3396.

Transport Canada (2020). *Minister Garneau Announces Extended Measures for Cruise Ships and Pleasure Craft in Canada*. Ottawa, ON: Transport Canada.

Tyack, P. L. (2008). Implications for marine mammals of large-scale changes in the marine acoustic environment. *J. Mamm.* 89, 549–558. doi: 10.1644/07-MAMM-S-307R.1

Veirs, S., Veirs, V., and Wood, J. D. (2016). Ship noise extends to frequencies used for echolocation by endangered killer whales. *PeerJ* 4:e1657.

von Biela, V. R., Arimitsu, M. L., Piatt, J. F., Heflin, B., Schoen, S. K., Trowbridge, J. L., et al. (2019). Extreme reduction in nutritional value of a key forage fish during the Pacific marine heatwave of 2014–2016. *Mar. Ecol. Prog. Ser.* 613, 171–182.

Wenz, G. M. (1962). Acoustic ambient noise in the ocean: spectra and sources. *J. Acoust. Soc. Am.* 34, 1936–1956.

Wild, L. A., and Gabriele, C. M. (2014). Putative contact calls made by humpback whales (M*egaptera novaeangliae*) in southeastern Alaska. *Can. Acoust.* 42, 23–31.

Williams, R., Erbe, C., Ashe, E., and Clark, C. W. (2015). Quiet (er) marine protected areas. *Mar. Pollut. Bull.* 100, 154–161.

Yazir, D., Şahin, B., Yip, T. L., and Tseng, P. H. (2020). Effects of COVID-19 on maritime industry: a review. *Int. Marit. Health* 71, 253–264.

Conflict of Interest: The authors declare that the research was conducted in the absence of any commercial or financial relationships that could be construed as a potential conflict of interest.

Copyright © 2021 Gabriele, Ponirakis and Klinck. This is an open-access article distributed under the terms of the Creative Commons Attribution License (CC BY). The use, distribution or reproduction in other forums is permitted, provided the original author(s) and the copyright owner(s) are credited and that the original publication in this journal is cited, in accordance with accepted academic practice. No use, distribution or reproduction is permitted which does not comply with these terms.

frontiers in Marine Science

ORIGINAL RESEARCH
published: 29 June 2021
doi: 10.3389/fmars.2021.674788

Changes in Underwater Noise and Vessel Traffic in the Approaches to Halifax Harbor, Nova Scotia, Canada

Heather Breeze[1], Shihan Li[2], Emmaline C. Marotte[1], James A. Theriault[3], Jessica Wingfield[1] and Jinshan Xu[1]*

[1] Bedford Institute of Oceanography, Fisheries and Oceans Canada, Dartmouth, NS, Canada, [2] Shihan Li Consulting, Halifax, NS, Canada, [3] Ocean Environmental Consulting, Halifax, NS, Canada

Over the past two years, researchers at Fisheries and Oceans Canada have been running an acoustic monitoring project at multiple study sites throughout Nova Scotia, Canada to investigate baleen whale presence and levels of underwater noise. At the onset of the COVID-19 pandemic, a passive acoustic monitor (PAM) was in place in the study site located in the approaches to Halifax Harbor, a major Canadian port. This provided a unique opportunity to determine if changes in vessel noise levels occurred after pandemic restrictions were put in place. To investigate this, we analyzed and compared acoustic data collected from March 28 to April 28 and August 6 to October 22 in both 2019 and 2020. We also investigated possible changes in vessel traffic from February 1 through April 28 and July 1 through July 28 in 2019 and 2020 using terrestrial-based automatic identification system (AIS) data provided by the Canadian Coast Guard and cargo information provided by the Port of Halifax. The acoustic data were analyzed in 1/3 octave frequency bands. For the 89.1–112 Hz frequency band, we found an 8.4 dB increase in the daily minimum sound pressure level (SPL) in April 2020 compared to April 2019 due the presence of a large crane vessel stationed near the mooring site. For the period of August to October, we found an approximately 1.7 dB reduction in the same metric from 2019 to 2020. The most noticeable change in vessel composition was the dramatic decrease in the number and occurrence of pleasure craft in July 2020 compared to the same period in 2019. While this analysis looked at only a single PAM and a limited amount of data, we observed changes in sound levels in the frequency band known to be associated with shipping as well as changes in vessel traffic; we conclude that these observed changes may be related to pandemic restrictions.

Keywords: commercial shipping, vessel traffic, underwater noise, passive acoustic monitoring, Nova Scotia, COVID-19, automatic identification system (AIS)

OPEN ACCESS

Edited by:
Kerri D. Seger,
Applied Ocean Sciences,
United States

Reviewed by:
Vanessa ZoBell,
Scripps Institution of Oceanography,
University of California, San Diego,
United States
Edison Barbieri,
Instituto de Pesca, Agência Paulista
de Tecnologia dos Agronegócios
(APTA), Brazil

****Correspondence:***
Heather Breeze
Heather.Breeze@dfo-mpo.gc.ca

Specialty section:
This article was submitted to
Marine Pollution,
a section of the journal
Frontiers in Marine Science

Received: *02 March 2021*
Accepted: *02 June 2021*
Published: *29 June 2021*

Citation:
Breeze H, Li S, Marotte EC, Theriault JA, Wingfield J and Xu J (2021) Changes in Underwater Noise and Vessel Traffic in the Approaches to Halifax Harbor, Nova Scotia, Canada. Front. Mar. Sci. 8:674788. doi: 10.3389/fmars.2021.674788

INTRODUCTION

The past 50 years have seen a significant worldwide increase in the size and number of vessels in merchant fleets (Hildebrand, 2009). Global ship numbers have risen by a factor of 3.5 and gross tonnage by a factor of 10 (Frisk, 2012). Within the same time period, rising ambient noise levels in certain areas of the world's oceans have been observed, suggesting an overall increase of at least

20 dB in low-frequency (10–500 Hz) ambient noise since pre-industrial conditions (Hildebrand, 2009). Studies have since attributed rising underwater ocean noise levels to an increase in global shipping (Andrew et al., 2002; Frisk, 2012), with some estimates of increases in ambient noise at low frequencies as high as 3 dB per decade in parts of the world's oceans (Andrew et al., 2002). The potential for adverse effects on marine life, particularly cetaceans, from this increase in anthropogenic underwater noise has been discussed by many authors (see e.g., National Research Council, 2003; Weilgart, 2007; Tyack, 2008; Erbe et al., 2019; Duarte et al., 2021). Acknowledging the growing concerns about the impacts of underwater noise coupled with limited information for Canadian waters, the Government of Canada has recently made greater efforts to better understand anthropogenic ocean noise, particularly from commercial shipping. This initiative is part of a broader program to address impacts of commercial shipping in Canadian waters called the Oceans Protection Plan (OPP; Fisheries and Oceans Canada, 2021).

As part of efforts under the OPP, an underwater passive acoustic monitoring project was launched in 2018 to better understand marine mammal and vessel noise occurrence at multiple, single-hydrophone data collection sites around coastal Nova Scotia. Monitoring locations were selected based on anecdotal or historic sightings of baleen whales and proximity to existing or proposed anthropogenic noise-generating activities. The Port of Halifax is a major Canadian port and its approaches were therefore selected as one of the monitoring sites for this project. Data collected from this site cover the period from late March 2019 to October 2020, with two interruptions due to difficulties in retrieving or deploying equipment.

Starting in early 2020, countries around the world sought to limit the spread of a novel coronavirus (COVID-19) by restricting various activities, thus creating reductions in industrial activity and manufactured products as well as disrupting the movement of people and goods. The global economy was estimated to shrink by 3.5% in 2020, with production plummeting in the second quarter of 2020 followed by some recovery to pre-pandemic levels by the end of 2020 (International Monetary Fund, 2021). The reduction in global trade activity was widely expected to have a corresponding decrease in marine shipping traffic, which has been borne out by recent studies in some areas (March et al., 2020; Thomson and Barclay, 2020). During the spring of 2020 when COVID-19 restrictions would have begun affecting vessel activity in and out of Halifax Harbor, a passive acoustic monitor was in place in the approaches of the harbor as part of the acoustic monitoring project just described. The data collected during this time provided an opportunistic occasion to examine local changes in vessel noise levels hypothesized to have occurred as a result of COVID-19 pandemic-related restrictions on maritime trade. To investigate this, we compared noise levels in subsets of acoustic data collected from the study site in 2019 and 2020, including the time period overlapping with the implementation of pandemic-related restrictions. We also examined shipping traffic data and cargo data from the Halifax Port Authority to determine changes in vessel presence and port-wide imports and exports. While available data limited our comparison to only certain time periods between just two years, our study represents a unique opportunity to investigate changes in underwater noise before and after the onset of the COVID-19 pandemic in one of Canada's busiest shipping ports.

MATERIALS AND METHODS

Study Area, Mooring Design, and Instrumentation

Acoustic data collection at the study site was initiated in 2019 as part of a larger passive acoustic monitoring study described above. A passive acoustic monitor (PAM) enclosed in a custom-configured subsea mooring was deployed 2 km off a headland in the vessel traffic separation zone between the incoming and outgoing shipping lanes in the approaches to the Port of Halifax (**Figure 1**). An important fishing harbor is located nearby and commercial fishing occurs in the general area; however, fish harvesters usually avoid setting gear in the shipping lanes, thus minimizing potential interactions between the PAM and fishing gear. Recreational vessels also frequent the area. Several navigational buoys are located in the area, including two "bell" buoys which ring with wave movements. For 2019 and 2020, sea surface temperatures recorded by a nearby oceanographic buoy ranged from −1.1°C in March 2019 to 19.1°C in September 2019 (SmartAtlantic Alliance, 2020). While no direct observations were made of the seafloor at the site, a nearby drop camera survey (within 5 km of the site) documented cobble and boulder deposits with large expanses of massive ledge formations and the researcher concluded that the deeper portions of the survey area (40–50 m depth) represented energetically active environments (Vandermeulen, 2018). Water depth at the deployment site was measured as 63 m using the deployment vessel's navigation system.

The PAM system consisted of a SoundTrap acoustic recorder (Ocean Instruments, models ST300 STD and ST500 STD) suspended in a modified lobster trap which was tethered to a pop-up submersible buoy manufactured by Fiomarine (**Figure 2**). The trap was approximately one-quarter the size and lacked the opening of a commercial lobster trap. It was weighted with standard trap weights to ensure the entire mooring remained stationary on the seafloor when deployed. Before deployment, the buoy was programmed with a release time and date. The buoy and was set up to float 1–2 m above the trap until the release mechanism was activated. The rope remained spooled on the buoy until the release event, minimizing the presence of rope in the water column and thus reducing the risk of entanglement to pelagic marine species. This relatively small and self-contained mooring design allowed the PAM to be deployed from small vessels. The mooring design used in the study represented a culmination of a series of design configurations gradually improved over the course of many deployments conducted as part of the broader acoustic monitoring program described earlier (see Theriault et al., 2018). Modifications were made over time to reduce possible sources of noise including careful selection of noise-reducing swivels and hardware and securing all attachment points. Analysis of previous recordings have shown

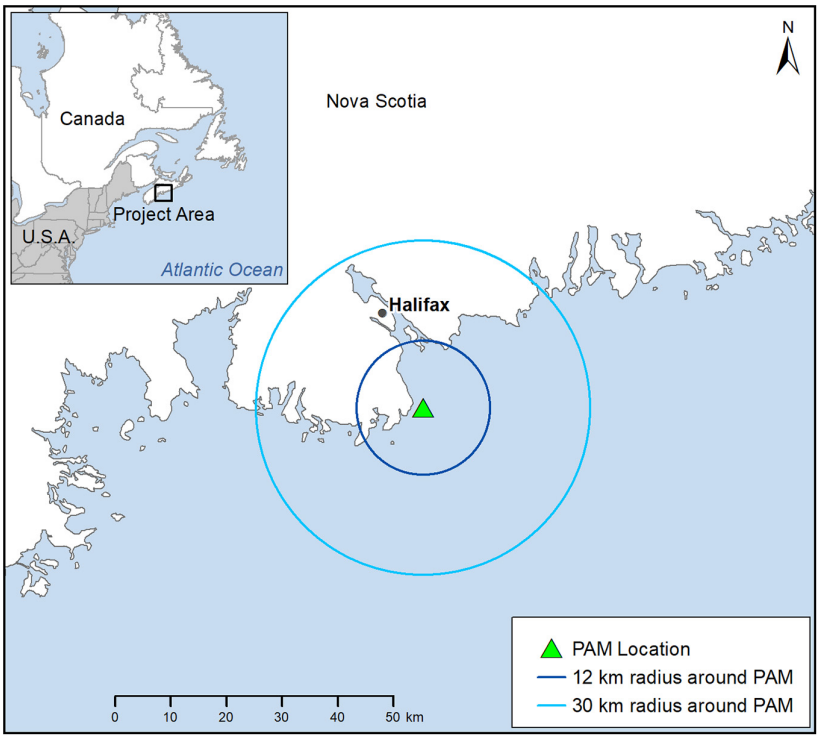

FIGURE 1 | The deployment location of the passive acoustic monitoring (PAM) system near the Port of Halifax. Shown are the 12- and 30-km radiuses around the mooring location that were used to examine shipping traffic and calculate noise energy from vessels.

that flow noise and other noise generated by the mooring itself has not been detected at levels significant enough to interfere with signals of interest. Furthermore, the signals of interest have a large wavelength of greater than 15 m and are unlikely to be attenuated by the cage nor by other components of the mooring; in actuality, the presence of the cage likely helps reduce flow noise by breaking up coherence thereby being somewhat advantageous to acoustic data collection.

FIGURE 2 | Components of the mooring used in the study. The Ocean Instruments SoundTrap acoustic recorder and battery case enclosed in a custom lobster trap (pictured on left) is tethered to a spooled Fiobuoy (pictured on right), a submersible pop-up buoy that enables surface retrieval of the entire system.

The SoundTrap was configured for continuous recording at a sampling rate of 24 kHz. Recorded audio files were automatically split into 30-min segments for ease of analysis. The SoundTraps were calibrated by the manufacturer and the sensitivity of the hydrophone systems was approximately −172.8 dB re 1 μPa/volt at 1 m at 250 Hz. The PAM was deployed at the site for periods of 8–10 weeks at which point it was recovered and immediately replaced with another mooring configured to the same specifications. In this way, near-continuous recording was achieved over periods of consecutive months. However, bad weather followed by the loss of equipment in the fall of 2019 resulted in a data gap between November 1, 2019 and February 20, 2020. A second data gap from April 28 to July 22, 2020 was caused by restrictions put in place during the COVID-19 pandemic which resulted in the temporary suspension of fieldwork.

Automatic Identification System Data

The automatic identification system (AIS) is an automated system for vessel tracking and identification to aid in navigation, collision avoidance, enforcement, and search and rescue. It is required on all vessels of 300 gross tonnage or more on an international voyage and vessels of 500 gross tonnage or more on

a domestic voyage (International Maritime Organization, 2015). In addition, most Canadian passenger vessels are required to carry an AIS transponder and many other vessels carry them for safety purposes (Navigation Safety Regulations, 2020). Ship-borne transponders automatically transmit information to terrestrial and satellite receivers. While vessels are underway, AIS messages are transmitted every 2 s (Class A devices) or 30 s (Class B devices). Messages are transmitted less frequently if the vessel is at anchor or stationary. AIS messages contain the vessel's position, speed over ground, heading, vessel type, and other fields.

Automatic identification system data were obtained from the Canadian Coast Guard's terrestrial AIS receiver network for an area within a 12-km radius of the PAM location (**Figure 1**). This area covers all the potential marine approaches to the Port of Halifax while excluding most docking areas within the port. Two time periods were selected for analysis in both 2019 and 2020: February 1 to April 28 and July 1 to 28. These periods were chosen because AIS data were readily available with no missing days in both years. The month of April also corresponded with the period for which there were acoustic data. The July period did not match the time for which acoustic data were available but did allow us to examine vessel patterns during a different season of the year.

The raw AIS messages were decoded using a Python script package developed at Fisheries and Oceans Canada.[1] Data fields of interest that were retained from the decoded messages for further analysis were the date and time (UTC), the vessel's latitude and longitude (decimal degrees), speed over ground (SOG, knots), and the unique Maritime Mobile Service Identity (MMSI) number. All analyses were completed using R version 3.6.3 (R Core Team, 2020). The packages "raster" (Hijmans, 2020), "ncdf4" (Pierce, 2019), and "rgdal" (Bivand et al., 2021) were used to load and extract data from the decoded AIS data files. The packages "padr" (Thoen, 2019), "Rmisc" (Hope, 2013), and "lubridate" (Grolemund and Wickham, 2011) were used in analyses and packages "ggplot2" (Wickham, 2016) and "egg" (Auguie, 2019) were used to create the figures.

There are often errors within AIS messages resulting from faulty equipment or human-related error when information has been entered manually (Harati-Mokhtari et al., 2007). To ensure the data used were as accurate as possible, we followed a similar quality control process to that of Metcalfe et al. (2018), which was a combination of methods described by the Marine Management Organisation (MMO), 2013), Coomber et al. (2016), and HELCOM (2008). First, the data were filtered to include only positional reports within a 12-km radius of the PAM location. Second, data points with invalid MMSI numbers (greater or less than nine digits) and MMSI numbers belonging to navigation aids, buoys, aircraft, and other non-vessels (<200,000,000 or >800,000,000) were removed (Coomber et al., 2016; Metcalfe et al., 2018). Finally, to exclude moored vessels from our analyses, data points for which the reported SOG was less than 1 knot were removed and a maximum speed cut off of 43 knots was imposed, as data points with speeds greater than this limit were rare and implausible for the corresponding vessel type. To characterize types of vessels using the area, valid MMSI numbers were entered into the IHS Sea-Web database to determine the vessel type (IHS Markit, 2021). If no information was found in that database, other web databases were searched, primarily MarineTraffic (2021). Vessels were then grouped into the following categories: cargo, fishing, passenger, pleasure craft, search and rescue, tanker, tug, and "other" (all remaining vessel types).

The temporal frequency at which AIS signals were emitted by vessels and subsequently received by terrestrial stations meant that there were no large spatial or temporal gaps in the dataset, which allowed us to analyze vessel presence without creating track lines. The data were summarized in two ways: (1) as the average number of unique vessels present per day in a given week and (2) as the average number of vessel occurrences per day in a given week. A vessel occurrence was defined as one or more AIS reports from a vessel occurring within a 1-h period within a 12-km radius of the mooring. If reports were received from multiple vessels during the same time period, they were calculated as multiple occurrences, e.g., AIS messages from three different vessels within the same 1-h period were considered three occurrences. As previously stated, data points with reported SOG values of less than 1 knot were excluded, and thus these measures refer only to the occurrence of vessels traveling faster than 1 knot. The occurrence of vessels not equipped with AIS transponders was unknown.

Vessel density for April 2019 and April 2020 was calculated based on the "EU Vessel density map detailed method" (European Marine Observation and Data Network, 2019). This method calculates the total time that vessels spend in pre-defined grid cells.

Cargo Statistics for the Port of Halifax

Quarterly cargo statistics for 2019 and 2020 were obtained from the Port of Halifax (2021). The port tracks container and non-containerized imports and exports at the facilities it manages as well as other facilities within the general area of Halifax Harbor.

Acoustic Data

After comparing the data collected from 2019 to 2020, it was determined that acoustic data had been successfully collected between the periods of March 28 to April 28 and August 6 to October 22 for both years. The 2020 time periods coincided with restrictions put in place as a result of the COVID-19 pandemic. The time series sound pressure wave data were processed with Short-time Fourier transform (STFT) into spectrogram data as a function of time and frequency with an FFT length of 32,768, overlap of 8,192, and Hann window applied. The spectrogram data had a time resolution of 1.024 s and a frequency resolution of 0.7324 Hz. The entire frequency band was divided into 1/3 octave bands for further analysis. Ship noise peaks at low frequencies (Wenz, 1962; Erbe et al., 2019), considered to be between 10 and 500 Hz for the purposes of this study, as per Hildebrand (2009). Consequently, the analysis focused on the normalized 1/3 octave band centered at 100 Hz (89.1–112 Hz). To quantify changes in sound pressure levels (SPLs) during the time periods of interest, the SPL of the 1/3 octave band centered at 100 Hz was averaged

[1]The Python script package was developed by Lanli Guo, Jinshan Xu, and Shihan Li and a report explaining the package, including the message types it decodes, performance and potential issues, is in preparation.

within this frequency band then the minimum, median, and maximum values were calculated for three different time scales: hourly, six-hourly, and daily.

An approach of temporal detection and classification based on the methodology described in Nystuen and Howe (2005) was adopted here as an auto detector of shipping traffic. To build the vessel noise detector, a circle with a 30-km radius around the PAM was defined (**Figure 1**). AIS data were used to identify and track individual vessels moving through the defined circle. The instantaneous SPL from two different times in the vessel's transit through the circle were selected from the data set (**Figure 3**): the start of the transit through the circle (i.e., "start time") and the point at which the vessel was closest to the PAM location ("closest point of approach"). The scatter plot of 1/3 octave bands centered at 100 Hz (89.1–112 Hz) and 500 Hz (447–562 Hz) are presented for both the "start time" and "closest point of approach." The vessel noise detector is built based on the different scatter distribution when there is vessel noise presenting.

The noise energy budget is estimated based on the following equation (Miller et al., 2008) for different frequency (f) and time (t):

$$I(f,t) = p(f,t)\,u(f,t) = \frac{p^2(f,t)}{\rho c}$$

with $\rho = 1.0273$ g/cm^3 as sea water density and $c = 1{,}500$ m/s as sound speed. The vessel noise detector was used to automatically find the portions of the acoustic recordings that were influenced by vessel noise, which we termed "shipping events." For all these events, the noise contributed by the vessel traffic was calculated by taking the average SPL of the periods before and after the shipping event and subtracting that from the SPL during the shipping event (**Figure 4**).

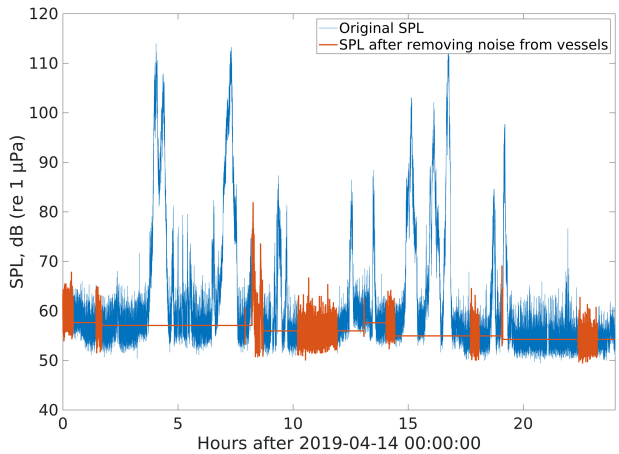

FIGURE 4 | An example from April 14, 2019 showing the estimation of the noise contribution from shipping traffic (in SPL) based on a single vessel detection algorithm. The lines are averaged SPL for the 1/3 octave band centered at 100 Hz.

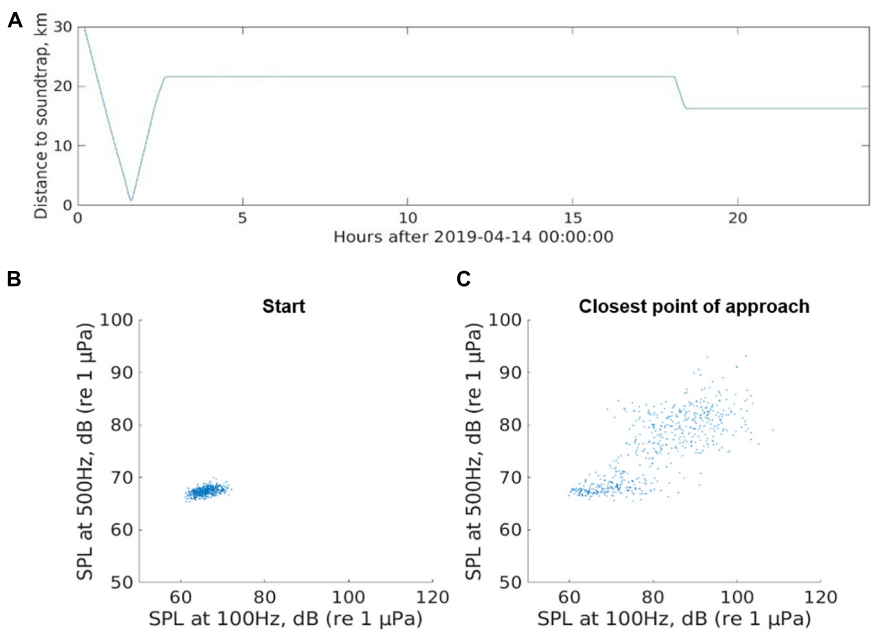

FIGURE 3 | An example of a ship event on April 14, 2019, showing the SPL changing with distance from the mooring location. The top panel **(A)** shows the vessel's distance from the mooring location over time within the selected date; the bottom panel shows the scatter plots between the 1/3 octave bands centered at 100 Hz and 500 Hz at the start **(B)** and closest point of approach **(C)** of the ship event (represented by the blue line in the top panel). The time periods used in the scatter plots were from 10 min before the start time until the start time, and 5 min before the closest point of approach to 5 min after the closest point of approach, respectively. The large dispersion of the scatter plot was a common pattern when vessels were near the mooring.

RESULTS

Vessel Traffic and Characteristics

Maps of vessel density (**Figure 5**) for April 2019 and 2020 show similar patterns for both years, with the inbound and outbound shipping lanes clearly visible. The other area of high vessel traffic in both years is activity to and from a fishing harbor. In 2020, there was irregular vessel activity in the area northeast of the mooring location. This was due to the presence of the *Thialf*, the second-largest crane vessel in the world (Palmeter, 2020). The crane vessel was using thrusters (dynamic positioning) to stay at the harbor mouth for much of April (pers. comm., M. MacIsaac, Exxon Mobil, Halifax, Nova Scotia, Canada, December 8, 2020).

Between February 1 and April 28, 2019, a total of 270 unique vessels occurred within a 12-km radius of the PAM site, while 218 unique vessels occurred during the same period in 2020. From July 1 to 28, 2019, 379 unique vessels were present, while 246 were present during the same period in 2020 (**Table 1**). When the February 1 to April 28 period was further broken down into the periods before and after the Province of Nova Scotia declared a state of emergency (March 22, 2020), the most noticeable difference was the decrease in the number of tanker vessels before March 22 in 2020 compared to the same period in 2019 (**Table 1**). In July, there were 128 fewer pleasure craft in 2020 than during the same period in 2019. Despite there being fewer unique vessels from February 1 to April 28, 2019 compared to the same period in 2020, the total number of vessel occurrences

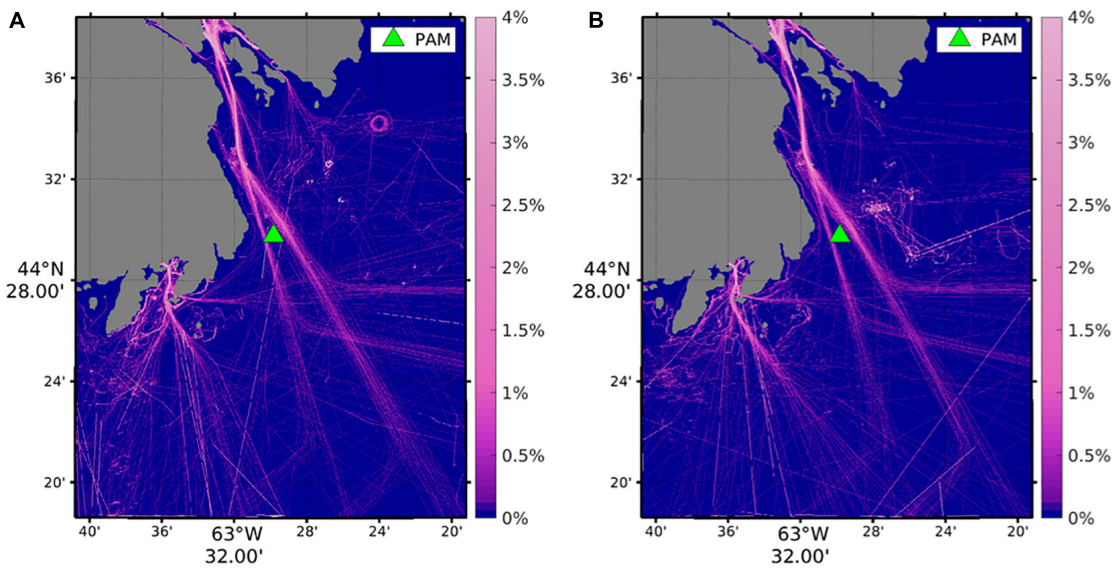

FIGURE 5 | Percentage of time vessels spend per grid cell, converted to vessel density per square kilometer, April 2019 **(A)** and April 2020 **(B)**. The green symbol is the location of the PAM. The movements of the *Thialf*, which stayed near the approaches to Halifax for the month of April 2020, and its support vessels are clearly visible to the northeast of the PAM location.

TABLE 1 | The number of unique vessels (UV) and vessel occurrences (VO) in each vessel type category within a 12-km radius of the PAM location from February 1 to March 21, March 22 to April 28, and July 1 to July 28, 2019 and 2020.

	February 1 to March 21		March 22 to April 28		July 1 to July 28	
Vessel Type	**2019 UV (VO)**	**2020 UV (VO)**	**2019 UV (VO)**	**2020 UV (VO)**	**2019 UV (VO)**	**2020 UV (VO)**
Cargo	88 (548)	79 (546)	72 (445)	67 (405)	58 (321)	55 (290)
Fishing	32 (789)	37 (960)	36 (870)	42 (884)	49 (834)	47 (762)
Tanker	26 (126)	7 (53)	16 (64)	9 (51)	7 (44)	11 (45)
Tug	10 (116)	11 (119)	15 (115)	11 (387)	11 (87)	18 (241)
Search and Rescue	2 (35)	3 (39)	7 (43)	3 (31)	3 (44)	4 (61)
Pleasure Craft	1 (7)	0 (0)	4 (12)	0 (0)	211 (1,191)	83 (443)
Passenger	1 (2)	2 (8)	2 (9)	0 (0)	13 (266)	2 (30)
Other	24 (563)	24 (603)	28 (539)	21 (547)	27 (550)	26 (528)
Total	184 (2,186)	163 (2,328)	180 (2,097)	153 (2,305)	379 (3,337)	246 (2,400)

"Other" includes vessels that did not fit within the other categories, such as navy ships, dive vessels, offshore construction vessels, cable laying ships, buoy tenders, and research vessels.

within the study area was greater in 2020 (4,633) compared to 2019 (4,283). The opposite was true for the July period, during which there were many more vessel occurrences in 2019 (3,337) compared to 2020 (2,400).

During the entire February 1 to April 28 period in both 2019 and 2020, fishing, cargo, and "other" vessels had the most occurrences in the study area. Fishing vessels were the most frequently occurring vessel type and occurred more frequently in 2020 than 2019. Cargo vessels occurred less frequently in 2020 than 2019, with a less than 1% decline in occurrence in the February 1 to March 21 period, and an 8.99% decrease in the March 22 to April 28 period. A peak in the average number of all vessel occurrences per day is noticeable during the week of April 5–11, with a more pronounced increase in 2020 than in 2019 (**Figure 6**). Part of that can be attributed to an increase in tug occurrence in 2020. Average daily occurrence of tugs increased in the week of April 5–11 and remained at a higher level throughout April. Tug occurrences in the March 22 to April 28, 2020 period were 236.22% higher in that period compared to the same period in 2019.

During the July period, there were fewer unique vessels present in 2020 compared to 2019 (**Table 1**) and lower average daily vessel occurrences (**Figure 7**). There were decreases in both the number of pleasure craft present and their number of occurrences during 2020 compared to 2019. A total of 211 unique pleasure craft occurred during a combined 1,191 h in 2019, while only 83 unique pleasure craft occurred during a combined 443 h in 2020, a 62.8% decrease. Passenger vessel occurrence also declined from 266 occurrences in 2019 to 30 occurrences in 2020, an 88.72% decrease. Cargo vessel presence had a much smaller decrease of 9.66%. Like in the spring period, tug occurrence increased in 2020 over 2019, in this case by 177.01%. This increase was particularly noticeable in the week of July 15–21 (**Figure 7**).

Changes in Cargo Imports and Exports

The cargo statistics for the Port of Halifax (**Table 2**) show that for the first two quarters of the year, the port had lower imports in 2020 than in 2019, but higher exports. However, imports rose in the third quarter of 2020, with imports higher in the third and fourth quarters of 2020 than the previous year. Exports were lower in the third quarter of 2020 than 2019 but increased in the fourth quarter to 40% over 2019 figures. As a result, the decrease in total cargo was less than 2% by weight over the previous year. However, for the quarters for which we obtained acoustic data (parts of Q2 and Q3), the change in cargo was greater: there was a 10.55% overall decrease in cargo in Q2 and a 5.08% decrease in cargo in Q3.

Levels of Underwater Noise

Spectrograms for the periods with acoustic data in both 2019 and 2020 are shown in **Figure 8**. Notably, the spectrogram of April 2020 shows higher SPLs between 30 Hz up to 5 kHz for an extensive period in that month. As seen in the AIS data, this SPL anomaly was likely attributable to the presence of a single vessel, *Thialf*, the second-largest crane vessel in the world which was using a dynamic positioning system to hold

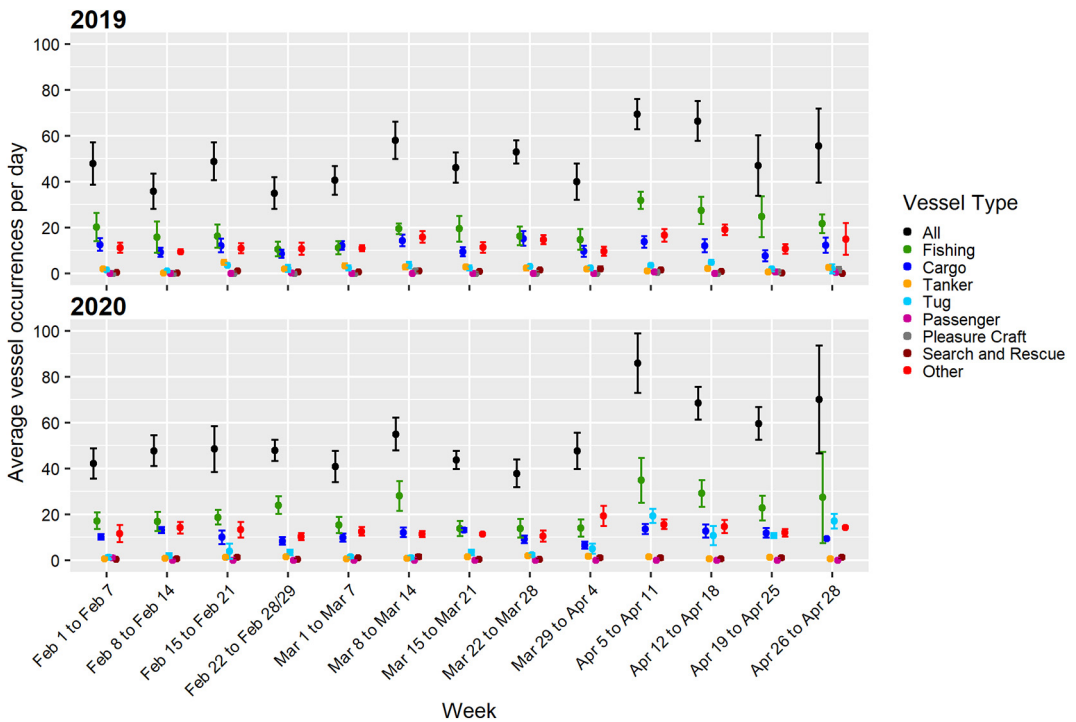

FIGURE 6 | Mean (±SE) daily vessel occurrence within a 12-km radius of the PAM location from February 1 to April 28, 2019 **(top)** and 2020 **(bottom)**. Averages were calculated over 7 days for all weeks except the week of April 26 for both years (3 days) and the week of February 22, 2020 (8 days).

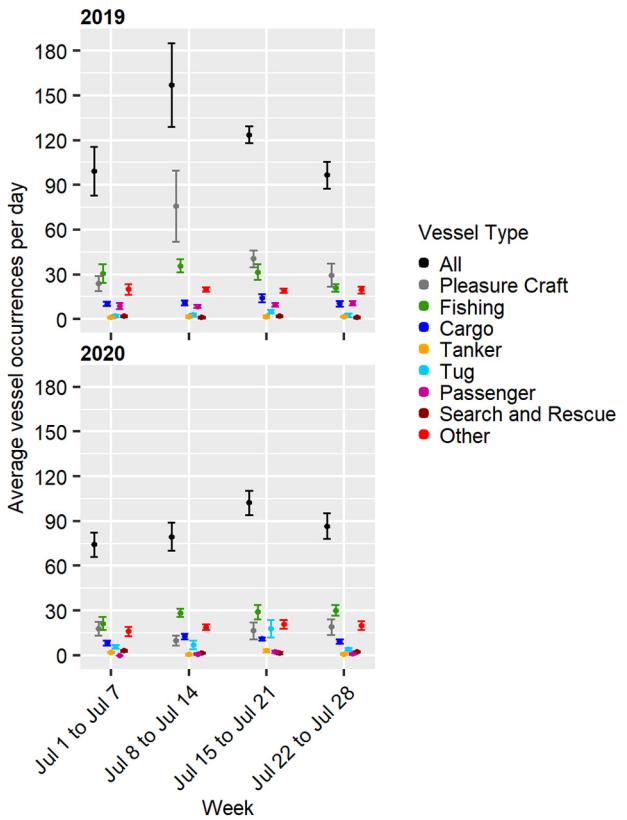

FIGURE 7 | Mean (±SE) daily vessel occurrence within a 12-km radius of the PAM location from July 1 to July 28, 2019 **(top)** and 2020 **(bottom)**. Averages were calculated over 7 days for all weeks.

TABLE 2 | Port-wide cargo, including Halifax Port Authority and non-Halifax Port Authority facilities (metric tons) (Port of Halifax, 2021).

	2019	2020	Change (%)
Imports			
Q1 (January–March)	1,113,641	881,348	−20.86
Q2 (April–June)	1,084,784	856,908	−21.01
Q3 (July–September)	946,242	1,053,374	11.32
Q4 (October–December)	1,000,168	1,009,131	0.9
Total	4,144,835	3,800,761	−8.30
Exports			
Q1 (January–March)	376,203	542,635	44.24
Q2 (April–June)	522,551	580,894	11.16
Q3 (July–September)	629,667	442,428	−29.74
Q4 (October–December)	466,236	655,697	40.61
Total	1,994,657	2,221,654	11.38
Total imports and exports (all quarters)	6,139,492	6,022,415	−1.91

station near the PAM location. In 2020, the daily minimum and daily median SPLs at 100 Hz in 2020 were more than 10 dB higher than in 2019 throughout much of the month of April, although daily maximum SPLs showed more similarity (**Figure 9** and **Table 3**). There were less obvious visual differences in the spectrograms in the August to October periods, although the 2019 period had more occurrences of intense low-frequency sound. An intense low-frequency event is visible on September 23, 2020, likely the post-tropical storm Teddy that made landfall in Nova Scotia on that date.

Plots of the minimum, maximum, and median SPL for the 1/3 octave band centered at 100 Hz from the continuous acoustic recording periods (i.e., March 28 to April 28, and August 6 to October 22) for both 2019 and 2020 are shown in **Figure 9**. The August to October periods were more similar between years than the April plots. Similar estimations for hourly and six-hourly time periods were carried out for these data sets and the differences between 2020 and 2019 in average SPL and errors with 95% confidence interval were calculated (**Table 3**). The paired *t*-test approach was used for calculating the 95% confidence interval for the difference in each statistic (minimum, maximum, and median) between 2019 and 2020. The *p*-value from the same hypothesis test is also shown in the table. At a significance level of 0.05, all *p*-values are significant except for the difference in maximum sound level between the August to October 2019 period and the August to October 2020 period. This suggests that among all these estimations, the minimum and median SPL showed noise reductions for all the hourly, six-hourly, and daily periods. The noise reductions for minimum and median SPL were statistically significant, with reductions of 2.244, 2.125, and 1.745 dB in the hourly, six-hourly, and daily minimum SPL, respectively.

Using the vessel noise energy estimation method described above, the daily noise energy introduced by shipping traffic averaged by the number of days in each week was calculated. Average daily vessel noise energy was higher in 2020 than 2019 for the first two weeks of the March to April period and lower in 2020 than 2019 for almost the entire period of August to October (**Figure 10**).

DISCUSSION

Restrictions aimed at reducing the spread of COVID-19 were initiated in January 2020 in China and spread to other locations around the world through the first few months of 2020. In Nova Scotia, restrictions on activities, including non-essential travel, went into effect on March 22, 2020 (Province of Nova Scotia, 2020). Over the course of 2020, news stories heralded the quieting of the oceans (see e.g., Sommer, 2020) and some studies have observed declines in vessel traffic and ocean noise (e.g., March et al., 2020; Thomson and Barclay, 2020). Our results parallel some of the findings related to vessel traffic but present a more complex picture in terms of commercial shipping and levels of underwater noise. Further comparisons with a greater number of pre-pandemic data years and data from multiple recording systems would have yielded a more complete understanding of the overall changes in vessel noise activity before and after the onset of the pandemic, but these data were not available.

March et al. (2020) found that there had been a reduction of marine traffic in 44.3% of the global ocean in April 2020, with major reductions in traffic density observed in European waters. However, they found that these changes varied between sectors,

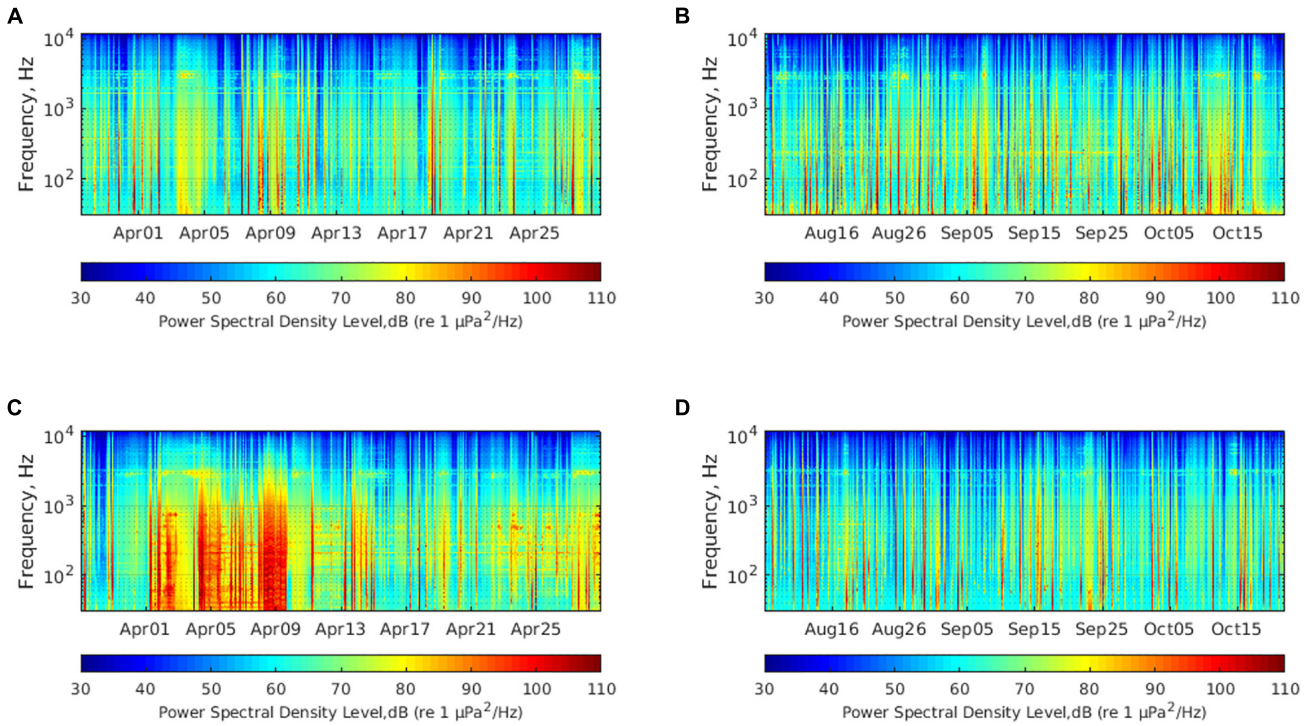

FIGURE 8 | Spectrograms from acoustic monitoring periods: March 28–April 28, 2019 **(A)**, August 6–October 22, 2019 **(B)**, March 28–April 28, 2020 **(C)**, and August 6–October 22, 2020 **(D)**.

with passenger vessel traffic sharply declining, particularly in tourist areas, while patterns of fishing vessel traffic varied, with increases in some areas (March et al., 2020). Our results are consistent with the findings of March et al. (2020) as we observed the highest decline in vessel occurrences in the pleasure craft and passenger vessel categories as compared to 2019. Additionally, the number of fishing vessels present near our mooring was similar or higher in 2020 than in similar periods in 2019. In Canada, commercial fishing was considered an essential function during the pandemic and was not subject to the same restrictions that would have limited tourism operations using passenger vessels. The pleasure craft that did occur were likely local vessels as border restrictions limited visitors from the United States and quarantine requirements deterred visitors from other provinces.

Tug hours increased substantially in 2020 in the periods we examined compared to 2019 and this change was partially attributable to the tugs tending to the *Thialf* throughout April 2020. Based on the available AIS data, the *Thialf* first arrived within the 12-km radius of the PAM on April 1, 2020, an appearance that coincides with the increase in tug occurrences in April 2020. However, the reason behind the more than doubling of tug occurrences in July 2020 (241) as compared to July 2019 (87) is not obvious from the datasets we examined.

The small decrease in cargo vessel occurrences in 2020 during the periods we examined might not have been representative of the full year. A previous study described Canada-wide reductions in imports and exports in the first two months of 2020 as compared to 2019 (2020 Statistics Canada data reported in Thomson and Barclay, 2020). While imports decreased in the Port of Halifax for the first quarter of 2020, exports greatly increased. Overall, cargo imports and exports varied greatly from 2019 figures and not always in the same direction. While overall quantity of cargo for the Port of Halifax decreased for the quarters we examined vessel presence, the limited amount of AIS data we looked at in detail made it difficult to draw strong conclusions. For example, the February 1 to March 21, 2020 period saw a decrease of 0.36% in cargo vessel occurrences from the previous year, yet the overall amount of cargo declined 4.42% in the first quarter of 2020. Including the AIS data for January may have shown a greater decrease in vessel occurrence; conversely, ships may have been on a fixed schedule and unable to adapt quickly to changes in demand.

Significant decreases in the minimum and median SPLs in the 1/3 octave band centered at 100 Hz were observed in the August to October 2020 period. Although our AIS data did not match that time period, it seems likely that these changes were due to decreased vessel traffic, as we found that the average daily noise energy introduced by shipping also decreased in that period. The decreases in SPL may have been associated with multiple vessel types. Pleasure craft (e.g., jet skis, yachts) represent a considerable noise source in some coastal areas (Samuel et al., 2005; Haviland-Howell et al., 2007). Hermannsen et al. (2019) found that non-AIS recreational vessels such as speedboats and sailing vessels elevated ambient noise in the 1/3 octave bands centered at 125 Hz, 2 kHz, and 16 kHz by up to 55, 47, and 51 dB, respectively, dominating the soundscape in a

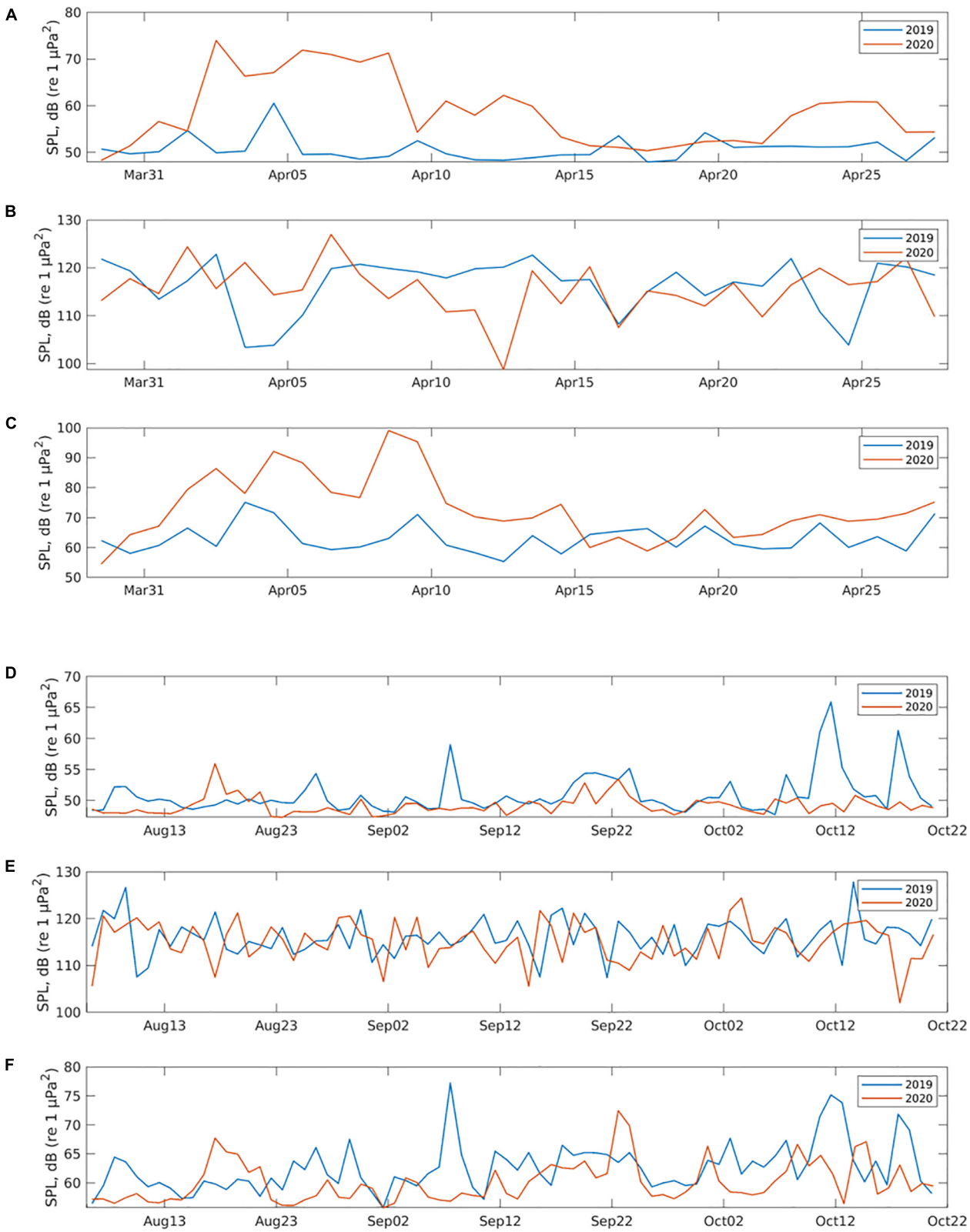

FIGURE 9 | Top panels show the daily moving average of minimum **(A)**, maximum **(B)**, and median **(C)** SPL for the 1/3 octave band centered at 100 Hz for March 28 to April 28 of 2019 and 2020. Bottom panels show the daily moving average of minimum **(D)**, maximum **(E)**, and median **(F)** SPL for the 1/3 octave band centered at 100 Hz for August to October of 2019 and 2020.

TABLE 3 | The 95% confidence interval (and *p*-value, "-" indicates the value is less than 0.0001) for the mean difference between 2020 and 2019 in minimum, maximum, and median sound pressure level for hourly, 6-h, and daily paired samples.

	March 28 to April 28			August to October		
	Minimum (dB)	**Maximum (dB)**	**Median (dB)**	**Minimum (dB)**	**Maximum (dB)**	**Median (dB)**
Hourly	10.6 ± 0.8 (–)	2.2 ± 1.6 (0.0001)	9.3 ± 0.9 (–)	−2.2 ± 0.3 (–)	−5.9 ± 0.9 (–)	−2.5 ± 0.4 (–)
6-h	10.0 ± 1.8 (–)	0.3 ± 2.7 (0.8)	9.5 ± 1.8 (–)	−2.1 ± 0.6 (–)	−4.0 ± 1.5 (–)	−2.1 ± 0.7 (–)
Daily	8.4 ± 2.8 (–)	−1.6 ± 2.6 (0.6)	9.9 ± 3.6 (–)	−1.8 ± 0.7 (–)	−0.8 ± 1.3 (0.1)	−2.4 ± 1.2 (–)

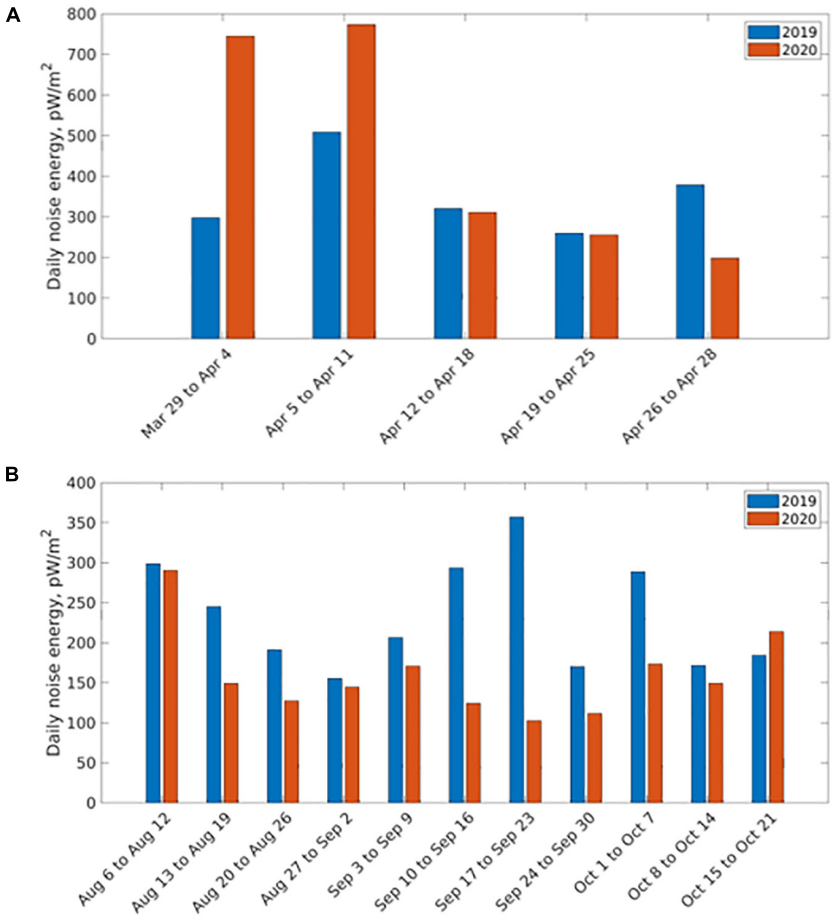

FIGURE 10 | The estimated noise energy by week for the 1/3 octave band centered at 100 Hz that can be attributed to vessels for **(A)** March 28 to April 28, 2019 and 2020 and **(B)** August 6 to October 22, 2019 and 2020.

coastal area and likely contributing to the disturbance of a local population of harbor porpoise. We observed a large decrease in pleasure craft occurrence in July 2020, which likely continued into the autumn as Nova Scotia extended its restrictions on social activities and visitors into that period. It is also likely that we underestimated the decrease in pleasure craft use since vessels not equipped with AIS transponders were not accounted for in the vessel occurrences reported above. Considering the potential for these types of water craft to elevate ambient noise levels, the reduction in pleasure craft likely contributed to the significant decrease in minimum and median SPL in the 1/3 octave band centered at 100 Hz that we observed in the August to October 2020 period.

Interestingly, this study revealed an unanticipated increase in underwater noise due to COVID-19 restrictions. The large crane ship *Thialf* did not dock directly at port facilities in Halifax due to concerns related to COVID-19 (Palmeter, 2020) and instead stayed near the approaches to the harbor for most of the month

of April 2020. The *Thialf* was visited by support vessels and used dynamic thrusters to maintain position. Thrusters may cause significant propeller cavitation and associated high levels of underwater noise (Erbe et al., 2013). Coupled with the noise generated by support vessel visits (e.g., tugs), the presence of the *Thialf* is believed to be the source of elevated underwater noise levels in the study area during the month of April 2020. The presence of high levels of localized noise over an extended period may present concerns for marine animals that frequent the outer margins of the harbor. Fin whales (*Balaenoptera physalus*) are known to occur in the study area (Hastings et al., 2014) and use low-frequency pulses to communicate (Nieukirk et al., 2004). Vessel noise overlaps in frequency with fin whale pulses which risks masking fin whale communication signals, an acoustic impact that has been observed in other baleen whale species (e.g., Hatch et al., 2012; Dunlop, 2016). Underwater noise associated with the presence of the crane ship, which would normally dock in the inner harbor where cetaceans are far less likely to occur, could have led to an unusual increase in levels of vessel noise that fin whales and other whale species typically encounter in the outer margins of Halifax Harbor during that time of year.

Thomson and Barclay (2020) observed reductions in underwater noise levels in weekly median SPL near the Port of Vancouver, which they suggested were related to reduced economic activity, including shipping traffic. While we observed statistically significant decreases in underwater noise during one acoustic monitoring period, overall our results demonstrate the dynamic and unpredictable nature of human activity in light of global disruptions brought on by the COVID-19 pandemic. Despite expectations of a decrease in vessel activity and, by extension, underwater vessel noise as a result of pandemic-related shutdowns, a temporary but significant increase in underwater noise was observed for part of the study period. While this observed increase was a consequence of COVID-19 restrictions, it nevertheless highlights the inadvertent impacts that may result from changes in human activity.

DATA AVAILABILITY STATEMENT

Data collected by Fisheries and Oceans Canada is made available to the public within two years, subject to some exceptions. The department's policy for scientific data can be found at the following url: https://www.dfo-mpo.gc.ca/about-notre-sujet/publications/science/datapolicy-politiquedonnees/index-eng.html. Requests to access the datasets should be directed to HB, Heather.Breeze@dfo-mpo.gc.ca.

AUTHOR CONTRIBUTIONS

HB, EM, and JT conceptualized the project. HB, EM, JT, and JW carried out the equipment preparation and fieldwork. HB, SL, JW, and JX carried out the data analysis. All authors contributed to the writing, review, and editing process.

FUNDING

This study was funded by Fisheries and Oceans Canada, a Canadian government department.

ACKNOWLEDGMENTS

We would like to thank Kasia Rozalska, Fisheries and Oceans Canada, for preparing **Figure 1**, and the captains and crew of the *CCGS Sigma-T*, *Lady Trish,* and *Pic! Pocket* for assistance in deploying and retrieving the passive acoustic monitors.

REFERENCES

Andrew, R. K., Howe, B. M., Mercer, J. A., and Dzieciuch, M. A. (2002). Ocean ambient sound: comparing the 1960s with the 1990s for a receiver off the California coast. *Acoust. Res. Lett.* 3, 65–70. doi: 10.1121/1.1461915

Auguie, B. (2019). *egg: Extensions for 'ggplot2': Custom Geom, Custom Themes, Plot Alignment, Labelled Panels, Symmetric Scales, and Fixed Panel Size. R package version 0.4.5*. Available online at: https://CRAN.R-project.org/package=egg (accessed February 10, 2021).

Bivand, R., Keitt, T., and Rowlingson, B. (2021). *rgdal: Bindings for the 'Geospatial' Data Abstraction Library. R package version 1.5-21*. Available online at: https://CRAN.R-project.org/package=rgdal (accessed February 10, 2021).

Coomber, F. G., D'Incà, M., Rosso, M., Tepsich, P., di Sciara, G. N., and Moulins, A. (2016). Description of the vessel traffic within the north Pelagos Sanctuary: inputs for Marine Spatial Planning and management implications within an existing international Marine Protected Area. *Mar. Policy* 69, 102–113. doi: 10.1016/j.marpol.2016.04.013

Duarte, C. M., Chapuis, L., Collin, S. P., Costa, D. P., Devassy, R. P., Eguiluz, V. M., et al. (2021). The soundscape of the Anthropocene ocean. *Science* 371:6529. doi: 10.1126/science.aba4658

Dunlop, R. A. (2016). The effect of vessel noise on humpback whale, *Megaptera novaeangliae*, communication behaviour. *Anim. Behav.* 111, 13–21. doi: 10.1016/j.anbehav.2015.10.002

Erbe, C., Marley, S. A., Schoeman, R. P., Smith, J. N., Trigg, L. E., and Embling, C. B. (2019). The effects of ship noise on marine mammals–A review. *Front. Mar. Sci.* 6:606. doi: 10.3389/fmars.2019.00606

Erbe, C., McCauley, R., McPherson, C., and Gavrilov, A. (2013). Underwater noise from offshore oil production vessels. *J. Acoust. Soc. Am.* 133, EL465–EL470. doi: 10.1121/1.4802183

European Marine Observation and Data Network (2019). *EU Vessel Density Map. Detailed Methods. V. 1.5*. Available online at: https://www.emodnet-humanactivities.eu/documents/Vessel%20density%20maps_method_v1.5.pdf (accessed February 21, 2021)

Fisheries and Oceans Canada (2021). *Mitigating the Impacts of Ocean Noise*. Available online at: https://www.dfo-mpo.gc.ca/oceans/noise-bruit/index-eng.html (accessed February 15, 2021)

Frisk, G. (2012). Noiseonomics: the relationship between ambient noise levels in the sea and global economic trends. *Sci. Rep.* 2:437. doi: 10.1038/srep00437

Grolemund, G., and Wickham, H. (2011). Dates and times made easy with lubridate. *J. Stat. Softw.* 40, 1–25. doi: 10.18637/jss.v040.io3

Harati-Mokhtari, A., Wall, A., Brooks, P., and Wang, J. (2007). Automatic Identification System (AIS): data reliability and human error implications. *J. Navig.* 60, 373–389. doi: 10.1017/s0373463307004298

Hastings, K., King, M., and Allard, K. (2014). "Ecologically and biologically significant areas in the Atlantic coastal region of Nova Scotia," in *Canadian*

Technical Report of Fisheries and Aquatic Sciences. 3107. Dartmouth, NS: Fisheries and Oceans Canada.

Hatch, L. T., Clark, C. W., Van Parijs, S. M., Frankel, A. S., and Ponirakis, D. W. (2012). Quantifying loss of acoustic communication space for right whales in and around a U.S. National Marine Sanctuary. *Conserv. Biol.* 26, 983–994. doi: 10.1111/j.1523-1739.2012.01908.x

Haviland-Howell, G., Frankel, A. S., Powell, C. M., Bocconcelli, A., Herman, R. L., and Sayigh, L. S. (2007). Recreational boating traffic: a chronic source of anthropogenic noise in the Wilmington, North Carolina Intracoastal Waterway. *J. Acoust. Soc. Am.* 122, 151–160. doi: 10.1121/1.2717766

HELCOM (2008). *Inaccuracies in AIS data – Effects on usability. Helsinki Commission (HELCOM) Expert Working Group for Mutual Exchange and Deliveries of AIS data. Document code: 9/1*. Helsinki: HELCOM, 4.

Hermannsen, L., Mikkelsen, L., Tougaard, J., Beedholm, K., Johnson, M., and Madsen, P. T. (2019). Recreational vessels without Automatic Identification System (AIS) dominate anthropogenic noise contributions to a shallow water soundscape. *Sci. Rep.* 9:15477. doi: 10.1038/s41598-019-51222-9

Hijmans, R. J. (2020). *raster: Geographic Data Analysis and Modeling. R package version 3.4-5*. Available online at: https://CRAN.R-project.org/package=raster (accessed February 10, 2021).

Hildebrand, J. A. (2009). Anthropogenic and natural sources of ambient noise in the ocean. *Mar. Ecol. Prog. Ser.* 395, 5–20. doi: 10.3354/meps08353

Hope, R. M. (2013). *Rmisc: Ryan Miscellaneous. R package version 1.5*. Available online at: https://CRAN.R-project.org/package=Rmisc (accessed February 10, 2021).

IHS Markit (2021). *Data from: Sea-Web*. London: IHS Markit.

International Maritime Organization (2015). *Revised Guidelines for the Onboard Operational Use of Shipborne Automatic Identification Systems (AIS). Resolution A.1106(29)*. Available online at: https://wwwcdn.imo.org/localresources/en/KnowledgeCentre/IndexofIMOResolutions/AssemblyDocuments/A.1106(29).pdf (accessed February 12, 2021).

International Monetary Fund (2021). *World Economic Outlook Update January 2021*. Available online at: https://www.imf.org/en/Publications/WEO/Issues/2021/01/26/2021-world-economic-outlook-update (accessed February 21, 2021)

March, D., Metcalfe, K., Tintoré, J., and Godley, B. (2020). *Tracking the Global Reduction of Marine Traffic During the COVID-19 pandemic. Research Square [Preprint]*. Available online at: https://www.researchsquare.com/article/rs-47243/v1 (accessed February 21, 2021)

Marine Management Organisation (MMO) (2013). *Spatial Trends in Shipping Activity. A Report Produced for the Marine Management Organisation (MMO). MMO Project No: 1042*. Newcastle: Marine Management Organisation, 46.

MarineTraffic (2021). *Data from: MarineTraffic*. Available online at: https://www.marinetraffic.com/ (accessed February 10, 2021).

Metcalfe, K., Bréheret, N., Chauvet, E., Collins, T., Curran, B. K., Parnell, R. J., et al. (2018). Using satellite AIS to improve our understanding of shipping and fill gaps in ocean observation data to support marine spatial planning. *J. Appl. Ecol.* 55, 1834–1845. doi: 10.1111/1365-2664.13139

Miller, J. H., Nystuen, J. A., and Bradley, D. L. (2008). Ocean noise budgets. *Bioacoustics* 17, 133–136. doi: 10.1080/09524622.2008.9753791

National Research Council (2003). *Ocean Noise and Marine Mammals*. Washington, DC: National Academies Press.

Navigation Safety Regulations (2020). *SOR/2020-216. Government of Canada Consolidated Regulations*. Available online at: https://laws-lois.justice.gc.ca/eng/regulations/ (accessed February 10, 2021).

Nieukirk, S. L., Stafford, K. M., Mellinger, D. K., Dziak, R. P., and Fox, C. G. (2004). Low-frequency whale and seismic airgun sounds recorded in the mid-Atlantic Ocean. *J. Acoust. Soc. Am.* 115, 1832–1843. doi: 10.1121/1.1675816

Nystuen, J. A., and Howe, B. M. (2005). "Ambient sound budgets," in *Proceedings of the Underwater Acoustics Measurements Conference*, Heraklion.

Palmeter, P. (2020). *Sable Decommissioning Plan Could be Stalled by COVID-19. April 8, 2020*. Available online at: https://www.cbc.ca/news/canada/nova-scotia/sable-decommissioning-plan-could-be-stalled-by-covid-19-1.5525917 (accessed December 2, 2020)

Pierce, D. (2019). *ncdf4: Interface to Unidata netCDF (version 4 or earlier) Format Data Files. R package version 1.17*. Available online at: https://CRAN.R-project.org/package=ncdf4 (accessed February 10, 2021).

Port of Halifax (2021). *Cargo Statistics*. Available online at: https://www.portofhalifax.ca/port-operations-centre/cargo-statistics/ (accessed February 17, 2021).

Province of Nova Scotia (2020). *State of Emergency Declared in Response to COVID-19, Seven New Cases*. Available online at: https://novascotia.ca/news/release/?id=20200322001 (accessed December 9, 2020).

R Core Team (2020). *R: A Language and Environment for Statistical Computing*. Vienna: R Foundation for Statistical Computing.

Samuel, Y., Morreale, S. J., Clark, C. W., Greene, C. H., and Richmond, M. E. (2005). Underwater, low-frequency noise in a coastal sea turtle habitat. *J. Acoust. Soc. Am.* 117, 1465–1472. doi: 10.1121/1.1847993

SmartAtlantic Alliance (2020). *Data from: SmartAtlantic Herring Cove Station*. Available online at: https://www.smartatlantic.ca/station_alt.html?id=halifax (accessed December 10, 2020)

Sommer, L. (2020). *Whales Get a Break as Pandemic Creates Quieter Oceans. Jul. 20, 2020*. Available online at: https://www.npr.org/2020/07/20/891854646/whales-get-a-break-as-pandemic-creates-quieter-oceans (accessed December 10, 2020)

Theriault, J. A., Flogeras, D., and Underwood, J. (2018). "Catching more than lobsters in traps: can citizen science be used to protect the North Atlantic right whale?," in *Poster presented at: 8th Detection, Classification, Localization, and Density Estimation Workshop* (Paris: Marine Mammals and Acoustics).

Thoen, E. (2019). *padr: Quickly Get Datetime Data Ready for Analysis. R Package Version 0.5.0*. Available online at: https://CRAN.R-project.org/package=padr (accessed February 10, 2021).

Thomson, D. J. M., and Barclay, D. R. (2020). Real-time observations of the impact of COVID-19 on underwater noise. *J. Acoust. Soc. Am.* 147, 3390–3396. doi: 10.1121/10.0001271

Tyack, P. L. (2008). Implications for marine mammals of large-scale changes in the marine acoustic environment. *J. Mammal.* 89, 549–558. doi: 10.1644/07-mamm-s-307r.1

Vandermeulen, H. (2018). "A drop camera survey of Sambro Ledges, Nova Scotia," in *Canadian Technical Report of Fisheries and Aquatic Sciences 3251* (Dartmouth, NS: Fisheries and Oceans Canada).

Weilgart, L. S. (2007). The impacts of anthropogenic ocean noise on cetaceans and implications for management. *Can. J. Zool.* 85, 1091–1116. doi: 10.1139/z07-101

Wenz, G. M. (1962). Acoustic ambient noise in the ocean: spectra and sources. *J. Acoust. Soc. Am.* 34, 1936–1956. doi: 10.1121/1.1909155

Wickham, H. (2016). *ggplot2: Elegant Graphics for Data Analysis*. New York, NY: Springer-Verlag.

Conflict of Interest: SL is self-employed and carries out research and data analysis in that role. JT is the president of Ocean Environmental Consulting.

The remaining authors declare that the research was conducted in the absence of any commercial or financial relationships that could be construed as a potential conflict of interest.

Copyright © 2021 Breeze, Li, Marotte, Theriault, Wingfield and Xu. This is an open-access article distributed under the terms of the Creative Commons Attribution License (CC BY). The use, distribution or reproduction in other forums is permitted, provided the original author(s) and the copyright owner(s) are credited and that the original publication in this journal is cited, in accordance with accepted academic practice. No use, distribution or reproduction is permitted which does not comply with these terms.

frontiers in Marine Science

ORIGINAL RESEARCH
published: 01 July 2021
doi: 10.3389/fmars.2021.689860

Soundscapes in the German Baltic Sea Before and During the Covid-19 Pandemic

Fritjof Basan, Jens-Georg Fischer and Dennis Kühnel*

Bundesamt für Seeschifffahrt und Hydrographie, Hamburg, Germany

Anthropogenic underwater noise has been identified as one of the main pressures on the marine environment. Considerable research efforts have been made to quantify acoustic soundscapes on different spatial and temporal scales in order to identify trends and investigate how this may impact the marine environment. Measures to reduce noise input into the seas from anthropogenic sources are under discussion, including the reduction of vessel speed or re-routing of shipping lanes. The decline in maritime transport as a consequence of the Covid-19 pandemic provides an opportunity to examine the associated extent of noise reduction. Here, we present the results of a "Before-After-Control-Impact" study where we analyzed acoustic data sets from two monitoring stations in the German Baltic Sea. Data were collected between 2013 and 2020. As part of an international initiative, coordinated by the International Quiet Ocean Experiment, monthly statistics (20 average sound pressure levels per 1/3 octave bands) were calculated from acoustic data collected during the pre-pandemic period (2013–2019), and were compared with data from the year 2020, during the Covid-19 pandemic. To account for varying natural conditions the measurements were sorted into categories of same prevailing sea state. Through this approach, measurements with equivalent natural noise impact are compared and any resulting differences are likely due to the variability in the anthropogenic noise. A decline in sound pressure of 13% (1.2 dB) for low frequencies (10 Hz–1 kHz) was observed at both stations, which corresponds to the reduced level of shipping activity.

Keywords: Baltic Sea, BACI, underwater acoustics, soundscapes, Covid-19

OPEN ACCESS

Edited by:
Edward Urban,
Scientific Committee on Oceanic Research, United States

Reviewed by:
Tetyana Margolina,
Naval Postgraduate School, United States
Haru Matsumoto,
Oregon State University, United States

****Correspondence:***
Fritjof Basan
fritjof.basan@bsh.de

Specialty section:
This article was submitted to Marine Ecosystem Ecology, a section of the journal Frontiers in Marine Science

Received: *01 April 2021*
Accepted: *08 June 2021*
Published: *01 July 2021*

Citation:
Basan F, Fischer J-G and Kühnel D (2021) Soundscapes in the German Baltic Sea Before and During the Covid-19 Pandemic. Front. Mar. Sci. 8:689860. doi: 10.3389/fmars.2021.689860

Abbreviations: AIS, Automatic Identification System; ARK, Arkona station; BACI, Before-After-Control-Impact; BIAS, Baltic Sea Information on the Acoustic Soundscape; BSH, Federal Maritime and Hydrographic Agency of Germany; DWD, German Weather Service; EEZ, Exclusive Economic Zone; EWAM, European Wave Model; FEB, Fehmarnbelt station; Fraunhofer IDMT, Fraunhofer Institute for Digital Media Technology; GES, Good Environmental Status; GT, Gross Tonnage; ICES, International Council for the Exploration of the Sea; ICON, Icosahedral Non-hydrostatic Weather and Climate Model; IMO, International Maritime Organization; IQOE, International Quiet Ocean Experiment; MarinEARS, Marine Explorer And Registry of Sound; MMSI, Maritime Mobile Service Identity; MSFD, Marine Strategy Framework Directive; PIMO, Pilot Monitoring of Continuous Sound in German Waters; SM2M/SM3M, Song Meter 2 Marine/Song Meter 3 Marine; SPL, Sound Pressure Level; TOB, Third-Octave-Band; TOL, Third-Octave-Level; TSG Noise, Technical Sub-Group on Underwater Noise; UBA, German Environment Agency.

INTRODUCTION

Since its global onset in 2020, the Covid-19 pandemic has led to exceptional developments around the world. Efforts, taken to slow down the outbreak have led to shutdowns in public life and economic activity and a reduction in human mobility (Gibney, 2020). This change in anthropogenic activities provides a rare opportunity to study man-made stressors on the environment on a global scale. Maritime shipping, one of the stressors on the marine environment, was directly affected by the pandemic due to travel restrictions and the decline of commercial shipping. The sharpest decline in maritime mobility was observed from March to June 2020, when severe restrictions were in place globally (Millefiori et al., 2020). Vessel traffic decreased in nearly 44.3% of the global ocean and in 77.5% of national waters during April 2020 (March et al., 2020). Consequently, the pressures associated with shipping, such as greenhouse gas emissions and underwater noise, were widely expected to decrease (Leaper, 2019).

Anthropogenic underwater noise has long been identified as one of the main pressures on the marine environment, with shipping noise mainly contributing to the ambient soundscape at lower frequencies; up to 500 Hz (Hildebrand, 2009) or up to 1 kHz (Merchant et al., 2012). Sounds in this frequency range experience little transmission loss due to a low absorption rate and can thus propagate over long distances, potentially affecting marine life over a wide area (Urick, 1983).

We show that the maritime mobility has also decreased in the Baltic German coastal waters. Further, we investigate whether the soundscape has changed correspondingly and thus sound pressure levels (SPLs) have decreased in lower frequency bands (<1 kHz).

Recordings from two underwater sound monitoring stations were used to assess the acoustic effects resulting from the economic impact of Covid-19. Both stations were initially set up as part of the Baltic Sea Information on the Acoustic Soundscape (BIAS) project from December 2013 to spring 2015. From 2017 to 2018, measurements were resumed as part of the BSH (Bundesamt für Seeschifffahrt und Hydrographie) project PIMO ("Pilot-Monitoring von Unterwasserschalleinträgen in die deutschen Meere") funded by the Federal Environmental Agency (UBA). Within the PIMO project, the concept of a long-term acoustic monitoring of the German EEZ in the context of the implementation of the Marine Strategy Framework Directive (MSFD) was developed (Fischer et al., 2019).

Since 2018, both stations have been are operated as part of the German national monitoring of underwater noise, required by the MSFD and conducted by the BSH.

As one of the MSFD's descriptors of Good Environmental State (GES), Descriptor 11 (D11) considers the energy introduced into the marine environment, which includes underwater sound. This sound shall not be at levels, that adversely affect the marine environment (European Commission (EC), 2008). The Technical Sub-Group on Underwater Noise (TSG Noise) has provided guidance on how the underwater sound should be monitored, indicating, that at least the two one-Third-Octave Bands (TOB) with center frequencies at 63and at 125 Hz need to be recorded (Dekeling et al., 2014). The two TOBs were chosen as a good proxies for the low-frequency sound generated by shipping activities, although this decision has led to disputes in the past (e.g., Hermannsen et al., 2014).

Fehmarnbelt (FEB), one of 36 monitoring stations contributing to the BIAS project, was the station which experienced the heaviest shipping traffic. It recorded the highest SPLs of all stations in 2014. Although Arkona (ARK) recorded substantially lower SPLs, it also lies in an area influenced by intense shipping pressure (Mustonen et al., 2019).

Due to changing responsibilities, funding opportunities and challenges of underwater sound monitoring, the data time series at both stations is interrupted. Nevertheless, the available acoustic data sets, collected between2013 and 2020, present an opportunity for a Before-After-Control-Impact (BACI) study on how the Covid-19 pandemic has affected the soundscape in the German Baltic Sea. It is conceivable that the averaged low-frequency SPLs at these two stations, which are dominated by vessel noise, may show decreases as the prevalence of shipping decreased during the pandemic.

In spring 2020 the International Quiet Ocean Experiment (IQOE) commenced an initiative to convene all underwater acoustic measuring institutions around the globe to contribute to a coordinated research effort on the effects of Covid-19 on the soundscape of the global ocean (Tyack et al., 2021). The study presented here is a contribution to this overall research effort.

Here, we examine whether maritime mobility decreased in the Baltic German coastal waters following the onset of the pandemic in 2020. Then, we used acoustic recordings from two underwater sound monitoring stations, recorded before and after March 1, 2020 to investigate whether the soundscape changed correspondingly and whether SPLs have decreased in lower frequency bands (<1 kHz) resulting from the economic impact of Covid-19.

We discuss how our findings relate to the results of an earlier BACI study, which investigated the change of the soundscape during the first weeks of the Covid pandemic at the Pacific coast of Canada (Thomson and Barclay, 2020) with a BACI study on the impact of Covid-19 on the soundscape at Montery Bay National Marine Sanctuary (Ryan et al., 2021); and with a BACI study that analyzed the acoustic effects of a voluntary commercial vessel slowdown trial in the Haro Strait (Joy et al., 2019).

MATERIALS AND METHODS

Measurement Stations

Data were collected at two locations in the German Baltic Sea: The FEB station and the ARK station. **Figure 1A** shows the position of the measurement stations and typical traffic conditions for this part of the Baltic Sea (AIS data provided by EMODnet Human Activities (EHA), 2019). The FEB station is located in a coastal area, only 6 km north of the island of Fehmarn in the center of the busy traffic separation scheme "Fehmarnbelt." The ARK station is located northeast of the island of Rügen—an area with less shipping activity. Both stations belong to the MARNET measuring network,

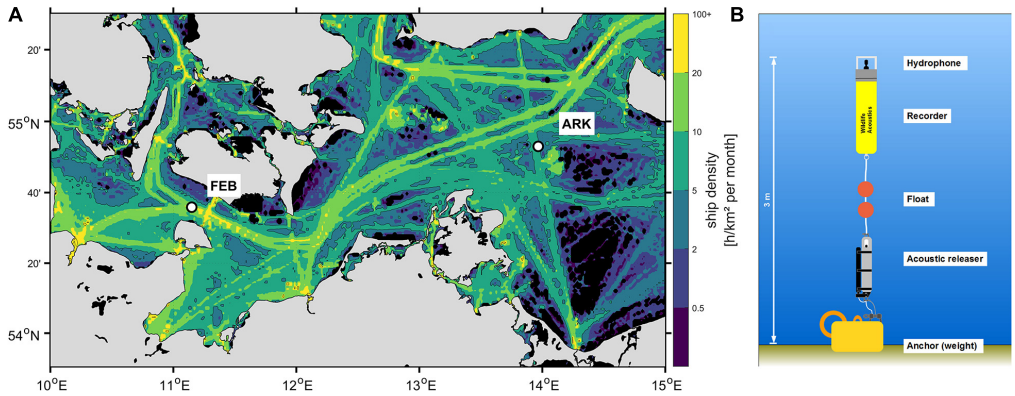

FIGURE 1 | Position **(A)** and station design **(B)** of FEB and ARK Measurement Station with AIS total density for May 2020 **(A)**. Ship density is expressed as time (in h) that ships have spent per km^2-grid cell per month (AIS data provided by EMODnet Human Activities (EHA), 2019). Black areas indicate no data availability.

managed by BSH, that measures temperature, salinity and surface currents in the German Bight and the western Baltic Sea (BSH, 2021). The Baltic Sea is a semi-enclosed basin, separated from the North Sea and the wider North Atlantic Ocean by the Kattegat and Skagerrak and the islands of Denmark (or Danish Straits). There is little tide, and wave action is limited, which tends to result in highly stratified physical oceanographic conditions with strong vertical salinity and temperature gradients (Dargahi et al., 2017). In summer stratification is strongest. Due to stronger solar radiation, warmer air temperatures and less wind-induced mixing a thermocline develops, separating the warm upper layer from the colder lower layers (Elken and Matthäus, 2008). In winter, the thermocline vanishes due to mixing processes induced by stronger winds, buoyancy loss from heat exchange with colder air temperatures and less solar radiation. The stratification in summer leads to stronger refraction and reflection of sound waves. Sound travels further during winter periods, when the water column is homogeneously mixed.

The autonomous recorder at FEB is installed ca. 100 m from the MARNET oceanographic buoy, which is also one of the navigational buoys marking the "Fehmarnbelt" traffic separation scheme. The ferry connection from Puttgarden to Rødby is ca. 14 km away, with usually three to four operating ferries and departures from both harbors every 30 min. The recorder, together with the hydrophone, is positioned 3 m above the seafloor in approximately 25 m depth. The mooring is attached to an achor weight and orientated vertically in the water column using appropriate buoyancy (**Figure 1B**). Typical measurement durations for these stations are 3–6 months, after which the device needs to be recovered for data download. In the BIAS project it was found that, on average, two vessels were present in a 5 km radius at any given time and more than eleven vessels (including ferries) were present in a 20 km radius (Mustonen et al., 2019). Due to the narrow Danish straits connecting the Baltic Sea and the North Sea the tidal influence is negligible. Although wind-driven surface currents can reach current speeds above 1.2 m/s, currents near the seabed rarely exceed 0.4 m/s (Brøker et al., 2014). This can cause significant flow noise impact on very low frequency bands up to 50 Hz, but was not further taken into account in this study (e.g., Haxel et al., 2013).

Arkona station is located between the Danish island of Bornholm and the German island of Rügen. Although compared to FEB, this station is located in a rather low-traffic location, it was still among the noisiest stations monitored during the BIAS project, and data at this site were clearly influenced by ship noise. ARK's station setup is identical to the setup at FEB (**Figure 1B**). Water depth at this station is about 45 m. Compared with FEB, the ARK monitoring location represents a more remote location of the open Baltic Sea. Open sea conditions occur more prevalently here, including higher sea states and stronger winds. During the monitoring in 2014, at least one vessel was found to be within a 10 km radius at all times (Mustonen et al., 2019). The construction and operation of offshore wind farms as well as the construction of gas pipelines are additional anthropogenic contributions to the ambient soundscape in this area. Flow noise is not considered to strongly influence sound recordings at ARK. Currents near the seafloor rarely exceed 0.1 m/s (Outzen, 2021).

Seasonal variations in SPLs are expected at both stations due to variability in physical oceanography and meteorology.

Acoustic Recordings

The acoustic data were collected using SM2M recorders (Wildlife Acoustics) fitted with "Low-Noise" hydrophones (HTI) from 2013 to 2015, and SM3M recorders (Wildlife Acoustics) fitted with "Standard" hydrophones (HTI) after 2016. The choice for low-noise hydrophones (from 2013 to 2015) instead of standard hydrophones (since 2016) had a considerable effect on the measurements, as the noise floor of low-noise hydrophones is substantially lower for high frequencies.

The difference in sensitivity can be up to 10 dB for frequencies higher than 1 kHz (Wildlife Acoustics (WA), 2017). Therefore, in this study, the comparison at high frequencies is associated with increased uncertainties. Far lower SPLs are measured at high frequencies using low-noise hydrophones instead of standard hydrophones. Since

high frequencies are less relevant for ship noise comparisons, in this study the focus is on lower frequencies (<1 kHz). A comparison of the low frequencies (dominated by ship noise) remains possible, as these are less affected by the choice of hydrophone.

All data were recorded using duty cycles of 15/45 min on/off and the sample rate was set at 32,000 samples per second, covering the frequency range up to 12.5 kHz. The hydrophones were mounted directly on the recorder body, so the system sensitivity was prone to effects such as body resonance and scattering from the flat surface (Crawford et al., 2020). However, since the housing of the instrument is only 91 cm long and has a diameter of 16.8 cm, these effects are not expected to significantly influence the beam pattern below 1 kHz (wavelength of 1.5 m). Instead, bottom reflections and scattering should have much larger effects.

Before each deployment, the systems were calibrated using an acoustic calibrator at 125 Hz (IEC, 2019). A laboratory calibration of the full spectrum could not be performed, although this would have been preferred since the frequency response curves of both the low-noise and the standard hydrophone are not flat (Wildlife Acoustics (WA), 2017). Given the strong roll-off in the sensitivity curve below 100 Hz SPLs in this frequency range are likely to be higher than those presented in this study, for both hydrophone types.

All recordings were processed to mean-square SPLs for TOBs—1/3-octave levels (TOLs)— using the tool "BSoundH" developed by Fraunhofer IDMT during the BSH project "Sound Mapping." The TOLs were computed with an integrated filter bank over time windows of 20 seconds.

To make the comparison more independent of natural changes due to seasonal variations, we compared the same calendar months from the pre-Covid (before March 2020) and during-Covid (March 2020 onward) period. If fewer than 14 days of data were available for a particular month, that month was not considered to be representative and was excluded from the analysis.

As a consequence, fewer months were available for comparison at the two stations (due to the lack of completeness of monthly data), but the resulting statistics are more robust. In total 13,329 individual recordings are available for FEB and 15,257 recordings are available for ARK (see **Table 1**).

To analyze the possible changes in the ship noise levels, two broadband levels—one below (10 Hz–1 kHz) and one above 1 kHz (1–12.5 kHz) are compared within the defined time periods before and after the Covid-19 onset. This frequency separation is based on the premise that vessel-emitted noise dominates in the lower frequency range. The limit for frequency bands, dominated by vessel noise, was set to 1 kHz in accordance with (Merchant et al., 2012). All frequencies from 1 to 12.5 kHz are expected to be mostly dominated by natural wind-driven noise (Hildebrand, 2009). To obtain these two broadband levels, the TOLs are computed for 20-s blocks and summed up in the respective frequency range, using quantities as described in Merchant et al. (2014). The monthly median broadband levels are compared in the following.

For a more detailed analysis in the frequency and time domain, the TOLs and the percentiles of the lower frequency band (10 Hz–1 kHz) for each month after March 2020 were compared with previous years.

To minimize the wind noise effects on our comparisons we additionally compared noise levels of the same sea state in the same calendar month across years. In this way only periods with the same natural conditions were compared with each other.

Wave Data

While comparing the same calendar months has the effect of removing some artifacts of seasonal variability, sea conditions during calendar months from different years may still differ due to finer scale variability in natural conditions. To consider this, the study compared periods of identical sea states within the same calendar month, before and after the Covid-19 onset. Wave height information for both stations was extracted from the European Wave Model (EWAM; WAMDI Group, 1988). This is an ocean wave forecast model for Europe based on the atmospheric model Icosahedral Non-hydrostatic Weather and Climate Model (ICON; Reinert et al., 2021). Data from both EWAM and ICON, were provided by the German Meteorological Service (DWD). The EWAM model was chosen as it provides comprehensive and continuous data coverage from 2013 to 2020. All hourly wave heights were sorted into sea state categories according to the Beaufort Sea State Code, ranging from 0 to 12 (The National Meteorological Library and Archive (NMLA), 2010). Periods with the same sea state were compared per calendar month, to compare equivalent levels of natural background noise and to identify changes in the anthropogenic noise levels. Due to small sample size, periods of sea state 5 or higher (significant wave height higher than 2 m) were excluded from the comparisons. For each sea state (0–4) the same calendar months before and during Covid-19 were compared.

Data on Marine Traffic

To verify the assumption that the Covid-19 outbreak led to a decrease in marine traffic, we compiled and examined monthly statistics of unique Maritime Mobile Service Identity (MMSI) numbers and International Maritime Organization (IMO) numbers within a 50 km radius around each respective

TABLE 1 | Available recordings before/and after the onset of the Covid-19 pandemic per calendar month and station; N/A indicates months, where no comparison was possible due to lack of data (2013–2020).

	Total	Mar	Apr	May	June	July	Aug	Sep
FEB	9247/4082	1135/466	720/687	2232/744	1440/720	1488/739	2232/726	N/A
ARK	11759/3498	N/A	N/A	1488/744	1440/720	2975/744	2976/744	2880/546

measurement station. These data were sourced from the vessel tracking service provider (VesselFinder®, 2020). These simple statistics are not an accurate measure of total traffic in an area; nevertheless, they provide a low-cost proxy for the relative trend in traffic levels. It remains impossible to separate individual ship types or ship passages solely from these data.

Unique MMSI numbers are assigned to all Automatic Identification System (AIS) on board ships. AIS systems have become more accessible during recent years and are not constrained to commercial shipping, but also are widely used among recreational vessels.

In contrast, IMO numbers are assigned to all propelled, sea-going, commercial vessels with a minimum of 100 GT (gross tonnage) and minimum length of 12 m—excluding most recreational vessels (IMO, 2014).

Consequently, unique MMSI numbers per area include all vessels carrying IMO numbers, but the IMO number statistics provide a focused overview of commercial shipping activities. Differences between MMSI numbers and IMO numbers per time period and area can be conditionally interpreted as a measure of recreational boating (although not all recreational vessels have AIS systems).

RESULTS

Analysis of Ship Traffic

To determine the effect of the pandemic on the levels of shipping activity at the two measurement stations, data on marine traffic were examined. For each year 2013–2020, monthly mean values of unique MMSI numbers (**Figure 2**) and unique IMO numbers (**Figure 3**) were compared and evaluated.

There was an observed reduction in marine traffic in 2020 (**Figure 3**). In the Fehmarnbelt, fewer unique MMSI numbers were registered between March and May 2020 than on average during the previous years (up to 21% fewer in April 2020), while more MMSI numbers than on average were registered from June to October (up to 21% more in August 2020). In the same area, the count of unique IMO numbers was below the average of the previous years during all months from March until October (up to 12% less commercial shipping during June 2020). From these data, a large-scale reduction in marine traffic could be observed between March and May 2020. Whilst the commercial shipping only slowly recovered to average levels during the second half of the year, more recreational boating (MMSI-IMO) than ever before was recorded in late 2020 at FEB. This effect can be explained by international travel restrictions that may have led to more national recreational boating than during previous years. Notably, the reduction of commercial traffic (from March to October 2020) coincides with the onset of the Covid-19 pandemic, followed by an increase in recreational boating from July to October 2020.

This observed pattern can only partially be seen in the vicinity of the ARK station. The lowest monthly mean of unique IMO numbers occurred during March to October 2020 (maximum difference of 12% compared to the average of previous years). The count of MMSI numbers was lower in 2020 than in previous years during the months March to August (up to 11% fewer in May compared to previous years), and a small increase (4% more compared to previous years) was observed during the autumn months. ARK is located further from the coast and is probably less attractive to recreational boating than the FEB; however, more commercial vessels are operating in this area. The data suggest an overall decrease in commercial shipping, but illustrate an increase in number of unique MMSI numbers for September and October. This increase in recreational boating might again be a reaction to international travel restrictions during summer and autumn 2020.

Analysis of Wave Data

Model results from months with available acoustic data show a long-term mean significant wave height of 0.7 ± 0.2 m at FEB and 1.1 ± 0.4 m at ARK. In comparison with previous years, the 2020 mean significant wave heights at ARK and FEB follow a similar seasonal pattern (**Figure 4**). During May and July 2020, exceptionally high sea states were modeled at both stations compared to previous years. The sea states during August and September 2020 were the lowest during the whole investigation period, also at both stations.

As anticipated, due to its proximity to shore, the sea states at FEB are considerably lower than at the ARK station. Thus, high-frequency SPLs (above 1 kHz) were observed to be higher at the ARK station.

Monthly Comparison for Low-Frequency and High-Frequency Bands

Since the start of the measurements at FEB in 2013, the lowest low-frequency SPLs were recorded in 2020, with an absolute minimum in July 2020 (**Figure 5A**). Although the number of unique MMSI numbers in July was 17% above the average, the number of unique IMO numbers was still 7% below the average of previous years. In August 2020, the decrease in the low-frequency band levels was not as pronounced as in previous months and at the same time an increase in marine traffic (both MMSI and IMO numbers) is evident. Low-frequency band levels (10 Hz–1 kHz) from January to March 2020 were in the range of previous measurements, but this period was before the most stringent measures against the spread of the pandemic came into effect. From April to August the low-frequency band levels were on average 1.2 dB below the mean of previous years—indicating a general decrease in low-frequency noise. This decrease corresponds to a decrease in sound pressure of 13%. For high-frequency band levels (1–12.5 kHz) such a clear decrease compared to previous years cannot be identified (**Figure 5B**). This meets our expectations, since a decrease in traffic should mainly affect the lower frequencies. In fact, the measurements from 2013 to 2015 show much lower high-frequency SPLs than all other years. The reason for this is most likely the different instrumentation that was being used during the BIAS project.

Similar effects could be identified at the ARK station. In contrast to the FEB station, the mean of unique MMSI numbers only increases to 4% above the pre-Covid-19 average in

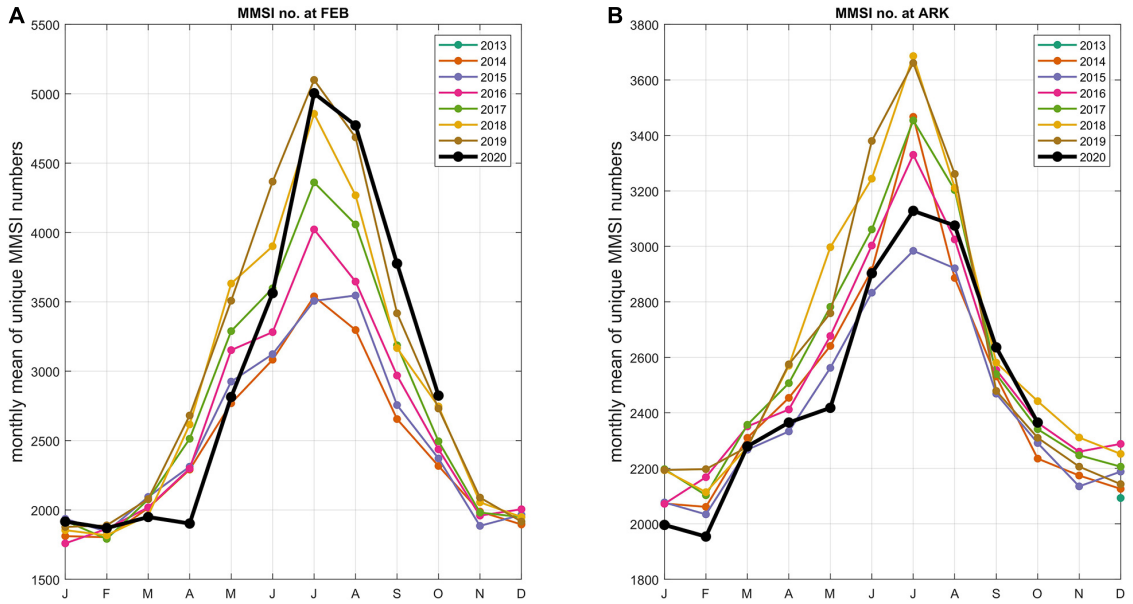

FIGURE 2 | Monthly mean of unique MMSI numbers per year within a 50 km radius around FEB-station **(A)** and ARK-station **(B)**, note the different scales in panels **(A)** and **(B)**.

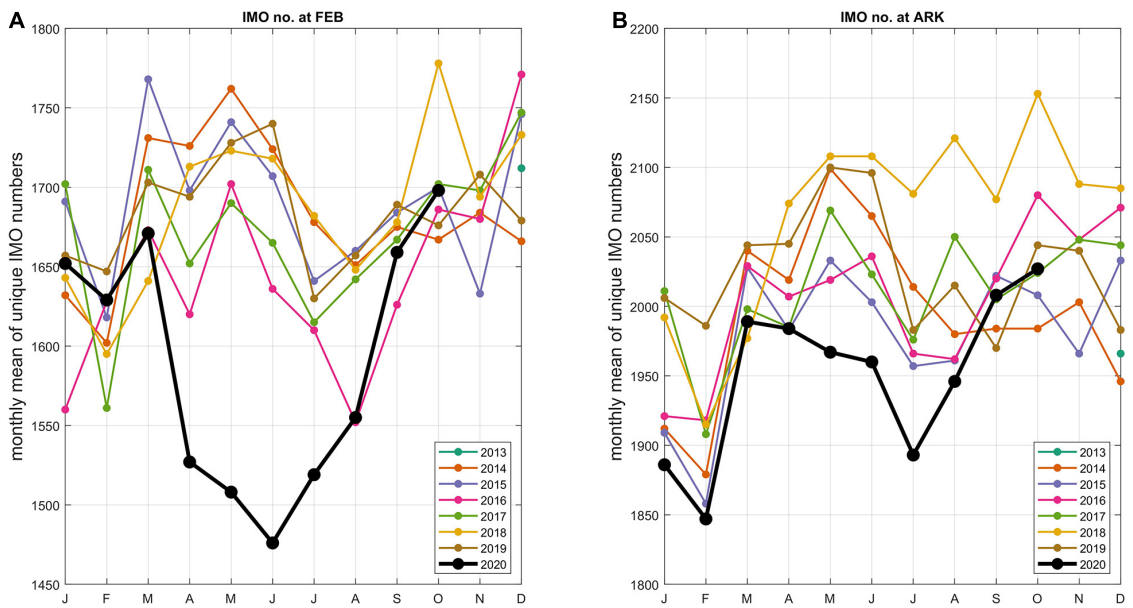

FIGURE 3 | Monthly mean of unique IMO numbers per year within a 50 km radius around FEB-station **(A)** and ARK-station **(B)**, note the different scales in panels **(A)** and **(B)**.

September and the mean of unique IMO numbers remains below pre-Covid-19 conditions until October 2020 (**Figure 6**). In the second half of the year commercial shipping recovered. Similar to the FEB station the low-frequency band noise after March 2020 was lower than during all previous years at ARK—indicating lowest received SPLs since the begin of recordings (**Figure 6A**). On average, the low-frequency noise was also 1.2 dB below the mean of the previous years, which corresponds to a reduction of sound pressure of 13%. Investigating the high-frequency band level (1 kHz to 12.5 kHz) (**Figure 6B**), the high SPLs in July and relatively low SPLs in August are obvious. This corresponds well with the high sea states modeled in July 2020 and the low sea states modeled in August 2020 (**Figure 2**). No divergent pattern for the period during Covid-19 from previous years can be identified. The high-frequency band levels are within the same range. Again, the high-frequency band levels from 2013 to 2015

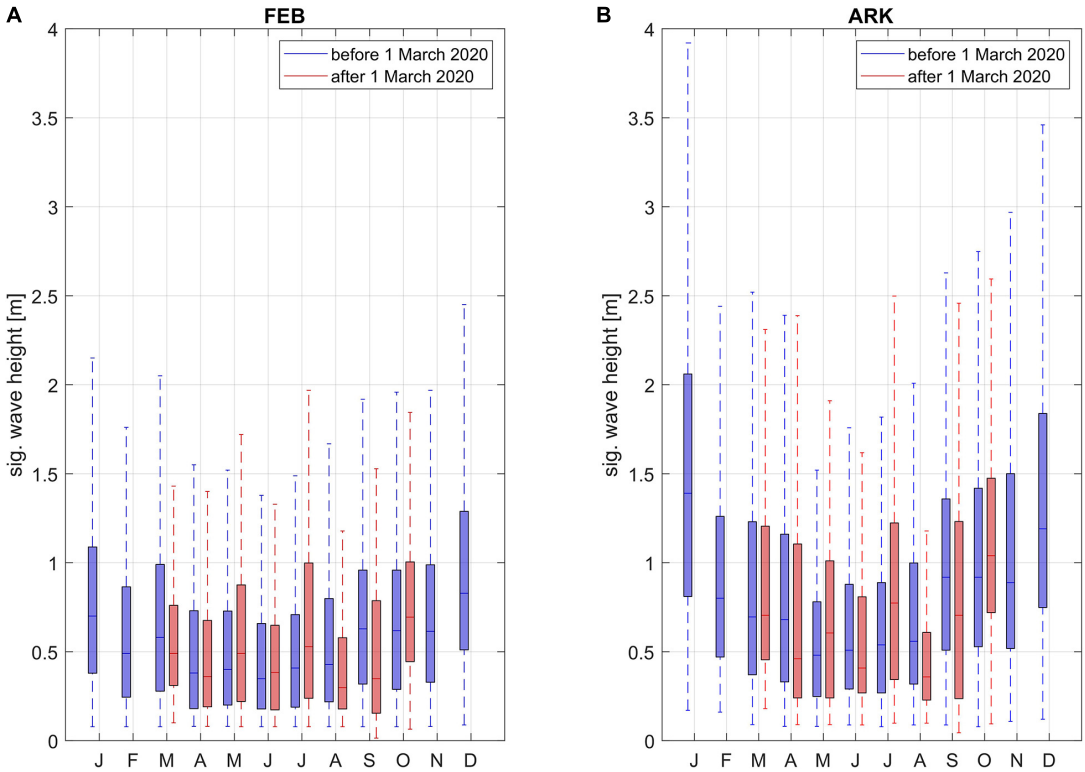

FIGURE 4 | Boxplots of significant wave height per month before (2013–2019; blue) and during (2020; red) Covid-19 pandemic at the CWAM's nearest grid points to FEB-station **(A)** and ARK-station **(B)**. Only months with available acoustic data were represented at both stations.

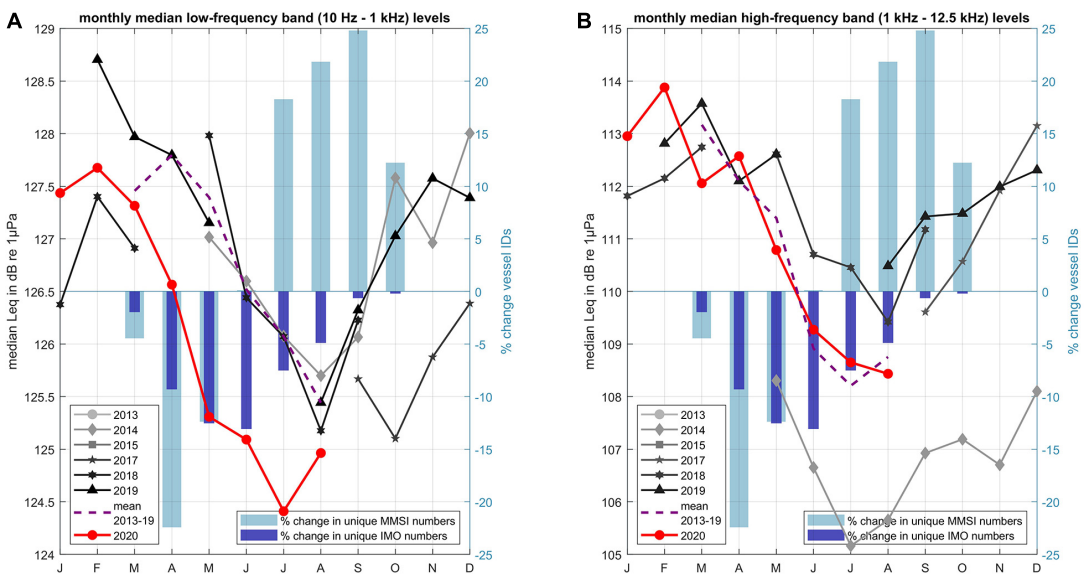

FIGURE 5 | Available monthly median broadband levels per year at FEB, medians of low frequency bands (10 Hz–1 kHz) **(A)**; Medians of high frequency bands (1–12.5 kHz) **(B)**; bars indicate percentage of marine traffic reduction after Covid-19 outbreak (mean 2013–2019 vs 2020), % reduction of unique MMSI numbers (light blue) and% reduction of unique IMO numbers (dark blue); average broadband levels of years before Covid-19 (dashed purple line), note the different scales for the broadband levels in panels **(A)** and **(B)**.

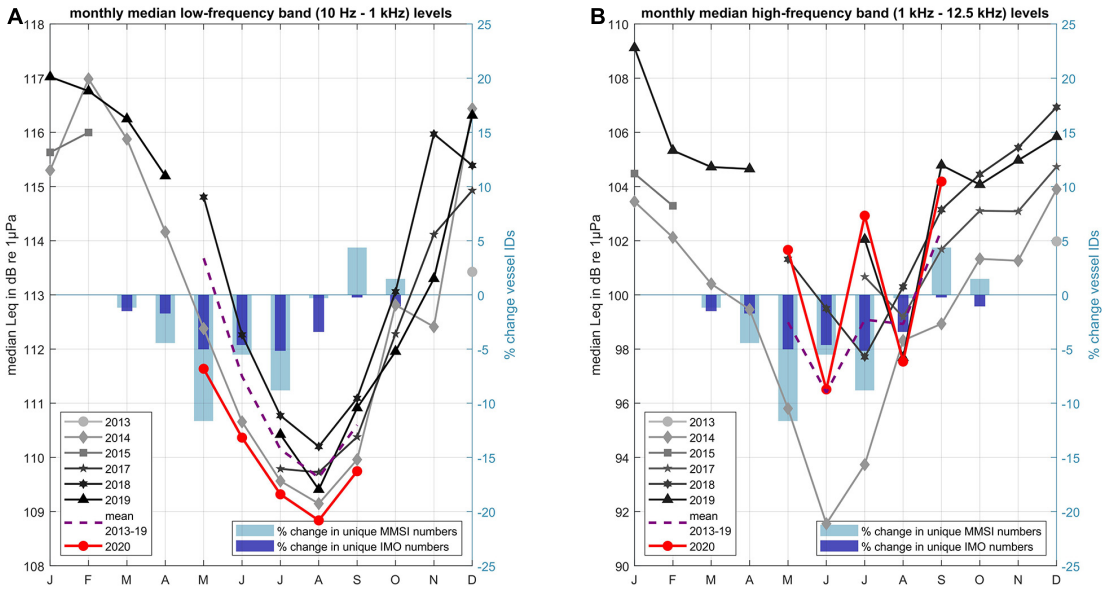

FIGURE 6 | Available monthly median broadband levels per year at ARK, medians of low frequency bands (10 Hz–1 kHz) **(A)**; Medians of high frequency bands (1–12.5 kHz) **(B)**; bars indicate percentage of marine traffic reduction after Covid-19 outbreak (mean 2013–2019 vs 2020), % reduction of unique MMSI numbers (light blue) and% reduction of unique IMO numbers (dark blue); average broadband levels of years before Covid-19 (dashed purple line), note the different scales for the broadband levels in panels **(A)** and **(B)**.

were substantially lower compared to all years, probably due to the usage of Low-Noise hydrophones during the BIAS project.

A Wilcoxon rank sum test was used to test if the differences of the monthly medians are significant. The test was chosen because none of the sets of recordings (for each month before and after the pandemic's onset) were distributed normally. Shapiro–Wilk tests were used to test for normality. At a 95% confidence level, it was found that all compared medians of SPLs differ significantly.

Monthly Comparison of Third-Octave Levels and Low Frequency Percentiles

Monthly medians per TOB were compared before and after the Covid-19 outbreak (**Figure 7**). For data before Covid-19 the medians per TOB were calculated for concatenated same calendar months. Comparisons for TOBs higher than 1 kHz do not consider data from 2014, since the instruments' sensitivities differ significantly in this frequency range and comparisons would not be meaningful. This leads to a sparser data coverage for the period before the pandemic for high frequencies. Excluding data from 2013 to 2015 data mainly affects high-frequency TOBs, reducing the positive deviation of 2020 data compared to data from previous years.

At FEB (**Figure 7A**) TOBs up to 100 Hz are distinctly lower than the median of previous years (up to 5 dB). The obvious decrease at the 200 Hz TOB of 4–5 dB can be explained by the installation of solar panels on the nearby FEB buoy, which made the use of a generator on the buoy almost redundant during 2020. TOLs for TOBs above 1 kHz from the years 2013 to 2015 were substantially lower than during other years. From April to August 2020 all low-frequency median TOLs (<100 Hz) as well as most high-frequency median TOLs (>100 Hz) are lower than before the pandemic. Reduction generally increases gradually with decreasing TOBs, except for the 200 Hz TOB. Highest reduction of up to 5.6 dB can be found in the 10 Hz TOB in July 2020.

The monthly TOL comparison for ARK (**Figure 7B**) indicates a distinct reduction in low-frequency SPLs. In contrast to FEB, a reduction is obvious for all TOBs up to 160 Hz. The highest reduction of SPL can be found for the 20 Hz band in May (-5.4 dB). The July measurements show higher TOLs (max. +3 dB at 1.6 kHz), which agrees well with the higher sea states during this month (**Figure 4B**). The smaller positive deviations in May and September cannot be explained by exceptional weather conditions or different instrumentation (deviations are present when including or excluding data from 2013 to 2015). As before, a Wilcoxon rank sum test was applied to test if observed differences in medians per TOB and month are significant. Only the difference at the 630 Hz TOB for May at ARK was found to be not statistically significant (at 95% confidence level).

Since a noise reduction is most evident for low frequencies, we further analyzed the temporal distribution of noise level changes in the low-frequency band (10 Hz–1 kHz). Therefore, the monthly differences of percentiles were compared (see **Figure 8**). Both stations show a general reduction of noise levels for the observed months. At FEB the strongest noise reductions are apparent in April and May 2020 (up to 5 dB) for low percentiles—indicating a reduction of background noise. The percentage of time with decreased noise levels increased from March to July to almost 90% and reduces to less than 50% in August (see **Figure 8A**). At ARK the strongest noise reduction is also observed in May (up to 2 dB) for low percentiles. The percentage

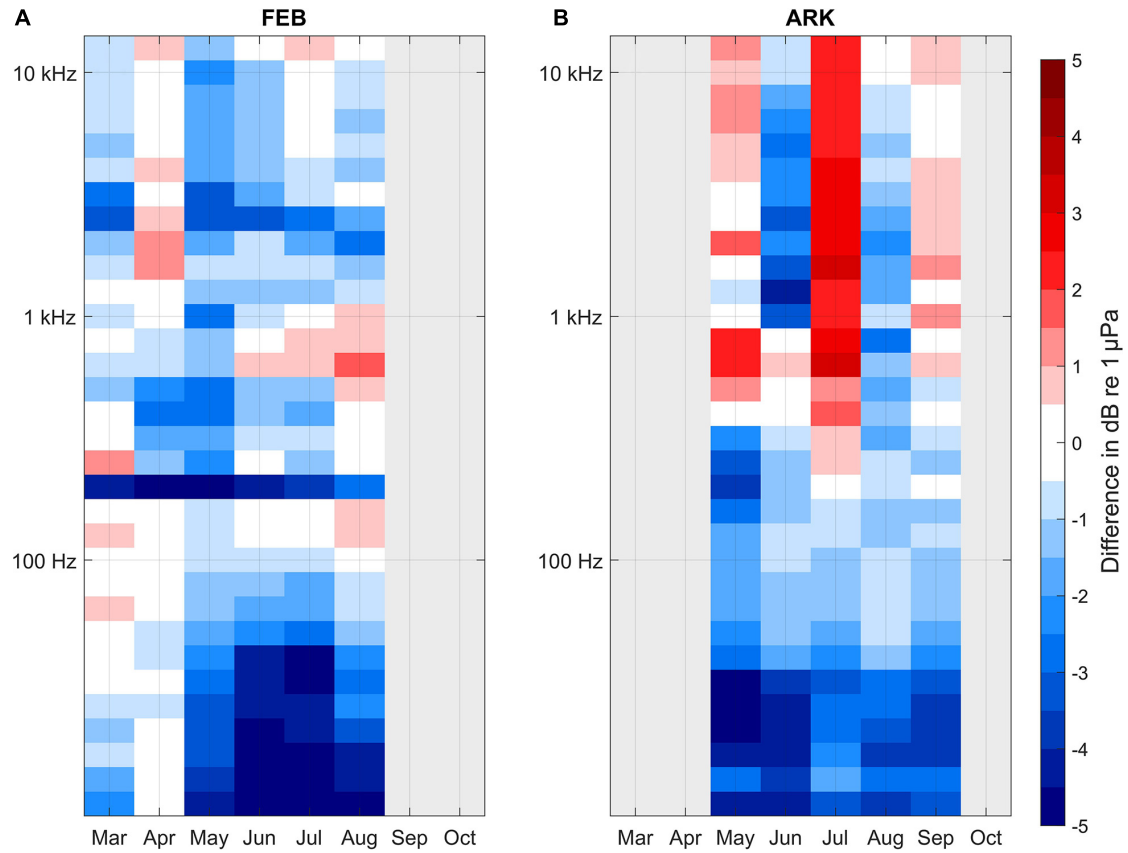

FIGURE 7 | Change of monthly median TOLs after outbreak of Covid-19 pandemic compared with previous years at FEB **(A)** and at ARK **(B)**. Light gray area indicates no data availability.

of time with reduced noise levels decreases in July, but stays above 70% during the whole assessment period. Small increases in noise levels at high percentiles can be observed in April at FEB and from May to August at ARK, indicating an increase of intermittent noise during these periods in 2020 compared with previous years.

Comparison for Periods of Same Sea State

Comparing noise levels of same sea state in same calendar months across years altered the observed noise reductions. At FEB, the mean difference (before and during Covid-19) in the low-frequency band is 1.1 dB and at ARK it is 1.9 dB. It appears, that including the sea state had a greater impact on the comparison at ARK, than it did for the comparison at FEB. The count of individual recordings, which have been compared per sea state and calendar month is summarized in **Tables 2**, **3**. For each calendar month and sea state a Wilcoxon rank sum test was performed in order to test whether the medians of the low-frequency band levels (before and after the pandemic's onset) are equal. The Wilcoxon rank sum test was chosen because none of the compared noise level sets were distributed normally. This was checked by performing a Shapiro-Wilk test for each set of noise levels per calendar month and sea state. At a 95% confidence level only the compared medians in March at FEB for sea state 4 did not differ significantly. For all other calendar months and sea states the differences between the medians are statistically significant. In **Figure 9**, the averages of the comparisons per sea state are shown for each calendar month (purple). Additionally, as a reference the monthly noise reductions as explained in section "Monthly Comparison for Low Frequency Bands and High Frequency Bands." are shown (green).

At FEB, considering the different sea states only altered the observed noise reduction in the low-frequency band by 0.1 dB. The pattern of the monthly differences is also not changed much when the sea states are included in the comparisons. The greatest difference between both methods is visible in March. The low sea states in March 2020 (see **Figure 4**) may have led to an overestimation of the observed noise reduction. In contrast to that the sea states in July 2020 were lower than during previous years, which might have led to an underestimation of the noise reduction. Although one would expect to also see an overestimation of noise reduction in August (very low sea states in 2020 compared with previous years), such a relation cannot be observed.

Comparing only time periods of equal sea states had a profound effect on the observed noise reduction at ARK

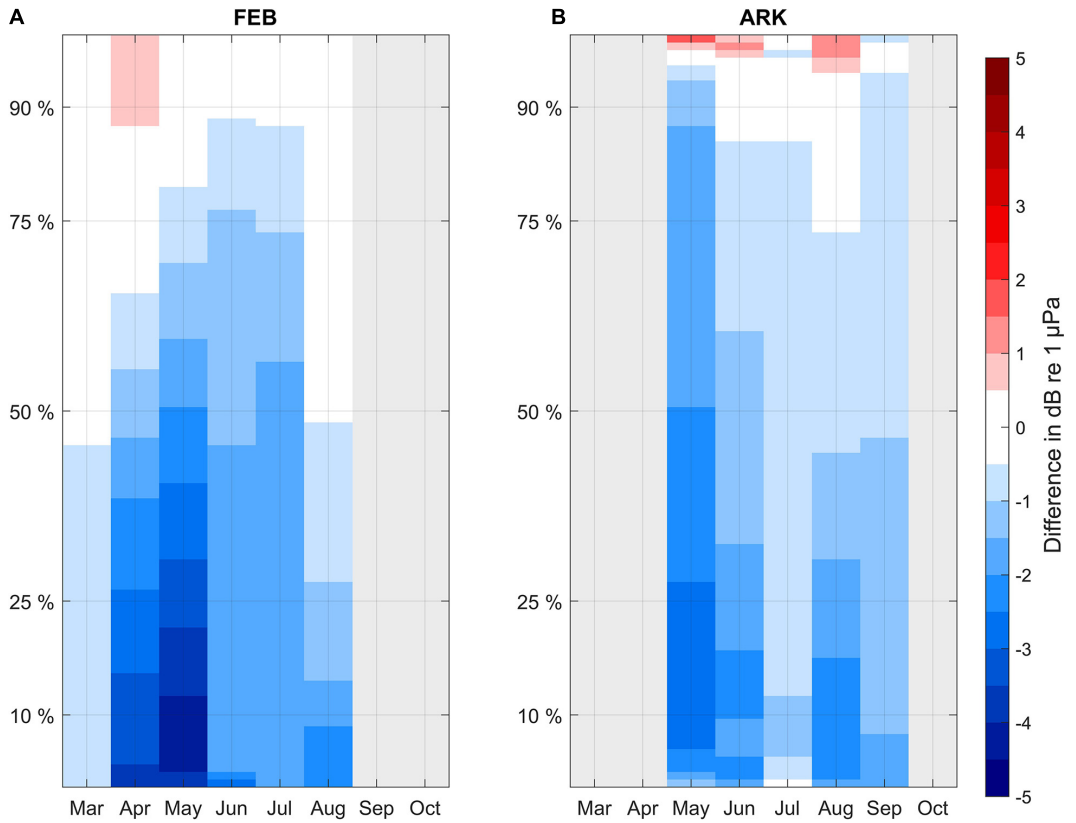

FIGURE 8 | Monthly differences of percentiles in the low-frequency band (10 Hz–1 kHz) for acoustic data measured before (2013–2019) and during Covid-19 pandemic (2020) at FEB **(A)** and at ARK **(B)**. Light gray area indicates no data availability.

TABLE 2 | Available recordings at FEB before/and after the onset of the Covid-19 pandemic per calendar month and sea state; N/A indicates months, where no comparison was possible due to lack of data (2013–2020).

FEB	Total	Mar	Apr	May	June	July	Aug	Sep
SS 0	468/381	31/3	58/66	112/97	48/109	116/45	103/61	N/A
SS 1	1016/643	103/56	121/135	248/78	124/108	136/96	284/170	N/A
SS 2	2579/1628	400/193	327/277	631/276	299/301	296/256	623/325	N/A
SS 3	1399/812	309/133	158/97	316/154	147/149	130/159	339/120	N/A
SS 4	790/596	257/71	56/105	181/139	98/53	66/182	132/46	N/A
SS 5	46/17	35/10	0/4	0/0	4/0	0/0	7/3	N/A
SS 6	0/0	0/0	0/0	0/0	0/0	0/0	0/0	N/A

TABLE 3 | Available recordings at ARK before/and after the onset of the Covid-19 pandemic per calendar month and sea state; N/A indicates months, where no comparison was possible due to lack of data (2013–2020).

ARK	Total	Mar	Apr	May	June	July	Aug	Sep
SS 0	3392/1569	N/A	N/A	302/311	299/302	979/305	907/301	905/350
SS 1	403/404	N/A	N/A	50/111	24/68	198/50	86/94	45/81
SS 2	1944/801	N/A	N/A	183/89	205/232	585/190	648/233	323/57
SS 3	1240/350	N/A	N/A	172/101	116/64	316/86	342/73	294/26
SS 4	949/352	N/A	N/A	37/132	69/38	151/107	248/43	444/32
SS 5	128/22	N/A	N/A	0/0	7/16	2/6	0/0	119/0
SS 6	29/0	N/A	N/A	0/0	0/0	0/0	0/0	29/0

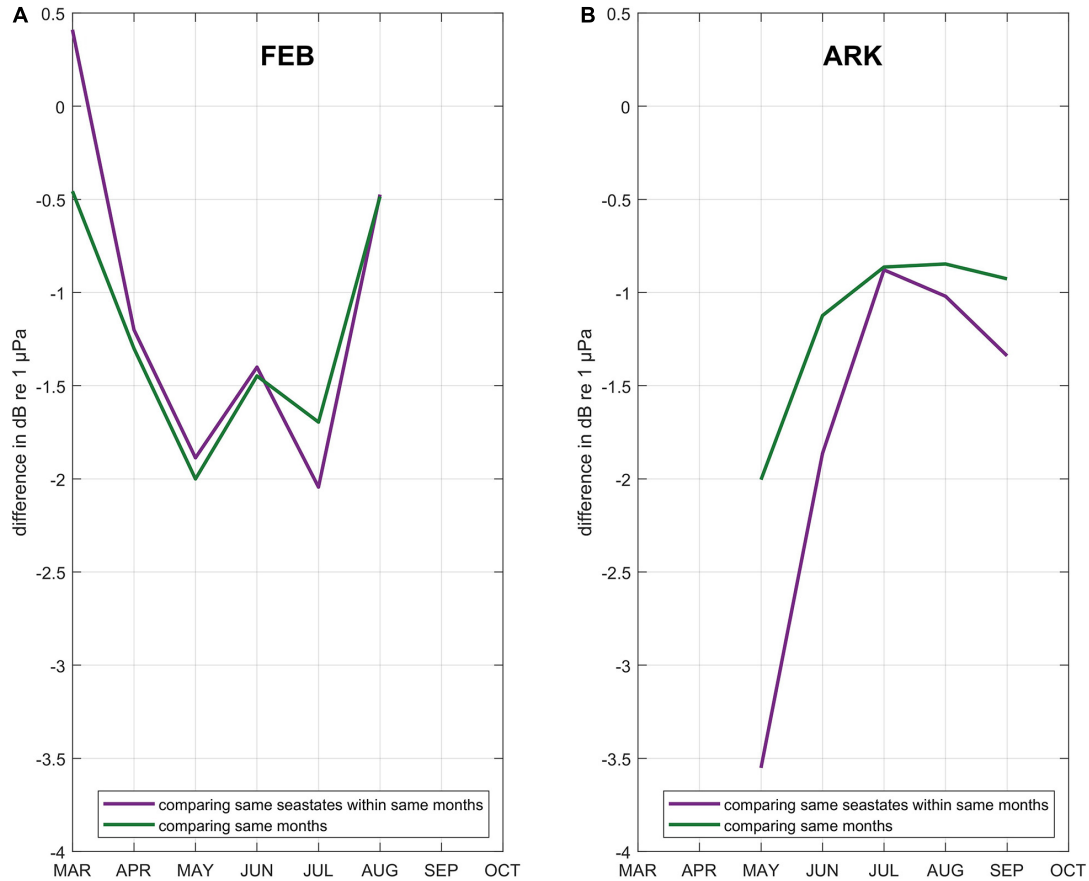

FIGURE 9 | Differences of medians of low frequency (10 Hz–1 kHz) sound pressure levels per calendar month (before and after March 1, 2020) at FEB **(A)** and at ARK **(B)**; all recordings per calendar month are compared (green); only periods of same sea state within same calendar month are compared with each other (purple).

increasing the median noise reduction (in the low-frequency band) by another 0.7–1.9 dB. For May, the noise reduction even increased by 1.5–3.5 dB, which corresponds well with observed high sea states during May 2020 (see **Figure 4**) and the low point of maritime traffic in 2020 (see **Figure 6**). For the other months no clear relations are apparent between the differences of sea states (between 2020 and previous years) and the differences of noise. It is notable, that differences between the two methods of comparison (considering sea states or not) are greatest during spring and autumn and smaller during summer months.

DISCUSSION

Monthly median TOLs for low frequencies (up to 1 kHz) were the lowest in 2020 since the start of the recordings in 2013 for both measurement stations. This coincides well with the onset of measures against the spread of the Covid-19 pandemic and the related decrease in commercial shipping. Analysis of our data has shown, that recreational boating also decreased during the first months of the pandemic, but increased significantly during the summer months at both stations. This increase might be associated with international travel restrictions and may have inhibited an even greater reduction of low frequency noise.

At the FEB station, the monthly SPLs for the low-frequency band (10 Hz–1 kHz) were on average 1.2 dB below the median levels of previous years of measurement. This corresponds to a reduction of the sound pressure of 13%. At the ARK station, a decrease of 1.2 dB in the low-frequency band was also observed, which is again equivalent to a decrease of 13% in sound pressure.

This is slightly less than the 1.5 dB reduction at 100 Hz (weekly power spectral density), which Thomson and Barclay (2020) described for the Pacific coast of Canada during the first weeks of the Covid-19 pandemic. Obviously, the observed metrics differ regarding their bandwidth and observation period so reductions are not directly comparable.

Ryan et al. (2021) have analysed the decrease in sound pressure in the 63 Hz TOB in the Monterey Bay National Marine Sanctuary following the Covid-19 pandemic onset. They report, that the mean TOL reduced by 1.9 dB re 1 μPa^2 Hz^{-1} in June 2020. The highest reductions of median 63 Hz -TOLs at FEB and ARK are similar (up to 1.9 dB in July at FEB and in May at ARK). Although not the same quantities were compared (medians instead of geometric means), the levels of reduction are of same magnitude.

To further put the observed reduction into perspective, it is worth mentioning the broadband (10 Hz–100 kHz) noise

reduction of 1.2 dB, that Joy et al. (2019) measured during a voluntary commercial vessel slowdown trial at the Lime Kiln listening station in the Haro Strait. Their decade band analysis even showed a 3.1 dB reduction in the 10–100 Hz band and a 2.3 dB reduction in the 100–1,000 Hz band. Although the given frequency ranges are again different, complicating direct comparisons, it is still noteworthy that similar or even higher rates of noise reduction were observed during the voluntary slowdown trial than during the extensive decrease in commercial shipping, that we have observed.

The reduction in sound pressure at FEB and ARK for some low TOBs was much higher than the average reduction at both stations. Considering all available data, at FEB a maximum reduction of 5.6 dB was recorded in July (at 10 Hz TOB). At ARK a maximum reduction of 5.4 dB in May (at 20 Hz TOB) was observed. Reductions of this magnitude correspond to a reduction of sound pressure of almost 50% for the respective TOB and month.

During the pandemic in 2020 the high-frequency band (1–12.5 kHz) at FEB was the lowest for all measurements taken after 2016. But this was not observed for the ARK station. The high-frequency band levels at ARK are within the range of the previous years. Data from before 2016 shows considerable low TOLs for high frequencies, which was associated with the lower noise floor at high frequencies of the used instrumentation. All measurements after 2016 were performed with the Standard hydrophone type, which has higher self-noise levels at high frequencies (up to 10 dB).

The analysis of the percentiles of the low-frequency band levels showed a noise reduction during most of the time after the onset of the Covid-19 pandemic at both stations. At FEB, the percentage of time with reduced noise levels increased from March to June and decreased thereafter, which corresponds with the increase of unique MMSI numbers in July. Whereas such a clear relation between traffic and noise reduction is not apparent at ARK, noise level reductions are evident during most of the time (up to 95% of the time).

To properly compare anthropogenic effects on the soundscape, it is necessary to ensure that time periods of same natural ambient noise were compared with each other. Monthly medians were compared to consider seasonal variations. To further consider variations within the same calendar months, periods of same sea state were compared. It was shown that this approach mainly altered results at the ARK station. The greatest effects of comparing only periods of same sea state could be observed during the windier autumn and spring months at ARK. At ARK, high sea states prevail more frequently compared to FEB. Therefore, it is concluded, that considering same sea states only is a method that is of less importance when analyzing coastal stations (like FEB), but becomes more relevant for offshore locations where higher sea states and stronger winds prevail.

The comparison of same sea states within same calendar months yielded a decrease in the low frequency band (10 Hz–1 kHz) of 1.1 dB at FEB and 1.9 dB at ARK (11 and 20% reduction of sound pressure, respectively). However, this method cannot be considered as more reliable than comparing only same calendar months. Although comparing periods of equal sea state may be a good proxy for identifying comparable natural conditions, this method does not necessarily contrast periods of comparable anthropogenic activity. Particularly with regard to the stations' proximity to the coast ferry passages, wind farm servicing, recreational boating or other activities may occur more often during the day than during the night.

Both presented methods are subject to uncertainties. Either it cannot be ensured, that periods of comparable natural conditions are compared (when comparing same calendar months only) or it cannot be ensured, that periods of same anthropogenic activity are compared (when considering only periods of same sea states). However, both methods yield results that indicate a comparable reduction of low-frequency noise levels during the first months of the Covid-19 pandemic.

Both stations continue to be operated by BSH as part of national underwater noise monitoring. As such, future measurements will further help to interpret and classify the results in terms of the relation of low frequency noise and shipping and countermeasures tackling anthropogenic noise can be evaluated. This study might further serve as a starting point to investigate ecological effects of the decrease in shipping noise due to the Covid-19 pandemic. Seizing the opportunity, BACI -studies on the distribution of noise sensitive species (e.g., the critically endangered harbor porpoise) before and during the pandemic could potentially complement studies like ours.

DATA AVAILABILITY STATEMENT

The raw data supporting the conclusions of this article will be made available by the authors, without undue reservation.

AUTHOR CONTRIBUTIONS

FB processed the measured data, performed the analysis, and designed the figures, and took the lead in writing the manuscript. J-GF supervised the project. DK and J-GF verified the results and were in charge of overall direction and planning. All authors designed and performed the measurements, discussed the results, and contributed to the final manuscript.

ACKNOWLEDGMENTS

We are immensely grateful to Ewan Edwards from Marine Scotland for his edits and comments that improved our manuscript significantly. We also thank our colleagues Martin Moritz, Kerstin Jochumsen, Kai Herklotz, Carina Juretzek, and Helmut Schmid from BSH, who provided insight and expertise that greatly assisted our research. We also owe gratitude to the Crew of the BSH research vessel DENEB, who enabled the data collection at both measurement sites. We further like to acknowledge the BSH project Sound Mapping (order number: 10044386), in which the tool BSoundH was developed, which was used for data processing in this study. In this regard we especially like to thank Stephanus Volke from Fraunhofer IDMT.

REFERENCES

Brøker, I., Hansen, I., and Middelboe, A. (2014). Eia for the fehmarnbelt crossing – the world's longest immersed tunnel. *Coast. Eng. Proc.* 1:47. doi: 10.9753/icce.v34.management.47

BSH. (2021). *Das Überwachungsmessnetz des BSH*. Available online at: https://www.bsh.de/DE/THEMEN/Beobachtungssysteme/Messnetz-MARNET/messnetz-marnet_node.html

Crawford, N., Robinson, S., and Wang, L. (2020). *Standard Procedure for Equipment Performance, Calibration and Deployment*. Belgium: European Union.

Dargahi, B., Kolluru, V., and Cvetkovic, V. (2017). Multi-Layered Stratification in the Baltic Sea: insight from a Modeling Study with Reference to Environmental Conditions. *J. Marine Sci. Eng.* 5:2. doi: 10.3390/jmse5010002

Dekeling, R., Tasker, M., Sandra, V. D. G., Ainslie, M., Andersson, M., André, M., et al. (2014). *Monitoring Guidance for Underwater Noise in European Seas, Part I: Executive Summary*. Luxembourg: Publications Office of the European Union.

Elken, J., and Matthäus, W. (2008). *Baltic Sea oceanography. Assessment of Climate Change for the Baltic Sea Basin*. Unite Kingdon: BALTEX.

EMODnet Human Activities (EHA). (2019). *Vessel ensity Map*. Available online at: https://www.emodnet-humanactivities.eu/search-results.php?dataname=Vessel+Density+(accessed March 23, 2021).

European Commission (EC). (2008). Directive 2008/56/EC of the European Parliament and of the Council *Establishing a Framework for Community Action in the Field of Marine Environmental Policy*. (Marine Strategy Framework Directive). Belgium: European Union.

Fischer, J., Kühnel, D., Basan, F., and Herklotz, K. (2019). *Pilot-Monitoring der Impulshaften und kontinuierlichen Unterwasserschalleinträge in Dem Deutschen Meere Unter der EU-Meeresstrategie-Rahmenrichtlinie (PIMO)*. Germany: Umweltbundesamt.

Gibney, E. (2020). Coronavirus lockdowns have changed the way Earth moves. *Nature* 580, 176–177. doi: 10.1038/d41586-020-00965-x

Haxel, J., Dziak, B., and Matsumoto, H. (2013). Observations of shallow water marine ambient sound: the low frequency underwater soundscape of the central Oregon coast. *J. Acoust. Soc. Am.* 05, 2586–2596. doi: 10.1121/1.4796132

Hermannsen, L., Beedholm, K., Tougaard, J., and Madsen, P. (2014). High frequency components of ship noise in shallow water with a discussion of implications for harbor porpoises (Phocoena phocoena). *J. Acoust. Soc. Am.* 136:1640. doi: 10.1121/1.4893908

Hildebrand, J. (2009). Anthropogenic and natural sources of ambient noise in the ocean. *Mar. Ecol. Progr. Ser.* 395, 5–20. doi: 10.3354/meps08353

IEC. (2019). *Underwater acoustics - IEC 60565-2:2019; Hydrophones - Calibration of hydrophones - Part 2: procedures for low frequency pressure calibration*. Switzerland: International Electrotechnical Commission.

IMO. (2014). Available online at: https://wwwcdn.imo.org/localresources/en/OurWork/IIIS/Documents/CL.2554-Rev-3_IMO%20Unique%20Company%20Identification%20Number%20Scheme.pdf (accessed February 11, 2021).

Joy, R., Tollit, D., Wood, J., MacGillivray, A., Li, Z., Trounce, K., et al. (2019). Potential Benefits of Vessel Slowdowns on Endangered Southern Resident Killer Whales. *Front. Mar. Sci.* 06:344. doi: 10.3389/fmars.2019.00344

Leaper, R. (2019). The Role of Slower Vessel Speeds in Reducing Greenhouse Gas Emissions, Underwater Noise and Collision Risk to Whales. *Front. Mar. Sci.* 6:505. doi: 10.3389/fmars.2019.00505

March, D., Metcalfe, K., Tintoré, J., and Godley, B. J. (2020). Tracking the global reduction of marine traffic during the COVID-19 pandemic. *Nat. Commun.* 12:2415.

Merchant, N., Fristrup, K. M., Johnson, M. P., Tyack, P. L., Witt, M. J., Blondel, P., et al. (2014). Measuring acoustic habitats. *Methods Ecol. Evol.* 6, 257–265.

Merchant, N. D., Witt, M. J., Blondel, P., Godley, B. J., and Smith, G. H. (2012). Assessing sound exposure from shipping in coastal waters using a single hydrophone and Automatic Identification System (AIS) data. *Mar. Poll. Bull.* 64, 1320–1329. doi: 10.1016/j.marpolbul.2012.05.004

Millefiori, L. M., Braca, P., Zissis, D., Spiliopoulos, G., Marano, S., Willett, P. K., et al. (2020). COVID-19 Impact on Global Maritime Mobility. *arXiv* 09.

Mustonen, M., Klauson, A., Andersson, M., Clorennec, D., Folegot, T., Koza, R., et al. (2019). Spatial and Temporal Variability of Ambient Underwater Sound in the Baltic Sea. *Sci. Rep.* 9:13237.

Outzen, O. (2021). *Report on the Oceanographic Conditions of Site O-1.3*. Available online at: https://pinta.bsh.de/2021/O-1.3 (accessed May 28, 2021).

Reinert, D., Prill, F., Frank, H., Denhard, M., Baldauf, M., Schraff, C., et al. (2021). *DWD Database Reference for the Global and Regional ICON and ICON-EPSForecasting System*. Germany: Deutscher Wetterdienst.

Ryan, J. et al. (2021). Reduction of Low-Frequency Vessel Noise in Monterey Bay National Marine Sanctuary During the COVID-19 Pandemic. *Frontiers in Marine Science*, 06, Issue 8.

The National Meteorological Library and Archive (NMLA). (2010). *Fact sheet 6 - The Beaufort Scale*. Avaialble online at: https://www.metoffice.gov.uk/binaries/content/assets/metofficegovuk/pdf/research/library-and-archive/library/publications/factsheets/factsheet_6-the-beaufort-scale.pdf (accessed 17 June, 2021).

Thomson, D., and Barclay, D. (2020). Real-time observations of the impact of COVID-19 on underwater noise. *J. Acoust. Soc. Am.* 147:3390. doi: 10.1121/10.0001271

Tyack, P. L., Miksis-Olds, J., Ausubel, J., and Urban, E. R. JR. (2021). Measuring ambient ocean sound during the COVID-19 pandemic. *Eos* 102. doi: 10.1029/2021EO155447

Urick, R. J. (1983). *Principles of Underwater Sound*. United states: McGraw-Hill.

VesselFinder® (2020). Available online at: https://www.vesselfinder.com/historical-ais-data.

WAMDI Group. (1988). The WAM model - a third generation ocean wave prediction model. *J. Phys. Oceanogr.* 18, 1775–1810. doi: 10.1175/1520-0485(1988)018<1775:twmtgo>2.0.co;2

Wildlife Acoustics (WA). (2017). *Song Meter SM3M Submersible and Deep Water Bioacoustics Recorder*. United States: Wildlife Acoustics, Inc.

Conflict of Interest: The authors declare that the research was conducted in the absence of any commercial or financial relationships that could be construed as a potential conflict of interest.

Copyright © 2021 Basan, Fischer and Kühnel. This is an open-access article distributed under the terms of the Creative Commons Attribution License (CC BY). The use, distribution or reproduction in other forums is permitted, provided the original author(s) and the copyright owner(s) are credited and that the original publication in this journal is cited, in accordance with accepted academic practice. No use, distribution or reproduction is permitted which does not comply with these terms.

frontiers in Marine Science

ORIGINAL RESEARCH
published: 02 July 2021
doi: 10.3389/fmars.2021.664724

Broad-Scale Responses of Harbor Porpoises to Pile-Driving and Vessel Activities During Offshore Windfarm Construction

Aude Benhemma-Le Gall[1], Isla M. Graham[1], Nathan D. Merchant[2] and Paul M. Thompson[1]*

[1] Lighthouse Field Station, School of Biological Sciences, University of Aberdeen, Cromarty, United Kingdom, [2] Centre for Environment, Fisheries and Aquaculture Science (Cefas), Lowestoft, United Kingdom

Offshore windfarm developments are expanding, requiring assessment and mitigation of impacts on protected species. Typically, assessments of impacts on marine mammals have focused on pile-driving, as intense impulsive noise elicits adverse behavioral responses. However, other construction activities such as jacket and turbine installation also change acoustic habitats through increased vessel activity. To date, the contribution of construction-related vessel activity in shaping marine mammal behavioral responses at windfarm construction sites has been overlooked and no guidelines or mitigation measures have been implemented. We compared broad-scale spatio-temporal variation in harbor porpoise occurrence and foraging activity between baseline periods and different construction phases at two Scottish offshore windfarms. Following a Before-After Control-Impact design, arrays of echolocation click detectors (CPODs) were deployed in 25 km by 25 km impact and reference blocks throughout the 2017–2019 construction. Echolocation clicks and buzzes were used to investigate porpoise occurrence and foraging activity, respectively. In parallel, we characterized broadband noise levels using calibrated noise recorders (SoundTraps and SM2Ms) and vessel activities using AIS data integrated with engineering records. Following an impact gradient design, we then quantified the magnitude of porpoise responses in relation to changes in the acoustic environment and vessel activity. Compared to baseline, an 8–17% decline in porpoise occurrence was observed in the impact block during pile-driving and other construction activities. The probability of detecting porpoises and buzzing activity was positively related to the distance from vessel and construction activities, and negatively related to levels of vessel intensity and background noise. Porpoise displacement was observed at up to 12 km from pile-driving activities and up to 4 km from construction vessels. This evidence of broad-scale behavioral responses of harbor porpoises to these different construction activities highlights the importance of assessing and managing all vessel activities at offshore windfarm sites to minimize potential impacts of anthropogenic noise.

Keywords: anthropogenic disturbance, cumulative impacts, offshore windfarm, passive acoustic monitoring, underwater noise, behavioral response, foraging, marine mammal conservation

OPEN ACCESS

Edited by:
Kerri D. Seger, Applied Ocean Sciences, United States

Reviewed by:
Roel Müller, Defense, Safety and Security, Netherlands Organization for Applied Scientific Research (TNO), Netherlands
Tristan Lippert, Aqustix, Germany

****Correspondence:***
Aude Benhemma-Le Gall
a.benhemma-legall.17@abdn.ac.uk

Specialty section:
This article was submitted to Marine Ecosystem Ecology, a section of the journal Frontiers in Marine Science

Received: *05 February 2021*
Accepted: *25 May 2021*
Published: *02 July 2021*

Citation:
Benhemma-Le Gall A, Graham IM, Merchant ND and Thompson PM (2021) Broad-Scale Responses of Harbor Porpoises to Pile-Driving and Vessel Activities During Offshore Windfarm Construction. Front. Mar. Sci. 8:664724. doi: 10.3389/fmars.2021.664724

INTRODUCTION

Offshore windfarm developments are currently expanding in response to global efforts to meet decarbonization targets. Many countries aim to generate significant proportions of electricity from offshore wind sources by 2030 (BEIS, 2019), but these developments must be in line with international conservation agreements such as the EU Habitats Directive 92/43/EEC and Environmental Impact Assessment 2014/52/EU Directives (Le Lièvre, 2019). This requires assessment and mitigation of construction, operation and decommissioning activities to reduce potential impacts on marine wildlife. In particular, there have been concerns over the effect of high levels of underwater noise from different anthropogenic activities on cetaceans, with potential to cause either injury or behavioral disturbance (Richardson et al., 1995; Dolman and Simmonds, 2010; Bailey et al., 2014).

Harbor porpoises (*Phocoena phocoena*), protected under the EU Habitats and Species Directive, are the most common cetacean species in offshore energy development sites within the North Sea (Thomsen et al., 2011; Hammond et al., 2013; Waggitt et al., 2020). Due to their high metabolic requirements, harbor porpoises are vulnerable to starvation (Wisniewska et al., 2016, 2018; Kastelein et al., 2019; Booth, 2020) and, as a consequence, could be especially vulnerable to anthropogenic disturbance. In exposed areas, such as offshore windfarm sites, individuals have to make trade-offs between using energy to leave the area or remaining in exposed areas and tolerating higher levels and/or rates of disturbance (Frid and Dill, 2002). These decisions are likely to be individual-based, context-dependent and site-specific, impacting individual activity budgets and fitness through reduced foraging performance (Booth, 2020). As such, animals may be responding to natural environmental variation, and a variety of different anthropogenic stressors such as fisheries, shipping noise and construction activity. In turn, either individually or in combination, this may have significant long-term biological consequences at a population level (Pirotta et al., 2014a).

The construction and operation of offshore windfarms involves a variety of vessels and activities that could each generate many types of anthropogenic noise that potentially disturb harbor porpoises or other marine mammals. Previously, however, impact assessments have focused on the loudest of these sources; impulsive noise from the pile-driving hammers used to install turbine foundations at most offshore windfarms (Madsen et al., 2006). Where these piling methods are used, mitigation typically involves either minimizing the likelihood that animals are within the injury zone when piling is initiated (Thompson et al., 2020), or using noise abatement techniques such as bubble curtains (Dähne et al., 2017). Extensive research conducted around North Sea windfarm sites has demonstrated that harbor porpoises may be displaced at distances of up to 26 km from piling (e.g., Tougaard et al., 2009; Brandt et al., 2011; Scheidat et al., 2011; Dähne et al., 2013; Haelters et al., 2015; Brandt et al., 2018). However, porpoises are also known to be displaced by vessel noise at distances of up to 7 km (Hermannsen et al., 2014; Dyndo et al., 2015; Wisniewska et al., 2018), with the level of response dependent upon vessel type and behavior (e.g., heading, speed) (Oakley et al., 2017; Hermannsen et al., 2019). Furthermore, even where animals are not displaced, porpoise foraging efficiency may be temporarily affected by exposure both to impulsive noise (Pirotta et al., 2014a; Sarnocińska et al., 2020) and vessel noise (Wisniewska et al., 2018).

Whilst previous studies recognized that construction vessel activity influenced porpoise displacement around pile-driving activities (Brandt et al., 2018; Graham et al., 2019), there remains uncertainty over the cumulative effects of different windfarm construction activities on displacement, foraging efficiency and population fitness. From a management perspective, this constrains efforts to assess and mitigate potential disturbance from windfarm construction activities other than pile-driving. For example, the installation of jackets, turbines and cables may also disturb animals by altering acoustic habitats through intense vessel activity (Merchant et al., 2012; Merchant et al., 2014). Consequently, there may be opportunities to better manage vessels throughout construction and operation to minimize cumulative impacts of shipping movements that could affect harbor porpoise occurrence and behavior. Furthermore, efforts to reduce impulsive noise levels during intermittent periods of pile-driving may result in longer-term noise from additional vessels. Better data on how harbor porpoises respond to different construction and operational phases of windfarm construction is therefore required to understand how different conservation interventions could affect broad-scale habitat displacement and foraging success, particularly within harbor porpoise Special Areas of Conservation (SAC) (JNCC and Natural England, 2019).

In this study, we aimed to compare broad-scale spatio-temporal variation in harbor porpoise occurrence and foraging activity between baseline periods and different phases of construction at two offshore windfarms in the Moray Firth, NE Scotland. The Beatrice offshore windfarm (commissioned in 2019) is composed of 84 (7 MW) turbines and two substations mounted on quadrapod jackets, while the Moray East offshore windfarm (to be commissioned in 2021) will have 100 (9.5 MW) turbines and three substations mounted on tripod jackets. Previous studies in this area used two complementary approaches to assess harbor porpoise responses to impulsive noise from seismic surveys (Thompson et al., 2013; Pirotta et al., 2014a) and pile-driving (Graham et al., 2019). First, Before-After Control-Impact (BACI) designs (Underwood, 1992; Smith, 2002) were used to determine whether variations in porpoise occurrence (Thompson et al., 2013) and activity (Pirotta et al., 2014a) were related to these anthropogenic disturbances. Second, impact gradient sampling designs (Ellis and Schneider, 1997) were also applied in each of these studies to estimate the spatial scale of effects (Graham et al., 2019). Here, we build on these studies, using a BACI design to determine how porpoise occurrence and activity were impacted during different construction phases, and a gradient design to explore how responses varied in relation to the distance from piling vessels as they undertook different activities. Finally, we characterized finer-scale variation in vessel activity and noise levels during different phases of construction and explored how these influenced spatio-temporal variation in porpoise occurrence and activity within the construction sites.

MATERIALS AND METHODS

Study Area and Context

The study was carried out in 2017, 2018, and 2019 during the construction of the Beatrice Offshore Windfarm and the first phase of construction at Moray East Offshore Windfarm (**Figure 1**). Beatrice was constructed between March 2017 and May 2019. From April 2017 to December 2017, an anchored piling vessel used impulsive pile-driving to install four 2.2 m diameter steel piles at 86 locations (Graham et al., 2019). Jackets were then installed onto each set of foundation piles between August 2017 and August 2018 using a jack-up vessel. This vessel was also used to install towers, nacelles and blades on each jacket, and the windfarm was fully operational in May 2019 (see **Figure 1**). Other activities such as boulder removal, inter-array and export cable installation and protection took place during

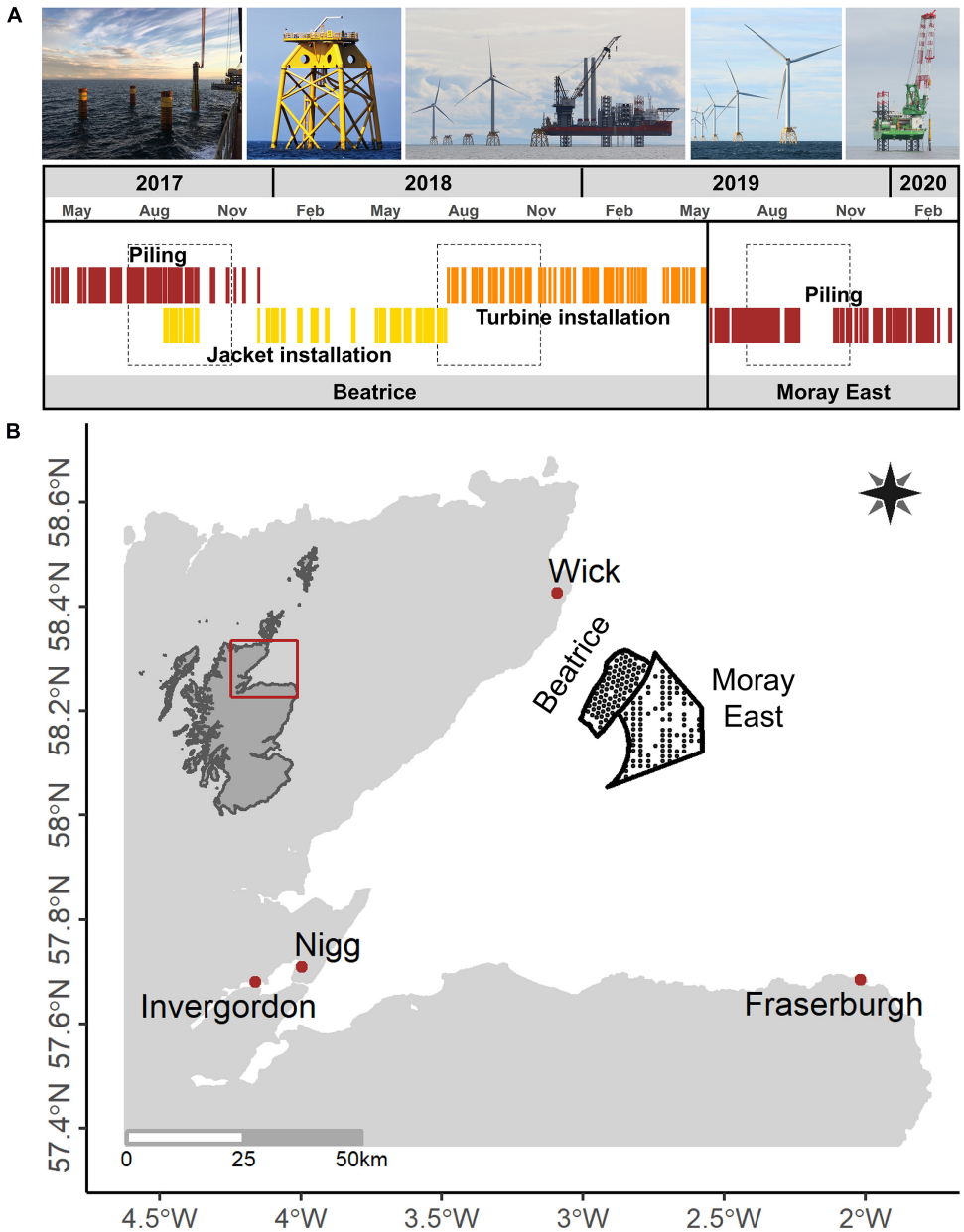

FIGURE 1 | (A) Timeline of key construction activities at two offshore windfarms, between 2017 and 2019, i.e., pile-driving at Beatrice and Moray East (in red), jacket foundation installation at Beatrice (in yellow), wind turbine installation at Beatrice (in orange); the time periods used in the Before-After Control-Impact models to compare baseline periods with key construction activities are represented with dashed rectangles. **(B)** Map showing the location of the Moray Firth in Scotland, the Beatrice and Moray East windfarm boundaries (black line) and turbine locations (black dots), and the harbors used as construction bases (red dots); Source (first picture): Beatrice Offshore Wind Limited.

the windfarm construction phase but were not investigated specifically in this study. Construction at Moray East started in May 2019 and the windfarm is anticipated to be fully operational in 2021. Between May and December 2019, a jack-up vessel used impulsive pile-driving to install three 2.5 m diameter steel piles at the first 90 Moray East locations. There was no overlap between the piling campaign and the jacket foundation installation phase at Moray East (see **Supplementary Table 1**).

Passive Acoustic Monitoring

Sampling Design and Data Collection

Following the sampling design used by Thompson et al. (2013), we investigated variation in harbor porpoise occurrence and buzzing activity using arrays of echolocation click detectors (V.0 and V.1 CPODs[1]). These devices were deployed (a) in a 25 km by 25 km impact and reference block throughout construction in 2017, 2018, and 2019 and (b) along a gradient of exposure from construction activities within the two windfarm sites (**Figure 2**). These data were also compared to baseline data that had been collected in 2010 and 2011 to support Environmental Impact Assessments (EIA) (Beatrice Offshore Windfarm Limited, 2012; Moray Offshore Renewables Limited, 2012). In parallel, calibrated noise recorders (Ocean Instruments SoundTrap and Wildlife Acoustics SM2M) were deployed at three locations to characterize variation in underwater noise levels (**Figure 3** and **Supplementary Figures 1A,B**).

Measuring Variation in Harbor Porpoise Occurrence

Echolocation click characteristics (e.g., time of occurrence, duration, center frequency, bandwidth) logged by the CPODs were processed and extracted with the manufacturer's software CPOD.exe (v2.044). The standard built-in "KERNO" classifier allocates click trains into one of four signal classes (Narrow Band High Frequency "NBHF," "Other cetaceans," "Boat Sonars" and "Unclassified") and one of four quality categories (high "Hi," moderate "Mod," low "Lo" and doubtful "?"). No information on the design of the classifier is currently available, but based on the manufacturer's CPOD manual (Tregenza, 2014), the classification algorithm searches for specific click parameters and inter-click intervals within trains (Clausen et al., 2019). High and moderate quality NBHF echolocation click trains of porpoise origin were extracted as Detection Positive Minutes per hour and then converted into presence-absence of porpoise detections per hour to assess hourly porpoise occurrence.

To extend endurance, CPODs are typically set up to log a maximum of 4,096 clicks per minute. This means that high levels of background noise can quickly saturate the CPODs and prevent any further data logging until the start of the next minute (Wilson et al., 2013). Additionally, the probability of detecting acoustic signals can be affected by the acoustic environment (Clausen et al., 2019). To estimate the distance at which CPODs were unlikely to saturate because of piling or construction vessel noise around each turbine site, we first extracted the number of unfiltered clicks (*Nall*) logged per minute by each device during the 10 months of piling activity in 2017. We then summarized these data in relation to distance from the piling vessel (**Supplementary Figure 2**) and took a conservative approach to prevent false-negative detections; discarding all data from CPODs within 2 km of the piling vessel and all hours with less than 60 min logged.

Estimating Variation in Harbor Porpoise Foraging Activity

We used variation in inter-click intervals (ICIs) to identify buzzes and provide a proxy for foraging activity (Pirotta et al., 2014b). The ICIs of logged NBHF click trains were calculated, normalized by natural log-transformation and categorized into three groups representing specific biological processes. The first group represents the high repetition rate click trains called buzzes that may be used for both foraging activity and social communication (Sorensen et al., 2018; Sarnocińska et al., 2020). Currently, it is not possible to distinguish between these two behaviors but, as in earlier studies (Pirotta et al., 2014a,b; Sarnocińska et al., 2020), we assumed that buzzes can be used as a proxy for foraging. The second group includes regular click trains and the third group represents the time between different click trains (Pirotta et al., 2014b). To identify the multimodal distribution of ICIs and allocate each ICI to one of the processes, Gaussian mixture models were fitted to the time series of ICIs, using the package *mixtools* (Benaglia et al., 2009) in R (v 3.6.0) (R Core Team, 2019). The number of component distributions k was initially set equal to three. However, at some locations, the low number of ICIs prevented the model from identifying the distribution centered on the buzz ICIs and so the number of components (k) was increased to four. If the model still did not discriminate the buzz ICI distribution using four components, data were pooled, so that datasets with higher proportions of buzz ICIs helped identify the buzz ICIs in datasets with overall lower numbers of detections. Additionally, when models did not converge after 1000 iterations, we increased the number of iterations to 2000 (and on one occasion reduced the convergence precision (epsilon) to 0.0001). Mixture models with 3 or 4 components were compared, choosing the model with the maximum loglikelihood. Results from the best model were then used to categorize each ICI into one of the three processes (e.g., **Supplementary Figure 3**) and the number of buzzes, regular and inter-train interval clicks were summarized per hour. The number of buzzes was converted into binary presence-absence of buzzes per hour, reducing the potential bias due to differences in sensitivity and detection range between acoustic devices and locations, respectively.

Before-After Control-Impact Analyses of Variation in Porpoise Occurrence and Foraging Activity in Relation to Different Phases of Windfarm Construction

For the BACI models, variation in both porpoise occurrence and foraging activity within each 25 km by 25 km block (**Figure 2**) were compared between the baseline and each monitoring phase. These analyses focused on data collected between July

[1] www.chelonia.co.uk

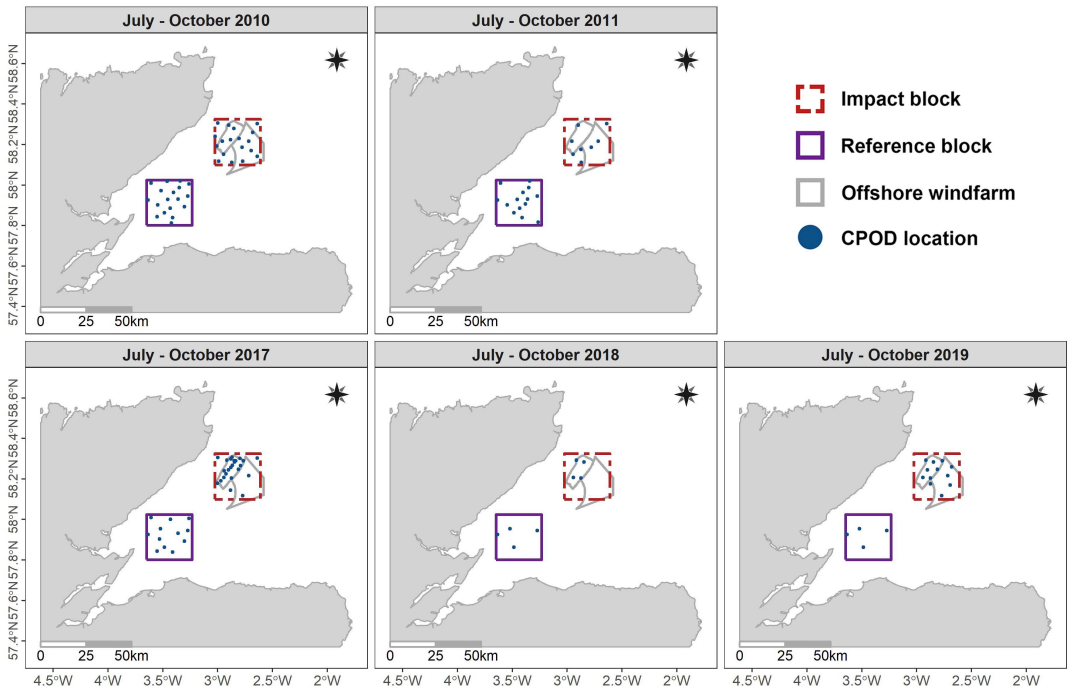

FIGURE 2 | Spatio-temporal distribution of echolocation click detectors (CPODs) within the reference and impact blocks and the offshore windfarms between 2010 and 2019.

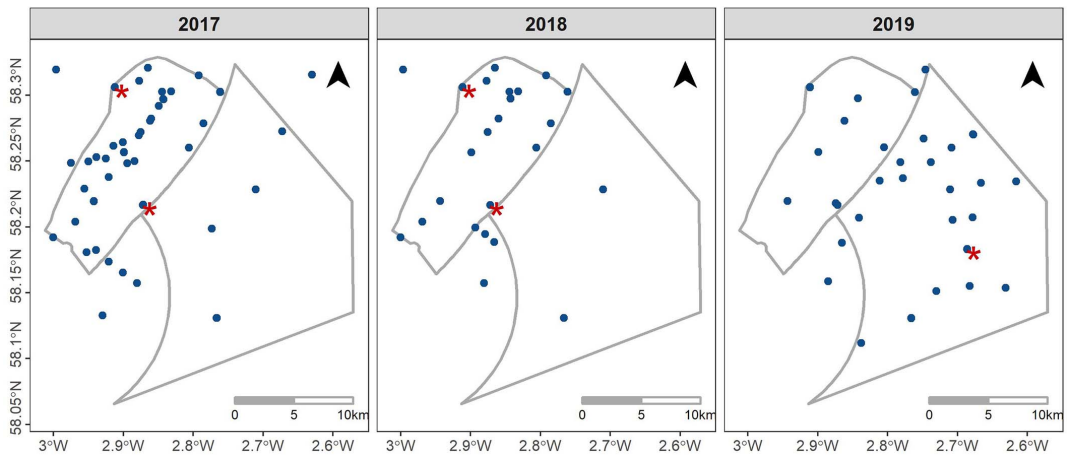

FIGURE 3 | Spatio-temporal distribution of the Passive Acoustic Monitoring array, CPODs (blue circles) and noise recorders (red stars), within and around the two offshore windfarms between 2017 and 2019.

TABLE 1 | Sampling effort used for the Before-After Control-Impact models.

Monitoring phases		Reference block		Impact block	
		# CPOD sites	# Days	# CPOD sites	# Days
Baseline	July–October 2010	18	110	18	122
	July–October 2011	15	110	9	123
Beatrice piling	July–October 2017	9	122	24	123
Beatrice turbine installation	July–October 2018	4	123	4	123
Beatrice operation – Moray East piling	July–October 2019	4	122	16	123

and October when comparable data were available in all years (see **Table 1**). Baseline data used in both windfarm EIAs were collected in 2010 and 2011 (Moray Offshore Renewables Limited, 2012). As seismic surveys were conducted in the current study's reference block between 1 and 11 September 2011, we excluded these data from the analyses. For the BACI modeling, the Beatrice piling phase was from July to October 2017, during which 221 piling events occurred at 52 turbine locations and 24 jackets were installed. The turbine installation phase was from July to October 2018, during which 32 turbines and the last 6 jackets were installed. The Moray East piling phase, from July to October 2019, included 165 piling events at 47 turbine locations. No further construction work occurred at Beatrice during this time period, but operations and maintenance vessels visited the site regularly once it became fully operational in May 2019 (**Figure 2**).

Spatial Scale of Porpoise Responses to Different Piling Vessel Activities

An impact gradient approach was used to assess finer scale variation in porpoise occurrence and buzzing activity in relation to distance from the piling vessels at both Beatrice and Moray East as they undertook different construction activities in 2017 and 2019. The position of each piling vessel was extracted from an Automatic Identification System (AIS) vessel-tracking dataset for the Moray Firth region. The mean and minimum distance between each CPOD and the piling vessel were then calculated for each monitoring hour, using the *sf* package (Pebesma, 2018). Information on the activity of the vessels was extracted from the developers' daily construction reports, and the factor "piling" or "no piling" was allocated to each hour monitored. Distance from the piling vessel was used as a proxy for the distance from construction activities (i.e., the noise/disturbance source), as the piling vessel was supported by two pilot vessels for anchoring, at Beatrice, and a tug bringing the piles on site. Hourly porpoise occurrence and buzzing activity were each modeled as a function of distance from the piling vessel in interaction with the vessel's activity ("piling"/"no piling") (**Table 2**).

Characterizing Vessel Activity

To characterize variation in the extent to which harbor porpoises were exposed to both piling vessels and other construction vessels, we integrated data from the developers' engineering records with AIS vessel-tracking data (Wright et al., 2019). AIS data for the entire Moray Firth were sourced at 5 min (2017) or 1 min (2018 and 2019) resolution from Astra Paging Ltd.[2] and Anatec Ltd.[3].

A 4 km by 4 km grid was created across the Moray Firth and the area of each grid cell calculated after any grid cells overlapping coastlines were cropped. AIS data were projected into WGS84 UTM 30N and then processed to produce hourly summaries a) within each of these grid cells and b) within a 5 km buffer around each of the passive acoustic monitoring sites. AIS data were interpolated every 5 min to calculate the time that each individual vessel stayed in a grid cell or buffer area. These data were then used to estimate measures of both vessel density and vessel intensity for each hour within each grid cell or buffer area. These two metrics provide complementary information highlighting variation in vessel behavior and distribution across the Moray Firth. At windfarm sites, construction-related vessels are often stationary for several hours, while other vessels (not involved in the construction) are likely to be transiting and consequently contribute less to the overall vessel intensity. Here, we defined vessel density as the number of individual vessels present in that hour per kilometer squared, and vessel intensity as the sum of residence times for all vessels present in that hour per kilometer squared. The minimum and mean distance from each CPOD or noise recorder to all vessels within each buffer area were also calculated and summarized for each hour and location.

Information on the vessels involved in the windfarm construction was extracted from the developers' weekly construction reports and used to filter AIS data to provide separate measures of vessel density and intensity (a) for construction vessels and (b) for other third-party marine traffic. To estimate the vessel density and intensity within each of the windfarm construction sites, these AIS data were filtered by location, and vessels were categorized following Table 1 in Metcalfe et al. (2018).

Variation in Background Noise Levels at the Construction Site

Underwater broadband noise recorders were deployed for periods of 2–6 months at three sites within the impact block to characterize noise levels in different phases of construction (**Table 3**, **Figure 4**, and **Supplementary Figure 1**). Recorders collected data at sampling rates of either 48 or 96 kHz, with duty cycle rates varying depending upon device and sampling

[2]www.astrapaging.com
[3]www.anatec.com

TABLE 2 | Sampling effort used for the gradient models, within the impact block, to assess harbor porpoise responses to pile-driving activities at Beatrice between March and December 2017 and Moray East between May and December 2019; mean harbor porpoise occurrence and mean foraging activity when porpoises were detected during and outside piling hours.

Windfarm (year)	Piling phase	Porpoise occurrence				Buzzing activity			
		# Site	# Day	# Hour	Mean per hour	# Site	# Day	# Hour	Mean per hour
Beatrice (2017)	No piling	34	204	54,467	0.319	34	204	17,387	0.279
	Piling	34	102	4,816	0.195	31	89	939	0.285
Moray East (2019)	No piling	29	219	83,841	0.458	23	219	29,166	0.348
	Piling	29	104	7,773	0.321	23	103	1,883	0.363

TABLE 3 | Sampling effort to investigate harbor porpoise responses to vessel activity and underwater broadband noise levels.

PAM devices	2017		2018		2019	
	# Site	# Day	# Site	# Day	# Site	# Day
CPOD	40	317	24	342	30	275
Noise recorder	2	128	2	252	1	97

rates (**Supplementary Table 2**). Data were processed in MATLAB following Merchant et al. (2015). Broadband noise levels were quantified between 25 Hz and 24 kHz to provide hourly root-mean-square (RMS) averaged sound pressure levels (SPL) in decibels (dB) relative to a reference pressure of 1 μPa (Kinsler et al., 1999; Merchant et al., 2015).

Modeling

BACI Models

To compare between the baseline and each construction phase, the hourly occurrence of porpoise detections and buzz detections were modeled as binomial response variables using six Generalized Linear Mixed-effects Models (GLMM). For each model, the link function was chosen based on the lowest Akaike Information Criterion (AIC), using either the *cloglog* or *probit* link function. The interaction between block and construction phase was used as the explanatory variable in all models.

Based on previous studies and preliminary data analyses, it was known that porpoises display diel and seasonal patterns in occurrence and foraging activity in this study area (Williamson et al., 2017; Graham et al., 2019). To focus on changes associated with the windfarm construction, month and diel phase were used as random factors in the BACI model. Diel phase (i.e., sunrise, day, sunset, or night) was allocated based on local sunrise and sunset times. Additionally, the CPOD location was also used as random effect to control for any site-specific environmental differences. To assess the significance of fixed effects and their interactions, a sequential analysis of deviance table (Type II Wald chi-square tests) was computed using the R package *car* (Fox and Weisberg, 2019). For each model, the response variable was predicted and the uncertainty (95% confidence intervals, CI) calculated using a bootstrapping approach (100 simulations) with the *bootMer* function of the *lme4* package (Bates et al., 2015). To validate models, we checked for temporal autocorrelation in model residuals using the partial auto-correlation function. The *DHARMa* package was used to verify the uniformity, dispersion, spatial and temporal autocorrelation of residuals (Hartig, 2020).

Impact Gradient Models

To investigate the spatial scale of the effects of pile-driving, vessel activity and underwater noise on harbor porpoise occurrence and foraging activity, hourly occurrence of porpoise detections and buzz ICIs were modeled as a function of: (1) the interaction between the distance from construction activities and piling

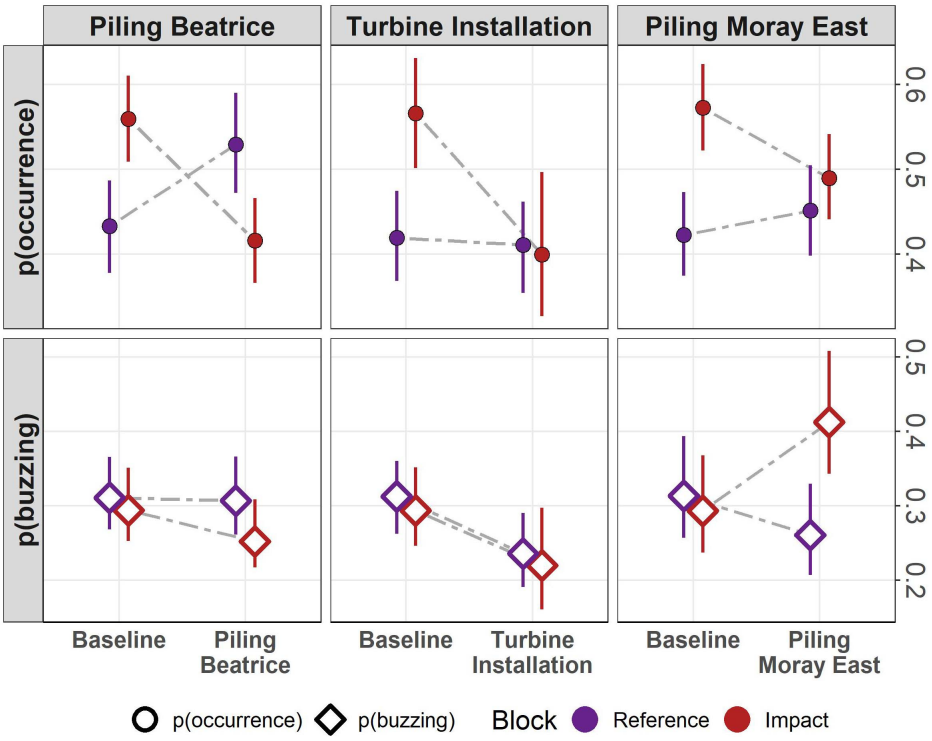

FIGURE 4 | The probability of harbor porpoise occurrence (circle) and buzzing activity (diamond) per hour between the reference (in purple) and impact (in red) blocks and between the baseline monitoring period and key construction activities (i.e., pile-driving and wind turbine installation at Beatrice offshore windfarm and pile-driving at Moray East offshore windfarm).

occurrence (*piling effect* models); (2) the interaction between the vessel intensity per hour and the mean distance from vessels (*vessel effect* models); (3) the averaged broadband sound pressure levels and piling occurrence (*noise effect* models).

For the *piling effect* models, we only considered sites within the impact block to investigate meso-scale response to construction activities. Additionally, we filtered the dataset to explore the magnitude of porpoise responses between 2 and 30 km from the piling vessel as it has been shown in other studies that a response to piling activities was apparent up to 26 km from piling (Tougaard et al., 2009; Dähne et al., 2013; Haelters et al., 2015; Brandt et al., 2016, 2018). Similarly, to investigate porpoise occurrence and activity in relation to broadband noise levels and the presence or absence of piling activity, we used data from the CPODs that were deployed at the same location as the noise recorders (**Figure 3**). Hours in which piling activities occurred within 2 km of these sites were not used in the *noise effect* models.

For the *vessel effect* models, we excluded hours in which piling activities occurred to focus only on the effect of vessels. To prevent masking effects of vessel noise on porpoise echolocation clicks, we followed Pirotta et al. (2014a) and excluded hours in which vessels were within 1 km of CPOD locations.

For the six models, binary generalized linear models with either a *probit* or *cloglog* link function were fitted using generalized estimating equations (GEE-GLMs), to account for temporal autocorrelation. The correlation structure was selected based on the lowest Quasi Information Criterion (QICr), resulting in using an "independence" correlation structure for all models. To determine whether the two-way interaction term should be retained, we used the *dredge* function of the *MuMIn* package, which ranks all model possibilities according to QIC (Barton, 2020). Year, Julian day and site ID were used to define a blocking variable in the GEE, allowing model residuals from each site within each day to be autocorrelated. Wald's tests were used to assess significance and bootstrapped coefficients from the GEE-GLM were used to estimate uncertainty (95% CI) and plot relationships between response and explanatory variables.

RESULTS

Variability in Porpoise Occurrence and Foraging Activity Between Different Phases of Windfarm Construction

In the BACI comparison, variation in harbor porpoise occurrence and foraging activity was best explained by the interaction between block and construction phase (**Figure 4**). The baseline probability of occurrence prior to any construction was around 0.42 in the reference block and 0.55 in the impact block, while the baseline probability of detecting buzz ICIs, when porpoises were present, was around 0.3 for both blocks. In comparison with the baseline, harbor porpoise occurrence significantly decreased by 14.3% in the impact block during the Beatrice piling phase (Wald test: $\chi^2 = 725.267$, $p < 0.001$) and by 8% during the Moray East piling phase (Wald test: $\chi^2 = 126.024$, $p < 0.001$). A decrease in porpoise occurrence (−16.7%) was also observed between the baseline and the Beatrice turbine installation phase (Wald test: $\chi^2 = 6.269$, $p = 0.012$). Despite these significant decreases, harbor porpoises were regularly detected within these construction sites throughout the monitoring period (**Supplementary Figure 4**).

When porpoises were present, the probability of detecting buzz ICIs also significantly decreased by 4.2% between the baseline and piling phase at Beatrice (Wald test: $\chi^2 = 14.216$, $p < 0.001$), although no significant change in buzzing activity was observed during turbine installation (Wald test: $\chi^2 = 0.009$, $p = 0.923$). In contrast, during the Moray East piling phase, the probability of detecting buzzing ICIs increased by 11% in the impact block but decreased by 5% in the reference block (Wald test: $\chi^2 = 176.517$, $p < 0.001$) (**Figure 4**).

Spatial Scale of Porpoise Responses to Different Piling Vessel Activities

During the construction period, finer-scale variation in harbor porpoise occurrence and foraging activity were best explained in the *piling effect* model by the interaction between the distance from the piling vessel and the presence or absence of piling (Beatrice: porpoise occurrence—Wald test: $\chi^2 = 482$, $p < 0.001$; buzzing activity—Wald test: $\chi^2 = 18.3$, $p < 0.001$. Moray East: porpoise occurrence—Wald test: $\chi^2 = 421$, $p < 0.001$; buzzing activity—Wald test: $\chi^2 = 6$, $p < 0.014$). During piling activity, the probability of porpoise occurrence increased significantly with distance from the source vessel in a similar fashion at both sites. When there was no piling activity, occurrence still decreased slightly closer to the vessel (−9.3% at Beatrice; −20.9% at Moray East) (**Figure 5**). During piling activities, when harbor porpoises were acoustically detected, buzzing activity at Beatrice decreased by 54% close to the piling vessel, but this effect was not as strong at Moray East (−40%). Again, when there was no piling activity, the probability of buzzing ICIs at both sites was slightly lower closer to the piling vessel (−19.6% at Beatrice; −22.7% at Moray East) (**Figure 5**).

Response of Porpoises to Vessel Activity at Windfarm Construction Sites

Figures 6A,B summarize the broad-scale spatial variation in the intensity and density of construction-related vessels across the Moray Firth between 2017 and 2019 (for further information on the overall vessel density and intensity across the Moray Firth between 2017 and 2019, see **Supplementary Figures 5A,B**). Over this period, median construction-related vessel density was 1.4 vessels.km^{-2} (range 0.06–64.8 vessels.km^{-2}) across the Moray Firth. Vessel density was highest in 2019 when both windfarms were under construction. Similarly, the median construction-related vessel intensity, across the Moray Firth, was 2.2 h.km^{-2} (range 0–29,006.8 h.km^{-2}). Most vessels occurred over the windfarm sites, but construction-related vessels also worked along export cable routes and between local ports and harbors, including Wick, Invergordon and Fraserburgh (**Figure 1B**).

In addition to the key offshore service vessels used for pile-driving and jacket or turbine installation, construction-related vessel traffic included fishing vessels working as guard vessels, passenger vessels for crew-transfers and some port service craft

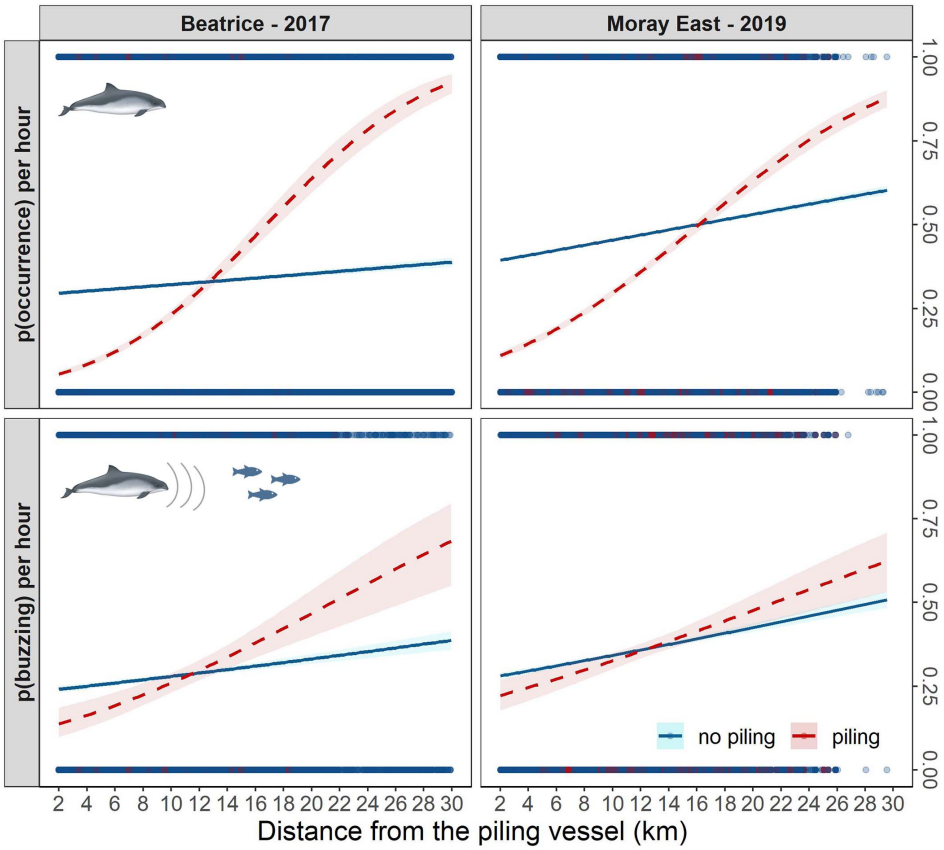

FIGURE 5 | The probability of harbor porpoise occurrence and buzzing activity per hour during (dashed red line) and outwith (blue line) pile-driving hours, in relation to distance from the pile-driving vessel at Beatrice (left) and Moray East (right); confidence intervals (shaded areas) estimated for uncertainty in fixed effects only; points represent the raw data distribution along the distance gradient during piling (red) and no piling (blue) activities; see the raw data frequency distribution in **Supplementary Figure 6**.

or unassigned vessels. Details of vessels used in each development are included in **Supplementary Table 3**.

Safety zones of 500–1,500 m were maintained around structures under construction, and of 50 m around installed structures waiting to be commissioned. Nevertheless, both the Beatrice and Moray East sites remained accessible to fishermen and other third-party vessel traffic throughout their construction. Within the two windfarm sites, the density of fishing, bulk carrier, cargo and unassigned vessels that were not involved in the construction ranged from 0.15 to 0.21 vessels.km^{-2} between 2017 and 2019. Fishing vessel density decreased at Beatrice in 2018 and 2019 and at Moray East in 2019. However, parallel increases in the intensity of fishing vessels suggested that the fishing vessels that were present spent more time in the area (**Table 4**).

During the 245- and 284-day pile-driving campaigns, the piling vessel was within the windfarm footprint for around 4,090 h (69.5% of the time) at Beatrice and 6,525 h (95.7% of the time) at Moray East. However, it should be noted that the piling vessel at Moray East was jacked-up for most of this time. The total number of hours in which piling occurred was around 437 h (7.4% of the time) at Beatrice and 773 h (11.3% of the time) at Moray East.

Estimates of vessel intensity around each of the passive acoustic monitoring sites were similar in 2017 and 2019 (**Figure 7A**), with the third quantile around 1.21–1.28 min.km^{-2} and a peak between 0.6 and 0.9 min.km^{-2}. Although the shape of the distribution of vessel intensities in 2018 was similar, the third quantile was around 1.78 min.km^{-2}, highlighting that vessel activity at Beatrice was higher during the installation of jackets and turbines. There was also spatial variability in vessel density and intensity between years and sites (**Figure 7B**). In 2017, the higher levels of vessel intensity occurred across Beatrice but in 2018 was more localized around the south-east boundary of the windfarm. In 2019, vessel intensity was spread across the two windfarm sites, but levels of vessel intensity remained highest at Beatrice (**Figure 7B**).

Based on the best fit *vessel effect* model, finer-scale variation in harbor porpoise occurrence within the windfarm sites was explained by the interaction between the vessel intensity and the mean vessel distance from each CPOD site within a 5 km buffer area (Wald test: $\chi^2 = 73.3$, $p < 0.001$) (**Figure 8A**). At a mean vessel distance of 2 km, porpoise occurrence decreased by up to 35.2% as vessel intensity increased, decreasing from 0.37 (95% CI: 0.36–0.39) when vessel intensity was zero

TABLE 4 | Density **(A)** and intensity **(B)** of vessels involved or not involved in the construction at Beatrice and Moray East offshore windfarms between 2017 and 2019, grouped by vessel category.

A	**Construction-related vessels**						**Non-construction vessels**					
Vessel density (N boat/km^2)	**Beatrice**			**Moray East**			**Beatrice**			**Moray East**		
Vessel category	**2017**	**2018**	**2019**	**2017**	**2018**	**2019**	**2017**	**2018**	**2019**	**2017**	**2018**	**2019**
Bulk carrier and cargo vessels	0.02	0.03	0.02	0.01	0.01	0.01	0.07	0.02	0.01	0.17	0.17	0.06
Fishing vessels	0.11	0.06	0.02	0.04	0.03	0.02	0.18	0.05	0.08	0.17	0.19	0.12
Military and law enforcement							0.01			0.01	0.00	
Non-port service craft	0.02	0.02		0.01	0.01		0.02	0.02	0.01	0.03	0.05	0.01
Offshore service vessels	0.08	0.15	0.06	0.04	0.07	0.03	0.03	0.02		0.05	0.03	0.01
Passenger vessels	0.01	0.11	0.10	0.00	0.03	0.04	0.04	0.04	0.02	0.12	0.13	0.02
Port service craft	0.15	0.09		0.05	0.05	0.01	0.02	0.02	0.02	0.05	0.04	0.04
Recreation vessels							0.09	0.06	0.06	0.08	0.09	0.13
Research vessels		0.01	0.02		0.00	0.00						
Tankers							0.02			0.04	0.04	0.02
Unassigned	0.09	0.11	0.05	0.06	0.07	0.04	0.15	0.15	0.02	0.16	0.21	0.08
Total	**0.47**	**0.58**	**0.26**	**0.21**	**0.28**	**0.15**	**0.63**	**0.37**	**0.21**	**0.88**	**0.96**	**0.48**
B	**Construction-related vessels**						**Other vessels**					
Vessel intensity (hour/km^2)	**Beatrice**			**Moray East**			**Beatrice**			**Moray East**		
Vessel category	**2017**	**2018**	**2019**	**2017**	**2018**	**2019**	**2017**	**2018**	**2019**	**2017**	**2018**	**2019**
Bulk carrier and cargo vessels	5.73	11.55	14.82	0.17	2.02	0.76	0.06	10.08	0.36	0.26	1.91	0.06
Fishing vessels	62.14	8.73	0.01	4.67	1.25	4.18	0.09	0.72	3.39	1.72	2.93	13.38
Military and law enforcement							0.00			0.01	0.00	
Non-port service craft	2.68	2.49		0.12	0.28		0.00	0.03	0.01	0.04	1.08	0.04
Offshore service vessels	43.27	194.06	82.53	4.36	36.00	19.41	63.16	1.99		2.09	0.23	0.39
Passenger vessels	0.07	77.28	85.35	0.03	0.45	0.20	0.02	8.03	0.03	0.44	0.34	0.10
Port service craft	62.08	10.47		4.57	0.73	0.01	0.27	0.01	0.23	0.15	0.07	0.29
Recreation vessels							0.05	0.02	0.02	0.11	0.15	0.17
Research vessels		0.04	1.57		0.07	0.33						
Tankers							0.01			0.21	0.23	0.01
Unassigned	34.10	115.42	25.13	18.20	14.22	18.13	0.07	4.72	0.18	7.62	23.10	1.79
Total	**210.07**	**420.05**	**209.41**	**32.13**	**55.01**	**43.03**	**63.75**	**25.60**	**4.23**	**12.65**	**30.04**	**16.23**

A white to red gradient was used with the highest values in vessel density and intensity represented in red.

(0 min.km^{-2}) to 0.02 (95% CI: 0.01–0.05) for a vessel intensity of 9.8 min.km^{-2}. Porpoise responses decreased as the mean vessel distance increased (−24% at 3 km) until no apparent response was observed at 4 km (+ 7.2%).

Vessel intensity also had a significant effect on the probability of buzzing (Wald test: $\chi^2 = 110$, $p < 0.001$). Throughout the 3 years, the probability of detecting buzzes in each hour that porpoises were present decreased by up to 24.5%, from 0.32 (95% CI: 0.32–0.33) when vessels were absent to 0.08 (95% CI: 0.06–0.11) for hours with a vessel intensity of 9.17 min.km^{-2} (**Figure 8B**). Mean distance to the vessel had no significant effect on the probability of detecting buzzes.

Variation in Occurrence and Foraging Activity of Porpoises in Relation to Noise

Both averaged broadband sound pressure levels in each hour (Wald test: $\chi^2 = 28.4$, $p < 0.001$) and piling occurrence (Wald test: $\chi^2 = 57.7$, $p < 0.001$) had significant effects on the probability of detecting harbor porpoises. Outside piling hours, porpoise detections decreased by 17% as SPL increased, decreasing from 0.44 (95% CI: 0.39–0.48) at 102 dB re 1 μPa to 0.26 (95%CI: 0.2–0.34) at 159 dB re 1 μPa. During piling activities, porpoise occurrence was initially lower (0.16 95% CI: 0.11–0.23 at 102 dB re 1 μPa) and decreased by 9% as SPL increased by 59 dB (0.07 95% CI: 0.04–0.12 at 159 dB re 1 μPa) (**Figure 9A**).

Similarly, variation in the probability of detecting buzzes was also explained by both SPL (Wald test: $\chi^2 = 19.53$, $p < 0.001$) and piling occurrence (Wald test: $\chi^2 = 8.73$, $p < 0.01$). However, while the probability of detecting buzzes decreased with increasing noise levels in either the presence or absence of piling, porpoises detected during piling exhibited higher levels of buzzing activity (**Figure 9B**). Outside piling hours, the probability of detecting buzzes decreased by up to 41.5% as the SPL increased, ranging from 0.44 (95% CI: 0.36–0.53) at 104 dB re 1 μPa to 0.03 (95% CI: 0.01–0.08) at 155 dB re 1 μPa. During piling hours, buzzing

occurrence decreased by up to 61.8% as the SPL increased, ranging from 0.76 (95% CI: 0.53–0.92) at 104 dB re 1 μPa to 0.15 (95% CI: 0.04–0.35) at 155 dB re 1 μPa (**Figure 9B**).

DISCUSSION

Uncertainties exist over the extent to which marine mammal occurrence and foraging activity varies through different phases of offshore windfarm construction. This, in turn, currently constrains efforts to balance the development of renewable energy to meet carbon reduction targets with the need to minimize disturbance to protected wildlife populations. Our BACI analyses provide evidence of broad-scale behavioral responses of harbor porpoises both to pile-driving and other construction-related activities (**Figure 4**). In addition, impact gradient analyses show that the magnitude of response varied depending on the activity type and distance from the disturbance source (**Figure 5**), and the cumulative pressure associated with vessels (**Figure 8**) and anthropogenic noise (**Figure 9**). Together, these analyses allowed us to quantify response levels during different construction contexts, while also highlighting that harbor porpoises continued to regularly use these sites throughout the 3-year construction period (**Supplementary Figure 4**). These findings now provide new data to parameterize energetics and population simulation models [e.g., DEPONS Nabe-Nielsen et al. (2018) and iPCoD Booth et al. (2017)] that can explore potential population-level consequences of these cumulative disturbances.

Changes in Porpoise Occurrence During the Two Piling Campaigns

As expected from previous studies of harbor porpoise responses to impulsive noise both at this (Thompson et al., 2013; Graham et al., 2019) and other (Tougaard et al., 2009; Brandt et al., 2011; Dähne et al., 2013; Haelters et al., 2015; Nabe-Nielsen et al., 2018). North Sea sites, our BACI analyses demonstrated a significant decrease in porpoise detections when pile-driving occurred at both the Beatrice and Moray East windfarm sites (**Figure 4**). In the BACI analyses, the observed changes in porpoise occurrence and buzzing activity between blocks and monitoring periods may be confounded by the varying sampling effort although similar relationships were found using the impact gradient analyses. In PAM based studies such as this, it is recognized that short-term decreases in acoustic detections could result from animals ceasing to vocalize rather than being displaced. However, given the high energetic requirements and foraging rates of harbor porpoises (Booth, 2020), the broader-scale changes observed here are most likely to result from avoidance behavior leading to lower densities over the impact block. In the German North Sea, the decrease in relative porpoise acoustic detection rates within 10 km of the pile-driving noise source, was associated with an increase in detection rates at 25 and 50 km distance, and matched the lower porpoise density, observed through visual aerial surveys, within 20 km of the noise source (Dähne et al., 2013). Similar findings were observed in response to seismic surveys over a range of 5–10 km in Thompson et al. (2013) and in response to a seal scarer in Brandt et al. (2013). In these studies, the aerial surveys supported the assumption that porpoises exposed to anthropogenic noise sources such as pile-driving, airgun and acoustic deterrent devices left the ensonified area rather than ceasing vocalizing. Consequently, even though our study relied solely on PAM data, decreases in acoustic detections in response to impulsive noise disturbance is likely to result from displacement. Approaches used for assessing the spatial scale of responses to piling have varied across studies. Nevertheless, our observed responses at distances of 10–15 km at both sites (**Figure 5**) are of a similar order of magnitude to results from the subset of Beatrice sites analyzed in Graham et al. (2019) and those from other North Sea windfarms (Tougaard et al., 2009; Brandt et al., 2011; Dähne et al., 2013; Haelters et al., 2015; Nabe-Nielsen et al., 2018). One limitation of using CPODs in these situations is that elevated background noise close to piling locations may affect detection probability (Clausen et al., 2019). When analyzing the magnitude of near-field responses to pile-driving (**Figure 5**), we accounted for this by excluding data from all CPOD locations that were within 2 km of the piling vessel.

Although patterns in porpoise detections were similar during the piling campaigns at the two Moray Firth sites, the magnitude of change in porpoise occurrence during the Moray East piling phase was lower than at Beatrice (**Figure 4**). Graham et al. (2019) showed that responses to pile driving noise at Beatrice diminished through 2017. The scale of response at Moray East in 2019 may therefore be smaller due to the increased tolerance of individuals remaining in the area (Bejder et al., 2009). However, little is known of broader-scale movement patterns of North Sea porpoises (see Sveegaard et al., 2011) and it is not currently possible to follow individual porpoises over multiple years. Thus, it remains unclear whether or not displaced individuals returned to impacted areas or whether porpoises exposed in 2017 were still present in subsequent years (Graham et al., 2019). Alternatively, variation in the magnitude of response in the two piling phases could result from local changes in habitat quality or other differences in the nature of the disturbance during pile-driving. For example, our impact block was large, and included both windfarms. Thus, during the 2019 Moray East piling phase, the northern part of the impact block also contained 86 operational structures within the Beatrice windfarm. Harbor porpoise occurrence in this part of the impact block could therefore have increased, as seen in the Egmond aan Zee windfarm in Dutch waters (Scheidat et al., 2011). Scheidat et al. (2011) suggest that such changes could result from increases in prey due to artificial reef effects within established windfarms, or because most shipping is excluded from Dutch windfarm sites; potentially allowing porpoises to shelter from vessel disturbance. However, our analysis of AIS data suggests that a sheltering effect is unlikely in the Moray Firth as there continued to be high levels of windfarm and third-party traffic over the Beatrice site in 2019 (**Figure 6**). Finally, the two piling campaigns used different installation infrastructure that may explain observed differences between the responses in 2017 and 2019. The piling vessel at Beatrice used eight anchors, requiring the presence of additional pilot and anchor-handling vessels, while an independent jack-up piling vessel was used at Moray East. Our study design did not

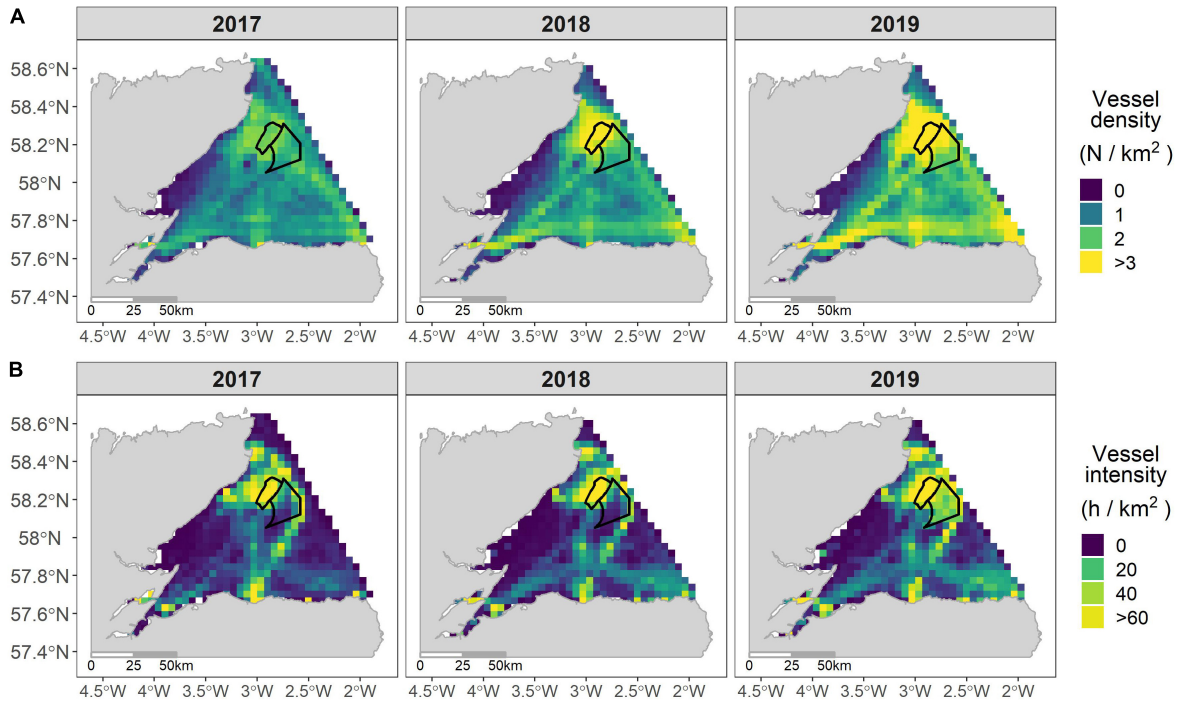

FIGURE 6 | Construction-related vessel density (number of vessels/km^2) **(A)** and intensity (h/km^2) **(B)** in the Moray Firth (4 × 4 km grid) between 2017 and 2019; Black lines are the boundaries of the two offshore windfarms in development; the upper limit of both the vessel density and intensity color scales is greater than 95th percentile.

enable us to discriminate between the fine and meso-scale spatio-temporal impact of this diverse range of construction-related activities, but these findings highlight the need for further work to explore how different pile installation techniques may affect the scale of response.

Changes in Porpoise Activity During the Two Piling Campaigns

Building on previous work that has focused on displacement during pile-driving, we also used information from the echolocation click characteristics to explore broad-scale changes in the activity of those porpoises that continued to use the windfarm sites. During an earlier seismic survey in this area, harbor porpoise occurrence decreased close to the noise source (Thompson et al., 2013), and animals remaining in exposed areas also exhibited a decrease in buzzing activity (Pirotta et al., 2014a). In the present BACI study, porpoises that remained in the impact block during pile-driving at Beatrice in 2017 also reduced their buzzing activity by 4.2% compared to baseline but, in contrast, buzzing activity during Moray East piling in 2019 was higher than baseline (**Figure 4**). As discussed in relation to differences in the magnitude of displacement during the two piling campaigns, differences in buzzing activity of porpoises remaining in the impact area may also result from local changes in habitat quality. The introduction of hard substrates (e.g., jacket foundations and scour protection) are likely to have enhanced the fine-scale habitat and changed fish assemblages, potentially increasing the prey availability for opportunistic and generalist feeders such as porpoises (Santos and Pierce, 2003) and explaining higher buzzing activity during this period. Better understanding of any reef effects following construction is now urgently required so that potential ecosystem benefits can be integrated into an evaluation of the lifetime cumulative impacts of windfarm construction and operation on these populations (King et al., 2015; Booth et al., 2017; Nabe-Nielsen et al., 2018).

Within the impact area, gradient analyses of data collected through both piling phases also suggest that the probability of detecting buzzes decreased by 54% with decreasing distance from the piling vessel (**Figure 5**), and by 61.8% as hourly RMS SPL increased from 104 to 155 dB re 1 μPa (**Figure 9B**). Thus, individuals remaining nearest exposed areas did spend less time buzzing, while porpoises displaced from exposed areas increased their buzzing activity, potentially compensating for lost foraging opportunities or increased energy expenditure. During extended periods of disturbance, porpoises must make trade-offs between fleeing, either permanently or temporarily, or remaining in areas that have a higher risk of disturbance or predation. Baseline distribution patterns suggest that the vicinity of both impact and reference areas represent high-quality feeding habitat (Brookes et al., 2013), and fleeing the area may incur high energetic costs and the risk of spending time in lower-quality habitat. Individual responsiveness to anthropogenic disturbances is therefore likely to be context-dependent and related to animal fitness (van Beest et al., 2018).

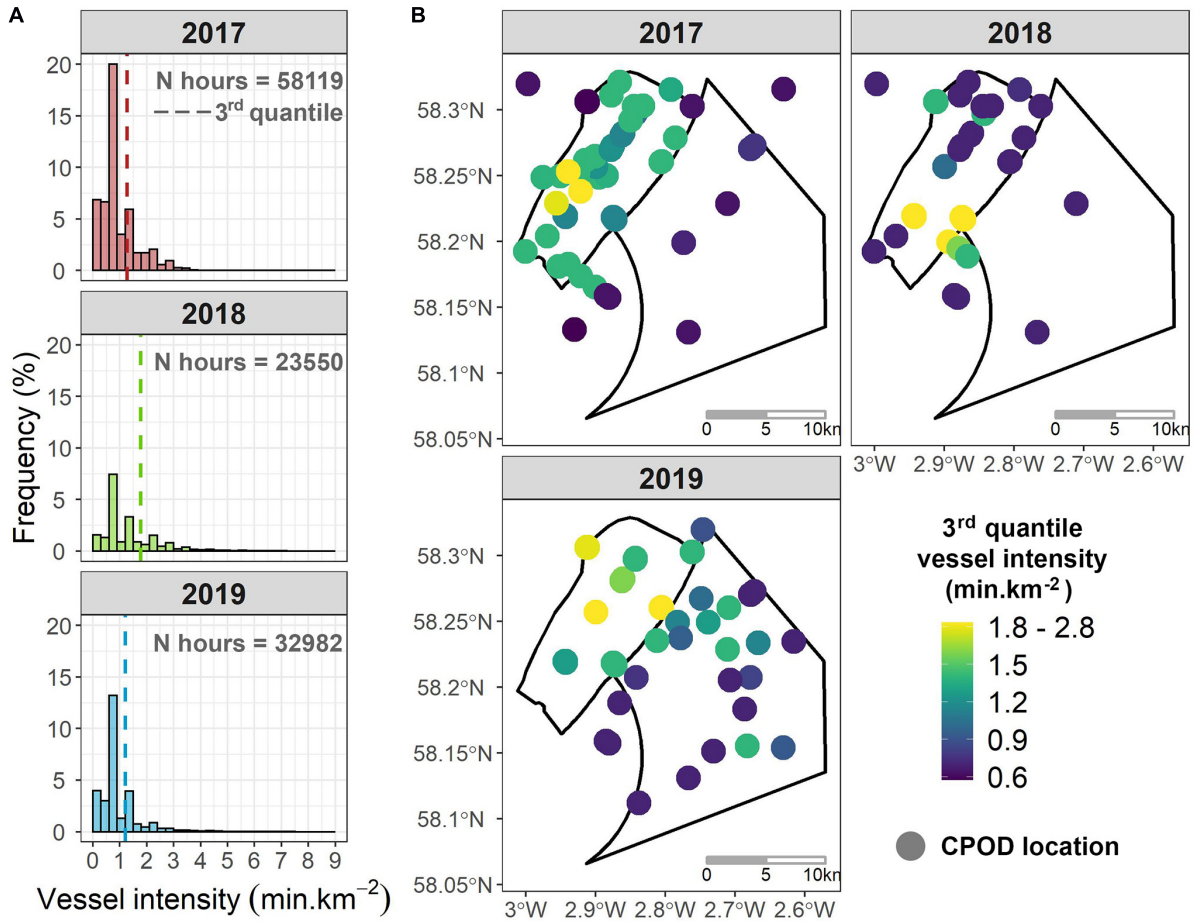

FIGURE 7 | (A) Histograms of the vessel intensity (min.km^{-2}) per hour in 2017 (pink), 2018 (green), 2019 (blue); dashed lines represent the third quantile of vessel intensity per hour; the sample size is showed by the number of hours monitored per year (N hours); **(B)** spatio-temporal distribution of the vessel intensity per hour within and around the two offshore windfarms between 2017 and 2019; the color gradient indicates the annual third quantile of vessel intensity within a 5 km buffer of each CPOD site.

Theoretically, individuals in poorer condition are less likely to leave high-quality habitats after a disturbance, as the energetic cost and risk of missing foraging opportunities may be too high (Gill et al., 2001; Beale and Monaghan, 2004; van Beest et al., 2018). In this seascape of fear, marine mammals can alter activity budgets according to perceived levels of predation risk (Wirsing et al., 2008), and are expected to perceive anthropogenic disturbance, such as pile-driving and vessel activity, as a form of predation (Frid and Dill, 2002). Consequently, porpoises in the vicinity of construction activities may reduce their buzzing activity as they adjust activity budgets to spend more time avoiding noise sources and less time engaged in foraging and/or social activities (Pirotta et al., 2014a; Wisniewska et al., 2018). Decreases in buzzing activity could also be explained by reduced prey availability or foraging performance as a result of the displacement or changed behavior of prey species in response to anthropogenic noise (Hassel et al., 2004; Mueller-Blenkle et al., 2010; Herbert-Read et al., 2017). Further field studies on the behavioral responses of different prey to pile-driving activities are required to understand the extent to which any spatio-temporal variation in the local prey availability and abundance may have indirect consequences on individual porpoise fitness (Hassel et al., 2004; Mueller-Blenkle et al., 2010).

Changes in Porpoise Occurrence and Activity in Relation to Vessels and Other Construction Activity

During the turbine installation phase, the broadscale BACI analysis showed that porpoise occurrence was also significantly lower at the impact block than during the baseline, even though no piling activities occurred (**Figure 4**). During this period (July–October 2018), various construction activities such as jacket foundation, turbine and cable installation occurred simultaneously at different locations within the windfarm, leading to high levels of vessel traffic (**Figures 7A,B**). Additionally, gradient analyses showed that the probability of detecting porpoises within the site decreased by up to 35.2% as vessel intensity increased, and as distance to the nearest vessel decreased (**Figure 8A**). Previous experimental studies

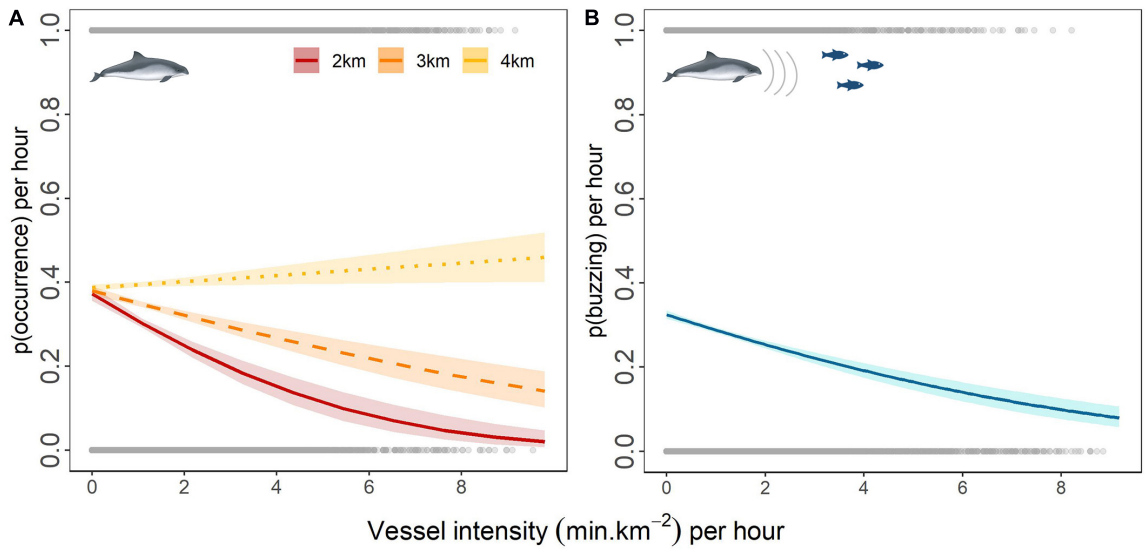

FIGURE 8 | The probability of harbor porpoise occurrence per hour in relation to vessel intensity per hour at a mean vessel distance of 2 km (red line), 3 km (dashed orange line), 4 km (dotted yellow line) **(A)**; the probability of buzzing activity per hour in relation to vessel intensity (blue line) **(B)**; confidence intervals (shaded areas) estimated for the uncertainty in fixed effects only; gray points represent the raw data distribution along the vessel intensity gradient; see the raw data frequency distribution in **Supplementary Figures 7, 8**.

demonstrated that captive harbor porpoises displayed strong behavioral responses when exposed to low levels of medium to high frequency vessel noise (Dyndo et al., 2015). Many vessels emit high frequency noises that overlap with frequency bands biologically relevant for porpoises, which may lead to acoustic masking and/or elicit adverse behavioral responses (Hermannsen et al., 2014). In our study, increased vessel activity led to a significant decrease in porpoise acoustic detections and activity (**Figures 8A,B**) at distances of up to 4 km (**Figure 8A**). However, studies using sound and movement recording tags that can detect finer-scale responses highlight that porpoise foraging may be disrupted at greater distances of up to 7 km (Wisniewska et al., 2018).

Using only data collected in the absence of pile-driving, we found that the probability of detecting porpoises decreased by up to 17% as the broadband sound pressure levels increased by 57 dB (**Figure 9A**). Increased levels of broadband noise emitted during other construction-related vessel activities may reduce the porpoise detection probability of CPODs (Clausen et al., 2019). However, to reduce the risk of vessel noise masking ultrasonic click detections and so the probability of false-negative detections, we discarded any hours with less than 60 min logged and during which vessels were within 1 km of CPODs (as Pirotta et al., 2014a), and additionally chose a coarse binary metric (i.e., presence/absence per hour) (Williamson et al., 2016). Thus, in this case, the decline in porpoise detections, in the absence of piling activities, is unlikely to be caused by a reduction in the effective detection area of the devices. In contrast, the decline in porpoise detections suggests that porpoises have exhibited a behavioral response to high levels of background noise associated with vessel and construction activities. In Wisniewska et al.'s (2018) study, tagged harbor porpoises responded to fast ferry passages by making deeper dives, increasing swimming effort, and ceasing echolocation and foraging for several minutes. Although these individuals lived in highly trafficked coastal waters, they did not seem to have habituated to vessel noise (Wisniewska et al., 2018). Similarly, throughout our 3-year monitoring, buzzing activity decreased by up to 24.5% as the vessel intensity increased in the study area (**Figure 8B**) and by up to 41.5% as the hourly RMS sound pressure levels increased from 104 to 155 dB re 1 μPa (**Figure 9B**). However, for the same levels of broadband noise, buzzing activity appeared to be higher during rather than in the absence of piling activities (**Figure 9B**). This increase in porpoise buzzing activity during piling may be indicative of behavioral changes in echolocation activity in response to noise (the Lombard effect). Harbor porpoises may increase the signal level of their clicks or the signal repetition rate (Branstetter et al., 2018) to compensate for the increased noise levels during social interactions (Sorensen et al., 2018) or foraging activity. Alternatively, adverse effects of piling noise on prey (e.g., Herbert-Read et al., 2017) may benefit predators by locally increasing prey availability and/or enhancing their foraging performance. Either way, these results highlight how chronic exposure to regular vessel activity and associated levels of anthropogenic noise could influence the foraging and/or social activity of those individuals which continue to use offshore construction sites during the pile-driving phase.

Vessel-tracking data provide a robust measure of the spatial distribution of windfarm construction vessels which are legally required to carry AIS. However, there are several reasons why these data may not fully capture variation in the soundscapes affecting species such as harbor porpoises and their prey. In coastal areas, many recreational vessels without AIS dominate

the anthropogenic soundscape (Hermannsen et al., 2019). This is less likely to be an issue offshore but reports from guard vessels indicate that local fishing boats without active AIS commonly used areas over and around the construction sites throughout our study period. Furthermore, although information on construction vessel locations was available, detailed information on variation in the activity of those vessels, which could affect their acoustic signature, was not. This could be particularly important for construction vessels that jacked up to install jacket foundations and turbines, and vessels which periodically used dynamic positioning. Greater understanding of how acoustic signatures vary between vessels, and in relation to speed or activity, could in future help identify ways in which vessel management plans could reduce broader scale disturbance during windfarm construction and operation.

In the absence of more detailed information on the acoustic signatures or activities of vessels detected using AIS, our recordings of broadband noise at three sample locations provide a valuable measure of broad-scale variation in noise exposure to animals through construction phases, and opportunities for comparison with other study systems (Hermannsen et al., 2014). Even here, though, these measures may be biased by proximity to particular vessels. To characterize this variation, we used an unweighted RMS SPL based on a sampling rate of 48 kHz. These frequencies are appropriate for characterizing long-term variation in shipping and pile-driving noise (Merchant et al., 2012, 2014; Thompson et al., 2020), and analysis of a higher sample rate recording at the site (**Supplementary Figure 10**) indicated that almost all of the acoustic energy from both pile driving and shipping noise was contained below 24 kHz (the highest acoustic frequency that can be measured at a sampling rate of 48 kHz). However, these 48 kHz recordings do not capture those higher frequencies that may be particularly important to porpoises (Tougaard et al., 2015). More focused investigation of porpoise behavioral responses to vessel noise would require an increase in sampling rate and focus on biologically significant spectral bands by using audiogram weighted SPL (Dyndo et al., 2015; Tougaard et al., 2015).

Management Implications

The planned expansion of offshore windfarms to meet decarbonization targets must proceed within frameworks for safeguarding protected wildlife populations and minimizing cumulative environmental impacts (Le Lièvre, 2019; Thompson et al., 2020). Efforts to understand and mitigate impacts on marine mammals have focused on the effects of impulsive noise produced during pile-driving. Whilst pile-driving does produce the highest amplitude noise, active piling occurred for <10% of the time in the 9–10-month piling phases at Beatrice and Moray East. Whilst responses to these short but intense periods of impulsive noise sources are of greater magnitude, we showed that harbor porpoise occurrence and buzzing activity also decreased in response to more chronic exposure to vessel traffic throughout construction. Further disturbance may also be expected from routine operation and maintenance vessels, although this may be offset by benefits resulting from the creation of new reef habitat. Further understanding of the relative importance of these different disturbance sources is now required if we are to assess the broader scale cumulative impact of construction, operation and decommissioning over the life cycle of an offshore windfarm. Our data should now be integrated into existing tools (e.g., Nabe-Nielsen et al., 2018) to explore the scale of these different disturbance impacts at both individual and population levels. This could then provide a framework that could be used

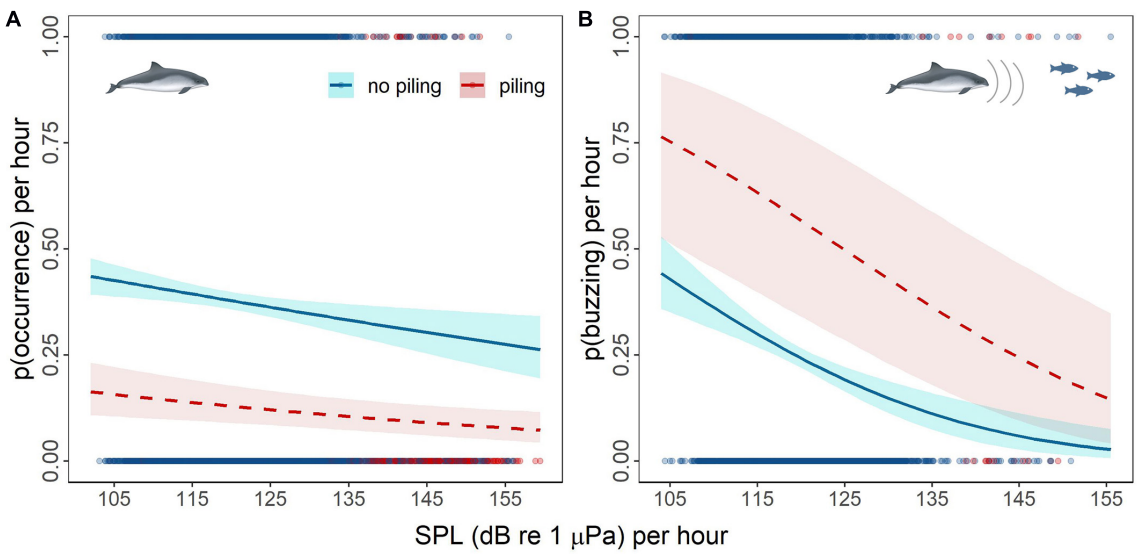

FIGURE 9 | The probability of harbor porpoise occurrence **(A)** and buzzing activity **(B)** per hour in relation to the broadband sound pressure level (SPL) per hour during (dashed red line) and outside (blue line) pile-driving hours; confidence intervals (shaded areas) estimated for the uncertainty in fixed effects only; points represent the raw data distribution along the SPL gradient during piling (red) and no piling (blue) activities; see the raw data frequency distribution in **Supplementary Figure 9**.

by policy makers to explore how cumulative impacts can be minimized by combining existing mitigation measures to reduce piling impacts with other regulatory measures to manage vessel traffic and other maritime activities occurring in or around construction sites.

DATA AVAILABILITY STATEMENT

The article's data and R code are available from the Dryad Digital Repository: https://doi.org/10.5061/dryad.v6wwpzgw4.

ETHICS STATEMENT

Ethical review and approval was not required for the animal study because this was a non-invasive, acoustic observational study of harbor porpoise responses to construction activities during the development of two commercial offshore windfarms. The authors had no control or influence over the duration or scheduling of construction activities including pile-driving. No animals were captured or tagged during this study and no research or animal ethical assessments were required. Porpoise responses were determined using remote passive acoustic devices on seabed moorings licensed for scientific use by Marine Scotland, and consented by the Crown Estate. Moorings were deployed and recovered using vessels with appropriate certification, accreditation and endorsements.

AUTHOR CONTRIBUTIONS

AB, PT, and IG conceived and designed the study based on data collection that has been led by PT and IG. NM analyzed all the noise data. AB processed the data, carried out the data analysis, and prepared all the tables and figures, under the supervision of IG and PT. AB drafted the manuscript. All authors contributed critically to the drafts and gave final approval for publication.

FUNDING

This study was partly funded by Beatrice Offshore Wind Ltd. and Moray Offshore Wind Farm (East) Ltd. using equipment previously purchased by UK Department of Energy and Climate Change, Scottish Government, Oil and Gas UK, COWRIE and Moray Offshore Renewables Ltd. PT and IG were core funded by University of Aberdeen. AB was core funded by the collaboration between University of Aberdeen and Marine Scotland Science through the MarCRF Ph.D. studentship. NM was core funded by Centre for Environment, Fisheries and Aquaculture Science.

ACKNOWLEDGMENTS

We thank Bill Ruck at Moray First Marine and University of Aberdeen's Lighthouse Field Station colleagues for support and assistance with data collection. We also thank the Beatrice Offshore Wind Ltd. and Moray Offshore Wind Farm (East) Ltd. teams for facilitating fieldwork and data collection during windfarm construction and providing details of the construction programs. We finally thank the members of MFRAG for their advice and two reviewers for their constructive comments.

SUPPLEMENTARY MATERIAL

The Supplementary Material for this article can be found online at: https://www.frontiersin.org/articles/10.3389/fmars.2021.664724/full#supplementary-material

REFERENCES

Bailey, H., Brookes, K. L., and Thompson, P. M. (2014). Assessing environmental impacts of offshore wind farms: lessons learned and recommendations for the future. *Aquat. Biosyst.* 10:8. doi: 10.1186/2046-9063-10-8

Barton, K. (2020). *MuMIn: Multi-Model Inference*. Available online at: https://CRAN.R-project.org/package=MuMIn (accessed August 24, 2020).

Bates, D., Machler, M., Bolker, B. M., and Walker, S. C. (2015). Fitting linear mixed-effects models using lme4. *J. Stat. Softw.* 67, 1–48.

Beale, C. M., and Monaghan, P. (2004). Behavioural responses to human disturbance: a matter of choice? *Anim. Behav.* 68, 1065–1069. doi: 10.1016/j.anbehav.2004.07.002

Beatrice Offshore Windfarm Limited (2012). *Beatrice Offshore Wind Farm Environmental Statement - Non Technical Summary*. Available online at: https://marine.gov.scot/sites/default/files/00392805.pdf (accessed August 28, 2020).

BEIS (2019). *Department of Business, Energy and Industrial Strategy*. Available online at: https://www.gov.uk/government/publications/offshore-wind-sector-deal (accessed May 28, 2020).

Bejder, L., Samuels, A., Whitehead, H., Finn, H., and Allen, S. (2009). Impact assessment research: use and misuse of habituation, sensitisation and tolerance in describing wildlife responses to anthropogenic stimuli. *Mar. Ecol. Prog. Ser.* 395, 177–185. doi: 10.3354/meps07979

Benaglia, T., Chauveau, D., Hunter, D. R., and Young, D. S. (2009). mixtools: an R package for analyzing finite mixture models. *J. Stat. Softw.* 32, 1–29. doi: 10.1007/978-0-387-35768-3_1

Booth, C. G. (2020). Food for thought: harbor porpoise foraging behavior and diet inform vulnerability to disturbance. *Mar. Mamm. Sci.* 36, 195–208. doi: 10.1111/mms.12632

Booth, C. G., Harwood, J., Plunkett, R., Mendes, S., and Walker, R. (2017). *Using the Interim PCoD Framework to Assess the Potential Impacts of Offshore wind Developments in Eastern English Waters on Harbour Porpoises in the North Sea*. Natural England Joint Report no 024. York: Natural England.

Brandt, M. J., Diederichs, A., Betke, K., and Nehls, G. (2011). Responses of harbour porpoises to pile driving at the Horns Rev II offshore wind farm in the Danish North Sea. *Mar. Ecol. Prog. Ser.* 421, 205–216. doi: 10.3354/meps08888

Brandt, M. J., Dragon, A. C., Diederichs, A., Bellmann, M. A., Wahl, V., Piper, W., et al. (2018). Disturbance of harbour porpoises during construction of the first seven offshore wind farms in Germany. *Mar. Ecol. Prog. Ser.* 596, 213–232. doi: 10.3354/meps12560

Brandt, M. J., Dragon, A. C., Diederichs, A., Schubert, A., Kosarev, V., Nehls, G., et al. (2016). *Effects of Offshore Pile Driving on Harbour Porpoise Abundance in the German Bight". Report Prepared for Offshore Forum Windenergie*. Hamburg: BioConsultSH.

Brandt, M. J., Höschle, C., Diederichs, A., Betke, K., Matuschek, R., Witte, S., et al. (2013). Far-reaching effects of a seal scarer on harbour porpoises, Phocoena

phocoena. *Aquat. Conserv. Mar. Freshw. Ecosyst.* 23, 222–232. doi: 10.1002/aqc.2311

Branstetter, B. K., Bowman, V. F., Houser, D. S., Tormey, M., Banks, P., Finneran, J. J., et al. (2018). Effects of vibratory pile driver noise on echolocation and vigilance in bottlenose dolphins (*Tursiops truncatus*). *J. Acoust. Soc. Am.* 143, 429–439. doi: 10.1121/1.5021555

Brookes, K. L., Bailey, H., and Thompson, P. M. (2013). Predictions from harbor porpoise habitat association models are confirmed by long-term passive acoustic monitoring. *J. Acoust. Soc. Am.* 134, 2523–2533. doi: 10.1121/1.4816577

Clausen, K. T., Tougaard, J., Carstensen, J., Delefosse, M., and Teilmann, J. (2019). Noise affects porpoise click detections - the magnitude of the effect depends on logger type and detection filter settings. *Bioacoustics* 28, 443–458. doi: 10.1080/09524622.2018.1477071

Dähne, M., Gilles, A., Lucke, K., Peschko, V., Adler, S., Krügel, K., et al. (2013). Effects of pile-driving on harbour porpoises (*Phocoena phocoena*) at the first offshore wind farm in Germany. *Environ. Res. Lett.* 8:025002. doi: 10.1088/1748-9326/8/2/025002

Dähne, M., Tougaard, J., Carstensen, J., Rose, A., and Nabe-Nielsen, J. (2017). Bubble curtains attenuate noise from offshore wind farm construction and reduce temporary habitat loss for harbour porpoises. *Mar. Ecol. Prog. Ser.* 580, 221–237. doi: 10.3354/meps12257

Dolman, S., and Simmonds, M. (2010). Towards best environmental practice for cetacean conservation in developing Scotland's marine renewable energy. *Mar. Policy* 34, 1021–1027. doi: 10.1016/j.marpol.2010.02.009

Dyndo, M., Wisniewska, D. M., Rojano-Donate, L., and Madsen, P. T. (2015). Harbour porpoises react to low levels of high frequency vessel noise. *Sci. Rep.* 5:11083.

Ellis, J. I., and Schneider, D. C. (1997). Evaluation of a gradient sampling design for environmental imapct assessment. *Environ. Monit. Assess.* 48, 157–172.

Fox, J., and Weisberg, S. (2019). *An R Companion to Applied Regression*. Thousand Oaks, CA: Sage.

Frid, A., and Dill, L. (2002). Human-caused disturbance stimuli as a form of predation risk. *Conserv. Ecol.* 6:11.

Gill, J. A., Norris, K., and Sutherland, W. J. (2001). Why behavioural responses may not reflect the population consequences of human disturbance. *Biol. Conserv.* 97, 265–268. doi: 10.1016/s0006-3207(00)00002-1

Graham, I. M., Merchant, N. D., Farcas, A., Barton, T. R., Cheney, B., Bono, S., et al. (2019). Harbour porpoise responses to pile-driving diminish over time. *R. Soc. Open Sci.* 6:190335. doi: 10.1098/rsos.190335

Haelters, J., Duliere, V., Vigin, L., and Degraer, S. (2015). Towards a numerical model to simulate the observed displacement of harbour porpoises *Phocoena phocoena* due to pile driving in Belgian waters. *Hydrobiologia* 756, 105–116. doi: 10.1007/s10750-014-2138-4

Hammond, P. S., Macleod, K., Berggren, P., Borchers, D. L., Burt, L., Canadas, A., et al. (2013). Cetacean abundance and distribution in European Atlantic shelf waters to inform conservation and management. *Biol. Conserv.* 164, 107–122. doi: 10.1016/j.biocon.2013.04.010

Hartig, F. (2020). *DHARMa: Residual Diagnostics for Hierarchical (Multi-Level/Mixed) Regression Models*. Available online at: https://CRAN.R-project.org/package=DHARMa (accessed May 29, 2020).

Hassel, A., Knutsen, T., Dalen, J., Skaar, K., Lokkeborg, S., Misund, O. A., et al. (2004). Influence of seismic shooting on the lesser sandeel (Ammodytes marinus). *ICES J. Mar. Sci.* 61, 1165–1173. doi: 10.1016/j.icesjms.2004.07.008

Herbert-Read, J. E., Kremer, L., Bruintjes, R., Radford, A. N., and Ioannou, C. C. (2017). Anthropogenic noise pollution from pile-driving disrupts the structure and dynamics of fish shoals. *Proc. R. Soc. B Biol. Sci.* 284, 20171627. doi: 10.1098/rspb.2017.1627

Hermannsen, L., Beedholm, K., Tougaard, J., and Madsen, P. T. (2014). High frequency components of ship noise in shallow water with a discussion of implications for harbor porpoises (*Phocoena phocoena*). *J. Acoust. Soc. Am.* 136, 1640–1653. doi: 10.1121/1.4893908

Hermannsen, L., Mikkelsen, L., Tougaard, J., Beedholm, K., Johnson, M., and Madsen, P. T. (2019). Recreational vessels without Automatic Identification System (AIS) dominate anthropogenic noise contributions to a shallow water soundscape. *Sci. Rep.* 9:15477.

JNCC, and Natural England, (2019). *Norfolk Vanguard Offshore Wind Farm Harbour Porpoise (Phocoena phocoena) Special Area of Conservation: Southern North Sea. Conservation Objectives and Advice on Operations*. Peterborough: JNCC.

Kastelein, R. A., Helder-Hoek, L., Jennings, N., van Kester, R., and Huisman, R. (2019). Reduction in body mass and blubber thickness of harbor porpoises (*Phocoena phocoena)* due to near-fasting for 24 Hours in four seasons. *Aquat. Mamm.* 45, 37–47. doi: 10.1578/am.45.1.2019.37

King, S. L., Schick, R. S., Donovan, C., Booth, C. G., Burgman, M., Thomas, L., et al. (2015). An interim framework for assessing the population consequences of disturbance. *Methods Ecol. Evol.* 6, 1150–1158. doi: 10.1111/2041-210x.12411

Kinsler, L. E., Frey, A. R., Coppens, A. B., and Sanders, J. V. (1999). *Fundamentals of Acoustics*. Hoboken, NJ: John Wiley & Sons.

Le Lièvre, C. (2019). Sustainably reconciling offshore renewable energy with Natura 2000 sites: an interim adaptive management framework. *Energy Policy* 129, 491–501. doi: 10.1016/j.enpol.2019.02.007

Madsen, P. T., Wahlberg, M., Tougaard, J., Lucke, K., and Tyack, P. (2006). Wind turbine underwater noise and marine mammals: implications of current knowledge and data needs. *Mar. Ecol. Prog. Ser.* 309, 279–295. doi: 10.3354/meps309279

Merchant, N. D., Fristrup, K. M., Johnson, M. P., Tyack, P. L., Witt, M. J., Blondel, P., et al. (2015). Measuring acoustic habitats. *Methods Ecol. Evol.* 6, 257–265.

Merchant, N. D., Pirotta, E., Barton, T. R., and Thompson, P. M. (2014). Monitoring ship noise to assess the impact of coastal developments on marine mammals. *Mar. Pollut. Bull.* 78, 85–95. doi: 10.1016/j.marpolbul.2013.10.058

Merchant, N. D., Witt, M. J., Blondel, P., Godley, B. J., and Smith, G. H. (2012). Assessing sound exposure from shipping in coastal waters using a single hydrophone and Automatic Identification System (AIS) data. *Mar. Pollut. Bull.* 64, 1320–1329. doi: 10.1016/j.marpolbul.2012.05.004

Metcalfe, K., Breheret, N., Chauvet, E., Collins, T., Curran, B. K., Parnell, R. J., et al. (2018). Using satellite AIS to improve our understanding of shipping and fill gaps in ocean observation data to support marine spatial planning. *J. Appl. Ecol.* 55, 1834–1845. doi: 10.1111/1365-2664.13139

Moray Offshore Renewables Limited (2012). *Environmental Statement Technical Appendix 4.4 A Marine Mammals Baseline*. Available online at: https://www.morayeast.com/download_file/216/219 (accessed August 28, 2020).

Mueller-Blenkle, C., McGregor, P. K., Gill, A. B., Andersson, M. H., Metcalfe, J., Bendall, V., et al. (2010). *Effects of Pile-Driving Noise on the Behaviour of Marine Fish. COWRIE Ref: Fish 06-08, Technical Report*. Cranfield: Cranfield University.

Nabe-Nielsen, J., van Beest, F. M., Grimm, V., Sibly, R. M., Teilmann, J., and Thompson, P. M. (2018). Predicting the impacts of anthropogenic disturbances on marine populations. *Conserv. Lett.* 11:e12563. doi: 10.1111/conl.12563

Oakley, J. A., Williams, A. T., and Thomas, T. (2017). Reactions of harbour porpoise (*Phocoena phocoena*) to vessel traffic in the coastal waters of South West Wales, UK. *Ocean Coast. Manag.* 138, 158–169. doi: 10.1016/j.ocecoaman.2017.01.003

Pebesma, E. (2018). Simple features for R: standardized support for spatial vector data. *R J.* 10, 439–446. doi: 10.32614/rj-2018-009

Pirotta, E., Brookes, K. L., Graham, I. M., and Thompson, P. M. (2014a). Variation in harbour porpoise activity in response to seismic survey noise. *Biol. Lett.* 10:20131090. doi: 10.1098/rsbl.2013.1090

Pirotta, E., Thompson, P. M., Miller, P. I., Brookes, K. L., Cheney, B., Barton, T. R., et al. (2014b). Scale-dependent foraging ecology of a marine top predator modelled using passive acoustic data. *Funct. Ecol.* 28, 206–217. doi: 10.1111/1365-2435.12146

R Core Team, (2019). *R: A Language and Environment for Statistical Computing*. Vienna: R Foundation for Statistical Computing.

Richardson, W., Greene, C., Malme, C., and Thompson, D. (1995). *Marine Mammals and Noise*. San Diego, CA: Academic Press.

Santos, M., and Pierce, G. (2003). The diet of harbour porpoise (*Phocoena phocoena*) in the northeast Atlantic. *Oceanogr. Mar. Biol.* 41, 355–390.

Sarnocińska, J., Teilmann, J., Balle, J. D., van Beest, F. M., Delefosse, M., and Tougaard, J. (2020). Harbor porpoise (*Phocoena phocoena*) reaction to a 3D seismic airgun survey in the North Sea. *Front. Mar. Sci.* 6:824. doi: 10.3389/fmars.2019.00824

Scheidat, M., Tougaard, J., Brasseur, S., Carstensen, J., Petel, T. V., Teilmann, J., et al. (2011). Harbour porpoises (*Phocoena phocoena*) and wind farms: a case study in the Dutch North Sea. *Environ. Res. Lett.* 6:025102. doi: 10.1088/1748-9326/6/2/025102

Smith, E. P. (2002). "BACI Design," in *Encyclopedia of Environmetrics*, eds A. H. El-Shaarawi, and W. W. Piegorsch (Chichester: John Wiley & Sons, Ltd).

Sorensen, P. M., Wisniewska, D. M., Jensen, F. H., Johnson, M., Teilmann, J., and Madsen, P. T. (2018). Click communication in wild harbour porpoises (*Phocoena phocoena*). *Sci. Rep.* 8:9702.

Sveegaard, S., Teilmann, J., Tougaard, J., Dietz, R., Mouritsen, K. N., Desportes, G., et al. (2011). High-density areas for harbor porpoises (*Phocoena phocoena*) identified by satellite tracking. *Mar. Mamm. Sci.* 27, 230–246. doi: 10.1111/j.1748-7692.2010.00379.x

Thompson, P. M., Brookes, K. L., Graham, I. M., Barton, T. R., Needham, K., Bradbury, G., et al. (2013). Short-term disturbance by a commercial two-dimensional seismic survey does not lead to long-term displacement of harbour porpoises. *Proc. Biol. Sci.* 280:20132001. doi: 10.1098/rspb.2013.2001

Thompson, P. M., Graham, I. M., Cheney, B., Barton, T. R., Farcas, A., and Merchant, N. D. (2020). Balancing risks of injury and disturbance to marine mammals when pile driving at offshore windfarms. *Ecol. Solut. Evid.* 1:e12034.

Thomsen, F., McCully, S. R., Weiss, L. R., Wood, D. T., Warr, K. J., Barry, J., et al. (2011). Cetacean stock assessments in relation to exploration and production industry activity and other human pressures: review and data needs. *Aquat. Mamm.* 37, 1–93. doi: 10.1578/am.37.1.2011.1

Tougaard, J., Carstensen, J., Teilmann, J., Skov, H., and Rasmussen, P. (2009). Pile driving zone of responsiveness extends beyond 20 km for harbor porpoises (*Phocoena phocoena* (L.)). *J. Acoust. Soc. Am.* 126, 11–14. doi: 10.1121/1.3132523

Tougaard, J., Wright, A. J., and Madsen, P. T. (2015). Cetacean noise criteria revisited in the light of proposed exposure limits for harbour porpoises. *Mar. Pollut. Bull.* 90, 196–208. doi: 10.1016/j.marpolbul.2014.10.051

Tregenza, N. (2014). *CPOD.exe: A Guide for Users*. Available online at: https://www.chelonia.co.uk/downloads/CPOD.pdf (accessed May 4, 2021).

Underwood, A. J. (1992). Beyond BACI: the detection of environmental impacts on populations in the real, but variable, world. *J. Exp. Mar. Biol. Ecol.* 161, 145–178. doi: 10.1016/0022-0981(92)90094-q

van Beest, F. M., Teilmann, J., Hermannsen, L., Galatius, A., Mikkelsen, L., Sveegaard, S., et al. (2018). Fine-scale movement responses of free-ranging harbour porpoises to capture, tagging and short-term noise pulses from a single airgun. *R. Soc. Open Sci.* 5:170110. doi: 10.1098/rsos.170110

Waggitt, J. J., Evans, P. G. H., Andrade, J., Banks, A. N., Boisseau, O., Bolton, M., et al. (2020). Distribution maps of cetacean and seabird populations in the North—East Atlantic. *J. Appl. Ecol.* 57, 253–269.

Williamson, L. D., Brookes, K. L., Scott, B. E., Graham, I. M., Bradbury, G., Hammond, P. S., et al. (2016). Echolocation detections and digital video surveys provide reliable estimates of the relative density of harbour porpoises. *Methods Ecol. Evol.* 7, 762–769. doi: 10.1111/2041-210x.12538

Williamson, L. D., Brookes, K. L., Scott, B. E., Graham, I. M., and Thompson, P. M. (2017). Diurnal variation in harbour porpoise detection — potential implications for management. *Mar. Ecol. Prog. Ser.* 570, 223–232. doi: 10.3354/meps12118

Wilson, B., Benjamins, S., and Elliott, J. (2013). Using drifting passive echolocation loggers to study harbour porpoises in tidal-stream habitats. *Endanger. Species Res.* 22, 125–143. doi: 10.3354/esr00538

Wirsing, A. J., Heithaus, M. R., Frid, A., and Dill, L. M. (2008). Seascapes of fear: evaluating sublethal predator effects experienced and generated by marine mammals. *Mar. Mamm. Sci.* 24, 1–15. doi: 10.1111/j.1748-7692.2007.00167.x

Wisniewska, D. M., Johnson, M., Teilmann, J., Rojano-Donate, L., Shearer, J., Sveegaard, S., et al. (2016). Ultra-high foraging rates of harbor porpoises make them vulnerable to anthropogenic disturbance. *Curr. Biol.* 26, 1441–1446. doi: 10.1016/j.cub.2016.03.069

Wisniewska, D. M., Johnson, M., Teilmann, J., Siebert, U., Galatius, A., Dietz, R., et al. (2018). High rates of vessel noise disrupt foraging in wild harbour porpoises (*Phocoena phocoena*). *Proc. Biol. Sci.* 285:20172314. doi: 10.1098/rspb.2017.2314

Wright, D., Janzen, C., Bochenek, R., Austin, J., and Page, E. (2019). Marine observing applications using AIS: automatic identification system. *Front. Mar. Sci.* 6:537. doi: 10.3389/fmars.2019.00537

Conflict of Interest: The authors have no known conflict of interest. This study was partly funded by two commercial developers, Beatrice Offshore Wind Ltd. and Moray Offshore Wind Farm (East) Ltd. However, these funding bodies had no input into data collection, analysis and interpretation nor into the paper redaction. The aims, scope and sampling design of the study were agreed by the statutory advisors represented on the Moray Firth Renewables Advisory Group (MFRAG) and the regulator Marine Scotland Licensing and Operations Team.

Copyright © 2021 Benhemma-Le Gall, Graham, Merchant and Thompson. This is an open-access article distributed under the terms of the Creative Commons Attribution License (CC BY). The use, distribution or reproduction in other forums is permitted, provided the original author(s) and the copyright owner(s) are credited and that the original publication in this journal is cited, in accordance with accepted academic practice. No use, distribution or reproduction is permitted which does not comply with these terms.

frontiers in Marine Science

REVIEW
published: 08 July 2021
doi: 10.3389/fmars.2021.674756

Restoration of Abundance and Dynamics of Coastal Fish and Lobster Within Northern Marine Protected Areas Across Two Decades

Even Moland[1,2], Albert Fernández-Chacón[2], Tonje Knutsen Sørdalen[2], David Villegas-Ríos[3,4], Susanna Huneide Thorbjørnsen[1,2], Kim Tallaksen Halvorsen[1], Mats Huserbråten[1], Esben Moland Olsen[1,2], Portia Joy Nillos Kleiven[1], Alf Ring Kleiven[1], Halvor Knutsen[1,2], Sigurd Heiberg Espeland[1,2], Carla Freitas[1,5] and Jan Atle Knutsen[1]*

[1] Institute of Marine Research, His, Norway, [2] Department of Natural Sciences, Centre for Coastal Research, University of Agder, Kristiansand, Norway, [3] Department of Ecology and Marine Resources, Instituto Mediterráneo de Estudios Avanzados (CSIC-UiB), Esporles, Spain, [4] Department of Ecology and Marine Resources, Instituto de Investigaciones Marinas (IIM-CSIC), Vigo, Spain, [5] Marine and Environmental Sciences Center (MARE), Funchal, Portugal

OPEN ACCESS

Edited by:
Juan Jacobo Schmitter-Soto, The South Border College (ECOSUR), Mexico

Reviewed by:
Corey Morris, Department of Fisheries and Oceans, Canada
Jennifer Caselle, University of California, Santa Barbara, United States
Hem Nalini Morzaria-Luna, Intercultural Center for the Study of Deserts and Oceans, United States

***Correspondence:**
Even Moland
even.moland@graduates.jcu.edu.au

Specialty section:
This article was submitted to Marine Ecosystem Ecology, a section of the journal Frontiers in Marine Science

Received: *01 March 2021*
Accepted: *15 June 2021*
Published: *08 July 2021*

Citation:
Moland E, Fernández-Chacón A, Sørdalen TK, Villegas-Ríos D, Thorbjørnsen SH, Halvorsen KT, Huserbråten M, Olsen EM, Nillos Kleiven PJ, Kleiven AR, Knutsen H, Espeland SH, Freitas C and Knutsen JA (2021) Restoration of Abundance and Dynamics of Coastal Fish and Lobster Within Northern Marine Protected Areas Across Two Decades. Front. Mar. Sci. 8:674756. doi: 10.3389/fmars.2021.674756

This article reviews a suite of studies conducted in a network of coastal Marine Protected Areas (MPAs) in Skagerrak, Southeast Norway. In 2006, Norway's first lobster reserves were implemented, with the aim of protecting European lobster (*Homarus gammarus*) through a ban on fixed gear. A before–after control-impact paired series (BACIPS) monitoring program was initiated to evaluate effects of protection on depleted lobster populations. Experimental trapping and capture-recapture techniques were combined to track demography of populations, also including movement of individuals within and beyond MPAs and adjacent control areas. Further, population genetics and parentage studies were applied, allowing for estimation of gene flow, and novel work on sexual selection in lobsters. Additional studies have evaluated MPA effects on coastal cod (*Gadus morhua*), and on commercially harvested labrids (*Ctenolabrus rupestris* and *Symphodus melops*) and anadromous brown trout (*Salmo trutta*). Together, these studies reported effects of protection pertaining to increased population density, survival, body size and phenotypic diversity, changes in emigration and interaction with surrounding fisheries, and alteration of selection pressure on morphological- and behavioral traits. Designation of MPAs in close collaboration with fishers and managers, long-term monitoring, inclusion of citizen science and evolving research protocols—also including fisheries data—have revealed novel effects of protection and harvesting on marine populations, thus providing substantial contributions to conservation science. Moreover, knowledge of MPA effects on coastal species has impacted harvest regulations showing the utility of MPAs as empirically documented management tools in Norway.

Keywords: acoustic telemetry, crustacean, displacement of effort, eco-evolutionary dynamics, fisheries management, marine reserve, rebuilding, spillover

INTRODUCTION

Fishing is well established as the driver having had the most impact on biodiversity in marine systems in the past 50 years (IPBES, 2019). Recognizing previous heavy exploitation as a reason for depressed levels of abundance is fundamental for taking appropriate management action. However, a lack of locally relevant scientific data on the potential contrast to the present-day depleted state of ecosystems has been considered an obstacle to set appropriate management targets for their recovery (Thurstan and Roberts, 2010). Chronic harvesting represents an impediment to observation of targeted species' natural population dynamics, life-history patterns and -strategies. Marine Protected Areas (MPAs)—areas in the sea that forbid some or all extractive activities are highly useful tools to obtain valuable baseline information on marine populations (Lubchenco et al., 2003; Fenberg et al., 2012; Baskett and Barnett, 2015). Studies conducted in conjunction with the introduction of MPAs have been shown to be useful tools for research and management (Claudet et al., 2008; Babcock et al., 2010; Edgar et al., 2014), e.g., allowing modeling of possible outcomes of different harvest regulations for Atlantic cod *Gadus morhua* (Fernández-Chacón et al., 2015), and demonstrating benefits of protecting large bodied European lobster *Homarus gammarus* (Sørdalen et al., 2018).

Replicated control vs. impact study designs are powerful tools in environmental impact assessment, and since the early beginnings of the marine conservation science discipline, studies using before–after control-impact (BACI) have been suggested (Jones et al., 1992). The strength of BACI-type approaches in environmental impact assessment is the unequivocal detection of change in an "impacted" site from before impact to after, when compared to a control location where the impact persists. In a marine conservation setting, the "impact" will typically be represented by the removal of one or more anthropogenic disturbances, such as all or part of the harvesting occurring in an ecosystem. Modifications and refinement of the analytical framework associated with the BACI approach (Stewart-Oaten et al., 1986) were described by Underwood (1992, 1994) who expanded on asymmetrical designs with multiple controls to account for spatial heterogeneity and temporal variance that has nothing to do with the human disturbance (or its removal). Russ (2002) proposed a replicated BACI-approach as the "gold standard" in marine conservation science. As more time-series information became available from marine conservation sites (Babcock et al., 2010), it supported a notion that time is essential both for development and discovery of MPA effects (Claudet et al., 2008; Kaplan et al., 2019; Barceló et al., 2021). The BACI framework was thus expanded to include before-after control-impact paired series (BACIPS), involving time series data collected inside and outside in replicated sites (Osenberg et al., 2011; Thiault et al., 2019). Importantly, as highly valuable by-products of unequivocally demonstrated population effects from BACI-type approaches, studies using the same populations in the "after" state can contribute to novel insights regarding less obvious effects of the contrasting management regimes such as restoration of selection pressures (see Sørdalen et al., 2018, 2020).

In the early 2000s, European lobster (*H. gammarus*) census indicators reached an all-time low for southern Norway—and as assessment indicated a population size likely lower than 10% of the historical maximum, the species was red listed as "near threatened" according to the IUCN (International Union for Conservation of Nature) criteria (Oug et al., 2006). Motivated by the dire situation lamented by fishers in Norway's south eastern Skagerrak region, and inspired by experiences gained from early protection trials in Lysekil, Sweden (Moland et al., 2013b), the first lobster reserves (as MPAs banning all gear types except hook-and-line) were established in Norway (Pettersen et al., 2009; Knutsen et al., unpublished). The objectives were to test whether spatial protection could indeed confer population benefits to lobster and provide information on the impact of the prevailing harvest pressure exerted on lobster in adjacent areas open to fishing. Additionally, it was proposed by participating scientists that partial protection imposed through the ban on fixed gear might confer quantifiable benefits to cod and potentially other harvested fish species. In 2004, population surveys began in proposed sites to evaluate their suitability, and from 2006 a replicated BACIPS design with paired lobster reserves and adjacent control areas have been monitored annually (see section "Study System and -Species"). Motivated by the early reported positive effects of MPAs on lobster, Tvedestrand municipality designated 15% of its coastal waters to protection in 2012 and became Norway's first to implement a no-take zone providing full protection for the fish and crustaceans assemblages. Since publication of the first scientific paper documenting the initial effects of protection on European lobster (and Atlantic cod) in 2013 (Moland et al., 2013a), there has been a steady growth in designations of lobster reserves as local management tools in Norway with 54 areas covering 84 km^2 implemented to date in total (Knutsen et al., unpublished).

Herein we review and summarize a suite of studies performed in conjunction with the designation of the first coastal MPAs in Southern Norway. Early effects of MPAs have been detected as indicated by population increases and shifts in age- and size-structure of protected populations. With time, the monitoring work has enabled (1) detection of longer-term demographic effects of protection, and (2) investigations into effects of the shifting selective "landscape" shaping individual traits disparately within protected and harvested populations. We discuss these findings considering MPA size and spacing in light of local population dynamics and -structure. We call for well managed MPAs as crucial to a holistic ecosystem approach to fisheries management, and as a nature-based solution to the challenge of restoring coastal populations and ecosystem function.

STUDY SYSTEM AND -SPECIES

Study System

Skagerrak is characterized by harboring a portfolio of once productive local fish and shellfish stocks in depleted states (Kleiven et al., 2012; Rogers et al., 2014; Cardinale et al., 2017). At present, Skagerrak is under high pressure from intensive bottom trawling for northern shrimp *Pandalus borealis* which

constitute the last economically viable fishery in this miniature deep sea (Knutsen et al., 2015; Kroodsma et al., 2018). In addition, environmental change influenced by land use in Skagerrak's large catchment is exacerbated by climate change (Frigstad et al., 2020).

Although several definitions of MPA networks exist, they commonly refer to an integrated system of multiple protected areas, often designed to conserve regional biodiversity, and ecosystem function across habitats (Olsen et al., 2013). The studies reviewed herein were conducted in a network—in the sense of a collection of independent MPAs located on the Norwegian Skagerrak coast, mostly in the outer coastal seascape, potentially connected by gene flow (**Figure 1**). Capture of lobster has been effectively banned in the MPAs through gear restrictions, with only hook and line fishing allowed in the partially protected areas also alleviating harvest pressure on several fish species (Pettersen et al., 2009; Moland et al., 2013a; Fernández-Chacón et al., 2015; Halvorsen et al., 2017). The first designated MPAs (**Figure 1** and **Table 1**, sites A–C, E) were established to generate knowledge on the development of lobster populations in areas unaffected by extractive fishing: Flødevigen in Agder county, the Bolærne archipelago at the mouth of the Oslo fjord in Vestfold and Telemark county, and the small island Kvernskjær in the Hvaler archipelago, in Viken county. Control areas are located adjacent to these and separated from MPAs by distances of 1,700, 850, and 2,250 m (from MPA center to control area center) in Flødevigen, Bolærne and Kvernskjær, respectively. A fourth MPA was established in Risør, in Agder county (**Figure 1** and **Table 1**, site C).

The fifth site covered by this review encompasses the sea areas of Tvedestrand municipality (**Figure 1** and **Table 1**, site D), which initiated a zoning plan with MPAs implemented in 2012. A larger MPA (4.9 km^2) was established in the municipality's outer coastal zone, motivated by the early successes in small-scale experimental MPAs in Skagerrak (Nillos Kleiven et al., 2019). Also included in the zoning and covered by this review is the no-take zone in the Tvedestrand fjord, prohibiting all types of fishing. Surrounded by MPAs allowing hook-and-line-type fishing gear, the no-take zone enables studying effects of protection on fish (**Figure 1** and **Table 1**). An acoustic telemetry array consisting of 56 acoustic receivers is deployed in the fjord, also including the no-take zone (for details, see Villegas-Ríos et al., 2017b; Thorbjørnsen et al., 2019; Freitas et al., 2021).

Since designation of the first set of MPAs, the areas have been subject to a range of studies designed to increase knowledge regarding the effects of protection for a collection of species that are targeted in Skagerrak fisheries (**Table 2**). Enforcement of MPAs is based on collaboration between the Directorate of Fisheries, the Coast Guard and local police. In these MPAs, only a few instances of poaching have been noted, mostly as a result of ignorance of MPA borders and regulations.

Study Species

European lobster (*H. gammarus*) (hereafter, lobster) is a large, long-lived sexually dimorphic crustacean and highly sought-after in Northern Europe's commercial and recreational fisheries. In response to declining catches, a variety of management measures have been adopted such as closed season, gear restriction, and minimum (25 cm) and maximum (32 cm, in Skagerrak only) legal-size limits. Lobsters are solitary, territorial and typically live within limited shorter-term (<1 years) home ranges (~0.02 km^2) once they settle into a suitable habitat (Moland et al., 2011; Skerritt et al., 2015). Longevity may span several decades (Sheehy et al., 1999). Spatial genetic structure throughout the species' range in Europe is limited, with only a weak differentiation between larger regions of the Swedish Skagerrak and the Atlantic areas to the west, with the population in Norway being a mix of these two (Ellis et al., 2017). In Skagerrak, the species is targeted in an intensive trap fishery, dominated by recreational fishers (Kleiven et al., 2012) exerting high levels of fishing mortality on legal lobsters (Wiig et al., 2013). Recent work combining an experimental evaluation of technological creep in the trap fishery with long-term CPUE time series suggest that coastal populations are in a severely depleted state compared to historical abundances (Kleiven et al., unpublished). Monitoring of lobster populations in MPAs and control areas (2005 to present, **Figure 1** and **Table 1**, sites A, B, E) consisted of a standardized capture-recapture sampling program conducted annually in mid-August to September. Lobsters were caught using mackerel-baited parlor pots placed at the bottom at depths between 8 and 30 m, tagged with external tags for individual identification and released at the capture locations (for more details, see Moland et al., 2013a; Sørdalen et al., 2018).

Coastal Atlantic cod (*G. morhua*) (hereafter, cod) is a demersal generalist predator with severely depleted populations in Skagerrak (Olsen et al., 2009; Knutsen et al., 2018; Barth et al., 2019; Perälä et al., 2020). The coastal cod population complex in Skagerrak consists of two genetically and biologically distinct but coexisting ecotypes. They both occur in the outer sections of the coast but gene flow among them is limited. Coastal cod typically exhibit stationary movement behaviors compared to more mobile oceanic populations (Rogers et al., 2014; Villegas-Ríos et al., 2017b). The "fjord" ecotype seems to be more sedentary and stationary than the "North Sea" ecotype (Kristensen et al., 2021). Among these populations, age at 50% maturity varies from 2 to 4 years; whereas body length (BL) at 50% maturity varies from 35 to 60 cm (Olsen et al., 2004; Roney et al., 2016). In Southern Norway, coastal cod is legally caught when greater than or equal to 40 cm minimum legal size (MLS) by the full range of gear (Fernández-Chacón et al., 2017). For the studies reviewed herein, cod (size range: 16–97 cm) were captured, from April to July (2005–2013), using fyke nets (Danish type, designed for eel capture), tagged with external tags for individual identification and released at the capture location. Tagging and recaptures occurred every year simultaneously at the MPA (**Figure 1** and **Table 1**, site E) and outside control areas (for more details, see Moland et al., 2013a; Fernández-Chacón et al., 2015).

Goldsinny wrasse (*Ctenolabrus rupestris*) and **corkwing wrasse** (*Symphodus melops*) are key mesopredators on rocky reef habitats and used as cleaner fish in salmonid aquaculture to control sea-lice infestations (Gjøsaeter, 2002; Halvorsen et al., 2020). The salmonid aquaculture industry demand for wild caught wrasse increased considerably from 2010, when salmon lice developed resistance to various delousing chemicals, and the

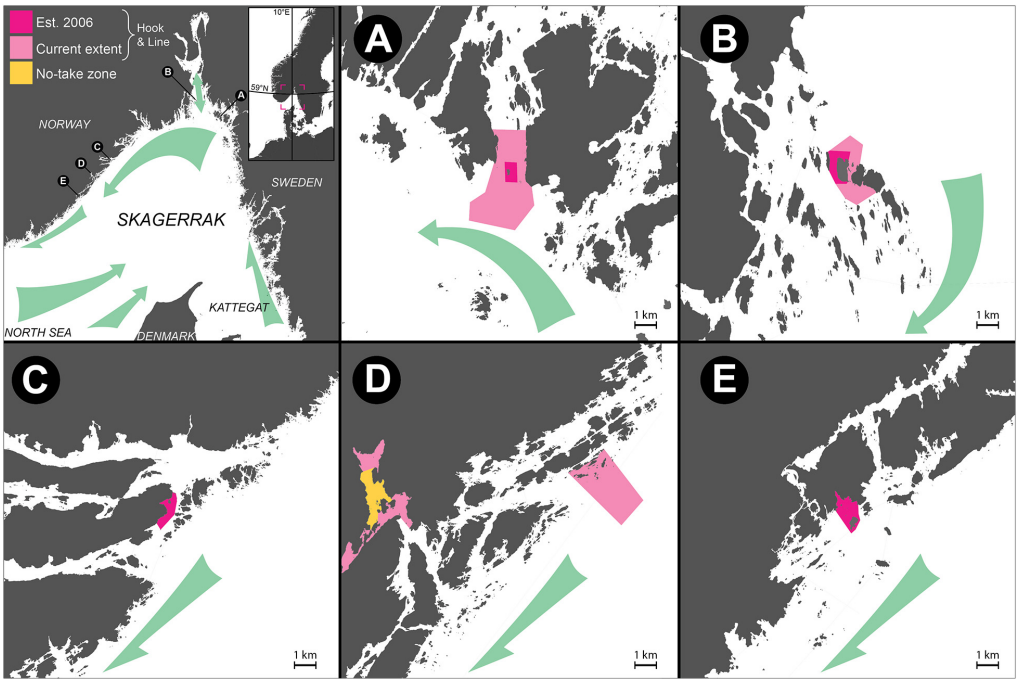

FIGURE 1 | Maps of MPAs in Skagerrak reviewed herein, drawn on equal scale, presented in sequence according to position along the Norwegian Coastal Current: **(A)** Kvernskjær, **(B)** Bolaerne, **(C)** Risør, **(D)** Tvedestrand, **(E)** Flødevigen. Colored squares in upper left corner represent an area equivalent to 1 km^2 in maps **(A–E)**. Dark pink polygons represent the MPAs established in 2006 (e.g., in **A–C,E**); areas expanded or implemented at later dates (**Table 1**) are in light pink, while the no-take zone is shown in yellow. Prevailing ocean currents and implied larval drift/gene flow is represented by green arrows. For information on control areas, see the studies listed in **Table 2**.

TABLE 1 | Name and location of MPAs used as study sites in the reviewed literature listed from East to West in Skagerrak.

Site	MPA name	MPA location	MPA size (km^2)	MPA est.	Regulation
A	Kvernskjær	59°02′ N, 10°58′ E	0.5 (4.5)	2006 (2020)	Hook-and-line
B	Bolærne	59°13′ N, 10°31′ E	0.7 (2.7)	2006 (2016)	Hook-and-line
C	Risør	58°43′ N, 9°14′ E	0.6	2006	Hook-and-line
D	Tvedestrand outer coast	58°36′ N, 9°8′ E	4.9	2012	Hook-and-line
	Tvedestrand inner fjord	58°35′ N, 9°0′ E	1.5	2012	Hook-and-line
	Tvedestrand NTZ	58°35′ N, 8°57′ E	1.5	2012	No-take zone
E	Flødevigen	58°25′ N, 8°45′ E	1.1	2006	Hook-and-line

*Information in parentheses: area included in MPA after expansion and year of MPA expansion. Site A–D: see also maps in **Figure 1**.*

fishery for wrasse as cleaner fish grew to its present size in absence of fundamental knowledge on demography and abundance of the targeted wrasse populations in Norwegian waters. To assess the consequences of harvesting, Halvorsen et al. (2017) sampled the wrasse populations in marine protected areas (**Figure 1** and **Table 1**, sites C–E) and adjacent control areas on the Skagerrak coast in Southern Norway. The survey was conducted toward the end of the fishing season in 2013, with fyke nets and baited traps set at shallow depths, mimicking the fishing methods of the commercial wrasse fishery. Recent mark-recapture work shows that these labrids have very high site fidelity and the spill-over to adjacent fished areas is probably minimal (Halvorsen et al., 2021).

Brown trout (*Salmo trutta*) is a salmonid fish that either spends its whole life in fresh water or adopts an anadromous strategy largely motivated by access to more food (Olsen et al., 2006; Thorstad et al., 2016). Anadromous trout are commonly known as sea trout. Sea trout were caught around the center islands of the Tvedestrand fjord both inside and outside the no-take zone (2013–2016, **Figure 1** and **Table 1**, site D). Individuals were captured in the fjord using a beach seine to minimize potential selective fishing of any behavioral type, and by electrofishing in the spawning river. Individuals were anaesthetized with clove oil before being tagged internally with an acoustic transmitter (Vemco V9P/V13P, for details, see Thorbjørnsen et al., 2019, 2021).

MPA IMPACTS

Population Density

The studies reviewed herein used catch-per-unit-effort (CPUE) as an indicator of abundance or population density in MPAs versus control areas (**Table 2**). Moland et al. (2013a) showed a 245% average increase in CPUE for lobster over the first 4 years

TABLE 2 | Species and MPA effects reported in the reviewed literature based on BACI-derived study designs.

Species	Effect	Design	References
Homarus gammarus	Limited adult export, high gene flow*	Whole network approach	Huserbråten et al., 2013
	CPUE increase, size increase	BACIPS	Moland et al., 2013a
	Size increase, Biomass spillover	BACIPS ACIPS	Thorbjørnsen et al., 2018
	Mating behavior difference	ACI	Sørdalen et al., 2018
	Abundance gradient, effort displacement	BACI/BAG	Nillos Kleiven et al., 2019
	Relaxed harvest selection, increased phenotypic complexity	BACIPS	Fernández-Chacón et al., 2020
	Relaxed harvest selection, trait rescue	ACIPS	Sørdalen et al., 2020
	Population increase, survival increase	BACIPS	Fernández-Chacón et al., 2021
Gadus morhua	CPUE increase, size increase	Assym. BACI	Moland et al., 2013a
	Survival increase, increase in emigration prob.	Assym. BACI	Fernández-Chacón et al., 2015
Ctenolabrus rupestris	CPUE difference	ACIPS	Halvorsen et al., 2017
Symphodus melops	CPUE difference, size- and age diff.	ACIPS	Halvorsen et al., 2017
Salmo trutta	Home range protection	ACI	Thorbjørnsen et al., 2019
	Selection difference	ACI	Thorbjørnsen et al., 2021

*BACIPS, before–after control-impact paired series; ACIPS, after control-impact paired series; ACI, after control-impact. Asymmetrical BACI: before–after control-impact design with one impact site and multiple control sites. BAG: before–after-gradient, Ellis and Schneider (1997). *High gene flow among the MPAs is suggested as a likely benefit, not an MPA effect per se.*

of protection, versus 87% increase in control areas. Recently, Fernández-Chacón et al. (2021) applied a robust design model to the capture-recapture time series data to estimate annual abundances (corrected for imperfect detection) in the same areas (2006–2014). The results indicated that abundance levels increased after protection—albeit highly variable among MPAs. It also confirmed that the CPUE-based estimates for the first 4 years were indeed a realistic approximation of the average abundance increase.

A CPUE-based indicator also demonstrated an effect of partial protection on fish. After implementation, the Flødevigen MPA acquired and retained the highest probability of catching at least one adult cod per research trap compared to the three outside control areas open to harvesting (for details, see Moland et al., 2013a), indicating a survival benefit to cod protected from all but hook-and-line gear (see section "Survival Benefits"). For the two wrasse species commercially harvested as cleaner fish, *C. rupestris* and *S. melops*, Halvorsen et al. (2017) demonstrated higher CPUE in MPAs (banning fixed gear types) relative to adjacent controls, indicating that the fishery to some extent depletes local site-specific populations in areas open to harvesting. MPAs generally had higher abundance of the two wrasses, with the CPUE of goldsinny being 33–65% higher within MPAs, while ranging from 16% lower to 92% higher in MPAs for corkwing. This was the first study to assess the impact of this fishery and demonstrated the value of MPAs when coastal areas are faced with new, and unexpected stressors from profitable industries.

Although often used in fisheries research and capture-based monitoring studies, CPUE can be a problematic indicator as it relies on the catchability of the species in question (Maunder et al., 2006). In addition, it is difficult to estimate the rate at which change in CPUE is related to the real and unobserved change in abundance. However, in balanced designs with temporally overlapping sampling and standardized effort as used herein, CPUE should yield meaningful information on changes in abundance with time. Spatial heterogeneity in population responses was evident in the studies utilizing the long-term monitoring data collected in the original lobster reserves (Moland et al., 2013a; Fernández-Chacón et al., 2020, 2021). This underscores the utility of proper design choices and adequate replication in studies assessing MPA-effects.

Long-Term Effects on Demography

Survival Benefits

Using an array of acoustic receivers, Huserbråten et al. (2013) provided early demonstration of residency and high annual survival rate of acoustically tagged lobster in the Kvernskjaer MPA (0.5 km^2). Population monitoring with capture-recapture allowed for modeling of vital rates in longer term studies. Moland et al. (2013b) found a linear positive trend in survival with body size in lobster in a Swedish MPA (Kåvra), with an additive effect of sex implying that females have lower natural mortality than males. Catchability (in research traps) was found to be higher in males in the same data, while the capture-recapture modeling applied to the data revealed that although caught less—and thus observed less than males in catches—the female population had higher survival, most likely due to lower growth rate and less risk prone behavior (Biro et al., 2014; Biro and Sampson, 2015). The same sex-specific differences in lobster survival and catchability were found in a recent study using capture-recapture data collected in the Norwegian Skagerrak (Fernández-Chacón et al., 2021), confirming this pattern for the species. In this case, they also reported, from one MPA that survival increased by 125.2 and 78.5% after protection for large-sized (>25 cm) males and females, respectively. Similarly, the capture-recapture data allowed Fernández-Chacón et al. (2015) to estimate the implicated survival increase conferred to cod, constituting 167 and 83% for small (<45 cm) and large cod (=45 cm), respectively (see **Figure 2C**) compared to "before," with no change in the control areas.

Recovery of Size Structure

Rebuilding of age- and size structure are hallmarks of lowered harvest pressure incurring lowered mortality in any harvested animal population (see Francis et al., 2007 and references therein). In southern Norway, at the onset of the monitoring

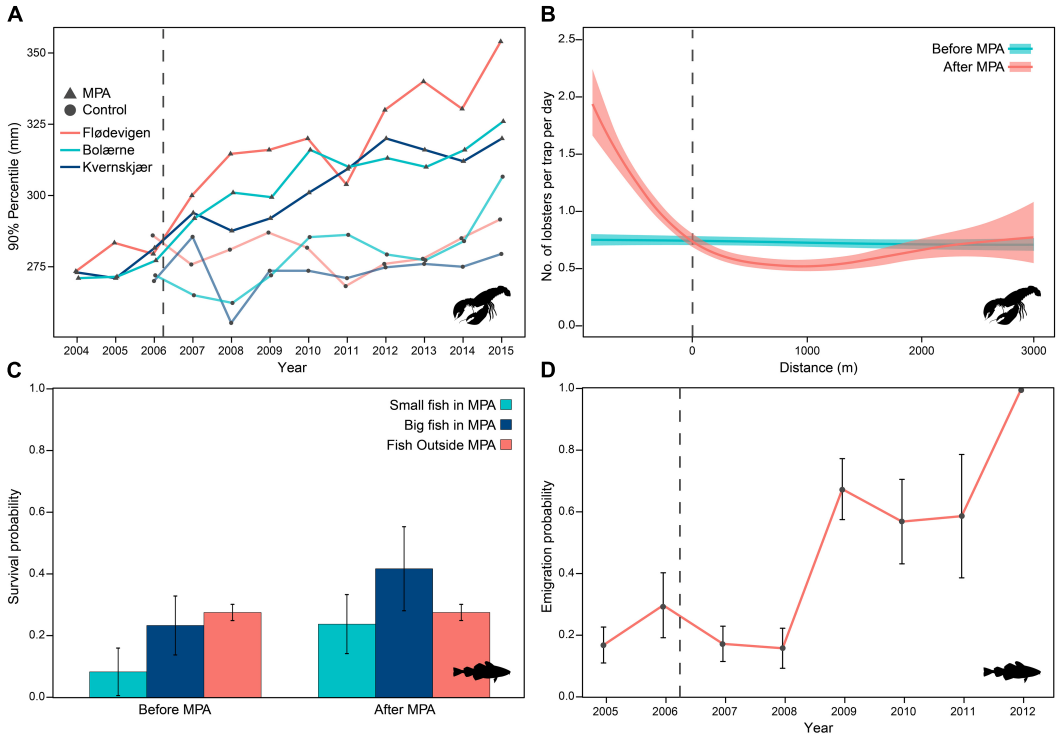

FIGURE 2 | Population effects of MPAs before and after MPA implementation: **(A)** size-structure indicator (90 percentile) of *H. gammarus* in three MPAs (triangles) and three control areas (circles) in Skagerrak (modified from Fernández-Chacón et al., 2020); **(B)** cross-border abundance gradient in *H. gammarus* (modified from Nillos Kleiven et al., 2019); **(C)** average survival rates of *G. morhua* in a MPA and multiple control areas; and **(D)** development in emigration probability of *G. morhua* tagged inside a MPA (modified from Fernández-Chacón et al., 2015).

time series, lobster was managed with a 24 cm total length (TL) minimum legal size (MLS). Harvested populations were thus characterized by few larger individuals. An increased average body size (13%) of lobster in MPAs relative to controls was evident after 4 years of protection from the annual lobstering season (Moland et al., 2013a), an effect somewhat dampened by introduction of a 25 cm MLS in 2008. Thorbjørnsen et al. (2018) presented "before" (2006) and "after" (2014) data on the demography of lobster in the three original MPAs, demonstrating a substantial widening of the size structure in the protected populations compared to the harvested before-state. By 2014, the average size increase in MPAs was 15% compared to 1% in control areas. More recently, Fernández-Chacón et al. (2020) analyzed body size data of tagged lobster sampled from 2004 to 2015 in all MPA-Control area pairs and reported a rapid change in the size structure characterized by an increase of the large-sized fraction of the population (see **Figure 2A**) with a subsequent increase in mean size. Overall, the diversity of sizes tended to increase inside protected areas. The study by Moland et al. (2013a) also detected a significant rebuilding of size-structure of cod inside one of the lobster reserves, where only hook and line fishing is allowed. Outside the reserves, both age- and size-structure of cod is severely truncated (see also, Olsen and Moland, 2011) as typically seen under intense harvest pressure (see "Harvest Selection on Phenotypes").

Interaction With Surrounding Fisheries

Emigration

The initially implemented MPAs were small (∼0.5–1.1 km^2), and since the onset of the research capture and tagging of lobster, recoveries have been reported from fishers operating outside of the MPAs or in adjacent control areas. Huserbråten et al. (2013) quantified the emigration from MPAs (**Figure 1** and **Table 1**, sites A, B, D) and found that during the initial 6 years of protection 4.7% of tagged individuals emigrated from MPA sites. Both Huserbråten et al. (2013) and Thorbjørnsen et al. (2018) reported a highly left skewed distribution of movement behaviors, with the majority of individuals recaptured (in research traps) close to their tagging location. However, movement up to 24 km away from tagging location was reported (range: 34–24,670 m) by fishers recovering tagged lobsters. Whereas emigration by lobsters seemed stable over time at ∼4–5% of tagged individuals during the first 4–6 years of protection, the capture-recapture data on cod in the Flødevigen MPA analyzed by Fernández-Chacón et al. (2015) revealed an increasing tendency (annual probability) for cod to emigrate with time after MPA establishment (**Figure 2D**). This was attributed to ontogenetic and/or density dependent movement of tagged individuals.

Spillover of Biomass

Benefits of MPAs have been reported as net contribution to spiny lobster fishery catches through spillover (Goñi et al., 2010).

Thorbjørnsen et al. (2018) compared cases of emigration and subsequent recovery by fishers for MPAs and control areas from 2006 to 2014. While there was no difference in movement rates between MPAs and control areas, the lobster emigrating from MPAs to fished areas were significantly larger (1.19 cm, $p < 0.005$) than lobsters emigrating from control areas.

Cross-Border Abundance Gradient

Nillos Kleiven et al. (2019) used experimental lobster fishing with randomized trap deployments in a wider area inside and around the outer Tvedestrand lobster MPA before and after implementation. The aim was to test for an effect gradient from inside- to far outside the MPA in a before-after-gradient (BAG) design (Ellis and Schneider, 1997). After 4 years, lobster abundance measured by CPUE increased significantly by a factor of 2.6 inside the MPA, with a decreasing gradient toward the border and into the fished areas outside. CPUE values in fished areas further away (3 km) remained similar to values before MPA establishment. However, a depression of population density developed at the MPA border compared to before data (**Figure 2B**). Using the effort data, the depression in density could be explained by the increased fishing effort close to the reserve border. The study thus demonstrated the effect of "fishing the line" (*sensu* Kellner et al., 2007)—possibly even penetrating into the MPA, and the need for effort control in areas surrounding MPAs.

Redistribution of Effort

In 2009, 3 years prior to implementation of the Tvedestrand zoning scheme, a study was carried out in which all traps deployed throughout the municipality seascape by commercial and recreational fishers during the first week of the lobstering season were registered. Repeating the same study in years 2, 3, and 4 after MPA implementation, Nillos Kleiven et al. (2019) were able to document a ∼80% increase of effort (trap numbers) in the total area, and pinpoint the appearance of fishing hotspots with a threefold increase in trap density. The highest increase was near the borders, indicating a shift in the preferred fishing areas.

Harvest Selection on Phenotypes

Body Size

Fernández-Chacón et al. (2020) provided size-dependent survival estimates of lobster in both MPA and control areas in Skagerrak, together with the shape of the relationship between survival and total body length. They documented significant negative relationships between survival and body size at the control areas but not in the MPAs, where the effect of body size was predominantly positive, and concluded that MPAs are a viable management approach for protecting against fisheries-induced selection, through the spatial refuge in both size-dependent and overall mortality.

Mating Patterns and Sexually Selected Traits

MPAs, in combination with control areas, can also be useful as field laboratories for understanding how fishing can affect mating systems of species. For instance, as lobsters have become more numerous and grown to larger sizes in the MPAs (Fernández-Chacón et al., 2020, 2021), the opportunity and scope for mate choice should also increase. In a parental assignment study conducted in Flødevigen, Sørdalen et al. (2018) found a female preference for males with larger body sizes, but that the relative size difference between females and males of mated pairs (the size-assortative mating pattern) were significantly larger in the reserve compared to mated pairs in the control area (**Figure 3A**). They also found positive selection differentials on male body- and claw size inside the MPA, but not in the control area, implying that size has less influence on male mating success in fished areas—most likely because fisheries-induced selection weakens female choice and the competition between males. Furthermore, estimations of sexual selection gradients on male traits uncovered selection to be acting strongest on relative claw size (claw size relative to body size), rather than on absolute claw and body size. This trait was later linked to an increased risk of being captured in the fishery (Moland et al., 2019), and the finding that male lobsters have up to 8% larger claws inside MPAs compared to similarly sized males in fished areas (Sørdalen et al., 2020). In sum, these findings strongly suggest that MPAs can be an effective means to preserve functional mating patterns, as well as restore and maintain diversity in sexually selected traits.

Behavioral Traits

A series of studies conducted in conjunction with the MPAs aimed to investigate the effects of protection beyond demography and life-history traits. Villegas-Ríos et al. (2017a) suggested that protection might induce behavioral changes in favor of less mobile phenotypes in the protected population resulting from three processes/assumptions. First, individuals differ in their tendency to move, and therefore to leave the MPA and be exposed to the fishery outside. This idea is now widely recognized as several studies have demonstrated repeatability of movement traits such as dispersal tendency or home range size in several fish and aquatic invertebrates, including cod and lobster (Harrison et al., 2015; Villegas-Ríos et al., 2017b; Moland et al., 2019). Second, individuals with a smaller home range would spend more time under protection and thus increase their fitness, as shown by Villegas-Ríos et al. (unpublished). However, the potential for protection depends on the location of the home range. Thorbjørnsen et al. (2019) showed that the degree of potential protection conferred to sea trout by a no-take zone increased with home range size in sea trout initially tagged outside of the no-take zone (**Figure 3B**). Last, movement traits must be at least partially heritable to affect population behavioral composition over time, which seems to be the case across species and taxa according to a recent metanalysis by Dochtermann et al. (2019). Using sea trout as a model species, Thorbjørnsen et al. (2021) showed that home range size represented a personality trait that also affected survival differently depending on how much time the fish spent in the reserve. Having a larger home range led to a decrease in survival for individuals spending more time in the reserve, while having a larger home range led to an increase in survival for individuals spending less time in the reserve. To preserve behavioral variation in a population, a mosaic of marine protected areas

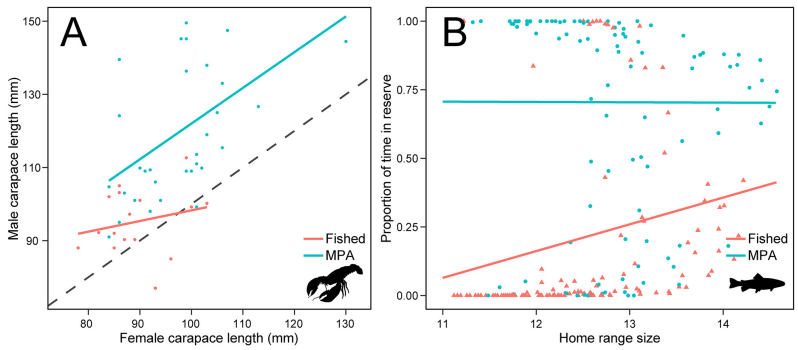

FIGURE 3 | Evidence of altered selection landscapes in MPAs: **(A)** size-assortative mating in *H. gammarus* inside and outside a lobster reserve. Data points are mating confirmed by genetic parentage studies on lobster populations in protected (blue) and harvested (orange) states. Stippled line denote isometry (Y = X) where females and males are equal in size (modified from Sørdalen et al., 2018); **(B)** disparate protection potential (proportion of time spent in a no-take MPA) with increasing home range size in *S. trutta* tagged inside (blue, circles) and outside (orange, triangles) of the no-take zone in Tvedestrand fjord (modified from Thorbjørnsen et al., 2019).

and areas open to harvest was suggested as a management tool (Thorbjørnsen et al., 2021).

DISCUSSION

Over the course of 16 years since the first before data were collected in designated experimental MPAs in Skagerrak, the network of MPAs described herein have allowed for substantial contributions to marine- and fisheries conservation science. Early effects of MPAs have been detected as population increases and positive shifts in age- and size-structure of protected populations. With time, the BACIPS-designed monitoring work has enabled detection of (1) longer-term demographic effects of protection, and (2) shifts in the selective landscape shaping phenotypic traits disparately within protected and harvested populations. Although the BACIPS-design has been used effectively in other MPA studies, e.g., in ecological evaluation of MPA networks (e.g., Grorud-Colvert et al., 2014; Thiault et al., 2019), they remain rare. In their seminal study, Claudet et al. (2008) showed that sufficient time (and size) is essential for MPA-effects to develop. Investment in long-term monitoring is thus a worthwhile priority for any entity tasked with evaluation of MPA-effects. In the Northern Channel Islands, California, there is evidence for trophic redundancy attained through restoration of predator abundance and -size structure, especially in older MPAs (Hamilton and Caselle, 2015; Caselle et al., 2018; Eisaguirre et al., 2020). However, using an extensive BACI time series, Malakhoff and Miller (2021) recently suggested that despite increased predator density, trophic cascades have yet to develop in California's northern Channel Island marine reserves after 15 years of protection. They suggested that more time, and/or recovery of more effective urchin predators might be needed to induce kelp forest trophic cascades. Long-term BACIPS monitoring studies are helpful in producing realistic expectations regarding the development of population- and ecological effects of MPAs.

Clawed and spiny lobsters have shown unequivocal positive response to protection in MPAs elsewhere (Shears et al., 2006; Goñi et al., 2010; Hoskin et al., 2011). Considering the recent and historical harvest pressure on coastal European lobster populations in Skagerrak (Kleiven et al., 2012; Kleiven et al., unpublished), it is likely that the positive effects of cessation of harvesting reported by studies reviewed herein were enabled by the combination of long-term historical depletion and high pre-closure fishing pressure in the sites (Jaco and Steele, 2020). While rebuilding of local lobster populations was the main goal when implementing the MPAs, the decreased harvest pressure in these areas also conferred effects on several fish species. Striving to test hypotheses of general interest to conservation science, we deem the study of lobster and sympatric fish species as case studies with attributes that are transferable to other aquatic species using the marine environment for all or part of their life cycle (e.g., Sørdalen et al., 2018, 2020; Thorbjørnsen et al., 2021). Two wrasse species, goldsinny (*Ctenolabrus rupestris*) and corkwing wrasse (*Symphodus melops*), both harvested to provide cleaner fish services in the salmonid aquaculture industry, showed moderate positive responses to protection in MPAs reviewed herein. Wrasse species targeted by fisheries have shown positive responses in other studies conducted in temperate MPAs, e.g., California sheephead *Semicossyphus pulcher* (Hamilton and Caselle, 2015; Jaco and Steele, 2020) and the Mediterranean wrasses *Coris julis* and *Symphodus doderleini* (Claudet et al., 2006). There is scope for further studies on the utility of MPAs to alleviate harvesting pressure and ensure ecosystem function and recruitment of wrasse species currently being heavily targeted by intensive fisheries in Southern and Western Norway.

Optimal MPA size and spacing has been a subject of much debate and scientific inquiry (see e.g., Gaines et al., 2010; Costello and Connor, 2019), also suggesting MPAs designed to benefit highly migratory species with known migration routes, aggregating behavior, and philopatry (Boerder et al., 2019). Interestingly, the relatively small Tvedestrand no-take zone was large enough to protect individual sea trout (Thorbjørnsen et al., 2019), hereby showing protective effects for an anadromous species. European lobster is generally a resident species showing high site-fidelity in shorter-term studies, both inside and outside

of MPAs (Moland et al., 2011; Huserbråten et al., 2013; Wiig et al., 2013). Due to a relatively long pelagic larval duration of 3–8 weeks, there is high potential for long distance dispersal (Manel et al., 2019). Using molecular techniques, Huserbråten et al. (2013) analyzed lobster tissue samples from the Skagerrak coastline spanning the MPA network (∼400 km, **Figure 1**). The work revealed high gene flow among populations which suggested a potential for downstream recruitment benefits from the MPAs in study. Although the initially implemented MPAs seemed to be of sufficient size to confer observable population effects, the recent trend has been establishment of somewhat larger MPAs in outer coastal areas of Skagerrak (Knutsen et al., unpublished). Two of the MPAs reviewed herein were subject to recent expansions (2016 and 2020) resulting from processes initiated by local management bodies to ensure management-relevant scaling of MPAs for lobster (see **Figure 1**). While Olsen and Moland (2011) demonstrated limited home range size of cod in a coastal seascape, the longer-term work by Fernández-Chacón et al. (2015) showed a tendency for increased annual emigration probability with time—thus indicating that the 1.1 km^2 Flødevigen MPA was too small to harbor coastal cod home ranges throughout- and past ontogeny. An effect of density dependence was also suggested as a partial explanation for the increased emigration probability. The sympatric cod ecotypes inhabiting coastal habitats in Skagerrak (Knutsen et al., 2018) seem to harbor differences in habitat, feeding ecology and movement behavior, where the "fjord" ecotype is associated with fjord habitat and benthic feeding ecology while the "North Sea" ecotype is associated with pelagic feeding and an higher tendency to migrate (Barth et al., 2019; Kristensen et al., 2021). There are knowledge gaps considering optimal design of MPAs tailored to these ecotypes' movement ecology. Commonly found occupying the outer coastal seascape, the "North Sea" ecotype is also overrepresented in cod samples from the bottom trawl fleet (Jorde et al., 2018). The more migratory behavior suggested for this ecotype might require larger, continuous fjord-to-deep-sea transect type MPAs to provide protection throughout the life cycle. Subject to intensive bottom trawling (Kroodsma et al., 2018), it is uncertain whether cod or other depleted demersal fish species might recover in Skagerrak under the present management regime (Cardinale et al., 2017). However, motivation to implement sufficiently large MPAs banning bottom trawling might be gleaned from Öresund, Sweden. Here, a ban on bottom trawling in effect since 1932 has allowed cod to prosper, also during periods of adverse environmental conditions, with size and age structure otherwise unseen at present in the Skagerrak-Kattegat neighborhood (Lindegren et al., 2010; Sundelöf et al., 2013).

Using data from the Tvedestrand fjord MPAs, Villegas-Ríos et al. (2017b) suggested that a small no-take zone could be maladaptive for fjord cod by favoring behavioral phenotypes characterized by small home ranges. While testing this hypothesis for sea trout in the Tvedestrand fjord, Thorbjørnsen et al. (2021) suggested a seascape mosaic of marine reserves, partially protected areas and areas open to harvest as a management tool to preserve behavioral variation in a sea trout population. Preserving behavioral variation is important to maintain a population's resilience to environmental change (Dingemanse et al., 2004). Fishes captured using hook-and-line can experience behavior selection against more active individuals (Alós et al., 2016), and MPA networks can help oppose this selection. Utilizing the same acoustic telemetry array in Tvedestrand fjord, Freitas et al. (2021) showed that summer peaks in sea surface temperature represent challenges for cod residing in a fjord environment, while ballan wrasse (*Labrus bergylta*) and Atlantic pollack (*Pollachius pollachius*) retained their movement behavior. During such periods, cod were confined to deeper, cooler water masses—away from shallow habitats preferred during autumn and winter. Future MPAs designed to protect cod and other demersal cold water species would benefit from being placed in sites that might act as "climate refugia" (Davis et al., 2021), where access to cool and well oxygenated water masses is likely to prolong habitat suitability in the face of increased environmental variability.

The recovery of size-structure and survival benefits reported from the studies conducted in the Norwegian Skagerrak all respond to a shift in size-selective mortality occurring within MPAs as a result of protection from fisheries. Baskett and Barnett (2015) reviewed the ecological and evolutionary consequences of marine reserves and noted the theoretical potential for protection against fisheries-induced evolution. Two findings reviewed herein support this notion. Using parental assignment, Sørdalen et al. (2018) showed a pattern of size-assortative mating in lobster which was much more pronounced in an MPA due to the recovery of size-structure. Moreover, relative claw size was found to be the best predictor of male mating success. This trait—large relative claw size—is both under sexual selection in natural states, and subject to harvest selection due to correlated behavioral traits that confer catchability in traps (Moland et al., 2019). Sørdalen et al. (2020) later showed that this sexually selected trait is rescued by absence of harvesting in MPAs. These pioneering studies resulted in significant advancement of our understanding of the contrasting effects of harvesting and protection on a long-lived species with complex behavioral and reproductive biology and led to introduction of a maximum legal size limit in the Skagerrak lobster fishery as of 2017.

In conclusion, the MPAs reviewed herein conferred multiple population effects on several species inhabiting the Skagerrak coastal seascape. Importantly, BACI-designed monitoring of MPA-control area pairs provided unequivocal demonstrations of local effects of protection on lobster populations. Importantly, as highly valuable by-products of unequivocally demonstrated population effects from BACI-type approaches, studies using the same populations in the "after" state can contribute to novel insights regarding more subtle effects of protection. Effects of protection on two wrasse species harvested as cleaner fish in salmonid aquaculture underscore the value of MPAs when coastal areas are faced with new and unexpected stressors from profitable industries. Namely, the opportunity to better understand and measure cumulative effects on coastal ecosystems through control-impact studies which in turn enable managers to make knowledge based-management decisions.

Effects of protection on European lobster in terms of conspicuous size increase and density increase manifested

as record breaking catches in research traps have created enthusiasm and optimism in the public eye, and thus provided an easily accessible entry to the concept of marine conservation and rebuilding potential in depleted coastal populations. This does not preclude the fact that allocation of areas in the coastal zone from fisheries to conservation purposes is still in an early phase in Norway and thus bound to be the subject of much debate among stakeholders. Nonetheless, MPAs in the form of small-scale lobster reserves—allowing hook and line fishing to continue—have provided a first introduction to the principles and potential benefits of marine conservation. Proper planning in close collaboration with fishers and managers, long-term scientific monitoring, inclusion of citizen science and evolving research protocols—also including fisheries data—have revealed novel effects of protection and harvesting on marine populations, with impact on harvest rules and the use of MPAs as empirically documented management tools in Norway.

AUTHOR CONTRIBUTIONS

EM and JK contributed equally to the conception and outline of the review. EM, AF-C, ST, DV-R, TS, KH, MH, AK, and EO wrote the manuscript. PNK, HK, SE, CF, and JK commented on versions of the draft. All authors contributed to manuscript revision, read, and approved the submitted version.

FUNDING

Long term monitoring of the MPAs in Skagerrak was funded by the Institute of Marine Research coastal ecosystems research program. Preparation of the manuscript was supported by the University of Agder through a priority research grant awarded to the Centre of Coastal Research (CCR). EO received funding from the Marine Science Program within the Research Council of Norway, grant no. 294926 (CODSIZE). DV-R received funding from the European Union's Horizon 2020 research and innovation programme under the Marie Sklodowska-Curie grant agreement No. 793627 (BEMAR) and from the programme IF_ERC from the Spanish National Research Council.

ACKNOWLEDGMENTS

We thank colleagues at the IMR Flødevigen marine research station for valuable assistance in field work and scientific cruises, as well as data management. We honor the late S.E. Enersen who worked side by side with JK in the early years of MPA site designation, implementation and monitoring. JK also trained a new generation of lobster researchers at IMR. EM and AK are indebted to their mentors G.P. Jones and G.R. Russ. We are thankful for the contributions from three referees who provided insightful reviews that improved the content of this review.

REFERENCES

Alós, J., Palmer, M., Rosselló, R., and Arlinghaus, R. (2016). Fast and behavior-selective exploitation of a marine fish targeted by anglers. *Sci. Rep.* 6:e38093. doi: 10.1038/srep38093

Babcock, R. C., Shears, N. T., Alcala, A. C., Barrett, N. S., Edgar, G. J., Lafferty, K. D., et al. (2010). Decadal trends in marine reserves reveal differential rates of change in direct and indirect effects. *Proc. Natl. Acad. Sci. U.S.A.* 107, 18256–18261. doi: 10.1073/pnas.0908012107

Barceló, C., White, J. W., Botsford, L. W., and Hastings, A. (2021). Projecting the timescale of initial increase in fishery yield after implementation of marine protected areas. *ICES J. Mar. Sci.* fsaa233. doi: 10.1093/icesjms/fsaa233

Barth, J. M., Villegas-Ríos, D., Freitas, C., Moland, E., Star, B., André, C., et al. (2019). Disentangling structural genomic and behavioural barriers in a sea of connectivity. *Mol. Ecol.* 28, 1394–1411. doi: 10.1111/mec.15010

Baskett, M. L., and Barnett, L. A. K. (2015). The ecological and evolutionary consequences of marine reserves. *Annu. Rev. Ecol. Evol. Syst.* 46, 49–73. doi: 10.1146/annurev-ecolsys-112414-054424

Biro, P. A., Adriaenssens, B., and Sampson, P. (2014). Individual and sex-specific differences in intrinsic growth rate covary with consistent individual differences in behaviour. *J. Anim. Ecol.* 83, 1186–1195. doi: 10.1111/1365-2656.12210

Biro, P. A., and Sampson, P. (2015). Fishing directly selects on growth rate via behaviour: implications of growth-selection that is independent of size. *Proc. Biol. Sci.* 282:20142283. doi: 10.1098/rspb.2014.2283

Boerder, K., Schiller, L., and Worm, B. (2019). Not all who wander are lost: improving spatial protection for large pelagic fishes. *Mar. Policy* 105, 80–90. doi: 10.1016/j.marpol.2019.04.013

Caselle, J. E., Davis, K., and Marks, L. M. (2018). Marine management affects the invasion success of a non-native species in a temperate reef system in California,. USA. *Ecol. Lett.* 21, 43–53. doi: 10.1111/ele.12869

Cardinale, M., Svenson, A., and Hjelm, J. (2017). The "easy restriction" syndrome drive local fish stocks to extinction: the case of the management of Swedish coastal populations. *Mar. Policy* 83, 179–183. doi: 10.1016/j.marpol.2017.06.011

Claudet, J., Osenberg, C. W., Benedetti-Cecchi, L., Domenici, P., Garcia-Charton, J. A., Perez-Ruzafa, A., et al. (2008). Marine reserves: size and age do matter. *Ecol. Lett.* 11, 481–489. doi: 10.1111/j.1461-0248.2008.01166.x

Claudet, J., Pelletier, D., Jouvenel, J.-Y., Bachet, F., and Galzin, R. (2006). Assessing the effects of marine protected area (MPA) on a reef fish assemblage in a northwestern Mediterranean marine reserve: identifying community-based indicators. *Biol. Conserv.* 130, 349–369. doi: 10.1016/j.biocon.2005.12.030

Costello, M. J., and Connor, D. W. (2019). Connectivity is generally not important for marine reserve planning. *Trends Ecol. Evol.* 34, 686–688. doi: 10.1016/j.tree.2019.04.015

Davis, T. R., Champion, C., and Coleman, M. A. (2021). Climate refugia for kelp within an ocean warming hotspot revealed by stacked species distribution modelling. *Mar. Environ. Res.* 166:105267. doi: 10.1016/j.marenvres.2021.105267

Dingemanse, N. J., Both, C., Drent, P. J., and Tinbergen, J. M. (2004). Fitness consequences of avian personalities in a fluctuating environment. *P. Roy. Soc. B.* 271, 847–852. doi: 10.1098/rspb.2004.2680

Dochtermann, N. A., Schwab, T., Anderson Berdal, M., Dalos, J., and Royauté, R. (2019). The heritability of behavior: a meta-analysis. *J. Hered.* 110, 403–410. doi: 10.1093/jhered/esz023

Edgar, G., Stuart-Smith, R., Willis, T., Kininmonth, S., Baker, S. C., Banks, S., et al. (2014). Global conservation outcomes depend on marine protected areas with five key features. *Nature* 506, 216–220. doi: 10.1038/nature13022

Eisaguirre, J. H., Eisaguirre, J. M., Davis, K., Carlson, P. M., Gaines, S. D., and Caselle, J. E. (2020). Trophic redundancy and predator size class structure drive differences in kelp forest ecosystem dynamics. *Ecology.* 101:e02993. doi: 10.1002/ecy.2993

Ellis, C. D., Hodgson, D. J., Daniels, C. L., Collins, M., and Griffiths, A. G. F. (2017). Population genetic structure in European lobsters: implications for connectivity, diversity and hatchery stocking. *Mar. Ecol. Prog. Ser.* 563, 123–137.

Ellis, J. I., and Schneider, D. C. (1997). Evaluation of a gradient sampling design for environmental impact assessment. *Environ. Monit. Assess.* 48, 157–172.

Fenberg, P. B., Caselle, J. E., Claudet, J., Clemence, M., Gaines, S. D., Antonio García-Charton, J., et al. (2012). The science of European marine reserves: status, efficacy, and future needs. *Mar. Policy* 36, 1012–1021.

Fernández-Chacón, A., Buttay, L., Moland, E., Knutsen, H., and Olsen, E. M. (2021). Demographic responses to protection from harvesting in a long-lived marine species. *Biol. Conserv.* 257:109094. doi: 10.1016/j.biocon.2021.109094

Fernández-Chacón, A., Moland, E., Espeland, S. H., Kleiven, A. R., and Olsen, E. M. (2017). Causes of mortality in depleted populations of Atlantic cod estimated from multi-event modelling of mark–recapture and recovery data. *Can. J. Fish. Aquat. Sci.* 74, 116–126. doi: 10.1139/cjfas-2015-0313

Fernández-Chacón, A., Moland, E., Espeland, S. H., and Olsen, E. M. (2015). Demographic effects of full vs. partial protection from harvesting: inference from an empirical before-after control-impact study on Atlantic cod. *J. Appl. Ecol.* 52, 1206–1215.

Fernández-Chacón, A., Villegas-Ríos, D., Moland, E., Baskett, M. L., Olsen, E. M., and Carlson, S. M. (2020). Protected areas buffer against harvest selection and rebuild phenotypic complexity. *Ecol. Appl.* 30:e02108. doi: 10.1002/eap.2108

Francis, R. C., Hixon, M. A., Clarke, M. E., Murawski, S. A., and Ralston, S. (2007). Ten commandments for ecosystem-based fisheries scientists. *Fisheries* 32, 217–233.

Freitas, C., Villegas-Ríos, D., Moland, E., and Olsen, E. M. (2021). Sea temperature effects on depth use and habitat selection in a marine fish community. *J. Anim. Ecol.* doi: 10.1111/1365-2656.13497

Frigstad, H., Kaste, Ø., Deininger, A., Kvalsund, K., Christensen, G., Bellerby, R. G. J., et al. (2020). Influence of riverine input on Norwegian coastal systems. *Front. Mar. Sci.* 7:332. doi: 10.3389/fmars.2020.00332

Gaines, S. D., White, C., Carr, M. H., and Palumbi, S. R. (2010). Designing marine reserve networks for both conservation and fisheries management. *Proc. Natl. Acad. Sci. U.S.A.* 107, 18286–18293. doi: 10.1073/pnas.0906473107

Gjøsaeter, J. (2002). Fishery for goldsinny wrasse (*Ctenolabrus rupestris*) (Labridae) with pots along the Norwegian Skagerrak coast. *Sarsia* 87, 83–90.

Goñi, R., Hilborn, R., Diaz, D., Mallol, S., and Adlerstein, S. (2010). Net contribution of spillover from a marine reserve to fishery catches. *Mar. Ecol. Prog. Ser.* 400, 233–243.

Grorud-Colvert, K., Claudet, J., Tissot, B. N., Caselle, J. E., Carr, M. H., Day, J. C., et al. (2014). Marine protected area networks: assessing whether the whole is greater than the sum of its parts. *PLoS One* 9:e102298. doi: 10.1371/journal.pone.0102298

Halvorsen, K. T., Larsen, T., Browman, H. I., Durif, C., Aasen, N., Vøllestad, L. A., et al. (2021). Movement patterns of temperate wrasses (Labridae) within a small Marine Protected area. *J. Fish Biol.*

Halvorsen, K. T., Larsen, T., Sørdalen, T. K., Vøllestad, L. A., Knutsen, H., and Olsen, E. M. (2017). Impact of harvesting cleaner fish for salmonid aquaculture assessed from replicated coastal marine protected areas. *Mar. Biol. Res.* 13, 359–369. doi: 10.1080/17451000.2016.1262042

Halvorsen, K. T., Sørdalen, T. K., Larsen, T., Browman, H. I., Rafoss, T., Albretsen, J., et al. (2020). Mind the depth: the vertical dimension of a small-scale fishery shapes selection on species, size and sex in wrasses. *Mar. Coast. Fish.* 12, 404–422. doi: 10.1002/mcf2.10131

Hamilton, S. L., and Caselle, J. E. (2015). Exploitation and recovery of a sea urchin predator has implications for the resilience of southern California kelp forests. *Proc. R. Soc. B* 282:20141817. doi: 10.1098/rspb.2014.1817

Harrison, P. M., Gutowsky, L. F. G., Martins, E. G., Patterson, D. A., Cooke, S. J., and Power, M. (2015). Personality-dependent spatial ecology occurs independently from dispersal in wild burbot (*Lota lota*). *Behav. Ecol.* 26, 483–492. doi: 10.1093/beheco/aru216

Hoskin, M. G., Coleman, R. A., von Carlshausen, E., and Davis, C. M. (2011). Variable population responses to the establishment of a temperate no-take zone. *Can. J. Fish. Aquat. Sci.* 68, 185–200. doi: 10.1139/F10-143

Huserbråten, M. B. O., Moland, E., Knutsen, H., Olsen, E. M., André, C., and Stenseth, N. C. (2013). Conservation, spillover and gene flow within a network of Northern European marine protected areas. *PLoS One* 8:e73388. doi: 10.1371/journal.pone.0073388

IPBES (2019). *Summary for Policymakers of the Global Assessment Report on Biodiversity and Ecosystem Services of the Intergovernmental Science-Policy Platform on Biodiversity and Ecosystem Services*, eds S. Díaz, J. Settele, E. S. Brondízio, H. T. Ngo, M. Guèze, J. Agard, et al. (Bonn: IPBES secretariat), 56.

Jaco, E. M., and Steele, M. A. (2020). Pre-closure fishing pressure predicts effects of marine protected areas. *J. Appl. Ecol.* 57, 229–240. doi: 10.1111/1365-2664.13541

Jones, G. P., Cole, R. C., and Battershill, C. N. (1992). "Marine reserves: Do they work?," in *Proceedings of the Second International Temperate Reef Symposium*, Auckland, 29–45.

Jorde, P. E., Kleiven, A. R., Sodeland, M., Olsen, E. M., Ferter, K., Jentoft, S., et al. (2018). Who is fishing on what stock: population-of-origin of individual cod (*Gadus morhua*) in commercial and recreational fisheries. *ICES J. Mar. Sci.* 75, 2153–2162. doi: 10.1093/icesjms/fsy080

Kaplan, K. A., Yamane, L., Botsford, L. W., Baskett, M. L., Hastings, A., Worden, S., et al. (2019). Setting expected timelines of fished population recovery for the adaptive management of a marine protected area network. *Ecol. Appl.* 29:e01949. doi: 10.1002/eap.1949

Kellner, J. B., Tetreault, I., Gaines, S. D., and Nisbet, R. M. (2007). Fishing the line near marine reserves in single and multispecies fisheries. *Ecol. Appl.* 17, 1039–1054. doi: 10.1890/05-1845

Kleiven, A. R., Olsen, E. M., and Vølstad, J. H. (2012). Total catch of a red-listed marine species is an order of magnitude higher than official data. *PLoS One* 7:e31216. doi: 10.1371/journal.pone.0031216

Knutsen, H., Jorde, P. E., Blanco Gonzalez, E., Eigaard, O. R., Pereyra, R. T., Sannaes, H., et al. (2015). Does population genetic structure support present management regulations of the northern shrimp (*Pandalus borealis*) in Skagerrak and the North Sea? *ICES J. Mar. Sci.* 72, 863–871. doi: 10.1093/icesjms/fsu204

Knutsen, H., Jorde, P. E., Hutchings, J. A., Hemmer-Hansen, J., Grønkjaer, P., Jørgensen, K. E. M., et al. (2018). Stable coexistence of genetically divergent Atlantic cod ecotypes at multiple spatial scales. *Evol. Appl.* 11, 1527–1539.

Kristensen, M. L., Moland, E., Koed, A., Källo, K., Olsen, E. M., Knutsen, H., et al. (2021). Disparate movement behaviour and feeding ecology in sympatric ecotypes of Atlantic cod. *Ecol. Evol.* accepted.

Kroodsma, D. A., Mayorga, J., Hochberg, T., Miller, N. A., Miller, K., Ferretti, F., et al. (2018). Tracking the global footprint of fisheries. *Science* 359, 904–908.

Lindegren, M., Diekmann, R., and Möllmann, C. (2010). Regime shifts, resilience and recovery of a cod stock. *Mar. Ecol. Prog. Ser.* 402, 239–253. doi: 10.3354/meps08454

Lubchenco, J., Palumbi, S. R., Gaines, S. D., and Andelman, S. (2003). Plugging a hole in the ocean: the emerging science of marine reserves. *Ecol. Appl.* 13, 3–7.

Malakhoff, K. D., and Miller, R. J. (2021). After 15 years, no evidence for trophic cascades in marine protected areas. *Proc. Biol. Sci.* 288:20203061. doi: 10.1098/rspb.2020.3061

Manel, S., Loiseau, N., Andrello, M., Fietz, K., Goñi, R., Forcada, A., et al. (2019). Long-distance benefits of marine reserves: Myth or Reality? *Trends Ecol. Evol.* 34, 342–354. doi: 10.1016/j.tree.2019.01.002

Maunder, M. N., Sibert, J. R., Fonteneau, A., Hampton, J., Kleiber, P., and Harley, S. J. (2006). Interpreting catch per unit effort data to assess the status of individual stocks and communities. *ICES J. Mar. Sci.* 63, 1373–1385. doi: 10.1016/j.icesjms.2006.05.008

Moland, E., Carlson, S. M., Villegas-Ríos, D., Wiig, J. R., and Olsen, E. M. (2019). Harvest selection on multiple traits in the wild revealed by aquatic animal telemetry. *Ecol. Evol.* 9, 6480–6491.

Moland, E., Olsen, E. M., Andvord, K., Knutsen, J. A., and Stenseth, N. C. (2011). Home range of European lobster (*Homarus gammarus*) in a marine reserve: implications for future reserve design. *Can. J. Fish. Aquat. Sci.* 68, 1197–1210.

Moland, E., Olsen, E. M., Knutsen, H., Garrigou, P., Espeland, S. H., Kleiven, A. R., et al. (2013a). Lobster and cod benefit from small-scale northern marine protected areas: inference from an empirical before-after control-impact study. *Proc. Biol. Sci.* 280:20122679.

Moland, E., Ulmestrand, M., Olsen, E. M., and Stenseth, N. C. (2013b). Long-term decrease in sex-specific natural mortality of European lobster within a marine protected area. *Mar. Ecol. Prog. Ser.* 491, 153–164.

Nillos Kleiven, P. J., Espeland, S. H., Olsen, E. M., Abesamis, R. A., Moland, E., and Kleiven, A. R. (2019). Fishing pressure impacts the abundance gradient of European lobsters across the borders of a newly established marine protected area. *Proc. Biol. Sci.* 286: 20182455.

Olsen, E. M., Carlson, S. M., Gjøsaeter, J., and Stenseth, N. C. (2009). Nine decades of decreasing phenotypic variability in Atlantic cod. *Ecol. Lett.* 12, 622–631.

Olsen, E. M., Johnson, D., Weaver, P., Goñi, R., Ribeiro, M. C., Rabaut, M., et al. (2013). *Achieving Ecologically Coherent MPA Networks in Europe: Science Needs and Priorities. Marine Board Position Paper 18*, eds K. E. Larkin and N. McDonough (Ostend: European Marine Board).

Olsen, E. M., Knutsen, H., Gjøsaeter, J., Jorde, P. E., Knutsen, J. A., and Stenseth, N. C. (2004). Life history variation among local populations of Atlantic cod (Gadus morhua) from the Norwegian Skagerrak coast. *J. Fish Biol.* 64, 1725–1730. doi: 10.1111/j.1095-8649.2004.00402.x

Olsen, E. M., Knutsen, H., Simonsen, J. H., Jonsson, B., and Knutsen, J. A. (2006). Seasonal variation in marine growth of sea trout, *Salmo trutta*, in coastal Skagerrak. *Ecol. Freshw. Fish* 15, 446–452.

Olsen, E. M., and Moland, E. (2011). Fitness landscape of Atlantic cod shaped by harvest selection and natural selection. *Evol. Ecol.* 25, 695–710.

Osenberg, C. W., Shima, J. S., Miller, S. L., and Stier, A. C. (2011). "Ecology – Assessing effects of marine protected areas: confounding in space and possible solutions," in *Marine Protected Areas: A Multidisciplinary Approach*, ed. J. Claudet (Cambridge: Cambridge University Press), 143–167.

Oug, E., Djursvoll, P., Aagaard, K., Brattegaard, T., et al. (2006). "Crustacea," in *Norwegian red list*, eds J. A. Kålås, Å. Viken, and T. S. Bakken (Trondheim: Artsdatabanken), 197–206.

Perälä, T., Olsen, E. M., and Hutchings, J. A. (2020). Disentangling conditional effects of multiple regime shifts on Atlantic cod productivity. *PLoS One* 15:e0237414. doi: 10.1371/journal.pone.0237414

Pettersen, A. R., Moland, E., and Olsen, E. M. (2009). "Lobster reserves in coastal Skagerrak – an integrated analysis of the implementation process," in *Integrated Coastal Zone Management*, eds E. Dahl, E. Moksness, and J. Støttrup (London: Wiley-Blackwell Publishing), 178–188.

Rogers, L. A., Olsen, E. M., Knutsen, H., and Stenseth, N. C. (2014). Habitat effects on population connectivity in a coastal seascape. *Mar. Ecol. Prog. Ser.* 511, 153–163.

Roney, N. E., Hutchings, J. A., Olsen, E. M., Knutsen, H., Albretsen, J., and Kuparinen, A. (2016). Fine-scale life-history structure in a highly mobile marine fish. *Evol. Ecol. Res.* 17, 95–109.

Russ, G. R. (2002). "Yet another review of marine reserves as reef fishery management tools," in *Coral Reef Fishes: Dynamics and Diversity in a Complex Ecosystem*, ed. P. F. Sale (San Diego, CA: Academic Press), 421–443.

Shears, N. T., Grace, R. V., Usmar, N. R., Kerr, V., and Babcock, R. C. (2006). Long-term trends in lobster populations in a partially protected vs. no-take Marine Park. *Biol. Conserv.* 132, 222–231. doi: 10.1016/j.biocon.2006.04.001

Sheehy, M. R. J., Bannister, R. C. A., Wickins, J. F., and Shelton, P. M. J. (1999). New perspectives on the growth and longevity of the European lobster (*Homarus gammarus*). *Can. J. Fish. Aquat. Sci.* 56, 1904–1915.

Skerritt, D. J., Robertson, P. A., Mill, A. C., Polunin, N. V. C., and Fitzsimmons, C. (2015). Fine- scale movement, activity patterns and home-ranges of European lobster *Homarus gammarus*. *Mar. Ecol. Prog. Ser.* 536, 203–219.

Sørdalen, T. K., Halvorsen, K. T., Harrison, H. B., Ellis, C. D., Vøllestad, L. A., Knutsen, H., et al. (2018). Harvesting changes mating behaviour in European lobster. *Evol. Appl.* 11, 963–977.

Sørdalen, T. K., Halvorsen, K. T., Vøllestad, L. A., Moland, E., and Olsen, E. M. (2020). Marine protected areas rescue a sexually selected trait in European lobster. *Evol. Appl.* 13, 2222–2233. doi: 10.1111/eva.12992

Stewart-Oaten, A., Murdoch, W. W., and Parker, K. R. (1986). Environmental impact assessment: "Pseudoreplication" in time? *Ecology* 67, 929–940.

Sundelöf, A., Wennhage, H., and Svedäng, H. (2013). A red herring from the Öresund (ICES40G2): the apparent recovery of the Large Fish Indicator (LFI) in the North Sea hides a non-trawled area. *ICES J. Mar. Sci.* 70, 1081–1084. doi: 10.1093/icesjms/fst117

Thiault, L., Kernaléguen, L., Osenberg, C. W., Lison, de Loma, T., Chancerelle, Y., et al. (2019). Ecological evaluation of a marine protected area network: a progressive-change BACIPS approach. *Ecosphere.* 10:e02576. doi: 10.1002/ecs2.2576

Thorbjørnsen, S. H., Moland, E., Huserbråten, M. B. O., Knutsen, J. A., Knutsen, H., and Olsen, E. M. (2018). Replicated marine protected areas (MPAs) support movement of larger, but not more, European lobsters to neighbouring fished areas. *Mar. Ecol. Prog. Ser.* 595, 123–133. doi: 10.3354/meps12546

Thorbjørnsen, S. H., Moland, E., Simpfendorfer, C., Heupel, M., Knutsen, H., and Olsen, E. M. (2019). Potential of a no-take marine reserve to protect home ranges of anadromous brown trout (*Salmo trutta*). *Ecol. Evol.* 9, 417–426. doi: 10.1002/ece3.4760

Thorbjørnsen, S. H., Moland, E., Villegas-Ríos, D., Bleeker, K., Knutsen, H., and Olsen, E. M. (2021). Selection on fish spatial personality differs between a no-take marine reserve and fished areas. *Evol. Appl.* doi: 10.1111/eva.13242

Thorstad, E. B., Todd, C. D., Uglem, I., Bjørn, P. A., Gargan, P. G., Vollset, K. W., et al. (2016). Marine life of the sea trout. *Mar. Biol.* 163:47. doi: 10.1007/s00227-016-2820-3

Thurstan, R. H., and Roberts, C. M. (2010). Ecological Meltdown in the Firth of Clyde, Scotland: two centuries of change in a coastal marine ecosystem. *PLoS One* 5:e11767. doi: 10.1371/journal.pone.0011767

Underwood, A. J. (1992). Beyond BACI: the detection of environmental impacts on populations in the real, but variable, world. *J. Exp. Mar. Biol. Ecol.* 161, 145–178. doi: 10.1016/0022-0981(92)90094-q

Underwood, A. J. (1994). On beyond BACI: sampling designs that might reliably detect environmental disturbances. *Ecol. Appl.* 4, 3–15. doi: 10.2307/1942110

Villegas-Ríos, D., Moland, E., and Olsen, E. M. (2017a). Potential of contemporary evolution to erode fishery benefits from marine reserves. *Fish Fish.* 18, 571–577. doi: 10.1111/faf.12188

Villegas-Ríos, D., Réale, D., Freitas, C., Moland, E., and Olsen, E. M. (2017b). Individual level consistency and correlations of fish spatial behaviour assessed from aquatic animal telemetry. *Anim. Behav.* 124, 83–94. doi: 10.1016/j.anbehav.2016.12.002

Wiig, J. R., Moland, E., Haugen, T. O., and Olsen, E. M. (2013). Spatially structured interactions between lobsters and lobster fishers in a coastal habitat: fine-scale behaviour and survival estimated from acoustic telemetry. *Can. J. Fish. Aquat. Sci.* 70, 1468–1476. doi: 10.1139/cjfas-2013-0209

Conflict of Interest: The authors declare that the research was conducted in the absence of any commercial or financial relationships that could be construed as a potential conflict of interest.

Copyright © 2021 Moland, Fernández-Chacón, Sørdalen, Villegas-Ríos, Thorbjørnsen, Halvorsen, Huserbråten, Olsen, Nillos Kleiven, Kleiven, Knutsen, Espeland, Freitas and Knutsen. This is an open-access article distributed under the terms of the Creative Commons Attribution License (CC BY). The use, distribution or reproduction in other forums is permitted, provided the original author(s) and the copyright owner(s) are credited and that the original publication in this journal is cited, in accordance with accepted academic practice. No use, distribution or reproduction is permitted which does not comply with these terms.

frontiers in Marine Science

ORIGINAL RESEARCH
published: 09 July 2021
doi: 10.3389/fmars.2021.660122

Changes in the Movement and Calling Behavior of Minke Whales (*Balaenoptera acutorostrata*) in Response to Navy Training

Ian N. Durbach[1,2], Catriona M. Harris[1], Cameron Martin[3], Tyler A. Helble[3], E. Elizabeth Henderson[3], Glenn Ierley[4], Len Thomas[1] and Stephen W. Martin[5]*

[1] Centre for Research into Ecological and Environmental Modelling, University of St Andrews, St Andrews, United Kingdom, [2] Centre for Statistics in Ecology, Environment and Conservation, University of Cape Town, Cape Town, South Africa, [3] Naval Information Warfare Center Pacific, San Diego, CA, United States, [4] Scripps Institution of Oceanography, University of California, San Diego, San Diego, CA, United States, [5] National Marine Mammal Foundation, San Diego, CA, United States

OPEN ACCESS

Edited by:
Juan Jacobo Schmitter-Soto, The South Border College (ECOSUR), Mexico

Reviewed by:
Nataly Castelblanco-Martínez, National Council of Science and Technology (CONACYT), Mexico
Frans-Peter Lam, Netherlands Organisation for Applied Scientific Research TNO, Netherlands

***Correspondence:**
Ian N. Durbach
id52@st-andrews.ac.uk

Specialty section:
This article was submitted to Marine Ecosystem Ecology, a section of the journal Frontiers in Marine Science

Received: 28 January 2021
Accepted: 16 June 2021
Published: 09 July 2021

Citation:
Durbach IN, Harris CM, Martin C, Helble TA, Henderson EE, Ierley G, Thomas L and Martin SW (2021) Changes in the Movement and Calling Behavior of Minke Whales (Balaenoptera acutorostrata) in Response to Navy Training. Front. Mar. Sci. 8:660122. doi: 10.3389/fmars.2021.660122

Many marine mammals rely on sound for foraging, maintaining group cohesion, navigation, finding mates, and avoiding predators. These behaviors are potentially disrupted by anthropogenic noise. Behavioral responses to sonar have been observed in a number of baleen whale species but relatively little is known about the responses of minke whales (*Balaenoptera acutorostrata*). Previous analyses demonstrated a spatial redistribution of localizations derived from passive acoustic detections in response to sonar activity, but the lack of a mechanism for associating localizations prevented discriminating between movement and cessation of calling as possible explanations for this redistribution. Here we extend previous analyses by including an association mechanism, allowing us to differentiate between movement responses and calling responses, and to provide direct evidence of horizontal avoidance responses by individual minke whales to sonar during U.S. Navy training activities. We fitted hidden Markov models to 627 tracks that were reconstructed from 3 years of minke whale (*B. acutorostrata*) vocalizations recorded before, during, and after naval training events at the U.S. Navy's Pacific Missile Range Facility, Kauai, Hawaii. The fitted models were used to identify different movement behaviors and to investigate the effect of sonar activity on these behaviors. Movement was faster and more directed during sonar exposure than in baseline phases. The mean direction of movement differed during sonar exposure, and was consistent with movement away from sonar-producing ships. Animals were also more likely to cease calling during sonar. There was substantial individual variation in response. Our findings add large-sample support to previous demonstrations of horizontal avoidance responses by individual minke whales to sonar in controlled exposure experiments, and demonstrate the complex nature of behavioral responses to sonar activity: some, but not all, whales exhibited behavioral changes, which took the form of horizontal avoidance or ceasing to call.

Keywords: naval sonar, passive acoustic monitoring, behavioral response, animal movement, minke whale

INTRODUCTION

Over the last few decades there has been increasing effort to study and understand the impacts of anthropogenic disturbance on marine mammals. In particular there has been a focus on the effects of underwater noise on individuals, both physiologically and behaviorally, and the potential for these effects to result in population-level consequences (e.g., National Research Council, 2005; Harris et al., 2018; Pirotta et al., 2018; Booth et al., 2020). Underwater noise has the potential to impact many different life functions due to the importance of sound in an environment where vision often has limited utility. For example, many marine mammal species rely on sound for foraging, socializing, navigating, mate finding, and predator avoidance (e.g., Tyack and Clark, 2000; Johnson et al., 2009; Parks et al., 2014; King and Janik, 2015; Erbe et al., 2016). One of the best studied sources of underwater noise, with respect to its effect on marine mammals, is naval sonar (see Harris et al., 2018, for review). Research was originally motivated by atypical mass stranding events apparently caused by naval sonar activities (D'Amico et al., 2009). More recently there has been increased regulatory requirements to quantify marine mammal behavioral responses to noise and consider the fitness consequences that, e.g., cessation of foraging, may have on individuals and populations (Pirotta et al., 2018).

Controlled exposure experiments (CEEs), which utilize a formal experimental design, have been one of the main approaches taken by field researchers trying to establish a causal relationship between sonar stimuli and behavioral responses (Southall et al., 2016). These studies use a suite of data collection methods to quantify the behavior of the study animal before, during, and after exposure to specific doses of sonar sound. CEEs can be logistically challenging and expensive to undertake and, therefore, sample sizes tend to be small for most studied species. This is certainly true for the minke whale (*Balaenoptera acutorostrata*), for which there have only been two sonar exposures achieved to date because of the logistical difficulties of conducting CEEs on this species (Kvadsheim et al., 2017). Minke whales are among the most abundant and wide-ranging baleen whales (Bannister, 2018), with individuals undertaking a seasonal migration between high latitudes, where they spend summer, and low latitudes, where they spend winter. Despite being listed as a species of Least Concern under the International Union for Conservation of Nature (IUCN) Red List (Cooke et al., 2018), the species is relatively poorly understood and, from the perspective of noise disturbance, they are of concern due to their involvement in the multi-species stranding event in the Bahamas in 2000 (Balcomb and Claridge, 2001). Minke whales can be difficult to track visually and it can be challenging to approach close enough to deploy telemetry devices. Two independent research teams have each conducted one sonar exposure on minke whales and the results were combined by Kvadsheim et al. (2017) to compare the responses of these two individuals. Despite being exposed in different geographical locations, in different contexts, and with different sonar signals, both individuals demonstrated similar avoidance responses (Kvadsheim et al., 2017). Interestingly, these two individual exposure events resulted in responses at lower received levels and of higher severity than has been observed for most other baleen whale individuals [e.g., blue whales (*Balaenoptera musculus*, Southall et al., 2019), humpback whales (*Megaptera novaeangliae*, Sivle et al., 2016)], indicating that perhaps minke whales should be treated differently from other baleen whales when assessing the risk of sonar exposure to this species. There is increasing evidence that the most commonly used approach for grouping species for e.g., noise impact assessment, whereby species are classified according to functional hearing groups, is not appropriate for assessing behavioral responses to sonar (Harris et al., 2018). It is therefore important to understand whether the results obtained thus far for minke whales are representative of the responsiveness of the species.

Given the complexity of the results emerging from CEE studies whereby there is high inter- and intra-species and individual variability in both response thresholds (i.e., the received level of sound at which an individual responds) and the type of responses exhibited (Southall et al., 2016; Harris et al., 2018), it is critical that findings are validated with larger datasets where possible. Opportunistic exposure studies provide an opportunity to test the predictions established by CEEs across larger scales, both spatial and temporal, but also with larger numbers of individual animals (e.g., McCarthy et al., 2011; Melcon et al., 2012; Moretti et al., 2014; Martin et al., 2015). Opportunistic exposure studies monitor responses of marine mammals to real-world naval training (as opposed to potentially somewhat artificial experimental) activities during which the researcher has no control over the use of the sonar or the doses received by individual animals. These studies have often been associated with U.S. Navy training and testing ranges where bottom-mounted hydrophone arrays located on the ranges can be used to monitor the presence and distribution of vocalizing marine mammals using passive acoustic monitoring (PAM), a non-invasive tool for wildlife monitoring that places one or more autonomous recording devices into marine or terrestrial environments and uses the recordings from these devices for monitoring purposes e.g., estimating species distribution or density (Sugai et al., 2019). Changes in presence or distribution can be used to evaluate the effects of discrete training events. Here it is important to distinguish between the experimental protocol used and the monitoring technology used to gather data. Controlled studies offer greater control over treatment effects i.e., exposure to sonar, but cost and logistical challenges constrain sample sizes and the realism of the simulated scenarios. Opportunistic exposure studies are relatively inexpensive to perform when conducted on existing instrumented Navy ranges, and sonar ship movements are unrelated to whale locations, but experimental control over sonar exposure is lacking. CEEs have primarily used telemetry devices, which collect high-frequency movement (and potentially other) data independent of animal calling, but add to the logistical challenge and cost as animals must first be tagged. Potential disturbance of the focal animal e.g., by the act of tagging and focal following, is also a concern. PAM is non-invasive, and large sample sizes can be obtained on Navy ranges at relatively low cost, but movement responses depend on paths reconstructed from localizations that are only observable while the animal is calling, and so can only be assessed for calling animals. There is also the potential that some animals near Navy ranges are, in

some way, habituated or sensitized to Navy activities and are not representative of individuals which have been exposed either less frequently, or not at all, to naval sonar.

Passive acoustic monitoring of the Pacific Missile Range Facility (PMRF) in Hawaii has provided an opportunity to complement the small sample of minke whales exposed to sonar using the CEE approach and to test the predictions from those studies. Findings from the CEEs described in Kvadsheim et al. (2017) allowed us to establish the prediction that minke whales may exhibit an avoidance response in relation to sonar exposure, which we tested using opportunistically collected PAM data. Minke whales produce characteristic boing calls (Rankin and Barlow, 2005; Helble et al., 2020a) that make them amenable to study using PAM. Boing calls produced by North Pacific minke whales have a peak frequency of ∼1.4 kHz, duration of 1–4.5 s, and inter-call interval of 6 min when calling individually, with some geographical variation in call characteristics (Thompson and Friedl, 1982; Rankin and Barlow, 2005; Oswald et al., 2011). These calls are detected seasonally around Hawaii and it is thought that they are made only by sexually active males and for the purposes of breeding. Relatively little is known about whether all sexually active males make this call, how frequently individuals call and the what the ratio of boing calling minke whales is to all other minke whales (females, juveniles, and calves).

Improvements in acoustic processing capabilities permit increasingly sophisticated analyses of PAM data. Harris et al. (2019a) analyzed a subset of the track data presented herein to establish whether there was a shift in the spatial distribution of calling minke whales before, during and after multi-platform naval training events. They concluded that there was a clear change in the spatial distribution of calling, with fewer tracks in the vicinity of the center of ship activity. However, the analysis they conducted did not allow conclusions to be drawn about whether this change in the spatial distribution of calling related to a silencing response or an avoidance response, or a combination of the two. The primary objective of the current paper is to distinguish call cessation from avoidance, and thus investigate whether minke whales exhibit a horizontal movement response away from sonar-producing ships. The methodological development that allows us to do this is the generation of acoustic tracks for individual whales from the localizations (Helble et al., 2015, 2016, 2020a,b Klay et al., 2015; Henderson et al., 2018; Harris et al., 2019a; Guazzo et al., 2020). In addition, we assessed whether minke whales were more likely to cease calling during sonar exposure, as changes in calling behavior have been reported in response to anthropogenic noise for a number of other baleen whale species [blue whales–Melcon et al., 2012; bowhead whales (*Balaena mysticetus*, Blackwell et al., 2013, 2015); humpback whales–Risch et al., 2012; Cerchio et al., 2014].

MATERIALS AND METHODS

Study Area

Data were collected from 47 time-synchronized, bottom-mounted range hydrophones on PMRF, approximately centered on the area where U.S. Navy training occurs offshore the island of Kauai, Hawaii, and separated from one another by 5–7 km at depths of 650–4750 m (**Figure 1**). The hydrophone array covers an area of approximately 1200 km^2. Minke whale call localization accuracy decreases as distance from the edge of the array increases (Helble et al., 2015). Previous studies (Harris et al., 2019a) assumed that all calls were detected and localized accurately, and therefore used a conservative study area. Here, advances in the estimation of localization errors allow us to incorporate these errors into our analyses and to therefore make use of the entire area in which calls can be localized.

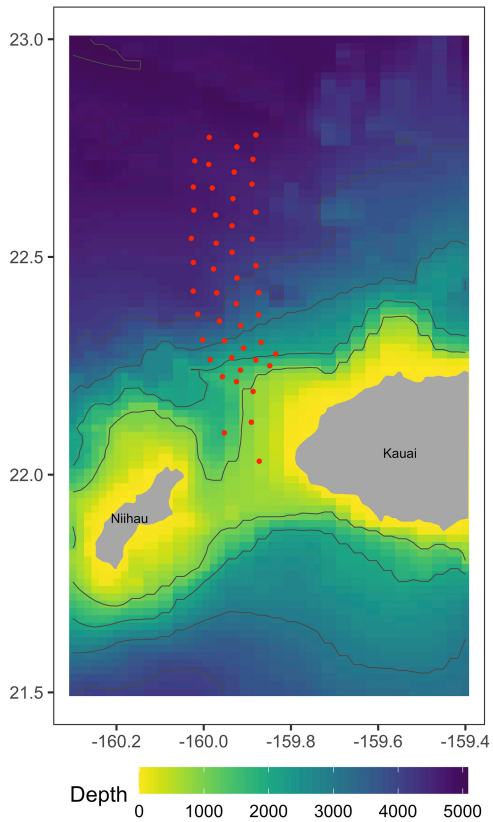

FIGURE 1 | Approximate locations of 47 recorded broadband hydrophones at the Pacific Missile Range Facility in Kauai, Hawaii. These hydrophones have the frequency response necessary to detect minke whale boing calls.

Processing of Passive Acoustic Monitoring Data

Full details of the detection, classification, and localization procedures can be found in Martin et al. (2015). In brief, minke whale boing calls were automatically detected and localized based on signal strengths and times of arrival at multiple hydrophones (**Figure 2A**). An association model then groups localizations that were sufficiently close in time and space into "tracks," based upon the species reported call rate and swim speeds (Klay et al., 2015, **Figure 2B**). Tracks were generated using specific criteria. Here, at least 8 hydrophones had to contribute to the localization solution, the maximum time between successive calls was 40 min., the

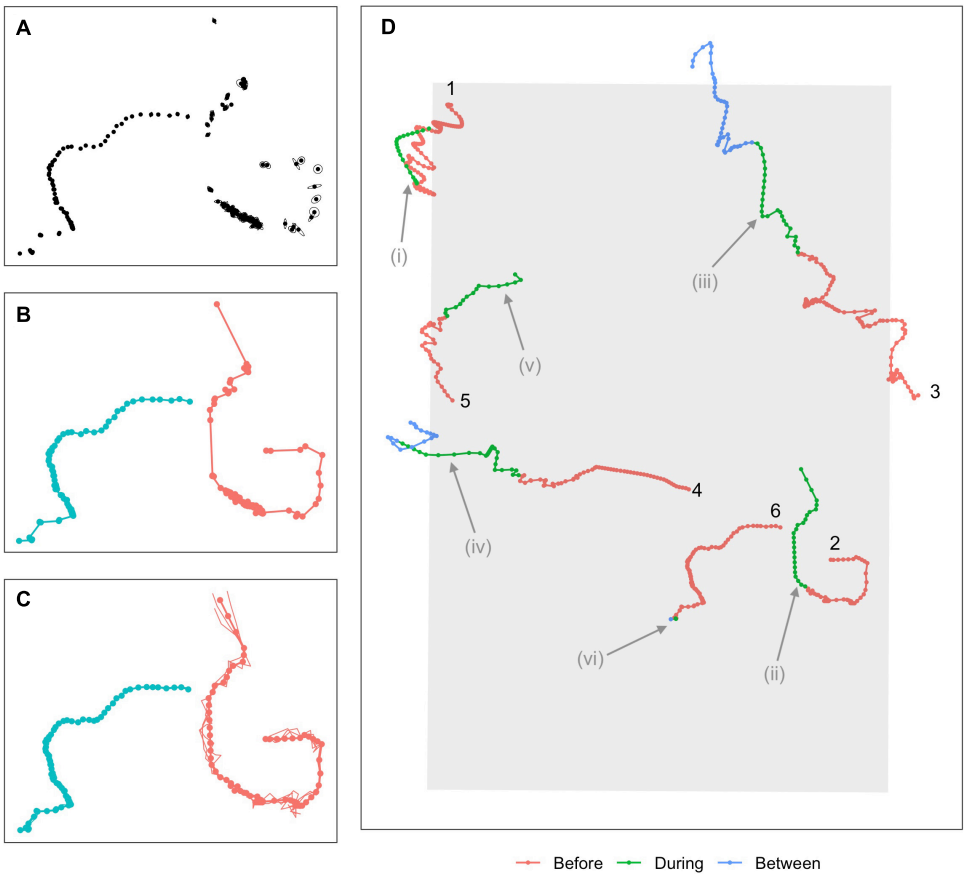

FIGURE 2 | Overview of modeling process. **(A)** Calls are first detected and localized, with associated measurement errors indicated by ellipses around each point. **(B)** An association algorithm groups localizations into tracks. **(C)** A continuous-time movement model is fitted to the tracks, allowing locations and associated location errors to be estimated at any time. Points show estimated mean locations at 5-min intervals ("single imputation"), connected by linear interpolation (thicker solid line). Thinner lines show three simulated plausible trajectories for each animal ("multiple imputation," points for these tracks suppressed for clarity). **(D)** A subset of six single-imputation tracks overlapping with the During sonar exposure phase, some of which demonstrate potential avoidance behavior. Colors indicate sonar exposure phase and a track ID number is used to indicate the beginning of the track. Potential avoidance responses include changes in headings (Tracks 1, 2, 3; possible changes indicated at i, ii, iii), increased speed (Tracks 4, 5; indicated at iv, v), more directional movement (Track 3, at iii), or cessation of calling (Track 6, at vi). Evidence of avoidance can be fairly clear (Tracks 1 and 2) but is often ambiguous or inconclusive (Tracks 3–5).

maximum change in latitude or longitude was 0.06°, and the least squares error of the actual and modeled times had to be under 0.075 s. A minimum of 12 calls were required in a track, which is based on one animal at the nominal call rate (1 call/∼5 min) over the course of an hour. A multi-hypothesis tracker (Baggenstoss, 2015) was used to remove any outlying localizations. The dataset used in the next stage of the analysis was made up of 62,323 localizations associated into 629 tracks. While the number of individual calling whales present at any point in time can be determined, it is not possible to determine whether any tracks separated in time by more than 40 min were from one or multiple individuals. The number of individual whales producing the 629 tracks is therefore unknown.

Error ellipses defining the observation error associated with each localization were derived employing elements of the geometric dilution of precision (DOP) methods developed for global positioning satellite system (GPS) navigation (Hofmann-Wellenhof et al., 2001). The whale position at the time of its call is analogous to the location of a GPS receiver at that time, with the bottom mounted hydrophones analogous to satellites in space. The method assumes direct path propagation from the whale to each hydrophone involved in the solution. This assumption is plausible for an area encompassing the hydrophone array plus a buffer zone out to approximately 5.5 times the water depth of the hydrophones in all directions (Urick, 1983; Rui et al., 2012). The two-dimensional (x, y) error of each tracked localization utilized only the first eight localizations to reduce potential indirect arrival paths. The geometric matrix A is an $n \times 4$ matrix of which the first three columns are the components of the unit vectors pointing from the estimated whale position to each of n hydrophones with the fourth column all ones. With the assumption that the measurement and modeled errors are the same for all simultaneous observations with a given standard deviation, the covariance matrix was then estimated as $(A^T A)^{-1}$. The PAM methods did not provide an estimated minke whale depth, so whales were assumed to be

near the surface when localized. Mean reported minke whale dive depths range from 18 to 36 m (Friedlaender et al., 2014; Henderson et al., 2018), far smaller than the depths at which hydrophones are deployed at PMRF (650–4750 m), suggesting our assumption is reasonable. The covariance data was utilized to calculate the error ellipse in the horizontal plane as well as the horizontal DOP (HDOP). The error ellipse was then scaled by the estimated timing accuracy for the processed data, with an assumption of one standard deviation timing error of 10 msec, or approximately 15 m. A minority of localizations (10%, 6924/70509) fell outside the area in which the direct path assumption is expected to hold, and for these observations the error ellipses may be underestimates. Rather than omit these localizations, we performed *post hoc* sensitivity checks of our conclusions to their inclusion (**Supplementary Material 2**).

Our localizations occurred irregularly in time and were subject to observation error, violating requirements of the Hidden Markov Models (HMMs) that we use later to model movement. A continuous-time correlated random walk model was therefore fitted to the localizations using the R (v 3.6.2; R Core Team, 2019) package crawl (Johnson et al., 2008; Johnson and London, 2018). The fitted model was used to obtain improved estimates of the localizations ("single imputation," following McClintock and Michelot, 2018) as well as 30 simulated versions of each track ("multiple imputation") at a temporal resolution of 5 min (**Figure 2C**). Single imputation tracks effectively smoothed out local variation due to observation error, and represented each track by a single set of best estimated locations. Multiple imputation tracks represented each track by 30 simulated trajectories, each of which was a plausible path the animal might have taken, i.e., that are consistent with the localizations and associated errors observed for that track. Subsequent inferences made were pooled across these simulated sets of tracks, propagating uncertainty arising from observation errors through the analysis (McClintock, 2017). Two tracks failed to converge and were removed from the analysis. The final dataset was made up of 77,390 localizations from 627 tracks (single imputation) or 30 × 627 tracks (multiple imputation).

Navy Sonar Training Activities

Submarine Command Course (SCC) training events are anti-submarine warfare (ASW) training activities conducted under realistic scenarios and involving diverse platforms including submarines, surface ships, helicopters, and maritime patrol aircraft (U.S. Department of the Navy, 2018). Various anthropogenic sounds of potential concern may be produced during training, including sounds from mid-frequency sonars, sonar countermeasures, high frequency sonars, torpedo sonars, and vessels and aircraft. Training events took place over the course of 3–4 days in each of February 2014, 2015, and 2017. The training activities were broadly comparable across the 3 years, in terms of the types of activities, center of ship activity, and the level of activity during the training activities (relating specifically to surface ship hull-mounted MFAS, active sonobuoys, and helo-dipping sonar, **Table 1**).

Precise data on the positions of individual ships including when and where they emit sonar during training activities are classified, but summary information was provided at 5-min intervals between the start and end times of each whale track that overlapped with the training event. We recorded whether any MFAS was produced in each 5-min interval and the type of MFAS produced (ship, other, both ship and other). The closest point of approach (CPA) was calculated between the whale and any participating ships (a) with sonar and (b) without sonar in each 5-min interval. As this information was calculated prior to the fitting of the continuous-time movement model, whale positions were only available at localization times. The bearing from the ship to the whale and the ship's heading at the CPA were also recorded. Bearing and heading information was discretized into four quadrants (i.e., north, east, south, and west) so that exact ship positions could not be recovered. Cumulative sound exposure was estimated using the Peregrine propagation model (Heaney and Campbell, 2016) to estimate transmission loss from a source to a receiver for received level estimation at each tracked whale position from all overlapping surface ship hull-mounted MFAS (i.e., AN/SQS-53C) transmissions. Due to security concerns, modeled MFAS exposure metrics were limited to the maximum sound exposure level received from a single transmission during a track (max SEL), and cumulative sound exposure level for each 5-min bin over the duration of a track (cSEL). The cSEL was estimated by summing the magnitude received level (μPa) from all surface ship hull-mounted MFAS transmissions in a 5-min bin. We applied a pragmatic decay estimate to the cSEL, which is otherwise a non-decreasing function of time. If consecutive time bins had exposures, a dynamic fractional amount of the cSEL from the prior bin was used for cumulation. If a succeeding bin did not have an exposure but the prior bin did have an exposure, a static decay of 30% was applied to the cSEL from the prior bin. If consecutive bins did not have exposures, a static decay of 10% was applied to the cSEL from the prior bin. If six consecutive bins did not have exposures the cSEL was reset to zero. All sonar exposure covariates were allocated to each location based on which 5-min bin the location fell into.

The training period was characterized by alternating phases of intermittent sonar activity and less active phases between events where ships repositioned in preparation for the next training event. We therefore distinguished between "During sonar exposure" phases of the training period, which begin at the first sonar transmission of a training event and end when no sonar activity is detected for the next 30 min, and "Between sonar exposure" phases that occur between these. Specific MFAS sources in the During phase are primarily surface ship hull mounted MFAS (i.e., AN/SQS-53C with a center frequency of approximately 3 kHz and a nominal source level of 235dB re1μPa (U.S. Department of the Navy, 2018), but also active MFAS sonobuoys (e.g., AN/SSQ-62) and helicopter (helo-) dipping MFAS sonar (AN/AQS/22). The final Between phase included 24 h after the last sonar transmission, to ensure vessels participating in the training activity had adequate time to depart the area (Harris et al., 2019a).

Times outside of the training period were divided into a Baseline phase that occurred at least 1 week before the event [duration = 6 days (2014), 30 days (2015), 21 days (2017), resulting in substantially fewer tracks in 2014]; a Before phase

TABLE 1 | Timing, number, and duration of bouts of sonar activity during naval training activities in 2014, 2015, and 2017.

	Start of first sonar bout	End of last sonar bout	Sonar bouts	Duration of bouts		
				Total	Mean (min)	SD (min)
2014	18 February 09:28	21 February 04:26	20	21.4	64.3	56.8
2015	16 February 00:30	19 February 16:12	16	23.8	89.3	75.1
2017	15 February 09:40	17 February 15:01	27	18.5	41.1	24.8

TABLE 2 | Start and end of survey period in each year, the number of tracks overlapping with each sonar exposure phase (columns headed "Baseline" to "After") and the number of unique tracks per study year ("Total").

	Start	End	Baseline	Before	During	Between	After	Total
2014	5 February	26 February	38	23	11	19	42	115
2015	8 January	24 February	181	40	35	75	44	329
2017	18 January	22 February	87	54	15	21	30	183
Locations			38626	15885	1527	8755	12597	77390

*The survey period includes all phases, with the training event itself taking up a relatively small part of this (see **Table 1**). The number of unique tracks per year is less than the sum across phases because tracks can span more than one phase. The final row gives the total number of imputed locations available in each phase.*

starting 1 week before and ending at first sonar transmission; and an After phase starting 24 h after the last sonar transmission (duration = 4 days for all years). A subset of illustrative whale tracks spanning multiple phases are shown in **Figure 2D**. There were no acoustic data indicative of sonar activity in Baseline, Before, or After phases.

The detection, classification, and localization algorithms resulted in the derivation of 627 unique tracks (115, 329, and 183 tracks for 2014, 2015, and 2017, **Table 2**). There was substantial overlap between the During and Between phases, because of the relatively short duration of the During phases: 54 tracks had localizations in both During and Between phases, out of 61 and 115 tracks with at least one During or Between localization respectively. There was also some overlap between Baseline and Before phases (9 tracks), Before and During/Between phases (11 tracks, of which 6 had localizations in all three phases), and After and During/Between phases (14 tracks, of which 1 had localizations in all three phases). The great majority of tracks fell within a single phase (546 of 627 tracks, 87%). The number of unique tracks overlapping in time with each phase is shown in **Table 2**.

Statistical Analysis

Changes in Movement Behavior

Hidden Markov Models have been widely applied to animal movement data from position- or displacement-sensing tags (Isojunno and Miller, 2015; DeRuiter et al., 2017), and have been specifically used to study avoidance behavior where the objects of avoidance (or attraction) were fixed in space (McClintock et al., 2012; Michelot et al., 2017) or moving with known locations (Mul et al., 2020). Here HMMs were applied to tracks derived from data derived from PAM to study the avoidance of objects whose locations are imprecisely known. Two steps were used to analyze movement responses. First, all tracks were used to evaluate broad-scale differences between sonar exposure phases. Then, observations in the During phase were used to assess specific effects to ship covariates, which are otherwise potentially obscured by the relative scarcity of During observations (1527/77,391). As model run times were substantial, promising candidate models were first identified by fitting HMMs (Zucchini et al., 2017) to speeds, turning angles, and whale headings between time-regular locations in single imputation tracks, using maximum likelihood (see **Figure 2** for a subset of typical input tracks). Tidal currents were not accounted for and so speeds are over the seafloor. The relatively long study period used here spans multiple tidal cycles. In this context, neglecting tidal currents (which can be significant, up to ∼1 m/s, but which are also subject to substantial local measurement error) is expected to introduce variance but no bias. We then refitted the two best candidate models, which were clearly preferred to all other models by Akaike's Information Criterion (AIC) weights, using 30 imputations of each track. Speeds were modeled using a gamma distribution for positive continuous values; turning angles and headings used a wrapped Cauchy distribution for circular response variables. Mean turning angles were fixed to zero to impose unbiased turning angles, with the remaining concentration parameter estimated by the HMM. To account for the possibility of headings changing between sonar exposure phases, the mean and concentration of each state-dependent heading distribution was allowed to depend on sonar exposure phase. State transition probabilities were modeled as a function of three covariates: sonar exposure phase, decaying cumulative SEL, and inverse distance to closest ship. Both continuous covariates were standardized to lie between zero and one, with any missing values replaced by zeros. Two different forms of the sonar exposure phase covariate were used: one including all five phases, and one comparing the During phase against all other phases. Obtaining a fitted model that was numerically stable enough to estimate standard errors for all effects required

constraining some model parameters. The effects of Baseline and Before phases on whale headings were combined in one movement state, and a prior distribution of $N(0,100)$ placed on the coefficient associated with the effect of the Baseline phase on whale heading in that state. This improved the numerical stability of the optimization routine (Mul et al., 2020). As the same prior constraint was used across all HMMs, these were still comparable using AIC. We restricted our analyses to models with two states in order to focus on detecting large-scale changes in movement behavior associated with training events. The great majority of our tracks fall into Baseline and Before phases, and although introducing additional states primarily captures extra detail in these phases, it does so at the expense of dividing the relatively small number of During tracks across more states. All HMMs were fitted using the R package momentuHMM (McClintock and Michelot, 2018). The two models selected by AIC were refitted using five sets of starting values to assess model sensitivity, with no improvements to the likelihood. Model fit was assessed by checking the pseudo-residuals for each of the state-dependent variables for non-normality and autocorrelation.

In our case ship position was classified and so recorded only indirectly and imprecisely, as described above. Furthermore, most localizations outside the During phase had no ship covariates at all, because to the best of our knowledge surface ships with hull-mounted sonar were not present at that time (if they were present the PAM data shows they were not using their sonar). HMMs need non-missing covariate values for any modeled response variables, and although replacement of missing values with plausible values is possible (for example, a large distance to ship, or a small cSEL), the relative scarcity of true non-missing covariate values makes their associated effects difficult to evaluate using the HMM just described. To assess whether the direction of whale movement was away from ships emitting sonar, the subset of the data for which ship covariate data was available was used. Based on the output of the HMM fitted to the entire dataset, we identified one state that described movement patterns that were consistent with a potential avoidance response and that accounted for the majority of observations in the During phase. Our second-stage analysis was restricted to those observations that had been allocated to this state in the most likely state sequence for each track, with the allocation performed by the Viterbi algorithm (Zucchini et al., 2017).

These data were challenging to model because whale heading was a circular response variable exhibiting considerable within-track autocorrelation, and potential explanatory variables were usually constant within track because of the discretization into quadrants, and so would be confounded with random intercepts in a mixed model. Data were therefore analyzed using four independent binary logistic regressions using Generalized Estimating Equations (Ziegler, 2011) applied to the single-imputation tracks. This provided a flexible way of modeling autocorrelation but required simplifying the response variable, as GEEs have not been developed for circular response variables and implementations for multinomial responses are limited in the kinds of correlation structures they can accommodate (Touloumis et al., 2013). Each GEE used one of the four cardinal directions (north, west, south, east) as a response variable, with headings in a particular direction (coded as a 1) or in any of the remaining three directions (coded as a 0) encoding that response variable. Continuous whale headings were discretized into the same four quadrants used to record the bearing of the whale relative to the closest ship. Models were fitted with the bearing of the whale relative to the closest MFAS ship, ship heading, cumulative SEL, and inverse distance to closest ship as potential covariates. As whales were overwhelmingly either to the north or west of ships (913/960 observations, 95%), relative bearing was encoded as a binary covariate (1 = whale to the north, 0 = whale to the west). Ship headings were only available within the same four quadrants used to express our other directional variables. We used individual track as the panel structure (i.e., allowing for autocorrelation in the headings), fitting models assuming independence, exchangeable or AR(1) correlation structures, and performing model selection by the Quasilikelihood Independence Criteria (QIC). Models were fitted using the R package geepack (Halekoh et al., 2006).

Changes in Calling Behavior

To assess whether cessation of calling was associated with sonar activity or with any behavioral movement states identified by the HMM, an extended Cox proportional hazards regression model was fitted. The event of interest was the occurrence of the last localization in each track, and the hazard rate at time t the instantaneous risk that an animal is not localized again, given that it had been localized up until t. The hazard rate was modeled as a function of sonar exposure phase, Viterbi-decoded movement states obtained from the two-state HMM, and their interaction. The last localization was interpreted as indicating that calling had ceased, although because our association rules impose a maximum time between successive calls of 40 min (as well as other restrictions, see section "Processing of Passive Acoustic Monitoring Data"), cessation is only confirmed for the following 40 min under the assumption that all calls are localized. Because sonar exposure phase varies over time, the time between the first and last localizations of each track was split into 5-min intervals, with covariate information available in each interval (Thomas and Reyes, 2014). Chi-squared tests of weighted residuals (Grambsch and Therneau, 1994) and a graphical inspection of residuals plots (Xue and Schifano, 2017) were used to assess the proportional hazards assumption (i.e., the use of time-independent model coefficients) and the adequacy of model fit. Models were fitted using the R package survival (Therneau, 2020).

RESULTS

The AIC-selected model (AIC weight 78%, next best model 22%) included sonar exposure phase both as a covariate on the transition probabilities and as a covariate on both the mean and concentration of the state-dependent distributions governing whale heading (**Supplementary Material 1**). The only other model with any meaningful support was one that replaced the binary During indicator with decayed cSEL (**Supplementary Material 1**) as a covariate on the transition probabilities.

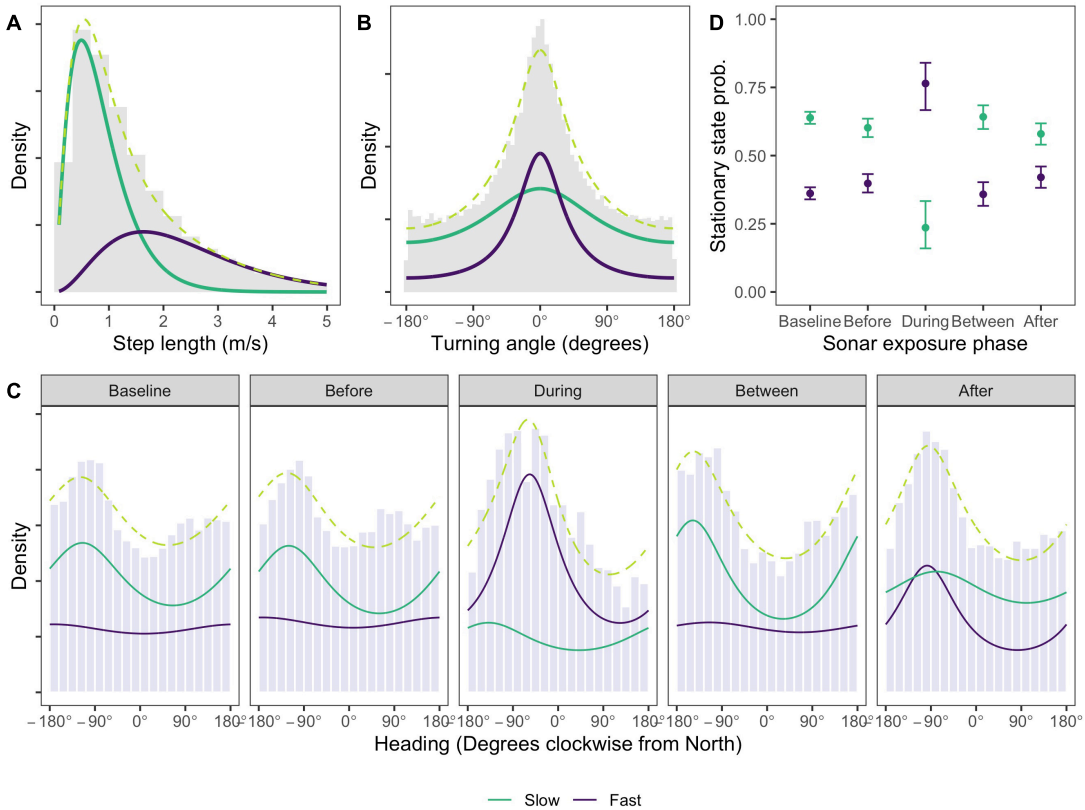

FIGURE 3 | Estimated state-dependent densities for **(A)** speed, **(B)** turning angle, **(C)** whale heading relative to North, and **(D)** the effect of sonar exposure phase on the probability that a location is found in a given state. Density values are uninformative and so suppressed. One state (green line) comprises slow, undirected movement, most commonly with a heading between south-east and north-west. A second state (purple line) involves faster, more directed travel which, during sonar exposure, is also characterized by more northerly headings that would typically take the whale away from the range of ship activity. Whales are much more likely to be observed in the second state during sonar exposure. Observed data is shown as gray histograms; the marginal distribution (dashed lime green line) shows the sum of the state-dependent densities. Heading densities in panel **(C)** are standardized within each sonar exposure phase to facilitate comparison between the phases, which have very different sample sizes (see **Table 1**).

Estimated state-dependent distributions of speed and turning angle indicated one state characterized by relatively slow, undirected movement (mean = 0.84 m/s, SD = 0.53 m/s, angular concentration κ = 0.18; **Figures 3A,B**, model results tabulated in **Supplementary Material 2**), and the other substantially faster, more directed movement (mean = 2.36 m/s, SD = 1.30 m/s, angular concentration κ = 0.52; **Figures 3A,B**). For brevity we refer to the two states as "slow" and "fast" movement, respectively. Movement in the Baseline and Before phases was most commonly in a west-south-west (WSW) direction when animals were in the slow movement state (Baseline: mean = 245°, 95% confidence interval (CI) = (240°; 250°), concentration κ = 0.13; Before: mean = 240°, 95% CI = (233°; 246°), concentration κ = 0.15; **Figure 3C**). In the fast movement state a very small concentration estimate implied a near-uniform distribution of headings in these phases (both phases: mean = 188°, 95% CI = (184°; 191°), concentration κ = 0.04; **Figure 3C**). During sonar, movement in the fast state became more northerly on average, and more concentrated (mean = 303°, 95% CI = (293°; 314°), concentration κ = 0.28; **Figure 3C**), with much fewer headings between south and east. Movement in the slow state was WSW on average but highly variable (mean = 221°, 95% CI = (133°; 309°), concentration κ = 0.13). Significant coefficients associated with the effect of the During indicator in the fast state indicated that both the mean and concentration of whale heading changed significantly during sonar activity for that state, relative to baseline activity (effect of During indicator on mean heading = 13.96, 95% CI = (7.28; 20.65); effect of During indicator on concentration = 2.31, 95% CI = (1.90; 2.72)). No significant effects were observed for the slow state, indicating that whale headings were not significantly changed by sonar exposure in this state (effect of During indicator on mean heading = −1.08, 95% CI = (−7.24; 5.06); effect of During indicator on concentration = −0.09, 95% CI = (−0.92; 0.74)). Distributions of whale headings in the Between phase became slightly more concentrated and southerly in the slow movement state, relative to the Baseline phase (concentration: between κ = 0.21 vs. baseline κ = 0.13; effect of Between indicator on concentration = 0.53, 95% CI = (0.36; 0.70); mean = 212°, 95% CI = (205°; 219°), effect of Between indicator on mean heading = −1.92, 95% CI = (−2.73, −1.11)). Headings in the fast movement state closely resembled those in the Baseline

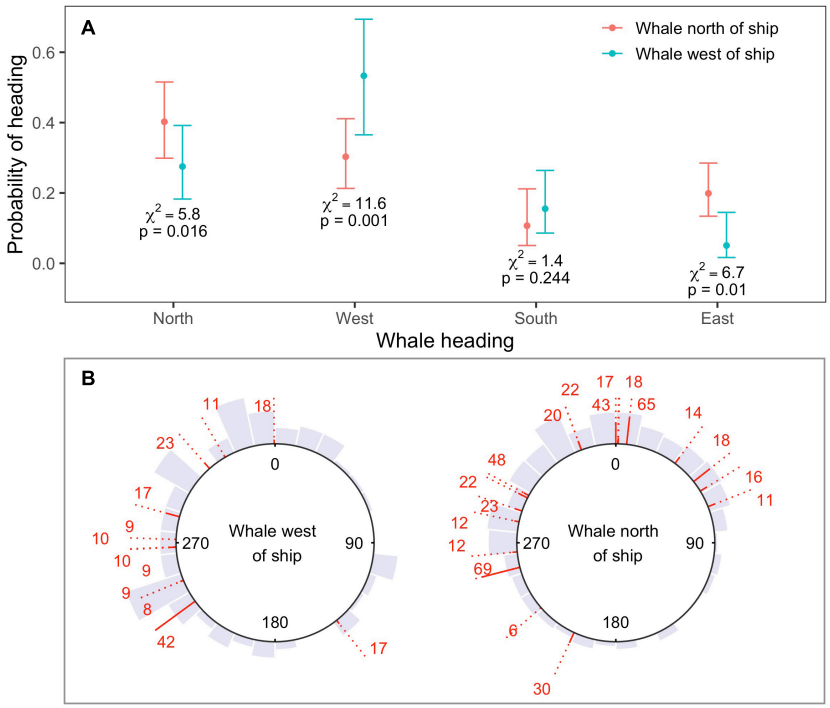

FIGURE 4 | (A) Estimated probability of heading north, west, south, or east as a function of whale bearing relative to ship, as obtained from four independent binomial GEEs (one model for each cardinal direction). Responses were consistent with movement away from sonar-producing ships. Whales were more likely to head north if whale bearing was to the north or east of the ship, and more likely to move west when whale bearing was to the west; **(B)** observed headings shown by gray histograms, for whales located to the west (left-hand plot) or north (right-hand plot) of the closest MFAS ship. Headings between start and end locations are shown for each track as red lines. The solid part of each line standardizes the length of the dotted line by track length. Sample sizes (number of 5-min intervals) are shown at each line end. Headings show substantial individual variability, but little or no north-easterly movement when whale bearing was to the west.

phase. More northerly and more concentrated headings were observed for fast movement state observations in the After phase, relative to baseline, although less so than During sonar activity (concentration: Between $\kappa = 0.27$ vs. Baseline $\kappa = 0.04$; effect of After indicator on concentration = 2.26, 95% CI = (1.90; 2.61); mean = 262°, 95% CI = (257°; 266°), effect of After indicator on mean heading = 13.36, 95% CI = (6.68, 20.05)).

The fast movement state is far more likely to occur in the During phase than in any other phase, and with relatively small differences between any other phases (**Figure 3D**). After assigning each location to its most likely state using the Viterbi algorithm (Zucchini et al., 2017), the fast movement state accounted for between 35 and 41% of locations in non-sonar phases, compared to 70% of locations in the During phase. Model checking (**Supplementary Material 2**) revealed no evidence of systematic deviations from model assumptions, although pseudo-residuals for speed and heading exhibited a moderate amount of residual autocorrelation. To check the robustness of our conclusions, the selected HMM was refitted to data thinned to one observation per 15 min to reduce autocorrelation, and found no meaningful differences (**Supplementary Material 2**). We also checked the sensitivity of our results to the interval used to impute tracks and to the slightly higher call rates that were observed in Between and During phases, again finding no substantive differences (**Supplementary Material 2**).

Changes in heading observed for locations in the fast movement state during sonar exposure were consistent with movement away from sonar-producing ships (**Figure 4A**). Whales were more likely to head north when their bearing was to the north of the closest sonar-producing ship, rather than to the west (N heading $\chi^2 = 5.8$, $p = 0.02$). Similarly, whales were more likely to head west, and less likely to head east, when their bearing was to the west of the closest ship, rather than north (West heading $\chi^2 = 11.6$, $p < 0.001$; East heading $\chi^2 = 6.7$, $p = 0.01$). Model selection by QIC favored the use of an AR(1) correlation structure for all four response variables, and whale bearing was the only significant covariate effect (**Supplementary Material 4**). Although the use of an independent model for each response direction meant that probabilities were not guaranteed to sum to one over all potential directions, this sum differed negligibly from one (1.01).

Headings showed substantial individual heterogeneity in the mean direction of movement as well as the variability around that mean (**Figure 4B**). Nevertheless, north-easterly movement was only observed for whales located to the north of the closest ship, for whom this movement would be away from the position of the ship (**Figure 4B**); whales whose bearing was to the west of the closest ship exhibited almost no north-easterly movement.

Whales were more likely to stop calling when they were in the fast movement state (Odds Ratio [OR] = 2.26, 95% CI = (1.92,

TABLE 3 | Estimates from a Cox proportional hazards model assessing the effect on sonar exposure phase and movement state on the cessation of calling.

Covariate	Coefficient	Odds ratio	95% CI	*z*	*p*
Before	−0.16	0.85	(0.68, 1.07)	−1.39	0.17
Between	0.14	1.15	(0.90, 1.47)	1.09	0.28
During	0.26	1.30	(0.79, 2.13)	1.03	0.30
After	0.16	1.17	(0.94, 1.45)	1.44	0.15
Slow state	−0.82	0.44	(0.37, 0.52)	−9.73	<0.001
During × Slow state	1.32	3.74	(1.71, 8.21)	3.29	<0.001

*Our experimental setup defines cessation of calling as no call detected in the next 40 min. Sonar activity is associated with cessation of calling through two pathways. Whales were more likely to cease calling when in the fast movement state, and this state was more likely during sonar activity (see **Figure 3**). Whales in a slow movement state were more likely to cease calling during sonar than in other exposure phases.*

2.67), $p < 0.001$; **Table 3**). Of the 627 tracks, 366 (58%) ceased calling during the fast movement state, although these account for only 39% of observations (30,080/77,391). While our previous analyses have shown that the faster movement state is more common in the During phase, once in the fast movement state whales were not significantly more likely to stop calling in the During phase than in other phases (OR = 1.30, 95% CI = (0.79, 2.13), $p = 0.30$). In contrast, whales in the slow movement state were more likely to stop calling in the During phase than in other phases (OR = 3.74, 95% CI = (1.71, 8.21), $p < 0.001$). Of the 261 tracks where cessation of calling was observed when the whale was in a slow movement state, 11 (4%) occurred in the During phase, while During phase observations account for fewer than 1% of all slow movement state observations (444/47,311). This suggests the possibility of two distinct mechanisms by which sonar activity may be associated with a cessation of calling–whales may change their movement behavior by transitioning into a faster movement state, which has a higher probability of call cessation regardless of exposure phase; or they may remain in a slow movement state but be more likely to stop calling than in other exposure phases. Model fit diagnostics showed global support for the proportional hazards assumption, but covariate-specific tests provided marginal statistical evidence ($p = 0.047$) for violations in the movement state covariate, suggesting the need for a time-varying coefficient (**Supplementary Material 5**). To test the sensitivity of our results to this violation, we fitted a model with coefficients for the movement state covariate and its interaction with the During period indicator separately estimated for two time regimes suggested by residual plots ($t \leq 90$ min, $t > 90$ min). This implements a simple "step function" form for the time-varying coefficient. Results did not change greatly, the only change being that the increased likelihood of call cessation associated with the faster movement state was essentially limited to tracks older than 90 min–the effect was not observed in earlier parts of the tracks (**Supplementary Material 5**).

DISCUSSION

Previous analyses of a subset of the data presented herein demonstrated a spatial redistribution of minke whale localizations in response to navy training activities that involved sonar emission (Harris et al., 2019a). However, methodological constraints meant that it was not possible to identify whether this redistribution was related to movement away from the range or to a cessation of calling on the range. Here we have directly modeled individual animal movement to conclusively demonstrate the presence of an avoidance response to ships emitting sonar. Movement became faster and more directed during sonar exposure than in baseline phases; the mean direction of movement differed during sonar exposure; and this change was consistent with movement away from sonar-producing ships. A separate analysis of calling responses showed that animals were more likely to cease calling during any sonar exposure.

The combined results of these analyses provide an improved understanding of the mechanisms underlying the spatial redistribution of calling minke whales described in Harris et al. (2019a). Harris et al. (2019a) reported a spatial shift in calling whales to the north and west of the range in both years analyzed, which can now be explained by the increased probability of individuals moving in a northerly or westerly direction during exposure. However, the reduction in overall calling on the range (Martin et al., 2015), and the reduction in the presence of calling whales in the center of the range (Harris et al., 2019a), are likely due to a more complex combination of responses. As has been shown here, response behavior may consist of both movement and calling responses. We found that whales were more likely to enter a fast movement state during sonar exposure, and that this state was associated with a greater chance of call cessation regardless of sonar exposure phase. Whales remaining in a slow movement state during sonar exposure were more likely to stop calling than in other exposure phases. One interpretation of these results is that there are two distinct response types–one involving changes in movement and calling behavior, and another involving changes in calling behavior only. An alternate interpretation is that in the former the movement response occurs before the calling response, while in the latter the calling response occurs first and we do not observe the movement response. Movement data that depends on PAM are insufficient to differentiate between these possibilities, which are potentially better suited to analysis using telemetry devices.

Opportunistic exposure studies have the potential to complement data from CEEs (and vice versa). They can allow for much larger sample sizes extending over larger spatial and temporal scales than is practical in CEEs, but at the expense of

experimental control. Using PAM as a monitoring technology offers similar advantages, with larger sample sizes relative to what can be achieved with telemetry devices–but movement responses depend on paths reconstructed from localizations that are only observable while the animal is calling. The frequency of localizations, and thus the temporal scale at which responses can be detected, depend on animal call rate. Despite these limitations, the analysis of data collected before, during and after training activities on PMRF has provided further evidence of an avoidance response of minke whales to sonar, a prediction established by CEEs (Kvadsheim et al., 2017). Not only have we demonstrated this response across many more individuals, but we have also provided a better indication of the potential duration of this response in the realistic context of a multi-day training activity. CEEs have primarily relied on fine-resolution telemetry tags (e.g., Dtags, Johnson and Tyack, 2003) which collect data over a limited time window before and after the exposure trial, and the exposure itself is generally on the order of tens of minutes to around an hour (Southall et al., 2016). This has made it difficult to relate the response durations observed in CEEs to possible impacts on the individual or population in terms of e.g., energy acquisition or reproduction. Here we showed that whales continued to be more likely to head toward the north-west, away from the range, in the period after naval training, suggesting some persistence in the effects of sonar. This again aligned with Harris et al. (2019a), who noted that it took a number of days before the minke whale distribution returned to baseline. Similar recovery times have been observed for beaked whales studied on navy ranges (Tyack et al., 2011; Henderson et al., 2016; Manzano-Roth et al., 2016). While effects persist in the period after naval training, we also showed that the most prominent changes in movement behavior–transitions to a fast, directed state with a distinct heading–generally do not persist in the phases between sonar events. Reasons for the greater persistence in the After period are not clear, but a slight increase in southerly movement observed between sonar events, when coupled with the propensity for north-westerly headings during sonar, suggests that some animals may reverse changes in their movements due to sonar immediately after the sonar event.

The effect of behavioral disruption on the individual, and ultimately the population, depends on whether the behavior ceases altogether during the sonar activity and for some time after, or whether animals move elsewhere and continue the behavior in sub-optimal conditions, or whether they move elsewhere and carry on as normal. In most other studies the behavior being disrupted has been foraging and therefore impacts have been discussed in terms of lost foraging opportunities (e.g., Moretti et al., 2014; Friedlaender et al., 2016; Sivle et al., 2016; Isojunno et al., 2017; Harris et al., 2019b). Effects of sonar on the foraging activities of other baleen whale species vary but consistent observations are (a) a high degree of individual variation in responses, (b) certain kinds of foraging (e.g., deep feeding) being more affected by sonar, (c) the importance of environmental context (e.g., prey distribution, bottom depth) in determining responses. Little is known about the effects of sonar on minke whale foraging. Kvadsheim et al. (2017) exposed one of two animals to MFAS off each of southern California and Norway. Exposed animals exhibited horizontal movement responses but no dive responses. Changes in foraging behavior could not be investigated, in one case because of a lack of foraging in the period leading up to exposure, and in the other case because sensors measuring lunging were not used. In our study the use of PAM also precludes an analysis of lunging and hence foraging behavior. However, the behavior being disrupted was most likely related to breeding as it is believed that the calling of minke whales in the Hawaii region at this time of year relates to males calling to attract mates, and the area is not as productive for feeding as other areas (e.g., Alaska). It may be that for the duration of the training activity, the noise levels on the range are too high for effective communication and therefore they either cease calling altogether or continue calling but move off the range. Alternatively, the response by males may be a response to females moving off the range (Harris et al., 2019a). Potential cessation of calling has been shown in this area both in Martin et al. (2015) and Harris et al. (2019a). It is unknown whether disruption of male mating behavior for a period of a few days each year could ultimately lead to reduced reproductive output for this population.

Kvadsheim et al. (2017) reported an avoidance threshold of 146–156 dB SPL re 1 μPa from the two CEEs conducted, and predicted this threshold could result in the significant reductions in minke whale vocalizations reported over the large PMRF training area reported in Martin et al. (2015). Through inclusion as covariates we attempted to determine the effect of SEL and distance to ships as two different "dose" metrics that may affect the probability of responding. We found little evidence for an effect of either of these covariates but this should not be taken as evidence for the absence of an effect or a dose-response relationship as this result is very likely due to coarse discretization of these covariates due to security-related issues. Future work to better understand the relationships between dose metrics and response includes implementing these analyses in a secure, Navy-classified environment utilizing full resolution on geometric covariates (e.g., ship heading, bearing from whale to ship) as well as utilizing the maximum SPL in all 5 min bins.

Our modeling process uses a lengthy data pipeline–calls are localized, associated, imputed regularly in time, and only then used as input for statistical analyses–and each step involves modeling assumptions and some degree of subjectivity. Three potential concerns are: (a) the use of some localizations that are far enough from the hydrophone array that the direct path assumption used to calculate localization errors may be violated; (b) tracks reconstructed by the continuous-time movement model may be sensitive to call rate, so that the same true animal trajectory may be reconstructed differently if that reconstruction happens during times of less frequent calling; (c) sensitivity of results to the choice of interval used to impute tracks. We refitted HMMs to datasets addressing each of these concerns, finding that our results and conclusions remained the same using: (a) a subset of tracks that restricted locations to lie within a smaller survey area in which the direct path assumption reliably holds; (b) tracks resampled to equalize call rates across sonar exposure phases; (c) tracks imputed at 15-min intervals (**Supplementary Material 2**).

Despite not being able to link the observed movement and calling responses to a sound exposure level or distance to ship, the scale of the observed response across many individuals and across years, provides further evidence of the sensitivity of minke whales to sonar exposure relative to other baleen whale species studied thus far [e.g., blue whales (*B. musculus*, Southall et al., 2019), humpback whales (*M. novaeangliae*, Sivle et al., 2016)]. We also found that an avoidance response is exhibited across different contexts, as the CEEs described in Kvadsheim et al. (2017) took place when the animals were in a foraging state rather than mating state. In conclusion, our results offer broad agreement with the conclusions drawn by Kvadsheim et al. (2017) regarding minke whale sensitivity to sonar, and showed that this sensitivity is exhibited across behavioral contexts.

DATA AVAILABILITY STATEMENT

The datasets presented in this article are not readily available because they contain classified information about U.S. Navy training. Requests to access the datasets should be directed to SM, steve.martin@nmmpfoundation.org.

ETHICS STATEMENT

Ethical review and approval was not required for the animal study because data on animal activity was entirely non-invasive and collected using passive acoustic monitoring during the course of U.S. Navy training activity taking place on the PMRF.

AUTHOR CONTRIBUTIONS

ID wrote the draft manuscript and performed the statistical analysis of the data with CH and LT. SM, CM, and EH collected that data. SM, CM, TH, and GI processed the passive acoustic data. All authors contributed to the article and approved the submitted version.

FUNDING

This research was funded by the U.S. Office of Naval Research under grant number N000141612859. The passive acoustic data were recorded under support by COMPACFLT for the Navy Marine Species Monitoring Program. The call association tracking algorithm was developed under a separate U.S. Office of Naval Research project (2011–2015 Advanced Detection, Classification and Localization, grant number: N0001414IP20037).

ACKNOWLEDGMENTS

We would like to thank the personnel at PMRF for their support in obtaining acoustic recordings, without which our analysis would not have been possible.

SUPPLEMENTARY MATERIAL

The Supplementary Material for this article can be found online at: https://www.frontiersin.org/articles/10.3389/fmars.2021.660122/full#supplementary-material

REFERENCES

Baggenstoss, P. M. (2015). A multi-hypothesis tracker for clicking whales. *J. Acoust. Soc. Am.* 137, 2552–2562. doi: 10.1121/1.4919370

Balcomb, K. C., and Claridge, D. E. (2001). A mass stranding of cetaceans caused by naval sonar in the Bahamas. *Bahamas J. Sci.* 5, 2–12.

Bannister, J. L. (2018). "Baleen whales (Mysticeti)," in *Encyclopedia of Marine Mammals*, 3rd Edn, eds B. Würsig, J. G. M. Thewissen, and K. M. Kovacs (London: Academic Press), 62–69. doi: 10.1016/b978-0-12-804327-1.00058-3

Blackwell, S. B., Nations, C. S., McDonald, T. L., Greene, C. R. Jr., Thode, A. M., Guerra, M., et al. (2013). Effects of airgun sounds on bowhead whale calling rates in the Alaskan Beaufort Sea. *Mar. Mammal Sci.* 29, E342–E365.

Blackwell, S. B., Nations, C. S., McDonald, T. L., Thode, A. M., Mathias, D., Kim, K. H., et al. (2015). Effects of airgun sounds on bowhead whale calling rates: evidence for two behavioral thresholds. *PLoS One* 10:e0125720. doi: 10.1371/journal.pone.0125720

Booth, C. G., Sinclair, R. R., and Harwood, J. (2020). Methods for monitoring for the population consequences of disturbance in marine mammals: a review. *Front. Mar. Sci.* 7:115. doi: 10.3389/fmars.2020.00115

Cerchio, S., Strindberg, S., Collins, T., Bennett, C., and Rosenbaum, H. (2014). Seismic surveys negatively affect humpback whale singing activity off northern Angola. *PLoS One* 9:e86464. doi: 10.1371/journal.pone.0086464

Cooke, J. G., Zerbini, A. N., and Taylor, B. (2018). *Balaenoptera Acutorostrata. IUCN Red List Threat. Species 2018 e.T2480A50350661*. Available online at: http://www.iucnredlist.org (accessed June 25, 2021).

D'Amico, A., Gisiner, R. C., Ketten, D. R., Hammock, J. A., Johnson, C., Tyack, P. L., et al. (2009). Beaked whale strandings and naval exercises. *Aqu. Mammals* 35, 452–472. doi: 10.1578/am.35.4.2009.452

DeRuiter, S. L., Langrock, R., Skirbutas, T., Goldbogen, J. A., Calambokidis, J., Friedlaender, A. S., et al. (2017). A multivariate mixed hidden Markov model for blue whale behavior and responses to sound exposure. *Ann. Appl. Stat.* 11, 362–392.

Erbe, C., Reichmuth, C., Cunningham, K., Lucke, K., and Dooling, R. (2016). Communication masking in marine mammals: a review and research strategy. *Mar. Pollut. Bull.* 103, 15–38. doi: 10.1016/j.marpolbul.2015.12.007

Friedlaender, A. S., Goldbogen, J. A., Nowacek, D. P., Read, A. J., Johnston, D., and Gales, N. (2014). Feeding rates and under-ice foraging strategies of the smallest lunge filter feeder, the Antarctic minke whale (*Balaenoptera bonaerensis*). *J. Exp. Biol.* 217, 2851–2854. doi: 10.1242/jeb.106682

Friedlaender, A. S., Hazen, E. L., Goldbogen, J. A., Stimpert, A. K., Calambokidis, J., and Southall, B. L. (2016). Prey-mediated behavioral responses of feeding blue whales in controlled sound exposure experiments. *Ecol. Appl.* 26, 1075–1085. doi: 10.1002/15-0783

Grambsch, P. M., and Therneau, T. M. (1994). Proportional hazards tests and diagnostics based on weighted residuals. *Biometrika* 81, 515–526. doi: 10.1093/biomet/81.3.515

Guazzo, R. A., Helble, T. A., Alongi, G. C., Durbach, I. N., Martin, C. R., Martin, S. W., et al. (2020). The Lombard effect in singing humpback whales: source levels increase as ambient ocean noise levels increase. *J. Acoust. Soc. Am.* 148, 542–555. doi: 10.1121/10.0001669

Halekoh, U., Højsgaard, S., and Yan, J. (2006). The R package geepack for generalized estimating equations. *J. Stat. Softw.* 15:56033.

Harris, C. M., Burt, M. L., Allen, A., Wensveen, P. J., and Miller, P. (2019b). Foraging behavior and disruption in blue (*Balaenoptera musculus*), Fin (Balaenoptera physalus) and humpback (*Megaptera novaeangliae*) whales in relation to sonar exposure: the challenges of generalizing responsiveness in species with high individual variability. *Aqu. Mammals* 45, 646–660. doi: 10.1578/AM.45.6.2019.646

Harris, C. M., Martin, S., Martin, C., Helble, T., Henderson, E., Paxton, C. G. M., et al. (2019a). Changes in the spatial distribution of acoustically-derived minke whale (*Balaenoptera acutorostrata*) tracks in response to navy training. *Aquat. Mammals* 45, 661–674. doi: 10.1578/AM.45.6.2019.661

Harris, C. M., Thomas, L., Falcone, E., Hildebrand, J., Houser, D., Kvadsheim, P., et al. (2018). Marine mammals and sonar: dose-response studies, the risk-disturbance hypothesis and the role of exposure context. *J. Appl. Ecol.* 55, 396–404. doi: 10.1111/1365-2664.12955

Heaney, K. D., and Campbell, R. L. (2016). Three-dimensional parabolic equation modeling of mesoscale eddy deflection. *J. Acoust. Soc. Am.* 139, 918–926. doi: 10.1121/1.4942112

Helble, T. A., Guazzo, R. A., Alongi, G. C., Martin, C. R., Martin, S. W., and Henderson, E. E. (2020b). Fin whale song patterns shift over time in the central North Pacific. *Front. Mar. Sci.* 7:587110. doi: 10.3389/fmars.2020.587110

Helble, T. A., Guazzo, R. A., Martin, C. R., Durbach, I. N., Alongi, G. C., Martin, S. W., et al. (2020a). Lombard effect: minke whale boing call source levels vary with natural variations in ocean noise. *J. Acoust. Soc. Am.* 147, 698–712. doi: 10.1121/10.0000596

Helble, T. A., Henderson, E. E., Ierley, G. R., and Martin, S. W. (2016). Swim track kinematics and calling behavior attributed to Bryde's whales on the Navy's Pacific Missile Range Facility. *J. Acoust. Soc. Am.* 140, 4170–4177. doi: 10.1121/1.4967754

Helble, T. A., Ierley, G. R., D'Spain, G. L., and Martin, S. W. (2015). Automated acoustic localization and call association for vocalizing humpback whales on the Navy's Pacific Missile Range Facility. *J. Acoust. Soc. Am.* 137, 11–21. doi: 10.1121/1.4904505

Henderson, E. E., Helble, T. A., Ierley, G., and Martin, S. (2018). Identifying behavioral states and habitat use of acoustically tracked humpback whales in Hawaii. *Mar. Mammal Sci.* 34, 701–717. doi: 10.1111/mms.12475

Henderson, E. E., Martin, S. W., Manzano-Roth, R. A., and Matsuyama, B. (2016). Occurrence and habitat use of foraging Blainville's beaked whales (*Mesoplodon densirostris*) in Hawaii. *Aquat. Mammals* 42, 549–562. doi: 10.1578/AM.42.4.2016.549

Hofmann-Wellenhof, B., Lichtenegger, H., and Collins, J. (2001). *GPS Theory and Practice*, 4rd Edn. Wien, NY: Springer-Verlag.

Isojunno, S., and Miller, P. J. O. (2015). Sperm whale response to tag boat presence: biologically informed hidden state models quantify lost feeding opportunities. *Ecosphere* 6, 1–46. doi: 10.1890/ES14-00130.1

Isojunno, S., Sadykova, D., DeRuiter, S. L., Curé, C., Visser, F., Thomas, L. J., et al. (2017). Individual, ecological, and anthropogenic influences on activity budgets of long-finned pilot whales. *Ecosphere* 8:e02044. doi: 10.1002/ecs2.2044

Johnson, D. S., and London, J. M. (2018). crawl: an R package for fitting continuous-time correlated random walk models to animal movement data. *Zenodo* doi: 10.5281/zenodo.596464

Johnson, D. S., London, J. M., Lea, M. A., and Durban, J. W. (2008). Continuous-time correlated random walk model for animal telemetry data. *Ecology* 89, 1208–1215. doi: 10.1890/07-1032.1

Johnson, M., de Soto, N. A., and Madsen, P. T. (2009). Studying the behavior and sensory ecology of marine mammals using acoustic recording tags: a review. *Mar. Ecol. Progr. Ser.* 395, 55–73. doi: 10.3354/meps08255

Johnson, M., and Tyack, P. L. (2003). A digital acoustic recording tag for measuring the response of wild marine mammals to sound. *IEEE J. Eng.* 28, 3–12. doi: 10.1109/joe.2002.808212

King, S. L., and Janik, V. M. (2015). Come dine with me: food-associated social signalling in wild bottlenose dolphins (*tursiops truncatus*). *Animal Cogn.* 18, 969–974. doi: 10.1007/s10071-015-0851-7

Klay, J., Mellinger, D. K., Moretti, D. J., Martin, S. W., and Roch, M. A. (2015). *Advanced Methods for Passive Acoustic Detection, Classification and Localization of Marine Mammals. Office of Naval Research Arlington, VA Technical Report*. Available online at https://www.onr.navy.mil/reports/FY15/mbklay.pdf (accessed 22 May 2021)

Kvadsheim, P. H., DeRuiter, S., Sivle, L. D., Godlbogen, J., Roland-Hansen, R., Miller, P. J. O., et al. (2017). Avoidance responses of minke whales to 1-4kHz naval sonar. *Mar. Poll. Bull.* 121, 60–68. doi: 10.1016/j.marpolbul.2017.05.037

Manzano-Roth, R., Henderson, E. E., Martin, S. W., Martin, C., and Matsuyama, B. M. (2016). Impacts of U.S. Navy training events on Blainville's beaked whale (*Mesoplodon densirostris*) foraging dives in Hawaiian waters. *Aqu. Mammals* 42, 507–518. doi: 10.1578/AM.42.4.2016.507

Martin, S. W., Martin, C. R., Matsuyama, B. M., and Henderson, E. E. (2015). Minke whales (*Balaenoptera acutorostrata*) respond to navy training. *J. Acoust. Soc. Am.* 137, 2533–2541. doi: 10.1121/1.4919319

McCarthy, E., Moretti, D., Thomas, L., DiMarzio, N., Morrissey, R., Jarvis, S., et al. (2011). Changes in spatial and temporal distribution and vocal behavior of Blainville's beaked whales (*Mesoplodon densirostris*) during multi-ship exercises with mid-frequency sonar. *Mar. Mammal Sci.* 27, E206–E226.

McClintock, B. T. (2017). Incorporating telemetry error into hidden Markov models of animal movement using multiple imputation. *J. Agric. Biol. Environ. Stat.* 22, 249–269. doi: 10.1007/s13253-017-0285-6

McClintock, B. T., King, R., Thomas, L., Matthiopoulos, J., McConnell, B. J., and Morales, J. M. (2012). A general discrete−time modeling framework for animal movement using multistate random walks. *Ecol. Monogr.* 82, 335–349. doi: 10.1890/11-0326.1

McClintock, B. T., and Michelot, T. (2018). momentuHMM: R package for generalized hidden Markov models of animal movement. *Methods Ecol. Evol.* 9, 1518–1530. doi: 10.1111/2041-210x.12995

Melcon, M. L., Cummins, A. J., Kerosky, S. M., Roche, L. K., Wiggins, S. M., and Hildebrand, J. A. (2012). Blue whales respond to anthropogenic noise. *PLoS One* 7:e32681. doi: 10.1371/journal.pone.0032681

Michelot, T., Langrock, R., Bestley, S., Jonsen, I. D., Photopoulou, T., and Patterson, T. A. (2017). Estimation and simulation of foraging trips in land-based marine predators. *Ecology* 98, 1932–1944. doi: 10.1002/ecy.1880

Moretti, D., Thomas, L., Marques, T., Harwood, J., Dilley, A., Neales, R., et al. (2014). A risk function for behavioral disruption of Blainville's beaked whales (*Mesoplodon densirostris*) from mid-frequency active sonar. *PLoS one* 9:e85064. doi: 10.1371/journal.pone.0085064

Mul, E., Blanchet, M. A., McClintock, B. T., Grecian, W. J., Biuw, M., and Rikardsen, A. (2020). Killer whales are attracted to herring fishing vessels. *Marine Ecology Progress Series* 652, 1–13.

National Research Council (2005). *Marine Mammal Populations and Ocean Noise*. Washington, DC: The National Academies Press.

Oswald, J. N., Au, W. W., and Duennebier, F. (2011). Minke whale (*Balaenoptera acutorostrata*) boings detected at the Station ALOHA Cabled Observatory. *J. Acoust. Soc. Am.* 129, 3353–3360. doi: 10.1121/1.3575555

Parks, S. E., Cusano, D. A., Stimpert, A. K., Weinrich, M. T., Friedlaender, A. S., and Wiley, D. N. (2014). Evidence for acoustic communication among bottom foraging humpback whales. *Sci. Rep.* 4:7508. doi: 10.1038/srep07508

Pirotta, E., Booth, C. G., Costa, D. P., Fleishman, E., Kraus, S. D., Lusseau, D., et al. (2018). Understanding the population consequences of disturbance. *Ecol. Evol.* 8, 9934–9946.

R Core Team (2019). *R: A Language and Environment for Statistical Computing*. Vienna: R Foundation for Statistical Computing.

Rankin, S., and Barlow, J. (2005). Source of the North Pacific 'boing' sound attributed to minke whales. *J. Acoust. Soc. Am.* 118, 3346–3351. doi: 10.1121/1.2046747

Risch, D., Corkeron, P. J., Ellison, W. T., and Van Parijs, S. M. (2012). Changes in humpback whale song occurrence in response to an acoustic source 200 km away. *PLoS one* 7:e29741. doi: 10.1371/journal.pone.0029741

Rui, D., Kun-De, Y., Yuan-Liang, M., and Bo, L. (2012). A reliable acoustic path: Physical properties and a source localization method. *Chinese Phys. B* 21:124301. doi: 10.1088/1674-1056/21/12/124301

Sivle, L. D., Wensveen, P. J., Kvadsheim, P., Lam, F.-P. A., Visser, F., Cure, C., et al. (2016). Naval sonar disrupts foraging behavior in humpback whales. *Mar. Ecol. Progr. Ser.* 562, 211–220. doi: 10.3354/meps11969

Southall, B. L., DeRuiter, S. L., Friedlaender, A., Stimpert, A. K., Goldbogen, J. A., Hazen, E., et al. (2019). Behavioral responses of individual blue whales (*Balaenoptera musculus*) to mid-frequency military sonar. *J. Exp. Biol.* 222:jeb190637. doi: 10.1242/jeb.190637

Southall, B. L., Nowacek, D. P., Miller, P. J. O., and Tyack, P. L. (2016). Experimental field studies to measure behavioral responses of cetaceans to sonar. *Endangered Species Res.* 31, 293–315. doi: 10.3354/esr00764

Sugai, L. S. M., Silva, T. S. F., Ribeiro, J. W. Jr., and Llusia, D. (2019). Terrestrial passive acoustic monitoring: review and perspectives. *BioScience* 69, 15–25. doi: 10.1093/biosci/biy147

Therneau, T. (2020). *survival. A Package for Survival Analysis in R. R package version 3.2-3*. Available online at: https://CRAN.R-project.org/package=survival (accessed April 26, 2021).

Thomas, L., and Reyes, E. M. (2014). Tutorial: survival estimation for Cox regression models with time-varying coefficients using SAS and R. *J. Stat. Softw.* 61(c1):24870.

Thompson, P. O., and Friedl, W. A. (1982). A long term study of low frequency sounds from several species of whales off Oahu, Hawaii. *Cetology* 45, 1–19.

Touloumis, A., Agresti, A., and Kateri, M. (2013). GEE for multinomial responses using a local odds ratios parameterization. *Biometrics* 69, 633–640. doi: 10.1111/biom.12054

Tyack, P. L., and Clark, C. W. (2000). *Communication and Acoustic Behavior of Dolphins and Whales. In Hearing by Whales and Dolphins*. New York, NY: Springer, 156–224.

Tyack, P. L., Zimmer, W. M. X., Morretti, D., Southall, B. L., Claridge, D. E., Durban, J. W., et al. (2011). Beaked whales respond to simulated and actual Navy sonar. *PLoS one* 6:e17009. doi: 10.1371/journal.pone.0017009

U.S. Department of the Navy (2018). *Hawaii-Southern California Training and Testing final environmental impact statement/Overseas environmental impact statement*. Pearl Harbor, HI: Naval Facilities Engineering Command, Pacific.

Urick, R. J. (1983). *Principles of Underwater Sound*. New York, NY: McGraw-Hill.

Xue, Y., and Schifano, E. D. (2017). Diagnostics for the Cox model. *Commun. Stat. Appl. Methods* 24, 583–604. doi: 10.29220/csam.2017.24.6.583

Ziegler, A. (2011). *Generalized Estimating Equations*. New York, NY: Springer Science and Business Media.

Zucchini, W., MacDonald, I. L., and Langrock, R. (2017). *Hidden Markov Models for Time Series: an Introduction Using R*. Boca Raton, FL: CRC press

Conflict of Interest: The authors declare that the research was conducted in the absence of any commercial or financial relationships that could be construed as a potential conflict of interest.

Copyright © 2021 Durbach, Harris, Martin, Helble, Henderson, Ierley, Thomas and Martin. This is an open-access article distributed under the terms of the Creative Commons Attribution License (CC BY). The use, distribution or reproduction in other forums is permitted, provided the original author(s) and the copyright owner(s) are credited and that the original publication in this journal is cited, in accordance with accepted academic practice. No use, distribution or reproduction is permitted which does not comply with these terms.

frontiers in Marine Science

ORIGINAL RESEARCH
published: 12 July 2021
doi: 10.3389/fmars.2021.664230

Far-Field Effects of Impulsive Noise on Coastal Bottlenose Dolphins

Oihane Fernandez-Betelu, Isla M. Graham, Kate L. Brookes†, Barbara J. Cheney, Tim R. Barton and Paul M. Thompson*

Lighthouse Field Station, School of Biological Sciences, University of Aberdeen, Aberdeen, United Kingdom

Increasing levels of anthropogenic underwater noise have caused concern over their potential impacts on marine life. Offshore renewable energy developments and seismic exploration can produce impulsive noise which is especially hazardous for marine mammals because it can induce auditory damage at shorter distances and behavioral disturbance at longer distances. However, far-field effects of impulsive noise remain poorly understood, causing a high level of uncertainty when predicting the impacts of offshore energy developments on marine mammal populations. Here we used a 10-year dataset on the occurrence of coastal bottlenose dolphins over the period 2009–2019 to investigate far-field effects of impulsive noise from offshore activities undertaken in three different years. Activities included a 2D seismic survey and the pile installation at two offshore wind farms, 20–75 km from coastal waters known to be frequented by dolphins. We collected passive acoustic data in key coastal areas and used a Before-After Control-Impact design to investigate variation in dolphin detections in areas exposed to different levels of impulsive noise from these offshore activities. We compared dolphin detections at two temporal scales, comparing years and days with and without impulsive noise. Passive acoustic data confirmed that dolphins continued to use the impact area throughout each offshore activity period, but also provided evidence of short-term behavioral responses in this area. Unexpectedly, and only at the smallest temporal scale, a consistent increase in dolphin detections was observed at the impact sites during activities generating impulsive noise. We suggest that this increase in dolphin detections could be explained by changes in vocalization behavior. Marine mammal protection policies focus on the near-field effects of impulsive noise; however, our results emphasize the importance of investigating the far-field effects of anthropogenic disturbances to better understand the impacts of human activities on marine mammal populations.

Keywords: anthropogenic noise, BACI, renewable energy, seismic exploration, acoustic disturbance, offshore wind farm, passive acoustic monitoring, marine mammal

OPEN ACCESS

Edited by:
Kerri D. Seger, Applied Ocean Sciences, United States

Reviewed by:
Isha Bopardikar, Indian Institute of Science Education and Research, Tirupati, India
Mario Barletta, Federal University of Pernambuco, Brazil

****Correspondence:***
Oihane Fernandez-Betelu
oihane.fernandez@abdn.ac.uk

†Present address:
Kate L. Brookes, Marine Laboratory, Marine Scotland Science, Aberdeen, United Kingdom

Specialty section:
This article was submitted to Marine Ecosystem Ecology, a section of the journal Frontiers in Marine Science

Received: *04 February 2021*
Accepted: *10 June 2021*
Published: *12 July 2021*

Citation:
Fernandez-Betelu O, Graham IM, Brookes KL, Cheney BJ, Barton TR and Thompson PM (2021) Far-Field Effects of Impulsive Noise on Coastal Bottlenose Dolphins. Front. Mar. Sci. 8:664230. doi: 10.3389/fmars.2021.664230

INTRODUCTION

Ambient noise in the marine environment has increased since the 1950s due to the rise of human activities at sea (Frisk, 2012). In response to the heightened concerns about the potential impacts of noise on marine life, many countries have reached international agreements to monitor underwater noise levels (Van der Graaf et al., 2012; OSPAR, 2017; Reeve, 2019). In Europe, the Marine Strategy

Framework Directive (MSFD) requires Member States to avoid sound sources that are likely to cause significant impact in the marine environment (Tasker et al., 2010). The MSFD sets out a series of indicators to assess the environmental status of an area, which for underwater noise is the proportion and spatial distribution of days on which sound sources exceed levels likely to entail significant impact.

Human activities such as pile-driving, seismic surveys and sonars produce some of the most powerful sounds underwater (Gordon et al., 2003). These impulsive sounds are defined as acute, broadband, transient signals with a rapid onset and a rapid decay (<1 s) and are considered particularly hazardous to marine mammals (Southall et al., 2007). However, during the propagation, the acoustic characteristics of sound change at rates that vary according to the specific environmental conditions. The greatest change in the acoustic characteristics of impulsive sounds occurs within ∼ 10 km from the source (Hastie et al., 2019) and, therefore, the hazardous characteristics of these sounds will vary with distance (Southall et al., 2007). Impulsive sounds have the potential to impact cetaceans through direct injury at shorter distances (here near-field) and through behavioral disturbance at longer distances (here far-field; Erbe et al., 2018). Measures to mitigate near-field effects from injury are widely adopted (Bröker et al., 2015; Verfuss et al., 2016). However, potential far-field behavioral effects and the longer-term consequences of any short-term disturbance remain challenging to assess (Pirotta et al., 2018). To date, most of the studies on the effect of impulsive noise on wild marine mammals have focused on harbor porpoises (*Phocoena phocoena*) and seals (*Phoca vitulina*) (e.g., Russell et al., 2016; Brandt et al., 2018; Graham et al., 2019). Other species, such as bottlenose dolphins (*Tursiops truncatus*), may react differently to this disturbance but information on this is sparse (David, 2006; Finneran et al., 2015; Graham et al., 2017). Due to the lack of empirical data, estimates of potential behavioral effects required for the regulation of marine energy developments have a high level of uncertainty for these animals (Merchant, 2019).

This uncertainty can be especially challenging where offshore energy developments are being considered within or near to areas used by protected cetacean populations. Over the last decade, three major energy developments have been undertaken in NE Scotland, near a Special Area of Conservation (SAC) that was established in the Moray Firth to protect bottlenose dolphins. These included a 2D seismic survey for oil and gas exploration in 2011, and the installation of foundation piles for two offshore wind farms in 2017 (Beatrice Offshore Wind Farm) and 2019 (Moray East Offshore Wind Farm), all of which are known to result in high levels of impulsive underwater noise (Madsen et al., 2006; Thomsen et al., 2011). The Habitats Directive (92/43/EEC) requires regulators to ensure that the Favorable Conservation Status of the SAC is maintained. Therefore, higher levels of assessment and protection were required prior to all three of these projects. The Appropriate Assessments undertaken by the regulator, concluded that there were no likely long-term impacts on the protected bottlenose dolphin population and permissions were granted (Berr, 2007; MS-LOT, 2014; MS-LOT and Marine Scotland Science, 2014). However, significant objections were raised during some of these processes, arguing that dolphins could be displaced from the southern coast of the Moray Firth, an important area for this population (Cheney et al., 2013).

Given the sensitivities surrounding this issue and the level of uncertainty in the predictions, we used passive acoustic monitoring (PAM) to investigate whether far-field effects of impulsive noise from these offshore activities resulted in displacement of dolphins from coastal waters in the southern Moray Firth. To do so, echolocation data loggers (CPODs) were deployed to study variation in dolphin detections in areas exposed to different levels of impulsive noise. First, year-to-year variability in dolphin occurrence was investigated in each of those areas. Second, Before-After Control-Impact analyses (BACI; Underwood, 1992; Smith, 2002) were performed at two temporal scales to assess potential differences in detections within these areas. At the medium temporal scale, the BACI analysis compared years in which impulsive noise from offshore activities was present or absent. At the small temporal scale, finer-scale patterns within years with offshore activity were explored by comparing days in which impulsive noise was present or absent. Lastly, during the construction of Moray East wind farm, a more extensive PAM array was deployed in the coastal area nearest this development to investigate whether dolphins were displaced away from it and toward the coast during piling days.

MATERIALS AND METHODS

Study Area and Moray Firth Projects

The study was carried out in the Moray Firth, a large triangular embayment of the North Sea that covers approximately 5,230 km^2. The seabed gradually slopes from the coast to depths of up to 200 m and, in the center, there is a shallow sand bank of 40–50 m depth called the Smith Bank (Eleftheriou et al., 2004). The Firth is frequented by a range of cetacean species (Thompson et al., 2015; Robinson et al., 2017; Risch et al., 2019) that includes animals from a protected population of bottlenose dolphins that uses the Moray Firth SAC (**Figure 1**). The distribution of this population is primarily coastal (Thompson et al., 2015) and, although individuals show interannual variability in their range (Pirotta et al., 2015b), the population shows high site fidelity at a broader scale (Cheney et al., 2014). The area most intensively used by these dolphins is the inner Moray Firth, in the south-western part of the Firth, which is considered to be their core area of distribution (Cheney et al., 2013). However, a large proportion of the population uses other areas further south along the east coast of Scotland, such as St Andrews Bay and the Tay Estuary (Arso Civil et al., 2019). The southern coast of the Moray Firth is also intensively used by these dolphins and acts as a corridor between the SAC in the Moray Firth and the other key areas around the east coast (Culloch and Robinson, 2008; Cheney et al., 2013; Arso Civil et al., 2019).

In 2011, between the 2nd and the 11th of September, 2D seismic surveys were undertaken within the central Moray Firth, at minimum distances of 18 and 42 km from the southern coast and inner Moray Firth, respectively (**Figure 1** and **Table 1**). They were conducted with a 470 cubic inch airgun array and a 5–6 s

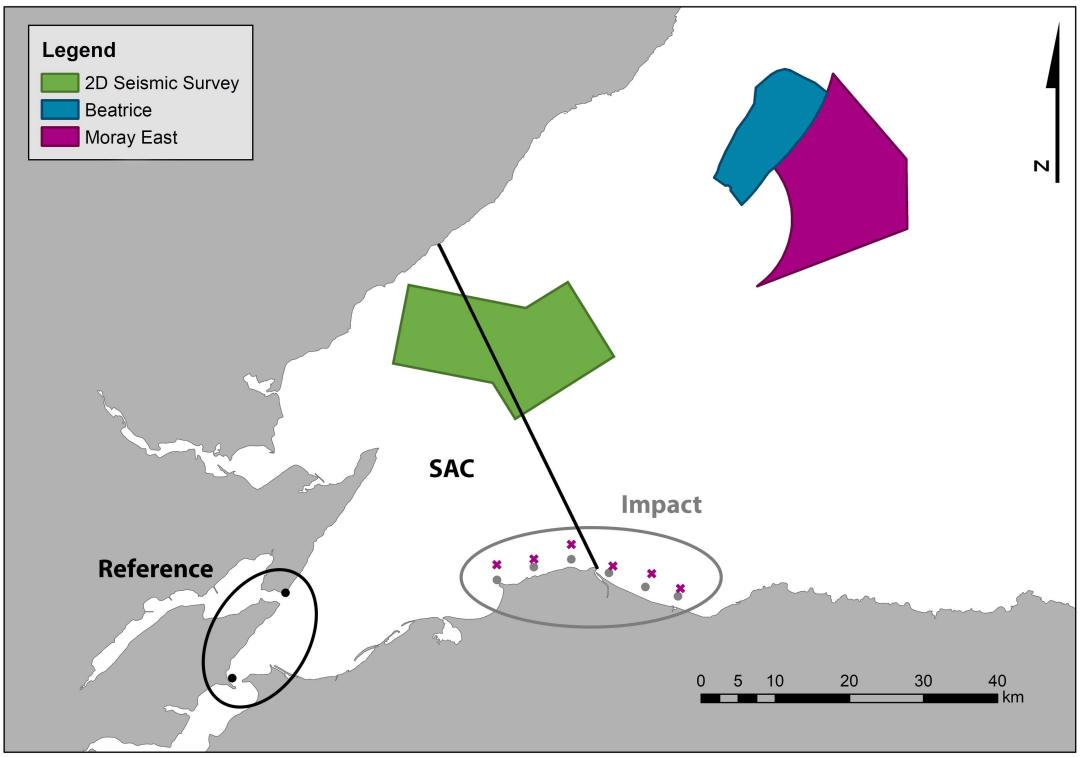

FIGURE 1 | Map of the Moray Firth showing the boundary of the Moray Firth SAC (solid line) and the areas in which different offshore projects were undertaken (2D seismic survey and Beatrice and Moray East wind farms). Circles (•): CPODs deployed from 2009 to 2019 (circled in black: *Reference Area* array; circled in gray: *Impact Area* array); X-shaped crosses (x): CPODs deployed in 2019 only (*Impact Outer* array).

shot interval (see Thompson et al., 2013 for survey details and modeled predictions of received noise levels). Between the 2nd April and the 2nd December 2017, the 344 pile foundations for the Beatrice wind farm were installed on the Smith Bank at least 53 km from the southern coast and 80 km from the inner Moray Firth. Each pile was hammered into the seabed using impulsive pile driving techniques with a maximum hammer energy of 2299 kJ (see Graham et al., 2019 for modeled predictions of received noise levels). On the 30th May 2019, construction started at the Moray East wind farm next to Beatrice; 264 pile foundations were installed between May and December 2019 (see MORL, 2016 for modeled predictions of received noise levels). Piles were installed using similar impulsive pile driving techniques and a maximum hammer energy of 2071 kJ (see **Supplementary Tables 1, 2** for detailed piling timelines from Beatrice and Moray East).

TABLE 1 | Summary table with distance to the offshore project and maximum predicted received noise levels expressed as unweighted single-pulse sound exposure levels (SEL: dB re 1 $\mu Pa^2 s$ (Thompson et al., 2013; MORL, 2016; Graham et al., 2019).

		Reference area	Impact area
2D seismic	Minimum distance (km)	42	18
	Max Received noise levels (SEL)	132	139
Beatrice	Minimum distance (km)	80	53
	Max Received noise levels (SEL)	100	128
Moray east	Minimum distance (km)	78	45
	Max Received noise levels (SEL)	93	141

Passive Acoustic Monitoring

Echolocation detectors (CPODs, Chelonia Ltd.) were used to collect information on temporal patterns of occurrence in areas known to be frequented by bottlenose dolphins (Cheney et al., 2014). CPODs were deployed between 2009 and 2019 following previously described techniques (Bailey et al., 2010a; Thompson et al., 2013; Graham et al., 2019). Two CPODs were deployed at sites within the inner Moray Firth where the impact was expected to be lowest; hereafter the *Reference Area* (**Figure 1**; Fernandez-Betelu et al., 2019). These reference sites were located at minimum distances of 42, 80, and 78 km from the seismic survey, Beatrice and Moray East wind farm developments, respectively. Six CPODs were deployed along the southern Moray Firth coast, the part of the dolphin population's coastal range that was closest to all three offshore activities, where the impact was expected to be highest, hereafter the *Impact Area* (Thompson et al., 2010). These impact sites were located at minimum distances of 18, 53, and 45 km from the seismic survey, Beatrice and Moray East wind farm developments, respectively. In 2019, during the construction of Moray East wind farm, six extra CPODs were deployed in the *Impact Area* at greater distances from the coast (from 3 to 4 km), hereafter *Impact Outer* area. With this array we aimed to investigate whether dolphins from

further out at sea were displaced toward the coast in the southern Moray Firth by impulsive noise. Although data were collected year round at some locations, data from November to April were excluded from all the analyses due to the low occurrence of dolphins during those months along the southern Moray Firth coast (Fernandez-Betelu et al., 2019).

CPOD data were downloaded and trainfiltered using the manufacturer's software[1] to identify which echolocation clicks were produced by dolphins. As recommended by the manufacturer, only click trains classified as high and moderate quality were used in this study. Since previous photo-ID, line transects and aerial surveys confirmed that the presence of other species of dolphins is rare in the studied sites (Thompson et al., 2015), all detected echolocation clicks were assumed to be produced by bottlenose dolphins. Detection Positive Hours per day (DPH) was the metric derived from the click train detections that we chose as the proxy for dolphin occurrence. DPH describes the number of hours in each day in which a dolphin click train was detected on each CPOD and is a robust proxy for studying odontocete occurrence (Brookes et al., 2013; Williamson et al., 2016). We used the statistical program R v. 3.5.1 (R Core Team, 2018) in all subsequent analyses.

Inter-Annual Variability in Dolphin Occurrence

Inter-annual variability in the occurrence of dolphins in the *Reference* and *Impact Areas* was characterized from a sub-set of comparable data from 4 long-term CPODs, two in each of the areas, that provided complete datasets for August and September from 2009 to 2019 (see timeline with CPOD deployments in **Supplementary Figure 1**). We calculated the DPH per day for these months and assessed the year-to-year variability in dolphin occurrence within these areas. Comparisons between years were made using non-parametric Kruskal-Wallis tests because data were not normally distributed.

Far-Field Effects on Bottlenose Dolphin Occurrence in Relation to Seismic and Wind Farm Projects: Medium and Small Temporal Scales

We performed BACI analyses (Underwood, 1992; Smith, 2002) to investigate whether there was a change in dolphin detections in the *Impact Area* relative to the more distant *Reference Area* during each offshore activity. In the BACI analyses we performed generalized linear mixed models (GLMM) with a Poisson family distribution and square root link function (Bolker et al., 2009). We used dolphin DPH as the response variable and included area (*Reference Area/Impact Area*) and period (*Baseline period/Activity period*) as fixed effects in interaction. At the medium temporal scale, the *Activity period* comprised years when offshore activities were undertaken and the *Baseline period* years without these offshore activities. At the small temporal scale, the *Activity period* included days in which impulsive noise was generated and the *Baseline period*, days in which impulsive noise was not generated (**Table 2**). We included CPOD location and day within a year as random intercepts to remove patterns in the residuals and improve the fit of GLMM models at both temporal scales.

[1] www.chelonia.co.uk

Far-Field Effect on Bottlenose Dolphin Occurrence in Relation to Moray East Wind Farm: Displacement From the Southern Moray Firth at a Fine Spatial Scale

During foundation installation at Moray East wind farm we investigated the occurrence of dolphins in the *Impact Area* at a fine spatial scale and assessed whether dolphins were displaced toward the coast during piling days. To do so, we assessed differences in dolphin DPH between the CPODs closer to the shore (*Impact Inner* array) and the CPODs further from the coast (*Impact Outer* array) in the impact area (**Figure 1**). We used GLMM and introduced array (*Impact Inner/Impact Outer*) and period (*Piling/Non-piling days*) as explanatory variables in interaction. CPOD location and day within a year were included as random intercepts.

RESULTS

CPODs were successfully deployed from 2009 to 2019 and provided more than 10,000 days of CPOD data. Gaps in the dataset occurred due to a combination of device failure and logistical constraints. Data from 2012 were removed from these analyses because only one CPOD was recovered that year from the *Impact Area* (**Supplementary Figure 1**).

TABLE 2 | Data used in the BACI analyses for the medium and small temporal scales.

			Baseline period	Activity period
Medium temporal scale	2D seismic	Dates	01–14 Sep	02–11 Sep
		Years	2009, 2010, 2013, 2014	2011
		Tot. ndays	60	10
	Beatrice	Dates	May–Sep	May–Sep
		Years	2014, 2015, 2016, 2018	2017
		Tot. ndays	611	153
	Moray East	Dates	May–Sep	May–Sep
		Years	2014, 2015, 2016, 2018	2019
		Tot. ndays	611	153
Small temporal scale	2D seismic	Dates	23 Aug–01 Sep, 12–21 Sep	02–11 Sep
		Years	2011	2011
		Tot. ndays	20	10 (16.4%)
	Beatrice	Dates	Non-piling days May–Sep	Piling days May–Sep
		Years	2017	2017
		Tot. ndays	68	85 (52.4%)
	Moray East	Dates	Non-piling days May–Sep	Piling days May–Sep
		Years	2019	2019
		Tot. ndays	101	52 (24.6%)

Table includes the total number of days in each of the periods (Baseline period/Activity period) and the percentage of days with impulsive noise in August and September in brackets.

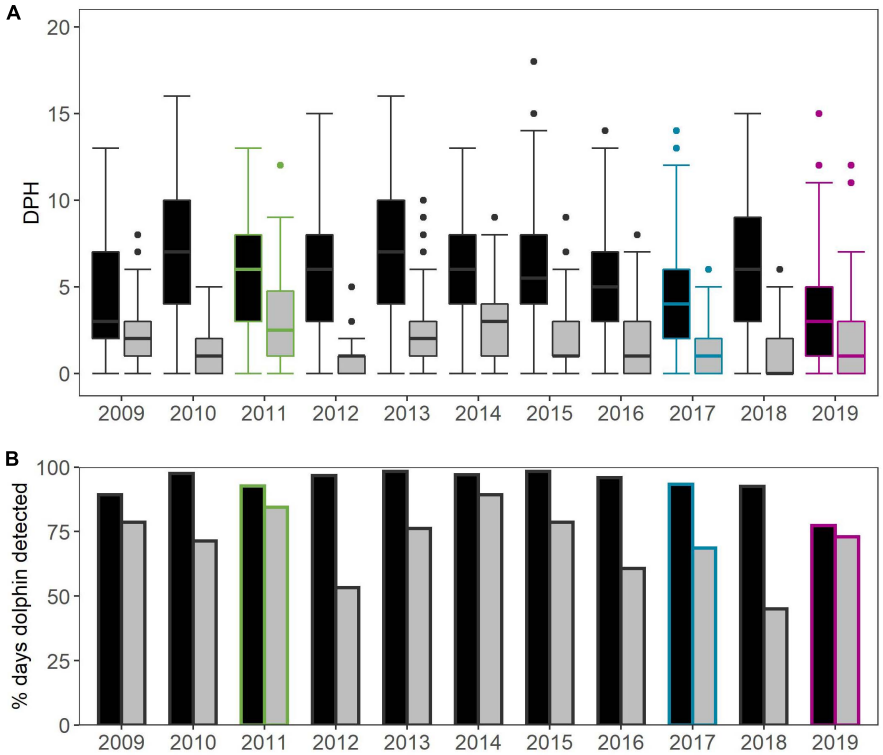

FIGURE 2 | Inter-annual variation in **(A)** dolphin Detection Positive Hours per day and **(B)** percentage of days that dolphins were detected in *Reference Area* (black) and *Impact Area* (gray). Data from August-September 2009 to 2019 from the 4 long-term CPODs. Colored borders indicate years when offshore activities took place (2011: 2D seismic survey; 2017: Beatrice wind farm construction; and 2019: Moray East wind farm construction).

Inter-Annual Variability in Dolphin Occurrence

The seismic survey, Beatrice and Moray East wind farm construction resulted in impulsive noise being produced within the Moray Firth on 16.4, 52.4, and 24.6% of days in August and September 2011, 2017, and 2019, respectively (**Table 2**).

For the comparable subset of data from August-September, there were significant inter-annual differences in the daily occurrence of dolphins (DPH) in both areas (**Figure 2A**). The median DPH ranged between 3 and 7 h in the *Reference Area* (X^2 = 102.26, df = 10, $p < 0.0001$) and between 0 and 3 h in the *Impact Area* (X^2 = 139.4, df = 10, p-value < 0.0001) (**Figure 3** and details in **Supplementary Table 3**). Dolphin detections were higher in the *Reference Area* than in the *Impact Area* during all years: dolphins were detected on 77–98% of the days in the *Reference Area*, compared to 45–89% of the days in the *Impact Area* (**Figure 2B**).

Far-Field Effects on Bottlenose Dolphin Occurrence in Relation to Seismic and Wind Farm Projects: Medium and Small Temporal Scales

At the medium temporal scale, the BACI analysis did not identify any consistent relationship between observed inter-annual variability and the occurrence of impulsive noise from these offshore activities (**Figure 4** and **Table 3**). There were significant impacts of both the seismic survey and Beatrice wind farm construction, but the effects were in opposite directions. For the seismic survey in 2011, dolphin detections in the *Impact Area* increased by 50% (to a median of 3 h per day) compared to baseline years but reduced by 100% (to a median of 0.5 h per day) in the *Reference Area* (GLMM: X^2 = 32.975, df = 1, $p < 0.001$). In contrast, during the Beatrice wind farm piling campaign in 2017, compared to baseline years, dolphin detections decreased by 50% in the *Impact Area* (to a median of 1 h per day) and decreased by 14% (to a median of 6 h per day) in the *Reference Area* (GLMM: X^2 = 39.342, df = 1, $p < 0.001$). Finally, when impact piling was conducted at Moray East wind farm in 2019, no significant difference in dolphin detections between areas was found compared to baseline years (GLMM: X^2 = 0.9451, df = 1, $p > 0.05$; **Figure 4** and **Table 3**).

At the small temporal scale, the BACI analysis identified a significant impact of all three offshore activities, with an increase in dolphin detections in the impact area during those days on which impulsive noise was generated (**Figure 5** and **Table 3**). For the seismic survey, an increase in dolphin detections of 200% (to a median of 3 h per day) was obtained in the *Impact Area* whereas a reduction of 90% (to a median of 0.5 h per day) was detected in the *Reference Area* (GLMM: X^2 = 38.861, df = 1, $p < 0.001$).

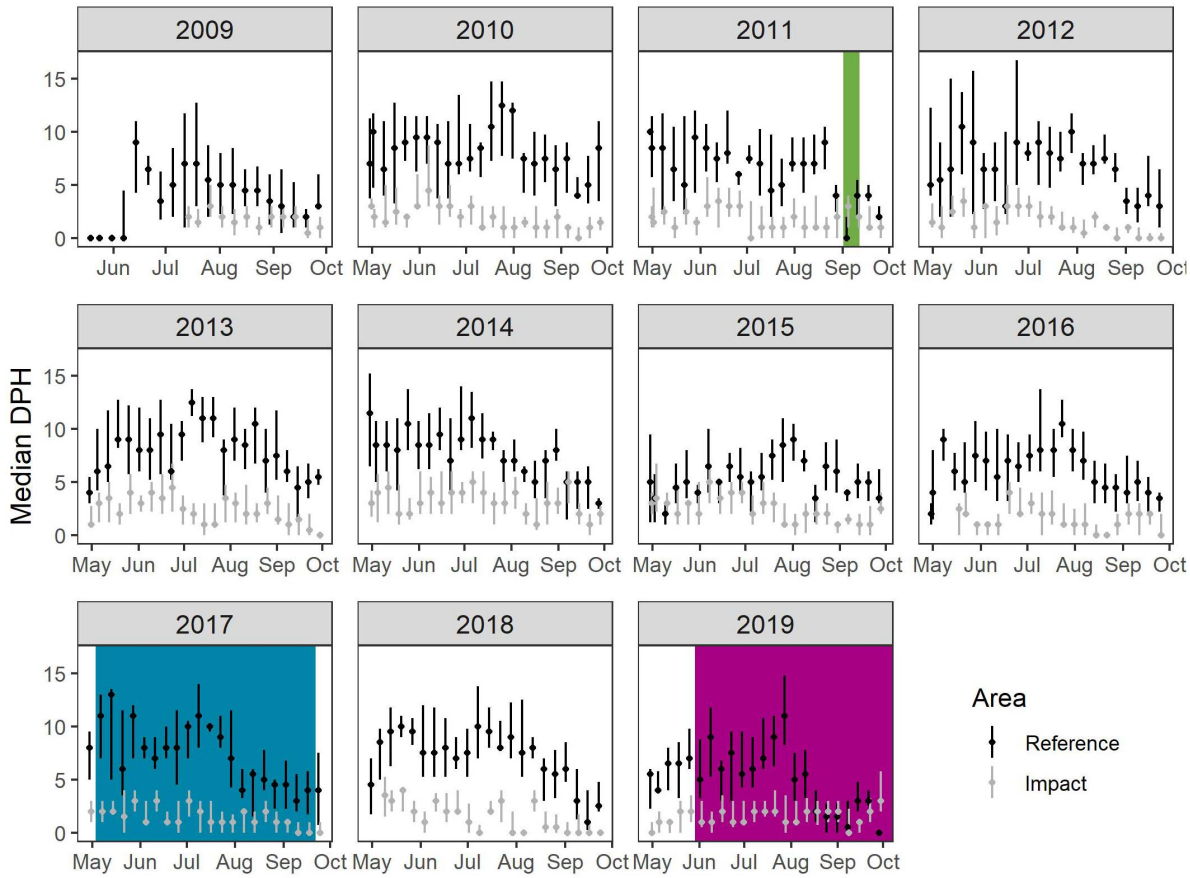

FIGURE 3 | Weekly median Detection Positive Hours (DPH) and inter-quartile ranges in the *Reference Area* (black) and *Impact Area* (gray) in each of the years studied. Colored areas indicate when offshore activities took place (green: 2D seismic survey; blue: Beatrice wind farm construction; magenta: Moray East wind farm construction).

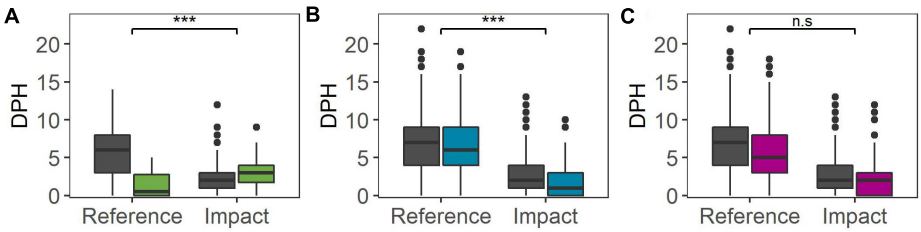

FIGURE 4 | Dolphin Detection Positive Hours (DPH) in the inner Moray Firth (*Reference Area*) and the southern Moray Firth (*Impact Area*) during the *Baseline period* (dark gray) and the *Activity period* (colored) at the medium temporal scale: **(A)** 2D seismic survey, **(B)** Beatrice wind farm construction and **(C)** Moray East wind farm construction. Significance of the interaction between period and area is indicated above the bar at the top: ***$P < 0.001$; n.s. $P > 0.05$.

During pile-driving at Beatrice wind farm, an increase in dolphin detections of 100% was found in the *Impact Area* (to a median of 2 h per day) whereas there was no change in the *Reference Area* (GLMM: $X^2 = 5.198$, df = 1, $p < 0.05$). For the Moray East wind farm development, dolphin detections increased by 100% (to a median of 2 h per day) in the *Impact Area* and increased by 20% (to a median of 6 h per day) in the *Reference Area* (GLMM: $X^2 = 4.807$, df = 1, $p < 0.05$; **Figure 5** and **Table 3**).

Far-Field Effect on Bottlenose Dolphin Occurrence in Relation to Moray East Wind Farm: Displacement From the Southern Moray Firth at a Fine Spatial Scale

There was a significant increase in dolphin detections during piling days in both *Impact Inner* and *Impact*

TABLE 3 | Results of the Poisson generalized linear mixed models used to investigate the effect of impulsive noise from offshore activities on the acoustic detection of dolphins at sites in the inner Moray Firth (*Reference Area*) and the southern Moray Firth (*Impact Area*) at the medium and small temporal scales and in the *Impact Inner* and *Impact Outer* arrays at the fine spatial scale.

			Estimate	Std. error	Df	*P*-Value
Medium temporal scale	2D seismic survey	*Intercept*	0.777	0.089	1	< 0.001
		Period	0.240	0.154	1	0.119
		Area	0.910	0.137	1	< 0.001
		Period:Area	−1.617	0.286	1	< 0.001
	Beatrice	*Intercept*	0.786	0.066	1	< 0.001
		Period	−0.338	0.046	1	< 0.001
		Area	1.078	0.127	1	< 0.001
		Period:Area	0.270	0.041	1	< 0.001
	Moray East	*Intercept*	0.786	0.069	1	< 0.001
		Period	−0.205	0.046	1	< 0.001
		Area	1.085	0.132	1	< 0.001
		Period:Area	0.039	0.040	1	0.331
Small temporal scale	2D seismic survey	*Intercept*	0.502	0.163	1	0.002
		Period	0.478	0.170	1	0.005
		Area	1.147	0.350	1	0.001
		Period:Area	−0.186	0.298	1	< 0.001
	Beatrice	*Intercept*	0.274	0.093	1	0.003
		Period	0.286	0.089	1	0.001
		Area	1.428	0.141	1	< 0.001
		Period:Area	−0.174	0.077	1	0.023
	Moray East	*Intercept*	0.385	0.121	1	< 0.001
		Period	0.327	0.086	1	< 0.001
		Area	1.209	0.208	1	< 0.001
		Period:Area	−0.162	0.074	1	0.028
Fine spatial scale	Moray East	*Intercept*	0.471	0.397	1	0.235
		Period	0.245	0.082	1	0.003
		Area	−2.211	0.603	1	< 0.001
		Period:Area	0.153	0.980	1	0.121

Outer arrays compared to non-piling days (GLMM: $X^2 = 8.932$, df = 1, $p = 0.003$; **Figure 6**). Dolphin detections were significantly higher at the *Impact Inner* array than at the *Impact Outer* array (GLMM: $X^2 = 14.659$, df = 1, $p < 0.001$). The interaction between array and period was not significant (GLMM: $X^2 = 2.406$, df = 1, $p > 0.05$; **Table 3**).

DISCUSSION

The analysis of 10 years of PAM data highlighted that dolphins used Moray Firth inshore areas regularly, albeit the extent of use varied from year to year without any consistent relationship to the impulsive noise generated by offshore activities. Nevertheless, at a fine temporal scale within offshore activity years, there was a significant change in dolphin occurrence depending upon the presence or absence of impulsive noise on different days.

The results of this study suggest that the impulsive noise generated by offshore activities did not cause any dolphin displacement from the southern coast of the Moray Firth. The southern coast is the closest area to the offshore activities within this bottlenose dolphin population's range (Arso Civil et al., 2019): the seismic survey took place 20–30 km away, and piling at Beatrice 50–70 km and Moray East 40–70 km, from the southern coast. Predicted maximum received noise levels were 139 dB and 128 dB re 1 $\mu Pa^2 s$ during the seismic survey and during piling at Beatrice wind farm, respectively (unweighted single pulse SEL; Thompson et al., 2013; Graham et al., 2019) and 141 dB re $\mu Pa^2 s$ in the worst-case scenario for Moray East wind farm (MORL, 2016). Our analyses showed that dolphins continued using the southern coast of the Moray Firth during the seismic survey and impact pile-driving. These results are in line with recent studies that found that displacement of marine mammals from impulsive noise sources only occurs at shorter distances. For instance, displacement of harbor porpoises and baleen whales, which are more sensitive to noise (Southall et al., 2019b), has been reported up to 20 km away from impulsive noise sources (Dähne et al., 2013; Dunlop et al., 2018; Graham et al., 2019; Southall et al., 2019a; Sarnocińska et al., 2020). There are no similar studies for bottlenose dolphins but, since they are less sensitive than baleen whales and harbor porpoises to noise, shorter ranges of displacement would be expected.

Contrary to expectations, the BACI analysis at the smaller temporal scale, showed an increase in dolphin detections on the southern Moray Firth coast on days with impulsive noise. Furthermore, this increase was consistent between all three offshore projects. The short-term increase in dolphin detections observed only at the smallest temporal scale is in line with

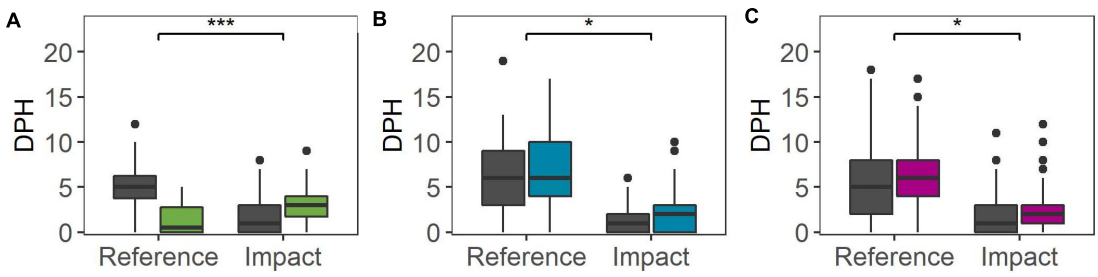

FIGURE 5 | Dolphin Detection Positive Hours (DPH) in the inner Moray Firth (*Reference Area*) and the southern Moray Firth (*Impact Area*) during the *Baseline period* (dark gray) and the *Activity period* (colored) on the small temporal scale: **(A)** 2D seismic survey, **(B)** Beatrice wind farm construction and **(C)** Moray East wind farm construction. Significance of the interaction between period and area is indicated above the bar at the top: ***$P < 0.001$; *$P < 0.05$.

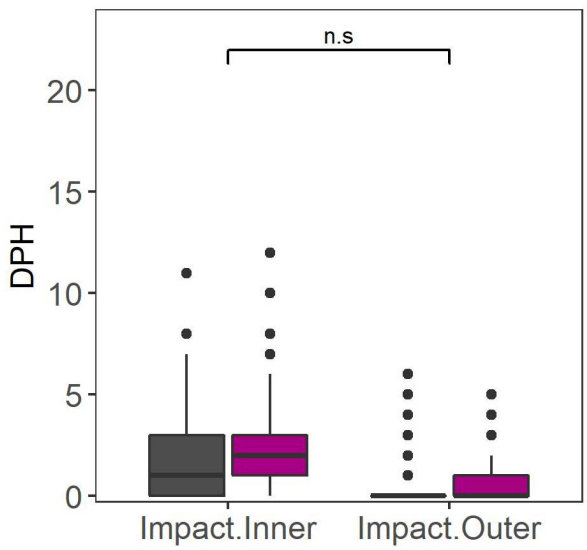

FIGURE 6 | Dolphin DPH for the *Impact Inner* and *Impact Outer* CPOD arrays in the *Impact Area* during the construction of Moray East wind farm (2019): non-piling days (dark gray) and piling-days (magenta). Significance of the interaction between period and array is indicated above the bar at the top: n.s. $P > 0.05$.

previous studies that found that behavioral alterations due to noise exposure last less than a day (Thompson et al., 2013; Van Beest et al., 2018). Our findings are consistent with those of Bailey et al. (2010b) who, based on criteria in Southall et al. (2007) suggested that dolphins in this study area might exhibit modifications in behavior at around 50 km away from a piling vessel. Acute noises can modify marine mammal group size and group behavior (Visser et al., 2016; Curé et al., 2021), which in turn can cause changes in vocalizations (Henderson et al., 2012). Therefore, one possible explanation for the observed increase in dolphin detections is that noise modified bottlenose dolphin group sizes or group behavior. Although whistle vocalization rates have been linked to group sizes (Quick and Janik, 2008), echolocation click rates cannot be directly linked to the size of bottlenose dolphin groups (Nuuttila et al., 2013). Since our study was based on echolocation data loggers, we cannot test whether the increase in noise levels modified dolphin group sizes. Moreover, since CPOD detections and the number of individuals are not directly linked (Nuuttila et al., 2013), it does not follow that the increase in detections observed here is indicative of changes in group size. Changes in marine mammal vocalizations due to distant (>20 km) anthropogenic noise sources have been observed previously (Risch et al., 2012; Blackwell et al., 2013; Shannon et al., 2016). Therefore, another explanation of the increase in detections is that dolphins might have changed their vocalization rate (Blackwell et al., 2015) or the amplitude of their calls (Holt et al., 2009; Parks et al., 2011) in response to the impulsive noise generated by the offshore activities. In an experiment with captive bottlenose dolphins, the playback of pile driving noise resulted in an increase in the number of clicks produced by these animals (Branstetter et al., 2018). Caution is required when extrapolating information from trained to wild animals, but an increase in the click rate could explain the observed increase in detections by our CPODs during the impulsive noise events. Results obtained from the fine scale spatial analysis during the construction of Moray East wind farm also support this hypothesis. No displacement from the outer toward the inner array was observed during piling days, while a subtle but consistent increase in dolphin detections was observed on both arrays. Research is needed to further investigate potential changes in the acoustic characteristics of bottlenose dolphin clicks during far-field impulsive noise events. Passive acoustic devices that collect information on marine mammal click characteristics could be deployed during future offshore developments to explore in more detail whether these activities can be linked to differences in dolphin click rates or click amplitude.

At the medium temporal scale, comparing dolphin occurrence to baseline years, the results were not consistent between offshore activities. During the seismic survey, an increase in dolphin detections was observed on the southern coast. During the construction of Beatrice wind farm, a decrease was detected in the same area and during the construction of Moray East wind farm, no significant difference was detected. In line with previous studies, dolphin detections overall were higher in the *Reference Area* of the inner Moray Firth, compared with the *Impact Inner* area on the southern coast, but the extent of use varied between years and through the season (Thompson et al., 2015; Fernandez-Betelu et al., 2019). The difference in detections at the medium temporal scale therefore seems likely to be related to the natural inter-annual variation in occurrence that was also reflected in our analyses here (**Figure 2**). Although potentially modified by anthropogenic factors, bottlenose dolphin occurrence is largely influenced by a range of natural drivers, such as prey abundance and oceanographic processes (Heithaus and Dill, 2002; Benjamins et al., 2015). Our results suggest that the effect of far-field noise is less important than these other natural drivers in affecting the occurrence of dolphins in this study area.

We used a BACI design to investigate the effect of impulsive noise on the coastal occurrence of dolphins. This methodology is based on the comparison of data from two similar areas (Impact and Control) in situations where only one of them is affected by a disturbance. However, finding control sites with similar ecological characteristics to impact sites, while being distant enough to be unaffected by the disturbance, is not always feasible (Underwood, 1992, 1994). The sites defined here as reference sites were chosen because they were located at greater distances from the developments but were still within the bottlenose dolphin population's range. However, a complete lack of disturbance cannot be assured there, hence the term *Reference* instead of *Control Area*. For instance, during the construction of Moray East wind farm an increase in detections was observed at both *Reference* and *Impact Areas* during piling days, potentially indicating that noise levels might also have affected dolphins at reference sites. Nevertheless, these 10 years of passive acoustic

monitoring data provided a robust dataset to investigate the effects of three offshore projects, while overcoming some of the limitations of the BACI design. The consistent results at the smallest temporal scale strengthened our hypothesis that a change in vocal behavior may have caused the observed increase in dolphin detections. While the contrasting results at the medium temporal scale from multiple offshore activities prevented us from suggesting misleading effects that might have been inferred from work conducted only during a single project. Overall, our analyses showed that long-term datasets such as this provide opportunities to detect relatively subtle differences in bottlenose dolphin behavior linked to the far-field impulsive noise generated by offshore activities.

Management Implications

Limited data on localized cetacean populations can constrain environmental assessments for new developments, particularly where these occur in or near protected areas. In the Moray Firth, concerns over the potential impacts of offshore developments on the protected population of bottlenose dolphins required additional research and survey effort in the area to inform licensing decisions.

The findings of this study support the Appropriate Assessments' conclusions that these offshore activities would not have a major impact on the bottlenose dolphin population using the SAC (Berr, 2007; MS-LOT, 2014; MS-LOT and Marine Scotland Science, 2014). Our results also concur with recent photo-ID studies of this dolphin population that showed increasing trends in both population size (Cheney et al., 2014) and vital rates (Cheney et al., 2019), supporting the lack of any large-scale impacts on the population. Our analysis showed that dolphins continued using the area of their range where the impact was expected to be highest when these projects took place. The monitoring of the far-field responses of dolphins provided evidence of potential short-term changes in vocalizations as reported for other marine mammal species (Gomez et al., 2016). Developers are required to perform marine mammal monitoring for several years to create a sufficient baseline and assess potential impacts (Diederichs et al., 2008). However, in places with high inter-annual variability in the presence of marine mammals, analyses using data from other years as a baseline may produce misleading results.

Marine mammal protection policies are focused on minimizing the near-field acute effects of impulsive noise (Bröker et al., 2015; Verfuss et al., 2016). While the risk of death or injury is limited to the first hundreds of meters from the sound source (Southall et al., 2019b), behavioral responses, such as changes in vocalizations, can occur at greater distances (hundreds of km) potentially affecting a greater number of animals (Risch et al., 2012). Here, we suggested that distant impulsive noise sources may have caused modifications of bottlenose dolphin vocalizations. Further research is now required to test this hypothesis and describe the extent of any change in more detail, given that moderate modifications of vocal behavior have the potential to affect foraging and individual vital rates (Southall et al., 2007). The challenge in future research will be linking modifications of vocal behavior to changes in energetic costs (Booth, 2020; Pirotta et al., 2021) and, ultimately, population level consequences (Pirotta et al., 2015a; Reed et al., 2020).

DATA AVAILABILITY STATEMENT

All data are available from the Dryad Digital Repository. All datasets and R code used for the analyses are available at: https://doi.org/10.5061/dryad.6hdr7sr17.

ETHICS STATEMENT

Ethical review and approval was not required for the animal study because this was a non-invasive, acoustic observational study of bottlenose dolphin responses to offshore seismic surveys and pile-driving. The authors had no control or influence over the duration or scheduling of offshore activities. No animals were captured or tagged during this study and no research or animal ethical assessments were required. Bottlenose dolphin responses to impulsive noise were determined using remote passive acoustic devices on seabed moorings licensed for scientific use by Marine Scotland, and consented by the Crown Estate. Moorings were deployed and recovered using vessels with appropriate certification, accreditation and endorsements.

AUTHOR CONTRIBUTIONS

OFB, IG, and PT designed the study based on data collection that had been led by IG, KB, and PT. TB managed data collection. IG and BC processed the raw data. All analyses were designed and conducted by OFB and supervised by IG. OFB led the writing of the manuscript. All authors reviewed and contributed critically to the drafts.

FUNDING

Financial support for this study was provided through a series of consortia funded projects that involved the UK Department of Energy and Climate Change (DECC), Scottish Government, Oil and Gas UK Ltd., COWRIE, NatureScot, The Crown Estate, Highlands and Islands Enterprise, Beatrice Offshore Wind Ltd., and Moray Offshore Wind Farm (East) Ltd. OFB was funded by the Fundación "la Caixa" (Becas Posgrado, 2015) and their support was greatly appreciated. The authors declare that this study received funding from three commercial developers: Oil and Gas UK Ltd., Beatrice Offshore Wind Ltd., and Moray Offshore Wind Farm (East) Ltd. However, these funding bodies had no input into the study design, data collection, analysis, interpretation of data, the writing of this article or the decision to submit it for publication.

ACKNOWLEDGMENTS

We would like to thank Bill Ruck, Moray First Marine and colleagues from the University of Aberdeen for assistance with the data collection. We are also grateful to Drs. Nathan Merchant and Adrian Farcas (CEFAS) for the provision of the data on the noise modeling and their valuable comments during the development of this work. The project benefited at all stages from input provided by the scientific steering groups and stakeholder groups established by UK and Scottish Governments to support the work conducted around these regional oil and gas and renewables projects.

SUPPLEMENTARY MATERIAL

The Supplementary Material for this article can be found online at: https://www.frontiersin.org/articles/10.3389/fmars.2021.664230/full#supplementary-material

REFERENCES

Arso Civil, M., Quick, N. J., Cheney, B., Pirotta, E., Thompson, P. M., and Hammond, P. S. (2019). Changing distribution of the east coast of Scotland bottlenose dolphin population and the challenges of area-based management. *Aquat. Conserv.* 29, 178–196. doi: 10.1002/aqc.3102

Bailey, H., Clay, G., Coates, E. A., Lusseau, D., Senior, B., and Thompson, P. M. (2010a). Using T-PODs to assess variations in the occurrence of coastal bottlenose dolphins and harbour porpoises. *Aquat. Conserv.* 20, 150–158. doi: 10.1002/aqc

Bailey, H., Senior, B., Simmons, D., Rusin, J., Picken, G., and Thompson, P. M. (2010b). Assessing underwater noise levels during pile-driving at an offshore windfarm and its potential effects on marine mammals. *Mar. Pollut. Bull.* 60, 888–897. doi: 10.1016/j.marpolbul.2010.01.003

Benjamins, S., Dale, A., Hastie, G., Waggitt, J., Lea, M.-A., Scott, B., et al. (2015). "Confusion reigns? A review of marine megafauna interactions with tidal-stream environments," in *Oceanography and Marine Biology: An Annual Review*, eds R. N. Hughes, D. J. Hughes, I. P. Smith, and A. C. Dale (Boca Raton, FL: CRC Press), 1–54. doi: 10.1201/b18733-2

Berr (2007). *Appropriate Assessment With Regard to 24th Offshore Oil and Gas Licensing Round (Inner Moray Firth)*. London: Berr.

Blackwell, S. B., Nations, C. S., McDonald, T. L., Greene, C. R., Thode, A. M., Guerra, M., et al. (2013). Effects of airgun sounds on bowhead whale calling rates in the Alaskan Beaufort Sea. *Mar. Mamm. Sci.* 29, E342–E365. doi: 10.1111/mms.12001

Blackwell, S. B., Nations, C. S., McDonald, T. L., Thode, A. M., Mathias, D., Kim, K. H., et al. (2015). Effects of airgun sounds on Bowhead whale calling rates: evidence for two behavioral thresholds. *PLoS One* 10:e0125720. doi: 10.1371/journal.pone.0125720

Bolker, B. M., Brooks, M. E., Clark, C. J., Geange, S. W., Poulsen, J. R., Stevens, M. H. H., et al. (2009). Generalized linear mixed models: a practical guide for ecology and evolution. *Trends Ecol. Evol.* 24, 127–135. doi: 10.1016/j.tree.2008.10.008

Booth, C. G. (2020). Food for thought: harbor porpoise foraging behavior and diet inform vulnerability to disturbance. *Mar. Mamm. Sci.* 36, 195–208. doi: 10.1111/mms.12632

Brandt, M., Dragon, A., Diederichs, A., Bellmann, M., Wahl, V., Piper, W., et al. (2018). Disturbance of harbour porpoises during construction of the first seven offshore wind farms in Germany. *Mar. Ecol. Prog. Ser.* 596, 213–232. doi: 10.3354/meps12560

Branstetter, B. K., Bowman, V. F., Houser, D. S., Tormey, M., Banks, P., Finneran, J. J., et al. (2018). Effects of vibratory pile driver noise on echolocation and vigilance in bottlenose dolphins (*Tursiops truncatus*). *J. Acoust. Soc. Am.* 143:429. doi: 10.1121/1.5021555

Bröker, K., Gailey, G., Muir, J., and Racca, R. (2015). Monitoring and impact mitigation during a 4D seismic survey near a population of gray whales off Sakhalin Island, Russia. *Endanger. Species Res.* 28, 187–208. doi: 10.3354/esr00670

Brookes, K. L., Bailey, H., and Thompson, P. M. (2013). Predictions from harbor porpoise habitat association models are confirmed by long-term passive acoustic monitoring. *J. Acoust. Soc. Am.* 134, 2523–2533. doi: 10.1121/1.4816577

Cheney, B., Corkrey, R., Durban, J. W., Grellier, K., Hammond, P. S., Islas-Villanueva, V., et al. (2014). Long-term trends in the use of a protected area by small cetaceans in relation to changes in population status. *Glob. Ecol. Conserv.* 2, 118–128. doi: 10.1016/j.gecco.2014.08.010

Cheney, B. J., Thompson, P. M., and Cordes, L. S. (2019). Increasing trends in fecundity and calf survival of bottlenose dolphins in a marine protected area. *Sci. Rep.* 9:1767. doi: 10.1038/s41598-018-38278-9

Cheney, B., Thompson, P. M., Ingram, S. N., Hammond, P. S., Stevick, P. T., Durban, J. W., et al. (2013). Integrating multiple data sources to assess the distribution and abundance of bottlenose dolphins *Tursiops truncatus* in Scottish waters. *Mamm. Rev.* 43, 71–88. doi: 10.1111/j.1365-2907.2011.00208.x

Culloch, R. M., and Robinson, K. P. (2008). Bottlenose dolphins using coastal regions adjacent to a special area of conservation in north-east Scotland. *J. Mar. Biol. Assoc. U. K.* 88, 1237–1243. doi: 10.1017/s0025315408000210

Curé, C., Isojunno, S., Siemensma, M. L., Wensveen, P. J., Buisson, C., Sivle, L. D., et al. (2021). Severity scoring of behavioral responses of sperm whales (*Physeter macrocephalus*) to novel continuous versus conventional pulsed active sonar. *J. Mar. Sci. Eng.* 9:444. doi: 10.3390/jmse9040444

Dähne, M., Gilles, A., Lucke, K., Peschko, V., Adler, S., Krügel, K., et al. (2013). Effects of pile-driving on harbour porpoises (*Phocoena phocoena*) at the first offshore wind farm in Germany. *Environ. Res. Lett.* 8:025002. doi: 10.1088/1748-9326/8/2/025002

David, J. A. (2006). Likely sensitivity of bottlenose dolphins to pile-driving noise. *Water Environ. J.* 20, 48–54. doi: 10.1111/j.1747-6593.2005.00023.x

Diederichs, A., Nehls, G., Dähne, M., Adler, S., Koschinski, S., and Verfuß, U. (2008). *Methodologies for Measuring and Assessing Potential Changes in Marine Mammal Behaviour, Abundance or Distribution Arising from the Construction, Operation and Decommissioning of Offshore Windfarms*. Husum: BioConsult SH Report to COWRIE Ltd.

Dunlop, R. A., Noad, M. J., McCauley, R. D., Kniest, E., Slade, R., Paton, D., et al. (2018). A behavioural dose-response model for migrating humpback whales and seismic air gun noise. *Mar. Pollut. Bull.* 133, 506–516. doi: 10.1016/j.marpolbul.2018.06.009

Eleftheriou, A., Basford, D., and Moore, D. C. (2004). *Report for the Department of Trade and Industry – Synthesis of Information on the Benthos of Area SEA 5*. Aberdeen.

Erbe, C., Dunlop, R., and Dolman, S. (2018). "Effects of noise on marine mammals," in *Effects of Anthropogenic Noise on Animals*, eds H. Slabbekoorn, R. J. Dooling, A. N. Popper, and R. R. Fay (New York, NY: Springer), 277–309.

Fernandez-Betelu, O., Graham, I. M., Cornulier, T., and Thompson, P. M. (2019). Fine scale spatial variability in the influence of environmental cycles on the occurrence of dolphins at coastal sites. *Sci. Rep.* 9:2548. doi: 10.1038/s41598-019-38900-4

Finneran, J. J., Schlundt, C. E., Branstetter, B. K., Trickey, J. S., Bowman, V., and Jenkins, K. (2015). Effects of multiple impulses from a seismic air gun on bottlenose dolphin hearing and behavior. *J. Acoust. Soc. Am.* 137, 1634–1646. doi: 10.1121/1.4916591

Frisk, G. V. (2012). Noiseonomics: the relationship between ambient noise levels in the sea and global economic trends. *Sci. Rep.* 2:437. doi: 10.1038/srep00437

Gomez, C., Lawson, J. W., Wright, A. J., Buren, A. D., Tollit, D., and Lesage, V. (2016). A systematic review on the behavioural responses of wild marine mammals to noise: the disparity between science and policy. *Can. J. Zool.* 94, 801–819. doi: 10.1139/cjz-2016-0098

Gordon, J. C. D., Gillespie, D., Potter, J., Frantzis, A., Simmonds, M. P., Swift, R., et al. (2003). A review of the effects of seismic survey on marine mammals. *Mar. Technol. Soc. J.* 37, 16–34. doi: 10.4031/002533203787536998

Graham, I. M., Merchant, N. D., Farcas, A., Barton, T. R., Cheney, B., Bono, S., et al. (2019). Harbour porpoise responses to pile-driving diminish over time. *R. Soc. Open Sci.* 6:190335. doi: 10.1098/rsos.190335

Graham, I. M., Pirotta, E., Merchant, N. D., Farcas, A., Barton, T. R., Cheney, B., et al. (2017). Responses of bottlenose dolphins and harbour porpoises to variations in piling noise during harbour construction. *Ecosphere* 8, 1–16.

Hastie, G., Merchant, N. D., Götz, T., Russell, D. J. F., Thompson, P., and Janik, V. M. (2019). Effects of impulsive noise on marine mammals: investigating range-dependent risk. *Ecol. Appl.* 29:e01906. doi: 10.1002/eap.1906

Heithaus, M. R., and Dill, L. M. (2002). Food availability and tiger shark predation risk influence bottlenose dolphin habitat use. *Ecology* 83, 480–491. doi: 10.1890/0012-9658(2002)083[0480:faatsp]2.0.co;2

Henderson, E. E., Hildebrand, J. A., Smith, M. H., and Falcone, E. A. (2012). The behavioral context of common dolphin (*Delphinus* sp.) vocalizations. *Mar. Mamm. Sci.* 28, 439–460. doi: 10.1111/j.1748-7692.2011.00498.x

Holt, M. M., Noren, D. P., Veirs, V., Emmons, C. K., and Veirs, S. (2009). Speaking up: killer whales (*Orcinus orca*) increase their call amplitude in response to vessel noise. *J. Acoust. Soc. Am.* 125, EL27–EL32. doi: 10.1121/1.3040028

Madsen, P. T., Wahlberg, M., Tougaard, J., Lucke, K., and Tyack, P. (2006). Wind turbine underwater noise and marine mammals: implications of current knowledge and data needs. *Mar. Ecol. Prog. Ser.* 309, 279–295. doi: 10.3354/meps309279

Merchant, N. D. (2019). Underwater noise abatement: economic factors and policy options. *Environ. Sci. Policy* 92, 116–123. doi: 10.1016/j.envsci.2018.11.014

MORL (2016). *Telford, Stevenson and MacColl Offshore Wind Farms – Piling Strategy*. Outer Moray Firth: MORL.

MS-LOT, and Marine Scotland Science (2014). *Appropriate Assessment for the Construction and Operation of the Beatrice Offshore Windfarm in the Outer Moray Firth*. Aberdeen.

MS-LOT (2014). Appropriate Assessment for the Construction and Operation of Three Offshore Generating Stations – The Telford, Stevenson and Maccoll Offshore Wind Farms In The Outher Moray Firth. Aberdeen: MS-LOT.

Nuuttila, H. K., Thomas, L., Hiddink, J. G., Meier, R., Turner, J. R., Bennell, J. D., et al. (2013). Acoustic detection probability of bottlenose dolphins, *Tursiops truncatus*, with static acoustic dataloggers in Cardigan Bay, Wales. *J. Acoust. Soc. Am.* 134, 2596–2609. doi: 10.1121/1.4816586

OSPAR (2017). *Distribution of Reported Impulsive Sounds* [Online]. Available online at: https://oap.ospar.org/en/ospar-assessments/intermediate-assessment-2017/pressures-human-activities/distribution-reported-impulsive-sounds-sea/ (accessed August 17, 2020).

Parks, S. E., Johnson, M., Nowacek, D., and Tyack, P. L. (2011). Individual right whales call louder in increased environmental noise. *Biol. Lett.* 7, 33–35. doi: 10.1098/rsbl.2010.0451

Pirotta, E., Booth, C. G., Cade, D. E., Calambokidis, J., Costa, D. P., Fahlbusch, J. A., et al. (2021). Context-dependent variability in the predicted daily energetic costs of disturbance for blue whales. *Conserv. Physiol.* 9:coaa137. doi: 10.1093/conphys/coaa137

Pirotta, E., Booth, C. G., Costa, D. P., Fleishman, E., Kraus, S. D., Lusseau, D., et al. (2018). Understanding the population consequences of disturbance. *Ecol. Evol.* 8, 9934–9946. doi: 10.1002/ece3.4458

Pirotta, E., Harwood, J., Thompson, P. M., New, L., Cheney, B., Arso, M., et al. (2015a). Predicting the effects of human developments on individual dolphins to understand potential long-term population consequences. *Proc. R. Soc. B* 282:20152109. doi: 10.1098/rspb.2015.2109

Pirotta, E., Thompson, P. M., Cheney, B., Donovan, C. R., and Lusseau, D. (2015b). Estimating spatial, temporal and individual variability in dolphin cumulative exposure to boat traffic using spatially explicit capture-recapture methods. *Anim. Conserv.* 18, 20–31. doi: 10.1111/acv.12132

Quick, N. J., and Janik, V. M. (2008). Whistle rates of wild bottlenose dolphins (*Tursiops truncatus*): influences of group size and behavior. *J. Comp. Psychol.* 122:305. doi: 10.1037/0735-7036.122.3.305

R Core Team (2018). *R: A Language and Environment for Statistical Computing*. Viena: R Core Team.

Reed, J., Harcourt, R., New, L., and Bilgmann, K. (2020). Extreme effects of extreme disturbances: a simulation approach to assess population specific responses. *Front. Mar. Sci.* 7:519845. doi: 10.3389/fmars.2020.519845

Reeve, L. L. N. (2019). "Transboundary pollution in the new legally binding instrument under the U.N. convention on the law of the sea: the case for anthropogenic underwater noise," in *Proceedings of the Oceans 2019 MTS/IEEE Seattle* (Piscataway, NJ: IEEE).

Risch, D., Corkeron, P. J., Ellison, W. T., and Van Parijs, S. M. (2012). Changes in humpback whale song occurrence in response to an acoustic source 200 km away. *PLoS One* 7:e29741. doi: 10.1371/journal.pone.0029741

Risch, D., Wilson, S. C., Hoogerwerf, M., van Geel, N. C. F., Edwards, E. W. J., and Brookes, K. L. (2019). Seasonal and diel acoustic presence of North Atlantic minke whales in the North Sea. *Sci. Rep.* 9:3571. doi: 10.1038/s41598-019-39752-8

Robinson, K. P., Bamford, C. C. G., Airey, A., Bean, T. S., Bird, C., Haskins, G. N., et al. (2017). Killer whale (*Orcinus orca*) occurrence in the Moray Firth, Northeast Scotland: incidental sightings, behavioural observations, and photo-identification. *Aquat. Mamm.* 43, 26–32. doi: 10.1578/AM.43.1.2017.26

Russell, D. J., Hastie, G. D., Thompson, D., Janik, V. M., Hammond, P. S., Scott-Hayward, L. A., et al. (2016). Avoidance of wind farms by harbour seals is limited to pile driving activities. *J. Appl. Ecol.* 53, 1642–1652. doi: 10.1111/1365-2664.12678

Sarnocińska, J., Teilmann, J., Balle, J. D., van Beest, F. M., Delefosse, M., and Tougaard, J. (2020). Harbor porpoise (*Phocoena phocoena*) reaction to a 3D seismic airgun survey in the North Sea. *Front. Mar. Sci.* 6:824. doi: 10.3389/fmars.2019.00824

Shannon, G., McKenna, M. F., Angeloni, L. M., Crooks, K. R., Fristrup, K. M., Brown, E., et al. (2016). A synthesis of two decades of research documenting the effects of noise on wildlife. *Biol. Rev.* 91, 982–1005. doi: 10.1111/brv.12207

Smith, E. P. (2002). "BACI design," in *Encyclopedia of Environmetrics*, eds A. H. El-Shaarawi and W. W. Piegorsch (Chichester: John Wiley & Sons Ltd), 141–148.

Southall, B. L., Bowles, A. E., Ellison, W. T., Finneran, J. J., Gentry, R. L., Greene, C. R. Jr., et al. (2007). Marine mammal noise exposure criteria. *Aquat. Mamm.* 33:411.

Southall, B. L., Deruiter, S. L., Friedlaender, A., Stimpert, A. K., Goldbogen, J. A., Hazen, E., et al. (2019a). Behavioral responses of individual blue whales (*Balaenoptera musculus*) to mid-frequency military sonar. *J. Exp. Biol.* 222:jeb190637. doi: 10.1242/jeb.190637

Southall, B. L., Finneran, J. J., Reichmuth, C., Nachtigall, P. E., Ketten, D. R., Bowles, A. E., et al. (2019b). Marine mammal noise exposure criteria: updated scientific recommendations for residual hearing effects. *Aquat. Mamm.* 45, 125–232. doi: 10.1578/am.45.2.2019.125

Tasker, M. L., Amundin, M., Andre, M., Hawkins, A., Lang, W., Merck, T., et al. (2010). *Marine Strategy Framework Directive Task Group 11 Report Underwater Noise and Other Forms of Energy*. Copenhagen: ICES.

Thompson, P. M., Brookes, K. L., and Cordes, L. S. (2015). Integrating passive acoustic and visual data to model spatial patterns of occurrence in coastal dolphins. *ICES J. Mar. Sci.* 72, 651–660. doi: 10.1093/icesjms/fsu110

Thompson, P. M., Brookes, K. L., Graham, I. M., Barton, T. R., Needham, K., Bradbury, G., et al. (2013). Short-term disturbance by a commercial two-dimensional seismic survey does not lead to long-term displacement of harbour porpoises. *Proc. R. Soc. B* 280:20132001. doi: 10.1098/rspb.2013.2001

Thompson, P. M., Lusseau, D., Barton, T., Simmons, D., Rusin, J., and Bailey, H. (2010). Assessing the responses of coastal cetaceans to the construction of offshore wind turbines. *Mar. Pollut. Bull.* 60, 1200–1208. doi: 10.1016/j.marpolbul.2010.03.030

Thomsen, F., McCully, S. R., Weiss, L. R., Wood, D. T., Warr, K. J., Barry, J., et al. (2011). Cetacean stock assessments in relation to exploration and production industry activity and other human pressures: review and data needs. *Aquat. Mamm.* 37, 1–93. doi: 10.1578/am.37.1.2011.1

Underwood, A. J. (1992). Beyond BACI: the detection of environmental impacts on populations in the real, but variable, world. *J. Exp. Mar. Biol. Ecol.* 161, 145–178. doi: 10.1016/0022-0981(92)90094-q

Underwood, A. J. (1994). On beyond BACI: sampling designs that might reliably detect environmental disturbances. *Ecol. Appl.* 4, 3–15. doi: 10.2307/1942110

Van Beest, F. M., Teilmann, J., Hermannsen, L., Galatius, A., Mikkelsen, L., Sveegaard, S., et al. (2018). Fine-scale movement responses of free-ranging harbour porpoises to capture, tagging and short-term noise pulses from a single airgun. *R. Soc. Open Sci.* 5:170110. doi: 10.1098/rsos.170110

Van der Graaf, A. J., Ainslie, M. A., André, M., Brensing, K., Dalen, J., Dekeling, R. P. A., et al. (2012). *European Marine Strategy Framework Directive-Good Environmental Status (MSFD GES): Report of the Technical Subgroup on Underwater Noise and Other Forms of Energy*. Brussels: European Union.

Verfuss, U. K., Sparling, C. E., Arnot, C., Judd, A., and Coyle, M. (2016). "Review of offshore wind farm impact monitoring and mitigation with regard to marine mammals," in *The Effects of Noise on Aquatic Life II*, eds A. N. Popper and A. Hawkins (New York, NY: Springer), 1175–1182. doi: 10.1007/978-1-4939-2981-8_147

Visser, F., Curé, C., Kvadsheim, P. H., Lam, F.-P. A., Tyack, P. L., and Miller, P. J. O. (2016). Disturbance-specific social responses in long-finned pilot whales, *Globicephala melas*. *Sci. Rep.* 6:28641. doi: 10.1038/srep28641

Williamson, L., Brookes, K. L., Scott, B. E., Graham, I. M., Bradbury, G., Hammond, P. S., et al. (2016). Echolocation detections and digital video surveys provide reliable estimates of the relative density of harbour porpoises. *Methods Ecol. Evol.* 7, 762–769. doi: 10.1111/2041-210X.12538

Conflict of Interest: The authors declare that the research was conducted in the absence of any commercial or financial relationships that could be construed as a potential conflict of interest.

Copyright © 2021 Fernandez-Betelu, Graham, Brookes, Cheney, Barton and Thompson. This is an open-access article distributed under the terms of the Creative Commons Attribution License (CC BY). The use, distribution or reproduction in other forums is permitted, provided the original author(s) and the copyright owner(s) are credited and that the original publication in this journal is cited, in accordance with accepted academic practice. No use, distribution or reproduction is permitted which does not comply with these terms.

frontiers in Marine Science

ORIGINAL RESEARCH
published: 26 July 2021
doi: 10.3389/fmars.2021.673565

Slower Ship Speed in the Bahamas Due to COVID-19 Produces a Dramatic Reduction in Ocean Sound Levels

Charlotte Dunn[1,2], James Theriault[3], Leigh Hickmott[2,4] and Diane Claridge[1,2]*

[1] Bahamas Marine Mammal Research Organisation, Abaco, Bahamas, [2] Sea Mammal Research Unit, Scottish Oceans Institute, University of St Andrews, St Andrews, United Kingdom, [3] Ocean Environmental Consulting, Halifax, NS, Canada, [4] Open Ocean Consulting, Petersfield, United Kingdom

As underwater noise from ship traffic increases, profound effects on the marine environment highlight the need for improved mitigation measures. One measure, reduction in ship speed, has been shown to be one of the key drivers in reducing sound source levels of vessels. In 2017, a study began to assess the impacts of increasing commercial shipping traffic on sperm whales in Northwest Providence Channel, northern Bahamas, an international trade route that primarily serves the southeast US. Ship data were collected from an Automatic Identification System (AIS) station combined with recordings from an acoustic recorder to measure underwater sound levels and to detect the presence of sperm whales. Here we analyze a subset of these data to opportunistically investigate potential changes in ship traffic before and during the COVID-19 pandemic. These data span one calendar year from October 2019 to October 2020. A pre-COVID-19 dataset of 121 days, from a recorder approximately 2 km from the shipping route was compared to a 134-day dataset collected during COVID-19 from the same site, comprising 2900 and 3181 ten-minute recordings, respectively. A dramatic decrease in ocean noise levels concurrent with changes in shipping activity occurred during the pandemic. The mean pre-COVID-19 power density level in the 111–140 Hz 1/3-octave band was 88.81 dB re 1 μPa (range 81.38–100.90) and decreased to 84.27 dB re 1 μPa (range 78.60–99.51) during COVID-19, equating to a 41% reduction in sound pressure levels (SPL). After differences in seasonal changes in wind speed were accounted for, SPL decreased during the pandemic by 3.98 dB (37%). The most notable changes in ship activity were significantly reduced vessel speeds for all ship types and fewer ships using the area during the pandemic. Vessel speed was highly correlated to SPL and the only ship-based variable that predicted SPLs. Despite the opportunistic nature [i.e., not a standard before-after-control-impact (BACI) study], this study provides a unique opportunity to assess the effectiveness of ship traffic management strategies, such as slowing ships down, to mitigate impacts on marine life in the study area, including local sperm whale populations.

Keywords: COVID-19, noise, sperm whales, ecosystem health, ship speed, marine mammal, shipping, automatic identification system

OPEN ACCESS

Edited by:
Edward Urban,
Scientific Committee on Oceanic Research, United States

Reviewed by:
Sofie Van Parijs,
Northeast Fisheries Science Center (NOAA), United States
William Halliday,
Wildlife Conservation Society, Canada

****Correspondence:***
Charlotte Dunn
cdunn@bahamaswhales.org

Specialty section:
This article was submitted to Marine Ecosystem Ecology, a section of the journal Frontiers in Marine Science

Received: *27 February 2021*
Accepted: *07 June 2021*
Published: *26 July 2021*

Citation:
Dunn C, Theriault J, Hickmott L and Claridge D (2021) Slower Ship Speed in the Bahamas Due to COVID-19 Produces a Dramatic Reduction in Ocean Sound Levels. Front. Mar. Sci. 8:673565. doi: 10.3389/fmars.2021.673565

INTRODUCTION

Anthropogenic noise is increasing globally and impacting marine soundscapes (Andrew et al., 2002; Hildebrand, 2009; Erbe et al., 2014; Duarte et al., 2021). Maritime trade is reliant on shipping networks linking all major global economies and where seaborne routes exist, marine soundscapes are altered by vessel noise. This noise pollution is proving detrimental to the lives of a plethora of marine organisms, including commercial fish (Sarà et al., 2007; Stanley et al., 2017) and whale species (Clark et al., 2009; Putland et al., 2017; Cholewiak et al., 2018). The number of commercial vessels, their size and speed, all have upward trends (Frisk, 2012; McKenna et al., 2012), creating ever increasing issues of noise pollution and for large marine animals, greater threat associated with ship strike (Rockwood et al., 2020), highlighting the need for improved mitigation measures to limit impacts on marine life.

The combined use of Automatic Identification System (AIS) and passive acoustic monitoring have revealed evidence of the impact that high volume, fast moving, large vessels have on the marine environments and their occupants (Vanderlaan and Taggart, 2009; van der Hoop et al., 2012; Putland et al., 2017; Joy et al., 2019). Changes in vessel behavior such as reduced speed can decrease sound source levels and the cumulative impact they have on soundscapes (McKenna et al., 2013; Putland et al., 2017; MacGillivray et al., 2019). Additionally, the risk of injury or death of large marine animals due to ship strike can also be reduced by modifications to vessel behavior, such as speed and route alterations (Gende et al., 2011; Conn and Silber, 2013; Crum et al., 2019).

The islands of The Bahamas lie just off the southeastern seaboard of the United States. They span over 1,222 km and consist of 700 islands with a variety of habitats and rich biodiversity including submarine canyons and deep-water channels, the world's third largest coral-reef system, carbon-sink seagrass beds, diverse marine megafauna with over 24 different marine mammal species, along with four species of turtle and over 40 species of shark. Northwest Providence Channel (NPC), in the northern Bahamas is strategically located, facilitating access of Atlantic shipping and Caribbean cruise ship fleets to Florida's major seaports and cruise ship hubs (www.MiamiDade.Gov, 2019; Rodrigue and Wang, 2020). The NPC route bisects two shallow-water bank systems, the Great Bahama and Little Bahama Banks, both of which are crucial for commercial and game fisheries in The Bahamas, notably for spiny lobster (*Panulirus argus*) and bonefish (*Albula vulpes*) (Fedler, 2010; Adams and Murchie, 2015; Sherman et al., 2018), and home to resident dolphin populations (Herzing, 1997; Durban et al., 2000; Fearnbach et al., 2012). Moreover, at least two locations along the bank edge of NPC are historical spawning aggregation sites of the endangered Nassau grouper (*Epinephelus striatus*) that may be impacted by increasing ship noise as it overlaps in frequency with sounds produced by this species during reproductive behavior (Scharer et al., 2012). The deep (>1,000 m) waters of the NPC are also utilized by many marine mammal species, with particular philopatry shown by sperm whale (*Physeter macrocephalus*) clans (Claridge et al., 2015; Joyce et al., 2017). In 2017, the Bahamas Marine Mammal Research Organisation (BMMRO) began a passive acoustic monitoring study in NPC to track sperm whale movement through the area to understand the overlap between sperm whale habitat use and commercial shipping traffic. An AIS station was installed to track ships within the study area.

At the end of December 2019, the World Health Organization (WHO) became aware of a new disease, COVID-19, caused by a new coronavirus called SARS-CoV-2, originating in the People's Republic of China and by mid-March 2020 the WHO reported the outbreak a pandemic (World Health Organization [WHO], 2020; Poon and Peiris, 2020). Global movement of people and goods altered dramatically, decreasing and even eliminating some commercial vessel-based activities, such as the cruise ship industry (Gössling et al., 2021). In The Bahamas, the first COVID-19 case was reported on 15th March 2020, and the government enacted emergency orders on 19th March 2020 (Government of The Bahamas, 2020). It was anticipated that the combination of restrictions of movement within The Bahamas, the United States and the wider Atlantic region in response to the COVID-19 pandemic would generate a shift in vessel traffic behavior in Bahamian waters. Soundscapes can be altered by both anthropogenic (Duarte et al., 2021) and environmental factors (e.g., wind speed and wave height) (Thomson and Barclay, 2020). Here, we use acoustic and AIS data collected for the sperm whale study, and available environmental data to opportunistically investigate potential changes to shipping activity and the ocean soundscape in the NPC during the COVID-19 pandemic.

MATERIALS AND METHODS

Acoustic Data Collection and Analysis

A passive acoustic recorder, SoundTrap ST500 from Ocean Instruments, was deployed on the seafloor at the southeastern-most tip of Little Bahama Bank off southern Abaco Island, northern Bahamas (25.803445, −77.112943, depth = 28.65 m) to record underwater sound levels including noise from ship traffic and marine life in NPC (**Figure 1**). The hydrophone was intentionally placed at <30 m to allow for safe scuba deployment and retrieval, yet with proximity to heavy shipping traffic to investigate use of the area by sperm whales and, as a secondary question, to detect noise that might impact a Nassau grouper spawning aggregation site. The device sampled at a rate of 144 kHz on a duty cycle of 10 min, every 60 min. This schedule was selected based on the recording capacity of the recorders 256 GB internal memory and the speed at which sperm whales traverse this area.

The hydrophone recorder was deployed on 15th October 2019, but the dataset does not begin until 29th October, the date our AIS tower was operational following hurricane Dorian, a category 5 storm that hit The Bahamas on 1st September. The recorder was retrieved on 29th February 2020 to download the data, recharge the batteries, and redeploy as soon as possible. However, COVID-19 stay-at-home orders were issued by the Government of The Bahamas soon thereafter which prevented redeployment until 1st June 2020. Despite lack of a continuous acoustic record from the start of the pandemic, these data still

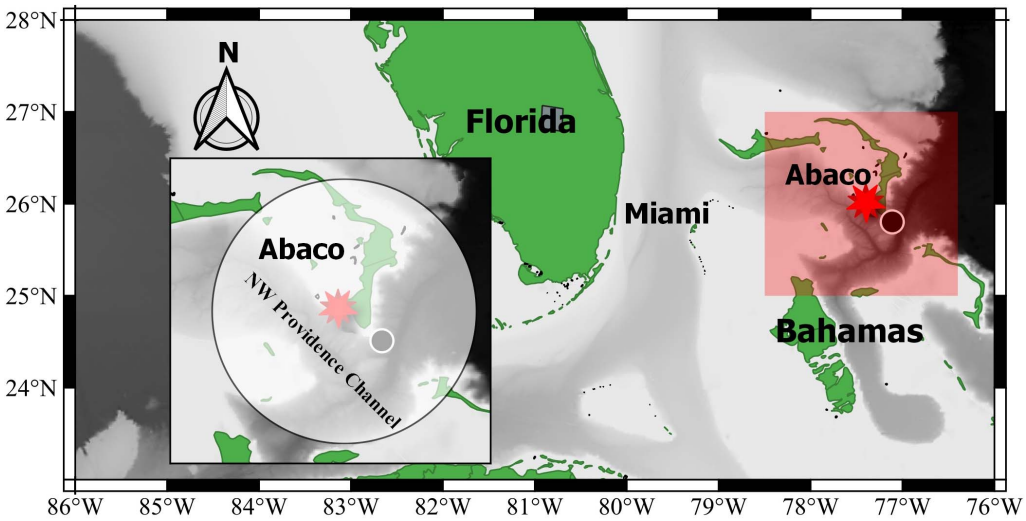

FIGURE 1 | A map of islands in the northern Bahamas, their proximity to the Florida panhandle and the study area, a circle indicating the average 93 km distance messages can be received at the Automatic Identification System (AIS) station, including locations of the AIS station ID 844 (red star) and ST500 hydrophone (black circle) off the southern end of Abaco Island. GEBCO (2020).

provide a unique opportunity to compare underwater sound levels in NPC pre-COVID-19 and during COVID-19.

To measure underwater sound levels, sound pressure level (SPL) measurements were made from the hydrophone recordings using the noise band monitor module in the open-source PAMGuard software version 2.01.05 BETA (Gillespie et al., 2009). Continuous underwater sound levels were measured in nine different standard 1/3-octave bands between 70 and 500 Hz in every 10 s period for each 10-min recording, as peak frequencies produced by commercial ships are typically over 100 Hz (Merchant et al., 2014). Sound levels in the nine different 1/3-octave bands were strongly correlated and therefore just one band was chosen that was representative of the environments sound levels, the 111–140 Hz 1/3-octave band. The binary files generated from PAMGuard were processed with Matlab_R2020b (Mathworks, Nantick, MA) to extract the sound levels as band energy (dB re 1 μPa), and a median sound level was calculated for each 10-min recording.

In situ environmental data at the recording site were not available so archived wind speed data was accessed at the National Data Buoy Center website (NOAA, National Data Buoy Center) for the weather buoy nearest the study site (station 41047 located at 27.5N, −71.5W), 590 km ENE from our hydrophone. Archived wind speeds (m/s) were averaged over an 8-min period by averaging "the simple scalar average of the wind speed observations[1]."

Marine Traffic Data

AIS data were collected using BMMRO's AIS station, ID 844 (26.0N, −77.4W; elevation 10 m). A MATLAB function was written to decode the AIS messages, and R scripts (R Core Team, 2020) were used to identify the unique number of vessels using the area, their speed, and their locations. The closest point of approach (CPA) of each unique vessel to the hydrophone was calculated using the great-circle-distance with the Vincenty (ellipsoid) method from the R package geosphere (version 1.5-10). Only messages which were complete and without error were considered in this analysis. The Marine Traffic website[2] provides information on ship type, size and tonnage (but not load) based on each vessel's Maritime Mobile Service Identity (MMSI) number. MMSI numbers transmitted by AIS to station 844 were matched to the Marine Traffic database to obtain vessel details. Two percent of the transmitted MMSI numbers did not have an associated entry in the Marine Traffic database, so these records were discarded for analyses that included ship type. AIS data without corresponding hydrophone recordings were also excluded (i.e., when the recorder was not deployed).

Study Area

Marine Traffic summary statistics for AIS station ID 844 showed that during the study period, the average reception distance from which a ship's message could be received was 93 km. The ST500 acoustic recorder was deployed 37 km from the AIS station, which provided confidence that the recorded acoustic data were representative of the ship traffic detected at the AIS station (**Figure 1**).

Statistical Analysis

To explore causation of changes in SPL between the pre- and during COVID-19 datasets, a generalized linear model (GLM) was used in the software package R, using the "glm" function in the lme4 package (Bates et al., 2012). A normal (Gaussian) error structure was chosen with SPL as the response variable, and six predictor variables, including continuous variables; number of

[1]https://www.ndbc.noaa.gov/wndav.shtml

[2]www.marinetraffic.com

ships, the log transform of the CPA distance, speed, and wind speed, and categorical variables; pre- or during COVID-19, and day or night. The day or night variable was added to include small recreational fishing vessels that may not have AIS. These vessels do not typically use the area at night, defined here as between 7 p.m. and 7 a.m. local time. Ship data were filtered to include ships within a 20 km radius of the recorder to include only the ships that were most likely affecting the sound levels on the hydrophone recordings, and ships that were present during recording periods (the first 10 min of every hour). Additionally, to focus our investigation on the effect of ship activity on the SPL, we also filtered the data to only include time periods when wind speeds were not greater than a "gentle breeze," or less than 5.5 m/s as described in Pensieri et al., 2015, as high wind speeds can dominate sound recordings making it difficult to discriminate the contributors to any changes in sound.

The Akaike Information Criterion (AIC) was used to select the best statistical model (Burnham and Anderson, 2002), or which models to average, if more than one model was appropriate. The "dredge" function from the MuMIn package was used for model selection, i.e., those with the smallest AIC values. For all models with an AIC difference of < 3 compared to the best model, model averaging was performed. Summed Akaike weights were used to estimate the relative importance of variables within the model (Burnham and Anderson, 2002).

RESULTS

Acoustic Data Collection and Analysis

The acoustic record spans a full calendar year; the pre-COVID-19 dataset consists of 121 days of recordings from 29th October 2019 to 29th February 2020, comprising 2900 ten-minute duration wav files. This was compared to the during COVID-19 dataset of 134 days of recordings from 1st June 2020 to 12th October 2020, and 3181 ten-minute duration wav files (**Table 1**).

Comparisons between datasets were calculated from all data, not just using the monthly averages shown in **Table 1**. The mean pre-COVID-19 power level in the 111–140 Hz 1/3-octave band was 88.81 dB re 1 μPa (range 81.38–100.90), compared to 84.27 dB re 1 μPa (range 78.60–99.51) for the during COVID-19 dataset, a resultant decrease of 4.54 dB. Using methods described by Urick (1983), the reported spectral level decrease of 4.54 dB equates to a soundscape sound pressure reduction of 41% during the pandemic compared to the pre-COVID-19 period. A Welch two-sample *t*-test showed the reduction in sound levels during the pandemic was highly significant ($p < 0.01$), with a 95% confidence interval of 4.39–4.68.

To focus the investigation on the effects of ship behavior on changes of SPL, the dataset was filtered to include only ships within 20 km of the recorder, that were present during the recorders' duty cycle, and wind speed was less than 5.5 m/s (Pensieri et al., 2015). During these time periods, average wind speeds for the pre-COVID dataset, i.e., fall/winter months, were higher (<2 m/s) than during the spring/summer months of the pandemic dataset. This filtering resulted in a 3.98 dB decrease in the spectral level which equates to a 37% soundscape sound pressure reduction, suggesting that although seasonal changes in wind speed during the pandemic contributed to a reduction in overall sound, anthropogenic causes were predominant.

Marine Traffic Data

Using AIS data, a comparison of commercial ship activity in the study area before and during the pandemic showed that while some uses of the area remained the same or were similar throughout the period, some changes did occur. A plot of ship

TABLE 1 | A summary of the dataset showing the number of days AIS data were recorded with corresponding hydrophone data, the number of unique vessels per month, the mean sound level detected at the acoustic recorder, the mean ship speed derived from the mean speeds for each vessel per month, the median Closest Point of Approach (CPA) of unique vessels per month and the average wind speed per month.

Month	# Days	# Unique vessels	Mean sound level (dB)	Mean speed (kts)	Median CPA (km)	Average wind speed (m/s)
Pre-COVID						
October 2019	3	88	85.06	12.28	3.55	5.33
November 2019	30	717	87.68	13.50	3.99	6.35
December 2019	28	640	89.62	14.24	3.98	7.50
January 2020	31	749	89.30	13.35	4.40	6.48
February 2020	29	626	89.05	13.80	4.37	6.58
Totals	**121**	**2,820**				
Overall averages			**88.14**	**13.43**	**4.06**	**6.45**
During COVID						
June 2020	31	534	85.97	11.68	5.07	4.51
July 2020	31	543	84.04	12.05	4.69	4.68
August 2020	31	461	84.02	12.80	4.54	4.16
September 2020	30	402	83.43	13.59	5.06	4.42
October 2020	12	545	83.39	12.28	4.51	5.12
Totals	**134**	**2,485**				
Overall averages			**84.17**	**12.48**	**4.77**	**4.58**

Totals and overall averages are in bold.

location data shows that the primary route used by ships to traverse the study area did not appear to differ before and during COVID-19 (**Figure 2**). This assumption was supported by similar CPA distances of ships to the hydrophone during both time periods for all ships (**Table 1**); the pre-COVID-19 median CPA was 4.09 km (range 0.02–289.98 km) compared to 4.77 km during-COVID-19 (range 0.11–274.41 km). However, the number of unique ships present in the pre-COVID-19 period was higher (n = 2,820) compared to during COVID-19 (n = 2,485).

In addition to fewer number of ships present during the pandemic, there were pronounced changes in ship activity between the two periods; the most notable change in ship behavior was that ships traveled at a slower speed as they passed through the study area during the pandemic (**Figure 3**). The mean speed of vessels using the AIS data in the pre-COVID-19 dataset was 13.77 kts (range 0–36.7), compared to 12.35 kts (range 0–29.2) during COVID-19. A Welch two-sample t-test showed the reduction in speed during the pandemic was highly significant ($p < 0.01$), with a 95% confidence interval of 1.42–1.41 kts. A simple Pearson correlation showed a strong (0.9) correlation between the ship speeds and sound levels for the pre-COVID-19 dataset and a strong (0.7) correlation during COVID-19.

Other COVID-related changes in ship activity were noted. Throughout the study AIS transmissions were received from 6 to 10 different ship types per month, with both the lowest and highest number of different ship types per month occurring in the pre-COVID-19 period. However, not all ship types were represented in the study area equally. Ship traffic primarily consisted of tankers and cargo ships (which include container ships), both before and during the pandemic, but both types were recorded more frequently during COVID-19 than in the pre-COVID-19 period (tankers: pre- 33%, during 39% and cargo: pre-39%, during 44%). Other changes in use of the area by vessel type included "Fishing" and "High Speed Craft" vessels present before the pandemic, but absent during COVID-19, and "Search and Rescue" vessels present during the pandemic but absent in the pre-COVID-19 dataset (**Figure 4**). Welch two-sample t-tests for each individual ship type (e.g., "Cargo," "Passenger," etc.) found vessel speeds were significantly greater in the pre-COVID-19 period (n = 2,569 ships) than during COVID-19 (n = 2,294 ships) regardless of ship type. This dataset only includes records with MMSI numbers which provides the ship type information.

To further investigate potential changes in ship activity pre- and during COVID-19, we investigated the amount of time ships spent in the area before and during the pandemic. The amount of time was similar for all types of ship with three exceptions (**Figure 5**). "Passenger" ships (predominantly cruise ships) initially remained in the study area for longer durations during the beginning of the COVID-19 study period, but then the time in the area declined to pre-COVID levels (pre-COVID-19: median 4, range 1–30; during COVID-19: median 5, range 1–27). The time "Special Craft" (e.g., fire-fighting vessels, supply vessels, and landing craft) spent in the study area followed an opposite pattern, with increasing time spent in the area during the pandemic (pre-COVID-19: median 2, range 1–16; during COVID-19: range 1–17, median 3). The most predominant ship types, tankers and cargo ships, used the area in the same way before and during the pandemic, spending 2 days or less in the study area. Both October datasets were omitted from this analysis, as neither contained a complete record of the entire month's activity.

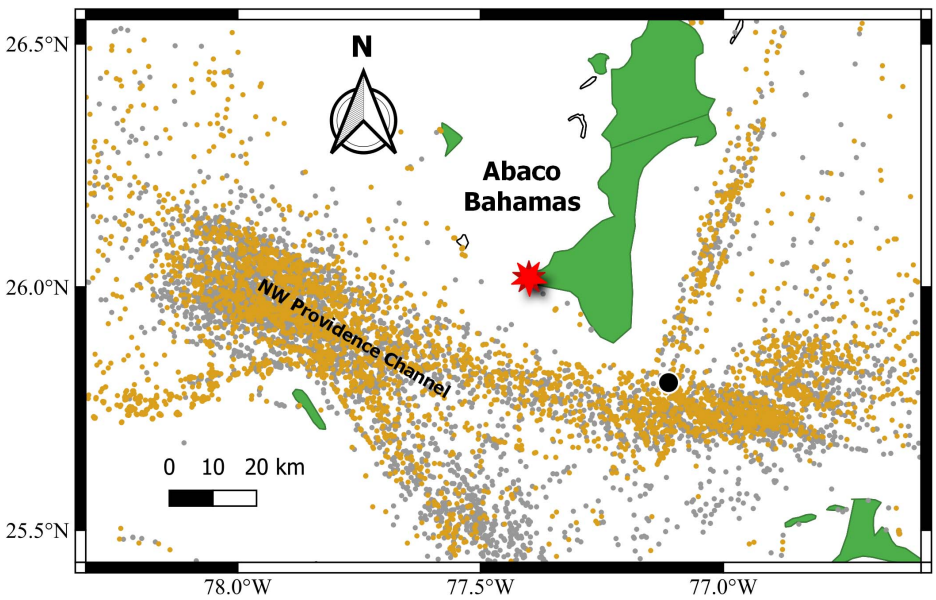

FIGURE 2 | Map of Northwest Providence Channel (NPC) depicting ship location messages transmitted and received by AIS receiver station 844 (red star) for the pre-COVID-19 time period (ship locations in gray, n = 6,449) and during COVID-19 (ship locations in orange, n = 5,692) during corresponding times when the ST500 hydrophone (black circle) was deployed. Each ship is represented by one location per day.

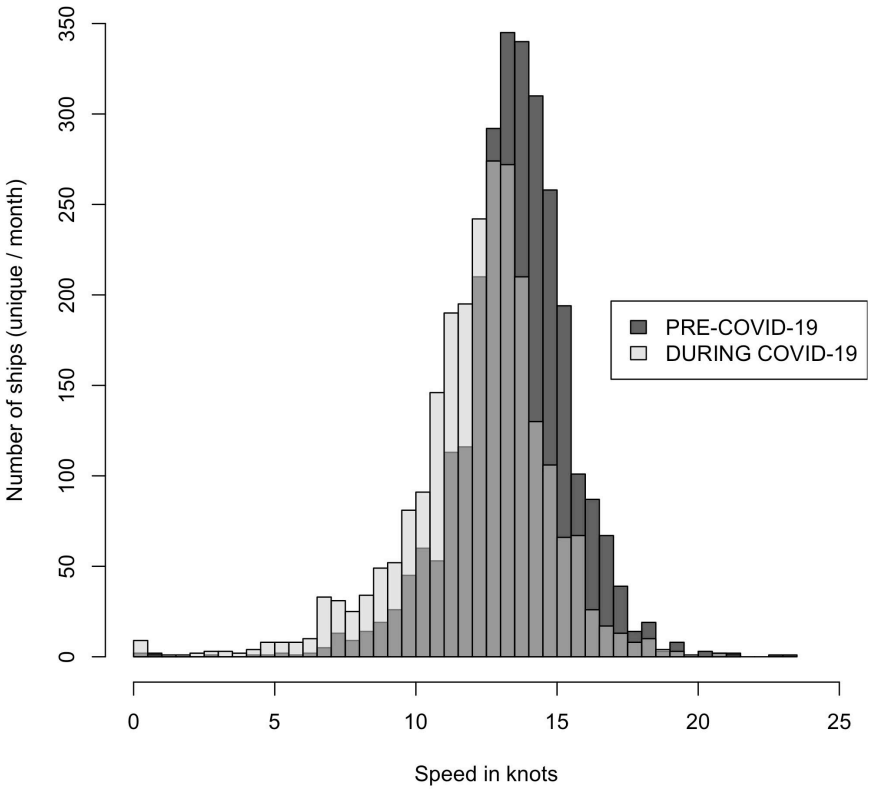

FIGURE 3 | A histogram presenting the number of ships/months and the mean ship speed for each unique ship per month PRE-COVID-19 (dark gray, n = 2,781) and during COVID-19 (light gray, n = 2,439). The gray central area is where the datasets overlap.

Statistical Analysis

GLMs were fit to two different datasets. A GLM using CPA (log transformed) and speed from only the ship closest to the hydrophone during each 10-min recording period had a higher AIC than a GLM that used mean CPA (log transformed) and mean speed of all ships present during each recording period. Therefore, the dredge function was performed on the preferred model, i.e., the GLM using mean values. The best model kept all but the day/night variable and the mean CPA (log-transformed), and the remaining four variables were all significant. Six models had an ΔAIC less than 3 from the best model, and the results from these six models were averaged and weighted by each model's Akaike weight. Model results indicate the most important variables (shown as the summed Akaike weights in **Table 2**) for predicting SPL were whether it was pre- or during the pandemic and mean ship speed. The positive relationship between ship speed and SPL shows that as ship speed increased, so too did SPL, as seen by the positive slope and standard error (**Table 2**).

DISCUSSION

The global spread of COVID-19 has had catastrophic impacts on the planet's human inhabitants. The pandemic's influence has been far reaching, dramatically altering lives, infrastructure and the fabric of societal norms. Global trade saw a steep downturn due to the pandemic, which in turn reduced and altered the nature of commercial shipping activity. Our study showed changes in commercial ship traffic in Northwest Providence Channel in The Bahamas during the pandemic and dramatically reduced ocean noise levels. After filtering for low wind speeds (because our interest is the effect of anthropogenic changes and not climatic variations during the pandemic), we found SPLs in the study area decreased by 3.98 dB which equates to a soundscape sound pressure reduction of 37% during the pandemic compared to the pre-COVID-19 period. Despite the opportunistic nature of the study [i.e., not a standard before-after-control-impact (BACI) study], we found robust evidence of concurrent changes in commercial shipping activity, most notably reduced vessel speeds and fewer ships using the area during the pandemic. However, our statistical analyses revealed vessel speed was the only ship-based variable that predicted SPLs, which has strong implications for management of ship activities in the area to reduce noise-related impacts on marine life.

In spite of the retrospective approach used in this study, its findings are consistent with other studies, implicating ship activities with changes in soundscapes. Globally ships have become the most widespread and predominant anthropogenic source of noise in the ocean (Erbe et al., 2019). Ship source levels are correlated with vessel speed (McKenna et al., 2012; Leaper, 2019; Ryan et al., 2021), but other characteristics such as vessel type, size, draft, and load can all affect noise emissions

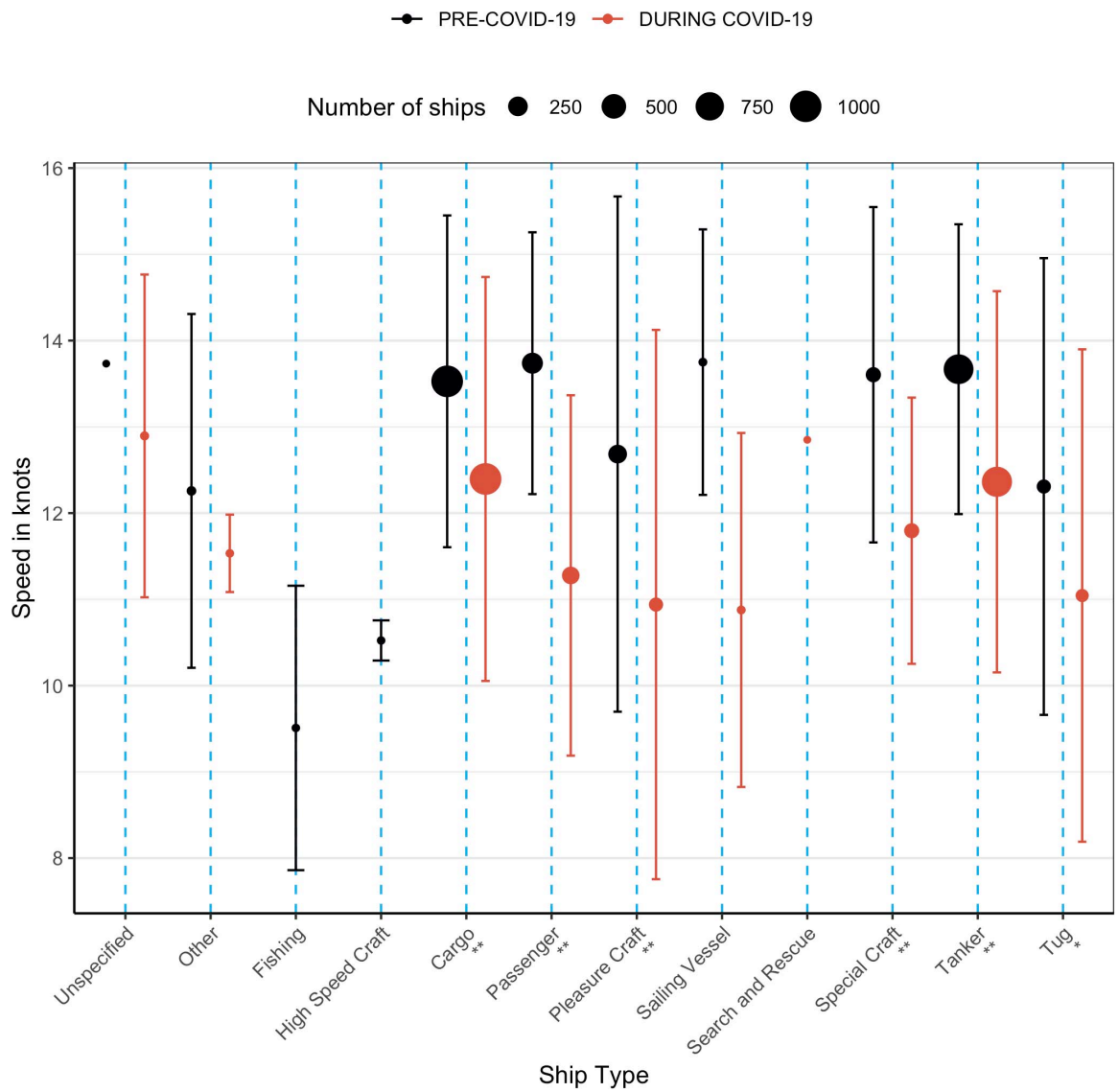

FIGURE 4 | Speed by ship type, pre- and during COVID-19, with the size of the point scaled to represent the number of ships, error bars representing the standard deviation of the mean speeds and the *p*-value of the *t*-test between datasets (*$p < 0.05$; **$p < 0.01$) for each ship type. Sample sizes were not large enough for Unspecified and Other ships to be included. The ship type "Special Craft" is made up of a variety of types (e.g., fire fighting vessels, supply vessels and landing craft).

from vessels (MacGillivray et al., 2019). To determine the factors influencing reduced SPLs found in our study, we investigated the effect of vessel speed, the number of ships and their distance to the recorder, and explored changes in ship type, and the amount of time ships spent in the study area pre- and during COVID-19. We found a significant reduction in vessel speeds during the pandemic, and multiple lines of evidence suggested slower vessel speed was the most predominant cause of the reduced SPL. Not surprisingly, speed was also strongly correlated to SPL both pre- and during COVID. However, other changes in ship activity also have to be considered.

We documented several other changes in ship activity during the pandemic. For example, there were 335 fewer ships using the area, however, the proportion of cargo ships and tankers, which represented most of the ship traffic (>70%), remained the same during the two periods. Other types of ships using the area and the time ships remained in the study area changed, although only slightly. Voluntary slowdown studies have provided detailed evidence for ship source levels (SL) versus speed for differing vessel categories (Joy et al., 2019). In our study, all ship types slowed down during the pandemic, but we were unable to determine which types had the greatest impact. Although direct correlation of SPL with average ship speed is complex and beyond the limits of this study, our finding of a median speed reduction of 1.42 kts could result in a reduction in SPL of 3.98 dB (e.g., see MacGillivray et al., 2019; Leaper, 2019). Given this and the strong predictive power that speed had on SPL in our study, we believe that slower ship speeds during the

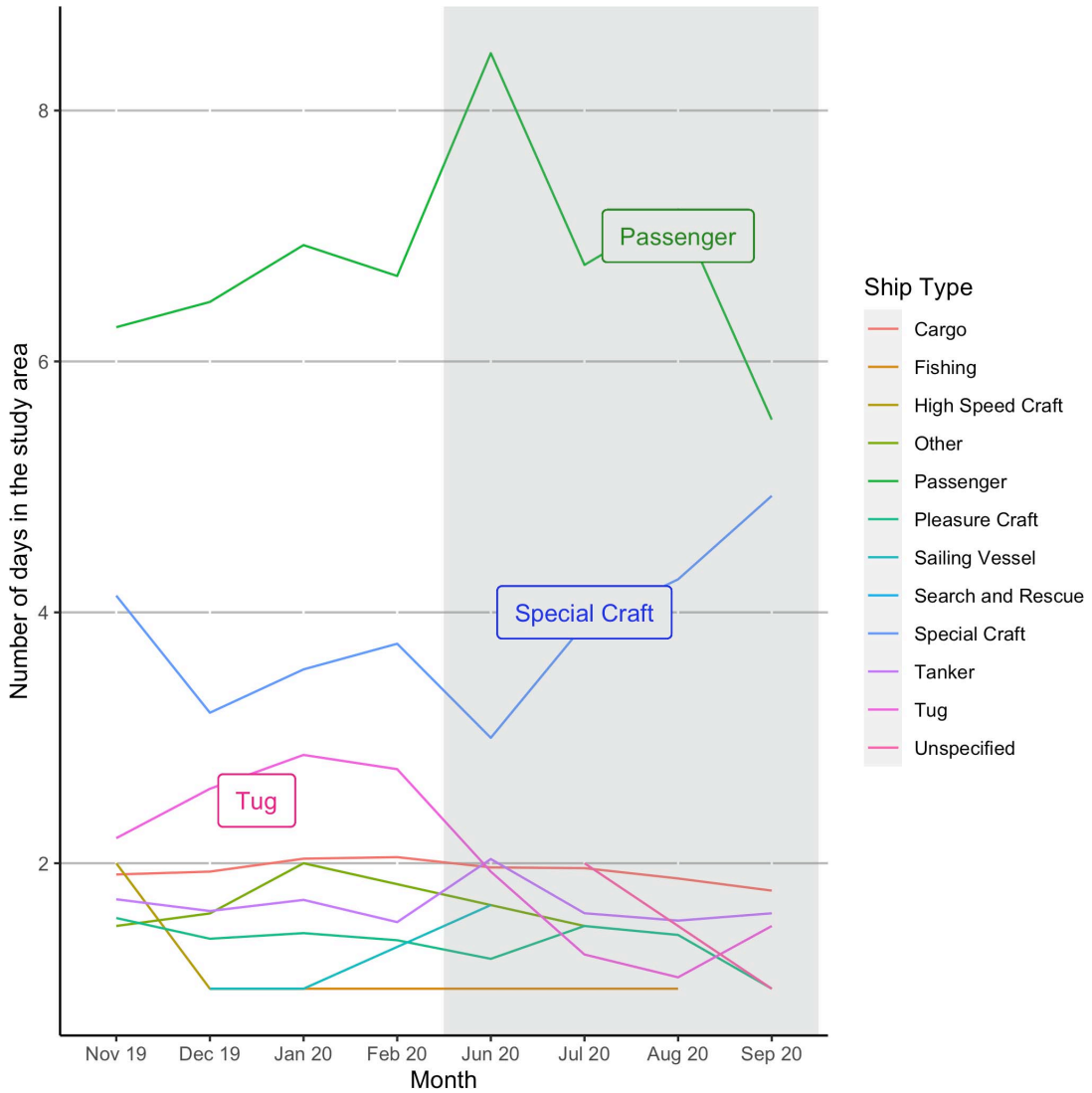

FIGURE 5 | The number of days ship types were present in the study area pre- and during COVID-19 (shaded gray), with the three ship types that had changes in behavior labeled on their respective line.

pandemic was the predominant anthropogenic cause of a quieter soundscape in NPC.

The opportunistic nature of this study presented some analysis challenges and limited our ability to carry out analyses that would further strengthen our conclusions. Firstly, the hydrophone was intentionally placed at a shallow enough depth that allowed scuba deployment and retrieval, yet with proximity to heavy shipping traffic to investigate use of the area by sperm whales, and, as a secondary question, to determine if it was a grouper spawning aggregation site. As such, we were unable to carry out analysis conducted in other studies, e.g., pairing the acoustic data with individual contributors of noise such as ships, as seen in MacGillivray et al., 2019, where single vessels were isolated and matched to their acoustic data by rejecting recordings when there were other AIS vessels within "six times the measured CPA of the vessel of interest." Similarly, Putland et al., 2017 rejected AIS vessels from their analyses that were not alone for at least 30 min. Most importantly, we were not able to calculate ship source levels. Extreme bathymetric changes in the study area (ranging from < 5 to $> 4{,}000$ m) suggest a complex acoustic environment, but we

TABLE 2 | Summed Akaike weights ($\Sigma\omega_i$), model averaged estimates and their standard errors and *p*-values for AIS and other data variables in the GLM model.

Variable	$\Sigma\omega_i$	Estimate	Std. Error	*P*-value
Pre/during COVID-19	1.00	3.75085	0.16732	<0.001
Mean speed	1.00	0.07981	0.02197	<0.001
Wind speed	0.94	0.14337	0.05170	<0.05
Number of ships	0.77	0.04502	0.03143	0.15
Day/Night	0.41	0.06545	0.11842	0.58
Mean CPA (log-transformed)	0.29	0.04251	0.20478	0.84

did not have a sound speed profile for the area, therefore we were not able to pair the hydrophone data with individual ships from the AIS data. However, the median CPA of ∼4 km for both datasets indicates most ships in this study were close enough to the hydrophone to account for the received SPLs but future work should include a sound propagation model.

Similarly, *in situ* environmental data must also be considered, particularly wind speed and wave height which both influence background sound (Thomson and Barclay, 2020). The data available to us for this study, however, was from a buoy 300 nm away from the recorder, and our datasets were seasonal. As expected, the winter months had higher winds, but the change in average windspeeds between the two periods was small and so was not expected to be a major driver of different sound levels. To limit wind effects we focused on comparing spectral sound levels in the 1/3 octave band from 111 to 140 Hz to avoid sensitivity to wind-generated distant noise (above 1 kHz, see Urick, 1983) and variation in acoustic propagation loss from surface reflection loss (Jones et al., 2009). After filtering out higher wind speeds (as our interest was changes in ship activity, not environmental), we showed a reduction in the SPL of the soundscape from only 41 to 37%. However, the statistical model still weighted the lower (filtered) wind speed as an important variable in predicting SPL. *In situ* data would better capture local conditions and its variability and should be included in future studies.

The presence or absence of smaller vessels could potentially have a significant influence on the NPC soundscape (see Hermannsen et al., 2019). Of specific concern during our study was that the acoustic recorder was located within a popular sport-fishing site used primarily by smaller vessels which do not possess AIS, and their presence was undocumented due to the opportunistic nature of this investigation. However, an extreme climatic event and the pandemic itself limited the number of non-AIS vessels in the study area. On the 1st September 2019 hurricane Dorian struck The Bahamas as a category 5 storm causing catastrophic damage to the northern Bahamas[3]. Ninety percent of boats and all marinas in the hurricane's path were destroyed, drastically decreasing sport-fishing activity. The pandemic further slowed the recovery and rebuilding efforts from hurricane Dorian as the Bahamian government imposed stay-at-home orders and travel restrictions throughout the country. As such, small vessel presence in the study area is expected to have remained low during COVID-19 resulting in little change during the study period. For these reasons, we consider the effect of smaller non-AIS vessels on the observed soundscape sound reduction during the pandemic likely to be negligible, as supported by the GLM analyses which used day/night as a proxy for fishing activity. However, as the area recovers from hurricane Dorian and pandemic restrictions are lifted, future studies will have to consider the influence of non-AIS vessels on noise levels at this site.

Marine environments have seen a steep rise in the degree with which they are altered by anthropogenic influences in recent decades. Noise pollution being non-visible, but dramatic in its effects is of particular concern. Ocean sound is increasing by 3 dB per decade (Wenz, 1962; Andrew et al., 2002), and thus a 3.98 dB reduction in SPLs found in this study is a considerable one, especially when considering the short timeframe in which the change occurred. In a theoretical sense, an ocean environment which relatively quickly became 37% quieter during COVID-19, may have returned the study site to a soundscape that has not existed for over a decade. This dramatic reduction in sound may have had an impact on marine life (Putland et al., 2017; Duarte et al., 2021), broadening communication space and reducing masking effects. For example, the critically endangered and commercially valuable Nassau grouper (Sadovy et al., 2018; Waterhouse et al., 2020) produces pulse trains (mean peak frequency 77.4 ± 30.3 Hz) and tonal sounds (mean peak frequency 99.0 ± 33.6 Hz) for predator avoidance and reproduction (Scharer et al., 2012). The quieter soundscape in NPC during the pandemic has the potential to permit better transmission of alarm sounds to conspecifics, leading to reduced predation risk and higher reproductive success through improved communication during spawning aggregations. Slower vessel speeds are also correlated to reduced collision rates for large marine animals, such as sharks, turtles, and whales (Rowat et al., 2006; Hazel et al., 2007; Casale et al., 2010; Pierce and Norman, 2016) so fewer large animals may have been injured by ship strikes during the pandemic.

Adult female sperm whales are year-round inhabitants of NPC (Claridge et al., 2015) raising concerns about the impact of increasing commercial shipping traffic in the region on this local population and has been the focus of an on-going study to investigate management needs. The reduction in ship speed, number of ships and SPLs during the pandemic provides a unique opportunity to assess the effectiveness of strategies to mitigate impacts, such as slowing ships. These large whales (female length 11 m and weight 15 tons; Whitehead, 2003) produce 10 Hz–30 kHz sounds for communication and foraging (Watkins, 1977; Madsen et al., 2002; Mohl et al., 2003; Whitehead, 2003; Rendell and Whitehead, 2004) and have long surfacing intervals after foraging dives (Gordon et al., 1992). Ship traffic not only presents a threat of ship strikes to large whales, but shipping noise can elevate stress levels (Rolland et al., 2012) while vessel presence can alter surfacing behavior and respiration rates (Gordon et al., 1992). Fewer vessels in NPC during the COVID-19 period (12% less), combined with a quieter environment (37% quieter) and average vessel speed decrease (1.42 kts slower) may allow individual whales to better detect and avoid approaching vessels, reducing the risk of ship strike, especially for naïve calves that spend more time at, or close to, the surface than adults (Gordon et al., 1992). The reduction in sound levels was evident in all bandwidths, including within the frequency range of sperm-whale vocalizations, which will have resulted in increasing the communication space for sperm whales using the study area. One counter influence of ship speed reduction is an increase in vessel residency in the area which may increase the risk of collision for animals, although it is unknown if slower, quieter vessels present a greater collision threat (Erbe et al., 2019). Quantifying how

[3]https://www.nhc.noaa.gov/archive/2019/DORIAN_graphics.php?product=5day_cone_with_line

the change in ship residency during the pandemic may have altered the risk of collision presents an interesting aspect for future research. However, maintaining slower ship speeds such as those recorded during the pandemic, but over longer periods could have positive population level effects, e.g., population growth for sperm whales and other marine life through increased survival and reproductive success. This study provides a unique opportunity for the investigation of the potential changes in sperm whale habitat use in the study area during the pandemic that could elucidate the extent to which changes in ship traffic activity impacted sperm whales in NPC, informing effective management directives.

CONCLUSION

Collecting persistent multi-sensor data such as AIS and acoustic data is greatly beneficial to studies of shifting environmental and anthropogenic change and can even drive policy and management directives, such as seen with the Port of Vancouver's ECHO Program in which ships voluntarily slowdown. Critically, such data collection regimes provide data acquisition and quantifiable metrics for events that are unplanned or unforeseen, such as the COVID-19 outbreak. These circumstances, although lacking experimental design, allow insights into events that hitherto could not be studied such as impacts of this anthropause, providing a unique opportunity to test prospective management directives. This study found that a relatively small decrease in ship speed (<2 knot) during transit of NPC led to a 37% SPL reduction in the marine soundscape, a level that would not have existed for a decade. These opportunistically collected data provide baseline information for future mitigation measures for the management of shipping through Bahamian waters. Vessel speed reduction will need to consider the trade-off between source level reduction, time spent in a region and if a ship can travel at speeds slower than their operational speed (McKenna et al., 2012). However, effective mitigation such as routing traffic away from prime habitat and slowing ships down could help maintain biodiversity of marine life, increase their resilience to other anthropogenic stressors like climate change, and aid in the recovery of commercial fish stocks and other vulnerable, threatened or endangered species in NPC.

Given the dramatic COVID-related alteration to the soundscape in the study area, it is important to continue data collection and assess whether and for how long these changes will persist. The reduction in vessel speed was likely driven by changes in global consumer demand and the supply infrastructure. Reduced consumer demand and the closure of retail sectors left retailers with large inventories. Increased transit times, longer routes and stowing of excess inventory on slower moving vessels while waiting for markets to reopen benefits importers and retailers, allowing them to delay payment for products paid on delivery (Saul et al., 2020). With the global roll out of vaccination programs, financial markets and global trade is beginning to rebound, directly influencing shipping activity. It is conceivable that as economies endeavor to recover, shipping traffic may increase, potentially to levels beyond historic records. Continued monitoring of vessel activity and acoustic output will provide crucial information to determine if these documented changes are short-lived or not, and to what extent dramatic shifts in soundscapes over periods of months have beneficial implications for soundscapes and the inhabitants of these environments. Reductions in anthropogenic noise such as we describe, but implemented using shipping management initiatives, will aid ecosystem health. Despite the opportunistic nature of this study our findings are useful to inform policy makers and assist governance of the shipping industry to effect protection measures for the marine environment and also provide an important baseline for establishing an acoustic budget in Northwest Providence Channel.

DATA AVAILABILITY STATEMENT

The raw data supporting the conclusions of this article will be made available by the authors, without undue reservation.

AUTHOR CONTRIBUTIONS

CD and DC: funding acquisition and field work. CD, JT, LH, and DC: conceptualization. CD and JT: data analysis. LH: writing first draft. All authors contributed to the writing—review and editing process.

FUNDING

Funding for the purchase of SoundTrap hydrophones and associated field work came from Field School, Sabine and Reinhold Probst, M Rogers, The Devereux Ocean Foundation and The Bahamian Environment Protection Foundation.

ACKNOWLEDGMENTS

We would like to thank Stephanie Archer for advice with the data plots, Stacy De Ruiter for guidance with modeling, Luke Rendell for help with the AIS parser, and the following for assistance with the deployment and retrieval of hydrophones and visual surveys of sperm whales; Field School staff and volunteers, Thomas Brown, Bahamian students from University of the Bahamas and overseas, Sabine and Reinhold Probst, Mark Kopp and Kim Rody, Tim and Rebekah Higgs, Enie Hensel, Michael Sheratt, and Jeremy Pleydell-Bouverie, The Bahamian Environment Protection Foundation, and the Perry Institute for Marine Science.

SUPPLEMENTARY MATERIAL

The Supplementary Material for this article can be found online at: https://www.frontiersin.org/articles/10.3389/fmars.2021.673565/full#supplementary-material

REFERENCES

Adams, A. J., and Murchie, K. J. (2015). Recreation fisheries as conservation tools for mangrove habitats. *Am. Fish. Soc. Symp.* 83, 43–56.

Andrew, R. K., Howe, B. M., Mercer, J. A., and Dzieciuch, M. A. (2002). Ocean ambient sound: comparing the 1960s with the 1990s for a receiver off the California coast. *Acoust. Res. Lett Online* 3, 65–70. doi: 10.1121/1.1461915

Bates, D., Machler, M., Bolker, B., and Walker, S. (2012). Fitting linear mixed-effects models using lme4. *J. Stat. Softw.* 67, 1–48.

Burnham, K. P., and Anderson, D. R. (2002). *Information and Likelihood Theory: A Basis for Model Selection and Inference. In: Model Selection and Multimodel Inference: A Practical Approach*. New York: Springer-Verlag, 49–79.

Casale, P., Affronte, M., Insacco, G., Freggi, D., Vallini, C., Pino d'Astore, P., et al. (2010). Sea turtle strandings reveal high anthropogenic mortality in Italian waters. *Aquat. Conserv. Mar. Freshw. Ecosyst.* 20, 611–620. doi: 10.1002/aqc.1133

Cholewiak, D., Clark, C. W., Ponirakis, D., Frankel, A., Hatch, L. T., Risch, D., et al. (2018). Communicating amidst the noise: modeling the aggregate influence of ambient and vessel noise on baleen whale communication space in a national marine sanctuary. *Endang. Species Res.* 36, 59–75. doi: 10.3354/esr00875

Claridge, D., Dunn, C., Ylitalo, G., Herman, D., Durban, J., and Parsons, K. (2015). *Behavioral Ecology of Deep- diving Odontocetes in The Bahamas. SERDP Project Number: RC-2114 Bahamas Marine Mammal Research Organisation, NOAA Alaska Fisheries Science Center – Final Technical Report Vers. 2*. Washington, DC: NOAA.

Clark, C. W., Ellison, W. T., Southall, B. L., Hatch, L., Van Parijs, S. M., Frankel, A., et al. (2009). Acoustic masking in marine ecosystems: intuitions, analysis, and implication. *Mar. Ecol. Prog. Ser.* 395, 201–222. doi: 10.3354/meps08402

Conn, P. B., and Silber, G. K. (2013). Vessel speed restrictions reduce risk of collision-related mortality for North Atlantic right whales. *Ecosphere* 4, 1–15.

Crum, N., Gowan, T., Krzystan, A., and Martin, J. (2019). Quantifying risk of whale–vessel collisions across space, time, and management policies. *Ecosphere* 10:e02713. doi: 10.1002/ecs2.2713

Duarte, C. M., Chapuis, L., and Collin, S. P. (2021). The soundscape of the Anthropocene ocean. *Science* 371;eaba4658. doi: 10.1126/science.aba4658

Durban, J. W., Parsons, K. M., Claridge, D. E., and Balcomb, K. C. (2000). Quantifying dolphin occupancy patterns. *Mar. Mamm. Sci.* 16, 825–828. doi: 10.1111/j.1748-7692.2000.tb00975.x

Erbe, C., Marley, S. A., Schoeman, R. P., Smith, J. N., Trigg, L. E., and Embling, C. B. (2019). The effects of ship noise on marine mammals-a review. *Front. Mar. Sci.* 6:606. doi: 10.3389/fmars.2019.00606

Erbe, C., Williams, R., Sandilands, D., and Ashe, E. (2014). Identifying modeled ship noise hotspots for marine mammals of canada's pacific region. *PLoS One* 9:e89820. doi: 10.1371/journal.pone.0089820

Fearnbach, H., Durban, J., Parsons, K., and Claridge, D. (2012). Seasonality of calving and predation risk in bottlenose dolphins on Little Bahama Bank. *Mar. Mamm. Sci.* 28, 402–411. doi: 10.1111/j.1748-7692.2011.00481.x

Fedler, T. (2010). *The economic impact of flats fishing in The Bahamas*. Nassau: Bahamas Flats Fishing Alliance, 16.

Frisk, G. (2012). Noiseonomics: the relationship between ambient noise levels in the sea and global economic trends. *Sci. Rep.* 2:437. doi: 10.1038/srep00437

GEBCO (2020). *General Bathymetric Chart of Oceans [online]*. Available online at: www.gebco.net (accessed February, 2021).

Gende, S. M., Hendrix, A. N., Harris, K. R., Eichenlaub, B., Nielsen, J., and Pyare, S. (2011). A Bayesian approach for understanding the role of ship speed in whale–ship encounters. *Ecol. Appl.* 21, 2232–2240. doi: 10.1890/10-1965.1

Gillespie, D., Dunn, C., Gordon, J., Claridge, D., Embling, C., and Boyd, I. (2009). Field recordings of Gervais' beaked whales Mesoplodon europaeus from the Bahamas. *J. Acoust. Soc. Am.* 125, 3428–3433. doi: 10.1121/1.3110832

Gordon, J., Leaper, R., Hartley, F. G., and Chappell, O. (1992). Effects of whale-watching vessels on the surface and underwater acoustic behaviour of sperm whales off Kaikoura, New Zealand. *Conserv. Te Papa Atawhai.* 48, 1–64.

Gössling, S., Scott, D., and Hall, M. C. (2021). Pandemics, tourism and global change: a rapid assessment of COVID-19. *J. Sustain. Tour.* 29, 1–20. doi: 10.1080/09669582.2020.1758708

Government of The Bahamas (2020). Available online at: https://www.bahamas.gov.bs (accessed February, 2021).

Hazel, J., Lawler, I., Marsh, H., and Robson, S. (2007). Vessel speed increases collision risk for the green turtle *Chelonia mydas*. *Endang. Spec. Res.* 3, 105–113. doi: 10.3354/esr003105

Hermannsen, L., Mikkelsen, L., Tougaard, J., Beedholm, K., Johnson, M., and Madsen, P. T. (2019). Recreational vessels without Automatic Identification System (AIS) dominate anthropogenic noise contributions to a shallow water soundscape. *Sci. Rep.* 9:15477. doi: 10.1038/s41598-019-51222-9

Herzing, D. L. (1997). The life history of free-ranging Atlantic spotted dolphins (*Stenella frontalis*): age classes, color phases and female reproduction. *Mar. Mamm. Sci.* 13, 576–595. doi: 10.1111/j.1748-7692.1997.tb00085.x

Hildebrand, J. A. (2009). Anthropogenic and natural sources of ambient noise in the ocean. *Mar. Ecol. Prog. Ser.* 395, 5–20. doi: 10.3354/meps08353

Jones, A., Sendt, J., Duncan, A. J., Clarke, Paul, A., and Maggi, A. (2009). *Modelling the Acoustic Re-flection Loss at the Rough Ocean Surface. Acoustics*. Sydney: Australian Acoustical Society.

Joy, R., Tollit, D., Wood, J., MacGillivray, A., Li, Z., Trounce, K., et al. (2019). Potential benefits of vessel slowdowns on endangered southern resident killer whales. *Front. Mar. Sci.* 6:344. doi: 10.3389/fmars.2019.00344

Joyce, T. W., Durban, J. W., Claridge, D. E., Dunn, C. A., Fearnbach, H., Parsons, K. M., et al. (2017). Physiological, morphological, and ecological tradeoffs influence vertical habitat use of deep-diving toothed-whales in the Bahamas. *PLoS One* 12:e0185113. doi: 10.1371/journal.pone.0185113

Leaper, R. (2019). The role of slower vessel speeds in reducing greenhouse gas emissions, underwater noise and collision risk to whales. *Front. Mar. Sci.* 6:505. doi: 10.3389/fmars.2019.00505

MacGillivray, A. O., Li, Z., Hannay, D. E., Trounce, K. B., and Robinson, O. M. (2019). Slowing deep-sea commercial vessels reduces underwater radiated noise. *J. Acoust. Soc. Am.* 146:340. doi: 10.1121/1.5116140

Madsen, P. T., Wahlberg, M., and Mohl, B. (2002). Male sperm whale (Physeter macrocephalus) acoustics in a high-latitude habitat: implications for echolocation and communication. *Behav. Ecol. Sociobiol.* 53, 31–41. doi: 10.1007/s00265-002-0548-1

McKenna, M., Wiggins, S., and Hildebrand, J. (2012). Relationship between container ship underwater noise levels and ship design, operational and oceanographic conditions. *Sci. Rep.* 3:1760. doi: 10.1038/srep01760

McKenna, M. F., Katz, S. L., Wiggins, S. M., Ross, D., and Hildebrand, J. A. (2012). A quieting ocean: unintended consequence of a fluctuating economy. *J. Acoust. Soc. Am.* 132, EL169–EL175. doi: 10.1121/1.4740225

Merchant, N. D., Pirotta, E., Barton, T. R., and Thompson, P. M. (2014). Monitoring ship noise to assess the impact of coastal developments on marine mammals. *Mar. Pollut. Bull.* 78, 85–89. doi: 10.1016/j.marpolbul.2013.10.058

Mohl, B., Wahlberg, M., and Madsen, P. (2003). The monopulsed nature of sperm whale clicks. *J. Acoust. Soc. Am.* 114:1143. doi: 10.1121/1.1586258

Pensieri, S., Bozzano, R., Nystuen, J. A., Anagnostou, E. N., Anagnostou, M. N., and Bechini, R. (2015). Underwater acoustic measurements to estimate wind and rainfall in the Mediterranean Sea. *Adv. Meteorol.* 2015:612512 . doi: 10.1155/2015/612512

Pierce, S. J., and Norman, B. (2016). *Rhincodon typus. The IUCN Red List of Threatened Species. e.T19488A2365291*. Gland: IUCN.

Poon, L. L. M., and Peiris, M. (2020). Emergence of a novel human coronavirus threatening human health. *Nat. Med.* 26, 317–319. doi: 10.1038/s41591-020-0796-5

Putland, R. L., Merchant, N. D., Farcas, A., and Radford, C. A. (2017). Vessel noise cuts down communication space for vocalizing fish and marine mammals. *Glob. Change Biol.* 24, 1708–1721. doi: 10.1111/gcb.13996

R Core Team (2020). *R: A Language and Environment for Statistical Computing*. Vienna: R Foundation for Statistical Computing.

Rendell, L., and Whitehead, H. (2004). Do sperm whales share coda vocalizations? Insights into coda usage from acoustic size measurement. *Anim. Behav.* 67, 865–874. doi: 10.1016/j.anbehav.2003.04.018

Rockwood, R. C., Adams, J., Silber, G., and Jahncke, J. (2020). Estimating effectiveness of speed reduction measures for decreasing whale-strike mortality in a high risk region. *Endang. Species Res.* 43, 145–166. doi: 10.3354/est01056

Rodrigue, J., and Wang, G. W. Y. (2020). Cruise shipping supply chains and the impacts of disruptions: the case of the Caribbean. *Res. Transp. Bus. Manag.* 2020:100551. doi: 10.1016/j.rtbm.2020.100551

Rolland, R. M., Parks, S. E., Hunt, K. E., Castellote, M., Corkeron, P. J., Nowacek, D. P., et al. (2012). Evidence that ship noise increases stress in right whales. *Proc. R. Soc. B.* 279, 2363–2368. doi: 10.1098/rspb.2011.2429

Rowat, D., Meekan, M. G., Engelhardt, U., Pardigon, B., and Vely, M. (2006). Aggregations of juvenile whale sharks (*Rhincodon typus*) in the Gulf of Tadjoura, Djibouti. *Environ. Biol. Fish.* 80, 465–472. doi: 10.1007/s10641-006-9148-7

Ryan, J. P., Joseph, J. E., Margolina, T., Hatch, L. T., Azzara, A., Reyes, A., et al. (2021). Reduction of low-frequency vessel noise in monterey bay national marine sanctuary during the COVID-19 pandemic. *Front. Mar. Sci.* 8:656566. doi: 10.3389/fmars.2021.656566

Sadovy, Y., Aguilar-Perera, A., and Sosa-Cordero, E. (2018). *Epinephelus Striatus: The IUCN Red List of Threatened Species. 2018*. Report no. e.T7862A46909843. Gland: International Union for Conservation of Nature and Natural Resources.

Sarà, G., Dean, J., D'Amato, D., Buscaino, G., Oliveri, A., Genovese, S., et al. (2007). Effect of boat noise on the behaviour of bluefin tuna *Thunnus thynnus* in the Mediterranean Sea. *Mar. Ecol. Prog. Ser.* 331, 243–253. doi: 10.3354/meps331243

Saul, J., Baertlein, L., and Dowsett, S. (2020). *Ocean Shipping Shrinks as Pandemic Pummels Retailers*. Available online at: https://www.reuters.com/article/us-health-coronavirus-shipping-retail/ocean-shipping-shrinks-as-pandemic-pummels-retailers-idUSKBN23C0MS (accessed February, 2021).

Scharer, M. T., Rowell, T. J., Nemeth, M. I., and Appeldoorn, R. S. (2012). Sound production associated with reproductive behaviour of Nassau grouper Epinephelus striatus at spawning aggregations. *Endang. Species Res.* 19, 29–38. doi: 10.3354/esr00457

Sherman, K. D., Shultz, A. D., Dahlgren, C. P., Thomas, C., Brooks, E., Brooks, A., et al. (2018). Contemporary and emerging fisheries in The Bahamas - Conservation and management challenges, achievements and future directions. *Fish. Manag. Ecol.* 25, 319–331. doi: 10.1111/fme.12299

Stanley, J. A., Van Parijs, S. M., and Hatch, L. T. (2017). Underwater sound from vessel traffic reduces the effective communication range in Atlantic cod and haddock. *Sci. Rep.* 7:14633. doi: 10.1038/s41598-017-14743-9

Thomson, D. J. M., and Barclay, D. R. (2020). Real-time observations of the impact of COVID-19 on underwater noise. *J. Acoust. Soc. Am.* 147:3390. doi: 10.1121/10.0001271

Urick, R. J. (1983). *Principles of Underwater Sound*. New York, NY: McGraw-Hill.

van der Hoop, J. M., Vanderlaan, A. S. M., and Taggart, C. T. (2012). Absolute probability estimates of lethal vessel strikes to North Atlantic right whales in Roseway Basin, Scotian Shelf. *Ecol. Appl.* 22, 2021–2033. doi: 10.1890/11-1841.1

Vanderlaan, A. S., and Taggart, C. T. (2009). Efficacy of a voluntary area to be avoided to reduce risk of lethal vessel strikes to endangered whales. *Conserv. Biol.* 23, 1467–1474. doi: 10.1111/j.1523-1739.2009.01329.x

Waterhouse, L., Heppell, S. A., Pattengill-Semmens, C. V., McCoy, C., Bush, P., Johnson, B. C., et al. (2020). Recovery of critically endangered Nassau grouper (Epinephelus striatus) in the Cayman Islands following targeted conservation actions. *Proc. Natl. Acad. Sci. U.S.A.* 117, 1587–1595. doi: 10.1073/pnas.1917132117

Watkins, W. A. (1977). Acoustic behavior of sperm whales. *Oceans* 20, 50–58.

Wenz, G. M. (1962). Acoustic ambient noise in the ocean: spectra and sources. *J. Acoust. Soc. Am.* 34, 1936–1956. doi: 10.1121/1.1909155

Whitehead, H. (2003). *Sperm Whales – Social Evolution in the Ocean*. London: The University of Chicago Press, Ltd.

World Health Organization [WHO] (2020). *Coronavirus Disease (COVID-19) Outbreak*. Available online at: https://www.who.int/emergencies/diseases/novel-coronavirus-2019/interactive-timeline/ (accessed February, 2021).

www.MiamiDade.Gov (2019). *PortMiami Port Guide 2018-2019*. Available online at: https://www.miamidade.gov/portmiami/library/stats-brochure-2019.pdf (accessed February, 2021).

Conflict of Interest: LH was employed by the company Open Ocean Consulting. JT volunteered with the company Ocean Environmental Consulting. Both authors freely donate their time as board members of the Bahamas Marine Mammal Research Organization.

The remaining authors declare that the research was conducted in the absence of any commercial or financial relationships that could be construed as a potential conflict of interest.

Publisher's Note: All claims expressed in this article are solely those of the authors and do not necessarily represent those of their affiliated organizations, or those of the publisher, the editors and the reviewers. Any product that may be evaluated in this article, or claim that may be made by its manufacturer, is not guaranteed or endorsed by the publisher.

Copyright © 2021 Dunn, Theriault, Hickmott and Claridge. This is an open-access article distributed under the terms of the Creative Commons Attribution License (CC BY). The use, distribution or reproduction in other forums is permitted, provided the original author(s) and the copyright owner(s) are credited and that the original publication in this journal is cited, in accordance with accepted academic practice. No use, distribution or reproduction is permitted which does not comply with these terms.

frontiers in Marine Science

ORIGINAL RESEARCH
published: 30 July 2021
doi: 10.3389/fmars.2021.664691

The Efficacy of Management Measures to Reduce Vessel Noise in Critical Habitat of Southern Resident Killer Whales in the Salish Sea

Rianna E. Burnham[1], Svein Vagle[1], Caitlin O'Neill[1] and Krista Trounce[2]*

[1] Institute of Ocean Sciences, Department of Fisheries and Oceans Canada, Sidney, BC, Canada, [2] Vancouver Fraser Port Authority, Vancouver, BC, Canada

The inland waters around southern Vancouver Island and northern Washington State, known as the Salish Sea, host critical habitat for endangered southern resident killer whales (SRKW). This is, however, a highly traversed area, with approaches to industrial ports and coastal cities, international shipping lanes, ferry routes, and considerable recreational vessel traffic. Vessel noise is a key threat to SRKW prosperity, and so conservation measures directed to mitigate its effects have been explored annually since 2017. Here, we describe trials undertaken in 2020, which included spatially limited slowdown zones, exclusion areas as Interim whale Sanctuary Zones (ISZs), and a lateral displacement of tug transits to increase the distance between their route and SRKW foraging areas. To assess each of the measures we first considered the level of mariner participation using data from the Automated Identification Systems (AIS), mandatory for commercial vessels. Knowing this, the changes in soundscape were examined, focused on impacts on broadband (10 Hz to 100 kHz) ambient noise and the frequencies used by SRKW for communication (500 Hz to 15 kHz) and echolocation (15 to 100 kHz). A control period of two-months prior to trial initiation was used to quantify the changes. High levels (> 80%) of compliance were found for each measure, except ISZs, where observance was low. Median reduction in speeds ranged from 0.2–3.5 knots. Resulting sound reductions were most notable in the lower frequencies, although reductions were also recorded in SRKW pertinent ranges. Tug displacement also reduced ambient noise in these frequencies, despite making up a small portion of the overall traffic. The management trials were effective in reducing potential impacts singularly and in concert. Greater awareness and stakeholder engagement may increase compliance and, therefore, the efficacy of measures in the future.

Keywords: Salish Sea, southern resident killer whales, critical habitat, vessel exclusion, slowdown, mitigation actions, soundscape monitoring, passive acoustics

OPEN ACCESS

Edited by:
Kerri D. Seger,
Applied Ocean Sciences (AOS),
United States

Reviewed by:
Brad Hanson,
National Marine Fisheries Service (NOAA), United States
Monika Shields,
Orca Behavior Institute (OBI),
United States

****Correspondence:***
Rianna E. Burnham
rianna.burnham@dfo-mpo.gc.ca

Specialty section:
This article was submitted to Marine Ecosystem Ecology, a section of the journal Frontiers in Marine Science

Received: *05 February 2021*
Accepted: *08 July 2021*
Published: *30 July 2021*

Citation:
Burnham RE, Vagle S, O'Neill C and Trounce K (2021) The Efficacy of Management Measures to Reduce Vessel Noise in Critical Habitat of Southern Resident Killer Whales in the Salish Sea. Front. Mar. Sci. 8:664691. doi: 10.3389/fmars.2021.664691

INTRODUCTION

Killer whales (*Orcinus orca*) frequent the coast of British Columbia. The inland waters around southern Vancouver Island and northern Washington State, collectively referred to as the Salish Sea, hosts both Bigg's (formerly transient) and resident killer whale ecotypes. Whereas the mammal-eating Bigg's killer whale population has increased (Towers et al., 2012), the piscivorous southern

resident killer whale (SRKW) population has declined to 75 individuals in recent years (Center for Whale Research, 2021) and are listed as Endangered under both the *Canadian Species at Risk Act* (SARA) and the American *Endangered Species Act* (ESA, Krahn et al., 2004; National Oceanic and Atmospheric Administration [NOAA], 2005). Swiftsure Bank and the Strait of Juan de Fuca, Haro Strait on the west side of San Juan Island, Boundary Pass, Swanson Channel, and southern portions of the Strait of Georgia are designated critical habitat for SRKW, and are areas they utilize frequently during the summer (Balcomb and Bigg, 1986; Krahn et al., 2004; Department of Fisheries and Oceans Canada [DFO], 2017b; Olson et al., 2018). Components of these sites, including high bathymetric relief with nearshore shallow reefs adjacent to deep water, and strong tidal currents to aggregate prey, are the foundations of foraging habitat (Groot et al., 1984; Heimlich-Boran, 1988; Hauser et al., 2007; Hanson et al., 2010; Olson et al., 2018).

Killer whales use sound as their principal means to sense their environment. They actively send and receive information on their surroundings using echolocation clicks, whistles, or calls. Echolocation is used to form a cognitive image of their surroundings and so plays a role in navigation, and prey location and capture (Ford, 1989; Au et al., 2004). The whistles and calls are used to communicate between conspecifics, or hunting groups. Acoustic additions from vessels are in the frequency ranges that SRKW use for communication and echolocation (Veirs et al., 2016), potentially impacting their ability to send and receive signals, or accurately interpret them. Indeed, vessel presence and acoustic disturbance have been identified as a key limiting factor to SRKW population recovery and survival (Weilgart, 2007; Lacy et al., 2017; Department of Fisheries and Oceans Canada [DFO], 2018; Raverty et al., 2020).

Critical habitats in the Salish Sea experience high rates of commercial vessel traffic transiting international shipping lanes to ports including Victoria, Vancouver, Tacoma, Port Angeles, and Seattle. Here, we present the results of management actions undertaken to limit acoustic impacts of vessels on SRKW in the area. Since 2017, several conservation measures have been implemented in areas designated as key foraging areas for SRKW. These include voluntary spatially delimited slowdown trials and alteration of vessel tracks in or near existing shipping lanes under the Enhancing Cetacean Habitat and Observation (ECHO) program, and mandated exclusion areas, Interim whale Sanctuary Zones (ISZs), implemented and managed by Transport Canada. All measures were implemented with the support of the Canadian and U.S. coast guards, marine transportation industries and Fisheries and Oceans Canada (DFO).

The voluntary slowdown measures were first applied in the summer of 2017 for a 31 km portion of Haro Strait in the Compulsory Pilotage Area (*Pilotage Act* 1985). Although the focus of the slowdown request was piloted commercial vessels over 350 gross tons, and pleasure craft over 500 gross tons, all vessels were encouraged to reduce their speed when it was safe and feasible. This initial trial found decreased speed effectively reduced source level noise for container ships, cruise vessels, vehicle carriers, tankers, and bulkers (MacGillivray et al., 2019). In 2019, the slowdown zone was increased to encompass Haro Strait and Boundary Pass completely, over a distance of 55 km. Participation has increased from 61% in the first year to consistently over 80% in 2018 and 2019, resulting in decreases in ambient noise particularly in the low frequencies (MacGillivray et al., 2017, 2019; Joy et al., 2019).

The initial lateral displacement trial in 2018 requested all outbound deep-sea vessels and both outbound and inbound tugs and barges operating in, or north of, the outbound shipping lane to move their transits southward within the bounds of the shipping lanes over a 63 km area in the Strait of Juan de Fuca. This was intended to move vessels away from areas frequented by SRKW, presumably to forage (Olson et al., 2018). Restricted movement was possible for piloted vessels, which moved their transit approximately 600 m southward, resulting in little effect on the ambient noise level. The transit of tugs through this area is not restricted to shipping lanes; their passage through Juan de Fuca is often closer to the coastline than the shipping lanes, even when not transiting port-to-port (Cominelli et al., 2019). Therefore, for the same trial an average shift of approximately 3900 m was possible from tugs (Vagle and Neves, 2019). Tugs showed high participation, significantly reducing noise in the higher frequencies of the soundscape (Vagle and Neves, 2019). Since 2019, trials have requested tugs and barges only to alter their vessel passage routes, resulting in as much as a 7 dB reduction in the broadband ambient noise, and 11.5 dB reduction of higher frequency noise, on a per-transit basis for the trial that year (Vagle, 2020).

Vessel exclusion zones, known as Interim whale Sanctuary Zones (ISZs) have been implemented in key SRKW foraging areas on Swiftsure Bank and in Swanson Channel, off Pender Island, and around East Point off Saturna Island since 2019 (Olson et al., 2018). Mandated to all vessel types, these measures were enforced by Parks Canada wardens (Author Pers. Obs., 2019). However, compliance especially for small, recreational vessels was low (Vagle, 2020).

Here, we report on the results from the most recent trials, undertaken through the summer and fall of 2020, using acoustic recordings made at Swiftsure Bank, Jordan River in the Strait of Juan de Fuca, Haro Strait, Boundary Pass, and Swanson Channel and Saturna Island in the southern Gulf Islands. The ambient noise levels during the trials are compared to pre-trial baselines, as well as noise levels and results from similar trials enacted in the summers of 2017-2019. Measures of the effectiveness of the trials are two-fold: First, the level of voluntary participation to the slowdown and displacement measures, and compliance to the exclusion zones by mariners are established. With this in mind, we then consider the changes in the sound fields between the control and trial conditions. The efficacy of measures are assessed on their own and jointly for reducing anthropogenic noise in areas used by SRKW in the Salish Sea. Comparison between voluntary and regulated actions are also possible. Although the analysis considers the effect of overall ambient noise changes resulting from the management measures, we also focus on soundscape changes in the frequency bands used by SRKW for foraging and communication. This assessment will help us refine future measures for enhanced success in achieving conservation goals.

MATERIALS AND METHODS

Several conservation measures aimed at mitigating vessel noise were in place during the summer of 2020. Vessel passage through the trial areas was characterized via Automatic Information System (AIS) data collected by Canadian Coast Guard terrestrial receivers. Class A AIS transceivers are mandatory for vessels over 300 tons (excluding fishing vessels) and for passenger vessels over 150 tons carrying more than 12 passengers. Also, towage and escort vessels of any tonnage must carry a Class A transceiver. Class A vessel data were primarily from larger commercial vessels, classified as bulkers, container ships, ferries, fishing vessels, government or research vessels, naval vessels, cruise ships, recreational vessels, tankers, tugs, vehicle carriers, or registered whale watching vessels. In addition, Class B vessel data were also used, which is typically transmitted from smaller vessels, often pleasure craft, fishing, or smaller commercial vessels that carry an AIS transceiver by choice. The AIS system transmits vessel name, identification number, type, and location every 5–30 s. These data were cleaned and binned into 5-min packages from which the pathway and speed of each vessel was interpolated. Passive acoustic moorings were deployed to monitor the soundscape in each of the trial areas subject to conservation measures. A recorder at Jordan River was previously assessed to best represent the lateral displacement request (Vagle and Neves, 2019; Vagle, 2020), located approximately halfway through the trial zone, and 5 km north of the outbound traffic lane (**Figure 1** and **Supplementary Table 1**). Each of the slowdown and ISZ areas had a designated mooring to monitor the changes in ambient noise recordings resulting from the measures (**Figure 1**). The efficacy of the mitigation actions was assessed through comparison to control, pre-trial periods two months immediately prior to trial initiation.

Management Actions

Vessel Slowdown 2020

A slowdown of bulkers, tankers, ferries and government vessels transit speed to 11 knots, and vehicle carriers, cruise, and container vessels to 14.5 knots, was requested for sections of shipping lanes crossing Swiftsure Bank, and through Haro Strait and Boundary Pass (**Figures 1–3**). Other vessel types, including government, naval and ferries vessels transiting the specified areas were also requested to slow down, however, the noise reduction related to changes in speed from commercial shipping were given greatest attention. These piloted vessels have shown participation resulting in notable sound level reductions in previous years (MacGillivray et al., 2017, 2019; Joy et al., 2019), and so remain the focus. The slow transit zone extended from Discovery Island in the south to East Point of Saturna Island to the north covering 55 km of Haro Strait and Boundary Pass (**Figures 1**, **2**). Monitoring for whales began in June, with measures initiated by a SRKW sighting on July 1, 2020. The

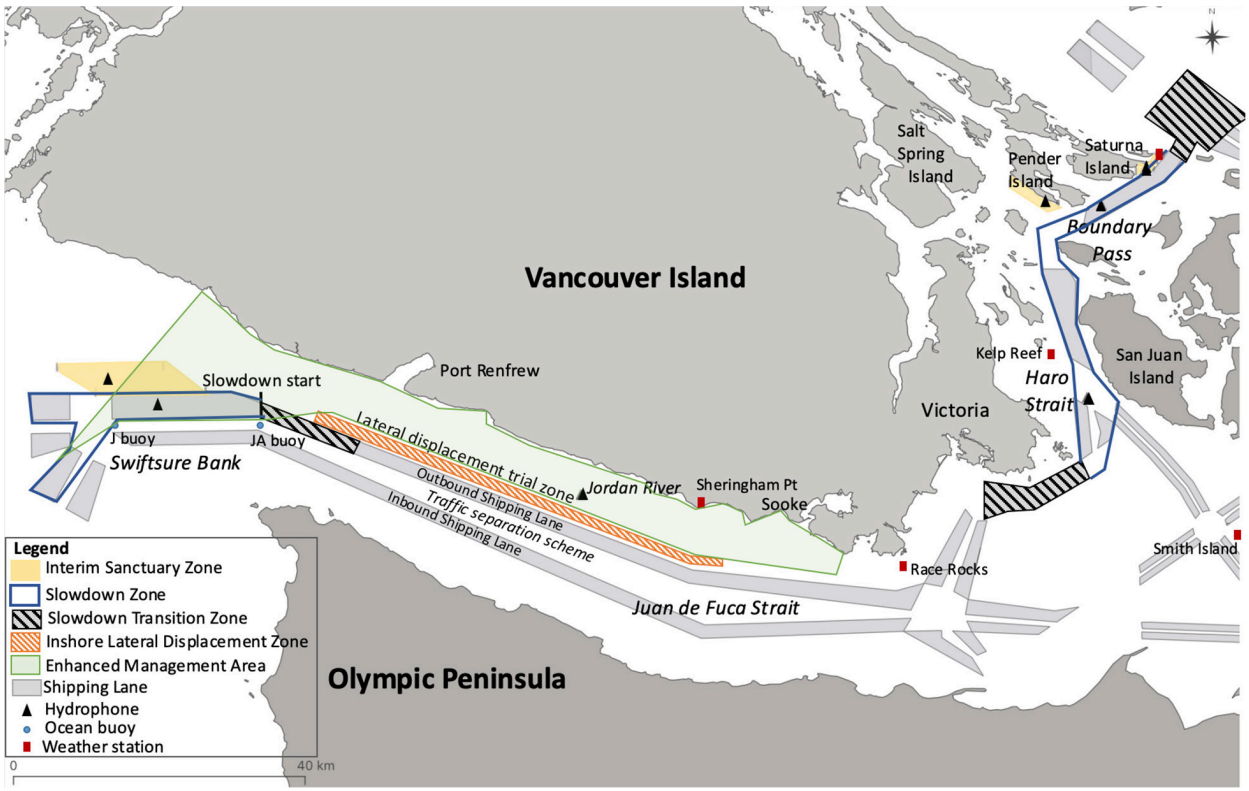

FIGURE 1 | The study area within the Salish Sea. Commercial shipping lanes are shown, as are the locations for all the management actions undertaken in the summer of 2020.

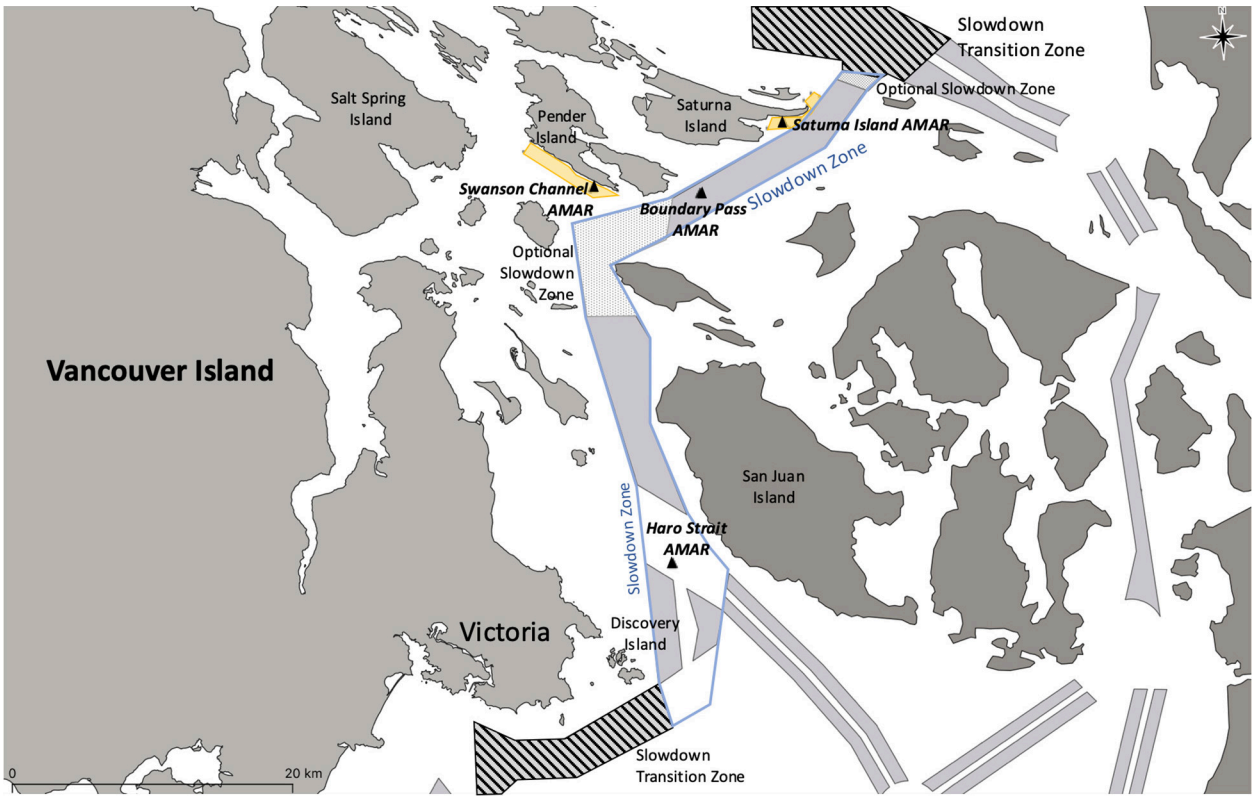

FIGURE 2 | The voluntary slowdown area in Haro Strait and Boundary Pass, and transition zones. The mooring locations used to assess the slowdown are shown with black triangles. Interim Sanctuary Zones (ISZs) are indicated in yellow.

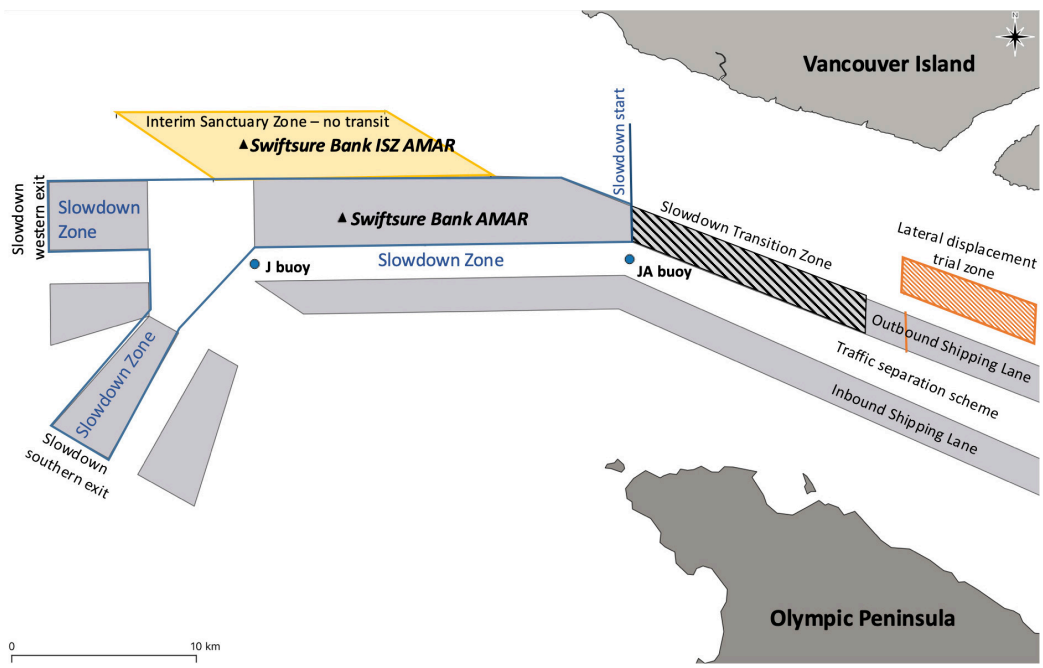

FIGURE 3 | The voluntary slowdown area and transition zones on Swiftsure Bank, with slowdown requested west of the JA buoy. The mooring locations used to assess the slowdown are shown with black triangles and labeled as AMAR. The Interim Sanctuary Zone (ISZ) is indicated in yellow, and the start of the lateral displacement trial zone in Juan de Fuca in orange.

trial ran until October 31, 2020 (**Table 1**). A similar slowdown request was also made for an area of Swiftsure Bank for outbound vessels over a 31–37 km stretch from the start of a transition zone just east of JA buoy to the end of the in- and outbound traffic separation scheme from August 1-October 31, 2020 (**Table 1** and **Figures 1**, **3**).

Lateral Displacement 2020

A more southerly transit route through the outbound shipping lane or a dedicated 1,500 m wide inshore lateral displacement zone, which maintained a 1000 m buffer from the traffic separation scheme (**Table 2** and **Figure 4**), was requested for tugs and barges. This trial was applied from June 1 to October 31, 2020, and was designed to move vessels away from presumed SRKW foraging areas, and concentrate traffic into the shipping lanes. This might have both acoustic benefits and reduce vessel-strike risk.

The tracks of each tug transit were examined, and the average distance for closest approach established. Change between the control and trial periods was examined through an independent t-test. The potential for change in sound pressure levels (SPL) for each tug passage, following a change in passage route into the lateral displacement zone, was also considered by examining the AIS data for vessels with multiple transits both before and during the trial.

TABLE 1 | Conservation measures enacted during the summer 2017–2020.

Measure	Description	Zone (km)	Trial dates
a) Voluntary Slowdown			
2017	All vessels through Haro Strait: 11 kts	31	Aug.7-Oct.6
2018	All vessels through Haro Strait	31	Jul. 2-Oct.31
	- Bulker, tankers, ferries, government: 12.5 kts		
	- Vehicle carrier, cruise ships, container ships: 15 kts		
2019	All vessels through Haro Strait and Boundary Pass	55	Jul.5-Oct.15
	- Bulker, tankers, ferries, government: 11.5 kts		
	- Vehicle carriers, cruise ships, container vessels: 14.5kts		
2020	All vessels through Haro Strait and Boundary Pass	55	Jul.1-Oct.31
	All vessels through zone on Swiftsure Bank	31-37	Aug.1-Oct.31
	- Bulker, tankers, ferries, government: 11.5 kts		
	- Vehicle carriers, cruise ships, container vessels: 14.5kts		
b) Voluntary Lateral displacement			
2018	Outbound deep-sea, in- and outbound Tugs	63	Aug.20-Oct.31
2019	All Tugs and barges move south	52	Jun17-Oct.31
2020	All Tugs and barges move south	52	Jun.1-Oct.31
c) Mandated Interim Sanctuary Zones			
2019	Area of vessel exclusion at Swiftsure Bank	~30 km^2	Jun.1-Nov.30
	Area of vessel exclusion in Swanson Channel	~2.5km^2	
	Area of vessel exclusion by Saturna Island	~1.8km^2	
2020	Area of vessel exclusion at Swiftsure Bank	~30 km^2	Jun.1-Nov.30
	Area of vessel exclusion in Swanson Channel	~2.5km^2	
	Area of vessel exclusion by Saturna Island	~1.8km^2	

TABLE 2 | Values of median speed for pre-trial and trial periods, and median speed change between periods for slowdown regions.

Median speeds (kts)	Pre-trial speed	Trial speed	Change	Requested speed
a) Swiftsure Bank				
Bulker	11.3	11.2	−0.2	11.5
Container ship	14.2	13.3	−0.9	14.5
Tanker	12.0	11.1	−0.9	11.5
b) Haro Strait				
Bulker	12.5	11.7	−0.8	11.5
Container ship	17.0	13.7	−3.3	14.5
Tanker	11.8	10.9	−0.9	11.5
c) Boundary Pass				
Bulker	12.7	11.4	−1.3	11.5
Container ship	17.4	13.9	−3.5	14.5
Tanker	12.0	11.2	−0.8	11.5

Speed through water values shown were derived from a frequency distribution of vessel count and speed. Requested slowdown speed is also shown.

Interim Sanctuary Zones (ISZ) 2020

Interim whale Sanctuary Zones (ISZs) on Swiftsure Bank, in Swanson Channel off Pender Island, and around East Point off Saturna Island were implemented between June 1 and November 30, 2020 (**Figure 1** and **Table 1**, **Supplementary Table 2**). The measures were assessed until October 31 to be in-line with the other management measures. The passages of vessels, per type, within the ISZs during the control and enforcement period were established from AIS data. The vessel transits per type within 8 km of the recorders positioned in the ISZs were also examined to better understand the vessel-derived noise additions to the recordings (**Figure 5**), with pre-trial and trial passage rate compared through independent t-tests.

Vessel Presence and Speed Assessment

The passage rate of vessels by type was determined from the AIS data and the number of transits reported to the Port of Vancouver. Impacts from COVID-19 restrictions, in force from April 6, 2020 were considered, whereby all commercial marine vessels with a capacity of more than 12 passengers were prohibited from engaging in non-essential activities, such as tourism or recreation; cruise ships with the capacity for overnight accommodations for 100 or more people were banned in Canadian waters and refused moorage in Canadian ports, and ferries were required to reduce the maximum number of passengers to 50% of capacity (gov.bc.ca; Transport Canada, 2020). The number of ferry transits between Canadian ports through the summer were quantified from information from BC Ferries (bcferries.ca). Ferries transiting between Canadian and American ports were absent throughout. Recreational boating was discouraged, but formal restrictions were eased in late June (June 24, gov.bc.ca).

Vessel presence, quantified from AIS track data, was used to assess participation in trials and establish the vessel-derived input

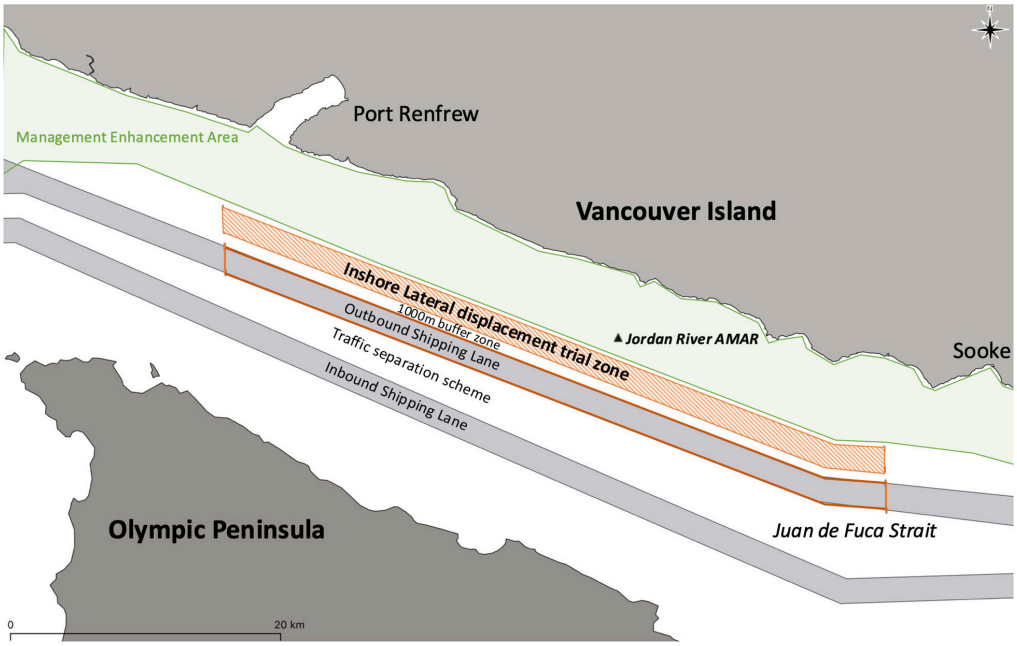

FIGURE 4 | The section of Juan de Fuca where tugs were requested to transit either in the 1500 m inshore lateral displacement zone or outbound shipping lane to take a more southern route. The hydrophone deployed at Jordan River used to assess the efficacy of this measure is shown as a black triangle and labeled as Jordan River AMAR.

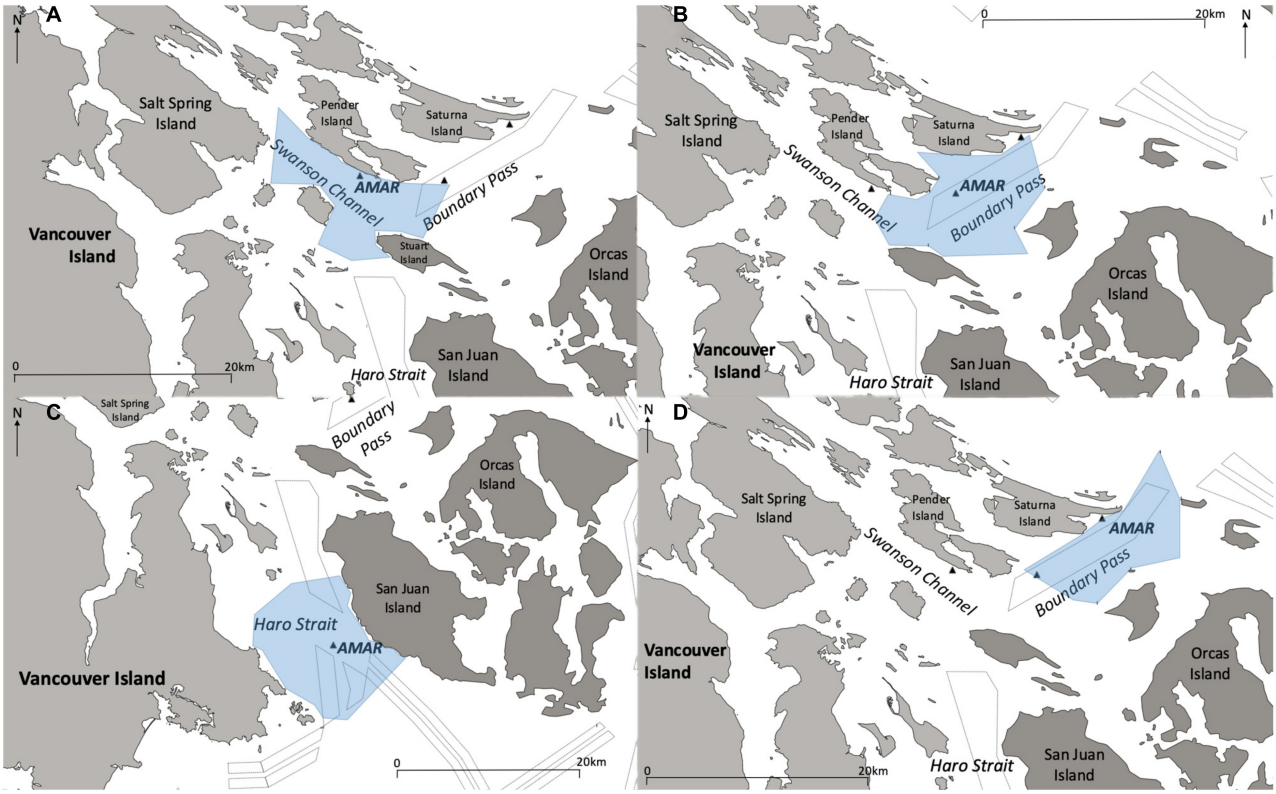

FIGURE 5 | Modified polygons of maximum extent of 8 km (blue shading) around the **(A)** Swanson Channel, **(B)** Boundary Pass, **(C)** Haro Strait, and **(D)** East Point, Saturna Island acoustic moorings (labeled AMAR) used to quantify vessel passages.

to the soundscape for both control and trial periods. For the slowdown trial areas in Haro Strait and Boundary Pass, and the ISZs on Saturna Island and in Swanson Channel the area over which the impact of vessels was considered was restricted by the geography, constrained by island or reef landmasses (**Figure 5**). In the more open water areas, vessel presence up to a maximum distance of 8 km was considered, to restrict the analysis to vessels within the shipping lanes, or waters immediately proximal to the trial zones (**Figure 5**). For the slowdown program at Swiftsure Bank, the analysis of vessels was restricted to the outbound traffic lane and a maximum distance of 8 km. The maximum distance of 8 km for the lateral displacement trial includes the waters from the Jordan River mooring to the outbound shipping lane, but not as distant as the inbound lane.

The 8 km limit is greater than the estimated detection range of SRKW communication calls in Juan de Fuca Strait and on Swiftsure Bank, which at its maximum was estimated to be 6.5 km (L_{10}, Swiftsure Bank during the summer; Mouy et al., 2020). Abiotic noise during the summer months is presumed to be lowest; however, we used the conservative 8 km distance to recognize that noise from wind, waves, water movement, and precipitation makes substantial additions to the soundscape (Vagle et al., 1990; Medwin et al., 1992; Richardson et al., 1995; Nystuen, 1996; Nystuen and Ma, 2002; Ma et al., 2005; Pensieri et al., 2015).

We quantified and compared vessels in these 8 km radius areas, or modified polygons (**Figure 5**) for slowdown and lateral displacement trials. For the ISZs on Swiftsure Bank, off Saturna Island, and in Swanson Channel the vessel assessment from AIS data was restricted to the area of exclusion (**Supplementary Table 2**). Vessels were aggregated into five classes: Class A deep-sea vessels, containing bulkers, container ships, tankers, and vehicle carriers; fishing vessels; tugs; passenger vessels, which included both ferries and cruise ships, and Class B vessels. In this analysis Class B was used to assess the presence of small vessels in each trial zone. The AIS data on the four Class A categories were used to quantify compliance with the slowdown trials. For the lateral displacement trial, only Class A tugs were used. For the ISZs, avoidance of all vessel types was considered, with Class B vessel movements highlighted.

The closest approach distance between each AIS-tracked vessel in these categories and the acoustic recorder was assessed and normalized to calculate the probability density functions of distance for pre-trial and trial transits. This analysis was applied to slowdown areas to confirm that any changes in the soundscape were a result of participation in the voluntary measure. For the lateral displacement, the passage distance of tugs were the focus of the analysis.

Individual vessel speed was derived to give speed over ground (SOG) from the time difference and distance between sequential 5-minute data points in the AIS data. This was corrected to speed through water (STW) by accounting for the speed and direction of surface currents retrieved from the WebTide model (Hannah et al., 2008).

The control-trial comparisons completed to assess the efficacy of each of the conservation measures used a pre-trial period of two months from the initiation date of the voluntary measure. For slowdown trials at Swiftsure Bank this control period was June 1-July 31, 2020, whereas for slowdown in Haro Strait and Boundary Pass, lateral displacement through Juan de Fuca Strait, and the Swiftsure Bank and Swanson Channel ISZs, control periods from April 1-May 31 2020 were used. Pre-trial recordings for the Saturna Island ISZ were limited to May 9-31, 2020 only.

Acoustic Recordings and Analysis

The underwater recordings were made using Autonomous Multichannel Acoustic Recorders (AMAR G4, JASCO Applied Sciences) equipped with GeoSpectrum Technologies M36-100 hydrophones mounted on a quiet mooring that positioned the hydrophone approximately 2 m above the sea floor. Each system was calibrated from 100 Hz to 250 kHz by the manufacturer, and then again at 250 Hz prior to each deployment. Continuous recordings were made at a sample rate of 256-kHz with 24-bit resolution and stored on internal SD memory cards as wav files. On retrieval, these wav files were processed with custom Python scripts, modified from those used by Merchant et al. (2015). One-minute power spectra were computed using a 1-s Hanning window, with a 50% overlap and Welch's averaging, from which sound pressure level (SPL) measures were calculated. Recordings from trial periods (**Table 1**) were compared to the baseline established from pre-trial recordings for all management actions.

Broadband ambient noise in the 10 Hz to 100 kHz frequency range was evaluated for changes between the pre-trial and trial recordings. This range represents the frequencies for which, if noise levels were increased, there may be behavioral or physiological implications for SRKW (Heise et al., 2017). Killer whale vocalizations are typically between 500 Hz and 15 kHz; noise in this range potentially could obscure conspecific calling or social behaviors, linked to group cohesion and coordination. Echolocation occurs in the frequency range of 15-100 kHz, therefore acoustic additions in this range could mask signal echoes, impairing navigation, orientation, and prey location and capture (Heise et al., 2017). Changes in soundscape and vessel presence were evaluated using the decadal bands 10–100 Hz, 100–1000 Hz, 1000–10,000 Hz and 10,000–100,000 Hz.

To evaluate the changes in ambient noise from each of the mitigation measures, a cumulative distribution function (CDF) SPL analysis was conducted. The L_5, L_{50} and L_{95} exceedance levels were obtained for each using only data that satisfied restrictions to minimize potential flow and wind noise in the recordings to better assess the input from vessels. Here L_{95} represents general baseline quiet ambient conditions exceeded 95% of the time, L_{50} represents the median and levels of noise 50% of the time, and L_5 gives the upper level of noise inputs, present for a small proportion (5%) of the recordings. The L_{50} exceedance level is used frequently in noise comparisons to represent typical sound levels (e.g., Klinck et al., 2012; Merchant et al., 2012), whereas the L_{95} and L_5 levels indicate the range of sound levels present, and help characterize both the background ambient noise level (L_{95}) and periods of elevated noise that may mask SRKW acoustic signals, or initiate behavioral change (Clark et al., 2009; Merchant et al., 2015).

Restrictions on the data analyzed were made to limit abiotic noise additions potentially obscuring the SPL changes resulting

from the management measures. Only recordings made during slack tides, when current estimates were less than 0.25 m/s, were used. Current estimates were accessed from Webtide (Hannah et al., 2008). Also, wind speeds could not exceed 5 m/s. Wind speed data were collected from lighthouse or weather buoy recordings. For Juan de Fuca Strait, the Sheringham Point light station (48.0500N, -123.8833W) was used; for Swiftsure Bank, wind measures were taken from the Cape Flattery/JA ocean buoy (48.4930N, -124.7260W); Smith Island (48.3206N, -122.8308W) wind recordings were used for Haro Strait, and for Boundary Pass, and for the ISZs at Swanson Channel and Saturna Island, wind speed data from East Point light station on Saturna Island (48.7800N, -123.0400W) were used. All of these weather stations (**Figure 1**) reported hourly.

Acoustic additions from small vessels may contribute significantly to the overall noise levels, and potentially mask the change in the sound field resulting from the conservation measures. The use of Class B data represented the minimum presence of small vessels, but many more were expected to be present and not be equipped with AIS transponders. In an effort to reduce the impact of these vessels in the soundscape assessments for the slowdown trials, a small vessel detection algorithm, based on the approach by Warner et al. (2020), was implemented. This small vessel detector aimed to identify small vessels both moving slowly and at speed in the acoustic data to be removed, but retain signals for vessels subject to the trial measures. The detector used hourly median SPL levels in three decadal bands, comparing observed SPL values to threshold SPL values in decibels (dB). Exceedances in SPL at or above the threshold values compared to hourly values were a determinant of small vessels (Warner et al., 2020). The frequency band 100–1000 Hz has previously been used successfully as an indicator of vessel presence (Merchant et al., 2012, 2015); for the small vessel detector an increased amplitude in this band by 6 dB, together with SPL elevated by 5 dB in the range 1–10 kHz, and by 23 dB in the 10–100 kHz compared to an hourly median indicated small vessels moving at speed. In addition, this same definition but with SPL in the 100–1000 Hz range exceeding the hourly median by 6 dB, but by no more than 9 dB represented small vessels moving slowly (Warner et al., 2020). The precision (95.4%) and efficacy of the detector was established for a test dataset by both manual review of the acoustic data, and comparison to visual observations noting the number of small vessels around the mooring during recording (Warner et al., 2020). Those sections of data indicated by the detector to include small vessels were omitted from the data analyzed for slowdown and lateral displacement trials. For the ISZs it was only times that these criteria were met that were used to determine the changes in the sound field as a result of Class B and small vessel presence.

RESULTS

Vessel Presence and Speed Assessment

The AIS data indicated that the vessel passages, by type, within the 8 km distances or modified polygons varied considerably between the sites (**Figures 6**, **7**). At Swiftsure Bank and Jordan River there was greater consistency between the control and trial periods (**Figure 6**). Deep-sea commercial traffic dominated Jordan River, with Class A vessels consistently about 50% of the transits within 8 km of the mooring by week (**Figure 6**). This contrasted with Haro Strait and Boundary Pass, which showed an increase of Class B vessels from May to peak in July to August, and then decline again in the late summer (**Figure 6**). This increase in smaller vessels was less pronounced at Swiftsure Bank, with a greater proportion of 'other' vessel additions (**Figure 6**). Tug traffic was present at all locations, but was most common on Swiftsure Bank, Jordan River, and Haro Strait. The level and proportional presence of each vessel type at each of these sites was consistent with the year before (Vagle, 2020).

Class B vessels dominated in the ISZs. The exclusion zone on Swiftsure Bank showed more variety in vessel composition over time compared to the other locations (**Figure 7**). Only Saturna Island showed periods when vessels were absent, with vessel presence for Swiftsure Bank and Swanson Channel actually elevated during the enforced exclusion period (**Figure 7**).

The proportion of time that each vessel type was at the closest point of approach, and likely the dominant noise source for 10-min periods, was aggregated and examined on a weekly basis. Class A vessels were closest to the mooring for 50% of the recording time in both control and trial periods at Swiftsure Bank and Jordan River. Proportions of the recordings with vessels within 8 km were greatest for moorings on Swiftsure Bank and Jordan River, consistently exceeding 60%. In Haro Strait and Boundary Pass, the AIS data showed tugs to pass closest to the moorings. Conversely, AIS data showed vessels to be present rarely more than 20% of the time per week at the mooring within the ISZ off Saturna Island.

Recordings from within the Swanson Channel ISZ may reflect the change in ferry traffic over the summer. Passage numbers from Otter Bay, the closest ferry terminal on Pender Island, and in proximity to the ISZ, showed ferry traffic decreased following the April COVID-19 restrictions. The summer months would normally see increases in ferry transits through the study area, however sailings between Vancouver Island and the lower mainland of British Columbia and the Gulf Islands were reduced or suspended as part of the pandemic response measures. As restrictions eased, sailings through the summer increased to 70% of 2019 levels. The number of transits were consistent throughout the trial period. The most notable change between years resulting from these restrictions was for cruise ships and ferries transiting across the American-Canadian border, which were totally absent for summer 2020 (Vancouver Fraser Port Authority, Unpublished data). This, however, did not overtly impact the results of the conservation measures trialed in this analysis.

The number of Class A commercial cargo vessel transits through the Salish Sea to the Port of Vancouver were generally unchanged when compared to previous years (Vancouver Fraser Port Authority, Unpublished data). Importantly, for the lateral displacement trial and comparison between years, the transits of tugs were also comparable to previous years. A notable short-term decline in passages in June-July was seen for vehicle carriers/roll-on-roll-off vessels only (Vancouver Fraser Port

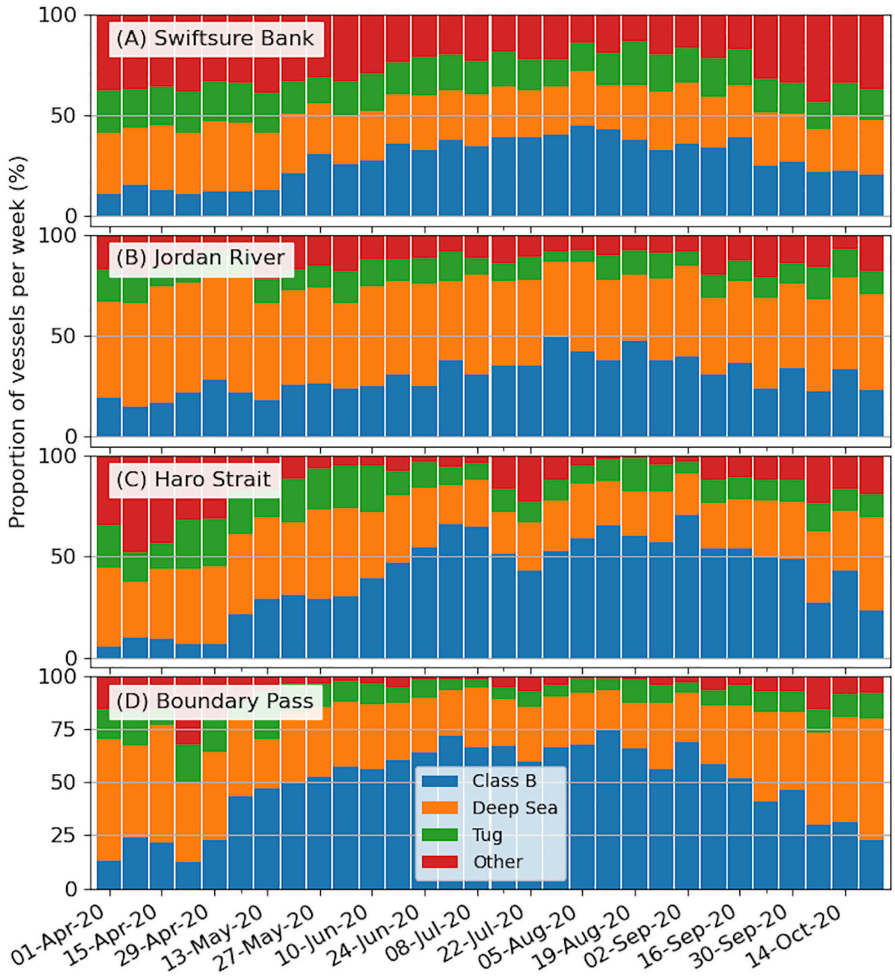

FIGURE 6 | Vessel passages by type within 8 km of the mooring expressed proportionally of weekly totals from AIS data for **(A)** Swiftsure Bank, **(B)** Jordan River, **(C)** Haro Strait, **(D)** Boundary Pass. The data were used to assess changes in the sound field based on vessel presence and participation. Trial for **(A)** Aug. 1-Oct. 31; **(B)** Jun. 1-Oct 31; **(C)** and **(D)** Jul. 1- Oct. 31.

Authority, Unpublished data). The AIS data showed a reduction of Class B vessels in Canadian waters in 2020 compared to previous years, perhaps due to COVID-19 restrictions and passage of recreational vessels between America and Canada being restricted throughout the summer.

Slow Down Participation

The AIS data showed the number of vessel transits through the slowdown zones at Swiftsure Bank and Haro Strait to Boundary Pass were consistent during trial periods and the control period. Therefore, any changes in the ambient noise fields resulted from either a change in the relative distance of the transit from the mooring, or changes in vessel speeds. The former was ruled out through the probability density analysis of closest approach, using the AIS data on weekly vessel passages. For Swiftsure Bank, vessels predominantly transited between 0.8-1.2 km from the mooring. This was consistent for both pre- and trial periods. A peak of vessel passages at a distance of approximately 10 km from the mooring was recorded for July 1-November 1, which, when vessels were considered by type, was attributed to tugs. Vessels were most likely to pass within 2 km of the mooring at Haro Strait, and within 1 km at Boundary Pass. The probability densities were again consistent between the pre- and trial periods. The AIS data showed participation in the slowdown measures to be greater in 2020 compared to all other trial years. This was also confirmed in the pilots' self-reporting; there were 1803 transits through the Haro Strait-Boundary Pass slow down zone, 91% of which pilots reported to have reduced their speed. At Swiftsure Bank, a non-piloted area, STW calculations suggested 82% of the 861 transits reduced speed to within one knot of the target speeds during the trial period (Vancouver Fraser Port Authority, Unpublished data).

The speed through water for each vessel was quantified and compared to an overall median value for vessels of the same type for each of the slowdown regions and passages within 8 km (**Table 2**). Most of the transit speeds fell within 5 knots above or below the pre-trial median speed. The most notable reduction of speed was by container ships that participated in the program

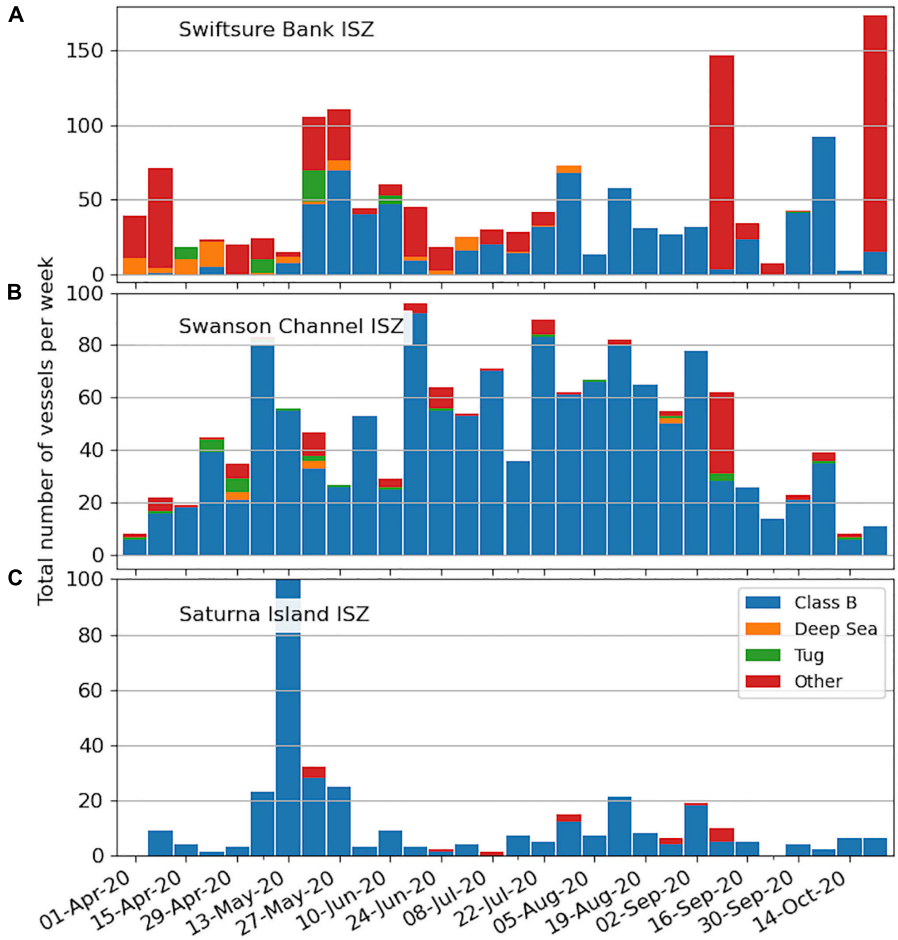

FIGURE 7 | Vessel passages within the Interim Sanctuary Zones (ISZz) at **(A)** Swiftsure Bank, **(B)** Swanson Channel, **(C)** Saturna Island expressed weekly from AIS data. The number of vessels, and the proportion of vessel type, is shown. Trial period for ISZs Jun. 1-Oct. 31, 2020.

in the Haro Strait-Boundary Pass trial area. The median speeds recorded at Swiftsure Bank for bulkers and container ships were, however, already below the requested slowdown speed in the pre-trial periods (**Table 2**).

Lateral Displacement Participation

The overall number of tugs transiting the Strait of Juan de Fuca was low compared to the number of other commercial vessels, therefore their impact on the overall noise field was also relatively low. The density of position reports of tugs in the lateral displacement zone in 2020 was greater than in 2019. The mean changes in distance from the Enhanced Management Area (**Figures 1**, **2**), protected for SRKW foraging, increased on average by 1.22 km from 2017, when no lateral displacement was enacted, to the 2020 lateral displacement (Vancouver Fraser Port Authority, Unpublished data). However, a large majority of the tug travel in this area was noted in the inbound and outbound shipping lanes, or south of the shipping lanes, in United States waters, outside of the trial period.

During the 2020 study period all tugs north of the outbound shipping lane, or within 8 km of the Jordan River mooring were tracked. During the pre-trial period (April 1-June 1) 24 different tugs and a total of 46 transits were considered. During the trial period (June 1-November 1) 32 different tugs were tracked with a total of 144 transits. This was a significant increase in average daily transit number between pre-trial and trial periods ($t(280.512) = 2.353$, $p = 0.019$, **Figure 8**). Overall, the mean transit distance of tugs from the mooring increased significantly (**Figure 8**; $t(2.029) = 168.051$, $p = 0.044$), by 463 m on average. Passages within 1.5 km of the mooring showed a considerable decrease during the trial period (**Figure 8**). Eighty-two percent of the tugs spent at least of 50% of their transit through the trial zone in the outbound lane or the lateral displacement zone. This was an increase from 76% of transits in the previous year. For tugs that made multiple transits ($n = 11$) in both the pre-trial and trial periods, the distances were either significantly increased ($n = 3$) or unchanged, and already at a distance consistent with the request ($n = 8$). The transit speeds of these vessels were also generally reduced in the displacement and enhanced management zones in Juan de Fuca Strait compared to those in shipping lanes or the traffic separation zone (Vancouver Fraser Port Authority, Unpublished data).

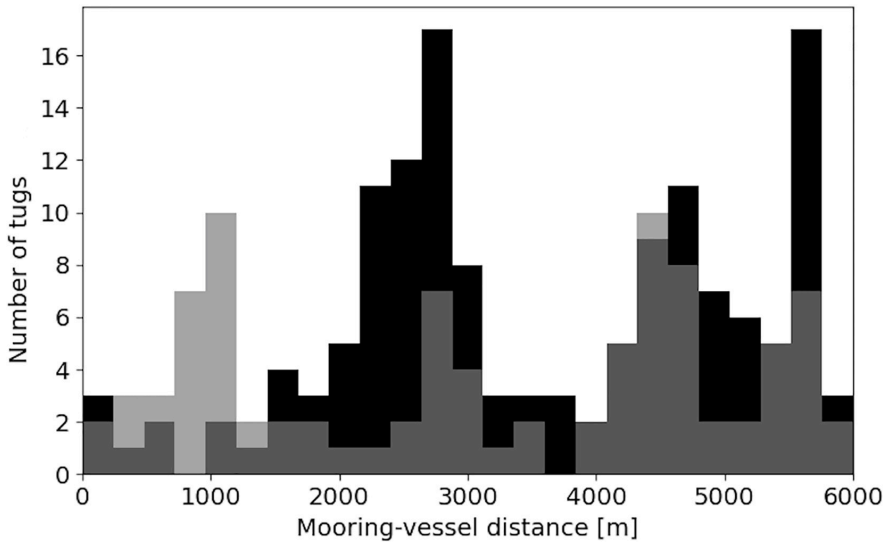

FIGURE 8 | Distribution of nearest approach distances for tugs as they passed the Jordan River mooring (positioned at zero) during the pre-trial period (light) and trial period (black). Darker gray represents where pre- and trial period results overlap.

ISZ Exclusion Compliance

Vessel passages through the ISZs were quantified and expressed for pre-trial and trial periods (**Figure 7**). Generally, the number of vessels (**Figure 7**), and proportion of time with vessels in the ISZs increased as the summer progressed. Swanson Channel showed Class B vessels consistently present, with this vessel type dominating proportionally. The number of vessels within the area around the mooring (**Figure 5**) significantly increased for the period that the ISZ measures were in place compared to the control period ($t(388.406) = 8.102$, $p < 0.001$), and generally increased throughout the summer also. Limited recording time in May, prior to the commencement of the exclusion zone measures, was available for Saturna Island to further act as a control. However, this pre-trial period did feature days with considerable vessel presence (**Figure 7**). In the week of May 13, 2020 AIS records showed several days with vessels present for at least 6 hours per day, and two days exceeding 16 hours from the AIS records. The traffic composition in the Swiftsure Bank ISZ was representative of its proximity to the commercial traffic lanes, as well as being an area use by Class B and smaller, recreational vessels.

Changes in Ambient Noise Levels

Data for periods when current speeds exceeded 0.25 m/s, wind speeds were more than 5 m/s, or when the small vessel detector signaled the presence of non-AIS tracked vessels were removed to more clearly evaluate the efficacy of the vessel slowdowns and lateral displacement. The low-current criterion reduced the number of available minutes of valid data by about 50%, except for the Swanson Channel ISZ where the reduction was only 6%. The corresponding reduction in available minutes due to the wind speed criterion varied between 16 and 46%. The reduction in available minutes to analyze as a result of the small vessel detector ranged between a low of 5% at Jordan River to a high of 18% in the Swanson Channel ISZ (see **Supplementary Table 4**). Therefore, the largest proportion of removals resulted from the restriction of abiotic noise in the ambient levels. Removals of small vessels, following the removal of high wind and current periods, were greatest in the ISZs at Swanson Channel (43%) and Saturna Island (57%), and least at the Swiftsure Bank slowdown mooring. Overall, this process left between 11-34% of the trial data to compare to equally filtered control data, with Jordan River the least affected and Swanson Channel the most. A similar removal of Class A vessels left between 20-62% of the data for an analysis of the changes in ambient noise levels for the Class B vessel presence in ISZs (see **Supplementary Table 4**).

The SPLs derived from the cumulative distribution functions (CDFs), and changes between trial and pre-trials periods showed a decrease in almost all locations and frequency ranges tested at the L_5, L_{50}, and L_{95} exceedance levels (**Table 3** and **Supplementary Table 3**). Considerable decreases were seen for median broadband soundscape frequencies during the slowdown and lateral displacement trial periods compared to the prior two months. Similar declines were seen for the frequency ranges relevant to SRKW (**Table 3**). For Swiftsure Bank, Boundary Pass, and Jordan River reductions were seen most notably in SPL values at median levels, whereas for Haro Strait these reductions were limited to periods when the noise levels were most elevated, at the L_5 exceedance level (**Table 3**). Lesser reductions in SPL were seen in the ISZ recordings when comparing data collected during the slowdown trials were compared to control periods. The ISZ measures on Swiftsure Bank did show notable decreases in the lowest frequencies in ambient noise (L_{95}) levels, unmatched by other moorings (**Supplementary Table 3**).

Slowdown trials at Swiftsure Bank and Boundary Pass resulted in reductions in median noise levels predominantly in the lowest frequency bands (**Supplementary Table 3**). The greatest broadband ambient noise reductions were at Swiftsure Bank as

TABLE 3 | The differences in SPL between pre-trial and trial periods at the L_5, L_{50}, L_{95} exceedance levels are shown for frequency ranges important to SRKW communication (500 Hz to 15 kHz) and echolocation (15–100 kHz).

SPL difference (dB)			
Frequency range (Hz)	**L_{95}**	**L_{50}**	**L_5**
a) Swiftsure Bank, slowdown trial			
10-100000	−0.7	−2.0	−4.9
500-15000	−3.7	−2.0	−0.6
15000-100000	−1.4	−2.2	−2.7
b) Haro Strait, slowdown trial			
10-100000	2.6	−1.6	−3.0
500-15000	0.8	0.2	−1.4
15000-100000	2.8	1.3	−1.6
c) Boundary Pass, slowdown trial			
10-100000	2.8	−2.3	−2.2
500-15000	−4.3	0.8	−0.2
15000-100000	−0.6	−4.3	−0.4
d) Jordan River, lateral displacement, tugs only			
10-100000	0.8	−1.4	−1.2
500-15000	−1.9	−1.9	−3.0
15000-100000	−0.9	−3.3	−4.7
e) Swiftsure ISZ			
10-100000	−4.3	1.8	2.3
500-15000	−4.0	−3.1	9.9
15000-100000	0.2	0.0	−3.6
f) Swiftsure ISZ, class B vessels only			
10-100000	−9.8	1.9	9.1
500-15000	−2.5	−2.2	13.8
15000-100000	−1.2	0.0	−0.4
g) Saturna Island ISZ			
10-100000	−1.2	2.2	2.7
500-15000	−2.4	−3.0	−1.0
15000-100000	−0.1	−0.8	−9.1
h) Saturna Island ISZ, class B vessels only			
10-100000	−2.6	−3.9	5.8
500-15000	−2.2	−8.5	−2.9
15000-100000	−0.1	−2.9	−16.4
i) Swanson Channel ISZ			
10-100000	−0.7	−1.0	0.3
500-15000	−2.1	−2.7	−1.7
15000-100000	0.0	−0.4	0.3
j) Swanson Channel ISZ, class B vessels only			
10-100000	0.5	0.9	3.7
500-15000	0.3	−0.1	1.5
15000-100000	0.2	1.8	2.7

The full soundscape range (10 Hz to 100 kHz) is shown for its potential to impact behavior.

a result of the slowdown action. Boundary Pass comparisons showed the greatest reduction in the SRKW communications band at the L_{95} level, more indicative of a change in background noise (**Table 3**). The greatest reduction in noise in echolocation frequencies came from the median SPL at the same mooring. The Haro Strait mooring showed a similar pattern of declines in SPL, with the more notable reductions seen at the L_5 exceedance level (**Table 3**).

The impact of tug movement in the lateral displacement zone was considered separately because the number of vessels was limited (n = 46 and n = 144, pre-trial and trial periods respectively), and only the impact of the closest approaches of these vessels was considered (**Table 3**). Considerable reductions were seen in the SRKW frequency ranges, with mid- to higher-frequency ranges showing the most noticeable decreases in SPL during the trial period (**Table 3** and **Supplementary Table 3**). The reductions possible from individual tug transits were also quantified. Sixteen individual vessels were identified in the AIS data to have made transits in the management zone in both the pre-trial and trial periods, 11 of these were multiple transits. Eight of these tugs made their journeys at a consistent distance from the mooring in both the control and trial periods, and were already at a distance that complied with the trial and use of the lateral displacement zone. Three of the tugs were found to alter their route in accordance to the lateral displacement trial request. The most significant change showed the closest approach distance in the pre-trial period to be 750 m, which was increased to 1760 m during the trial period. This increase of more than 1 km distance from the mooring reduced overall soundscape levels in the broadband frequency 10 Hz to 100 kHz from 130.6 dB re 1 μPa to 125.3 dB re 1 μPa (−5.3 dB change). Similar reductions in the SRKW communication band (−4.7 dB) and echolocation band (−5.6 dB) were recorded. In both of the SRKW communication frequency ranges, greater reductions were found at Jordan River than could be attributed from changes in tug traffic alone. However, the reverse was true for the reduction in broadband ambient noise, with overall no change at this mooring when all vessel types were considered.

Inclusion of the changes in Class B vessels only for the ISZs in this analysis focused on smaller vessels. Reductions in SPL were considerable in the highest frequency ranges at Saturna Island, whereby changes considering Class B vessels only far outweighed those found when including Class A traffic (**Supplementary Table 3**). This pattern was reversed for Swanson Channel, suggesting that Class B vessels remained in the exclusion zone during the trial period (**Figure 7** and **Table 3**). Although background and median noise levels were reduced for recordings made in the Swiftsure ISZ when measures were in place, these reductions were focused in the low frequencies. The removal of Class A vessels from the recordings showed even greater reductions in these low-frequencies and ambient noise levels (**Table 3**). This was also seen for the Swanson Channel ISZ, with few reductions found at this mooring for the Class B vessel comparison of trial to control (**Figure 5**). Saturna Island ISZ, however, showed much greater reductions when considering only Class B vessels, focused in the mid- to high-frequencies and SRKW bands (**Table 3**).

DISCUSSION

Large scale changes in the acoustic environments of cetaceans are an increasing concern (Tyack, 2008). Vessel presence, and vessel-derived acoustic disturbance is one of three main

factors listed as limiting the population recovery for SRKW (Weilgart, 2007; Lacy et al., 2017; Department of Fisheries and Oceans Canada [DFO], 2018). Whale habitat use in the Salish Sea is associated with the abundance of their salmonid prey (Nichol and Shackleton, 1996; Baird et al., 2005), foraging, or traveling between foraging and wintering habitats (Balcomb and Bigg, 1986; Krahn et al., 2004). The management experiments discussed here encompassed known SRKW summer habitat on Swiftsure Bank, in portions of Juan de Fuca Strait, Haro Strait and the west side of San Juan Island, Swanson Channel, Boundary Pass, and southern portions of the Strait of Georgia (Department of Fisheries and Oceans Canada [DFO], 2017a,b; Olson et al., 2018).

Killer whales use their acoustic senses for navigation and foraging, as well as to maintain contact between conspecifics. Marine traffic creates disturbances that modify behavior, degrades marine environments, and effectively fragments habitat (Pirotta et al., 2019). Noise from vessels has the potential to affect the whales' ability to perform critical life processes through masking. The management measures outlined here are aimed to reduce the impact from vessels. In particular, reducing noise additions to the frequency ranges used by SRKW in echolocation and calling. Also, changes in the spatial extent over which they can communicate or echolocate impacts navigation, foraging success, and group cohesion. Decreased foraging success, for an already nutritionally stressed population (Ford et al., 2009) is a serious challenge to survival.

Compensation techniques in calling, including louder vocalizations, and in altered frequencies, help SRKW maintain acoustic contact in the presence of small vessels as noted by Holt et al. (2009, 2011). This may, however, also alter their energetic balance, expending more energy to call more consistently (Noren et al., 2013; Holt et al., 2015). However, through metabolic studies with dolphins, Noren et al. (2017) suggest the energetic cost of altered acoustics use, especially for echolocation, is negligible compared to other behaviors that might result from vessel presence. Changes in behavior or avoidance of noise sources in foraging areas (Lusseau et al., 2009; Noren et al., 2009, 2016) resulting from the perception of anthropogenic noise as a risk (Tyack, 2008) may further compound its energetic implications. The cumulative cost of these responses is heightened for SRKW as a prey-limited species.

Assessing the efficacy of mitigation programs should take into account both the rate of compliance by vessels to changes in their speed and/or route, and then, knowing the rate of participation in a trial, quantify the reductions of noise in the sound field. All the measures enacted were aimed to balance the effective change in SPL and compliance. Efficacy also should be measured in the frequencies relevant to the focal species for these measures, as we have done using the frequency ranges for SRKW communication and echolocation.

Adaptations of the conservation actions have been made since the trials began in 2017 to both increase participation and reductions in ambient noise level. For the slowdown trials, for example, changes in the trial start time, area, and speed restrictions have resulted in increased noise reductions. As well, the proportion of vessels participating in the trial in 2020 surpassed previous years. The initiation of measures has been based on sightings of SRKW in the Salish Sea since 2018. The whales follow the 'in-migration' of northern Chinook salmon *(Oncorhynchus tshawytscha)* populations, which typically occurs from April to September (Waples et al., 2004). Chinook salmon is the near-sole prey for this period for SRKW, with fish from the Fraser River comprise up to 90% of their diet at this time in these inland waters (Hanson et al., 2010, 2021); however, there have been large fluctuations in salmon abundance and survival in the Salish Sea (Ruff et al., 2017), and stocks are depleted (Nelson et al., 2019). These losses have been linked to habitat degradation, over-harvest, and changing ecosystem conditions (Lawson, 1993; Ruckelshaus et al., 2002; Peterson and Schwing, 2003; Ward et al., 2015). In recent years, SRKW have reduced their residency times in the Salish Sea, and have been noted to have been absent between April and June, entering these waters increasingly later in the summer (Shields et al., 2018; Hanson et al., 2021).

Vessel presence was most altered by COVID-19 restrictions in pre-trial rather than trial periods, although restrictions and advisories to limit travel remained in place throughout. The week-by-week reductions in noise levels in the Strait of Georgia reported by Thomson and Barclay (2020) in January to April 2020 were not seen in our data, nor were the reductions in commercial vessel traffic they reported in comparison to previous years. We, therefore, have not made any attempt to correct the comparison between the control and trial periods to account for these restrictions.

For Boundary Pass and Haro Strait, pilot-reported participation (91%) exceeded that of previous years, including 2019 where the request was the same for distance and speed. The reductions in broadband ambient noise were similar to previous trial years (Joy et al., 2019; MacGillivray et al., 2019). However, the greatest SPL changes were noted in the lower frequencies in prior studies. During the 2020 trial there were also reductions in the mid- to high-frequencies for median and background (L_{95}) exceedance levels for Boundary Pass, and in the upper sound limits in Haro Strait (L_5; **Table 3** and **Supplementary Table 3**). Previous trials had not noted SPL reductions for frequencies greater than 15 kHz. This may result from the removal of small vessels from the analysis, which typically add to higher frequencies, and are seasonally increased during the trial period (**Figure 6**). The slowdown at Swiftsure Bank was introduced in 2020, and showed a high rate of participation. However adjustment in transit speeds from pre-trial to trial were not as great as those for the slowdown zone in the inner waters, especially for container vessels (**Table 2**). Despite this, changes in median ambient noise levels were recorded, predominantly in the low frequencies (**Supplementary Table 3**), with the change between the control and trial period in these frequencies greater than those calculated for Haro Strait and Boundary Pass. The changes in noise levels at frequencies pertinent to SRKW (Branstetter et al., 2017; Heise et al., 2017) showed greatest change at Boundary Pass for the slowdown measures, and were at their least in the adjoining Haro Strait (**Table 3**). The differences in acoustic levels and changes in ambient noise between the slowdown trial zones could be attributed to differing topography, distances between moorings and vessel passage, and water

property profiles (Warner et al., 2020), as well as the different composition of vessel traffic (**Figure 6**).

Noise emissions differ by vessel class. Container ships emit the greatest sound levels of the Class A vessels tracked in this study. Each transit has the capacity to elevate noise relative to ambient by approximately 20 dB, focused in the 125 Hz to 20 kHz range (Veirs et al., 2016). Similar levels have been noted for bulkers and cargo vessels (Veirs and Veirs, 2006; Veirs et al., 2016). The greater proportion of deep-sea and tug traffic at Swiftsure Bank compared to the Haro Strait and Boundary Pass zone (**Figure 6**), may have instigated the larger reduction in low-frequency bands despite the reduction of speed between zones. Regressions between the source level of vessel emissions and speed (SOG) have shown a linear relationship in the order of 0.93 dB per knot (1.8 dB per m/s) for broadband source levels for the vessels transiting through the slowdown zones, likely to vary within a range of 0.2-3.4 dB dependent on vessel class (Veirs et al., 2016). Our examination of SPL change was done through aggregate vessel classes, but several other factors may influence the acoustic output other than speed, including the vessel draft, size, loading, and maintenance schedule (International Maritime Organization [IMO], 2014).

A reduction in speed by deep-sea and passenger vessels to 11 knots minimizes the amount of lost whale foraging time in excess of 10% (Joy et al., 2019). Although a reduction of speed results in lower acoustic inputs, it also extends transit times, and so has the potential to increase the overall exposure time to vessel noise for SRKW. However, notable increases in the percentage of time with Class A vessels in proximity to the moorings was not seen at the commencement or during the slowdowns, suggesting that the benefits in reducing the overall sound exposure levels in the whales' soundscape in these areas was not at the expense of SRKW exposure time.

The lateral displacement trial of tugs and barges has shown both a good rate of participation, and reduction of the noise in both the broadband and higher frequencies in all years. The results shown here build on previous success (Vagle and Neves, 2019; Vagle, 2020). The reduction in noise as a result of moving tugs away from SRKW critical habitats was noticeable. The reductions were not as great as noted in 2019 for the trial reported here, but compares well to the initial results in 2018 which had reductions between 4.3–5.8 dB resulting from altered tug transit routes (Vagle and Neves, 2019). The reductions in 2019 were aided by a general reduction in shipping traffic (Vagle, 2020). The probability of closest approach in the trial period was increased from within 2 km of the mooring, with higher participation in displacement trial in 2020 than in previous years. Moreover, tugs were generally taking a route more distant to the mooring outside of the trial. It should be noted that some of the tug transits were port-to-port and so would not be subject to the lateral displacement measures. These were not included in the transit numbers used to measure participation, but they would still be present in the AIS and acoustic data streams.

The physical presence and proximity of vessels has been demonstrated to hinder foraging behaviors, with changes in dive patterns and lost feeding opportunities reported (Williams et al., 2006, 2009, 2014; Lusseau et al., 2009; Noren et al., 2009; Holt et al., 2021). The greater maneuverability of tugs compared to other vessel types has allowed a shift in transit routes resulting in an increased distance between them and SRKW foraging habitat (Department of Fisheries and Oceans Canada [DFO], 2017a,b). This is more feasible than a complete rerouting of shipping lanes. By putting greater space between the areas used by the whales and the vessel transit routes, the displacement measures reduce the disturbance from physical presence, while also decreasing the risk of vessel strikes. The significance of individual tugs voluntarily altering their routes was seen with reductions of approximately 5 dB in both the overall soundscape and SRKW frequencies used for calling and echolocation, resulting directly from an increase of 1 km in transit distance from the mooring.

Following the results of these trials, modeling exercises have been used to assess further mitigation actions. An additional westward shift of the existing traffic lanes through Haro Strait, and southward shift of the outbound lane through Juan de Fuca Strait, for example, has been suggested to further reduce noise levels in areas critical for SRKW (Matthews et al., 2018). In areas where safe transit lanes are limited, as they are in the Salish Sea, the creation or alteration of shipping lanes may not be possible. Instead, re-direction of some vessel types or speed reductions are more easily achieved and can succeed in reducing the vessel impacts (Vanderlaan and Taggart, 2007; Conn and Silber, 2013; Laist et al., 2014). This is also true for species whose presence and movements are less predictable, or show changes in presence over space and time as is increasingly noted for SRKW in the Salish Sea (Hanson et al., 2021).

Exclusion of vessels from the ISZs had the lowest levels of compliance. Swiftsure Bank showed very little change, if any, between the proportion and time spent by vessels between pre-trial and test periods. However, there were considerable reductions in the ISZ recordings. This suggests that the recordings at this mooring may also be affected by the slowdown measures in place in the traffic lane proximal to the ISZ (**Figures 1**, **3** and **Table 3**). This could also be indicated by the most notable changes in SPL being focused in the lower-frequencies, even when focusing on changes in the presence of Class B vessels in the ISZ (**Supplementary Table 3**). The presence of commercial vessel was low (**Figure 7**), and the probability density analysis showed Class A vessels did not travel within 2 km of the ISZ mooring, which further suggests the changes may be a result of the proximal slowdown. The ISZs in the Gulf Islands also typically showed low compliance, although the time with, and presence of vessels (**Figure 7**) was much less than the management area on Swiftsure Bank. The noise reductions at Swanson Channel were focused in the low-frequencies, and those representing vessel presence. Changes from pre-trial were greatest only when considering Class A vessels, suggesting that Class B and recreation vessels may be prevalent while the ISZ was in place, which was confirmed by the AIS data (**Figure 7**). The change in ferry passages over time, as COVID-19 restrictions were eased through the summer, was considered principally for its effect on the sound field in the Swanson Channel ISZ. On a more regional scale, as considered

here, ferries can make substantial additions to the soundscape. The number of ferry transits to Otter Bay and through the Gulf Islands were consistent between July and October 2020. The recordings from the Swanson Channel mooring showed decreases in SPL despite the increase of traffic, both from ferries and smaller recreational vessels (**Figure 7**). The Saturna Island ISZ showed the lowest vessel presence during the trial period (**Figure 7**). However, the comparison between this and baseline levels in the month before, especially for Class B vessels (**Table 3** and **Figure 7**) indicates an inflated reduction due to intense vessel activity just before the commencement of the exclusion. This is believed to be a result of the installation and testing of an underwater listening station from mid- to late-May. The pre-trial period was half of the other ISZs, as recordings prior to May 9 were not available. For the ISZs, as with all the management measures assessed, we were only able to demonstrate the compliance by AIS-tracked vessels. Assessment of changes in behavior by recreational mariners is much harder to measure, and remains a significant gap in our analysis. Whether the contributions from small vessels would surpass those of commercial vessels, especially on localized scales, is currently not possible to establish. However, their addition to the sound field could be considerable based on their high number, high speed, and use of coastal areas in the Salish Sea. Unchanged or increased SPL levels in the decadal bands compared to the control pre-trial recordings, especially in the 100–1000 Hz range (**Supplementary Table 3**), considered with the proportional composition of vessel traffic at each site (**Figure 7**) suggests that the use of the management zones by smaller Class B and recreational vessels remained high, or indeed increased, as the summer and trial period progressed. Until the presence and acoustic additions of small vessels are better characterized, we may underestimate the impacts of vessel noise on cetacean species, especially those in coastal waters.

Our conclusions are limited by the reliance on AIS data to characterize vessel presence, especially when establishing compliance to ISZs. Many vessels known to use these areas, such as pleasure craft and fishing vessels, are not required to transmit AIS data. Even for vessels where transceivers are required, the cooperation of vessel captains is needed. For terrestrial AIS there are gaps in coverage between base stations as the broadcasts are approximately line-of-sight, which may reduce the reliability of the spatial data. The broadcasts are also subject to human error in data input, data corruption, signal noise, and instrument failure (Aarsæther and Moan, 2009; McGillivary et al., 2009; Silber and Bettridge, 2010; Robards et al., 2016).

Our ambient noise recordings have shown that considerable changes in SPLs can be exacted with relatively small changes. The change in slowdown measures between years by 0.5 to 1 knot, depending on vessel type, showed increased reductions between 2018 and 2019 (Joy et al., 2019). As well, the altered route of tugs and barges, a relatively small component of the vessel traffic through Juan de Fuca Strait and other management areas, reduced noise in the sound field. Also, we found changes by single vessels can have a noteworthy impact. Most significantly, all trial zones showed reductions in the SRKW communication and echolocation frequency ranges (**Table 3**).

The limitations of vessel transit speed and route alteration, as analyzed here, are operational measures designed to reduce the vessel noise impacts on an endangered species using habitat areas deemed critical for its survival. A reduction in anthropogenic noise reduces the impact of lost echolocation and communication ability that is required for locating and capturing prey. An alternative approach would be source-based, whereby vessel design is altered from the outset, or the existing fleet is retrofitted to reduce their source levels (Veirs et al., 2017). A more regular maintenance schedule is also an effective means of reducing a vessel's acoustic impact (International Maritime Organization [IMO], 2014). Operational measures can be enacted more proactively, and are typically applied on a local scale and for shorter times. Source-base initiatives are longer term measures that are being considered by the ECHO program and its collaborators, with the potential for port incentives to be provided to the quieter vessels. These would have a more global and long-term effect.

A combination of both source and operational measures will be the most effective route for decreasing the additions of noise in the acoustic environment in the Salish Sea. A clear and coordinated approach for managers, with additional effort given to raising mariners' awareness, is needed to maintain and increase participation. Additional measures such as vessel convoying and greater restrictions in timing or transit zones are yet to be fully explored. This may increase the length of quiet periods between vessel transits for SRKW.

A high level of stakeholder collaboration and regulatory incentive to follow management directives was key to the successes experienced in similar management programs in other critical whale habitats (Wiley et al., 2013; Ebdon et al., 2019). In other regions where speed reductions are in place, vessel compliance is reported directly to the operating company (e.g., Right Whale Corporate Responsibility Card for vessels in Stellwagen Bank) or openly online (e.g., the Whale Safe Tool for vessels in the Santa Barbara Channel) to increase adherence to the speed limits in future transits.

The high rates of voluntary participation in the slowdown and displacement trials we describe here suggests there is promise in the application of these measures to reduce human impact on the soundscape, even without regulatory backing. Commercial vessel noise and disturbance has been identified as the greatest threat to SRKW success, after the decline in prey availability (Lacy et al., 2017). Whereas Chinook stock enhancements and increased habitat quality involve complex solutions over time, the measures described here can have an immediate benefit on whales transiting or foraging in the Salish Sea. Enforcement at current levels may increase compliance further, and prevent compensatory behavior to try and make up lost time by increasing speed in other areas, for example. In this study, voluntary measures demonstrated a higher-level of compliance than those mandated, although a program to heighten awareness of the measures may further increase voluntary participation before the introduction of more regulatory measures are needed. The enforcement of the ISZ would also greatly benefit from increased awareness as to the location and rationale of the conservation measures. What is yet to be determined are the full behavioral

implications that each of these measures has on SRKW. Increased knowledge of whale response, and both short- and long-term consequences of vessel-based acoustic disturbance will enhance the accurate design, prioritization, and implementation of effective management plans.

DATA AVAILABILITY STATEMENT

The raw data supporting the conclusions of this article will be made available by the authors, without undue reservation.

AUTHOR CONTRIBUTIONS

RB and SV led the conception and design of the work, data collection and analysis, and analyzed and interpreted the data. CO'N provided technical expertise in the field and with the AMAR systems for data collection. KT provided details from the POV on the trials, vessel transits and participation. RB drafted the work. All authors revised, provided review and revisions, and final approval of the work.

FUNDING

This work was funded by the Government of Canada's Ocean Protection Plan.

ACKNOWLEDGMENTS

The authors would like to thank Peter Van Buren, Christie Morrison and Harald Yurk for help with acquiring the data and time spent in the field. Thanks also must go to the officers and crew on CCGS VECTOR for all their help with servicing our hydrophone moorings in the Salish Sea.

SUPPLEMENTARY MATERIAL

The Supplementary Material for this article can be found online at: https://www.frontiersin.org/articles/10.3389/fmars.2021.664691/full#supplementary-material

Supplementary Table 1 | Hydrophone mooring locations and the management measures they are used to assess.

Supplementary Table 2 | Coordinates for the extents of the Interim Sanctuary Zones in 2020.

Supplementary Table 3 | Comparison of sound pressure levels (SPLs) at the L_5, L_{50}, L_{95} exceedance levels in decadal bands, overall soundscape (10 Hz-100 KHz) and frequency ranges important to SRKW. The absolute SPL values and differences between in SPL for pre-trial and trial periods are shown.

Supplementary Table 4 | Iterative filtering process of data vessel minutes (VM) to remove tide noise, then wind noise then small vessel (Class B) noise. Analyzed Class A VM are those representing the presence of tanker, bulkers, container ships, or vehicle carriers. Class B VM the removal of Class A presence is done before the removal of tide- or wind-effected vessel minutes.

REFERENCES

Aarsæther, K. G., and Moan, T. (2009). Estimating navigation patterns from AIS. *J. Navig.* 62, 587–607. doi: 10.1017/s0373463309990129

Au, W. W. L., Ford, J. K. B., Horne, J. K., and Allman, K. A. N. (2004). Echolocation signals of free- ranging killer whales (*Orcinus orca*) and modeling of foraging for chinook salmon (*Oncorhynchus tshawytscha*). *J. Acoust. Soc. Am.* 115, 901–909. doi: 10.1121/1.1642628

Baird, R. W., Hanson, M. B., and Dill, L. M. (2005). Factors influencing the diving behaviour of fish eating killer whales: sex differences and diel and interannual variation in diving rates. *Can. J. Zool.* 83, 257–267. doi: 10.1139/z05-007

Balcomb, K. C., and Bigg, M. A. (1986). "Population biology of three resident killer whale pods in Puget Sound and off southern Vancouver Island," in *Behavioural Biology of Killer Whales*, eds B. C. Kirkevold and J. S. Lockard (New York, NY: Alan R. Liss), 85–95.

Branstetter, B., St Leger, J., Acton, D., Stewart, J., Houser, D., Finneran, J. J., et al. (2017). Killer whale (*Orcinus orca*) behavioral audiograms. *J. Acoust. Soc. Am.* 141:2387. doi: 10.1121/1.4979116

Center for Whale Research (2021). *Southern Resident Orca Community Demographics, Composition of Pods, Births and Deaths Since 1998*. Harbor, WA: Center for Whale Research.

Clark, C., Ellison, W., Southall, B., Hatch, L., Van Parijs, S. M., Frankel, A., et al. (2009). Acoustic masking in marine ecosystems: intuitions, analysis, and implication. *Mar. Ecol. Prog. Ser.* 395, 201–222. doi: 10.3354/meps08402

Cominelli, S., Leahy, M., Devillers, R., and Hall, G. B. (2019). Geovisualization tools to inform the management of vessel noise in support of species' conservation. *Ocean. Coastal. Mang.* 169, 113–128. doi: 10.1016/j.ocecoaman.2018.11.009

Conn, P. B., and Silber, G. K. (2013). Vessel speed restrictions reduce risk of collision-related mortality for North Atlantic right whales. *Ecosphere* 4, 1–16. doi: 10.1890/ES13-00004.1

Department of Fisheries and Oceans Canada [DFO] (2017a). *Evaluation of the Scientific Evidence to Inform the Probability of Effectiveness of Mitigation Measures in Reducing Shipping-Related Noise Levels by Southern Resident Killer Whales*. DFO Can. Sci. Advis. Sec. Sci. Advis. Rep. 2017/041. Ottawa: DFO.

Department of Fisheries and Oceans Canada [DFO] (2017b). *Identification of Habitats of Special Importance to Resident Killer Whales (Orcinus orca) off the West Coast of Canada*. DFO Can. Sci. Advis. Sec. Sci. Advis. Rep. 2017/011. Ottawa: DFO.

Department of Fisheries and Oceans Canada [DFO] (2018). *Recovery Strategy for the Northern and Southern Resident Killer Whales (Orcinus orca) in Canada*. Ottawa: Fisheries & Oceans Canada, 10–84.

Ebdon, P., Riekkola, L., and Constantine, R. (2019). Testing the efficacy of ship strike mitigation for whales in the Hauraki Gulf, New Zealand. *Ocean Coast. Manag.* 184:10503.

Ford, J. K. B. (1989). Acoustic behaviour of resident killer whales (*Orcinus orca*) off Vancouver Island, British Columbia. *Can. J. Zool.* 67, 727–745. doi: 10.1139/z89-105

Ford, J. K. B., Ellis, G. M., Olesiuk, P. F., and Balcomb, K. C. (2009). Linking killer whales survival and prey abundance: food limitation in the oceans' apex predator? *Biol. Lett.* 6, 139–142.

Groot, C., Margolis, L., and Bailey, R. (1984). "Does the route of seaward migration of Fraser River sockeye salmon (Oncorhynchus nerka) smolts determine the route of return migration of the adults?," in: *Mechanisms of migration in fishes*, eds J. D. McCleave G. P. Arnold J. J. Dodson, and W.H. Neill (New York, NY: Plenum Press), 283–292.

Hannah, C. G., Dupont, F., Collins, A. K., Dunphy, M., and Greenberg, D. (2008). Revisions to a Modelling System for Tides in the Canadian Arctic Archipelago. *Can. Tech. Rep. Hydrogr. Ocean Sci.* 259, 6–62.

Hanson, M., Baird, R., Ford, J., Hempelmann-Halos, J., Van Doornik, D., Candy, J., et al. (2010). Species and stock identification of prey consumed by endangered southern resident killer whales in their summer range. *Endang. Sp. Res.* 11, 69–82. doi: 10.3354/esr00263

Hanson, M. B., Emmons, C. K., Ford, M. J., Everett, M., Parsons, K., Park, L. K., et al. (2021). Endangered predators and endangered prey: seasonal diet of

Southern Resident killer whales. *PLoS One* 16:e0247031. doi: 10.1371/journal.pone.0247031

Hauser, D. D., Logsdon, M. G., Holmes, E. E., Van Blaricom, G. R., and Osborne, R. W. (2007). Summer distribution patterns of southern resident killer whales *Orcinus orca*: core areas and spatial segregation of social groups. *Mar. Ecol. Prog. Ser.* 351:301. doi: 10.3354/meps07117

Heimlich-Boran, J. R. (1988). Behavioral ecology of killer whales (*Orcinus orca*) in the Pacific Northwest. *Can. J. Zool.* 66, 565–578. doi: 10.1139/z88-084

Heise, K. A., Barrett-Lennard, L. G., Chapman, N. R., Dakin, D. T., Erbe, C., Hannay, D. E., et al. (2017). Proposed metrics for the management of underwater noise for Southern Resident killer whales. *Coastal Ocean Rep. Ser.* 2:30.

Holt, M. M., Noren, D. P., Dunkin, R. C., and Williams, T. M. (2015). Vocal performance affects metabolic rate in dolphins: implications for animals communicating in noisy environments. *J. Exp. Biol.* 218, 1647–1654.

Holt, M. M., Noren, D. P., and Emmons, C. K. (2011). Effects of noise levels and call types on the source levels of killer whale calls. *J. Acoust. Soc. Am.* 130, 3100–3106. doi: 10.1121/1.3641446

Holt, M. M., Noren, D. P., Veirs, V., Emmons, C. K., and Veirs, S. (2009). Speaking up: killer whales (*Orcinus orca*) increase their call amplitude in response to vessel noise. *J. Acoust. Soc. Am.* 125, EL27–EL32. doi: 10.1121/1.3040028

Holt, M. M., Tennessen, J. B., Ward, E. J., Hanson, B. E., Emmons, C. K., Giles, D. A., et al. (2021). Effects of vessel distance on sex on the behavior of Endangered killer whales. *Front. Mar. Sci.*:582182. doi: 10.3389/fmars.2020.582182

International Maritime Organization [IMO] (2014). *Guidelines for The Reduction of Underwater Noise from Commercial Shipping to Address Adverse Impacts on Marine Life. The Marine Environment Protection Committee, MEPC. 1/Circ.833*. London: IMO.

Joy, R., Tollit, D., Wood, J., MacGillivray, A., Li, Z., Trounce, K., et al. (2019). Potential benefits of vessel slowdowns on endangered southern resident killer whales. *Front. Mar. Sci.* 6:344. doi: 10.3389/fmars.2019.00344

Klinck, H., Nieukirk, S. L., Mellinger, D. K., Klinck, K., Matsumoto, H., and Dziak, R. P. (2012). Seasonal presence of cetaceans and ambient noise levels in polar waters of the North Atlantic. *J. Acoust. Soc. Am.* 132, EL176–EL181.

Krahn, M. M., Ford, M. J., Perrin, W. F., Wade, P. R., Angliss, R. P., Hanson, M. B., et al. (2004). *2004 Status review of southern resident killer whales (Orcinus orca) under the Endangered Species Act. Technical Memo 2004, NMFS-NWFSC-62*. Seattle, WA: U.S. Dept. Commerce, NOAA.

Lacy, R. C., Williams, R., Ashe, E., Balcomb, K. C. III, Brent, L. J. N., Clark, C. W., et al. (2017). Evaluating anthropogenic threats to endangered killer whales to inform effective recovery plans. *Sci. Rep.* 7:14119.

Laist, D. W., Knowlton, A. R., and Pendleton, D. (2014). Effectiveness of mandatory vessel speed limits for protecting North Atlantic right whales. *Endanger. Species Res.* 23, 133–147. doi: 10.3354/esr00586

Lawson, P. W. (1993). Cycles in ocean productivity, trends in habitat quality, and restoration of salmon runs in Oregon. *Fisheries* 18, 6–10. doi: 10.1577/1548-8446(1993)018<0006:ciopti>2.0.co;2

Lusseau, D., Bain, D. E., Williams, R., and Smith, J. C. (2009). Vessel traffic disrupts the foraging behavior of southern resi- dent killer whales *Orcinus orca*. *Endang. Species. Res.* 6, 211–221. doi: 10.3354/esr00154

Ma, B. B., Nystuen, J. A., and Lien, R.-C. (2005). Prediction of underwater sound levels from rain and wind. *J. Acoust. Soci. Am.* 117, 3555–3565. doi: 10.1121/1.1910283

MacGillivray, A., Li, Z., and Yurk, H. (2017). *Modelling of Cumulative Vessel Noise for Haro Strait Slowdown Trial: Phase 1: Pre-trial Interim Report. Document Number 01443. Version 1.0*. Tokyo: JASCO.

MacGillivray, A. O., Li, Z., Hannay, D. E., Trounce, K. B., and Robinson, O. (2019). Slowing deep-sea commercial vessels reduces underwater radiated noise. *J. Acoust. Soc. Am.* 146, 340–351. doi: 10.1121/1.5116140

Matthews, M.-N. R., Alavizadeh, Z., Hannay, D. E., Horwich, L., and Frouin-Mouy, H. (2018). *Assessment of Vessel Noise within the Southern Resident Killer Whale Critical Habitat: Final Report. Document number 01618, Version 2.1*. Canada: Transport Canada/Government of Canada.

McGillivary, P. A., Schwehr, K. D., and Fall, K. (2009). "Enhancing AIS to improve whale-ship collision avoidance and maritime security," in *Proceedings of the OCEANS 2009, MTS/IEEE Biloxi - Marine Technology for Our Future: Global and Local Challenges*, Biloxi, MS, 1–8.

Medwin, H., Nystuen, J. A., Jacobus, P. W., Ostwald, L. H., and Snyder, D. E. (1992). The anatomy of underwater rain noise. *J. Acoust. Soc. Am.* 92, 1613–1623. doi: 10.1121/1.403902

Merchant, N. D., Fristrup, K. M., Johnson, M. P., Tyack, P. L., Witt, M. J., Blondel, P., et al. (2015). Measuring acoustic habitats. *Methods Ecol. Evol.* 6, 257–265. doi: 10.1111/2041-210X.12330

Merchant, N. D., Witt, M. J., Blondel, P., Godley, B. J., and Smith, G. H. (2012). Assessing sound exposure from shipping in coastal waters using a single hydrophone and Automatic Identification System (AIS) data. *Mar. Poll. Bull.* 64, 132–1329. doi: 10.1016/j.marpolbul.2012.005.004

Mouy, X., Wladichuk, J. L., and Austin, M. E. (2020). *Modelling Acoustic Detection Ranges of Resident Killer Whales. Document 02241, Version 1.0*. Ottawa: Fisheries and Oceans Canada.

National Oceanic and Atmospheric Administration [NOAA] (2005). *Endangered and Threatened Wildlife and Plants: Endangered Status for Southern Resident Killer Whales*. Department of Commerce. Rules and Regulations. 50 CFR Part 224. Washington, DC: NOAA.

Nelson, B. W., Shelton, A. O., Anderson, J. H., Ford, M. J., and Ward, E. J. (2019). Ecological implications of changing hatchery practises in Chinook salmon in the Salish Sea. *Ecosphere* 10:e02922.

Nichol, L. M., and Shackleton, D. M. (1996). Seasonal movements and foraging behaviour of northern resident killer whales (*Orcinus orca*) in relation to the inshore distribution of salmon (*Oncorhynchus* spp.) in British Columbia. *Can. J. Zool.* 74, 983–991. doi: 10.1139/z96-111

Noren, D., Holt, M. M., Dunkin, R. C., and Williams, T. M. (2017). Echolocation is cheap for some mammals: dolphins conserve oxygen while producing high-intensity clicks. *J. Exp. Mar. Bio. Ecol.* 495:1002. doi: 10.1016/j.jembe.2017.07.002

Noren, D. P., Holt, M. M., Dunkin, R. C., and Williams, T. M. (2013). The metabolic cost of communicative sound production in bottlenose dolphins (*Tursiops truncatus*). *J. Exp. Biol.* 216, 1624–1629. doi: 10.1242/jeb.083212

Noren, D. P., Holt, M. M., Dunkin, R. C., Thometz, N. M., and Williams, T. M. (2016). Comparative and cumulative energetic costs of odontocete responses to anthropogenic disturbance. *Proc. Meetings on Acou.* 27:040008 doi: 10.1121/2.0000299

Noren, D. P., Johnson, A. H., Rehder, D., and Larson, A. (2009). Close approaches by vessels elicit surface active behaviors by southern resident killer whales. *Endang. Species Res.* 8, 179–192. doi: 10.3354/esr00205

Nystuen, J. A. (1996). Acoustic rainfall analysis: rainfall drop size distribution using the underwater sound field. *J. Atmosph. Ocean. Tech.* 13, 74–84. doi: 10.1175/1520-0426(1996)013<0074:arards>2.0.co;2

Nystuen, J. A., and Ma, B. (2002). "Using ambient sound to passively monitor sea surface processes," in *Proceedings of the Sixth Pan Ocean Remote Sensing Conference (PORSEC)*, eds B. P. Pasaribu, R. Kaswadji, I. W. Nurjava, and J. L. Gaol (New York, NY: PORSEC Association), 9–14.

Olson, J. K., Wood, J., Osborne, R. W., Barrett-Lennard, L., and Larson, S. (2018). Sightings of southern resident killer whales in the Salish Sea 1976-2014: the importance of a long-term opportunistic dataset. *Endang. Species. Res.* 37, 105–118. doi: 10.3354/esr00918

Pensieri, S., Bozzano, R., Nystuen, J. A., Anagnostou, E. N., Anagnostou, M. N., and Bechini, R. (2015). Underwater acoustic measurements to estimate wind and rainfall in the Mediterranean Sea. *Adv. Meteorol.* 2015:612512.

Peterson, W. T., and Schwing, F. B. (2003). A new climate regime in northeast Pacific ecosystems. *Geophys. Res. Lett.* 30:4.

Pirotta, V., Grech, A., Jonsen, I. D., Laurance, W. F., and Harcourt, R. G. (2019). Consequences of global shipping traffic for marine giants. *Front. Ecol. Environ.* 17, 39–47. doi: 10.1002/fee.1987

Raverty, S., St. Leger, J., Noren, D. P., Burek-Huntington, K., Rotstein, D. S., Gulland, F. M. D., et al. (2020). Pathology findings and correlations with body condition index in stranded killer whales (*Orcinus orca*) in the northeastern Pacific and Hawaii from 2004 to 2013. *PLoS One* 15:e0242505. doi: 10.1371/journal.pone.0242505

Richardson, W. J., Greene, C. R. Jr., Malme, C. I., and Thomson, D. (1995). *Marine Mammals and Noise*. San Diego, CA: Academic Press.

Robards, M. D., Silber, G. K., Adams, J. D., Arroyo, J., Lorenzini, D., Schwehr, K., et al. (2016). Conservation science and policy applications of the marine vessel automatic identification system (AIS)–a review. *Bull. Mar. Sci.* 92, 75–103. doi: 10.5343/bms.2015.1034

Ruckelshaus, M. H., Levin, P., Johnson, J. B., and Kareiva, P. M. (2002). The Pacific salmon wars: what science brings to the challenge of recovering species. *Ann. Rev. Ecol. System.* 33, 665–706. doi: 10.1146/annurev.ecolsys.33.010802.150504

Ruff, C. P., Anderson, J. H., Kemp, I. M., Kendall, N. W., and Mchugh, A. (2017). Salish Sea Chinook salmon exhibit weaker coherence in early marine survival trends than coastal populations. *Fish. Ocean.* 26, 625–637. doi: 10.1111/fog.12222

Shields, M. W., Lindell, J., and Woodruff, J. (2018). Declining spring usage of core habitat by endangered fish-eating killer whales reflects decreased availability of their primary prey. *Pac. Cons. Biol.* 24, 189–193. doi: 10.1071/PC17041

Silber, G. K., and Bettridge, S. (2010). *Vessel Operations in Right Whale Protection Areas in 2009. NOAA Technical Memorandum NMFS-OPR-44*. Silver Spring, MD: NOAA.

Thomson, D. J. M., and Barclay, D. R. (2020). Real-time observations of the impact of COVID-19 on underwater noise. *J. Acoust. Soc. Am.* 147:3390. doi: 10.1121/10.0001271

Towers, J. R., Ford, J. K. B., and Ellis, G. M. (2012). Digital photo-identification dataset management and analysis: testing protocols using a commercially available application. *Can. Tech. Rep. Fish. Aquat. Sci.* 2978, 6–16.

Transport Canada (2020). *Minister Garneau Announces Extended Measures for Cruise Ships and Pleasure Craft in Canada*. Ottawa, ON: Transport Canada.

Tyack, P. (2008). Implications for marine mammals of large-scale changes in the marine acoustic environment. *J. Mammal.* 89, 549–558. doi: 10.1644/07-mamm-s-307r.1

Vagle, S. (2020). Evaluation of the efficacy of the Juan de Fuca lateral displacement trial and Swiftsure Bank plus Swanson Channel interim sanctuary zones, 2019. *Can. Tech. Rep. Hydrogr. Ocean Sci.* 332, 6–60.

Vagle, S., Large, W. G., and Farmer, D. M. (1990). An evaluation of the WOTAN technique of inferring oceanic winds from underwater ambient sound. *J. Atmosph. Ocean. Tech.* 7, 576–595. doi: 10.1175/1520-0426(1990)007<0576:aeotwt>2.0.co;2

Vagle, S., and Neves, M. (2019). Evaluation of the effects on underwater noise levels from shifting vessel traffic away from Southern Resident Killer Whale foraging areas in the Strait of Juan de Fuca in 2018. *Can. Tech. Rep. Hydrogr. Ocean Sci.* 329, 6–64.

Vanderlaan, A. S. M., and Taggart, C. T. (2007). Vessel collisions with whales: the probability of lethal injury based on vessel speed. *Mar. Mamm. Sci.* 23, 144–156. doi: 10.1111/j.1748-7692.2006.00098.x

Veirs, S., Veirs, V., Williams, R., Jasny, M., and Wood, J. (2017). A key to quieter seas: half of ship noise comes from 15% of the fleet. *PeerJ* 6:e26525v1.

Veirs, S., Veirs, V., and Wood, J. (2016). Ship noise in an urban estuary extends to frequencies used for echolocation by endangered killer whales. *PeerJ* 3:e955v3. doi: 10.7287/peerj.preprints.955v3

Veirs, V., and Veirs, S. (2006). *Average Levels and Power Spectra of Ambient Sound in the Habitat of Southern Resident Orcas*. Washington, DC: NOAA/NMFS/NWFSC.

Waples, R. S., Teel, D. J., Myers, J. M., and Marshall, A. R. (2004). Life-history divergence in Chinook Salmon: historic contingency and parallel evolution. *Evolution* 58, 386–403. doi: 10.1111/j.0014-3820.2004.tb01654.x

Ward, E. J., Anderson, J. H., Beechie, T. J., Pess, G. R., and Ford, M. J. (2015). Increasing hydroplogic variability threatens depleted anadromous fish populations. *Glob. Change Biol.* 21, 2500–2509. doi: 10.1111/gcb.12847

Warner, G. A., Wood, J. D., MacGillivray, A. O., Li, Z., Frouin-Mouy, H., Tollit, D., et al. (2020). "Chapter 1. Hydroacoustic monitoring," in *Proceedings of the ECHO Program 2019 Voluntary Vessel Slowdown Hydroacoustic Studies: Final Report* (Washington, DC: NOAA).

Weilgart, L. (2007). The impacts of anthropogenic ocean noise on cetaceans and implications for management. *Can. J. Zool.* 85, 1091–1116. doi: 10.1139/z07-101

Wiley, D., Hatch, L., Thompson, M., Schwehr, K., and MacDonald, C. (2013). Marine sanctuaries and marine planning: protecting endangered marine life. *Proc. Mar. Saf. Secur. Counc.* 70, 10–15.

Williams, R., Bain, D. E., Smith, J. C., and Lusseau, D. (2009). Effects of vessels on behavior patterns of individual Southern Resident killer whales *Orcinus orca*. *Endang. Species Res.* 6, 199–209. doi: 10.3354/esr00150

Williams, R., Erbe, C., Ashe, E., Beerman, A., and Smith, J. (2014). Severity of killer whale behavioral responses to ship noise: a dose–response study. *Mar. Poll. Bull.* 79, 254–260. doi: 10.1016/j.marpolbul.2013.12.004

Williams, R., Hedley, S. L., and Hammond, P. S. (2006). Modeling distribution and abundance of Antarctic baleen whales using ships of opportunity. *Ecol. Soc.* 11:28.

Conflict of Interest: The authors declare that the research was conducted in the absence of any commercial or financial relationships that could be construed as a potential conflict of interest.

Publisher's Note: All claims expressed in this article are solely those of the authors and do not necessarily represent those of their affiliated organizations, or those of the publisher, the editors and the reviewers. Any product that may be evaluated in this article, or claim that may be made by its manufacturer, is not guaranteed or endorsed by the publisher.

Copyright © 2021 Burnham, Vagle, O'Neill and Trounce. This is an open-access article distributed under the terms of the Creative Commons Attribution License (CC BY). The use, distribution or reproduction in other forums is permitted, provided the original author(s) and the copyright owner(s) are credited and that the original publication in this journal is cited, in accordance with accepted academic practice. No use, distribution or reproduction is permitted which does not comply with these terms.

frontiers in Marine Science

REVIEW
published: 05 August 2021
doi: 10.3389/fmars.2021.674594

Distance-Based Sampling Methods for Assessing the Ecological Effects of Offshore Wind Farms: Synthesis and Application to Fisheries Resource Studies

Elizabeth T. Methratta[1,2]*

[1] IBSS Corporation, Silver Spring, MD, United States, [2] Northeast Fisheries Science Center, National Oceanic and Atmospheric Administration – National Marine Fisheries Service, Woods Hole, MA, United States

Renewable energy, sustainable seafood, and a healthy marine ecosystem are integral elements of a sustainable blue economy. The rapid global advancement of offshore wind coupled with its potential to affect marine life compels an urgent need for robust methodologies to assess the impacts of this industry on fisheries resource species. Basic Before-After-Control-Impact (BACI) and Control-Impact (CI) designs are the most common experimental designs used to study the effects of offshore wind development on fisheries resources. These designs do not account for spatial heterogeneity which presents a challenge because empirical evidence shows that impact gradients occur at wind farms, with larger effect sizes close to turbine foundations that attenuate with increasing distance. Combining the before-after sampling design with distance-based methods could provide a powerful approach for characterizing both the spatial and temporal variance associated with wind development. Toward enhancing future monitoring designs for fisheries resource species at offshore wind farms, this paper aims to: (1) examine distance-based sampling methods that have been or could potentially be used to study impacts on fisheries resources at offshore wind farms including distance-stratified BACI, distance-stratified CI, Before-After-Gradient (BAG), and After-Gradient (AG) methods; (2) synthesize the methods and findings of studies conducted to date that have used distance-based methods to examine ecological impacts of offshore wind development for benthic macroinvertebrates, finfish, birds, and small mammals; (3) examine some of the central methodological elements and issues to consider in developing distance-based impact studies; and (4) offer recommendations for how to incorporate distance-based sampling methods into monitoring plans at offshore wind farms.

Keywords: BACI, gradient, BAG, marine renewable energy, methodology, sampling design

OPEN ACCESS

Edited by:
Juan Jacobo Schmitter-Soto, The South Border College (ECOSUR), Mexico

Reviewed by:
Stephen Buckland, University of St Andrews, United Kingdom
Mauro Sinopoli, Stazione Zoologica Anton Dohrn Napoli, Italy

***Correspondence:**
Elizabeth T. Methratta
Elizabeth.Methratta@noaa.gov

Specialty section:
This article was submitted to Marine Ecosystem Ecology, a section of the journal Frontiers in Marine Science

Received: *01 March 2021*
Accepted: *13 July 2021*
Published: *05 August 2021*

Citation:
Methratta ET (2021) Distance-Based Sampling Methods for Assessing the Ecological Effects of Offshore Wind Farms: Synthesis and Application to Fisheries Resource Studies. Front. Mar. Sci. 8:674594. doi: 10.3389/fmars.2021.674594

INTRODUCTION

Offshore wind is a rapidly advancing industry around the world. Along the Atlantic coast of the United States, there are currently 17 commercial leases (**Figure 1**), and additional areas on the Pacific coasts of California and Hawaii are being explored for possible development. The potential effects of wind development on marine fisheries resource species (i.e., finfish and shellfish

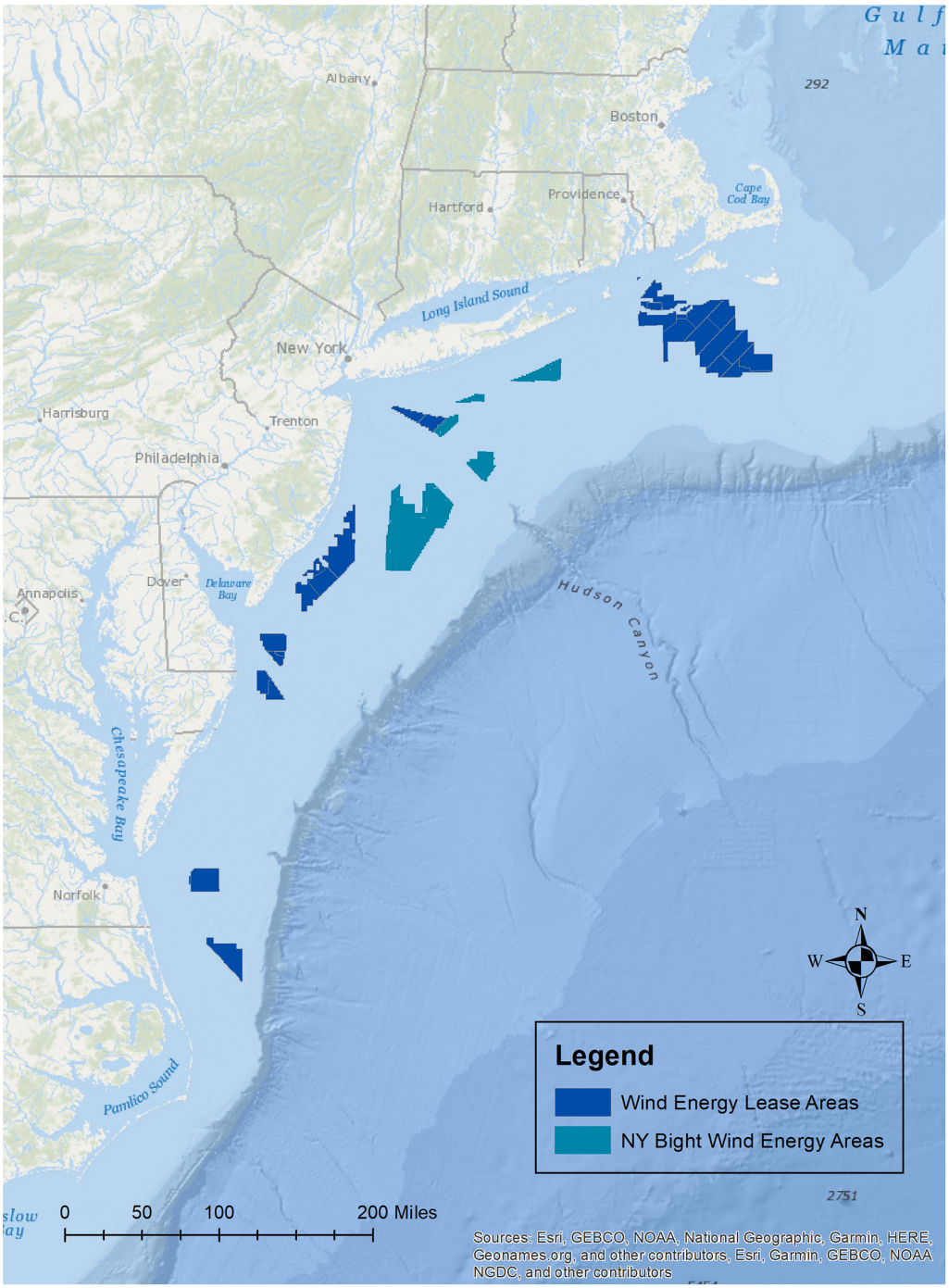

FIGURE 1 | Map of the current offshore wind lease areas off of the Atlantic coast of the United States, and the New York Bight wind energy areas to be leased.

including mollusks and crustaceans), and their habitats have gained major attention because of their ecological and economic importance and because of the implications that these effects may have for fishing communities (Gill et al., 2020; Methratta et al., 2020; Perry and Heyman, 2020). Effects on these taxa may occur through several impact producing factors (IPFs) that occur during each stage of development and that span multiple spatial and temporal scales (**Figure 2**; Degraer et al., 2019, 2020; Dannheim et al., 2020; Gill et al., 2020; Hutchison et al., 2020; Mooney et al., 2020). Robust methods to detect biological responses to these IPFs are needed in order to inform mitigation practices and fisheries management (Wilding et al., 2017).

Statistically robust monitoring designs are essential for detecting the ecological impacts of anthropogenic development

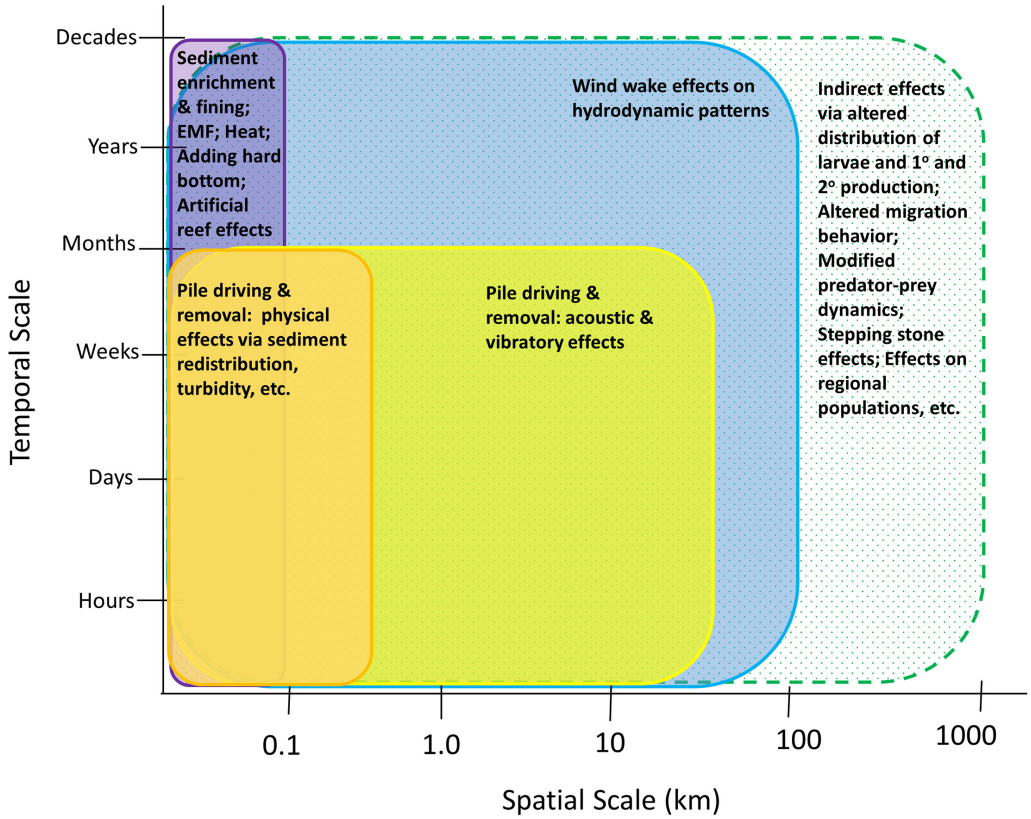

FIGURE 2 | Hypothesized spatial and temporal scales of IPFs that may affect fisheries resource species during the construction and operation phases. Solid bars indicate IPFs and their effects; the hatched bar indicates the potential scales of indirect effects.

in marine ecosystems (Franco et al., 2015; Van Hoey et al., 2019; Christie et al., 2020). Perhaps the method that has received the most attention and application is the Before-After-Control-Impact or BACI design (Green, 1979) which samples a treatment and control site prior to and after the intervention and then identifies impacts through statistical comparisons of sampling locations and time periods. In marine ecosystems, BACI has proven to be a useful tool in demonstrating effects due to such anthropogenic interventions as sewage spills, aquaculture, and fisheries exclusion (Smith et al., 1999; Aguado-Giménez et al., 2012; Moland et al., 2013).

Basic BACI and Control-Impact (CI; similar to BACI but samples after the intervention only) are the most common experimental designs used to study effects on fisheries resource species at offshore wind farms (OWFs) (Methratta, 2020). Typically sites are selected through a simple random process within the impact and control locations; in some instances sampling stations are kept within a specific environmental envelope to reduce variability among sites (e.g., similar depths or distances from shore). A strength of BACI is its emphasis on baseline data collection which enables comparisons between pre and post-intervention patterns. Although common, BACI and CI studies have generally reported either weak or inconsistent effects of OWFs on fisheries resource species (e.g., Vandendriessche et al., 2015). The limitations of the BACI design in the OWF context (i.e., the assumption of spatial homogeneity, the uncertainly of the scale of OWF effects, and the difficulty in finding suitable controls) (**Table 1**; Methratta, 2020) have spurred an interest in enhancing or replacing the BACI experimental design (Lindeboom et al., 2015).

Distance-based designs, in which samples are collected at relative distances from the OWF structures (Ellis and Schneider, 1997), offer several methodological advantages. Notably, they directly address issues of spatial heterogeneity and scale and can eliminate the need for a control (**Table 1**). The limited number of distance-based studies that have been conducted for fisheries resource species have revealed spatial gradients in the effects that OWFs have on these species following construction, with larger effect sizes near the structures that attenuate with increasing distance (e.g., Wilhelmsson et al., 2006; Methratta and Dardick, 2019). Lacking baseline information, these studies are unable to compare post-construction patterns with the reference condition, making it difficult to determine with certainty how the intervention interacted with the pre-construction ecosystem to drive the patterns observed. This highlights the need to collect robust baseline data to assess impacts at OWFs.

Impact assessment in aquatic and terrestrial ecosystems has long benefited from distance-based methods (e.g., Whittaker, 1967; Ellis and Schneider, 1997; Buckland et al., 2015). In coastal marine ecosystems, distance-based methods have demonstrated

TABLE 1 | Comparison of pros and cons of the simple BACI design with enhanced sampling methods that include distanced-based sampling.

Methodological issue	Basic BACI	Distance-stratified BACI	Distance-stratified CI	After-gradient (AG)	Before-after-gradient (BAG)
Control site selection	−	−	−	+	+
Spatial heterogeneity	−	+	+	+	+
Spatial scale	−	+	+	+	+
Comparison of post-construction to baseline	+	+	−	−	+

Plus sign indicates an advantage of the design and a negative sign indicates a challenge of the design.

gradients around artificial reefs (e.g., Davis et al., 1982; Reeds et al., 2018), oil and gas platforms (Ellis and Schneider, 1997), and area closures (Harmelin-Vivien et al., 2008) in the distribution, abundance, and diversity of marine organisms. As with OWF investigations, these studies often collect data only after the intervention, focusing primarily on post-intervention spatial variation with less attention paid to pre vs. post intervention changes. Although in some instances post-intervention sampling is the only practicable option because structures are already in place at the time that a monitoring plan is conceived, the absence of "before" data limits the information that can be gained from the study. Combining the before-after sampling design with distance-based methods can provide a powerful approach for characterizing both the spatial and temporal variance associated with OWF development.

Toward enhancing future monitoring designs for fisheries resource species at offshore wind farms, the goals of this paper are to: (1) examine distance-based sampling methods that have been or could potentially be used to study impacts on fisheries resources at OWFs including distance-stratified BACI, distance-stratified CI, Before-After-Gradient (BAG), and After-Gradient (AG) methods; (2) synthesize the methods and findings of studies conducted to date that have used distance-based methods to examine ecological impacts for benthic macroinvertebrates, demersal finfish, birds, and small mammals; (3) examine some of the methodological elements and issues central to developing distance-based impact studies; and (4) offer recommendations for incorporating distance-based sampling methods into monitoring plans at OWFs.

BEFORE-AFTER-CONTROL IMPACT DESIGN: OVERVIEW AND APPLICATION TO OFFSHORE WIND STUDIES

The Before-After-Control-Impact (BACI) design has been the cornerstone of experimental design in the field of ecological impact assessment for nearly four decades (e.g., Smokorowski and Randall, 2017). In that time, recommendations have been made for sample size selection, statistical analysis, and outcome interpretation (Underwood, 1992, 1994; Stewart-Oaten and Bence, 2001). Some of the central issues surrounding BACI discussed widely in the literature have included pseudoreplication (sensu Hurlbert, 1984), spatial autocorrelation, and temporal autocorrelation, with recommendations made for alternate designs such as paired control-impact sites (Stewart-Oaten et al., 1986), use of random time points (Underwood, 1991), and use of multiple controls (Underwood, 1991, 1992, 1993, 1994). Although no definitive consensus emerged from these papers on the best way to resolve the issues associated with BACI designs, these discussions have provided ecologists with a broader perspective of BACI issues and a larger suite of tools with which to modify the BACI design to answer specific questions in their systems. This is important because BACI remains one of the most popular methodologies in ecological impact assessment.

At OWFs, simple BACI and CI designs are the most common design used to study ecological impacts for fisheries resource species. In general, these studies have sought to examine how a single wind farm affects abundance, biomass, diversity, size, distribution, or community composition. Interactions with wind development, although typically studied as an overarching "wind farm effect," are in reality an aggregate of multiple IPFs that may be operating in the system during each phase of development (Degraer et al., 2019; Dannheim et al., 2020; Gill et al., 2020; Hutchison et al., 2020; Mooney et al., 2020). Generally, studies using these designs have reported either weak or inconsistent effects for fish species (e.g., Vandendriessche et al., 2015). There are numerous reasons for this including that: the simple BACI design does not explicitly address spatial heterogeneity; the scales of IPFs and their direct and indirect ecological effects are often not known; and it is often difficult to find suitable control locations (Methratta, 2020). That our understanding of wind farm interactions with fisheries resource species remains limited despite more than two decades of offshore wind development worldwide suggests that the approaches used to study these effects need to be enhanced.

DISTANCE-BASED SAMPLING METHODS AT OFFSHORE WIND FARMS

Before-After Designs

Distance-Stratified BACI

A distance-stratified BACI design is similar to a simple BACI design except that the impact area would be spatially stratified with respect to distance from the turbines and sites then randomly selected within these strata. As a before-after design, BACI is able to compare post-construction patterns to baseline conditions and to potentially distinguish impacts from other dynamic factors (e.g., fishing pressure) when data on those factors are available (Christie et al., 2020). Enhancing BACI by creating

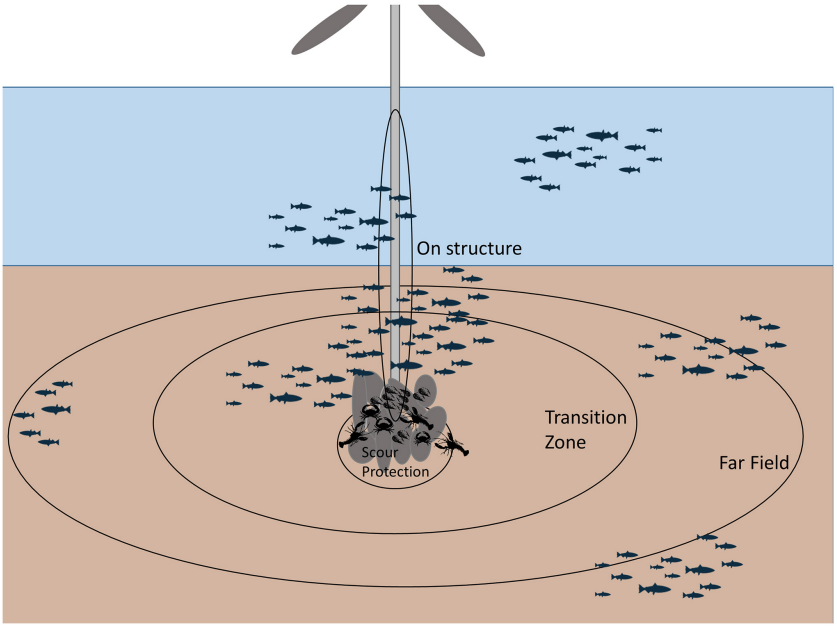

FIGURE 3 | Diagram of gradient-based sampling design with data collected on-structure, within the scour protection, within a transition zone, and at a far-field distance.

distance strata would address spatial heterogeneity and allow for an exploration of the scale of effect (**Table 1**). However, this design retains the difficulties of finding suitable control locations and the reliance upon these controls to assess impacts. Although spatially stratified BACI is not a common approach for offshore wind studies, stratifying the BACI design by habitat has been reported. For example, Degraer et al. (2013) used a habitat-stratified BACI design to explore ecological responses in the two dominant habitats present within a wind farm (i.e., sand banks and gullies). In doing so, this study was able to partition out the variance attributable to habitat differences and demonstrate a significant positive wind farm effect on epibenthic biomass, sea star (*Asterias rubens*) density, and sole (*Solea solea*) density in sand bank habitats that did not occur in gully habitats (Degraer et al., 2013).

Before-After-Gradient (BAG)

A BAG design samples at relative distances from the turbines in both the pre and post construction time periods (**Figure 3**; **Table 1**; Ellis and Schneider, 1997). As a before-after design, BAG retains the advantage of spatially stratified BACI in being able to compare post-construction patterns to baseline conditions and has the potential to distinguish impacts from other dynamic factors operating in and around the project area when these data are also available (Christie et al., 2020). BAG also has the additional advantage of not requiring a control location. Holding sampling effort constant, BAG has the potential to have greater statistical power compared to the basic BACI design because the variance associated with both spatial and temporal heterogeneity can be included in the explanatory terms of statistical models rather than being relegated to the error term (Mackenzie et al., 2013). There are no published examples of a BAG design for fisheries resource species at OWFs; however, this design has emerged as a leading approach in studying how small mammals and birds are affected by wind development (e.g., Thompson et al., 2010; Joint Nature Conservation Committee [JNCC], 2015) and has also been proposed as a method to study sea turtles at wind farms (Kraus et al., 2019). A related method, the Before-During-Gradient (BDG) design, samples distances both before and during the impact and has been used to examine effects of pile driving on small mammals (Tougaard et al., 2009; Dähne et al., 2013).

After-Construction Only Designs

Distance-Stratified Control-Impact (CI)

Like distance-stratified BACI, distance-stratified CI would rely on a control to assess impacts. Because this design would sample only during the post-construction time period, baseline data are lacking, and thus pre and post construction patterns cannot be compared. Post-construction temporal variation could be explored if sampling were repeated through time. Nevertheless, in instances where the study design is conceived only after the turbines are installed, this approach could be useful for characterizing spatial patterns and effects. There are no reported examples of this design being used for fisheries resource studies at OWFs.

After-Gradient (AG)

As with BAG, an After-Gradient (AG) design (Ellis and Schneider, 1997) samples at relative distances from the turbines and does not require a control; however, samples are collected in the post-construction time period only (e.g.,

Petersen and Fox, 2007; **Table 1**; **Figure 3**). As with distance-stratified CI, this design lacks the ability to compare post-construction effects to baseline conditions; however, there are several reported examples of its utility for characterizing post-construction spatial patterns and effects (e.g., Bergström et al., 2013; Stenberg et al., 2015). Post-construction spatio-temporal changes can also be explored if multiple time points are sampled after the intervention. This design has been used in the study of finfish, benthic invertebrates, and birds at wind farms (e.g., Coates et al., 2014).

WHAT HAS BEEN LEARNED FROM DISTANCE-BASED SAMPLING AT OFFSHORE WIND FARMS SO FAR?

The current state of knowledge of spatial patterns at OWFs learned through the application of distance-based methods is synthesized in this section for benthic invertebrates (**Table 2**), demersal finfish (**Table 3**), small marine mammals (**Table 4**), and birds (**Table 5**). Each study summarized in **Tables 2–5** reported an analysis of data collected for discrete distance categories, along continuous transects, or of tagged animals or echolocation clicks at relative distances from the turbines. Across taxa, distance-based studies have found distinct patterns along spatial gradients.

Benthic Invertebrates

The primary distance-based sampling method for benthic invertebrates has been the After-Gradient design (**Table 2**). For sediment macrofauna, these studies have generally shown that sediment grain size increases with increasing distance from turbine structures while species abundance, density, and richness as well as sediment organic content decreases with increasing distance (Wilhelmsson and Malm, 2008; Coates et al., 2014; Griffin et al., 2016; Lefaible et al., 2019; Braeckman et al., 2020; HDR, 2020; Hutchison et al., 2020; Lu et al., 2020). Changes in sediment characteristics and benthic community composition near the foundations are attributed to deposition of organic materials that fall from the structures (De Mesel et al., 2015). For epibenthic invertebrates, changes in communities along spatial gradients have also been observed with distance-based methods. Wilhelmsson et al. (2006) found an increased percent cover of mussels (*Mytilus trossulus*) and decreased percent cover of algae (*Polysiphonia fucoides and Rhodomela confervoides*) closer to turbines. Griffin et al. (2016) reported that communities shifted from species more characteristic of hard bottom environments at the turbines (e.g., European lobster, *Homarus gammarus*; Edible crab, *Cancer pagurus*) to those more characteristic of soft bottoms (e.g., Norwegian Lobster, *Nephrops norvegicus*) further away from turbines. Studies by Lefaible et al. (2018, 2019) and Braeckman et al. (2020) found higher macroinvertebrate abundances and distinct patterns of community structure nearer to the turbine structures for two wind farms that were approximately 16 km apart; however, the dominant species near the turbines differed between the two wind farms. At Block Island Wind Farm in the United States, dense aggregations of blue mussels (*Mytilus edulis*) were reported under and around the foundations compared to distances further away 4 years following construction (HDR, 2020; Hutchison et al., 2020).

Finfish

All distance-based studies of finfish at OWFs have used an After-Gradient design (**Table 3**). These studies have consistently demonstrated strong directional effects on demersal or reef-associated finfish. Reported effects have included higher levels of abundance and density at or very close to turbines ($\leq$50 m) for species such as two-spotted goby (*Gobiusculus flavescens*), sand goby (*Pomatoschistus Minutus*), cod (*Gadus morhua*), eel (*Anguilla anguilla*), shorthorn sculpin (*Myoxocephalus scorpius*), goldsinny wrasse (*Ctenolabrus rupestris*), and *Scyliorhinus* species (Wilhelmsson et al., 2006; Bergström et al., 2013; Reubens et al., 2013; Griffin et al., 2016). Species richness, taxa richness, and species diversity were generally higher closer to turbine structures (Stenberg et al., 2015; Griffin et al., 2016), although Wilhelmsson et al. (2006) found lower species diversity closer to turbines due to the dominance of two-spotted goby (*Gobiusculus flavescens*) in the community. Concurrent with an AG study that collected samples at distances ranging from 20 to 140 m from the turbines, Bergström et al. (2013) also conducted a BACI study; the BACI study sampled randomly selected sites ranging from 130 to 1,350 m from turbine foundations and found no effects of offshore wind development on the fish community. The contrasting outcomes of these concurrent studies highlight the importance of the spatial scale of sampling and the possibility that important effects could be missed if the nearest sampling stations are $>$100+ m from turbine foundations.

Peer-reviewed field studies of pelagic finfish and invertebrates at offshore wind farms are scarce in the literature. Although pelagic fish have been reported to occur at turbines (e.g., Mavraki et al., 2019), studies that have included pelagic species have generally not employed distance-based methods and have not reported clear patterns in relation to OWF structures (Stenberg et al., 2015; Floeter et al., 2017; van Hal et al., 2017; Karama et al., 2021). In laboratory settings, the IPFs associated with OWF development have demonstrable effects on pelagic species (Jones et al., 2021; Klimely et al., 2021). Although rare in the OWF literature, pelagic species have been the frequent focus of research at other manmade offshore structures including oil and gas platforms and artificial reefs where clear evidence of an aggregation effect has been demonstrated (e.g., Munnelly et al., 2020). The spatial and temporal patterns of finfish including pelagic species at manmade structures other than wind turbines is the subject of many recent reviews (Bolser et al., 2020; Munnelly et al., 2020; Paxton et al., 2020; Snodgrass et al., 2020). Much more research is needed in order to understand the scope, scale, and magnitude of effect that OWF development has on pelagic fish and invertebrate species and distance-based methods could aid these efforts.

Marine Mammals

Distance-based approaches, including After-Gradient, Before-After-Gradient, and Before-During-Gradient designs, have demonstrated changes in activity patterns, spatial variation in recovery times, and spatial variability in relative density in

TABLE 2 | Studies of benthic invertebrates that used a gradient design to examine the effects of OWF development.

Gradient design type	Groups studied	OWF factor studied	Distances from turbine (m) or (km)	Biological indices measured	Sampling modality	Analytical method	References
AG	Benthic community species; sediment enrichment	Physical presence of turbine foundations; habitat modification	15, 25, 50, 100 and 200 m distance, starting from the edge of the scour protection boulders	Biomass or ash free dry weight by species; total abundance, total number of species, sediment grain size, organic matter content	Van Veen grab	Multivariate and univariate permutational ANOVA	Coates et al. (2014)
AG	Fish and macroinvertebrates including European lobster (*Homarus gammarus*), Norway lobster (*Nephrops norvegicus*) and edible crab (*Cancer pagurus*); motile crustaceans, large predatory fish, bottom dwellers	Physical presence of turbine foundations; addition of hard-bottom habitat	0 m, 100 m, 4000 m	Species relative abundance (N_{max} or maximum number of fish recorded at any one time), diversity, age structure	Stereo BRUV	ANOVA; Kruskal–Wallis ANOVA with Dunn's comparisons	Griffin et al. (2016)
AG	Macrobenthic community including annelids, nematoda, crustaceans, and mollusks	Physical presence of turbine foundations; habitat modification	30–49 m, 50–69 m, and 70–90 m	Sediment grain size and organic content; macrofaunal community composition, abundance, evenness, diversity, dominance	Smith McIntyre grab sampler; paired with seabed video to provide broader contextual information of the surrounding area	ANOVA; Kruskal–Wallis with Tukey–Kramer comparisons; ANOSIM and Permanova+; PERMDISP	HDR (2019, 2020)
AG	Macrobenthic community including amphipods, polychaetes, annelids, nemerteans	Physical presence of turbine foundations; habitat modification	37.5 m (near) and 350–500 m (far)	Grain size distribution; total organic content; biomass; abundance; diversity; evenness	Van Veen grab	ANOVA; PERMANOVA; PERMDISP; PCO; SIMPER; CLUSTER; DistLM	Lefaible et al. (2018, 2019); Braeckman et al. (2020)
AG	Macroinvertebrates including annelids, mollusks, arthropods, echinoderms	Physical presence of turbine foundations; habitat modification	15, 25, 50, 100, and 200 m.	Abundance, sediment grain size, organic matter content	Van Veen grab	PERMANOVA; BIOENV	Lu et al. (2020)
AG	Macrobenthic community including crustaceans and mollusks; both epibiota and motile invertebrates and algae	Physical presence of turbine foundations; addition of hard-bottom habitat; habitat modification	0 m, 2 m, and 20 m	Biomass; assemblage structure	Diver collected samples using a quadrat and a putty knife	ANOSIM; SIMPER; Wilcoxon Matched Pairs Test, ANCOVA	Wilhelmsson and Malm (2008)
AG	Species included two-spotted goby (*Gobiusculus flavescens*) and sand goby (*Pomatoschistus minutus*); cottids; sessile attached inverts and algae	Physical presence of turbine foundations; addition of hard-bottom habitat	0 m; 1–5 m; 20 m; controls = 500 m and 1000 m	Fish abundance; percent cover of dominant sessile species	Visual scuba	Wilcoxon's Matched Pairs Test; ANOSIM and SIMPER	Wilhelmsson et al. (2006)

TABLE 3 | Studies of finfish that used a gradient design to examine the effects of OWF development.

Gradient design type	Groups studied	OWF factor studied	Distances from turbine (m) or (km)	Biological indices measured	Sampling modality	Analytical method	References
AG	Eel (*Anguilla anguilla*); cod (*Gadus morhua*); shorthorn sculpin (*Myoxocephalus scorpius*); gold-sinny wrasse (*Ctenolabrus rupestris*); eelpout (*Zoarces viviparus*); flounder (*Platichthys flesus*); black goby (*Gobius niger*); other less abundant species	Physical presence of turbine foundations; habitat modification	Transects running from 20 to 140 m from turbines; additional samples at 1350 m	Abundance	Fyke nets	GLM	Bergström et al. (2013)
AG	Fish and macroinvertebrates including European lobster (*Homarus gammarus*), Norway lobster (*Nephrops norvegicus*) and edible crab (*Cancer pagurus*); motile crustaceans, large predatory fish, bottom dwellers	Physical presence of turbine foundations; habitat modification	0 m, 100 m, 4000 m	Species relative abundance, diversity, age structure	Stereo BRUV	ANOVA; Kruskal–Wallis ANOVA with Dunn's comparisons	Griffin et al. (2016)
AG	Atlantic cod (*Gadus morhua*)	Physical presence of turbine foundations;	20 distances: 5, 10, 15, 20, 25, 30, 35, 40, 45, 50, 60, 70, 80, 90, 100, 110, 120, 130, 140, 150 m	Average relative percentages of detections	Acoustic telemetry of tagged fish	Qualitative summary of detection data	Reubens et al. (2013)
AG	Demersals; rocky reef species; most common species were whiting *Merlangius merlangus;* dab *Limanda limanda,* and sandeels *Ammodytidae* spp.	Physical presence of turbine foundations; habitat modification	near (0 to 100 m), middle (120 to 220 m) and far (230 to 330 m)	Abundance	Demersal multi-mesh gillnets	GLMM	Stenberg et al. (2015)
AG	Multiple species including dab *Limanda limanda;* sole *Solea solea*; cod (*G. morhua*), edible crab (*Cancer pagurus*)	Physical presence of turbine foundations; habitat modification	0–15 (scour); 15–25 m (transition zone); >25–589 m	Abundance per 10s	Dual-Frequency Identification Sonar (DIDSON)	Zero inflated negative binomial (ZINB) model	van Hal et al. (2017)
AG	Two-spotted goby (*Gobiusculus flavescens*) and sand goby (*Pomatoschistus minutus*); cottids; fish; sessile attached inverts and algae	Physical presence of turbine foundations; habitat modification	0 m; 1–5 m; 20 m; controls = 500 m and 1000 m	Fish abundance; percent cover of dominant sessile species	Visual scuba	Wilcoxon's Matched Pairs Test; ANOSIM and SIMPER	Wilhelmsson et al. (2006)

TABLE 4 | Studies of marine mammals that used a gradient design to examine the effects of OWF development.

Gradient design type	Groups studied	OWF factor studied	Distances from turbine (m) or (km)	Biological indices measured	Sampling modality	Analytical method	References
BAG	Harbor porpoise *Phocoena phocoena*	Acoustic effects of pile driving	2.5 km 3.2 km, 4.8 km, 10.1 km, 17.8 km, 21.2 km	Porpoise positive minutes per hour (PPM/h)	Passive acoustic monitoring	GAM	Brandt et al. (2011)
BAG	Harbor seals *Phoca vitulina*	Acoustic effects of pile driving	Data from satellite and GPS tags	Presence via telemetry	Satellite tags; GPS phone tags	CReSS	Russell et al. (2016)
BAG and BDG	Harbor porpoise *Phocoena phocoena*	Acoustic effects of pile driving and wind farm operation	<4 km, 7.5 km, 21 km	Interval between encounters	Passive acoustic monitoring	GLMM	Tougaard et al. (2009)
BDG	Harbor porpoise *Phocoena phocoena*	Acoustic effects of pile driving	12 distances from 1 to 50 km away from pile driving; 8–10.8; 7.4–9.8; 2.3–4.6; 3.0–4.2; 0.5–2.5; 2.3–4.7; 4.5–7.0; 2.5–4.5; 7.2–9.2; 23–25; 25.2–26; 48.7–50.5 km	Detection-positive 10 min (10 min periods with at least one porpoise click train detection); waiting times (interval length of periods of more than 10 min without detections given in minutes)	Passive acoustic monitoring with 12 positions	GAM; GLMM; GAMM	Dähne et al. (2013)
BG	Harbor porpoise *Phocoena phocoena*		Parallel transects at 10 km intervals running across wind farm and outside wind farm	Animal density	Aerial visual survey	GLM; ANOVA; GAMM	Gilles et al. (2009)

response to pile driving activity primarily for harbor porpoise (*Phocoena phocoena*) at OWFs (Tougaard et al., 2009; Brandt et al., 2011; Dähne et al., 2013; **Table 4**). These studies placed passive acoustic monitoring devices at multiple distances from the source of impact and recorded echolocation clicks produced by passing animals before and then during (Dähne et al., 2013), after (Brandt et al., 2011), or both during and after (Tougaard et al., 2009) pile driving. In response to pile driving, porpoise activity was reduced by 100% for the first hour and remained below typical levels for 24–72 h out to a distance of 2.6 km from the pile driving site (Brandt et al., 2011). The period of inactivity decreased with increasing distance out to 17.8 km, and at 22 km and beyond, there was no measurable change in activity (Brandt et al., 2011). Dähne et al. (2013) reported a reduced detection rate within 10.8 km of pile driving and increased activity at 25 km and 50 km suggesting displacement of animals. Displacement was also reported by Tougaard et al. (2009) but there was no spatial gradient detected which the authors suggest is because the impact of pile driving on harbor porpoise extended beyond the 20 km extent of the study. Russell et al. (2016) used satellite and GPS phone tags to monitor the movement of harbor seals before and during pile driving and during operation, finding that animals were displaced as much as 25 km during pile driving but that there was no measureable displacement during operation. A pre-construction aerial gradient survey conducted by Gilles et al. (2009) identified spatial and seasonal gradients in porpoise density and potential foraging hotspots in areas where OWFs are currently licensed or planned.

Marine Birds

Displacement following wind farm construction is the most common response reported for distance-based studies (primarily AG and BAG studies) of avian species at OWFs with reductions in abundance up to 92% reported in some instances (Petersen et al., 2004, 2014; Welcker and Nehls, 2016; Mendel et al., 2019) although attraction has been reported for some species (Welcker and Nehls, 2016; **Table 5**). Utilizing aerial digital, aerial visual, or ship-based visual surveys, these studies have generally found that density increased with increasing distance from wind farms. A reduction in loon (Red throated loon *Gavia stellate* and Black-throated loon *G. arctica*) density out to 16 km was observed by Mendel et al. (2019) while Petersen et al. (2004, 2014) found a reduction in divers (i.e., loons) (Red-throated diver *Gavia stellata* and Black-throated Divers *Gavia arctica*) out to 14 km and in Common scoter (*Melanitta nigra*) out to 10 km. Conversely, some studies have demonstrated attraction to OWFs for some species including Herring Gull (*Larus argentatus*), Little Gull (*Hydrocoloeus minutus*), and Arctic/Common tern (*Sterna paradisaea/Sterna hirundo*) (Petersen et al., 2004) perhaps for foraging opportunities. Welcker and Nehls (2016) identified the distance at which there was an asymptote in bird densities for several groups including alcids, divers, and little gulls. In a study of migratory patterns of several species

TABLE 5 | Studies of avian species that used a gradient design to examine the effects of OWF development.

Gradient design type	Groups studied	OWF factor studied	Distances from turbine (m) or (km)	Biological indices measured	Sampling modality	Analytical method	References
BAG	Waterbird species including cormorant *Phalacrocorax carbo*; geese *Anserini*; dabbling ducks *Anas* sp.; eider *Somateria mollissima*; other diving ducks such as red-breasted merganser *Mergus serrator*; gulls *Laridae*; passerines *Passeriformes*	Physical presence of turbines at an operating wind farm	Parallel transects at 0 m, 50 m, 100 m, 200 m, 300 m, 400 m, 500 m, 1000 m; 2000 m; 3000 m; 4000 m; 5000 m; 6000 m from the most easterly row of turbines	Flock size; orientation of migration routes; probability that waterbird passes through OWF	Stationary visual observers; ship-board radar	GLM	Kahlert et al. (2004)
BAG	Loons (*Gavia* spp.); red throated loon (*Gavia stellata*) and black-throated loons (*G. arctica*)	Physical presence of turbines at an operating wind farm	Transects running through wind farm; 3 km and 10 km radii out to 20 km away	Density	Aerial and ship-board visual survey	GAM; GAMM	Mendel et al. (2019)
BAG	Several species; Most abundant were common scoter *Melanitta nigra* and herring gull *Larus argentatus*	Physical presence of turbines at an operating wind farm	Parallel transects at 2 km intervals running across wind farm and outside wind farm	Density	Aerial visual survey	Chi-squared comparison of Jacobs selectivity index (D)	Petersen et al. (2004)
BAG	Several species including divers (*Gavia* spp.), common scoter (*Melanitta nigra*), long tailed duck (*Clangula hyemalis*), herring gull (*Larus argentatus*), little gull (*Larus minutus*), kittiwake (*Laridae*), terns (*Sterna* spp.), and auks (*Alcidae*)	Physical presence of turbines at an operating wind farm	Parallel transects at 2 km intervals running across wind farm and outside wind farm	Number of individuals and flocks	Aerial visual survey	Kolmogorov–Smirnov comparison of pre and post cumulative distribution functions over distance	Petersen et al. (2006)
BAG	Long tailed duck (*Clangula hyemalis*)	Physical presence of turbines at an operating wind farm	Parallel transects at 2 km intervals running across wind farm and outside wind farm	Density	Aerial visual survey	GAM	Petersen et al. (2011)
BAG	Common scoters *Melanitta nigra;* and red-throated diver/black-throated diver *Gavia stellate* and *G. arctica*	Physical presence of turbines at an operating wind farm	Parallel transects; at 2 km intervals running across wind farm and 4 km outside	Density	Aerial visual survey	CReSS	Petersen et al. (2014)
AG	Red- and black-throated diver *Gavia stellate and G. arctica;* guillemot *Uria aalge;* razorbill *Alca torda* and *Arctic Sterna pardisaea;* and common tern *S. hirundo*; distance analysis on common scoter *Melanitta nigra*	Physical presence of turbines at an operating wind farm	Parallel transects at 2 km intervals running across wind farm and outside wind farm	Number of individuals and flocks	Aerial visual survey	Kolmogorov–Smirnov test to compare several years of cumulative distribution functions constructed over distance	Petersen and Fox (2007)

(Continued)

TABLE 5 | Continued

Gradient design type	Groups studied	OWF factor studied	Distances from turbine (m) or (km)	Biological indices measured	Sampling modality	Analytical method	References
AG	Lesser black-backed gulls *Larus fuscus*	Physical presence of turbines at an operating wind farm	GPS data gridded to 250 × 250 m spatial cells	Presence/absence via GPS fixes	Tracking of GPS-tagged birds	GAM	Vanermen et al. (2020)
AG	Divers; gannets (*Morus bassanus*); little gulls (*Hydrocoloeus minutus*); common gulls (*Larus canus*); lesser black-backed gulls (*Larus fuscus*); herring gulls (*Larus argentatus*); great black-backed gulls (*Larus marinus*); kittiwakes (*Rissa tridactyla*); terns; alcids	Physical presence of turbines at an operating wind farm	Parallel transects at 3 km intervals running across and through wind farm	Number of individuals and clusters	Ship-board visual survey	GAM	Welcker and Nehls (2016)

of waterbirds, Kahlert et al. (2004) reported that these species avoided the wind farm particularly at closer distances (**Table 5**). Spatial heterogeneity within a wind farm was demonstrated by Vanermen et al. (2020) for lesser black-backed gulls which tended to avoid flying or perching in the wind farm center, but commonly perched on turbines at the edge of the wind farm.

METHODOLOGICAL ELEMENTS TO CONSIDER IN DESIGNING A DISTANCE-BASED STUDY FOR FINFISH AND INVERTEBRATES

There are numerous methodological elements to consider in designing a monitoring plan for finfish and shellfish at OWFs (ROSA, 2021). This section focuses on four elements that are specific to distance-based sampling, using existing studies as examples. Many other elements such as sample size determination, statistical power, temporal sampling interval, and selection of the biological indicators to be measured are also extremely important elements of experimental design and are covered elsewhere in detail (e.g., Buckland et al., 2015; Franco et al., 2015; Schweiger et al., 2016; Wilding et al., 2017; Van Hoey et al., 2019).

Selection of Distance Intervals

Matching both the spatial extent and resolution of sampling with that of ecological responses to OWF development is key to detecting impact gradients (Wiens, 1989). Previous studies that utilized distance-based sampling for fisheries resource species at OWFs have either taken continuous measures along transects (e.g., van Hal et al., 2017), taken samples at discrete distances along transects, or within spatial strata at increasing distances from turbines (e.g., Bergström et al., 2013; Coates et al., 2014; **Tables 2–5**). Selection of distance intervals for discrete sampling requires consideration of the mobility of the study animals, the spacing of turbines, the distribution of habitat within the wind farm prior to and after construction, and the assumptions made about how study animals associate with wind farm structures and natural habitats. To date, narrower distance bands that are closer to OWF structures have been used for species that have limited motility or are sessile in adult phases; wider distance bands that extend further from the foundations have been used for species with moderate motility (e.g., at the structure, within the scour protection, within a transition zone, and at a far-field distance) (**Figure 3** and **Tables 2–5**). In developing a continuous transect monitoring approach, additional considerations include the distance between transects, the directionality of transects, and how close transects come to the foundations. For both discrete and continuous sampling, the directionality of sampling relative to the turbine is an important consideration as oceanographic and environmental conditions may vary locally and regionally around turbine foundations (Hasager et al., 2015; Boon et al., 2018; van Berkel et al., 2020).

Perhaps the most important consideration in choosing distance intervals at which to sample relative to turbine structures is the hypothesis being considered and the underlying mechanism(s) believed to be driving potential changes. This is needed for both basic monitoring aimed at assessing the aggregate "wind farm effect" and targeted research projects that focus on specific, mechanism-based research questions (Hutchison et al., 2020). For targeted research studies examining the effect of a specific IPF, the choice of distance-based sampling intervals can be informed by understanding how the IPF varies across the wind farm area and the relationship between the IPF and the biological indices to be measured (Gill et al., 2020). **Figure 2** depicts hypothesized spatial and temporal scales for IPFs

that may affect fisheries resources and highlights that while direct effects may occur at scales similar to the IPFs driving them, the scales of indirect effects may extend further.

Although the distance-from-turbine effect has emerged in the literature as a consistent pattern across wind farms for finfish, benthic invertebrates, and sediment composition, some OWF-related IPFs may occur over much larger spatial scales (10s of km) (e.g., Mooney et al., 2020; van Berkel et al., 2020; **Figure 2**) and may therefore require a distance-based sampling strategy with broader spatial extent, resolution, and sampling intervals. For instance, hydrodynamic changes due to the presence of a wind farm occur over both local and broad scales; Locally, downstream turbulence, surface wave energy, and upwelling patterns are modified as currents pass by structures (Bakoday-Paskyabi et al., 2018), while at broad scales wind wakes may affect regional patterns of vertical stratification (Carpenter et al., 2016) up to 10s of km from the wind farm with potential implications for nutrient distribution, primary, and secondary production. This underscores the importance of considering the scale at which underlying mechanism(s) are hypothesized to be acting. In the case of ecological impacts due to hydrodynamic changes, distance-based sampling relative to individual turbines, the wind farm itself, and to other wind farms in the region may be relevant.

Sampling Modalities

Choosing a sampling modality for fisheries resources that can be used in close proximity to turbine structures or in areas where sub-bottom cables occur presents logistical challenges. Traditional fisheries sampling methods such as bottom trawl or dredge are problematic because of the large areas over which they integrate data, potential interactions with structures, and the amount of physical disturbance that they would cause over the footprint of the wind farm to achieve the necessary level of sampling effort and precision. Sampling modalities that provide accurate and precise estimates of the abundance and distribution of the target species of interest while minimizing disturbance to the ecosystem are highly desirable. Another important consideration is choosing gear types that can be readily calibrated with gear used in regional long term monitoring programs so that data collected at OWFs can be integrated with those collected in wider regional surveys (e.g., Streich et al., 2018). Studies targeting benthic invertebrates have primarily sampled with grab samplers, diver collected samples, diver visual observation, or baited remote underwater video (BRUV) (**Table 2**). For finfish, some distance-based studies at OWFs have used traditional methods such as visual diver observation, fyke nets, and gillnets while others have employed more modern approaches such as BRUV, acoustic telemetry, and dual-frequency identification (DIDSON) sonar (**Table 3**). All of these sampling modalities were capable of sampling on or very near turbine foundations.

The development of wind energy in the offshore zone presents an opportunity to develop new and advance existing innovative technologies for research and monitoring. Examples of sampling technologies that have been used to study ecological patterns at and around manmade structures in the ocean and which could be useful for gradient studies at OWFs include hydroacoustics (Degraer et al., 2013; Reynolds et al., 2018) and remotely operated vehicles outfitted with cameras (Ajemian et al., 2015; Wetz et al., 2020). With advances in areas such as machine learning, meta-barcoding, and unmanned research vessels, new monitoring technologies are also emerging such as eDNA (Stoekle et al., 2020), autonomous vehicles combined with camera or passive acoustic technologies (Zemeckis et al., 2019; National Oceanic and Atmospheric Association [NOAA], 2020), and video systems that are integrated with motion-detection and computer vision (Sheehan et al., 2020). Regular monitoring of environmental variables that drive the distribution and abundance of natural resources at wind farms is also essential and could potentially be achieved in coordination with existing ocean observing platforms (Wilkin et al., 2017).

Statistical Approaches

A wide variety of statistical methods have been used to evaluate significant ecological impacts in distance-based studies at OWFs (**Tables 2–5**). Key considerations in selecting an analytical approach are the assumptions made regarding the relationships among dependent and independent variables and their continuous covariables. In instances where linear or non-linear relationships are assumed, Generalized Linear Models (GLMs; McCullagh and Nelder, 1989) can be used as in Bergström et al. (2013) who applied GLMs to demonstrate declining abundance with distance from the turbine for total fish, cod (*G. morhua*), eel (*Anguilla anguilla*), shorthorn sculpin (*Myoxocephalus Scorpius*), and gold-sinny wrasse (*Ctenolabrus rupestris*). Curved or non-linear relationships can also be accommodated by Generalized Additive Models (GAMs) (Hastie and Tibshirani, 1990; Wood, 2006). GAMs have been employed to analyze bird and mammal data collected in distance-based studies at OWFs where they have revealed distinct spatial patterns (Brandt et al., 2011; Petersen et al., 2011; **Tables 4**, **5**). Mackenzie et al. (2013) pointed out that with GAMs, the p-values calculated assume that there is no spatial-temporal correlation among model residuals which can be problematic when there are unexplained patterns in the model. Generalized Additive Mixed Models (GAMMs), an extension of GAMs that incorporates random effects, allow for non-linear relationships with covariables as well as spatial-temporal correlation within sampling units (e.g., transects) (Zuur et al., 2009). GAMMs have also been employed to demonstrate spatial patterns of effect at OWFs for birds and small mammals (Dähne et al., 2013; Mendel et al., 2019). Winiarski et al. (2014) used a density surface model approach that estimated bird abundance over each section of a survey transect, and then employed GAM to model transect segment-level abundance as a function of environmental covariates. Another analytical approach, Complex Regional Spatial Smoother (CReSS), offers a further advantage of spatial adaptability, allowing for greater flexibility in the modeled relationship with covariables throughout the covariable range by focusing on the portions of the range where model residuals are greatest (Scott-Hayward et al., 2013). This method was used by Petersen et al. (2014) to demonstrate the reduction

and displacement of divers at an OWF. Additionally, non-parametric and multivariate approaches such as PERMANOVA, ANOSIM, and SIMPER (Clarke and Gorley, 2006; Anderson et al., 2008) have been employed to uncover abundance and community level differences along gradients of impact at OWFs particularly for benthic invertebrates and finfish (**Tables 2**, **3**; e.g., Wilhelmsson and Malm, 2008; Coates et al., 2014; Lu et al., 2020).

Collection of Data Along an Impact Gradient Prior to the Impact

A common reasoning for not selecting a before-after distance-based sampling design such as BAG is the difficulty in collecting data along a distance-from-turbine gradient prior to the construction of the turbines. This difficulty arises because often the specific locations of turbines and associated scour protection zones are not precisely known >2 years in advance of construction when baseline studies would occur. Changes in the turbine design or layout are often made by developers during the permitting process (e.g., engineering innovations that occur during the permitting process may lead to larger, more efficient turbines that are preferred by developers). Changes also occur because of conflicts among stakeholders regarding the spacing of turbines or placement of transit lanes (e.g., Baird and Associates, 2019; RODA, 2020). One solution is to resolve these conflicts and make a final selection about the turbine design and layout well in advance of the start of construction. Alternatively or perhaps additionally, data collection throughout the development area during 2+ years of baseline studies could be used to develop spatially explicit models that generate a predicted surface of the abundance and distribution of target species which could provide the "before" data in impact assessment models (Petersen et al., 2011, 2014; Winiarski et al., 2014).

DISCUSSION

Offshore wind is becoming an integral component of the blue economy worldwide. Innovative and robust study methodologies are needed to develop a comprehensive and mechanism-based understanding of the interactions between OWFs and marine ecosystems (Wilding et al., 2017). In the United States, commercial scale offshore wind development is imminent and there is an opportunity, before large scale development commences, to develop methodologies that are able to measure ecological effects and distinguish them from natural variation and other concurrent factors that affect populations. Combining a before-after sampling design with distance-based methods could provide a powerful approach for characterizing both the spatial and temporal variance associated with wind development in the ocean.

Before-after designs offer the unique ability to make comparisons of post-construction patterns with the reference condition, enabling an examination of how the intervention may have driven the patterns observed. Understanding how the biological and physical environment changes following the intervention could provide the basis for the development of mechanistic hypotheses to be tested at OWFs. This is important for understanding not only changes from baseline due to the direct effects of wind development, but also those due to indirect effects that change in response to wind development (e.g., changes in the distribution of fishing effort) if those data are available. In instances when studies are only conceived after construction has occurred, AG and distanced-stratified CI could be useful in elucidating effects during the operational phase.

Of the designs explored here, BAG offers several methodological advantages: It can evaluate spatial heterogeneity and the spatial scale of effect, does not require a control, and compares pre-construction with post-construction patterns, making it arguably the most robust and most versatile of the distance-based methods. These advantages have elevated BAG to becoming a recommended design in the study of birds (Jackson and Whitfield, 2011; Joint Nature Conservation Committee [JNCC], 2015) and small mammals (Thompson et al., 2010; Bailey et al., 2014) at OWFs. Nevertheless, there remains no published examples of BAG studies for finfish or invertebrates. Several applications of the AG design at wind farms are reported in the literature, and these studies have yielded important information on demersal finfish and benthic invertebrates during OWF operation.

Distance-stratified BACI may be useful in answering research questions about effects that are expected to occur over a limited, well-defined spatial extent and when suitable controls can be identified. For example, hypotheses regarding the direct effects of adding hard bottom habitat on the abundance of slow moving or sessile species could be explored with this method because hard bottom habitat added (i.e., turbine foundations and scour protection) occurs in distinct areas that could be readily stratified with regard to distance and compared to a control. The difficulty of finding a suitable control in a busy multi-use coastal ocean remains, and this obstacle is made even more challenging by the shifting environmental baselines that oceans are facing (Kleisner et al., 2017). This challenge can be ameliorated by careful baseline sampling to ensure that controls are sufficiently similar to impact locations, and by the measurement of co-variables at both control and impact locations that may be important in driving patterns of abundance and distribution of target species.

Localized effects at the scale of a single wind farm may seem relatively small and inconsequential compared to the broader expanse of the ocean and ecosystem level processes. However, the potential for local-scale effects to have regional and/or ecosystem level implications could occur through a variety of processes including larval transport (Krone et al., 2013; Slavik et al., 2018), stepping stone effects (Coolen et al., 2020), consumption of reef-associated species by mobile predators (Reubens et al., 2014; Russell et al., 2016), and the translocation of carbon derived from reef-associated species beyond the footprint of the wind farm and into the regional ecosystem (Reubens et al., 2014; Carey et al., 2020; Degraer et al., 2020; **Figure 2**). The potential for such effects has been borne out by predictive models. For example, using a coupled hydrodynamic-ecosystem model, Slavik et al. (2018) found that OWF development in the southern North Sea may

increase regional abundance of blue mussels (*Mytilus edulis*) and subsequently affect regional changes in primary production and water clarity. Barbut et al. (2020) used a coupled particle tracking-hydrodynamic model to demonstrate the potential for offshore wind development to overlap with flatfish spawning grounds in the North Sea, showing that this overlap could affect population dynamics. In a desktop analysis, Coolen et al. (2019) projected that having 5,000 turbines and associated scour structures in the Dutch North Sea by the year 2050 would have the potential to increase the Dutch edible crab population by 50 million individuals and the Atlantic cod population by hundreds of thousands. Satellite imagery shows that wind wakes (i.e., the effect of reduced wind speed on wave generation) can extend 10s of km from wind farms (Hasager et al., 2015). Changes in wave heights driven by wind wakes may impact the transport of suspended matter, affecting nutrient distribution with impacts extending to primary production and shellfish production (Carpenter et al., 2016; Boon et al., 2018). These studies suggest that offshore wind development has the potential to have non-trivial ecosystem level effects that extend far beyond the local scale of the footprint of an individual wind farm.

A regionally coordinated framework for research and monitoring could help to place local scale patterns within the context of the regional ocean through several pathways (Carey et al., 2020; Gill et al., 2020; Methratta et al., 2020; ROSA, 2021). First, using robust methodologies, a regional framework can inform our understanding of how local scale impacts on abundance, distribution, and vital population rates scale up to the regional level at which populations are managed (e.g., Barbut et al., 2020). Second, a regional framework is key to disentangling wind development impacts from effects caused by broader scale regional or ecosystem level scale phenomena such as changes in water temperature or primary production (e.g., Kleisner et al., 2017). Next, it could facilitate an integration of data collected at OWFs with those collected by long term regional scientific surveys (Methratta et al., 2020). Lastly, a regional framework could support the integration of accurate and precise estimates of biological indicators that can be used to inform the assessment of cross-sector tradeoffs within an integrated ecosystem assessment framework (Samhouri et al., 2014).

CONCLUSION AND RECOMMENDATIONS

Coupling before-after methods with distance-based sampling could provide a powerful approach to studying OWF effects on fisheries resources. The sampling frameworks and statistical methods for such an approach are most advanced in the study of marine mammals and birds at OWFs. The rich knowledge base that exists for mammalian and avian research methods could provide a valuable resource for researchers studying effects on finfish and invertebrates at wind farm installations.

Toward the goal of enhancing the development and application of distance-based sampling of fisheries resources at OWFs, the following recommendations are made: (1) Select a sampling design such as BAG that has the ability to analyze spatial variability both before and after construction; (2) Define testable hypotheses based on specific IPFs; (3) Develop assumptions about the spatial scale of effects and the distance intervals to be studied based on the focal mechanism(s); (4) Collect baseline data to inform local-scale site selection, develop hypotheses, and enable pre vs. post construction comparisons. Baseline data collection should occur for a period of time that is long enough to characterize patterns of natural variation prior to construction; (5) In defining sampling distances for distance-based sampling designs, consider at minimum the ecology of the target species, the spatial patterns of the underlying mechanism(s) hypothesized to be playing a potential role, baseline data on habitat distribution and environmental variables, and turbine spacing; (6) Measure environmental co-variables along with biological responses and include these as covariates in statistical models; (7) Nest local scale distance-based studies into a regionally coordinated framework for research and monitoring that utilizes standardized approaches (e.g., sample size determination, experimental design, sampling gears, sampling protocol) across wind projects within a region. Conducted consistently across wind farms within a region, such an approach could provide an unparalleled ability to distinguish wind farm impacts from natural variation, synthesize results and draw valuable conclusions that can inform fisheries management and decisions; (8) Establish a standard set of analytical methodologies that integrate information from local to regional to ecosystem scales; (9) Continue to develop and advance innovative research, monitoring, and observing technologies and platforms that provide accurate and precise estimates of biological indices and environmental covariates while minimizing disturbance to the ecosystem; (10) Broaden opportunities for sharing ideas and methodological innovations across areas of ecological research.

AUTHOR CONTRIBUTIONS

EM conceived the idea for this work, conducted the review and synthesis of the literature, and wrote this manuscript.

ACKNOWLEDGMENTS

I am grateful to the NOAA NMFS Offshore Wind Team and members of the International Council for the Exploration of the Sea, Working Group on Offshore Wind Development and Fisheries (ICES WGOWDF) for many thoughtful discussions on offshore wind and fisheries interactions. I am also grateful to Michael Fogarty, Andrew Lipsky, and the peer-reviewers assigned by the journal for providing constructive comments that improved this manuscript. The views expressed herein are those of the author and do not necessarily reflect the views of the Department of Commerce or its sub-agencies.

REFERENCES

Aguado-Giménez, F., Piedecausa, M. A., Guitérrez, J. M., García-Charton, J. A., Belmonte, A., and García-García, B. (2012). Benthic recovery after fish farming cessation: A "beyond-BACI" approach. *Mar. Poll. Bull.* 64, 729–738. doi: 10.1016/j.marpolbul.2012.02.012

Ajemian, M. J., Wetz, J. J., Shipley-Lozano, B., and Stunz, G. W. (2015). Rapid assessment of fish communities on submerged oil and gas platform reefs using remotely operated vehicles. *Fish. Res.* 167, 143–155. doi: 10.1016/j.fishres.2015.02.011

Anderson, M. J., Gorley, R. N., and Clarke, K. R. (2008). *PERMANOVA+ for PRIMER: Guide to Software and Statistical Methods*. Plymouth: PRIMER-E.

Bailey, H., Brookes, K. L., and Thompson, P. M. (2014). Assessing environmental impacts of offshore wind farms: lessons learned and recommendations for the future. *Aquat. Biosys.* 10:8. doi: 10.1186/2046-9063-10-8

Baird, W. F., and Associates (2019). *Letter to the US Coast Guard*. Available online at: https://static1.squarespace.com/static/5a2eae32be42d64ed467f9d1/t/5dd3d3e476d4226b2a83db25/1574163438896/Proposed+1x1+layout+from+RI-MA+Leaseholders+1+Nov+19+%281%29.pdf. (Accessed date January 8, 2021).

Bakoday-Paskyabi, M., Fer, I., and Reuder, J. (2018). Current and turbulence measurements at the FINO1 offshore wind energy site: analysis using 5-beam ADCPs. *Ocean Dyn.* 68, 109–130. doi: 10.1007/s10236-017-1109-5

Barbut, L., Vastenhoud, B., Vigin, L., Degraer, S., Volckaert, F. A. M., and Lacroix, G. (2020). The proportion of flatfish recruitment in the North Sea potentially affected by offshore wind farms. *ICES J. Mar. Sci.* 77, 1227–1237. doi: 10.1093/icesjms/fsz050

Bergström, L., Sundqvist, F., and Bergström, U. (2013). Effects of an offshore wind farm on temporal and spatial patterns in the demersal fish community. *Mar. Ecol. Prog. Ser.* 485, 199–210. doi: 10.3354/meps10344

Bolser, D. G., Egerton, J. P., Grüss, A., Loughran, T., Beyea, T., McCain, K., et al. (2020). Environmental and structural drivers of fish distributions among petroleum platforms across the U.S. Gulf of Mexico. *Mar. Coast. Fish.* 12, 142–163. doi: 10.1002/mcf2.10116

Boon, A. R., Caires, S., Wijnant, I. L., Verzijlbergh, R., Zijl, F., Schouten, J. J., Muis, S. (2018). *Assessment of system effects of large-scale implementation of offshore wind in the southern North Sea*. (Delft: Deltares).

Braeckman, U., Lefaible, N., Bruns, E., and Moens, T. (2020). "Turbine-related impacts on macrobenthic communities: An analysis of spatial and temporal variability," in *Environmental impacts of offshore wind farms in the Belgian Part of the North Sea: Empirical evidence inspiring priority monitoring research and management*, eds S. Degraer, R. Brabant, B. Rumes, and L. Virgin (Brussels: Royal Belgian Institute of Natural Sciences, OD Natural Environment, Marine Ecology and Management Section), 61–78.

Brandt, M. J., Diederichs, A., Betke, K., and Nehls, G. (2011). Responses of harbour porpoises to pile driving at the Horns Rev II offshore wind farm in the Danish North Sea. *Mar. Ecol. Prog. Ser.* 421, 205–216. doi: 10.3354/meps08888

Buckland, S. T., Rexstad, E. A., Marques, T. A., and Oedekoven, C. S. (2015). *Distance Sampling: Methods and Applications*. New York, NY: Springer.

Carey, D. A., Wilber, D. H., Read, L. B., Guarinello, M. L., Griffin, M., and Sabo, S. (2020). Effects of the Block Island Wind Farm on coastal resources lessons learned. *Oceanography* 33, 70–81. doi: 10.5670/oceanog.2020.407

Carpenter, J. R., Merckelbach, L., Callies, U., Clark, S., Gaslikova, L., and Baschek, B. (2016). Potential impacts of offshore wind farms on North Sea stratification. *PLoS One* 2016:160830. doi: 10.1371/journal.pone.0160830

Christie, A. P., Abecasis, D., Adjeroud, M., Alonso, J. C., Amano, T., and Anton, A. (2020). Quantifying and addressing the prevalence and bias of study designs in the environmental and social sciences. *Nat. Comm.* 11:6377. doi: 10.1038/s41467-020-20142-y

Clarke, K., and Gorley, R. (2006). *PRIMER V6: User Manual/Tutorial*. Plymouth: PRIMER-E.

Coates, D. A., Deschutter, Y., Vincx, M., and Vanaverbeke, J. (2014). Enrichment and shifts in macrobenthic assemblages in an offshore wind farm area in the Belgian part of the North Sea. *Mar. Environ. Res.* 95, 1–12. doi: 10.1016/j.marenvres.2013.12.008

Coolen, J. W. P., Boon, A. R., Crooijmans, R., Pelt, H., Kleissen, F., Gerla, D., et al. (2020). Marine stepping stones: Connectivity of *Mytilus edulis* populations between offshore energy installations. *Molec. Ecol.* 29, 686–703. doi: 10.1111/mec.15364

Coolen, J. W. P., Lengkeek, W., van der Have, T., and Bittner, O. (2019). *Upscaling positive effects of scour protection in offshore wind farms*. Netherlands: Wageningen Marine Research, doi: 10.18174/475354

Dähne, M., Gilles, A., Lucke, K., Peschko, V., Adler, S., Krügel, K., et al. (2013). Effects of pile-driving on harbour porpoises (*Phocoena phocoena*) at the first offshore wind farm in Germany. *Environ. Res. Lett.* 8:025002. doi: 10.1088/1748-9326/8/2/025002

Dannheim, J., Bergström, L., Birchenough, S. N. R., Brzana, R., Boon, A. R., Coolen, J. W. P., et al. (2020). Benthic effects of offshore renewables: identification of knowledge gaps and urgently needed research. *ICES J. Mar. Sci.* 77, 1092–1108. doi: 10.1093/icesjms/fsz018

Davis, N., VanBlaricom, G. R., and Dayton, P. K. (1982). Man-made structures on marine sediments: effects on adjacent benthic communities. *Mar. Biol.* 70, 295–303. doi: 10.1007/bf00396848

De Mesel, I., Kerckhof, F., Norro, A., Rumes, B., and Degraer, S. (2015). Succession and seasonal dynamics of the epifauna community on offshore wind farm foundations and their role as stepping stones for non-indigenous species. *Hydrobiologia* 756, 37–50. doi: 10.1007/s10750-014-2157-1

Degraer, S., Brabant, R., and Rumes, B. (2013). *Environmental impacts of offshore wind farms in the Belgian part of the North Sea: Learning from the past to optimise future monitoring programmes*. Brussels: Royal Belgian Institute of Natural Sciences, Operational Directorate Natural Environment, Marine Ecology and Management Section, 239.

Degraer, S., Brabant, R., Rumes, B., and Vigin, L. (2019). *Environmental Impacts of Offshore Wind Farms in the Belgian Part of the North Sea: Marking a Decade of Monitoring, Research and Innovation*. Brussels: Royal Belgian Institute of Natural Sciences, OD Natural Environment, Marine Ecology and Management, 134.

Degraer, S., Carey, D. A., Coolen, J. W. P., Hutchison, Z. L., Kerckhof, F., Rumes, B., et al. (2020). Offshore wind farm artificial reefs affect ecosystem structure and functioning: A synthesis. *Oceanography* 33, 48–57. doi: 10.5670/oceanog.2020.405

Ellis, J. I., and Schneider, D. C. (1997). Evaluation of a gradient sampling design for environmental impact assessment. *Environ. Monitor. Assess.* 48, 157–172.

Floeter, J., Beusekom, V., Auch, D., Callies, U., Carpenter, J., Dudeck, T., et al. (2017). Pelagic effects of offshore wind farm foundations in the stratified North Sea. *Prog. Oceanogr.* 156, 154–173. doi: 10.1016/j.pocean.2017.07.003

Franco, A., Quintino, V., and Elliott, M. (2015). Benthic monitoring and sampling design and effort to detect spatial changes. *Ecol. Indic.* 57, 298–304. doi: 10.1016/j.ecolind.2015.04.040

Gill, A. B., Degraer, S., Lipsky, A., Mavraki, N., Methratta, E., and Brabant, R. (2020). Setting the context for offshore wind development effects on fish and fisheries. *Oceanography* 33, 118–127. doi: 10.5670/oceanog.2020.411

Gilles, A., Scheidat, M., and Siebert, U. (2009). Seasonal distribution of harbor porpoises and possible interference of offshore wind farms in the German North Sea. *Mar. Ecol. Prog. Ser.* 383, 295–307. doi: 10.3354/meps08020

Green, R. H. (1979). *Sampling design and statistical methods for environmental biologists*. New York, NY: John Wiley and Sons.

Griffin, R. A., Robinson, G. J., West, A., Gloyne-Phillips, I. T., Richard, K., and Unsworth, F. (2016). Assessing fish and motile fauna around offshore windfarms using stereo baited video. *PLoS One* 11:e01. doi: 10.1371/journal.pone.0149701

Harmelin-Vivien, M., Le Diréach, L., Bayle-Sempere, J., Charbonnel, E., García-Charton, J. A., and Ody, D. (2008). Gradients of abundance and biomass across reserve boundaries in six Mediterranean marine protected areas: Evidence of fish spillover? *Biol. Cons.* 141, 1829–1839. doi: 10.1016/j.biocon.2008.04.029

Hasager, C. B., Vincent, P., Badger, J., Badger, M., Di Bella, A., Peña, A., et al. (2015). Using satellite SAR to characterize the wind flow around offshore wind farms. *Energies* 8, 5413–s5439. doi: 10.3390/en8065413

Hastie, T. J., and Tibshirani, R. J. (1990). *Generalized Additive Models*. London: Chapman & Hall.

HDR (2019). Benthic Monitoring during Wind Turbine Installation and Operation at the Block Island Wind Farm, Rhode Island – Year 2. Final Report to the U.S. Department of the Interior, Bureau of Ocean Energy Management, Office of Renewable Energy Programs. *OCS Study BOEM* 318:49701.

HDR (2020). *Benthic and Epifaunal Monitoring During Wind Turbine Installation and Operation at the Block Island Wind Farm*. Rhode Island: Final Report to the US Department of the Interior, Bureau of Ocean Energy Management, Office of Renewable Energy Programs.

Hurlbert, S. H. (1984). Pseudoreplication and the design of ecological field experiments. *Ecol. Monogr.* 54, 187–211. doi: 10.2307/1942661

Hutchison, Z. L., Gill, A. B., Sigray, P., Haibo, H., and King, J. W. (2020). Anthropogenic electromagnetic fields (EMF) influence the behavior of bottom-dwelling marine species. *Sci. Rep.* 10:4219. doi: 10.1038/s41598-020-60793-x

Jackson, D., and Whitfield, P. (2011). Guidance on survey and monitoring in relation to marine renewables deployments in Scotland. *Scot. Nat. Herit. Mar. Scot.* 2011:4.

Joint Nature Conservation Committee [JNCC] (2015). *Seabird Displacement Impacts from Offshore Wind Farms: report of the MROG Workshop*. JNCC Report No 568, Scotland: JNCC Peterborough.

Jones, I. T., Peyla, J. F., Clark, H., Song, Z., Stanely, J. A., and Mooney, T. A. (2021). Changes in feeding behavior of longfin squid (*Doryteuthis pealeii*) during laboratory exposure to pile driving noise. *Mar. Env. Res.* 165:105250. doi: 10.1016/j.marenvres.2020.105250

Kahlert, J., Petersen, I. K., Fox, A. D., Desholm, M., and Clausager, I. (2004). Investigations of birds during construction and operation of Nysted offshore wind farm at Rødsand. *NERI Rep.* 2004, 1–88. doi: 10.1016/b978-0-12-410422-8.00001-7

Karama, K. S., Matsushita, Y., Inoue, M., Kojima, K., Tone, K., Nakamura, I., et al. (2021). Movement pattern of red seabream *Pagrus major* and yellowtail *Seriola quinqueradiata* around offshore wind turbine and the neighboring habitats in the waters near Goto Islands, Japan. *Aquacult. Fish.* 6, 300–308. doi: 10.1016/j.aaf.2020.04.005

Kleisner, K. M., Fogarty, M. J., McGee, S., Hare, J. A., Moret, S., Peretti, C. T., et al. (2017). Marine species distribution shifts on the U.S. Northeast Continental Shelf under continued ocean warming. *Prog. Oceanogr.* 153, 24–36. doi: 10.1016/j.pocean.2017.04.001

Klimely, A. P., Putman, N. F., Keller, B. A., and Noakes, D. (2021). A call to assess the impacts of electromagnetic fields from subsea cables on the movement ecology of marine migrants. *Conserv. Sci Pract.* 3:e436. doi: 10.1111/csp2.436

Kraus, S. D., Kenney, R. D., and Thomas, L. (2019). *A Framework for Studying the Effects of Offshore Wind Development on Marine Mammals and Turtles. Report for the Massachusetts Clean Energy Center, Boston, MA 02110, and the Bureau of Ocean Energy Management. May 2019*, Vol. 20. Boston, MA: Bureau of Ocean Energy Management.

Krone, R., Gutow, L., Brey, T., Dannheim, J., and Schroeder, A. (2013). Mobile demersal megafauna at artificial structures in the German Bight – Likely effects of offshore wind farm development. *Est. Coast. Shelf Sci.* 125, 1–9. doi: 10.1016/j.ecss.2013.03.012

Lefaible, N., Braeckman, U., and Moens, T. (2018). "Effects of wind turbine foundations on surrounding macrobenthic communities," in *Environmental Impacts of Offshore Wind Farms in the Belgian Part of the North Sea: Assessing and Managing Effect Spheres of Influence*, eds S. Degraer, R. Brabant, B. Rumes, and L. Virgin (Brussels: Royal Belgian Institute of Natural Sciences, OD Natural Environment, Marine Ecology and Management Section), 57–77.

Lefaible, N., Colson, L., Braeckman, U., and Moens, T. (2019). Effects of turbine-related impacts on macrobenthic communities within two offshore wind farms during the operational phase. Brussels: Royal Belgian Institute of Natural Sciences. 47–63.

Lindeboom, H., Degraer, S., Dannheim, J., and Gill, A. B. (2015). Offshore wind park monitoring programmes, lessons learned and recommendations for the future. *Hydrobiologia* 756, 169–180. doi: 10.1007/s10750-015-2267-4

Lu, Z., Zhan, X., Guo, Y., and Ma, L. (2020). Small-scale effects of offshore wind-turbine foundations on macrobenthic assemblages in Pinghai Bay, China. *J. Coast. Res.* 36, 139–147. doi: 10.2112/jcoastres-d-19-00051.1

Mackenzie, M. L., Scott-Hayward, L. A. S., Oedekoven, C. S., Skov, H., Humphreys, E., and Rexstad, E. (2013). Statistical Modelling of Seabird and Cetacean data: Guidance Document. *Univ. Andr. Contr. Mar. Scot.* 2013:05.

Mavraki, N., Degraer, S., Moens, T., and Vanaverbeke, J. (2019). Functional differences in trophic structure of offshore wind farm communities: a stable isotope study. *Mar. Env. Res.* 157:104868. doi: 10.1016/j.marenvres.2019.104868

McCullagh, P., and Nelder, J. A. (1989). *Generalized Linear Models*, 2nd Edn. London: Chapman and Hall.

Mendel, B., Schwemmer, P., Peschko, V., Muller, S., Schwemmer, H., Mercker, M., et al. (2019). Operational offshore wind farms and associated ship traffic cause profound changes in distribution patterns of Loons (*Gavia* spp.). *J. Environ. Manage.* 231, 429–438. doi: 10.1016/j.jenvman.2018.10.053

Methratta, E. T. (2020). Monitoring fisheries resources at offshore wind farms: BACI vs. BAG designs. *ICES J. Mar. Sci.* 2020:26. doi: 10.1093/icesjms/fsaa026

Methratta, E. T., and Dardick, W. R. (2019). Meta-analysis of finfish abundance at offshore wind farms. *Rev. Fish. Sci. Aqua.* 27, 242–260. doi: 10.1080/23308249.2019.1584601

Methratta, E. T., Hawkins, A., Hooker, B. R., Lipsky, A., and Hare, J. A. (2020). Offshore wind development in the Northeast US Shelf Large Marine Ecosystem: Ecological, human, and fishery management dimensions. *Oceanography* 33, 16–27. doi: 10.5670/oceanog.2020.402

Moland, E., Olsen, E. M., Knutsen, H., Garrigou, P., Espeland, S. H., Kleiven, A. R., et al. (2013). Lobster and cod benefit from small-scale northern marine protected areas: inference from an empirical before-after control-impact study. *Proc. Royal Soc. B.* 280:20122679. doi: 10.1098/rspb.2012.2679

Mooney, T. A., Andersson, M. H., and Stanley, J. (2020). Acoustic impacts of offshore wind energy on fishery resources: An evolving source and varied effects across a wind farm's lifetime. *Oceanography* 33, 82–95. doi: 10.5670/oceanog.2020.408

Munnelly, R. T., Reeves, D. B., Chesney, E. J., and Baltz, D. M. (2020). Spatial and temporal influences of nearshore hydrography on fish assemblages associated with energy platforms in the Northern Gulf of Mexico. *Estua. Coasts* 44, 269–285. doi: 10.1007/s12237-020-00772-7

National Oceanic and Atmospheric Association [NOAA] (2020). *Scientists collecting data on commercial fish species in wind energy lease areas*. Available online at: www.fisheries.noaa.gov/feature-story/scientists-collecting-data-commercial-fish-species-wind-energy-lease-areas-0. (Accessed date July 1, 2021)

Paxton, A. B., Shertzer, K. W., Bacheler, N. M., Kellison, G. T., Riley, K. L., and Taylor, J. C. (2020). Meta-analysis reveals artificial reefs can be effective tools for fish community enhancement but are not one-size-fits-all. *Front. Mar. Sci.* 7:282. doi: 10.3389/fmars.2020.00282

Perry, R. L., and Heyman, W. D. (2020). Considerations for offshore wind energy development effects on fish and fisheries in the United States: A review of existing studies, new efforts, and opportunities for innovation. *Oceanography* 33, 28–37. doi: 10.5670/oceanog.2020.403

Petersen, I. K., Christensen, T. K., Kahlert, J., Desholm, M., and Fox, A. D. (2006). *Final Results of Bird Studies at the Offshore Wind Farms at Nysted and Horns Rev, Denmark*. Horns Rev: National Environmental Research Institute, Ministry of the Environment, 166.

Petersen, I. K., Clausager, I., and Christensen, T. J. (2004). "Bird numbers and distribution on the Horns Rev Offshore Wind Farm Area. Annual Status Report 2003," in *Report commissioned by Elsam Engineering A/S 2003*, (Denmark: National Environmental Research Institute).

Petersen, I. K., MacKenzie, M., Rextad, E., Wisz, M. S., and Fox, A. D. (2011). *Comparing Pre- and Post-Construction Distributions of Long-Tailed Ducks Clangula Hyemalis in and Around the Nysted Offshore Wind Farm, Denmark: A Quasi Designed Experiment Accounting for Imperfect Detection, Local Surface Features and Autocorrelation*. 17.

Petersen, I. K., Nielsen, R. D., and Mackenzie, M. L. (2014). *Post-construction evaluation of bird abundances and distributions in the Horns Rev 2 offshore wind farm area, 2011 and 2012*. Denmark: Aarhus University, DCE – Danish Centre for Environment and Energy, 51.

Petersen, K., and Fox, A. D. (2007). *Changes in bird habitat utilization around Horns Rev 1 offshore wind farm, with particular emphasis on Common Scoter*. Nagpur: National Environmental Institute.

Reeds, K. A., Smith, J. A., Suthers, I. M., and Johnston, E. L. (2018). An ecological halo surrounding a large offshore artificial reef: Sediments, infauna, and fish foraging. *Mar. Environ. Res.* 141, 30–38. doi: 10.1016/j.marenvres.2018.07.011

Reubens, J. T., Degraer, S., and Vincx, M. (2014). The ecology of benthopelagic fishes at offshore wind farms: A synthesis of 4 years of research. *Hydrobiologia* 727, 121–136. doi: 10.1007/s10750-013-1793-1

Reubens, J. T., Pasotti, F., Degraer, S., and Vincx, M. (2013). Residency, site fidelity, and habitat use of Atlantic cod (*Gadus morhua*) at an offshore wind farm using

acoustic telemetry. *Mar. Environ. Res.* 90, 128–135. doi: 10.1016/j.marenvres.2013.07.001

Reynolds, E. M., Cowan, J. H. Jr., Lewis, K. A., and Simosen, K. A. (2018). Method for estimating relative abundance and species composition around oil and gas platforms in the northern Gulf of Mexico. *U.S.A. Fish. Res.* 201, 44–55. doi: 10.1016/j.fishres.2018.01.002

RODA (2020). *Letter to NOAA Fisheries*. Available online at: https://rodafisheries.org/wp-content/uploads/2020/01/200103-MA_RI-layout-proposal.pdf. (Accessed date January 8, 2021).

ROSA (2021). Available online at: https://www.rosascience.org/. (Accessed date January 11, 2021).

Russell, D. J., Hastie, G. D., Thompson, D., Janik, V. M., Hammond, P. S., Scott-Hayward, L. A., et al. (2016). Avoidance of wind farms by harbour seals is limited to pile driving activities. *J. Appl. Ecol.* 53, 1642—1652. doi: 10.1111/13652664.12678

Samhouri, S. F., Haupt, A. J., Levin, P. S., Link, J. S., and Shuford, R. (2014). Lessons learned from developing integrated ecosystem assessments to inform marine ecosystem-based management in the USA. *ICES J. Mar. Sci.* 71, 1205–1215. doi: 10.1093/icesjms/fst141

Schweiger, A. H., Severin, D. H. I., Steinbauer, M. J., Dengler, J., and Beierkuhnlein, C. (2016). Optimizing sampling approaches along ecological gradients. *Methods Ecol. Evo.* 7, 463–471. doi: 10.1111/2041-210x.12495

Scott-Hayward, L., Mackenzie, M. L., Donovan, C. R., Walker, C. G., and Ashe, E. (2013). Complex Region Spatial Smoother (CReSS). *J. Comp. Graph. Stat.* 2, 340–360. doi: 10.1080/10618600.2012.762920

Sheehan, E. V., Bridger, D., Nancollas, S. J., and Pittman, S. J. (2020). PelagiCam: a novel underwater imaging system with computer vision for semi-automated monitoring of mobile marine fauna at offshore structures. *Environ. Mon. Assess.* 192:11. doi: 10.1007/s10661-019-7980-4

Slavik, K., Lemmen, C., Zhang, W., Kerimoglu, O., Klingbeil, K., and Wirtz, K. W. (2018). The large scale impact of offshore wind farm structures on pelagic primary production in the southern North Sea. *Hydrobiologia* 845, 35–53. doi: 10.1007/s10750-018-3653-5

Smith, A. K., Ajani, P. A., and Roberts, D. E. (1999). Spatial and temporal variation in fish assemblages exposed to sewage and implications for management. *Mar. Environ. Res.* 47, 241–260. doi: 10.1016/s0141-1136(98)00120-2

Smokorowski, K. E., and Randall, R. G. (2017). Cautions on using the before-after-control-impact design in environmental effects monitoring programs. *FACETS* 2, 212–232. doi: 10.1139/facets-2016-0058

Snodgrass, D. J. G., Orbesen, E. S., Walter, J. F., Hoolihan, J. P., and Brown, C. A. (2020). Potential impacts of oil production platforms and their function as fish aggregating devices on the biology of highly migratory fish species. *Rev. Fish. Biol. Fish.* 30, 405–422. doi: 10.1007/s11160-020-09605-z

Stenberg, C., Stottrup, J. G., van Deurs, M., Berg, C. W., Dinesen, G. E., Mosegaard, H., et al. (2015). Long-term effects of an offshore wind farm in the North Sea on fish communities. *Mar. Ecol. Prog. Ser.* 528, 257–265. doi: 10.3354/meps11261

Stewart-Oaten, A., and Bence, J. R. (2001). Temporal and spatial variation in environmental impact assessment. *Ecol. Monogr.* 71, 305–339. doi: 10.1890/0012-9615(2001)071[0305:tasvie]2.0.co;2

Stewart-Oaten, A., Murdoch, W. W., and Parker, K. R. (1986). Environmental impact assessment: "Pseudoreplication" in time? *Ecology* 67, 929–940. doi: 10.2307/1939815

Stoekle, M. Y., Adolf, J., Charlop-Powers, Z., Dunton, K. J., Hinks, G., and VanMorter, S. M. (2020). Trawl and eDNA assessment of marine fish diversity, seasonality, and relative abundance in coastal New Jersey, USA. *ICES J. Mar. Sci.* 2020:225. doi: 10.1093/icesjms/fsaa225

Streich, M. K., Ajemian, M. J., Wetz, J. J., and Stunz, G. W. (2018). Habitat-specific performance of vertical line gear in the western Gulf of Mexico: a comparison between artificial and natural habitats using a paired-video approach. *Fish. Res.* 204, 16–25. doi: 10.1016/j.fishres.2018.01.018

Thompson, P. M., Lusseau, D., Barton, T., Simmons, D., Rusin, J., and Bailey, H. (2010). Assessing the responses of coastal cetaceans to the construction of offshore wind turbines. *Mar. Poll. Bull.* 60, 1200–1208. doi: 10.1016/j.marpolbul.2010.03.030

Tougaard, J., Carstensen, J., Teilmann, J., Skov, H., and Rasmussen, P. (2009). Pile driving zone of responsiveness extends beyond 20 km for harbor porpoises (*Phocoena phocoena* (L.). *J. Acoust. Soc. Amer.* 126, 11–14.

Underwood, A. J. (1991). Beyond BACI: experimental designs for detecting human environmental impacts on temporal variations in natural populations. *Aust. J. Mar. Freshw. Res.* 42, 569–587. doi: 10.1071/mf9910569

Underwood, A. J. (1992). Beyond BACI: the detection of environmental impacts on populations in the real, but variable, world. *J. Exp. Mar. Biol. Ecol.* 161, 145–178. doi: 10.1016/0022-0981(92)90094-q

Underwood, A. J. (1993). The mechanics of spatially replicated sampling programmes to detect environmental impacts in a variable world. *Aust. J. Ecol.* 18, 99–116. doi: 10.1111/j.1442-9993.1993.tb00437.x

Underwood, A. J. (1994). On beyond BACI: sampling designs that might reliably detect environmental disturbances. *Ecol. Appl.* 4, 3–15. doi: 10.2307/1942110

van Berkel, J., Burchard, H., Christensen, A., Mortensen, L. O., Svenstrup Petersen, O., and Thomsen, F. (2020). The effects of offshore wind farms on hydrodynamics and implications for fishes. *Oceanography* 33, 108–117. doi: 10.5670/oceanog.2020.410

van Hal, R., Griffioen, A. B., and van Keeken, O. A. (2017). Changes in fish communities on a small spatial scale, an effect increased habitat complexity by an offshore wind farm. *Mar. Environ. Res.* 126, 26–36. doi: 10.1016/j.marenvres.2017.01.009

Van Hoey, G., Wischnewski, J., Craeymeersch, J., Dannheim, J., Enserink, L., Guerin, L., et al. (2019). Methodological elements for optimizing the spatial monitoring design to support regional benthic ecosystem assessments. *Environ. Monitor. Assess.* 191:423. doi: 10.1007/s10661-019-7550-9

Vandendriessche, S., Derweduwen, J., and Hostens, K. (2015). Equivocal effects of offshore wind farms in Belgium on soft substrate epibenthos and fish assemblages. *Hydrobiologia* 756, 19–35. doi: 10.1007/s10750-014-1997-z

Vanermen, N., Courtens, W., Daelemans, R., Lens, L., Muler, W., Van de Walle, M., et al. (2020). Attracted to the outside: a meso-scale response pattern of lesser black-backed bulls at an offshore wind farm revealed by GPS telemetry. *ICES J. Mar. Sci.* 77, 701–710. doi: 10.1093/icesjms/fsz199

Welcker, J., and Nehls, G. (2016). Displacement of seabirds by an offshore wind farm in the North Sea. *Mar. Ecol. Prog. Ser.* 554, 173–182. doi: 10.3354/meps11812

Wetz, J. J., Ajemian, M. J., Shipley, B., and Stunz, G. W. (2020). An assessment of two visual survey methods for documenting community structure on artificial platform reefs in the Gulf of Mexico. *Fish. Res.* 225:105492. doi: 10.1016/j.fishres.2020.105492

Whittaker, R. H. (1967). Gradient analysis of vegetation. *Biol. Rev.* 42, 207–264.

Wiens, J. A. (1989). Spatial scaling in ecology. *Funct. Ecol.* 3, 385–397. doi: 10.2307/2389612

Wilding, T. A., Gill, A. B., Boon, A., Sheehan, E., Dauvin, J. C., Pezy, J. P., et al. (2017). Turning off the DRIP ('Data-rich, information-poor') – rationalizing monitoring with a focus on marine renewable energy developments and the benthos. *Renew. Sustain. Energy Rev.* 74, 848–859. doi: 10.1016/j.rser.2017.03.013

Wilhelmsson, D., and Malm, T. (2008). Fouling assemblages on offshore wind power plants and adjacent substrata. *Estuar. Coast. Shelf Sci.* 79, 459–466. doi: 10.1016/j.ecss.2008.04.020

Wilhelmsson, D., Malm, T., and Öhman, M. C. (2006). The influence of offshore windpower on demersal fish. *ICES J. Mar. Sci.* 63, 775–784. doi: 10.1016/j.icesjms.2006.02.001

Wilkin, J., Rosenfeld, L., Allen, A., Baltes, R., Baptista, A., He, R., et al. (2017). Advancing coastal ocean modeling, analysis, and prediction for the US Integrated Ocean Observing System. *J. Operat. Oceanogr.* 12, 115–126. doi: 10.1080/1755876X.2017.1322026

Winiarski, K., Burt, M. L., Rexstad, E., Miller, D. L., Trocki, C. L., Paton, P. W. C., et al. (2014). Integrating aerial and ship surveys of marine birds into a combined density surface model: A case study of wintering Common Loons. *Condor.* 116, 149–161. doi: 10.1650/CONDOR-13-085.1

Wood, S. N. (2006). *Generalized Additive Models: An Introduction with R*. London: Chapman & Hall.

Zemeckis, D. R., Dean, M. J., DeAngelis, A. I., Van Parijs, S. M., Hoffman, W. S., Baumgartner, M. F., et al. (2019). Identifying the distribution of Atlantic cod spawning using multiple fixed and glider-mounted acoustic technologies. *ICES J. Mar. Sci.* 76, 1610–1625. doi: 10.1093/icesjms/fsz064

Zuur, A. F., Ieno, E. N., Walker, N. J., Saveliev, A. A., and Smith, G. M. (2009). *Mixed Effect Models and Extensions in Ecology with R*. Berlin: Springer Science & Business Media, LLC.

Conflict of Interest: EM was employed by IBSS Corporation.

Publisher's Note: All claims expressed in this article are solely those of the authors and do not necessarily represent those of their affiliated organizations, or those of the publisher, the editors and the reviewers. Any product that may be evaluated in this article, or claim that may be made by its manufacturer, is not guaranteed or endorsed by the publisher.

Copyright © 2021 Methratta. This is an open-access article distributed under the terms of the Creative Commons Attribution License (CC BY). The use, distribution or reproduction in other forums is permitted, provided the original author(s) and the copyright owner(s) are credited and that the original publication in this journal is cited, in accordance with accepted academic practice. No use, distribution or reproduction is permitted which does not comply with these terms.

frontiers in Marine Science

ORIGINAL RESEARCH
published: 23 August 2021
doi: 10.3389/fmars.2021.696136

The Behavioural Impacts of Commercial Swimming With Whale Tours on Humpback Whales (*Megaptera novaeangliae*) in Hervey Bay, Australia

Stephanie H. Stack[1,2]*, Kate R. Sprogis[2], Grace L. Olson[1], Florence A. Sullivan[1], Abigail F. Machernis[1] and Jens J. Currie[1]

[1] Pacific Whale Foundation, Wailuku, HI, United States, [2] Pacific Whale Foundation Australia, Urangan, QLD, Australia

OPEN ACCESS

Edited by:
Renata Sousa-Lima, Federal University of Rio Grande do Norte, Brazil

Reviewed by:
Aldo S. Pacheco, National University of San Marcos, Peru
Jorge Urbán Ramírez, Universidad Autónoma de Baja California Sur, Mexico

****Correspondence:***
Stephanie H. Stack
research@pacificwhale.org

Specialty section:
This article was submitted to Marine Ecosystem Ecology, a section of the journal Frontiers in Marine Science

Received: *16 April 2021*
Accepted: *20 July 2021*
Published: *23 August 2021*

Citation:
Stack SH, Sprogis KR, Olson GL, Sullivan FA, Machernis AF and Currie JJ (2021) The Behavioural Impacts of Commercial Swimming With Whale Tours on Humpback Whales (Megaptera novaeangliae) in Hervey Bay, Australia. Front. Mar. Sci. 8:696136. doi: 10.3389/fmars.2021.696136

Swim-with-whale tourism has expanded across several countries globally, with humpback whales (*Megaptera novaeangliae*) being the most commonly targeted species of baleen whale. Behavioural responses from humpback whales to swim-with-whale tours have been reported, however, responses are likely context-dependent. In 2014, swimming with humpback whales began in Hervey Bay, Queensland, Australia, an important resting ground and migratory stopover for humpback whales. The behavioural responses of humpback whales to this swim-with-whale industry have not been examined in Queensland, preventing informed management of this industry. The aims of this study were to: (1) examine short-term behavioural responses in whales *before, during,* and *after* swim-with-whale tours, and (2) investigate behavioural responses of whales throughout swim-with-whale tours compared to whale watch tours. Data were collected on board a commercial vessel, where *before, during* and *after* data were collected during swim-with-whale tours (250 h) and whale watch tours (150 h). Within the swim-with-whale tours, behavioural changes were detected *before, during,* and *after* the vessel approached and placed swimmers in the water on a mermaid line, with the majority of significant changes occurring in the *during* and *after* phases. The number of direction changes made by the whales was highest when swimmers were in the water and the whales did not resume undisturbed behaviour after the swimmers exited the water. There was a 50% reduction in the proportion of time that whales spent resting during swim-tours compared to during whale watch tours. In both tour types, the time spent engaging in various behaviours was impacted by the distance between the vessel and the whale(s). These results support the conclusion that the behaviour of humpback whales in Hervey Bay was altered in response to swim-with-whale tourism. As humpback whales are capital breeders with limited energy reserves, reducing disturbance to them is of high importance for their continued population recovery and for the sustainability of the marine tourism industry. In Australia,

where swim-with-whale tourism is becoming more established, robust education and enforcement programs, combined with continued monitoring of population dynamics through scientific research, are needed to minimise impacts to the population and guide adaptive management strategies.

Keywords: swim-with-whale, whale watching, in-water interactions, *Megaptera novaeangliae*, behavioural responses, anthropogenic impacts, before-during-after study design

INTRODUCTION

Whale watching has grown into a global marine industry that has created significant environmental, educational, scientific, and socioeconomic benefits for coastal communities around the world (Hoyt, 2001; O'Connor et al., 2009). Generating over $2 billion USD annually, the whale watch industry has placed an economic value to whales and dolphins and the types of interactions people have with them (Parsons, 2012). Over the past few decades, as the interest and value of the industry has grown, commercial operations have diversified the ways in which they facilitate interactions between members of the public and whales and dolphins in the wild (Samuels et al., 2000; Hoyt, 2001; Rose et al., 2005). One form of interaction that has emerged is the "swim-with" industry in which humans enter the water and attempt to closely observe free-ranging whales and dolphins (Samuels and Bejder, 2004; Rose et al., 2005). One of the first known commercial swim-with-whale programs developed during the mid-1900s off the Great Barrier Reef, Australia, after dwarf minke whales (*Balaenoptera acutorostrata*) began interacting with snorkelers (Arnold, 1997; Birtles et al., 2002; Valentine et al., 2004). Since then, the swim-with-whale industry has expanded across several countries globally (Hendrix and Rose, 2014). Worldwide, humpback whales (*Megaptera novaeangliae*) and dwarf minke whales are the most frequently targeted species for swim-with-whale activities (Gero et al., 2016). Humpback whales are commonly targeted as they are a cosmopolitan species and are easy to access as they migrate along coastal landmasses (Hendrix and Rose, 2014). Other large whale species are also sought after for close, in-water interactions, including blue (*Balaenoptera musculus*), fin (*Balaenoptera physalus*), and southern right (*Eubalaena australis*) whales (Hendrix and Rose, 2014). The list of locations and targeted species continues to grow as the swim-with-whale industry rapidly expands around the world (Stack and Serra, 2021). The design of swim-with commercial operations varies regionally in the type of permitted approach for vessels and swimmers for vessels and swimmers. The types of permitted approaches include floating at the surface with or without a tether, diving underwater on a breath hold and/or scuba diving (Stack and Serra, 2021).

Despite the growing industry, limited research has evaluated the impacts of swim-with-whale tourism on large baleen whale species. In some locations and for some species, behavioural responses from swim-with-whale activities have been evaluated. Off Argentina, southern right whales decreased their proportion of time spent resting and increased the proportion of time spent travelling, with mothers and calves being most sensitive to the presence of swimmers (Lundquist et al., 2013). Off the Kingdom of Tonga, Kessler et al. (2013) reported that humpback whales moved away from swim-with-whale tour groups more quickly when swimmers were loud and splashing on the surface of the water. Fiori et al. (2019) noted that humpback whales, particularly mother-calf pairs, exhibited vertical avoidance strategies, such as increasing the duration of dives and increasing the proportion of time spent diving. Off Western Australia, migrating humpback whales adopted both horizontal and vertical avoidance strategies in response to swim-with-whale activities by increasing their swim speeds, swimming more erratically, changing their heading away from the vessel and altering their dive patterns (Sprogis et al., 2020). Likewise, off Reunion Island, humpback whales were less likely to continue resting when swimmers were in the water (Hoarau et al., 2020). Impacts from swim-with-whale tourism likely differ from typical whale watch tourism, due to closer vessel approaches to the whales to place swimmers in the water and the presence of swimmers in the water. Several factors are involved in the response of whales to swim-with-whale activities, including the vessel approach type, group composition (if a calf is present), and location type (i.e., breeding ground, migration route, or feeding ground (Machernis et al., 2018; Sprogis et al., 2020). Importantly, disturbance to whales from the marine tourism industry increases the energetic consequences on whales (Lusseau and Bejder, 2007), thus reducing any disturbance is of high importance for both these capital breeders with limited energy reserves and the sustainability of the swim-with-whale industry. Overall, current research suggests that the rate at which swim-with-whale operations are expanding may not be sustainable for the targeted population on which they rely (Gero et al., 2016).

Examining the short-term behavioural responses of humpback whales to swim-with-whale activities across different locations and with differing approach types from operators is of importance as swimming with these large whales poses risks to the safety of humans. Dangerous encounters between humpback whales and humans have been documented off Western Australia, Réunion Island and the Kingdom of Tonga (Fiori et al., 2019; Barra et al., 2020; Hoarau et al., 2020; Sprogis et al., 2020). These agonistic behaviours include tail fluke thrashes, peduncle throws and pectoral fin slaps (Sprogis et al., 2020). Swimmers have sustained injuries such as broken bones, bruises, and scratches (Fiori et al., 2019; Sprogis et al., 2020), generally from pectoral shears and fluke thrashes, which are common behaviours directed toward swimmers by humpback whales (Barra et al., 2020). Safety incidents have occurred while swimming with mother and calves (Barra et al., 2020; Hoarau et al., 2020), where either the mother or the calf can cause an injury to swimmers.

Thus, due to the high-risk of human injuries it is important to manage the industry correctly to ensure the safety of swimmers.

The swim-with-whale industry began on the east coast of Australia in 2013 off Mooloolaba, Queensland. In response to this, and in an effort to jumpstart the regional economy, the Queensland government initiated a trial swim-with-whale commercial tourism program in Hervey Bay in 2014. After an incident-free three-year trial, in 2017, the Australian Government and Queensland Department of National Parks permitted the swim-with-whale program to become a permanent activity in Hervey Bay. During the 2014–2016 trial period, Fraser Coast Tourism and Events, Inc. convened with a group of stakeholders to develop a Code of Conduct for swimming with whales in Hervey Bay. These guidelines were developed by the tour operators and submitted to the Queensland Parks and Wildlife Service in 2018 (Fraser Coast Tourism and Events, 2018). The Code of Conduct reinforces the existing national and state legislation and guidelines for operation, including the marine park management and permitting conditions. The stipulations for how the activity must be conducted in Hervey Bay include that free swimming/snorkeling is not permitted. Instead of freely swimming in the water, the passengers must hold onto a "mermaid line" that is attached to the vessel at one end or remain on a submerged swim platform. The Code of Conduct also states that when placing swimmers in the water, "minimum distances of vessels must comply with the minimum legal requirement defined as no approach zone for vessels: 100 m from the whale" in line with the Australian National Guidelines for Whale and Dolphin Watching (Department of the Environment and Energy, 2017). There are no limits on the number of available commercial licenses, and all existing whale watch and dive operators were offered the opportunity to add swimming with the whales to their Commercial Activity Agreement. There are currently eight authorised tour vessels that offer swim-with-whale tours in Hervey Bay; some operators focus solely on swim-with-whale tours while others combine a mix of swim-with-whale and traditional whale watch tours.

Hervey Bay acts as important habitat for breeding stock E-1 on their southern migration in the austral winter after departure from their tropical breeding grounds on the Great Barrier Reef (Smith et al., 2012). The bay is shallow, sheltered and serves as a mid-migratory stopover, especially for mother and calves (Corkeron et al., 1994; Franklin et al., 2011, 2018; Stack et al., 2019). Migratory stopover grounds, such as Hervey Bay, offer shelter and a place for humpback whales to rest, which supports energy conservation and offers increased opportunities for nursing a calf (Videsen et al., 2017; Bejder et al., 2019). Thus, reducing human-induced disturbance to humpback whales is particularly important in Hervey Bay.

In a recent survey of global swim-with-whale operations, it was recommended that detailed studies should be conducted in each location containing swim-with-whale operations to examine the impact on individuals, groups, and populations of cetacean species to evaluate management options (Gero et al., 2016). These recommendations have been further supported by the International Whaling Commission (IWC) Scientific Committee. The IWC Scientific Committee acknowledge that: (1) the effects of swim-with-whale programs will vary among targeted species and populations, (2) further research into the impacts of swim-with-whale programs are required, and (3) a precautionary approach toward management of swim-with-whale programs should be implemented until the impacts are better understood (International Whaling Commission, 2000; International Whaling Commission , 2004). To meet this need, in this study we examined the short-term behavioural impacts of swim-with-whale tourism in Hervey Bay. Specifically, we: (1) assessed the effects (behavioural activity and changes in swimming direction) *before, during,* and *after* swimmers entered the water on a mermaid line with juvenile and adult whales, and (2) examined any differences in whale behaviours between whale watch and swim-with-whale tours. Furthermore, we identified any factors which influenced short-term behavioural changes in whales in response to swimmers; and identified any management issues associated with swim-with-whale tourism. It is hypothesised that: (1) swim-with-whale tours will cause behavioural changes in whales in the *during* phase compared to *before* and *after*, and that (2) short-term responses in swim-with-whale tours will be greater in magnitude compared to whale watch tours.

MATERIALS AND METHODS

Study Site and Species

This study was conducted from July through September in 2018, 2019, and 2020 in Hervey Bay, Queensland (25°00′S, 152°52′E; **Figure 1**). Hervey Bay is a shallow bay, generally < 18 m depth, which is composed of a sand and mud bottom. The E-1 humpback whale population migrates along the east coast of Australia between May and December to and from their Antarctic feeding grounds (Franklin et al., 2012; Andrews-Goff et al., 2018). On their southern migration, whales enter Hervey Bay from approximately early August to mid-October (Franklin et al., 2011). Humpback whales predominantly occupy the eastern portion of Hervey Bay, in Platypus Bay (Corkeron et al., 1994), which is a general use area in the Great Sandy Marine Park. There is a seasonal change in pod characteristics in the bay relating to the sexual and maturational classes; this is evident in arrival patterns. Juvenile whales and mature females are first to arrive in August, by mid-season larger groups of mature adults arrive, and by mid-late season mother-calf pairs arrive (Franklin et al., 2011). Whales may reside in the bay for 2–3 days, with some having extended stays for over a month (Stack et al., 2019). When leaving the bay, the whales exit north and continue their southern migration on the eastern side of K'gari (Fraser Island) (Franklin et al., 2018). Breeding stock E-1 has recovered well from the commercial whaling era, and is currently estimated at >25,545 whales (2015 estimate; 95% confidence interval 21,631–27,851) and has been increasing at an estimated 10.9% per annum (Noad et al., 2019).

Swim-With-Whale Tour Regulations

All trips and approaches to whales were conducted following the Australia National Guidelines for Whale and Dolphin Watching

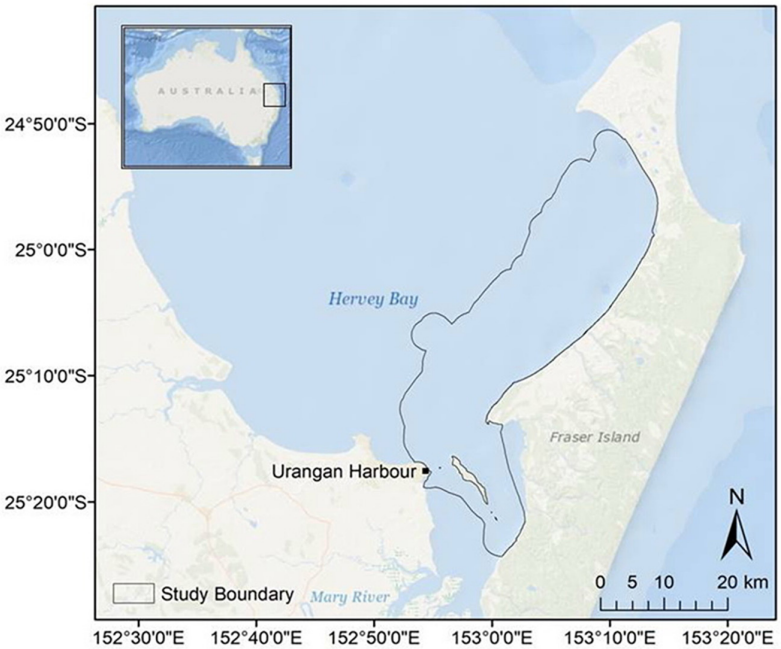

FIGURE 1 | The study area of Hervey Bay, Queensland, and its location along the east coast of Australia (insert). The vessel departed from Urangan Harbour and transited the nearshore protected waters west of K'gari (Fraser Island) within the study area outlined in black.

2017 (Department of the Environment and Energy, 2017) and Commercial Activity Agreement guidelines, which are outlined in detail below.

Commercial Activity Agreement and Code of Conduct

The main initial safety concern from the Queensland Government for the swim-with-whale tourism industry was from encounters between humans and sharks. After a review on sharks in the region (Pepperell and Williams, 2014), swim-with-whale activities were deemed safe by the Queensland Government and permitted for the 2014 whale season in Hervey Bay. Currently, the Queensland Government Commercial Activity Agreement provides the following limitations for licensed swim-with-whale operators (Department of the Environment and Energy, 2017):

- Free-swimming with whales is not permitted, and "immersive whale watching activities" are permitted via holding a mermaid line (a line that is secured to the vessel at one end, not to exceed 20 m in length) and/or duckboard method (e.g., sitting or lying on a submerged or semi-submerged swim platform aboard the vessel).
- The maximum number of swimmers allowed in the water at any one time is 10 persons, including guides.
- Immersive whale watching is prohibited at any time where a calf has been identified.
- A person must not enter the water closer than 100 meters (m) from a whale and, a person in the water within this 100 m distance, must not move toward a whale.
- The vessel engine must be stopped before the swimmers are placed in the water.

Compliance with these regulations is unknown and, to date, Queensland Marine Parks have not monitored the swim-with-whale industry in Hervey Bay. As the Code of Conduct is industry driven (not a government initiative), safety is based on the operators Safety Management System (SMS) through the Australian Maritime Safety Authority.

Whale Watch Tour Regulations

The Queensland Government currently requires all commercial whale watch operators to abide by the following regulations (Department of the Environment and Energy, 2017), which were followed by the vessel used during this study.

- The 'caution' zone is an area surrounding a whale or dolphin in which boats cannot travel at speeds of more than six knots or speeds that create a wake. The caution zone extends out 300 m from a whale.
- Within a caution zone there are areas designated as 'no approach' zones that boats cannot enter. These are the areas closest to an animal and directly in front of and behind an animal. For a whale, the no approach zone surrounds the animal for 100 m and extends 300 m in front of and behind the animal.
- A boat cannot enter a caution zone if three boats are already present within the caution zone of an animal.

Compliance with the regulations is unknown; however, Queensland Marine Parks does routinely monitor the whale watch industry.

Data Collection for Whale Watch and Swim-With-Whale Tours

Humpback whale behavioural observations were collected from a rigid-hull inflatable boat (RHIB), 12.5 m in length, with four Yamaha 300 hp outboard petrol engines. This same vessel was used to conduct both commercial swim-with-whale tours and whale watch tours at different times throughout the day departing from Urangan Harbor. Data on swim-with-whale operations were collected *before, during,* and *after* swimmers entered the water, to examine if there were any short-term changes in the whales' behaviour. Additionally, data were collected from the same vessel platform during traditional whale watch tours to compare the behavioural responses of whales between whale watching and the *during* phase of the swim-with-whale tours.

The swim-with-whale tours were specifically designed to adhere to the license conditions and Code of Conduct, including having <10 swimmers (including the swim guide) in the water, approaching the target whale at 100 m to place swimmers in the water and not swimming with groups with calves. Humpback whale calves in Hervey Bay range from a few weeks to a few months old (Stack et al., 2019). For this study, we defined a calf as described in the Australian National Guidelines; an individual whale visually estimated to be approximately 50% of the length of the accompanying whale and maintaining a constant and close relationship (e.g., as in Chittleborough, 1965) with the adult whale, who is assumed to be the mother (Department of the Environment and Energy, 2017; Stack et al., 2019).

TABLE 1 | For the purpose of this study, the humpback whale behavioural states were defined as diving, resting, travelling, surface active, and socialising.

Behavioural state	Description	Associated behavioural events
Diving	Whales take visible dives and remain submerged for an extended period of time.	Fluke up dive Fluke down dive Round out dive Sudden deep dive
Surface Active	Whales displayed energetic behaviours observed from the surface with or without a clear direction of travel* *if not directed toward another whale	Breach Peduncle throw Tail slap Head slap Pectoral fin slap
Resting	Individuals remain stationary at the surface or mill at the surface without a clear direction of travel.	Logging Milling/Resting
Socialising	Whales visibly interact with one another; includes surface active behaviours directed toward another whale with or without a clear direction of travel.	Active milling Surface active behaviours, if directed toward another whale.
Travelling	All animals in the group travel in a consistent direction.	Slow travel Medium travel Fast travel Sudden Burst of Speed Change of Direction (in any direction, e.g., toward and away from the vessel)
Other	Any behaviour not covered by the other categories	Spy hop Mugging the vessel

The list of all observed behaviours with the associated category for behavioural state are listed here and are adapted from Lundquist et al. (2013) and Fiori et al. (2019).

The transit time from Urangan Harbour to Platypus Bay was 30–45 min. Both swim-with-whale and whale watch tours had a transit speed of ∼25–28 knots, and humpback whales were searched for with the naked eye. Two dedicated researchers were on board for both swim-with-whale and whale watch tours. When a whale(s) was sighted, the vessel slowed to ∼15 knots until it reached the focal individual/group. Data for both swim-with-whale and whale watch tours began from around approximately 400 m distance. One researcher measured the distance to the whales using a Bushnell Legend 1200 ARC rangefinder throughout the encounter, where the distance between the whale and vessel varied, however the group was never actively approached by the vessel <100 meters. Whales were opportunistically photographed with a Canon DSLR camera (100–400 mm lens) to obtain photo-identification data on targeted whales dorsal fin and/or tail fluke to identify unique markings (Kaufman et al., 1987; Stack et al., 2019). Photo-ID matching was completed within each season to determine if the same whales were subjected to swim-with-whale tours on more than one occasion to avoid non-independent observations. The second researcher recorded the time, GPS location (lat/long), environmental conditions and behaviour of the whales during each phase (before, during, after) and throughout encounters on the whale watch tours. Data on the environmental conditions included the Beaufort sea state, where swims were only conducted during good weather conditions with low swell (Beaufort ≤ 3). Behavioural observations (Altmann, 1974) were classified into five states (**Table 1**), which were mutually exclusive and wholly inclusive (i.e., a group could not simultaneously be in multiple behavioural states, and behavioural states encompassed all possible observed activities). When there was a group of whales, the behavioural state was based on the predominant group behaviour. Additional behavioural data included recording: (i) group size and composition (juvenile, adult, mother-calf), (ii) changes to group composition, i.e., affiliations and disaffiliations, (iii) the overall behavioural state and changes that occurred (**Table 1**), and (iv) details on whale behavioural events associated with behavioural state (**Table 1**). Direction changes were recorded each time they occurred and were defined as a whale at the surface changing its heading by 90 degrees or more, irrespective of the boat position.

For swim-with-whale tours, data were collected as a *before, during,* and *after* study design. In the *before* phase, the skipper approached the target whales slowly from a distance (∼300 m) and data on the natural/control behaviour of the whales was recorded for 15 min. The distance between the whale and vessel varied in the *before* phase, however the group was never actively approached <100 m. It should be noted that in some cases, the whales actively approached the vessel in the *before* phase and the vessel remained in neutral to avoid engine noise as much as possible (thus the whales were closer than 100 m in the *before* phase in some instances). In the *before* phase, the captain determined if the whales were suitable to place swimmers in the water. Whale groups were deemed 'suitable' when they were not swimming quickly and had a calm demeanour, i.e., were not displaying any aggressive behaviours. In the *during* phase, the skipper approached the whales at 100 m and endeavoured to place

the swimmers in the water. In some cases, the whales were already within 100–150 m of the vessel and swimmers were placed in the water without manoeuvring. Swimmers were never placed in the water when the whales were closer than 100 m from the vessel. Once the skipper decided to make a swim attempt, the engine was turned off, a step ladder was lowered, a mermaid line (made of braided nylon, 20 m length, with pool noodles attached along the length of the rope to add flotation) was placed in the water and 1–10 people (with masks and snorkel, no fins) entered the water slowly and calmly. Participants were asked to hold onto the mermaid line and float, and not actively swim. The duration of the *during* phase generally lasted as long as the whales remained in the vicinity of the swimmers. The *after* phase consisted of an additional 15 min focal follow recording the behaviour of the whales, whilst the swimmers were back on board and the skipper kept the vessel at a distance ∼300 m to continue observations. It should be noted that in some cases, the whales actively approached the vessel in the *after* phase and the vessel remained in neutral to avoid engine noise as much as possible and waited for the whales to move beyond 300 m. The 15 min duration of the *before* and *after* phases was chosen to maximise the time recording the whale's behaviour and to allow for the time constraints of a three hour swim-with-whale tour.

Data Analysis

Comparison Among *Before, During, After* Phases Within Swim-With-Whale Tours

To determine potential changes in whale behaviour arising from swimmers in the water during swim-with-whale tours, the proportion of time spent in each behavioural state and frequency of direction changes/hour while travelling were calculated *before, during,* and *after* swimmers entered the water. We did not attempt to separate the effects of the vessel from the effects of swimmers in the water because under the Commercial Activity Agreement terms and Code of Conduct, the swimmers would never be present without the vessel.

The proportion of time spent in each behavioural state was calculated for each phase (*before, during,* and *after*), by dividing the time observed in a particular behavioural state by the total phase time. The proportion of time spent resting, socialising, surface active, and travelling was determined by summing the amount of time spent in each of the associated behavioural events reported in **Table 1** at a one-minute resolution. Socialising behaviours were restricted to observations that were specifically toward conspecifics. The proportion of time spent diving was determined by calculating the time between an associated behavioural event for diving (**Table 1**) and the subsequent re-surfacing of the group. The frequency of whale directional changes/hour was calculated by dividing the observed counts of direction changes while whales were travelling (**Table 1**) for each observation phase by the time spent in that phase and then converting this to direction changes per hour. The total number of samples included in the final models for *before, during,* and *after* data for swim-with-whale tours included data on focal groups with a minimum of 15 min observation time in all three phases, and group size remaining constant throughout the encounter (i.e., no affiliation or disaffiliations). To minimize impacts of environmental variables, only data where Beaufort sea state ≤ 3 were used in subsequent analysis.

Comparison Between Whale Watch and Swim-With-Whale Tours

To determine any potential differences of tour type on whale behaviour and swimming direction changes, data collected in the *during* phase (swimmers in the water) of swim with tours and aboard whale watch tours were examined. For whale watching, the engines were mostly left on transiting slowly or in neutral (occasionally switched off, e.g., when listening to whales) and *during* swim-with-whale tours, the engines were either switched off or placed in neutral. To determine potential changes in whale behaviours, the proportion of time spent in each behavioural state (1-min resolution) and frequency of direction changes/hour were quantified for each encounter and compared. The proportion of time spent in each behavioural state was calculated by dividing the time observed in a particular behavioural state by the total time spent with the group. For swim-with-whale tours, the total time was for the *during* phase only. The frequency of direction changes/hour was calculated by dividing the observed counts of direction changes by the total time spent with the group and then converting this to direction changes per hour. As regulations do not permit swim-with-whale tours with calf groups, any mother-calf data collected on whale watch tours were excluded to ensure the comparative analysis between the tour types included whales of the same age-classes and composition. To determine whether the tour type affected whales' behavioural activity level, we tested for significant differences in the pooled proportion of time spent in each behavioural state on whale watch tours and the *during* phase of swim-with-whale tours using a Z-test for proportions (Welch, 1937). The total number of samples included in the model were the total number of swim-with-whale tours and the total number of observations on whale watch tours where Beaufort sea state ≤ 3, group size remained constant throughout the encounter (i.e., no affiliation or disaffiliations), no calves were present, and at least 15 min of observation time.

Generalised Additive Modelling

All statistical analyses and subsequent figures were completed using *R* version 4.0.1 (R Core Team, 2020). To ensure accurate representation of whale behaviour, only phases with an observation time of $\geq$15 min were included in analysis. The frequency of direction changes/hour and the proportion of time whales spent in five behavioural states (**Table 1**; diving, resting, surface active, socialising, travelling) were modelled as a function of explanatory variables using generalised additive models (GAMs) developed in the mgcv package (Wood, 2004, 2017). GAMs allowed for the evaluation of non-normal response variables and testing of potential non-linear relationships.

To determine the potential impact within swim-with-whale tours, the proportion of time spent in each behavioural state and the frequency of direction changes/hour were modeled as a function of: whale group size (excluding groups with calves), average distance between the whale(s) and the vessel over the encounter (in m, the number of distance points ranged from 3 to 34, $SE = 14$), phase (*before, during, and after;* as a categorical

TABLE 2 | Summary of top GAM models showing the relationship between the number of direction changes, and the proportion of time spent surface active, resting, diving, and socialising *before, during*, and *after* swim-with-whale tours.

	Number of direction changes	Proportion of time surface active	Proportion of time resting	Proportion of time diving	Proportion of time socialising	Proportion of time travelling
Intercept	–0.69***	–1.54***	–3.97***	0.21	–1.53***	–1.41***
Year	–	–1.30**	–	–	1.21*	–
Phase – *Before*	–	–	–	–	–	–
Phase – *During*	–	–	–	–	–	–
Group size	–	–	–	–0.38*	–	–
Distance between vessel and whale(s)	–	–	–	–	–	–
Interaction between distance to whale(s) and phase *(Before)*	s(2.57)***	–	s(5.19)	s(1.49)	–	s(1.00)
Interaction between distance to whale(s) and phase *(During)*	s(6.77)***	–	s(4.26)	s(4.24)	–	s(1.00)**
Interaction between distance to whale(s) and phase *(After)*	s(2.40)*	–	s(1.00)*	s(1.77)	–	s(1.28)
Deviance explained (%)	56.0	10.2	25.0	20.4	9.1	10.1
Number of observations	126	126	126	126	126	126

*Rows represent candidate explanatory variables and columns represent response variables considered for each of the six separate models. Cells with a "–" indicate terms dropped from the final model. Values represent the parametric coefficient estimates for factors and the degree of smoothing [s(edf)] for smooth terms included in the final model. The significance value is represented as ***p = 0–0.001; **p = 0.001–0.01; *p = 0.01–0.05.*

variable), and year. In addition, to determine any differences between swim-with-whale tours and whale watching tours, the proportion of time spent in each behavioural state and the frequency of direction changes/hour were modeled as a function of: trip type (swim-with-whale, whale watching), whale group size (excluding groups with calves), average distance between the whale(s) and the vessel over the encounter, and year.

All models were fitted using penalized regression splines (Wood and Augustin, 2002) with default smoothing values (10 knots) in each spline and smoothing parameters estimated using generalised cross validation (GCV) score. To account for overdispersion, a quasibinomial family with a logit link was selected for models investigating the proportion of time spent in each behavioural state, and a quasipoisson family with a log link was applied for modelling frequency of direction changes/hour. This approach introduces a dispersion parameter, (ϕ), into the model which describes additional variance in the data that cannot be explained by a binomial or poisson distribution alone.

Model selection procedures followed Wood (2001), where a fully saturated model was initially fit for each response variable including interaction terms, and a final model was selected based on the GCV score and percent of deviance explained. The most parsimonious model was selected by decreasing the GCV score and increasing the deviance explained. With the exception of categorical variables, all continuous terms were initially fit with a smoother. Terms were tested for and removed if there were (1) non-significant linear terms with a parameter coefficient near 0; or (2) non-significant smoothed terms with estimated degrees of freedom (edf) close to 1. Smoother terms were retained for interactions between a categorical variable and continuous variable when at least one level of the interaction term met the criteria listed above. This allowed for the evaluation of the significant non-linear levels of the interaction term, despite some levels having an edf = 1 (Nisbet et al., 2018). The linear form of the term was retained if the smoothed term was dropped, had an edf near 0, did not decrease the GCV score and/or the deviance explained did not increase. Multicollinearity in explanatory variables was tested (>0.7 was deemed multicollinear per González-Suárez et al. (2013), and if present, the term with the least support for inclusion in the final model, based on the model selection criteria listed above, was dropped.

Model fit was evaluated through visual inspection of residual plots and diagnostic information produced using the gam.check function (Wood, 2001). Models were checked for overdispersion and autocorrelation to ensure modelling assumptions were met. Only models with significant relationships between response and explanatory variables are presented graphically in the subsequent results and included for discussion.

RESULTS

Summary Statistics for Swim-With-Whale and Whale Watch Tours

Over the course of three field seasons, from 2018 to 2020, data were recorded during 75 swim-with-whale tours (=250 h) and 48 whale watch tours onboard the tour vessel (=150 h). A total of 324 humpback whale groups were observed across both tour types, of which 127 groups (42 from swim-with-whale tours, 85 from whale watch tours) had a minimum observation time of $\geq$15 min and were used in subsequent analysis. The mean duration of time for observations during whale watch tours was 29 min (SD $\pm$ 12), and for swim-with-whale tours was 28 min (SD $\pm$ 16) *before*, 26 min (SD $\pm$ 13) *during,* and 28 min (SD $\pm$ 17) *after*. Whale group sizes ranged from one to six whales, with a median of two (SD $\pm$ 0.98) across both swim-with-whale tours and whale watch tours. There were 209

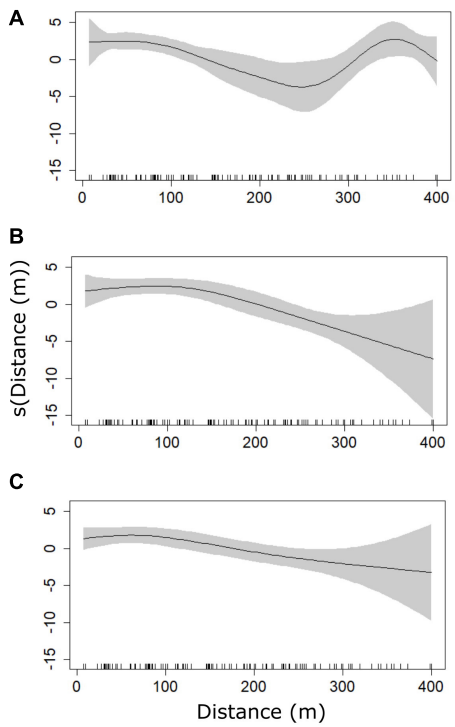

FIGURE 2 | Results from the best fit generalized additive model for the frequency of direction changes/hour made by humpback whales [Freq. Direct. Chang. = β_0 + s(phase:distance) + Error] showing model parameter estimates for the interaction between distance from the whale and phase type **(A)** *before*, **(B)** *during,* and **(C)** *after*. The dashed lines and shaded area represent the 95% confidence intervals of the parameter estimate. The vertical lines represent the data points combined for *before, during,* and *after* phases (rug-plot).

individual whales photographed during swim-with-whale tours of which none were re-sighted during swim-with-whale tours within each field season.

Comparison Among Phases (*Before, During, After*) Within Swim-With-Whale Tours

The frequency of direction changes/hour and the proportion of time spent resting, diving, and travelling were found to be significantly impacted by the interaction between phase (*before, during,* and *after*) and distance from whale to vessel (**Table 2**). There were no detectable changes in the proportion of time spent socialising or being surface active among phases of swim-with-whale tours (**Table 2**).

Direction changes were observed in 71% (30 of 42) of groups in the *before, during,* and *after* observations. The best fit model explaining the frequency of direction changes/hour observed within swim-with-whale tours explained 56.0% of the deviance and included the interaction term between phase and distance between whale and vessel (**Table 2**). The frequency of direction changes/hour varied significantly with distance for all phases (p-value = *before* < 0.001, *during* < 0.001, *after* 0.015; **Figure 2A**), with an increase in frequency of heading changes as the distance between the vessel and whale(s) decreased in the *during* and *after* phases (**Table 2** and **Figures 2B,C**). The frequency of direction changes/hour in the *before* phase varied with distance (**Figure 2A**) and was lowest when the vessel was 250 m from the whale group.

Surface activity was observed in 60% (25 of 42) of groups in the *before, during,* and *after* observations. The best fit model for the proportion of time that whale groups spent being surface active explained 10.2% of the deviance and included a term for year (**Table 2**). Surface activity was found to be significantly lower in 2020 (p-value = 0.007) relative to other years (**Table 2**). The phase, group size and distance from the vessel did not have a significant effect on the proportion of time spent surface active (**Table 2**).

Resting behaviour was observed in 24% (10 of 42) of groups in the *before, during,* and *after* observations. The best fit model explaining the proportion of time spent resting within swim-with-whale tours explained 25% of the deviance and included the interaction term between phase and distance between whale groups and vessel (**Table 2**). The proportion of time resting varied with distance throughout swim-with-whale tours (**Figures 3A–C**) and significantly decreased (p-value = 0.048) with distance *after* the vessel left (**Figure 3C**). The year, phase, and group size did not have a significant effect on the proportion of time resting (**Table 2**).

Diving was observed in 90% (38 of 42) of groups in the *before, during,* and *after* observations. The best fit model for the proportion of time diving included terms for group size and the interaction term between phase and distance between whale and vessel, which explained 20% of the deviance (**Table 2**). Group size had a significant effect on the proportion of time diving (p-value = 0.014); as group size increased, the proportion of time diving decreased (**Table 2**). The proportion of time diving varied with distance throughout swim-with-whale tours (**Figures 4A–C**) and was most variable *during* swim-with-whale tours however there was an equal chance of diving (**Figure 4B**). Phase, year, and distance from the vessel did not have a significant effect on the proportion of time spent diving (**Table 2**).

Socialising was observed in 38% (16 of 42) of groups in the *before, during,* and *after* observations. The best fit model explaining the proportion of time socialising within swim-with-whale tours included a term for year, and explained 9% deviance (**Table 2**). The time spent socialising varied significantly between years (p-value = 0.025), while phase, group size, and distance from the vessel did not have a significant effect (**Table 2**).

Travelling was observed in 33% (14 of 42) of groups in the *before, during,* and *after* observations. The best fit model explaining the proportion of time spent travelling within swim-with-whale tours explained 10% of the deviance and included the interaction term between phase and distance between whale and vessel (**Figure 5** and **Table 2**). The proportion of time spent travelling varied significantly with distance *during* swim-with-whale tours (p-value = 0.007), with whales travelling more when vessels remained further away (**Figure 5B**). The phase, year,

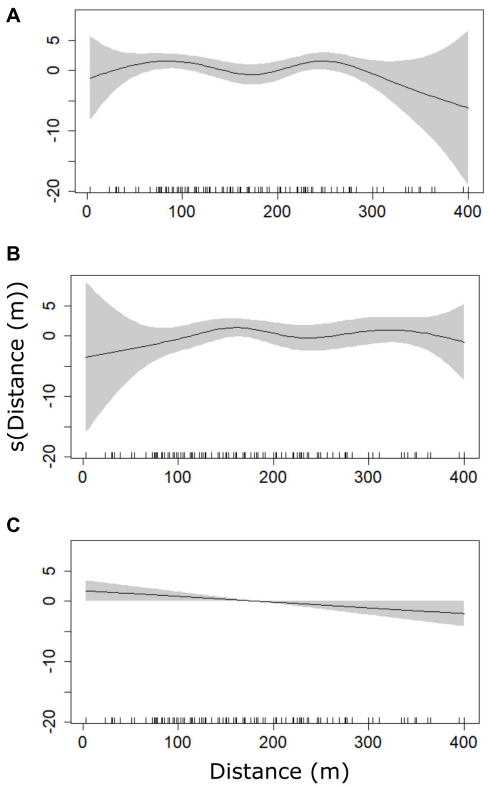

FIGURE 3 | Results from the best fit generalised additive model for the proportion of time humpback whales spent resting [Prop. Rest. = β_0 + s(phase:distance) + Error] showing model parameter estimates for the interaction between distance from the whale and phase type **(A)** *before* (note beyond 300 m there are fewer data points thus the confidence intervals are larger and interpretation beyond 300 m is cautioned), **(B)** *during,* and **(C)** *after* (linear). The shaded area represents the 95% confidence intervals of the parameter estimate. The vertical lines represent the data points combined for *before, during,* and *after* phases (rug-plot).

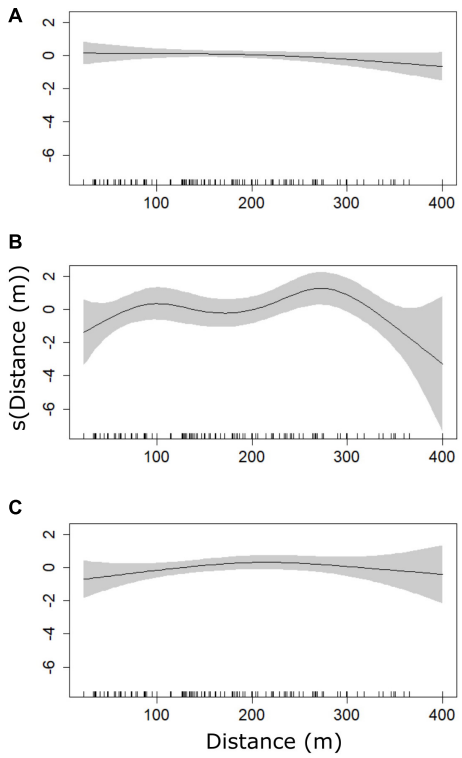

FIGURE 4 | Results from the best fit generalised additive model for the proportion of time humpback whales spent diving [Prop. Div. = β_0 + group size + s(phase:distance) + Error] showing model parameter estimates for the interaction between distance from the whale and phase type **(A)** *before*, **(B)** *during,* and **(C)** *after*. The dashed lines and shaded area represent the 95% confidence intervals of the parameter estimate. The solid horizontal lines represent the mean. The vertical lines represent the data points combined for *before, during,* and *after* phases (rug-plot).

group size, and distance from the vessel did not have a significant effect on the proportion of time spent travelling (**Table 2**).

Comparison Between Whale Watch and Swim-With-Whale Tours

The average distance between whale groups and the vessel during whale watch tours was 157 m (*SD* = 98, range = 12–400 m, *n* = 85). The distance between whales and the vessel in the *during* phase of swim-with-whale tours averaged 212 m (*SD* = 188, range = 5–400 m, *n* = 42). Within swim-with-whale tours, the distance between whale groups and the vessel was on average 160 m (*SD* = 92 m, range = 5–400 m, *n* = 42) *before,* 212 m (*SD* = 115, range = 5–400 m, *n* = 42) *during*, and 170 m (*SD* = 105 m, range = 3.5–400 m, *n* = 42) *after* approaches. Results from the best fit GAMs found the frequency of direction changes/hour as well as the proportion of time spent resting and travelling were significantly impacted by the interaction between tour type and distance from whale groups to vessel (**Table 3**). No detectable changes in the proportion of time spent being surface active, diving, or socialising were detected between whale watch and swim-with-whale tours (**Table 3**).

Whale direction changes were observed in 70 whale groups, with 94 occurrences during whale watch tours and 121 occurrences during swim-with-whale tours. The best fit model explained 49.2% of the deviance and included terms for year and the interaction between tour type and distance between whale(s) and vessel (**Table 3**). The frequency of direction changes/hour decreased with distance for both tour types (**Figures 6A,B**), and was found to be significant (*p*-value = 0.028) for whale watch tours (**Figure 6A**). The frequency of direction changes/hour was found to be significantly lower in 2020 (*p*-value = 0.013) relative to 2018 and 2019 (**Table 3**).

Surface active behaviours were recorded in 61% (52 of 85) of groups observed from whale watch tours and 21% (9 of 42) of groups *during* swim-with-whale tours. There was no detectable difference in the mean proportion of time spent conducting surface active behaviours between tour types (*Z*-test for two proportions: $Z = 2.58$, $p = 0.108$). The best fit model for the proportion of time that whale groups spent being surface active explained 23.8% of the deviance and included terms for tour

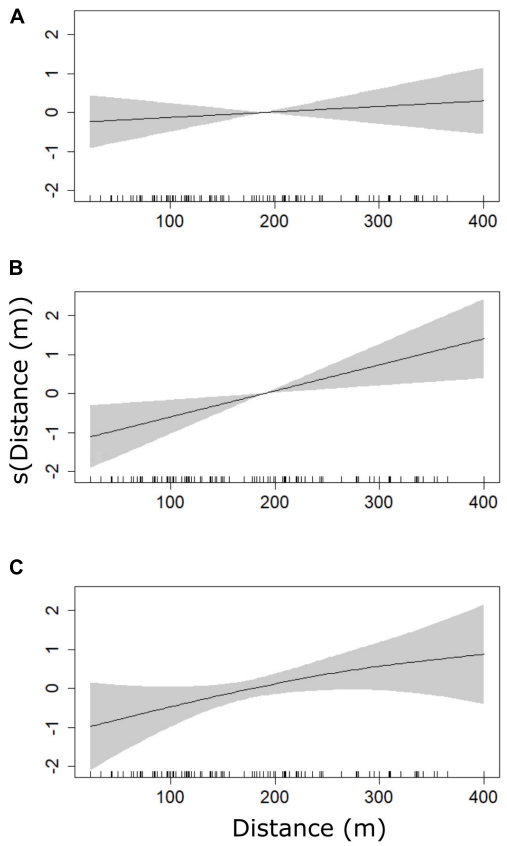

FIGURE 5 | Results from the best fit generalised additive model for the proportion of time humpback whales spent travelling [Prop. Travel. = β_0 + s(phase:distance) + Error] showing model parameter estimates for the interaction between distance from the whale and phase type **(A)** *before* (linear), **(B)** *during* (linear), and **(C)** *after*. The dashed horizontal lines represent the 95% confidence intervals of the parameter estimate. The solid horizontal lines represent the mean. The vertical lines represent the data points combined for *before, during,* and *after* phases (rug-plot).

type, year, and the interaction between tour type and distance between whale(s) and vessel (**Table 3** and **Figures 7A–C**). During swim-with-whale tours, the amount of time spent surface active decreased when compared to whale watch tours (p-value = 0.09, **Table 3** and **Figure 7A**). On whale watch tours, surface activity increased as vessel distance from the whale group increased (p-value = 0.065; **Figure 7B**). The proportion of time conducting

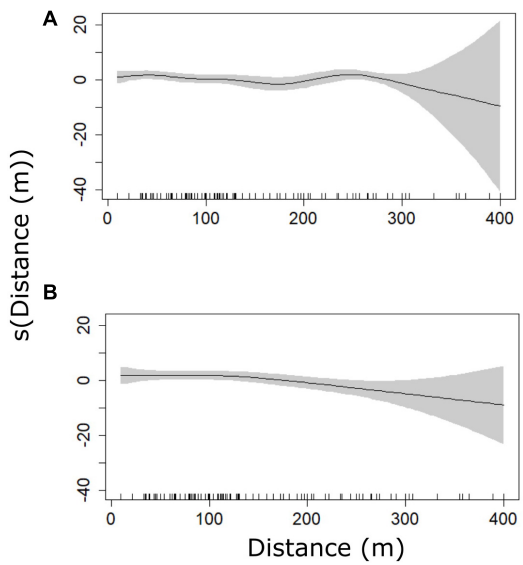

FIGURE 6 | Results from the best fit generalized additive model for the frequency of direction changes/hour made by humpback whales [Freq. Direct. Chang. = β_0 + year + s(tour type:distance) + Error] showing model parameter estimates for the interaction between distance from the whale and tour type for **(A)** whale watch and **(B)** swim-with-whale tours. Note beyond 300 m there are fewer data points thus the confidence intervals are larger and interpretation beyond 300 m is cautioned. The dashed horizontal lines represent the 95% confidence intervals of the parameter estimate. The solid horizontal lines represent the mean. The vertical lines represent the data points combined for whale watch and swim-with-whale tours (rug-plot).

TABLE 3 | Summary of top GAM models showing the relationship between the number of direction changes, and the proportion of time spent surface active, resting, diving, socialising, and travelling during swim-with-whale tours and whale watch tours.

	Number of direction changes	Proportion of time surface active	Proportion of time resting	Proportion of time diving	Proportion of time socialising	Proportion of time travelling
Intercept	0.83	–0.96***	–4.02***	–0.79*	–3.90***	–1.58***
Year	–1.29*	–1.52**	0.98	–1.06**	–	–
Group size	–	–	–	–0.43**	0.60***	–
Trip type	–	–1.09	–	–	–	–
Distance between vessel and whale(s)	–	–	–	–	–	–
Interaction between distance to whale(s) and trip type *(whale watch vessel)*	S(6.32)*	s(3.45)	s(4.12)*	s(1.00)	–	s(1.84)
Interaction between distance to whale(s) and trip type *(swim with vessel)*	S(2.40)	s(1.00)	s(1.00)	s(2.82)	–	s(1.00)**
Deviance explained (%)	49.2	23.8	27.2	25.6	15.4	11.6
Number of observations	127	127	127	127	127	127

*Rows represent candidate explanatory variables and columns represent response variables for each of the six separate models. Cells with a "–" represent terms dropped from the final model. Values represent the parametric coefficient estimates for factors and the degree of smoothing [s(EDF)] for smooth terms included in the final model. The significance value is represented as ***p = 0–0.001; **p = 0.001–0.01; *p = 0.01–0.05.*

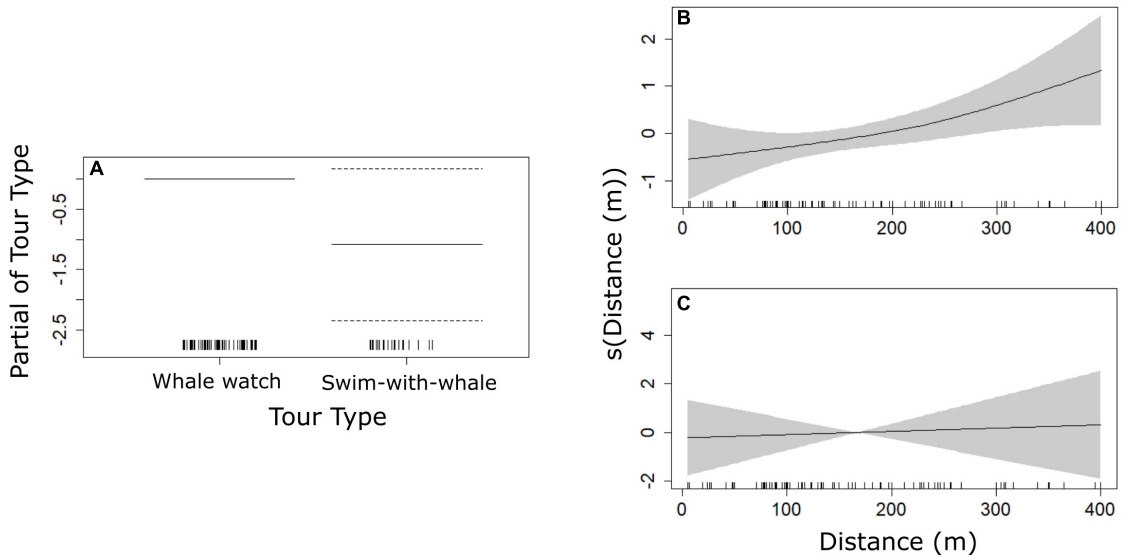

FIGURE 7 | Results from the best fit generalised additive model for the proportion of time humpback whales spent surface active [Prop. Surf. Activ. = β_0 + tour type + year + s(tour type:distance) + Error] showing model parameter estimates for **(A)** tour type and **(B)** distance between whale watch vessel and whale(s) (note < 100 m and >250 m there are fewer data points thus the confidence intervals are larger and interpretation is cautioned), and **(C)** distance between swim-with-whale vessel and whale(s) (linear; edf = 1). The dashed horizontal lines represent the 95% confidence intervals of the parameter estimate. The solid horizontal lines represent the mean. The vertical lines represent the data points combined for whale watch and swim-with-whale tours (rug-plot).

surface active behaviours was found to be significantly lower in 2020 (p-value = 0.005) relative to other years (**Table 3**).

Resting behaviour was recorded in 22% (19 of 85) of groups observed from whale watch tours and 12% (5 of 42) of groups *during* swim-with-whale tours. There was a 50% reduction in the proportion of time spent resting *during* swim-with-whale tours compared to whale watch tours, with the proportion of time spent resting found to be significantly less *during* swim-with-whale tours (Z-test for two proportions: Z = 4.287, p-value = 0.038). The best fit GAM model for the mean proportion of time resting explained 27.2% of the deviance, and included terms for year and the interaction term between tour type and distance between whale and vessel (**Figures 8A,B** and **Table 3**). The proportion of time resting was influenced significantly by distance of the whale watch vessel (p-value = 0.012; **Table 3**), with resting times ranging from 0 to 92% of the encounter and lowest when distances were beyond 100 m (**Figure 8A**).

Diving behaviour was recorded in 74% (63 of 85) of groups observed from whale watch tours and 47% (20 of 42) of groups *during* swim-with-whale tours. The proportion of time spent diving was not significantly different *during* swim-with-whale tours compared to whale watch tours (Z-test for two proportions: Z = 0.32, p = 0.57). The best fit model for the proportion of time that whale groups spent diving explained 25.6% of the deviance and included terms for year, group size, and the interaction between tour type and distance between the whale(s) and vessel (**Table 3**). The proportion of time spent diving varied with distance between tour types (**Table 3** and **Figure 9**) however, was not significant (p-value = 0.07) for whale watch tours. The proportion of time spent diving significantly decreased with an increase in group size (p-value = 0.006), and was significantly lower in 2020 (p-value = 0.002) relative to other years (**Table 3**).

Socialising was recorded in 39% (33 of 85) of groups observed from whale watch tours and 17% (7 of 42) of groups *during* swim-with-whale tours. The mean proportion of time spent socialising was not significantly different *during* swim-with-whale tours compared to whale watch tours (Z-test for two proportions: Z = 0.262, p = 0.61). The best fit model for the proportion of time that whale groups spent socialising explained 15.4% of the deviance and found a significant increase (p-value < 0.0001) with increasing group size (**Table 3**).

Travelling was recorded in 71% (60 of 85) of groups observed from whale watch tours and 26% (11 of 42) of groups *during* swim-with-whale tours. No detectable difference was found between the proportion of time spent travelling between tour types (Z-test for two proportions: Z = 2.36, p = 0.13). The best fit model for the proportion of time that whale groups spent travelling explained 11.6% of the deviance and included an interaction term between tour type and distance between whale(s) and vessel (**Table 3** and **Figures 10A,B**). During swim-with-whale tours, whales spent significantly more time travelling (p-value = 0.003) when vessels remained further away (**Table 3** and **Figure 10B**).

DISCUSSION

In this study, we examined short-term behavioural responses of humpback whales to swim-with-whale tours on a resting ground in Hervey Bay. A *before, during,* and *after* study design was implemented where the *during* phase constituted of swimmers

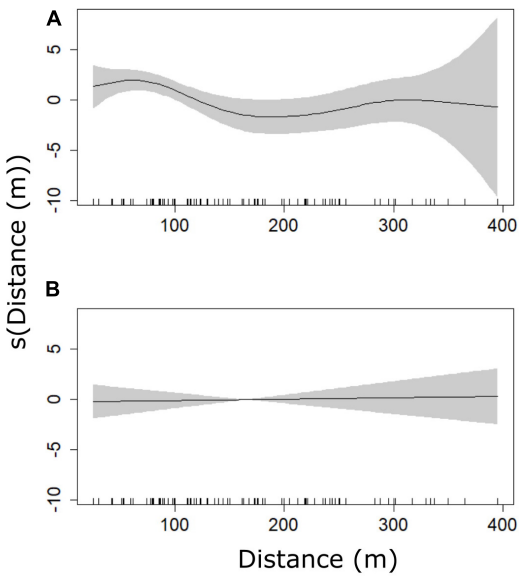

FIGURE 8 | Results from the best fit generalised additive model for the proportion of time humpback whales spent resting [Prop. Rest. = β_0 + year + s(tour type:distance) + Error] showing model parameter estimates for the interaction between distance from the whale and tour type for **(A)** whale watch (note beyond 300 m there are fewer data points thus the confidence intervals are larger and interpretation beyond 300 m is cautioned) and **(B)** swim-with-whale tours (linear; edf = 1). The dashed horizontal lines represent the 95% confidence intervals of the parameter estimate. The solid horizontal lines represent the mean. The vertical lines represent the data points combined for whale watch and swim-with-whale tours (rug-plot).

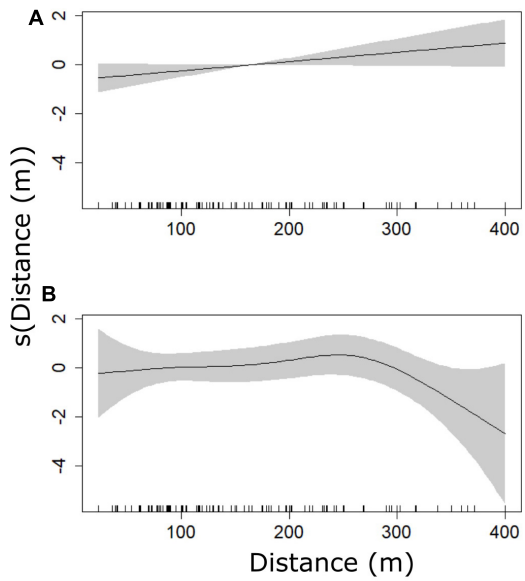

FIGURE 9 | Results from the best fit generalised additive model for the proportion of time humpback whales spent diving [Prop. Div. = β_0 + year + group size + s(tour type:distance) + Error] showing model parameter estimates for the interaction between distance from the whale and tour type for **(A)** whale watch (linear; edf = 1) and **(B)** swim-with-whale tours (note beyond 350 m there are fewer data points thus the confidence intervals are larger and interpretation beyond 350 m is cautioned). The dashed horizontal lines represent the 95% confidence intervals of the parameter estimate. The solid horizontal lines represent the mean. The vertical lines represent the data points combined for whale watch and swim-with-whale tours (rug-plot).

being placed in the water holding a mermaid line. Additionally, humpback whale behaviours in the *during* phase of swim-with-whale tours were compared to behaviours exhibited during traditional boat-based whale watch tours. Within the swim-with-whale tours, behavioural changes were detected in the *before, during,* and *after* phases, with the majority of significant changes occurring in the *during* and *after* phases. Whales also exhibited a higher frequency of direction changes and a 50% reduction in resting during swim-with tours compared to whale watch tours, demonstrating clear differences in the behavioural responses to the two tour types. These results support the conclusion that the natural behaviour of humpback whales in Hervey Bay was altered in response to swim-with-whale tourism.

Comparison between tour types (swim-with-whale and whale watch) demonstrated that the behavioural changes in the whales were largely related to the distance between whale(s) and the vessel, with an interaction term between tour type and distance to whale present in five of the six models investigated. The average vessel distance in the *during* phase of swim-with-whale tours was 212 m and during whale watch tours was 157 m. Given that this area has been described as a resting ground, resting is the predominant behaviour that is expected however the proportion of time spent resting during both tour types was low (6% of time during whale watch tours and 3% *during* swim-with-whale tours). These results suggest that humpback whales were more disturbed during swim-with-whale tours than during whale watch tours, but the low proportion of time spent resting overall is of concern and should be investigated further.

It is unclear if the presence of the swimmers is the factor that the whales are responding to and/or to the closer distance of the vessel. One caveat to this study is that the experimental design did not allow for data collection on humpback whale behaviour in the absence of boat-based tourism (i.e., control data), therefore behavioural changes could not be declared different from their natural behaviour, and should not be definitively attributed to boat approaches and/or swimmer placement. Some additional factors to consider when evaluating swim-with-whale impacts include the type of vessel approach, the sound level of the engine(s), the group composition and reproductive status of the whales, and the geographic location (i.e., calving ground, migration route, feeding ground). In this study, we used the same vessel platform and captains in order to minimise these differences and replicate the tour types as closely as possible.

Our findings add to the growing body of literature that show impacts on whale behaviour arising from commercial swim-with-whale tourism (e.g., Lundquist et al., 2013; Fiori et al., 2019; Hoarau et al., 2020; Sprogis et al., 2020). Here, we offer a comparison of how whale behavioural responses to swim-with-whale tours differ from those observed during traditional boat-based whale watch tours. There are several short-term behavioural responses reported on whales from the swim-with tourism industry (reviewed in Machernis et al., 2018),

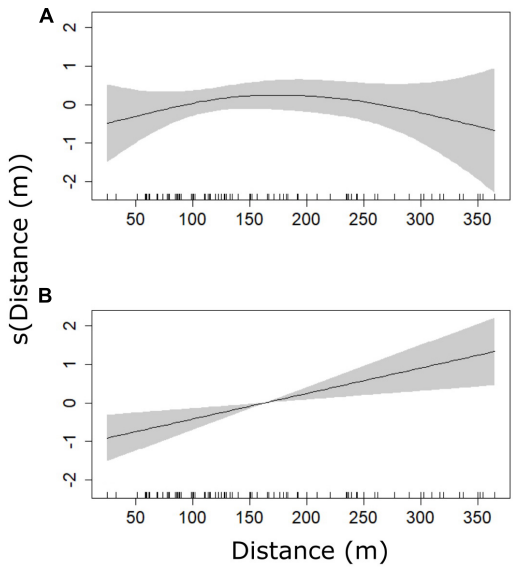

FIGURE 10 | Results from the best fit generalised additive model for the proportion of time humpback whales spent travelling [Prop. Travel. = β_0 + s(tour type:distance) + Error] showing model parameter estimates for the interaction between distance from the whale and tour type for **(A)** whale watch (note < 100 m and > 250 m there are fewer data points thus the confidence intervals are larger and interpretation is cautioned) and **(B)** swim-with-whale tours (linear; edf = 1). The dashed horizontal lines represent the 95% confidence intervals of the parameter estimate. The solid horizontal lines represent the mean. The vertical lines represent the data points combined for whale watch and swim-with-whale tours (rug-plot).

including an increase in surface active behaviours, respiration rate and swim speed, and a less direct path of travel (Kessler et al., 2013; Fiori et al., 2019, 2020; Hoarau et al., 2020; Sprogis et al., 2020). Changes in the amount of time spent resting and travelling have been described as a direct sign of disturbance, but changing direction has also been noted as a tactic for humpback whales to avoid predators and evade a perceived threat (Schaffar et al., 2013). The results in Hervey Bay are different to previous studies for resting, travelling, and surface active behaviours, but still show an alteration in behaviour is occurring during swim-with-whale tours. Previous research has shown that behavioural changes can be energetically costly for whales (e.g., Lusseau and Bejder, 2007; Braithwaite et al., 2015; Villagra et al., 2021), therefore the observed high frequency of direction changes may mean that humpback whales in Hervey Bay are experiencing an increase in their energy expenditure in response to swim-with-whale tours. Further research is needed to quantify these energetic impacts and if long-term consequences are apparent. The responses observed to swim-with-whale tours may not only require additional energetic costs, but also indicate an increased level of physiological disturbance that could interfere with normal whale behaviour (Schaffar et al., 2013; Fiori et al., 2019).

Our results highlight the importance of studying the impacts of swim-with-whale tourism in each region where it is offered, because the effects on the target animals likely differ for each species, population segment, and geographic area. Hervey Bay is a mid-migratory stopover where a portion of the population segment diverts and spends time during the southern migration, after departing the breeding grounds (Franklin et al., 2011; Stack et al., 2019). Humpback whales use Hervey Bay to rest, socialise, and nurse their calves prior to their migration to their Antarctic feeding grounds. Adult whales may also use this region for mating opportunities based on observations of competition pods (Bryden et al., 1989; Corkeron, 1995). Given this, it is unsurprising that the behavioural changes observed differed to those reported in other studies that examined behavioural responses to swim-with-whales tourism (Lundquist et al., 2013; Fiori et al., 2019; Sprogis et al., 2020). Furthermore, demonstrating any kind of vertical avoidance would be difficult in this environment given the low depth profile of Hervey Bay.

In Hervey Bay, placing swimmers in the water with a humpback whale calf is not permitted. This decision is based on the Marine Park Act 2004, where it is specified "there is no swimming with whales at any time where a calf has been identified" (Marine Parks Act 2004, 2017). This decision is in alignment with the International Whaling Commission (International Whaling Commission, 2014) and Australian National Guidelines (Department of the Environment and Energy, 2017), which do not endorse swimming with mother and calves. Accordingly, no swimming with calves was observed by researchers in Hervey Bay during this study. This is, however, not the case in other locations in Australia (e.g., Sprogis et al., 2020), and around the world (e.g., Fiori et al., 2019), where swimming with calves occurs, even in areas where it has been advised against. It is of great importance to limit disturbance on mother-calf pairs as they are the most sensitive to disturbance (Sprogis et al., 2020) and, over extended periods of time, increases in energy expenditure could become biologically significant for mothers with a dependent calf (Cartwright and Sullivan, 2009; Ejrnæs and Sprogis, 2021). Thus, in Hervey Bay it is of importance to retain best practice guidelines on not swimming with calves to reduce disturbance to the whales, but also to avoid injury to humans from high-risk situations with mother and calves (as documented in Sprogis et al., 2017, 2020; Fiori et al., 2019; Barra et al., 2020; Hoarau et al., 2020).

Management Recommendations

If the swim-with industry was to grow in areas where swimming with whales is not yet permitted, we recommend a precautionary approach to developing this activity. Resource managers should assume that disturbance is taking place unless it can be proven otherwise. The results of this study demonstrate that, when following all legal regulations and the Code of Conduct, swim-with-whale tourism causes humpback whales to change their behaviour and is generally more invasive than traditional boat-based whale watching. Developing a Code of Conduct among operators is an admirable step, however, the existence of guidelines alone is not sufficient at mitigating the potential for disturbance (Wiley et al., 2008). It is recommended that guidelines be accompanied by annual trainings with permit holders and a commitment to review and refresh the guidelines at a particular interval of time and/or when new information becomes available. In addition to education about the guidelines,

an increased monitoring presence and enforcement of the rules is needed to ensure that the guidelines that exist are being followed.

Disturbance to whales from tourism can cause deviations from natural whale behaviours that can have energetically costly consequences for these migratory whales (e.g., Lusseau and Bejder, 2007). Although the whales are not exhibiting a typical horizontal avoidance (swimming away), if the presence of the swimmers or vessels causes the whales to change their behaviour in any measurable manner, this will have an increased energetic cost for the whales. If humpback whales in Hervey Bay are changing their natural behaviours as a result of swim-with-whale tours, whether to avoid or to approach the vessel and/or the swimmers, they will spend more time swimming and changing directions and proportionally less time resting. This will affect the amount of stored energy they have available to complete their southern migration. As humpback whales are capital breeders with limited energy reserves, reducing disturbance is of high importance for their continued population recovery and for the sustainability of the marine tourism industry. As climate change continues to affect prey distribution and abundance (Bengtson Nash et al., 2018; Seyboth et al., 2021), whales may have to travel farther to seek out their prey, making these energetic impacts even more important to study and mitigate.

The pressure created by social media to get close to wildlife is an emerging trend that is partially driving this industry growth (Pagel et al., 2020a). Interviews conducted with swim-with-whale tour operators in the South Pacific revealed that skilled wildlife photographers and social media influencers were the type of passengers most likely to ignore safety rules and guidelines in order to get closer to wildlife (Pagel et al., 2020b). Such behaviour increases the potential for wildlife harassment and can elicit a behavioural response from wild animals that could pose a safety hazard for the swimmers (Pagel et al., 2020b). Managing tourism expectations through responsible advertising and clear messaging about the regulations and best practices is important so operators do not feel pressured into breaking regulations or getting closer than necessary.

Overall, swim-with-whale tourism poses a considerable risk to human safety due to the close proximity of large, powerful whales that can be unpredictable in their movements and behaviours. These tours also pose a greater risk to whale safety over traditional boat-based whale watching, due to close approaches by vessels and swimmers. In this study, several safety incidences were recorded including: (1) one whale exhibited numerous head slaps in sequence at approximately 100 m distance while swimming away from the vessel; (2) while initiating a swim with two juvenile whales, the guide was swimming the mermaid line out (no other passengers in the water yet) and one of the whales approached the guide to approximately 50 m distance and did a peduncle throw; (3) while there were six swimmers in the water with two adult whales, one whale performed a peduncle throw at approximately 100 m distance, in the direction of the swimmers. In other regions, researchers have reported a high rate of aggressive behaviours observed from humpback whales while swimmers were in the water and serious injuries to swimmers have occurred (Barra et al., 2020; Fiori et al., 2020; Sprogis et al., 2020). Despite the legal measures designed to minimise the safety risk to swimmers in Queensland, there were incidences where whale behaviour posed a risk to the safety of the swimmers. These incidents highlight the inherent danger that is present when swimming with large whales.

CONCLUSION

This study highlights that commercial swim-with-whale tours that abide by all legal regulations and the Code of Conduct have behavioural responses from humpback whales in Hervey Bay, Australia and that they are generally more invasive than traditional boat-based whale watching. It is unknown whether these short-term behavioural responses can have detrimental effects at the population-level and this should be further investigated. In areas where a swim-with-whales industry is already established, care must be taken to manage passenger expectations and be as non-invasive as possible. Commercial swim-with-whale tours have a greater motivation than traditional whale watch tours to get as close as possible to the whales in order to satisfy their customers' expectations for swim experiences, and these close approaches are shown to have a behavioural impact on the target whales. Robust education and enforcement programmes, combined with continued monitoring of population dynamics through scientific research, are needed to minimise detrimental impacts to the population and guide adaptive management strategies. In regions where this industry does not yet exist, countries should follow the precautionary principle and assume that impacts will occur. The commercial swimming with whales industry, where it exists, should be managed and guidelines refined until the point where the safety issues are addressed and there are no detectable impacts to whale behaviour. Furthermore, this activity should be ceased if swimmer injuries occur and/or, at any point, population-level effects are detected from the cumulative impact of repeated disturbance.

DATA AVAILABILITY STATEMENT

The raw data supporting the conclusions of this article will be made available by the authors, without undue reservation.

ETHICS STATEMENT

The animal study was reviewed and approved by Queensland Government Animal Ethics Committee.

AUTHOR CONTRIBUTIONS

SS conceived and conceptualized the study. SS, GO, JC, and KS conducted the fieldwork. SS, FS, and JC conducted the data processing and analysis. SS, KS, and JC carried out the interpretation. All the authors contributed to the writing and editing of the manuscript as well as commenting on various drafts of the manuscript.

FUNDING

Funding for this work was provided by Pacific Whale Foundation. The funder was not involved in the study design, collection, analysis, interpretation of data, the writing of this article or the decision to submit it for publication.

ACKNOWLEDGMENTS

We extend our thanks to the two reviewers whose feedback greatly improved the manuscript. We would like to thank Andrew Ellis for his assistance and support in executing this study, as well as the Ocean Defender captains Scott Whitcombe and Millie Stell, and the PacWhale Eco-Adventures Australia naturalists who assisted with this study. Thank you to Jessica McCordic, Antara May, Suzie Vallance, Jaimi Raveneau, Luke Spinks, Tine Haslam Nielsen, and Romy Levin for their valuable contributions to the data collection. Sincere thanks to the captains and crew of the Hervey Bay Whale Watch fleet for your generosity in hosting our researchers. Thank you to the Hervey Bay Harbour View Caravan Park for their accommodation support for Pacific Whale Foundation Australia researchers.

REFERENCES

Altmann, J. (1974). Observational study of behavior: sampling methods. *Behaviour* 49, 227–267. doi: 10.1163/156853974x00534

Andrews-Goff, V., Bestley, S., Gales, N. J., Laverick, S. M., Paton, D., Polanowski, A. M., et al. (2018). Humpback whale migrations to Antarctic summer foraging grounds through the southwest Pacific Ocean. *Sci. Rep.* 8:12333. doi: 10.1038/s41598-018-30748-4

Arnold, P. W. (1997). Occurrence of dwarf minke whales (*Balaenoptera acutorostrata*) on the northern great barrier reef, Australia. *Rep. Int. Whal. Commun.* 47, 419–424.

Barra, T., Bejder, L., Dalleau, M., Delaspre, S., Landes, A. E., Harvey, M., et al. (2020). Social media reveal high rates of agonistic behaviors of humpback whales in response to swim-with activities off Reunion Island. *Tour. Mar. Environ.* 15, 191–209. doi: 10.3727/154427320X15960647825531

Bejder, L., Videsen, S., Hermannsen, L., Simon, M., Hanf, D., and Madsen, P. T. (2019). Low energy expenditure and resting behaviour of humpback whale mother-calf pairs highlights conservation importance of sheltered breeding areas. *Sci. Rep.* 9:771. doi: 10.1038/s41598-018-36870-7

Bengtson Nash, S. M., Castrillon, J., Eisenmann, P., Fry, B., Shuker, J. D., Cropp, R. A., et al. (2018). Signals from the south; humpback whales carry messages of Antarctic sea-ice ecosystem variability. *Glob. Change Biol.* 24, 1500–1510. doi: 10.1111/gcb.14035

Birtles, R., Arnold, P., and Dunstan, A. (2002). Commercial swim programs with dwarf minke whales on the northern Great Barrier Reef, Australia: some characteristics of the encounters with management implications. *Aust. Mammal.* 24:23. doi: 10.1071/AM02023

Braithwaite, J. E., Meeuwig, J. J., and Hipsey, M. R. (2015). Optimal migration energetics of humpback whales and the implications of disturbance. *Conserv. Physiol.* 3:cov001. doi: 10.1093/conphys/cov001

Bryden, M. M., Corkeron, P. J., and Slade, R. W. (1989). *Humpback Whales (Megaptera novaeangliae) in Hervey Bay, Queensland 1988. Report to the Australian National Parks and Wildlife Service, Canberra*. Canberra: Australian Nature Conservation Agency.

Cartwright, R., and Sullivan, M. (2009). Behavioral ontogeny in humpback whale (*Megaptera novaeangliae*) calves during their residence in Hawaiian waters. *Mar. Mamm. Sci.* 25, 659–680. doi: 10.1111/j.1748-7692.2009.00286.x

Chittleborough, R. G. (1965). Dynamics of two populations of the humpback whale, Megaptera novaeangliae (Borowski). *Aus. J. Mar. Freshw. Res.* 16, 33–128. doi: 10.1071/MF9650033

Corkeron, P. J. (1995). Humpback whales (*Megaptera novaeangliae*) in Hervey Bay, Queensland: behaviour and responses to whale-watching vessels. *Can. J. Zool.* 73, 1290–1299. doi: 10.1139/z95-153

Corkeron, P., Brown, M., Slade, R., and Bryden, M. (1994). Humpback whales, *Megaptera novaeangliae* (Cetaceaa : Balaenopteridae), in Hervey Bay, Queensland. *Wildl. Res.* 21:293. doi: 10.1071/WR9940293

Department of the Environment and Energy (2017). *Australian National Guidelines for Whale and Dolphin Watching 2017. Commonwealth of Australia*. Washington, DC: Department of the Environment and Energy.

Ejrnæs, D., and Sprogis, K. R. (2021). Ontogenetic changes in energy expenditure and resting behaviour of humpback whale mother-calf pairs examined using unmanned aerial vehicles. *Wildl. Res.* doi: 10.1071/WR20186 [Epub ahead of print].

Fiori, L., Martinez, E., Orams, M. B., and Bollard, B. (2019). Effects of whale-based tourism in Vava'u, Kingdom of Tonga: behavioural responses of humpback whales to vessel and swimming tourism activities. *PLoS One* 14:e0219364. doi: 10.1371/journal.pone.0219364

Fiori, L., Martinez, E., Orams, M. B., and Bollard, B. (2020). Using unmanned aerial vehicles (UAVs) to assess humpback whale behavioral responses to swim-with interactions in Vava'u, Kingdom of Tonga. *J. Sustain. Tour.* 28, 1743–1761. doi: 10.1080/09669582.2020.1758706

Franklin, T., Franklin, W., Brooks, L., and Harrison, P. (2018). Site-specific female-biased sex ratio of humpback whales (*Megaptera novaeangliae*) during a stopover early in the southern migration. *Can. J. Zool.* 96, 533–544. doi: 10.1139/cjz-2017-0086

Franklin, T., Franklin, W., Brooks, L., Harrison, P., Baverstock, P., and Clapham, P. (2011). Seasonal changes in pod characteristics of eastern Australian humpback whales (*Megaptera novaeangliae*), Hervey Bay 1992-2005. *Mar. Mamm. Sci.* 27, E134–E152. doi: 10.1111/j.1748-7692.2010.00430.x

Franklin, W., Franklin, T., Brooks, L., Gibbs, N., Childerhouse, S., Smith, F., et al. (2012). Antarctic waters (Area V) near the Balleny Islands are a summer feeding area for some eastern Australian Breeding Stock E(i) Humpback Whales (*Megaptera Novaeangliae*). *J. Cetacean Res. Manage.* 12, 321–327.

Fraser Coast Tourism and Events (2018). *Fraser Coast Industry Code of Practice: Immersive Whale Interactions in the Great Sandy Marine Park*. Queensland: Fraser Coast Tourism and Events.

Gero, S., Pace, S., Kaufman, G., Parsons, E. C. M., Ritter, F., Sironi, M., et al. (2016). Initial survey of global commercial swim-with-whale operations. *J. Cetacean Res. Manage.* SC/66b/WW/02.

González-Suárez, M., Gómez, A., and Revilla, E. (2013). Which intrinsic traits predict vulnerability to extinction depends on the actual threatening processes. *Ecosphere* 4:art76. doi: 10.1890/ES12-00380.1

Hendrix, T., and Rose, N. A. (2014). "Swim-with-whales tourism – an updated review of commercial operations," *Paper SC/65b/WW03 Presented to the IWC Scientific Committee 12–24 May*, 6.

Hoarau, L., Dalleau, M., Delaspre, S., Barra, T., and Landes, A. E. (2020). Assessing and mitigating humpback whale (*Megaptera Novaeangliae*) disturbance of whale-watching activities in Reunion Island. *Tour. Mar. Environ.* 15, 173–189. doi: 10.3727/154427320X15943326793398

Hoyt, E. (2001). *Whale Watching 2001: Worldwide Tourism Numbers, Expenditures, and Expanding Socioeconomic Benefits : A Special Report from the International Fund for Animal Welfare*. Yarmouth Port, MA: International Fund for Animal Welfare.

International Whaling Commission (2000). "Report of the Sub-Committee on Whalewatching, Annex M," *52nd Meeting of the International Whaling Commission*, Adelaide, June–July 2000.

International Whaling Commission (2004). *Report of the Workshop on the Science for Sustainable Whalewatching*. Cape Town South Africa: Breakwater Lodge, 6–9 March 2004.

International Whaling Commission (2014). Report of the scientic committee. Annex M. report of the sub-committee on whalewatching. *J. Cetacean Res. Manage* 16, 380–392.

Kaufman, G., Smultea, M., and Forestell, P. (1987). Use of lateral body pigmentation patterns for photographic identification of east Australian (Area V) humpback whales. *Cetus* 7, 5–13.

Kessler, M., Harcourt, R., and Heller, G. (2013). Swimming with whales in Tonga: sustainable use or threatening process? *Mar. Policy* 39, 314–316. doi: 10.1016/j.marpol.2012.12.013

Lundquist, D., Sironi, M., Würsig, B., Rowntree, V., Martino, J., and Lundquist, L. (2013). Response of southern right whales to simulated swim-with-whale tourism at Península Valdés, Argentina. *Mar. Mamm. Sci.* 29, E24–E45. doi: 10.1111/j.1748-7692.2012.00583.x

Lusseau, D., and Bejder, L. (2007). The long-term consequences of short-term responses to disturbance experiences from whalewatching impact assessment. *Int. J. Comp. Psych.* 20, 228–236.

Machernis, A. F., Powell, J. R., Engleby, L., and Spradlin, T. R. (2018). *An Updated Literature Review Examining the Impacts of Tourism on Marine Mammals Over the Last Fifteen Years (2000-2015) to Inform Research and Management Programs*. Washington, DC: National Oceanic and Atmospheric Administration.

Marine Parks Act 2004. (2017). *Marine Parks Act 2004. State of Queensland*. 124. Available online at: https://www.legislation.qld.gov.au/view/pdf/inforce/current/act-2004-031 (Accessed February 2, 2021)

Nisbet, R., Elder, J., and Miner, G. (2018). *Handbook of Statistical Analysis and Data Mining Applications*. Cambridge, MA: Academic Press, 864.

Noad, M. J., Kniest, E., and Dunlop, R. A. (2019). Boom to bust? Implications for the continued rapid growth of the eastern Australian humpback whale population despite recovery. *Popul. Ecol.* 61, 198–209. doi: 10.1002/1438-390X.1014

O'Connor, S., Campbell, R., Cortez, H., and Knowles, T. (2009). *Whale Watching Worldwide: Tourism Numbers, Expenditures and Expanding Economic Benefits (Special Report From the International Fund for Animal Welfare)*. Yarmouth, MA: Economists at Large, 228.

Pagel, C. D., Orams, M. B., and Lück, M. (2020a). Experienced photographer's behaviour during commercial swim-with-wildlife tours: comparative case studies of three operations in the South Pacific. *Curr. Issues Tour.* 24, 1–13. doi: 10.1080/13683500.2020.1828312

Pagel, C. D., Orams, M., and Lück, M. (2020b). #biteme: Considering the potential influence of social media on in-water encounters with marine wildlife. *Tour. Mar Environ.* 15, 249–258. doi: 10.3727/154427320X15754936027058

Parsons, E. C. M. (2012). The negative impacts of whale-watching. *J. Mar. Biol.* 2012, 1–9. doi: 10.1155/2012/807294

Pepperell, J., and Williams, S. (2014). *Swimming with Humpback Whales-Potential Risks from Sharks, Report to Queensland Parks and Wildlife Service Department of National Parks, Recreation, Sport and Racing*. Queensland: Pepperell Research, 14.

R Core Team (2020). *R: A Language and Environment for Statstical Computing*. Vienna: Foundation for Statistical Computing.

Rose, N. A., Weinrich, M., Iñíguez, M. A., and Finkle, M. (2005). "Swimwith-whales tourism – an updated review of commercial operations," in *Paper SC/57/WW6 Presented to the IWC Scientific Committee* 20–24 June.

Samuels, A., and Bejder, L. (2004). Chronic interaction between humans and free-ranging bottlenose dolphins near Panama City Beach, Florida, USA. *J. Cetacean Res. Manage* 6, 69–77.

Samuels, A., Bejder, L., and Heinrich, S. (2000). *A Review of the Literature Pertaining to Swimming with Wild Dolphins*. Bethesda, MD: Marine Mammal Commission.

Schaffar, A., Madon, B., Garrigue, C., and Constantine, R. (2013). Behavioural effects of whale-watching activities on an Endangered population of humpback whales wintering in New Caledonia. *Endanger. Species Res.* 19, 245–254. doi: 10.3354/esr00466

Seyboth, E., Félix, F., Lea, M., Dalla Rosa, L., Watters, G. M., Reid, K., et al. (2021). Influence of krill (*Euphausia superba*) availability on humpback whale (*Megaptera novaeangliae*) reproductive rate. *Mar. Mamm. Sci.* 12805. doi: 10.1111/mms.12805

Smith, J. N., Grantham, H. S., Gales, N., Double, M. C., Noad, M. J., and Paton, D. (2012). Identification of humpback whale breeding and calving habitat in the Great Barrier Reef. *Mar. Ecol. Prog. Ser.* 447, 259–272. doi: 10.3354/meps09462

Sprogis, K. R., Bejder, L., and Christiansen, F. (2017). *Swim-with-Whale Tourism Trial in the Ningaloo Marine Park, Western Australia. Report to the Department of Parks and Wildlife, Western Australia*. Murdoch, WA: Murdoch University, 49.

Sprogis, K. R., Bejder, L., Hanf, D., and Christiansen, F. (2020). Behavioural responses of migrating humpback whales to swim-with-whale activities in the Ningaloo Marine Park, Western Australia. *J. Exp. Mar. Biol. Ecol.* 522, 151254. doi: 10.1016/j.jembe.2019.151254

Stack, S. H., and Serra, S. (2021). "Summary of swim-with-whales tourism around the globe," in *Paper SC/68C/WW/03 Presented to the IWC Scientific Committee*, 27 April–14 May, 8.

Stack, S. H., Currie, J. J., McCordic, J. A., Machernis, A. F., and Olson, G. L. (2019). Distribution patterns of east Australian humpback whales (*Megaptera novaeangliae*) in Hervey Bay, Queensland: a historical perspective. *Aust. Mammal.* 42:16. doi: 10.1071/AM18029

Valentine, P. S., Birtles, A., Curnock, M., Arnold, P., and Dunstan, A. (2004). Getting closer to whales—passenger expectations and experiences, and the management of swim with dwarf minke whale interactions in the Great Barrier Reef. *Tour. Manag.* 25, 647–655. doi: 10.1016/j.tourman.2003.09.001

Videsen, S. K. A., Bejder, L., Johnson, M., and Madsen, P. T. (2017). High suckling rates and acoustic crypsis of humpback whale neonates maximise potential for mother–calf energy transfer. *Funct. Ecol.* 31, 1561–1573. doi: 10.1111/1365-2435.12871

Villagra, D., García-Cegarra, A., Gallardo, D. I., and Pacheco, A. S. (2021). Energetic effects of whale-watching boats on humpback whales on a breeding ground. *Front. Mar. Sci.* 7:600508. doi: 10.3389/fmars.2020.600508

Welch, B. L. (1937). On the z-test in randomized blocks and Latin squares. *Biometrika* 29, 21–52. doi: 10.2307/2332405

Wiley, D. N., Moller, J. C., Pace, R. M., and Carlson, C. (2008). Effectiveness of voluntary conservation agreements: case study of endangered whales and commercial whale watching. *Conserv. Biol.* 22, 450–457. doi: 10.1111/j.1523-1739.2008.00897.x

Wood, S. N. (2001). mgcv: GAMs and Generalized Ridge Regression for R. *R News* 1, 20–25.

Wood, S. N. (2004). Stable and efficient multiple smoothing parameter estimation for generalized additive models. *J. Am. Stat. Assoc.* 99, 673–686. doi: 10.1198/016214504000000980

Wood, S. N. (2017). *Generalized Additive Models: An Introduction With R*, 2nd Edn. Boca Raton, FL: Chapman and Hall.

Wood, S. N., and Augustin, N. H. (2002). GAMs with integrated model selection using penalized regression splines and applications to environmental modelling. *Ecol. Modell.* 157, 157–177. doi: 10.1016/S0304-3800(02)00193-X

Conflict of Interest: The authors declare that the research was conducted in the absence of any commercial or financial relationships that could be construed as a potential conflict of interest.

Publisher's Note: All claims expressed in this article are solely those of the authors and do not necessarily represent those of their affiliated organizations, or those of the publisher, the editors and the reviewers. Any product that may be evaluated in this article, or claim that may be made by its manufacturer, is not guaranteed or endorsed by the publisher.

Copyright © 2021 Stack, Sprogis, Olson, Sullivan, Machernis and Currie. This is an open-access article distributed under the terms of the Creative Commons Attribution License (CC BY). The use, distribution or reproduction in other forums is permitted, provided the original author(s) and the copyright owner(s) are credited and that the original publication in this journal is cited, in accordance with accepted academic practice. No use, distribution or reproduction is permitted which does not comply with these terms.

frontiers in Marine Science

ORIGINAL RESEARCH
published: 25 August 2021
doi: 10.3389/fmars.2021.654184

Spatial Analysis of Beaked Whale Foraging During Two 12 kHz Multibeam Echosounder Surveys

Hilary Kates Varghese[1], Kim Lowell[1], Jennifer Miksis-Olds[1,2], Nancy DiMarzio[3], David Moretti[3] and Larry Mayer[1]*

[1] Center for Coastal and Ocean Mapping, University of New Hampshire, Durham, NH, United States, [2] Center for Acoustic Research and Education, School of Marine Science and Ocean Engineering, University of New Hampshire, Durham, NH, United States, [3] Ranges, Engineering and Analysis Department, Naval Undersea Warfare Center, Newport, RI, United States

To add to the growing information about the effect of multibeam echosounder (MBES) operation on marine mammals, a study was conducted to assess the spatial foraging effort of Cuvier's beaked whales during two MBES surveys conducted in January of 2017 and 2019 off of San Clemente Island, California. The MBES surveys took place on the Southern California Antisubmarine Warfare Range (SOAR), which contains an array of 89 hydrophones covering an area of approximately 1800 km^2 over which foraging beaked whales were detected. A spatial autocorrelation analysis of foraging effort was conducted using the Moran's I (global) and the Getis-Ord Gi* (local) statistics, to understand the animals' spatial use of the entire SOAR, as well as smaller areas, respectively, within the SOAR *Before, During,* and *After* the two MBES surveys. In both years, the global Moran's I statistic suggested significant spatial clustering of foraging events on the SOAR during all analysis periods (*Before, During,* and *After*). In addition, a Kruskal-Wallis (comparison) test of both years revealed that the number of foraging events across analysis periods were similar within a given year. In 2017, the local Getis-Ord Gi* analysis identified hot spots of foraging activity in the same general area of the SOAR during all analysis periods. This local result, in combination with the global and comparison results of 2017, suggest there was no obvious period-related change detected in foraging effort associated with the 2017 MBES survey at the resolution measurable with the hydrophone array. In 2019, the foraging hot spot area shifted from the southernmost corner of the SOAR *Before*, to the center *During,* and was split between the two locations *After* the MBES survey. Due to the pattern of period-related spatial change identified in 2019, and the lack of change detected in 2017, it was unclear whether the change detected in 2019 was a result of MBES activity or some other environmental factor. Nonetheless, the results strongly suggest that the level of detected foraging during either MBES survey did not change, and most of the foraging effort remained in the historically well-utilized foraging locations of Cuvier's beaked whales on the SOAR.

Keywords: BACI, multibeam echosounder, beaked whale behavior, spatial autocorrelation, GLC approach

OPEN ACCESS

Edited by:
Renata Sousa-Lima, Federal University of Rio Grande do Norte, Brazil

Reviewed by:
Jay Barlow, Southwest Fisheries Science Center (NOAA), United States
Elizabeth Henderson, SPAWAR Systems Center Pacific (SSC Pacific), United States

****Correspondence:***
Hilary Kates Varghese
hkatesvarghese@ccom.unh.edu

Specialty section:
This article was submitted to Marine Ecosystem Ecology, a section of the journal Frontiers in Marine Science

Received: *15 January 2021*
Accepted: *26 July 2021*
Published: *25 August 2021*

Citation:
Kates Varghese H, Lowell K, Miksis-Olds J, DiMarzio N, Moretti D and Mayer L (2021) Spatial Analysis of Beaked Whale Foraging During Two 12 kHz Multibeam Echosounder Surveys. Front. Mar. Sci. 8:654184. doi: 10.3389/fmars.2021.654184

INTRODUCTION

It is well understood that underwater anthropogenic sound can impact marine life (Hildebrand, 2005; Wright et al., 2007; Gomez et al., 2016). The exact effect will vary based on a multitude of factors (National Research Council, 2005) including but not limited to, characteristics inherent to the animal, the specific characteristics of the source of noise (Southall et al., 2007), the proximity of the animal to the source (Richardson et al., 1995; Erbe and Farmer, 2000; Falcone et al., 2017), whether the source and/or the animal is moving, and the behavioral state of the animal (Isojunno et al., 2016). The effect may also vary with different species (Miller et al., 2012) and among individuals of the same species (Sivle et al., 2015). Therefore, carefully controlled studies are necessary (Popper et al., 2020) to build an understanding about which species, behaviors, contexts, and interactions are most vulnerable to negative impacts during exposure to various anthropogenic underwater sound sources. Significant work has focused on understanding factors that lead to acute injury and death (Ketten, 2014; Kastelein et al., 2017), but arguably an equally concerning effect is behavioral change to a group or population that may ultimately lead to injury, death, or population decline (Johnson, 2012). This would include potential changes to important behaviors for an animal's livelihood such as foraging (Croll et al., 2006; McCarthy et al., 2011; Manzano-Roth et al., 2016), mating (Blom et al., 2019), and migrating (Malme et al., 1984).

Much of the work addressing the effect of anthropogenic noises on marine life has focused on marine mammals, for which the research has been heavily motivated by the protection of marine mammals under the Marine Mammal Protection Act (Marine Mammal Commission, 2015). One of the most vulnerable groups of marine mammals to anthropogenic noise appears to be beaked whales, as evidenced by the numerous strandings often linked to naval training exercises (Frantzis, 1998; Evans and England, 2001; D'Amico and Pittenger, 2009; Fernandez et al., 2012). As a result, there have been several studies investigating beaked whale foraging behavior during exposure to mid-frequency active sonar (MFAS) used during naval training exercises (McCarthy et al., 2011; Tyack et al., 2011; DeRuiter et al., 2013; Manzano-Roth et al., 2016; Falcone et al., 2017; DiMarzio et al., 2019). Several of these studies capitalized on the use of expansive hydrophone arrays found on United States Navy training ranges that are capable of receiving the echolocation clicks of foraging beaked whales (Jarvis et al., 2014). A Group Vocal Period (GVP), which represents a group of beaked whales foraging together in time and space, is a set of species-specific echolocation click trains associated to a central hydrophone of the foraging event (McCarthy et al., 2011). The GVP has been used as a proxy to assess foraging behavior across different time periods related to MFAS activity (McCarthy et al., 2011; Manzano-Roth et al., 2016; DiMarzio et al., 2019).

The spatial extent of the U.S. Navy hydrophone arrays extends over a couple thousand square-kilometer area. The MFAS and beaked whale foraging studies utilizing these arrays has included a temporal analysis (DiMarzio et al., 2019) in addition to a spatial analysis in some cases (McCarthy et al., 2011; Manzano-Roth et al., 2016). In the McCarthy et al. (2011) and Manzano-Roth et al. (2016) MFAS studies, heat maps of where the foraging events took place *Before, During,* and *After* MFAS activity were generated to provide insight into how the spatial use of the hydrophone arrays changed during the analysis periods. The lack of a more robust spatial analysis was likely the result of a clear temporal and spatial change in beaked whale foraging effort due to MFAS activity that did not require statistics to validate the obvious visual response reflected in the heat maps. The temporal analyses showed that the number of foraging events decreased on the array *During* MFAS activity, while the spatial analyses showed that most of the foraging effort shifted toward the edge (Manzano-Roth et al., 2016) or completely off the hydrophone array (McCarthy et al., 2011).

While it is clear that MFAS has an impact on beaked whales, the question has arisen as to the potential impact of other sonar signals on marine mammals, in particular, scientific echosounders. There have been several observational studies that suggest marine mammals react to high frequency scientific echosounders, either ceasing echolocation transmissions (Cholewiak et al., 2017), or increasing their heading variance (Quick et al., 2017). In 2008, there was a stranding event of melon-headed whales off of Madagascar that was associated in time with an offshore deep-water multibeam echosounder (MBES) mapping project 65 km away from the stranding site, though it was never conclusively determined to be the cause of the stranding (Southall et al., 2013). The increase in prevalence of these systems due to their expanding use in scientific work, geophysical surveys, and ocean mapping efforts has warranted further investigation of the potential effects echosounders may have on marine mammals.

This paper builds off of a recent study investigating the effect of deep-water MBES (12 kHz) activity on Cuvier's beaked whale foraging behavior (Kates Varghese et al., 2020), of which the analysis was modeled after similar MFAS work (McCarthy et al., 2011). Kates Varghese et al. (2020) presented a temporal assessment of foraging behavior *Before, During,* and *After* two MBES surveys conducted over the Southern California Antisubmarine Warfare Range (SOAR) hydrophone array of the U.S. Navy Southern California Offshore Range (SCORE). The temporal assessment of beaked whale foraging *During* MBES did not show a clear change in behavior with regards to MBES activity like that of the MFAS studies. Only one of the four metrics (number of GVPs, number of clicks per GVP, GVP duration, and click rate per GVP) used to assess foraging behavior changed *During* MBES activity; there was an increase in the number of GVPs per hour. A finer temporal analysis of each survey showed that the increase in the number of GVPs occurred during only one of the two surveys (Kates Varghese et al., 2020). And the number of GVPs increased again after the survey was complete, thereby providing no clear indication that the change was associated with the anthropogenic activity like that of the MFAS studies. Moreover, the increase in the number of GVPs during the MBES survey was a stark contrast to the decrease in the number of GVPs seen during the MFAS exercises.

In the MBES study, it was unclear through the temporal analysis alone whether the increase in the number of GVPs

during one of the two MBES survey periods was associated with the MBES activity. In order to provide a more complete picture of the potential effect of deep-water MBES as a sound source on beaked whale foraging behavior, a spatial analysis of beaked whale foraging behavior was conducted herein for the same two MBES surveys as the Kates Varghese et al. (2020). In the MFAS studies, spatial distribution maps of foraging events were used and provided another perspective on the effect that MFAS had on beaked whale foraging behavior. Not only did many of the animals decrease vocalizations but they visibly changed where they were predominantly foraging (McCarthy et al., 2011; Manzano-Roth et al., 2016), and sometimes left the U.S. Navy range where the MFAS was actively transmitting (Tyack et al., 2011), clearly indicating a response to the MFAS activity. Here a robust spatial analysis, beyond spatial distribution maps, was conducted to provide greater insight and to complement the temporal results in a comprehensive understanding of the potential impact of MBES on beaked whale foraging. In particular, the Global-Local-Comparison Approach (GLC) method described in Kates Varghese et al. (in review) was used, which was developed to robustly assess spatial marine mammal behavior across large-scale hydrophone arrays using spatial statistics and analysis of variance tests.

MATERIALS AND METHODS

This work utilized data from 89 hydrophones from the SOAR hydrophone array. The bottom-mounted hydrophones placed two to six km apart are found at depths ranging from 840 to 1750 m over an area of approximately 1800 km^2 off of San Clemente Island, California. The SOAR is shallowest along San Clemente Island in the southeast region, near which a shallow canyon is found before dropping off to 1500 m or greater over most of the rest of the range (**Figure 1**). The omnidirectional hydrophones were sampled at 96 kHz, and had a receiver bandwidth between 50 Hz and 48 kHz (DiMarzio and Jarvis, 2016). Due to their high site fidelity at the SOAR (Falcone et al., 2017), Cuvier's beaked whales and echolocation clicks from these animals, transmitted during foraging events, are routinely detected on the SOAR hydrophones.

As a follow-on to earlier work assessing the effect of MBES activity on the temporal aspects of Cuvier's beaked whale foraging behavior (Kates Varghese et al., 2020), the same detection and data processing schemes used in that study were used here. Echolocation clicks from several marine mammal species at the SOAR were detected using a class-specific support vector machine. Those that were classified as Cuvier's beaked whale foraging clicks were formed into click trains on a per hydrophone basis. Then a MATLAB-based autogrouper program used a set of rules based on the time and location of the click trains to form the GVPs (DiMarzio et al., 2018; Moretti, 2019). A GVP may be detected on multiple hydrophones, but the hydrophone that records the highest click density is defined as the center hydrophone of the event. The center hydrophone was used as the location of a GVP in this study. The maximum detection range of Blainville's beaked whale clicks was measured at 6.5 km at a U.S. Navy range in the Bahamas by cross-correlating the pattern of clicks identified on a DTAG, produced by the tagged animal, against the click patterns on surrounding bottom-mounted range hydrophones (Ward et al., 2008). These animals have a similar click source level and dive behavior to Cuvier's beaked whales (Johnson et al., 2004; Tyack et al., 2006). Previous studies at the SOAR have used an estimated horizontal detection distance of 6.3 km in defining a spatial range for Cuvier's beaked whale clicks detected from a single group (Kates Varghese et al., 2020). This detection range was assumed to be true for this study as well. The number of GVPs, per hydrophone, was used as a proxy to assess spatial foraging effort. For complete details on the detection and processing of GVPs see DiMarzio et al. (2018) and for its application to this work see the Materials and Methods section of Kates Varghese et al. (2020).

The method and data of this research study provide the opportunity to assess the change in overall spatial foraging behavior amongst Cuvier's beaked whales on the SOAR, i.e., the "foraging effort." This broad-stroke term is used because it emphasizes that this approach is agnostic to group size and composition, as both attributes can be ephemeral, in addition to other unknown factors such as foraging rates. Past studies of Cuvier's beaked whales have shown that this species is known

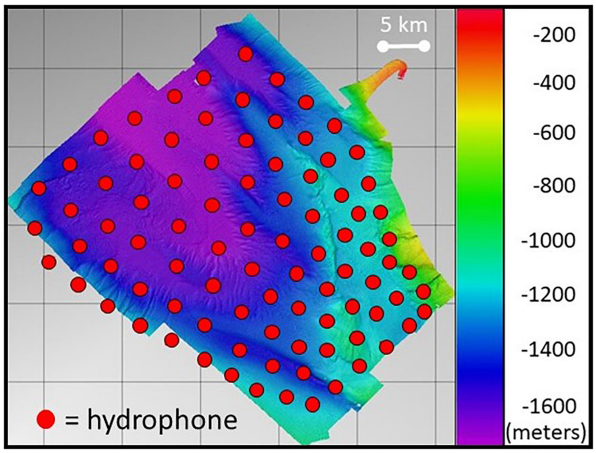

FIGURE 1 | Bathymetry of the SOAR with overlaid 89 hydrophone (red circles) sensors in the array. Depth scale is in meters. Reproduced from Kates Varghese et al. (2020) with the permission of the Acoustical Society of America.

TABLE 1 | MBES signal attributes and the estimated value for the 2017 and 2019 MBES surveys.

MBES signal attribute	Estimated value
Source Level (SPLrms)	239–242 dB re 1 μPa m
Center Frequency of Transmission	11–13.25 kHz
Transmission length	on the order of 100 ms
Time between pulses	6–7 s
Beam width (−3dB relative to reported source level) and geometry	1° along-track by ∼150° across-track; directed vertically toward seafloor

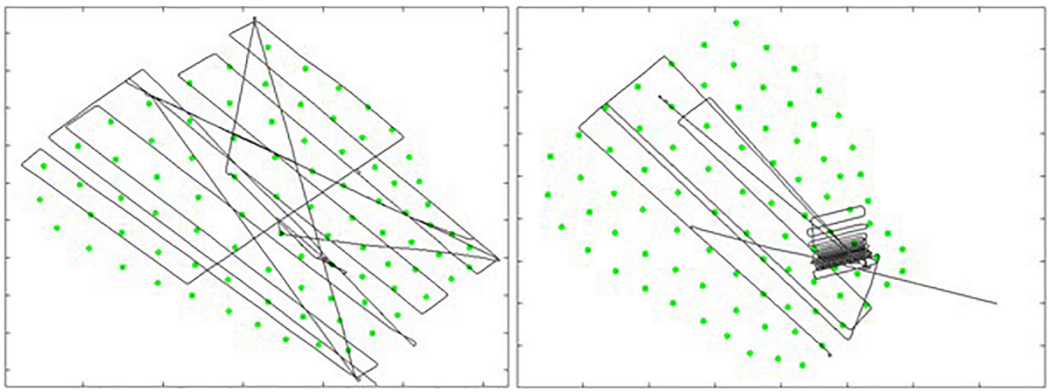

FIGURE 2 | Track lines from the 2017 (left) and 2019 (right) MBES surveys.[1] (Reproduced from Kates Varghese et al. (2020) with the permission of the Acoustical Society of America).

to forage in small groups that can vary in composition (Moulins et al., 2007) and change in size (McSweeney et al., 2007). Animals may leave one foraging group and begin foraging with another. A group of animals may leave an area, while another group arrives, and numerous groups could be foraging simultaneously in a particular location (Falcone et al., 2009). Frequently at SOAR it appears that multiple small groups are foraging in the same general area, ensonifying some common hydrophone. Therefore it is important to note that a GVP represents a single detected period of a group of beaked whales foraging, but a GVP is not tied to a specific group of animals. The formation of GVPs is an automated process based on a fixed set of rules, but the group of individuals it represents may differ. Thus this is not an assessment of specific individuals or the behavior of a specific group, rather overall group-level foraging effort.

Two MBES surveys were conducted, one in January 2017 (Mayer, 2017; Smith, 2019) and the other in January 2019 (Mayer, 2019), as part of a MBES characterization project for the Kongsberg EM 122, a deep water MBES. Both surveys utilized the UNOLS research vessel *Sally Ride* and its hull-mounted EM 122 (12 kHz center frequency) operating with typical parameters used for mapping a deep-water environment such as the SOAR (**Table 1**). The survey in 2017 followed a characteristic mowing-the-lawn pattern across the entire SOAR (**Figure 2** left), whereas the efforts of the 2019 characterization survey required a tighter mowing-the-lawn pattern confined to the canyon in the southeastern corner of the SOAR in addition to a few cross-range lines (**Figure 2** right). These surveys served as an opportunity to assess the effect of MBES on the spatial foraging effort of Cuvier's beaked whales. Because the exact movement of a vessel and hull-mounted MBES will vary from survey to survey based on the needs of the operation, the assessment of the two surveys provided a chance to observe potential variability in beaked whale spatial foraging effort during two separate MBES surveys.

[1]A video recreating the GVP detections and MBES survey track-lines in approximately ten minute intervals on the SOAR hydrophone array is provided for both the 2017 and 2019 data sets in the **Supplementary Materials**.

In order to assess the effect of MBES activity on the spatial foraging effort of Cuvier's beaked whales, the number of GVPs were summed by hydrophone over each analysis period: *Before, During,* and *After* for each of the two MBES surveys. The same analysis periods assessed in the temporal analysis (Kates Varghese et al., 2020) were used here for consistency (**Tables 2**, **3** for the 2017 and 2019 surveys, respectively). In the 2017 survey, each analysis period was 47 h long, whereas in 2019, each analysis period was 52 h long. These analysis periods were based on and equivalent to the length of time that the MBES was operating in each year.

Though it was not explicitly addressed in this study, previous research has shown that environmental and oceanographic conditions can affect prey availability on various spatiotemporal scales, impacting marine predator-prey relationships (Sims et al., 2006; Thayer and Sydeman, 2007; Embling et al., 2012; Santora et al., 2014; Cox et al., 2018). Based on this knowledge, it was expected that environmental conditions and prey distributions that could drive the beaked whales' spatial use of the SOAR would vary on a timescale of less than two years (the time between the two surveys). Thus each survey year was assessed individually.

The GLC approach (Kates Varghese et al., in review), a spatial assessment for analyzing marine mammal behavior on large hydrophone arrays, was used here. This method included two statistical spatial analyses: a global and local approach, as well as comparison analysis of variance tests and visualization tools for interpreting the statistical results. The global analysis used the Moran's I statistic (Moran, 1948) to provide a coarse assessment of the type of spatial distribution, i.e., clustered, random, or dispersed, of the foraging events over the SOAR as a whole. The local approach used the Getis-Ord Gi* statistic (Getis and Ord, 1992), a local indicator of spatial association (Anselin, 1995), which identifies where relative hot and cold spots of foraging activity occurred on a per hydrophone basis. The comparison analysis used the Kruskal-Wallis test (Kruskal and Wallis, 1952) to identify order-of-magnitude differences in the number of GVPs per hydrophone among analysis periods.

TABLE 2 | Analysis period times and details of the 2017 data set.

Analysis period	Date time	Details
Before	1/2/17 08:15–1/4/17 07:15	47 h period ending 25 h before MBES activity started on the array
During	1/5/17 08:15–1/7/17 07:15	47 h, MBES activity on the array
After	1/8/17 08:15–1/10/17 07:15	47 h period starting 25 h after MBES activity ended on the array

TABLE 3 | Analysis period times and details of the 2019 data set.

Analysis Period	Date Time	Details
Before	1/1/19 12:00–1/3/19 16:00	52 h period ending 20 h before MBES activity started on the array
During	1/4/19 12:00–1/6/19 16:00	52 h, MBES activity on the array
After	1/7/19 12:00–1/9/19 16:00	52 h period starting 20 h after MBES activity ended on the array

Global Analysis

In order to assess the spatial distribution of the foraging events over the entire SOAR, the global statistic, Moran's I, was used. Moran's I measures the overall spatial autocorrelation of a data set, producing a value between (−1, 1). A value of negative one corresponds to perfect dispersion (**Figure 3** left), a value of positive one corresponds to perfect clustering of like values (**Figure 3** right), and zero represents no autocorrelation, or a perfectly random distribution (**Figure 3** middle).

Moran's I is given by the formula:

$$I = \frac{N}{W}\frac{\sum_i \sum_j w_{i,j}(x_i - \overline{x})(x_j - \overline{x})}{\sum_i (x_i - \overline{x})^2}$$

where $W = \sum_{i=1}^{n}\sum_{j=1}^{n} w_{i,j}$ with $w_{i,j}$ being the weighting between the ith and j^{th} hydrophone and w represents the neighbor weighting matrix of i rows and j columns. x_i refers to the ith hydrophone value, in this case the number of GVP of the ith hydrophone and $\overline{x}$ is the mean number of GVPs over all of the hydrophones. A queen's contiguity neighbor weighting rule was used here as was recommended for similar data in Kates Varghese et al. (in review). The queen criterion defines neighbors as spatial units that share a boundary with the hydrophone of interest (i.e., all hydrophones immediately horizontal, vertical, or diagonal). Thus, the maximum number of neighbors an interior hydrophone could have is eight, whereas edge and corner hydrophones will have fewer.

The Moran's I statistic for each analysis period was converted to a z-score. To aid in the interpretation of the global results, p-values were computed for each z-score. The smaller the p-value, the greater the discrepancy between the observed data and the null hypothesis being tested (Tanha et al., 2017). The null hypothesis for the Moran's I analysis was that the spatial distribution of GVPs under consideration, for any of the analysis periods, was no different from random (I = 0). Alternatively, it was hypothesized that the spatial distribution was clustered (I = +1) during each analysis period, *Before, During,* and *After*, since beaked whales are known to primarily forage in the deepest part of the SOAR (Falcone et al., 2009; Schorr et al., 2014; DiMarzio et al., 2019; Southall et al., 2019). The Moran's I statistic, along with the p-value, was used to make a statement about whether the GVPs were clustered or not.

Local Analysis

If global spatial correlation – clustering or dispersion – was detected, the Getis-Ord Gi* (Gi*) local statistic was also computed. The Gi* statistic was found for each hydrophone using the formula:

$$G_i^* = \frac{\sum_{j=1}^{n} w_{i,j}x_j - \overline{X}\sum_{j=1}^{n} w_{i,j}}{S\sqrt{\frac{n\sum_{j=1}^{n} w_{i,j}^2 - (\sum_{j=1}^{n} w_{i,j})^2}{(n-1)}}}, \text{ where } S = \sqrt{\frac{\sum_{j=1}^{n} x_j^2}{n} - (\overline{X})^2} \text{ and}$$

$\overline{X} = \frac{\sum_{j=1}^{n} x_j}{n}$ and the remaining variables were the same as described for the Moran's I statistic. This statistic was used to understand where, i.e., on which specific hydrophones, the spatial correlation (relative hot or cold spots) occurred within the SOAR. For example, to be a relative hot spot, a hydrophone must be surrounded by other hydrophones that also exhibit a high number of GVPs and vice-versa for a relative cold spot. What constitutes a high or low number of GVPs will change depending on the specific set of data, their distribution and variance, which are all considered in the Gi* calculation.

P-values associated with each Gi* statistic, which is itself a z-score, were computed to help understand how the observed Gi* results differed from the null hypothesis. The null hypothesis was that GVPs were randomly distributed and thus that there were no relative hot or cold spots of foraging activity. A small p-value indicated a greater discrepancy from this null hypothesis suggesting a spatial anomaly – i.e., an area of congregation or absence. Since there are 89 hydrophones on the SOAR, alternative hypotheses were not made about individual hydrophones.

FIGURE 3 | From Kates Varghese et al. (in review). Spatial configurations that would result in ideal Moran's I values: *left* – perfect dispersion, Moran's I value = −1; *middle* – perfect randomness, Moran's I value = 0; *right* – perfect clustering, Moran's I value = +1.

However, it was hypothesized that the northwest part of the SOAR, which has the deepest depths, and where the animals are historically known to forage (Falcone et al., 2009; Schorr et al., 2014; DiMarzio et al., 2019; Southall et al., 2019), would be an area of high foraging activity (i.e., hot spots), while the shallow area in the southeast along San Clemente Island would have low foraging activity (i.e., cold spots). It was hypothesized that the relative hot and cold spots, with respect to foraging, would remain in these respective areas throughout the three analysis periods, which would indicate the spatial distribution of GVPs did not change during MBES activity.

Comparison Analysis

Although the spatial statistics provided insight into spatial changes on the SOAR, they did not provide information about differences in scale, i.e., the average number of GVPs per hydrophone occurring on the SOAR in the various analysis periods. In addition to, or in the absence of a spatial change, understanding potential order-of-magnitude differences in the number of GVPs detected provided further information about the extent of change. Following the GLC approach from Kates Varghese et al. (in review) for similar data, the Kruskal-Wallis test was used to compare the magnitude of observations among different analysis periods. For both years of study, the null hypothesis was that there was no difference in the number of GVPs per hydrophone on the SOAR among the analysis periods. Difference plots of the hydrophone array were also generated to show spatially what the relative change (e.g., increase, decrease, or no change) was in the number of GVPs between consecutive analysis periods.

The GLC approach is further developed and described in more detail in Kates Varghese et al. (in review).

RESULTS

2017

Of the 47 h analyzed for each of the three analysis periods in 2017, there were 127 GVPs detected across the 89 hydrophones *Before,* 135 *During,* and 148 *After*. The results of the global analysis are provided in **Table 4**. For all analysis periods of 2017, the Moran's I value suggested strong spatial clustering of GVPs on the SOAR.

The total number of GVPs detected and the respective Gi* z-score for each hydrophone was calculated and is shown in the map presented in the first and second columns, respectively, of **Figure 4** for each analysis period of 2017. To aid in the designation and interpretation of hot and cold spots in the Gi* results, *p*-values equal to or less than 0.1, or equal to and more than 0.9 were mapped along-side the Gi* results (**Figure 4**, column 3). Hydrophones with *p*-values of 0.1 or less provided the strongest evidence of hot spots on the Gi* plot, while a *p*-value of 0.9 or more provided the strongest evidence of a cold spot on the Gi* plot. Exact Gi* and *p*-values for all hydrophones are provided in the data section of this publication. Ultimately, a critical alpha level of 0.05 was used to guide the final interpretation of the Gi* results. Because of the two-tailed nature of this analysis (hot and cold spots), the authors focused on areas with *p*-values less than or equal to 0.025 (hot) or greater than or equal to 0.975 (cold) in the descriptive interpretation of the Gi* results that follows.

In each analysis period, there was a clustering (i.e., a group of several adjacent hydrophones) of hot spots in the northwest corner of the SOAR (**Figure 4**, column 3), overlapping the deeper waters of the SOAR (**Figure 1**). This result matched expectations since this area has historically been noted as favorable foraging grounds for these animals due to the deep-water conditions (Falcone et al., 2009; Schorr et al., 2014), providing ideal habitat for the squid that Cuvier's beaked whales prey upon (Santos et al., 2001). The exact cluster of hot spot hydrophones shifted slightly between analysis periods. However, based on the recommendation of Kates Varghese et al. (in review) in the development of the GLC approach, the general area of hot/cold spot clusters should be compared rather than employing a precise comparison of individual hydrophones. Since many of the hydrophones in the hot spot cluster were the same across analysis periods and remained in the same general area in the deepest part of the SOAR, this result suggested no obvious change occurred in spatial foraging effort in the 2017 study.

With respect to where there were very few GVPs, there was one cold spot hydrophone in the central-western part of the SOAR in the *Before* period and a small cluster of hydrophones signifying cold spots in the southeast corner of the SOAR *During* and *After*. Overall the southeastern corner – the relatively shallow and historically least-used area (Falcone et al., 2009; Schorr et al., 2014) – was not a high-use area for foraging beaked whales (**Figure 4**, column 1). Thus, the Gi* analysis further suggested no obvious spatial change occurred in beaked whale foraging effort among analysis periods in 2017 at a local level. This finding was supported by the difference plots for which the spatial distribution of hydrophones that exhibited no change, increase, or decrease in the number of GVPs appeared random (**Figure 5**).

Not only was there no overall change in the spatial location of relative hot/cold spots among analysis periods, but the Kruskal-Wallis comparison test revealed that the total number of GVPs per hydrophone among the three analysis periods were similar [H (2) = 1.24, p = 0.5369].

Overall the GLC spatial analysis of the 2017 study showed a consistent pattern, both globally and locally, in spatial clustering of GVPs and a similar number of GVPs for non-MBES and MBES analysis periods.

TABLE 4 | Global analysis results by analysis period for 2017, including Moran's I value (I), the z-score (z_I), and the associated *p*-value.

Analysis period	Moran's I (I)	z-score (z_I)	*p*-value	Conclusion
Before	0.2472	4.6851	<0.001	Clustered
During	0.2108	4.0260	<0.001	
After	0.3706	6.9217	<0.001	

A positive I indicates a clustered distribution, a negative I represents a dispersed distribution, and the p-value associated with each.

2019

Fifty-two hours of hydrophone data were analyzed for each of the three analysis periods in 2019. There were 60 GVPs detected

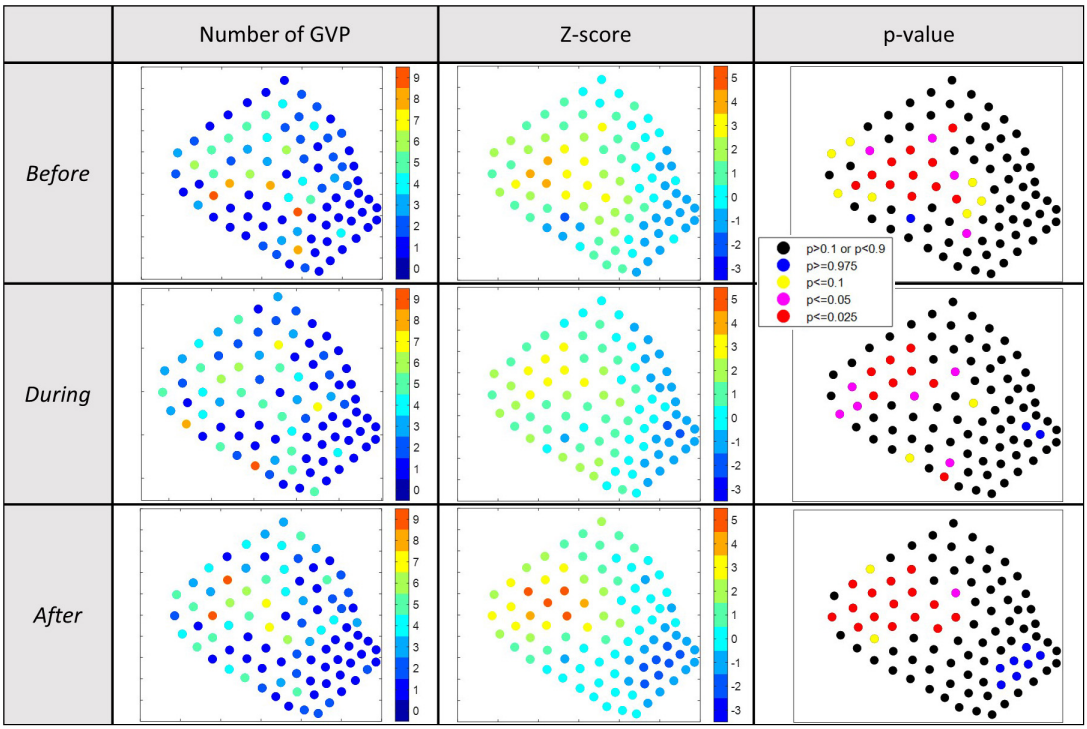

FIGURE 4 | Results of the 2017 Gi* analysis for local hot/cold spots. Column 1: visual depiction of the number of GVPs by hydrophone; column 2: visual depiction of the Gi* z-values by hydrophone; column 3: visual depiction of the *p*-values associated with the Gi* results by hydrophone. $p < 0.025$ were considered relative hot spots, whereas $p > 0.975$ were considered relative cold spots. Each row represents a different analysis period: top-*Before*; middle-*During*; bottom-*After*.

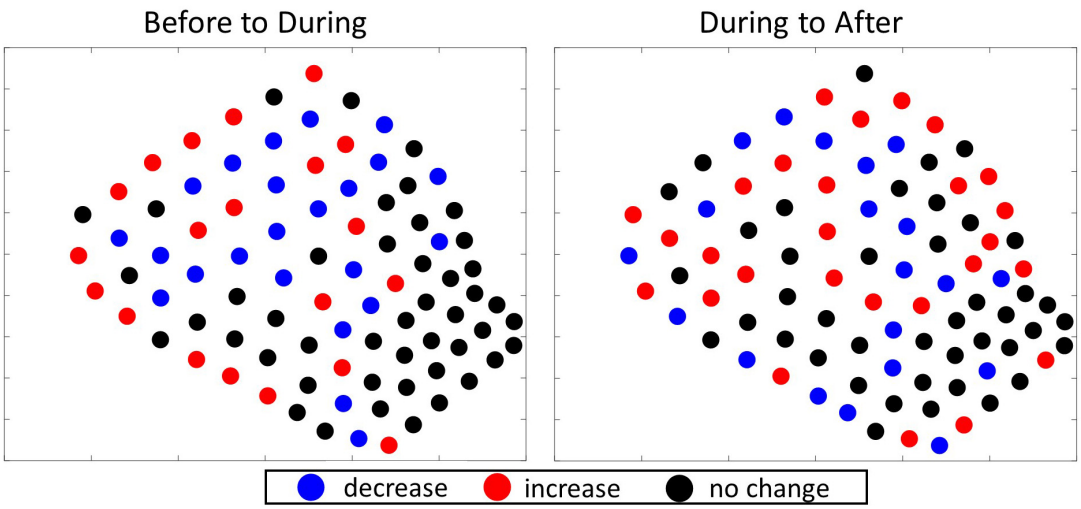

FIGURE 5 | Difference plots showing the direction of change in the number of GVPs per hydrophone from one period to the next of the 2017 survey. *Left*: difference plot showing change from *Before* to *During*; *Right*: difference plot showing change from *During* to *After*.

Before, 93 *During,* and 77 *After*. The global analysis results are provided in **Table 5**. For each of the three analysis periods the Moran's I value strongly suggested GVPs were spatially clustered on the SOAR.

The total number of GVPs detected, the Gi* z-score, and associated *p*-values were calculated and are shown by hydrophone in **Figure 6**, columns 1–3, respectively. Exact Gi* and *p*-values for all hydrophones are provided in the data section of this publication. A similar interpretation of **Figure 6** was conducted as described for the interpretation of the 2017 local results. There were no obvious cold spots identified in the 2019 analysis periods, suggesting widespread use of the SOAR by

TABLE 5 | Global analysis results by analysis period for 2019, including Moran's I value (I), the z-score (z_I), and the associated *p*-value.

Analysis period	Moran's I (I)	z-score (z_I)	*p*-value	Conclusion
Before	0.1105	2.2082	0.0139	Clustered
During	0.2078	3.9711	<0.001	
After	0.1265	2.4991	0.0064	

A positive I indicates a clustered distribution, a negative I represents a dispersed distribution, and the p-value associated with each.

foraging beaked whales in 2019 (**Figure 6**). There were distinct hot spot clusters identified in each analysis period. In the *Before* period the hot spot cluster was in the southwestern corner of the SOAR, *During* MBES activity the hot spot cluster was in the center, and *After* MBES activity there were several hot spot hydrophones in the center and a cluster of hot spot hydrophones in the southwestern corner of the SOAR (**Figure 6**). These results suggested that local spatial foraging effort did change during the 2019 study, a finding that was supported by a distinguishable spatial pattern visible in the 2019 difference plots (**Figure 7**). That is, there was a cluster of hydrophones in the center of the SOAR that all recorded an increase in GVPs from *Before* to *During* (**Figure 7** *left*), while from *During* to *After* (**Figure 7** *right*) there was a cluster of hydrophones in the center that all decreased in the number of GVPs.

The Kruskal-Wallis comparison test showed that the number of GVPs per hydrophone were similar between the three analysis periods [H (2) = 3.95, p = 0.1387].

Overall the GLC spatial analysis of the 2019 study showed foraging effort was consistently clustered, and the overall magnitude of foraging effort was similar throughout the 2019 analysis periods. But, the location of the foraging hot spot cluster changed through time.

DISCUSSION

The global analysis revealed that GVPs on the SOAR were notably clustered spatially in all analysis periods in both 2017 and 2019. In addition, the comparison tests for both years revealed that the overall number of GVPs detected per hydrophone was equivalent among analysis periods within each year. These results suggest that no obvious range-wide change in foraging effort occurred during MBES activity. The local results for the two surveys were not the same. In 2017, foraging hot and cold spots were, respectively, identified in the same general area of the SOAR during all three analysis periods. In 2019, foraging hot spots were identified in each analysis period, but the location shifted through time. Like the temporal analysis of foraging behavior during the two MBES surveys (Kates Varghese et al., 2020), the difference in local spatial results between the two years brings in to question whether the MBES activity (i.e., different spatial usage of the SOAR) could have contributed to the differences identified, or if the differences were related to variability in some other factor, such as prey distribution during the two years of study.

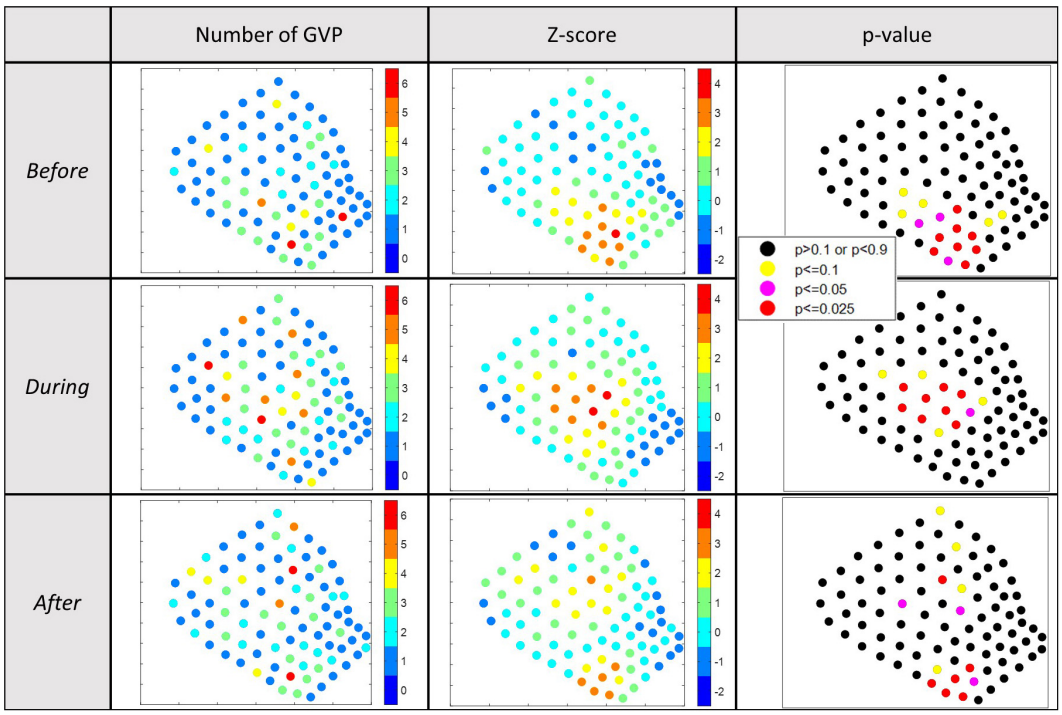

FIGURE 6 | Results of the 2019 Gi* analysis for local hot/cold spots. Column 1: visual depiction of the number of GVPs by hydrophone; column 2: visual depiction of the Gi* z-values by hydrophone; column 3: visual depiction of the *p*-values associated with the Gi* results by hydrophone. $p < 0.025$ were considered relative hot spots, whereas $p > 0.975$ were considered relative cold spots. Each row represents a different analysis period: top-*Before*; middle-*During*; bottom-*After*.

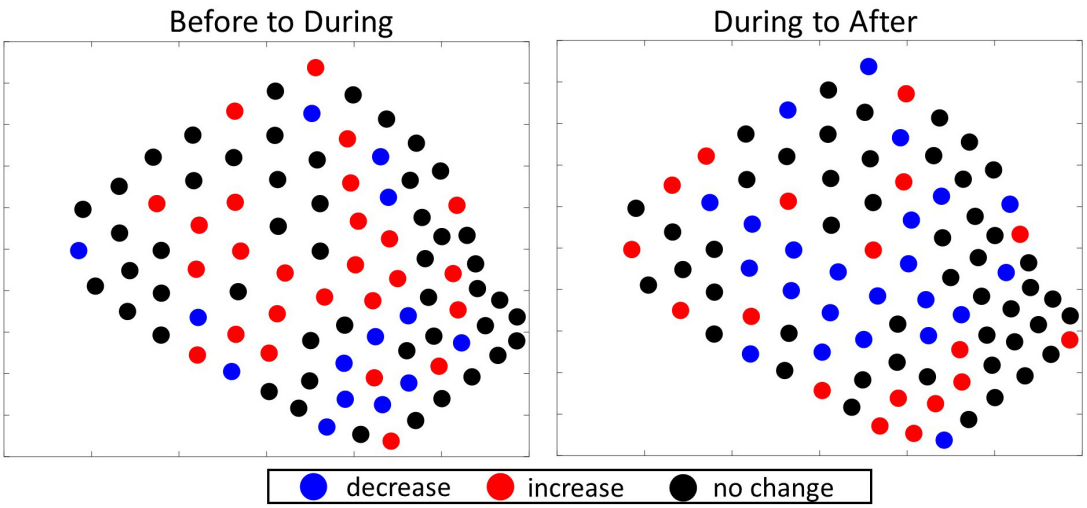

FIGURE 7 | Difference plots showing the direction of change in the number of GVPs per hydrophone from one period to the next of the 2019 survey. *Left*: difference plot showing change from *Before* to *During*; *Right*: difference plot showing change from *During* to *After*.

The results of the 2017 local analysis identified relative hot and cold spots in the same general area of the SOAR, but during each period on a slightly different set of hydrophones in the array. There are likely multiple interacting reasons for the slight difference in cluster locations. Firstly, even if the animals tend to forage in the same area throughout time, it is within reason to expect some amount of variation due to the natural variability in behavior (e.g., the animals are mobile, peaks and lulls in foraging are observed even in the absence of anthropogenic activity) (Schorr et al., 2014; Falcone et al., 2017), and because a cluster likely represents numerous groups foraging, each with their own movements over the wider area. Additionally, there may have been small changes in the distribution of prey, due to varying environmental conditions, which could have affected exact foraging locations. Lastly, the Gi* statistic, the statistic used in the local analysis, is a function not only of the number of GVPs at a specific hydrophone, but of its neighboring hydrophones as well. This can lead to a slightly different spatial z-score pattern, despite a generally very similar spatial data set. For this reason Kates Varghese et al. (in review) recommended that it is most appropriate to interpret change in spatial behavior using the GLC approach more holistically than on a single hydrophone basis to account for some of the sensitivity in the Gi* statistic. Most of the GVPs occurred in the northwest and north-central parts of the array and were lacking in the southeast. Since many of the hot spot hydrophones overlapped from one period to the next, there was no indication from this analysis that the area used for foraging had changed in an obvious way that would suggest the 2017 MBES survey had an effect.

The interpretation of the local analysis result for 2019 was less clear. *Before* the MBES survey, a distinct cluster of foraging hot spots was identified in the southwestern corner of the SOAR, *During* the survey a distinct cluster of foraging hot spots was identified in the center, and *After* there was a distinct hot spot cluster in the southwestern corner and potentially another hot spot cluster in the center of the SOAR. In general, the hot spot clusters had minimal overlap across abutting analysis periods, suggesting there was a change in foraging effort at the local level. But the pattern of two potential hot spot clusters identified in the *After* period was perplexing. Specifically, the potential cluster in the center of the array *After* was not as obvious as other clusters, raising the question of whether the center of the SOAR was in fact a highly used area by the animals during this period. Whether it was or not would provide information that could help in ruling out certain potential drivers of the 2019 result.

Referring to the spatial distribution of the 2019 raw data, z-scores, and difference plots provided further insight in interpreting the local result. The spatial distribution of high versus low GVP values *After* appeared random in the center area, suggesting it was only a few hydrophones where many GVPs occurred and not the entire area. In addition, the z-scores of hydrophones in the center in the *After* period were lower in comparison to all of the other hot spot clusters from any of the 2019 analysis periods – i.e., the center area hydrophones of the *After* period had a z-score value of mostly twos, while all other hot spots had z-scores of mostly threes or fours. This suggests that although there were a high number of GVPs in the center, it was not the most highly used area relative to the rest of the SOAR. In fact, the southwestern corner had higher z-score values during the same period. In examining the difference plots, none of the center hot spot hydrophones increased in the number of GVPs from *During* to *After,* and most of the GVP values on surrounding hydrophones in the center either decreased or stayed the same, whereas those in the southwestern corner had an increase in GVPs detected. Again, this result suggests that the center was not as active as the southwestern corner of the SOAR *After* the survey. Together, these results best support the interpretation that the center area was no longer as favored by the animals for foraging as it was in the *During* period.

If the spatial change was due to the MBES survey, one would expect a more discrete difference between each set of analysis periods, and thus a clear change back to the southwestern corner *After*. For example, in the McCarthy et al. (2011) in which the analysis periods abutted temporally, there was a distinct spatial change between the *Before, During,* and *After* analysis periods. In a finer temporal analysis of the spatial data, the researchers found that the animals returned to their normal spatial use of the range after 35 h. In the study herein, there were 20 h between each set of analysis periods in 2019, and each analysis period lasted 52 h. If the MBES was the cause of spatial change, assuming a similar response time as in the MFAS study, the temporal spacing in this study (i.e., time between analysis periods plus the duration of an analysis period) should have been more than adequate to capture distinct differences in foraging effort location. If the spatial change was due to a factor that was primarily a function of time rather than related to the MBES survey, one might expect a more gradual spatial change across all three analysis periods. But what occurred was a distinct change in foraging effort (i.e., relative hot spots) location from *Before* to *During* and a spatial pattern suggestive of a gradual change from *During* to *After*, a response somewhere in between the two scenarios that were expected. Thus, it is not readily obvious what the cause of the shift was.

There is no standard definition of what constitutes a meaningful shift in habitat use, especially in the context of response to anthropogenic activity or some other external factor. A meaningful shift in habitat use depends on a number of factors including the behavioral or ecological context for which the shift occurs, the species, suitable habitat connectivity, among many other factors. In the case where a group of animals is negatively affected by a disturbance, there may exist circumstances where either no suitable alternative habitat exists for the animals to move to, or the animals endure the disturbing activity despite potential and realized biological consequences (Claridge, 2013; Moretti, 2019). In addition the degree to which an easily observable response, such as behavior change, correlates with a meaningful effect, such as biological or physiological change, is not often known (Beale, 2007). Our ability to understand the degree to which a measured behavioral response is indicative of something meaningful requires comprehensive integration of the information available regarding the factors under which the behavioral change took place, as well as consideration of other known analogs. With this in mind, potential explanations for the observed shift in spatial use of the SOAR by beaked whales were explored.

Since the 12 kHz MBES sound is within the hearing range of beaked whales (Cook et al., 2006; Pacini et al., 2011), one explanation for a shift in foraging location is that the whales were disturbed by the anthropogenic activity on the SOAR, e.g., vessel presence, vessel noise, or MBES activity. In the case of a disturbance, movement would be expected away from the disturbing activity. This was the case with beaked whales in response to other sources within their hearing range, such as MFAS (McCarthy et al., 2011; Manzano-Roth et al., 2016) and acoustic pingers (Carretta et al., 2008). In both the McCarthy et al. (2011) and Manzano-Roth et al. (2016) studies, where a clear negative response to MFAS activity was concluded, the number of GVPs of Blainville's beaked whales was reduced and the majority of foraging shifted to the edge or off the range during MFAS activity. In the case of the acoustic pingers (10–12 kHz), bycatch of several beaked whale species was reduced to zero after the implementation of the pingers on gillnets in the California drift gill net fishery (Carretta et al., 2008). Neither of these were similar to the result seen here.

Alternatively, a shift in foraging effort location could also be due to attraction of the whales to the anthropogenic activity. During the first 24 h of the 2019 MBES survey (i.e., roughly half of the *During* period) the MBES survey was confined to the southeast corner of the SOAR (see **Figure 2** and the supplementary results of Kates Varghese et al. (2020) for a detailed description of the MBES surveys). Therefore, one might expect if the whales were attracted to the MBES sound that they might move to the southeast corner. Yet, this was not where the foraging hot spots were found. The remainder of the *During* period involved lines that ran across the center of the SOAR in a "mowing-the-lawn" pattern. Given that the MFAS study results (McCarthy et al., 2011; Manzano-Roth et al., 2016) are viewed as an avoidance response, where many of the animals moved to the edge or off the range, one might view a shift in foraging effort to the center of the SOAR during anthropogenic activity as movement toward, or an attraction to, the activity. In this case it is worth considering the sound propagation of the deep-water MBES on the SOAR. MBES transmit sound toward the seafloor in a beam that is narrow along-track (1°) and broad (∼150°) across-track (Lurton, 2016; Kates Varghese et al., 2019a). As a result, most of the energy is directed toward the seafloor directly below the vessel as lines are run over the survey area, reducing the acoustic footprint relative to an omni-directional or horizontally transmitting source (Lurton and DeRuiter, 2011; Lurton, 2016). A preliminary examination of some of the acoustic data from the hydrophone array from the 2017 survey revealed that the signal from the MBES was only detectable above the noise floor when the vessel was within 10–15 kilometers, or roughly 2–3 hydrophones, from a given hydrophone (Mayer, 2019; Kates Varghese et al., 2019b). The acoustic data from the array was not available for the 2019 survey as of the writing of this paper, but it is reasonable to expect that the sound propagation during the 2019 survey was similar to the 2017 survey since the survey utilized the same vessel, MBES, and was conducted in a similar sea state (Mayer, 2019). Since the MBES was not stationary during the survey, a distance of 10–15 km or less between the vessel and a group of foraging whales was likely only met a small portion of the time. Based on this, one might expect that if the whales heard and were attracted to the MBES that the spatial pattern of their foraging would more closely follow the track lines. This would likely lead to the detection of a more random spatial pattern in the local results than the clustering in the center seen here. Thus it does not seem probable that an attraction to the sound was the cause of the spatial change. However, a full analysis of the soundscape with respect to the distribution of GVPs would be needed to rule this out completely.

Another explanation for a shift in foraging location is due to a change in prey distribution, since foraging behavior in beaked

whales is heavily driven by prey dynamics (Benoit-Bird et al., 2016, 2020; Southall et al., 2019). The anthropogenic activity could have disturbed or attracted the prey, leading to a change in their distribution (Fewtrell and McCauley, 2012), followed by a change in where the whales foraged. Beaked whales primarily forage on deep-water squid (Santos et al., 2001) and some fish, both of which are thought to primarily detect low-frequency (<1 kHz) acoustic signals (in addition to particle motion) (Mooney et al., 2010; Popper and Hawkins, 2018). Thus it seems unlikely that such prey species would respond to the 12 kHz MBES signal. It is possible that the prey could detect and respond to vessel noise, which is lower in frequency (<1 kHz). Prey distribution and patchiness can also vary naturally due to normal prey movement over time and/or in response to spatially variable and temporally changing environmental conditions (Benoit-Bird et al., 2013, 2020). In fact, recent work has shown that within the SOAR, prey fields are heterogeneous over small distances (Southall et al., 2019). It is also possible that a specific prey patch was depleted by foraging whales, resulting in their movement to another prey patch elsewhere on the SOAR. Backscatter data from sonar systems can be used to identify squid and other prey items in the water column (Moline and Benoit-Bird, 2016; Southall et al., 2019), and be used to explore these prey distribution hypotheses. However, the signal needed to achieve an adequate estimate of biological organisms at the depths relevant to beaked whale foraging is not feasible from a traditional hull-mounted MBES (Moline and Benoit-Bird, 2016), like the one used in this study. Given the results of this study and the hypotheses explored here, the most probable explanation of the 2019 result is linked to the strong relationship between foraging behavior and prey field dynamics. Without complementary prey field information this cannot be concluded with certainty.

Although there was a change in the spatial use of the array in 2019 and the cause remains unclear there are a few key observations to take away from the 2019 survey. First, the most highly utilized location by the foraging animals (i.e., relative foraging hot spot) remained in the deeper area of the SOAR during all analysis periods. Despite the deeper waters being identified in past studies as the area where these animals forage (Falcone et al., 2009; Schorr et al., 2014), there may still be negative implications for a shift within this area (i.e., from the southwest to the center). Southall et al. (2019) found that even within small areas of the SOAR (the west versus the east for example) prey density can be quite different, which can have huge repercussions on the energetic costliness of an induced spatial change from favorable to unfavorable foraging grounds (Moretti, 2019). However, the number of GVPs detected during the MBES survey period was no different than the non-survey periods. Assuming there was no change in the number of animals foraging, this would suggest that there was not an overall change in foraging effort. Furthermore, the fine-scale temporal analysis of the 2019 survey showed no difference in two other GVP characteristics (i.e., number of clicks per GVP, and click rate per GVP) during the MBES survey versus non-MBES periods (Kates Varghese et al., 2020). These results further suggest that there was little change in how the animals were foraging. If there were obvious differences in the number of GVPs and intrinsic characteristics (i.e., number of clicks, click rate) of the GVP, this might suggest there was a change in the quality of the prey field with respect to foraging. In the absence of prey distribution data for this study, these results suggest that the spatial change identified may not be associated with a high energetic cost to the animals. Future studies assessing MBES impact should integrate prey field assessments to verify this. This is extremely important in being able to assess the biological and ecological relevance of a change in behavior.

The spatial change in the 2019 study and absence of change in 2017 raises the question, why was there a difference between the two years? Both surveys were conducted in January, removing potential seasonal differences in beaked whale ecology that might affect behavior. The surveys were also conducted using the same vessel and 12 kHz MBES, and occurred for similar lengths of time (47 h in 2017 versus 52 h in 2019). The only known difference between the two surveys were the line plans. The 2017 survey was conducted in a mowing-the-lawn pattern across the full length of the array, whereas the 2019 survey used a tighter mowing-the-lawn pattern confined to the southeast corner of the SOAR before conducting a few full-length passes across the middle of the SOAR. As discussed previously, the spatial change found in the 2019 study does not appear to be driven by MBES activity, so it would seem unlikely that the different line plans were the reason for the inter-annual differences. However, without further evaluation of some or all of the hypotheses posed here, this hypothesis should not be disregarded. It should be noted though that while the "mowing the lawn" survey conducted in 2017 is representative of a typical MBES mapping survey, the localized MBES survey in 2019 was conducted particularly to assess the beam pattern of the MBES system and is not at all representative of the use of MBES in deep-water ocean mapping work.

It is worth drawing attention to the spatial distribution of GVPs in the non-MBES periods before the surveys were conducted. These were also dissimilar between the two years. In 2017, there was relatively minimal GVP activity in the southeast portion of the SOAR, whereas in 2019 there was more widespread use of the entire SOAR. These patterns were seen throughout each respective year, suggesting that there was simply variation in the use of the SOAR by the animals from one year to the next. If the spatial distribution *Before* MBES activity was different between the two years, one cannot therefore assume that the difference between the two years was related to the anthropogenic activity or differences related to the operation of the MBES. Again, since prey distribution heavily dictates where these animals forage, there were very likely differences between prey patches in the two years that led to differences in use of the range both during and outside of periods of anthropogenic activity. Though, this may not be the only possible explanation for differences in spatial use of the SOAR between the two years.

Finally, it is important to keep in mind that the spatial statistics used here can only detect patterns at the resolution of the hydrophone array. Any potential changes in the spatial use of the array that happened on a scale finer than the hydrophone spacing of two to six kilometers were not detected. Spatial change in foraging behavior may occur on a different spatial resolution than was measured here and may have a different

consequence on foraging animals. Animal tagging studies and those that focus on individual behavior provide a necessary understanding of finer-scale changes in behavior and potential impacts of anthropogenic noises and should be undertaken with respect to MBES impact where possible in the future.

CONCLUSION

The overall findings of this spatial analysis align with the conclusions of the temporal assessment (Kates Varghese et al., 2020): foraging effort did not change in a stereotyped way that would suggest that the MBES surveys had a clear negative effect. In both years of study, neither the range-wide or order-of-magnitude comparisons revealed any obvious differences in beaked whale foraging during the MBES surveys. In the 2017 MBES survey there was no indication that the overall foraging effort changed spatially on a local level. *During* the 2019 MBES survey there was a change detected in the local spatial use of the SOAR. The change was a shift in the most foraging activity toward the center of the range, which was unlike the typical avoidance response seen several times in studies assessing beaked whale foraging response to MFAS. It was also a shift that remained in the deep-water area of the SOAR, thought to be favorable foraging grounds for beaked whales. This best supports the prey-dependence hypothesis as the cause of spatial change. However, the cause of this change and its overall impact cannot be stated with certainty. Future studies targeting the hypotheses posed here are needed to understand the 2019 result completely and should integrate animal tagging, prey field, and soundscape assessments to establish a more comprehensive picture.

DATA AVAILABILITY STATEMENT

The datasets presented in this article are not readily available because of security concerns related to the hydrophone locations. The processed data without the hydrophone locations are available with this manuscript. The raw data may be available on a case-by-case basis. Requests to access the datasets should be directed to ND, nancy.dimarzio@navy.mil.

AUTHOR CONTRIBUTIONS

DM, ND, LM, JM-O, and HK were involved in the coordination of the field component of this study. ND processed the acoustic data and provided the GVP data for this analysis. HK through the guidance of KL performed the reported analyses. JM-O, KL, and LM provided guidance to HK on the interpretation and communication of the findings of this work. All authors discussed the results and contributed to the final manuscript.

FUNDING

This material was based upon work supported by the National Science Foundation under grant no. 1524585 and NOAA grant no. NA15NOS4000200 provided to the Center for Coastal and Ocean Mapping at the University of New Hampshire.

ACKNOWLEDGMENTS

This study was possible thanks to collaborations with the Scripps Institute of Oceanography and the Office of Naval Research for ship time on the *R/V Sally Ride* and the U.S. Navy for the time on the SOAR range. Thank you to Stephanie Watwood at the Naval Undersea Warfare Center for supporting this project.

SUPPLEMENTARY MATERIAL

The Supplementary Material for this article can be found online at: https://www.frontiersin.org/articles/10.3389/fmars.2021.654184/full#supplementary-material

REFERENCES

Anselin, L. (1995). Local indicators of spatial association – LISA. *Geogr. Anal.* 27, 93–115. doi: 10.1111/j.1538-4632.1995.tb00338.x

Beale, C. M. (2007). The behavioral ecology of disturbance responses. *Int. J. Comp. Psychol.* 20, 111–120.

Benoit-Bird, K. J., Battaile, B. C., Heppell, S. A., Hoover, B., Irons, D., Jones, N., et al. (2013). Prey patch patterns predict habitat use by top marine predators with diverse foraging strategies. *PLoS One* 8:e53348. doi: 10.1371/journal.pone.0053348

Benoit-Bird, K. J., Southall, B. L., and Moline, M. A. (2016). Predator-guided sampling reveals biotic structure in the bathypelagic. *Proc. Biol. Sci.* 283:20152457. doi: 10.1098/rspb.2015.2457

Benoit-Bird, K. J., Southall, B. L., Moline, M. A., Claridge, D. E., Dunn, C. A., Dolan, K. A., et al. (2020). Critical threshold identified in the functional relationship between beaked whales and their prey. *Mar. Eco. Prog. Ser.* 654, 1–16. doi: 10.3354/meps13521

Blom, E. L., Kvarnemo, C., Dekhla, I., Schold, S., Andersson, M. H., Svensson, O., et al. (2019). Continuous but not intermittent noise has a negative impact on mating success in a marine fish with paternal care. *Nat. Sci. Rep.* 9:5494. doi: 10.1038/s41598-019-41786-x

Carretta, J. V., Barlow, J., and Enriquez, L. (2008). Acoustic pingers eliminate beaked whale bycatch in a gill net fishery. *Mar. Mamm. Sci.* 24, 956–961. doi: 10.111/j.1748-7692.2008.00218.x

Cholewiak, D., DeAngelis, A., Palka, D., Corkeron, P., and Van Parijs, S. (2017). Beaked whales demonstrate a marked acoustic response to the use of shipboard echosounders. *R. Soc. Open Sci.* 4:170940. doi: 10.1098/rsos.170940

Claridge, D. E. (2013). *Population Ecology of Blainville's Beaked Whales (Mesoplodon Densirostris)*. Ph.D. Thesis. St Andrews: University of St. Andrews.

Cook, M. L. H., Varela, R. A., Goldstein, J. D., McCulloch, S. D., Bossart, G. D., Finneran, J. J., et al. (2006). Beaked whale auditory evoked potential hearing measurements. *J. Comp. Physiol. A* 192, 489–495. doi: 10.1007/s00359-005-0086-1

Cox, S. L., Embling, C. B., Hosegood, P. J., Votier, S. C., and Ingram, S. N. (2018). Oceanographic drivers of marine mammal and seabird habitat-use across shelf-seas: a guide to key features and recommendations for future research and conservation management. *Estuar. Coast. Shelf Sci.* 212, 294–310. doi: 10.1016/j.ecss.2018.06.022

Croll, D. A., Clark, C. W., Calambokidis, J., Ellison, W. T., and Tershy, B. R. (2006). Effect of anthropogenic low-frequency noise on the foraging

ecology of *Balaenoptera* whales. *Anim. Conserv.* 4, 13–27. doi: 10.1017/S1367943001001020

D'Amico, A., and Pittenger, R. (2009). A brief history of active sonar. *Aquat. Mamm.* 35, 426–434. doi: 10.1578/AM.35.4.2009.426

DeRuiter, S. L., Southall, B. L., Calambokidis, J., Zimmer, W. M. X., Sadykova, D., Falcone, E. A., et al. (2013). First direct measurements of behavioral responses by Cuvier's beaked whales to mid-frequency active sonar. *Biol. Lett.* 9:20130223. doi: 10.1098/rsbl.2013.0223

DiMarzio, N., and Jarvis, S. (2016). *Temporal and Spatial Distribution and Habitat Use of Cuvier's Beaked Whales on the U.S. Navy's Southern California Antisubmarine Warfare Range (SOAR): Data Preparation*. Newport: Naval Undersea Warfare Center.

DiMarzio, N., Jones, B., Moretti, D., Thomas, L., and Oedekoven, C. (2018). *Marine Mammal Monitoring on Navy Ranges (M3R) on the Southern California Offshore Range (SOAR) and the Pacific Missile Range Facility (PMRF)— 2017*. Newport: Naval Undersea Warfare Center.

DiMarzio, N., Watwood, S., Fetherston, T., and Moretti, D. (2019). *Marine Mammal Monitoring on Navy Ranges (M3R) on the Southern California Anti-Submarine Warfare Range (SOAR) and the Pacific Missile Range Facility (PMRF) 2018*. Newport: Naval Undersea Warfare Center.

Embling, C. B., Illian, J., Armstrong, E., van der Kooij, J., Sharples, J., Camphuysen, K. C. J., et al. (2012). Investigating fine-scale spatio-temporal predator-prey patterns in dynamic marine ecosystems: a functional data analysis approach. *J. Appl. Ecol.* 49, 481–492. doi: 10.1111/j.1365-2664.2012.02114.x

Erbe, C., and Farmer, D. M. (2000). Zones of impact around icebreakers affecting beluga whales in the Beaufort Sea. *J. Acoustic. Soc. Am.* 108, 1332–1340. doi: 10.1121/1.1288938

Evans, D. L., and England, G. R. (2001). *Joint Interim Report Bahamas Marine Mammal Stranding Event of 15-16 March 2000, U.S.* Washington, DC: Department of Commerce and Secretary of the Navy.

Falcone, E. A., Schorr, G. S., Douglas, A. B., Calambokidis, J., Henderson, E., McKenna, M. F., et al. (2009). Sighting characteristics and photo-identification of Cuvier's beaked whales (Ziphius cavirostris) near San Clemente Island, California: a key area for beaked whales and the military? *Mar. Biol.* 156, 2631–2640. doi: 10.1007/s00227-009-1289-8

Falcone, E. A., Schorr, G. S., Watwood, S. L., DeRuiter, S. L., Zerbini, A. N., Andrews, R. D., et al. (2017). Diving behaviour of Cuvier's beaked whales exposed to two types of military sonar. *R. Soc. Open Sci.* 4:170629. doi: 10.1098/rsos.170629

Fernandez, A., Sierra, E., Martin, V., Mendez, M., Sacchinnin, S., Bernaldo de Quiros, Y., et al. (2012). Last "atypical" beaked whales mass stranding in the Canary Islands (July, 2004). *J. Mar. Sci. Res. Dev.* 2:107. doi: 10.4172/2155-9910.1000107

Fewtrell, J. L., and McCauley, R. D. (2012). Impact of air gun noise on the behavior of marine fish and squid. *Mar. Pollut. Bull.* 64, 984–993. doi: 10.1016/j.marpolbul.2012.02.009

Frantzis, A. (1998). Does acoustic testing strand whales? *Nature* 392:29. doi: 10.1038/32068

Getis, A., and Ord, J. K. (1992). The analysis of spatial association by use of distance statistics. *Geogr. Anal.* 24, 189–206. doi: 10.1111/j.1538-4632.1992.tb00261.x

Gomez, C., Lawson, J. W., Wright, A. J., Buren, A. D., Tollit, D., and Lesage, V. (2016). A systematic review on the behavioural responses of wild marine mammals to noise: the disparity between science and policy. *Can. J. Zool.* 94, 801–819. doi: 10.1139/cjz-2016-0098

Hildebrand, J. (2005). "Impacts of Anthropogenic sound," in *Marine Mammal Research: Conservation Beyond Crisis*, eds J. E. Reynolds II, W. F. Perrin, R. R. Reeves, S. Montgomery, and T. J. Ragen (Baltimore, MD: The Johns Hopkins University Press), 101–124.

Isojunno, S., Cure, C., Kvadsheim, P. H., Lam, F. P. A., Tyack, P. L., Wensveen, P. J., et al. (2016). Sperm whales reduce foraging effort during exposure to 1-2 kHz sonar and killer whale sounds. *Ecol. Appl.* 26, 77–93. doi: 10.1890/15-0040

Jarvis, S. M., Morrisey, R. P., Moretti, D. J., DiMarzio, N. A., and Shaffer, J. A. (2014). Marine mammal monitoring on navy ranges (M3R): a toolset for automated detection, localization, and monitoring of marine mammals in open ocean environments. *Mar. Technol. Soc. J.* 48, 5–20. doi: 10.4031/mtsj.48.1.1

Johnson, C. E. (2012). "Regulatory assessments of the effects of noise: moving from threshold shift and injury to behavior," in *The Effects of Noise on Aquatic Life*, eds A. N. Popper and A. Hawkins (New York, NY: Springer), 563–565. doi: 10.1007/978-1-4419-7311-5_127

Johnson, M., Madsen, P. T., Zimmer, W. M. X., Aguilar de Soto, N., and Tyack, P. L. (2004). Beaked whales echolocate on prey. *Proc. Biol. Sci.* 271, S383–S386.

Kastelein, R. A., Helder-Hoek, L., Van de Voorde, S., von Benda-Bechmann, S., Lam, F. P. A., Jansen, E., et al. (2017). Temporary hearing threshold shift in a harbor porpoise (*Phocoena phocoena*) after exposure to multiple airgun sounds. *J. Acoust. Soc. Am.* 142, 2430–2442. doi: 10.1121/1/5007720

Kates Varghese, H., Miksis-Olds, J., DiMarzio, N., Lowell, K., Linder, E., Mayer, L. A., et al. (2020). The Effect of two 12 kHz Multibeam mapping surveys on the foraging behavior of cuvier's beaked whales off of Southern California. *J. Acoustic. Soc. Am.* 147, 3849–3858. doi: 10.1121/10.0001385

Kates Varghese, H., Smith, M. J., Miksis-Olds, J. L., and Mayer, L. (2019a). Regulation consideration of ocean mapping multibeam echo sounders: a square peg in a round hole. *J. Ocean Technol.* 14, 40–46.

Kates Varghese, H., Smith, M. J., Miksis-Olds, J. L., and Mayer, L. (2019b). The contribution of 12 kHz multibeam sonar to a southern California marine soundscape. *J. Acoustic. Soc. Am.* 145:1671. doi: 10.1121/1.5101132

Ketten, D. R. (2014). Sonars and strandings: are beaked whales the aquatic acoustic canary? *Acoust. Today* 10, 45–55.

Kruskal, W. H., and Wallis, W. A. (1952). Use of ranks in one-criterion variance analysis. *J. Am. Stat. Assoc.* 47, 583–621. doi: 10.1080/01621459.1952.10483441

Lurton, X. (2016). Modelling of the sound field radiated by multibeam echosounders for acoustical impact assessment. *Appl. Acoust.* 101, 201–221. doi: 10.1016/j.apacoust.2015.07.012

Lurton, X., and DeRuiter, S. (2011). Sound radiation of seafloor-mapping echosounders in the water column, in relation to the risks posed to marine mammals. *Int. Hydrogr. Rev.* 6, 7–17.

Malme, C. I., Miles, P. R., Clark, C. W., Tyack, P., and Bird, J. E. (1984). *Investigations of the Potential Effects of Underwater Noise From Petroleum-Industry Activities on Migrating Gray-Whale Behavior*. Phase 2: January 1984 Migration Report Number: PB-86-218377/XAB; BBN-5586. Cambridge, MA: U.S. Department of Energy Office of Scientific and Technical Information.

Manzano-Roth, R., Henderson, E., Martin, S., Martin, C., and Matsuyama, B. (2016). Impacts of U.S. navy training events on Blainville's beaked whale (*Mesoplodon densirostris*) foraging dives in Hawaiian waters. *Aquat. Mamm.* 42, 507–528. doi: 10.1578/am.42.4.2016.507

Marine Mammal Commission (2015). *The Marine Mammal Protection Act of 1972 As Amended*. Bethesda, MD: NOAA National Marine Fisheries Service.

Mayer, L. (2017). *Performance and Progress Report University of New Hampshire/National Oceanic and Atmospheric Administration Joint Hydrographic Center 2017*. NOAA Grant No. NA15NOS4000200. Available online at: https://ccom.unh.edu/sites/default/files/progress_reports/2017-jhc-ccom-progress-report-web.pdf (accessed December 23, 2020).

Mayer, L. (2019). *University of New Hampshire/National Oceanic and Atmospheric Administration Joint Hydrographic Center 2019 Performance and Progress Report*. NOAA Grant No. NA15NOS4000200. Available online at: https://ccom.unh.edu/sites/default/files/progress_reports/2019-jhc-ccom-full-annual-report.pdf (accessed December 23,2020).

McCarthy, E., Moretti, D., Thomas, L., DiMarzio, N., Morrissey, R., Jarvis, S., et al. (2011). Changes in spatial and temporal distribution and vocal behavior of Blainville's beaked whales (*Mesoplodon densirostris*) during multiship exercises with mid-frequency sonar. *Mar. Mamm. Sci.* 27, E206–E226. doi: 10.1111/j.1748-7692.2010.00457.x

McSweeney, D. J., Baird, R. W., and Mahaffy, S. D. (2007). Site fidelity, associations, and movements of Cuvier's (*Ziphius cavirostris*) and Blainville's (*Mesoplodon densirostris*) beaked whales off the island of Hawai'i. *Mar. Mamm. Sci.* 23, 666–687. doi: 10.1111/j.1748-7692.2007.00135.x

Miller, P. J. O., Kvadsheim, P. H., Lam, F. P. A., Wensveen, P. J., Antunes, R., Alves, A. C., et al. (2012). The severity of behavioral changes observed during experimental exposures of Killer (*Orcinus orca*), long-finned pilot (*Globicephala melas*), and Sperm (*Physeter microcephalus*) whales to naval sonar. *Aquat. Mamm.* 38, 362–401. doi: 10.1578/AM.38.4.2012.362

Moline, M. A., and Benoit-Bird, K. (2016). Sensor fusion and autonomy as a powerful combination for biological assessment in the marine environment. *Robot* 5:4. doi: 10.3390/robotics5010004

Mooney, T. A., Hanlon, R. T., Christensen-Dalsgaard, J., Madsen, P. T., Ketten, D. R., and Nachtigal, P. (2010). Sound detection by the longfin squid (Loligo pealeii) studied with auditory evoked potentials: sensitivity to low-frequency particle motion and not pressure. *J. Exp. Biol.* 213, 3748–3759. doi: 10.1242/jeb.048348

Moran, P. A. P. (1948). The interpretation of statistical maps. *J. R. Stat. Soc. Ser. B Stat. Methodol.* 10, 243–251. doi: 10.1111/j.2517-6161.1948.tb00012.x

Moretti, D. J. (2019). *Estimating the Effect of Mid-Frequency Active Sonar on the Population Health of Blainville's Beaked Whale (Mesoplodon densirostris) in the Tongue of the Ocean*. Ph.D. Dissertation. St. Andrews: University of St. Andrews.

Moulins, A., Rosso, M., Nani, B., and Wurtz, M. (2007). Aspects of the distribution of Cuvier's beaked whale (Ziphius cavirostris) in relation to topographic features in the Pelagos Sanctuary (north-western Mediterranean Sea). *J. Mar. Biol. Assoc. U. K.* 87, 177–186. doi: 10.1017/S0025315407055002

National Research Council (2005). *Marine Mammal Populations and Ocean Noise: Determining When Noise Causes Biologically Significant Effects.* Washington, DC: The National Academies Press. doi: 10.17226/11147

Pacini, A. F., Nachtigall, P. E., Quintos, C. T., Schofield, T. D., Look, D. A., Levine, G. A., et al. (2011). Audiogram of a stranded Blainville's beaked whale (*Mesoplodon densirostris*) measured using auditory evoked potentials. *J. Exp. Biol.* 214, 2409–2415. doi: 10.1242/jeb.054338

Popper, A. N., and Hawkins, A. D. (2018). The importance of particle motion to fishes and invertebrates. *J. Acoust. Soc. Am.* 143, 470–488. doi: 10.1121/1.5021594

Popper, A. N., Hawkins, A. D., and Thomsen, F. (2020). Taking the animals' perspective regarding anthropogenic underwater sound. *Trends Ecol. Evol.* 35, 787–794. doi: 10.1016/j.tree.2020.05.002

Quick, N., Scott-Hayward, L., Sadykova, D., Nowacek, D., and Read, A. (2017). Effects of a scientific echo sounder on the behavior of short finned pilot whales (*Globicephala macrorhynchus*). *Can. J. Fish. Aquat. Sci.* 74, 716–726. doi: 10.1139/cjfas-2016-0293

Richardson, W., Malme, J., Green, C., and Thomson, D. (1995). *Marine Mammals and Noise*. San Diego, CA: Academic Press,

Santora, J. A., Schroeder, I. D., Field, J. C., Wells, B. K., and Sydeman, W. J. (2014). Spatio-temporal dynamics of ocean conditions and forage taxa reveal regional structuring of seabird-prey relationships. *Ecol. Appl.* 24, 1730–1747. doi: 10.1890/13-1605.1

Santos, M. B., Pierce, G. J., Herman, J., Lopez, A., Guerra, A., Mente, E., et al. (2001). Feeding ecology of Cuvier's beaked whale (*Ziphius cavirostris*): a review with new information on the diet of this species. *J. Mar. Biol. Assoc. U.K.* 81, 687–694. doi: 10.1017/s0025315401004386

Schorr, G. S., Falcone, E. A., Moretti, D. J., and Andrews, R. D. (2014). First long-term behavioral records from Cuvier's Beaked Whales (*Ziphius cavirostris*) reveal record-breaking dives. *PLoS One* 9:e92633. doi: 10.1371/journal.pone.0092633

Sims, D. W., Witt, M. J., Richardson, A. J., Southall, E. J., and Metcalf, J. D. (2006). Encounter success of free-ranging marine predator movements across a dynamic prey landscape. *Proc. Biol. Sci.* 273, 1195–1201. doi: 10.1098/rspb.2005.3444

Sivle, L. D., Kvadsheim, P. H., Cure, C., Isojunno, S., Wensveen, P. J., Lam, F. P. A., et al. (2015). Severity of expert-identified behavioural responses of Humpback Whale, Minke Whale, and Northern Bottlenose Whale to naval sonar. *Aquat. Mamm.* 41, 469–502. doi: 10.1578/AM.41.4.2015.469

Smith, M. J. (2019). *Analysis of the Radiated Sound Field of a Deep-Water Multibeam Echo Sounder Using a Navy Hydrophone Array*. Master's Thesis, University of New Hampshire, Durham. Available online at: https://unh.idm.oclc.org/login?url=https://www.proquest.com/dissertations-theses/analysis-radiated-sound-field-deep-water/docview/2273838102/se-2?accountid=14612 (accessed July 31, 2021).

Southall, B., Bowles, A., Ellison, W., Finneran, J., Gentry, R., Greene, C. Jr., et al. (2007). Marine mammal noise exposure criteria: initial scientific recommendations. *Aquat. Mamm.* 33:4.

Southall, B. L., Benoit-Bird, K. J., Moline, M. A., and Moretti, D. (2019). Quantifying deep-sea predator-prey dynamics: implications of biological heterogeneity for beaked whale conservation. *J. Appl. Ecol.* 56, 1040–1049. doi: 10.1111/1365-2664.13334

Southall, B. L., Rowles, T., Gulland, F., Baird, R. W., and Jepson, P. D. (2013). *Final Report of the Independent Scientific Review Panel investigating Potential Contributing Factors to a 2008 Mass Stranding of Melon-Headed Whales in Antsohihy, Madagascar*. Available online at: https://www.cascadiaresearch.org/Hawaii/Madagascar_ISRP_Final_report.pdf (accessed December 1, 2019).

Tanha, K., Mohammadi, N., and Janani, L. (2017). P-value: what is and what is not. *Med. J. Islam. Repub. Iran* 31:65. doi: 10.14196/mjiri.31.65

Thayer, J. A., and Sydeman, W. J. (2007). Spatio-temporal variability in prey harvest and reproductive ecology of a piscivorous seabird, *Cerorhinca monocerata*, in an upwelling system. *Mar. Ecol. Pro. Ser.* 329, 253–265. doi: 10.3354/meps329253

Tyack, P. L., Johnson, M., Aguilar Soto, N., Sturlese, A., and Madsen, P. T. (2006). Extreme diving of beaked whales. *J. Exp. Biol.* 209, 4238–4253. doi: 10.1242/jeb/0205

Tyack, P. L., Zimmer, W. M. X., Moretti, D., Southall, B. L., Claridge, D. E., Durban, J. W., et al. (2011). Beaked whales respond to simulated and actual navy sonar. *PLoS one.* 6:e17009. doi: 10.137/journal.pone.0017009

Ward, J., Morrissey, R., Moretti, D., DiMarzio, N., Jarvis, S., Johnson, M., et al. (2008). Passive acoustic detection and localization *of Mesoplodon densirostris* (Blainville's beaked whale) vocalizations using distributed bottom-mounted hydrophones in conjunction with a digital tag (dtag) recording. *Can. Acoustic.* 36, 60–66.

Wright, A. J., Soto, N. A., Baldwin, A. L., Bateson, M., Beale, C. M., Clark, C., et al. (2007). Do marine mammals experience stress related to anthropogenic noise? *Int. J. Comp. Psychol.* 20, 274–316.

Conflict of Interest: The authors declare that the research was conducted in the absence of any commercial or financial relationships that could be construed as a potential conflict of interest.

Publisher's Note: All claims expressed in this article are solely those of the authors and do not necessarily represent those of their affiliated organizations, or those of the publisher, the editors and the reviewers. Any product that may be evaluated in this article, or claim that may be made by its manufacturer, is not guaranteed or endorsed by the publisher.

Copyright © 2021 Kates Varghese, Lowell, Miksis-Olds, DiMarzio, Moretti and Mayer. This is an open-access article distributed under the terms of the Creative Commons Attribution License (CC BY). The use, distribution or reproduction in other forums is permitted, provided the original author(s) and the copyright owner(s) are credited and that the original publication in this journal is cited, in accordance with accepted academic practice. No use, distribution or reproduction is permitted which does not comply with these terms.

frontiers in Marine Science

ORIGINAL RESEARCH
published: 07 September 2021
doi: 10.3389/fmars.2021.705204

Contextualizing Thermal Effluent Impacts in Narragansett Bay Using Landsat-Derived Surface Temperature

Jonathan Benoit and Baylor Fox-Kemper*

Department of Earth, Environmental and Planetary Sciences (DEEPS), Brown University, Providence, RI, United States

This work utilizes remotely sensed thermal data to understand how the release of thermal pollution from the Brayton Point Power Station (BPPS) affected the temperature behavior of Narragansett Bay. Building upon previous work with Landsat 5, a multi-satellite analysis is conducted that incorporates 582 scenes from Landsat 5, Landsat 7, and Landsat 8 over 1984–2021 to explain seasonal variability in effluent impacts, contrast data after the effluent ceased in 2011, identify patterns in temperature before and after effluent ceased using unsupervised learning, and track how recent warming trends compare to the BPPS impact. Stopping the thermal effluent corresponds to an immediate cooling of 0.26 ± 0.1°C in the surface temperature of Mt. Hope Bay with respect to the rest of Narragansett Bay with greater cooling of 0.62 ± 0.2°C found near Brayton Point; though, cooling since the period of maximal impact (1993–2000) totals 0.53 ± 0.2°C in Mt. Hope Bay and 1.04 ± 0.2°C at Brayton Point. During seasons with lower solar radiation (winter) and lower mean river input (autumn and late summer), the BPPS effluent impact is more prominent. The seasonal differences between the high impact and low impact periods indicate that river input played an important role in the heat balance when emissions were lower, but surface fluxes dominated when emissions were higher. Putting the BPPS effluent in context, Landsat data indicates that Narragansett Bay warmed 0.5–1.2°C over the period of measurement at an average rate of 0.23 ± 0.1°C/decade and that net warming in Mt. Hope Bay is near zero. This trend implies that Narragansett Bay has experienced climatic warming over the past four decades on the scale of the temperature anomaly in Mt. Hope Bay caused by the BBPS effluent.

Keywords: Narragansett Bay, Brayton Point Power Station, thermal pollution, remote sensing, Landsat, climate change, surface temperature

OPEN ACCESS

Edited by:
Juan Jacobo Schmitter-Soto, The South Border College (ECOSUR), Mexico

Reviewed by:
Bo Nordell, Luleå University of Technology, Sweden
Sheila Madrak, San Diego Miramar College, United States

****Correspondence:***
Jonathan Benoit
jonathan_benoit@brown.edu

Specialty section:
This article was submitted to Marine Pollution, a section of the journal Frontiers in Marine Science

Received: *04 May 2021*
Accepted: *11 August 2021*
Published: *07 September 2021*

Citation:
Benoit J and Fox-Kemper B (2021) Contextualizing Thermal Effluent Impacts in Narragansett Bay Using Landsat-Derived Surface Temperature. Front. Mar. Sci. 8:705204. doi: 10.3389/fmars.2021.705204

1. INTRODUCTION

1.1. Background

The Brayton Point Power Station (BPPS) was a coal-fueled power station in Massachusetts that operated from 1963 to 2017. This power station was New England's largest fossil-fuel burning power station as well as a source of thermal pollution into Mt. Hope Bay, a northeastern embayment of Narragansett Bay (see **Figure 1**). Water from nearby rivers was used as a coolant for the power plant and heated 7–10°C above ambient river temperature before being released back into the

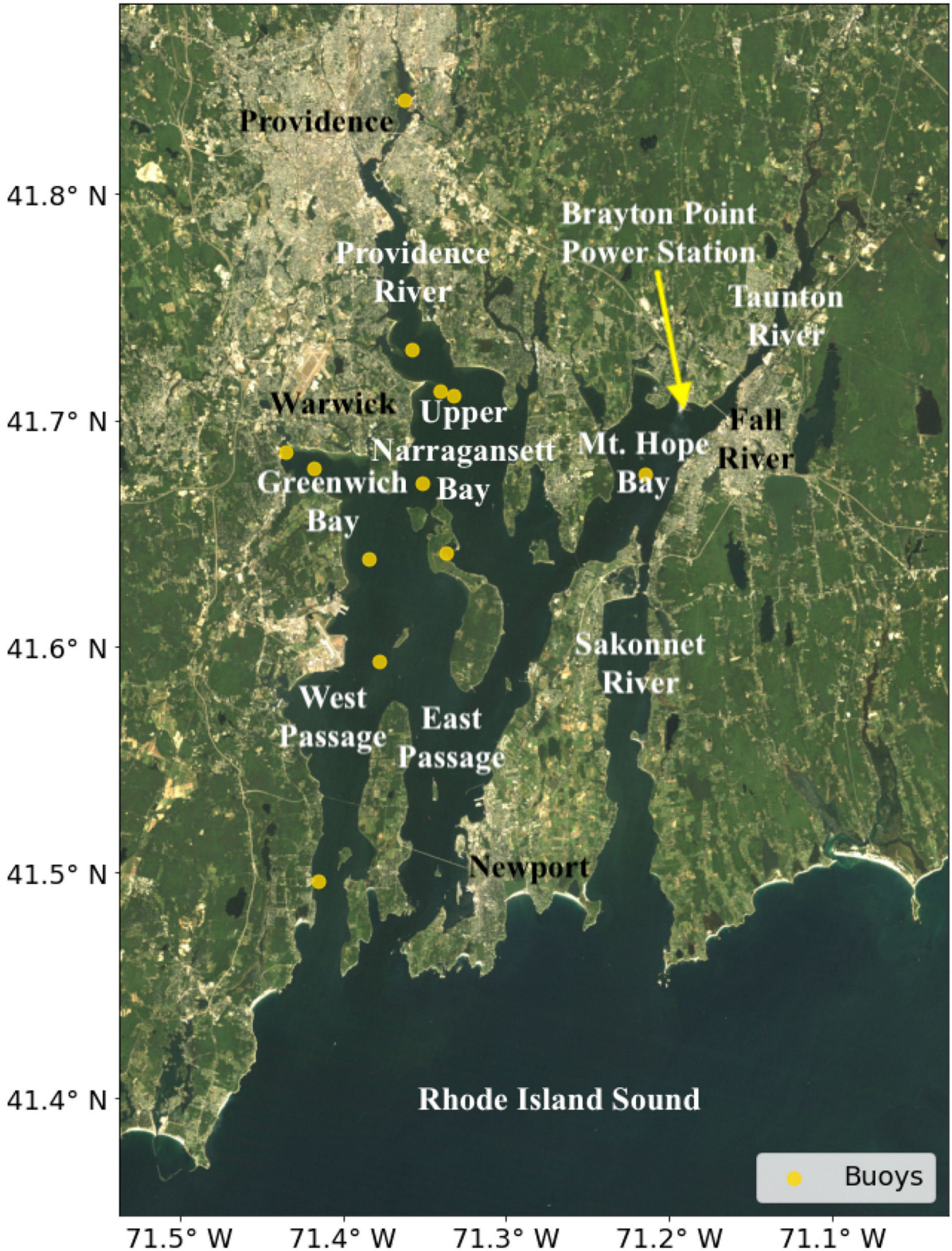

FIGURE 1 | Narragansett Bay shown in true color by a Landsat 5 scene on September 7th, 1984 with labeled regions and buoy locations. A plume of atmospheric discharge is faintly visible traveling southward from the Brayton Point Power Station.

environment. The EPA's New England Office and Department of Environmental Protection issued a new water discharge permit in 2003 that required the BPPS to drastically reduce thermal effluent release, though appeals were not resolved until 2007 and thermal effluent release did not stop until October 2011 when two cooling towers became operational. The BPPS later shut down operations completely in May 2017, and the cooling towers were demolished on April 27, 2019. Before regulations were tightened, the BPPS released nearly one billion gallons of water daily—enough to replace the entire volume of Mt. Hope Bay 3.5 times over a year—and released 44 petajoules (12 TWh) of heat annually into Mt. Hope Bay (United States Environmental Protection Agency, 2003). Comparing the heat released to the energy of incoming solar and longwave radiation and the effluent volume flux to the volume of river input contextualizes the scale of this impact. Using forcing data from the Ocean State Ocean Model (OSOM: Sane et al., 2020)—an application of the Regional Ocean Modeling System (ROMS) to Narragansett Bay and Rhode Island Sound—to facilitate this comparison, one billion gallons corresponds to 0.3–3.1% of the upper Taunton River input. The greatest relative volume of effluent occurs from July to October when river transport is the smallest. In terms of heat, the thermal effluent power, when spread across Mt. Hope Bay's surface, is equivalent to 7–16% of the incoming shortwave plus longwave radiation from the sun and atmosphere (the range reflects seasonal solar variability).

1.2. Previous Work

Using 14 Landsat 5 Thematic Mapper (TM) scenes, Mustard et al. (1999) found that Mt. Hope Bay had a heat anomaly of 0.8°C when compared to other upper-estuary regions and had anomalous seasonal temperature behavior characterized by delayed cooling in autumn and late summer. Further work found that the heat budget in Mt. Hope Bay is dominated by air-sea fluxes and that the BPPS effluent accounts for 25% of the total heating during winter and 15% during the summer (Fan and Brown, 2006). This work accounted for seasonal differences in effluent output, which is greater in winter and lower in summer, due to corresponding changes in energy demand and found that river input, in addition to surface exchanges, is a significant source of cooling during summer. Mustard et al. (2001) found that the effect of the thermal effluent on Mt. Hope Bay during the winter and spring are minimal as evidence of the thermal plume in satellite imagery is rarer during these seasons. With ∼20 years of *in situ* and satellite data taken since many of these studies, this work aims to use longitudinal thermal data across the Landsat satellite series to analyze the post-effluent response in Mt. Hope Bay and contextualize the BPPS impact amid temperature trends in Narragansett Bay.

1.3. Narragansett Bay Context

Monitoring of coastal marine ecosystems is critical to appreciate and mitigate the environmental challenges they face. Of particular concern, severe hypoxic events have been observed in Narragansett Bay historically (Deacutis et al., 2006; Melrose et al., 2007). Though nutrient release from rivers and wastewater treatment plants—as well as physical conditions controlling mixing and stratification—play primary roles in Narragansett Bay hypoxia, increases in temperature have been linked to increased susceptibility to hypoxia in coastal marine ecosystems as well (Pörtner et al., 2005; Miller and Harding, 2007; Conley et al., 2009; McBryan et al., 2013; Oviatt et al., 2017). Additionally, temperature plays an important role in biogeochemical cycling and ecosystem functioning by controlling the rates of chemical reactions, the timing of seasonal algal blooms, and spawning behavior (Valiela et al., 1997; Harley et al., 2006). With compounding ecological stressors such as climate change, overfishing, and increased predator prevalence, the effect of the BPPS effluent on declining fish populations has been difficult to isolate, though some studies have found local declines specific to Mt. Hope Bay and distinct rapid evolution in fish living near the BPPS thermal effluent (Gibson, 2002; DeAlteris et al., 2006; Dayan et al., 2019).

1.4. Climate Context

Due to the southward flow of the Labrador Current and polar amplification associated with climate warming in the source waters, the coastal shelf near the northeastern United States is particularly vulnerable to ocean warming and has warmed at a rate up to three times faster than the global sea surface temperature trend (MERCINA Working Group et al., 2015; Saba et al., 2016; Dupigny-Giroux et al., 2018; Neto et al., 2021). Near and within Narragansett Bay, long-term instrumental and palaeoceanographic records indicate that the region has warmed at a rate of 0.06–0.26 °C/decade in the past century (Shearman and Lentz, 2010; Smith et al., 2010; Salacup et al., 2019). Records of climatic temperature trends are often taken from few locations or coarse-resolution satellites, limiting the capture of change in spatially varying estuarine dynamics along a heterogeneous coast. The Landsat satellites (United States Geological Survey, 2021) provide decades of temperature data at finer than 120 m resolution, allowing for detailed spatial consideration of recent trends (Ding and Elmore, 2015). The derived temperature measurements taken by Landsat are less precise than on satellites designed specifically to measure sea surface temperature (SST); however, large near-shore and coastal variations in temperature permit Landsat accuracy to capture within-estuary variability. Additionally, estimation of temperature uncertainties by calibration to *in situ* buoy measurements over the same decades ensures appropriate consideration of uncertainty when using Landsat data in this work (Emery et al., 2001).

1.5. Estuarine Flow

To understand effluent and climatic impact on a dynamic estuarine system, the oceanographic processes at play are important to consider as well. In a shallow and well-mixed estuary such as Narragansett Bay, circulation is governed by diurnal tides, salinity-governed stratification, and river input (Geyer and MacCready, 2014). Because the northern embayments of Narragansett Bay are shallow and isolated from tidal mixing with shelf waters, they experience greater seasonal temperature extremes than deeper locations with significant oceanic influence (Mustard et al., 1999). Important for pollutant analysis, flushing timescales represent how long it takes to

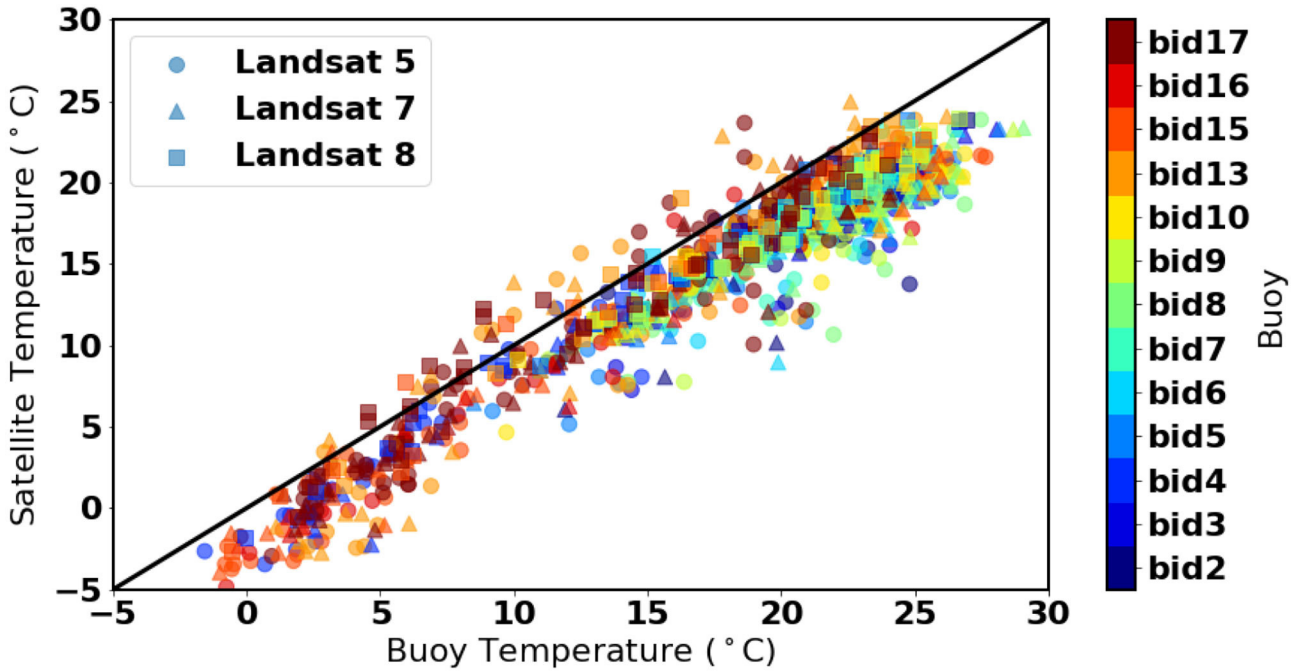

FIGURE 2 | Comparison between Landsat-derived temperature and surface *in situ* buoy measurements. The black line represents a 1:1 relationship for reference.

replace water masses in an estuary with water from rivers. Flushing timescales can be calculated for a body in an estuary by dividing the volume of water in the body by the rate of river input (Monsen et al., 2002). Observational and model-based studies indicate the surface flushing timescale of Narragansett Bay ranges from 14 to 33 days while the local flushing timescale in Mt. Hope Bay ranges from a single tidal cycle to ∼30 days depending on mean river input—which varies seasonally—and tidal magnitude—which varies monthly (Abdelrhman, 2005; Rogers, 2008; Sane et al., 2020).

Mt. Hope Bay flushing dynamics are dominated by input from the Taunton River and output into the Sakonnet River and East Passage. Though the extent of the thermal plume from the BPPS at any given time depends on the stage of the tidal cycle, the thermal effluent is dispersed throughout Mt. Hope Bay over the course of a tidal cycle and the temperature anomaly persists between cycles (Mustard et al., 2001). Satellite data is limited in measuring thermal plumes because satellites only measure surface temperature, which may exaggerate the plume's effect if the thermal plume is buoyant and presents as a surface lens of warmer water. However, due to year-round wind-driven and tide-driven mixing, as well as seasonal and diurnal convective mixing, Narragansett Bay is often well-mixed vertically, only having significant (haline) stratification—as evidenced by hypoxia—when river input is high and wind-driven mixing is low during acute periods in the spring and early summer (Torgersen et al., 1997). The most significant effluent effects are found outside of these high stratification periods, so an exaggerated surface plume would have to come primarily from temperature-driven buoyancy, which is unlikely in an estuary where salinity differences are large enough to govern stratification and where persistent stratification is challenged by nighttime convection. Further, this analysis focuses on temperature anomalies over many years, so any detected plume persists in the face of mixing and convection long enough to skew the repeat observations.

2. METHODS

2.1. Satellite Data

Earth-observing satellites measure outgoing electromagnetic radiation at a variety of wavelengths. Tuned to wavelengths longer than the visible range, thermally sensitive sensors on these satellites measure radiation that is strongly affected by surface temperature. By using principles from Planck's Law, the radiation measured by satellites can be converted to brightness temperature assuming that the surface is a black body (Mustard et al., 1999). While this data is useful, long-wavelength light cannot penetrate deeply into bodies of water, so water temperature determined through this method only represents the top 10μm, or skin, of the water's surface, meaning that satellite-derived thermal data can differ from the bulk water temperature when mixing is weak (Emery et al., 2001). A good correlation between satellite-derived temperature and *in situ* temperatures near the surface is expected, though satellite data is often cooler than *in situ* temperature because of evaporative cooling and can vary depending on wind conditions (Schneider and Mauser, 1996).

The USGS Landsat Surface Reflectance Tier 1 (United States Geological Survey, 2021) data products for Landsat 5, Landsat

TABLE 1 | Calibration terms for Landsat satellites: The bias term represents the mean difference between satellite and buoy surface temperature and the error term represents one standard deviation of this difference.

	Landsat 5	Landsat 7	Landsat 8
Bias (°C)	3.36	3.34	1.92
Measurement error (°C)	1.9	1.9	1.3

The bias term was added to calibrate all scenes from the corresponding satellite, and the error term estimates the measurement error of any individual pixel measurement.

7, and Landsat 8 are used in this analysis and include calculated brightness temperature for the thermal bands of each satellite. These thermal bands are Landsat 5 Thematic Mapper (TM) and Landsat 7 TM band 6, tuned to 10.40–12.50μm at 120 m/pixel and 60 m/pixel resolution, respectively, and Landsat 8 Thermal Infrared Sensor (TIRS) band 10, tuned to 10.60–11.19μm at 100 m/pixel resolution. The combination of these three satellites provides a continuous record from 1984 to the present with Landsat 5 operational from March 1984 to June 2011, Landsat 7 from April 1999 to the present, and Landsat 8 from February 2013 to the present. Each satellite passes over any specific location every 16 days, with an 8 day offset between satellites that operate simultaneously, and their sun-synchronous orbits ensure that all data over Narragansett Bay is taken at ∼15:30 GMT. However, the availability of data is much less frequent due to clouds and the scheduling of data processing. All data were resampled to 30 m/pixel resolution using cubic convolution before being accessed through Google Earth Engine.

Narragansett Bay falls within path 12, row 31 of the WRS-2 reference system. Landsat scenes over this location also include much of southeastern New England, Boston Bay, parts of Long Island Sound, and much of the coastal shelf south of Rhode Island. From the available 887 Landsat scenes in this location, all scenes with <50% cloud cover over Narragansett Bay are removed, resulting in 582 usable scenes for this analysis with an average of 23 days between observations. These selected scenes are then land and cloud masked by using a land mask from Hansen et al. (2013) and cloud quality attributes in the data.

2.2. Satellite Calibration and Atmospheric Correction

One problem faced when using satellite remote sensing to image land and water surfaces is how to account for absorption and emission of radiation from the atmosphere. The approach here is to quantify average satellite bias and uncertainties due to atmospheric and other effects by comparing to *in situ* surface buoy data. This analysis is done separately for each satellite because the thermal band on Landsat 8 is tuned to different wavelengths than the thermal bands on Landsat 5 and Landsat 7. The mean bias between satellite and buoy measurements is added to all data from the corresponding satellite, and the standard deviation of the mean differences after adding the bias represents the measurement uncertainty at any pixel, which quantifies typical variations that cause the buoy and bias-corrected satellite measurements to disagree. This bias correction calibrates the satellites against a consistent baseline of *in situ* data by quantifying the accuracy (bias) and precision (measurement uncertainty) of each satellite. After bias correction, the distributions of the differences between satellite and buoy measurements are nearly centered Gaussian distributions, so the use of standard deviation is appropriate. The measurement uncertainty of data using this method decreases with the number of scenes averaged together (assuming they represent different weather and thus are independent, consistent with the 23 day sampling period), though sampling uncertainty proves to be important as well.

To make the satellite comparison to *in situ* data, surface buoy data taken between 15:00 and 16:00 GMT on the dates of satellite flyby are compared to satellite-derived temperature averaged between non-masked pixels within 200 m of the buoy locations. The *in situ* data comes from a network of buoys in Narragansett Bay operated by the Rhode Island Department of Environmental Management (Rhode Island Department of Environmental Management, 2015) as shown in **Figure 1**. Data from 2003 to 2015 were used to conduct this analysis because all three Landsat satellites were operational for a portion of this period and the buoy network was dense at that time. In total, 1,261 buoy measurements were compared to Landsat data from 13 RI DEM buoys with 382 of those measurements compared to Landsat 5, 646 to Landsat 7, and 233 to Landsat 8.

The satellite to buoy comparison is depicted in **Figure 2** with the calculated biases and measurement uncertainties given in **Table 1**. All satellites show a high correlation between remotely sensed and *in situ* temperature with correlation coefficients >0.96. Satellite-derived temperature is found to be cooler than *in situ* temperature typically, which is consistent with other studies that used Landsat to quantify surface water temperature (Schneider and Mauser, 1996; Mustard et al., 1999). The Landsat 5 and Landsat 7 biases and uncertainties are similar, while the Landsat 8 bias and uncertainty differ significantly. This result is consistent with the fact that the Landsat 8 TIRS thermal band is tuned to different wavelengths than the Landsat 5 and Landsat 7 TM bands. To confirm the accuracy of this method, mean temperature values over all of Narragansett Bay during the periods the satellites overlap are compared as measured by different satellites (**Figure 3**). Only considering measurement uncertainty, the mean values fall inside of the margin of error for the comparison between Landsat 7 and Landsat 8 over 2013–2020 but outside the margin or error for Landsat 5 and Landsat 7 over 1999–2013. Considering sampling uncertainty, both cross-satellite comparisons fall within the margins of error, indicating that sampling uncertainty is important for this analysis. The sampling uncertainties are estimated by bootstrapping the mean temperature over all cloud-free pixels in Narragansett Bay.

After correction, satellite data are used in this analysis to determine climatic change and changes due to reduced thermal pollution. The overall warming trend detected in this analysis is unlikely to be an artifact of satellite calibration as the more recent satellites measured cooler temperatures on average and satellites are shown to be consistent within their uncertainties. To ensure a robust consideration of both sampling and measurement

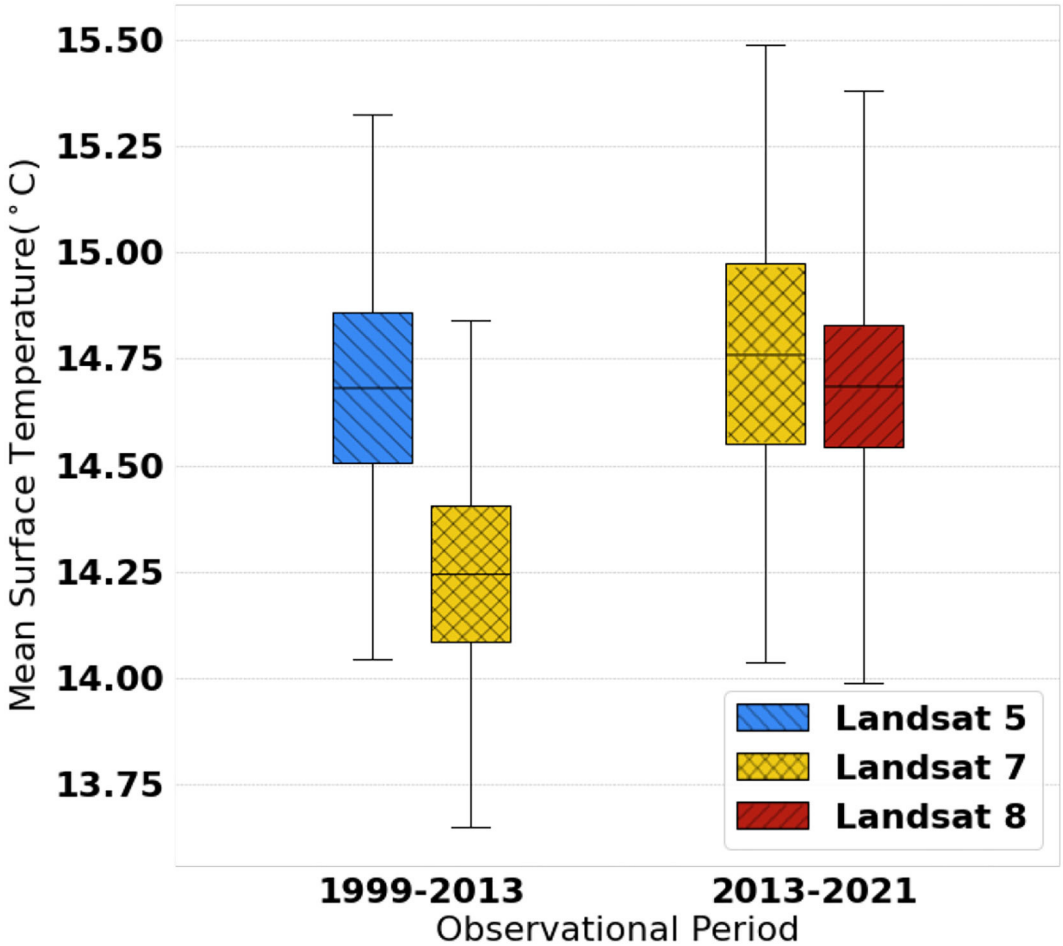

FIGURE 3 | Assessment of inter-satellite calibration by comparing surface temperature averaged over all of Narragansett Bay for overlapping time periods of each satellite. The central bars represent the means while the box edges represent propagated measurement uncertainty (from **Table 1**) and the whiskers represent sampling uncertainty estimated by bootstrapping.

uncertainty in these changes, Gaussian noise is added to all data based on measurement uncertainty before bootstrapping is conducted on the trends as described in section 2.4.

2.3. Climatology

Once the scenes are filtered, masked, and bias-corrected, a climatology is created that accounts for the non-uniform temporal spacing of the data following methods similar to Fisher and Mustard (2004): all scenes are arranged by day of year and, on a per-pixel basis, a harmonic curve of the form of Equation (1.1) is fit to the data as visualized in **Figure 4**. The constant term, α, captures the mean annual temperature while the combination of the cosine and sine coefficients, β and γ, respectively, allow for phase shift and amplitude fitting. The period of the harmonic function is fixed at one year. The harmonic curve fitting method is appropriate because seasonal temperature variability in Narragansett Bay primarily follows a sinusoidal shape (Shearman and Lentz, 2010; Salacup et al., 2019).

After fitting, more readily interpreted coefficients, A and ϕ, describing amplitude and phase shift of a single sine function as shown in Equation (1.2) are calculated from β and γ using Equations (2) and (3). **Figure 5** maps the resulting fitted parameters after pixel-wise regression for the 1984–2010 period. Note that the upper bay and rivers tend to have a warmer temperature, larger amplitude seasonal cycle, and precede the seasonal cycle in deeper water by about 15 days. The impact of the BPPS effluent is visible over this period as there is heightened mean temperature and a delayed seasonal cycle near Brayton Point.

$$T = \alpha + \beta \sin\left(\frac{2\pi}{365}t\right) + \gamma \cos\left(\frac{2\pi}{365}t\right) \tag{1.1}$$

$$= \alpha + A \sin\left(\frac{2\pi}{365}[t - \phi]\right) \tag{1.2}$$

$$A = -\sqrt{\beta^2 + \gamma^2}\frac{\beta}{|\beta|} \tag{2}$$

$$\phi = \frac{365}{2\pi}\left[\pi - \tan^{-1}\left(\frac{\gamma}{\beta}\right)\right] \tag{3}$$

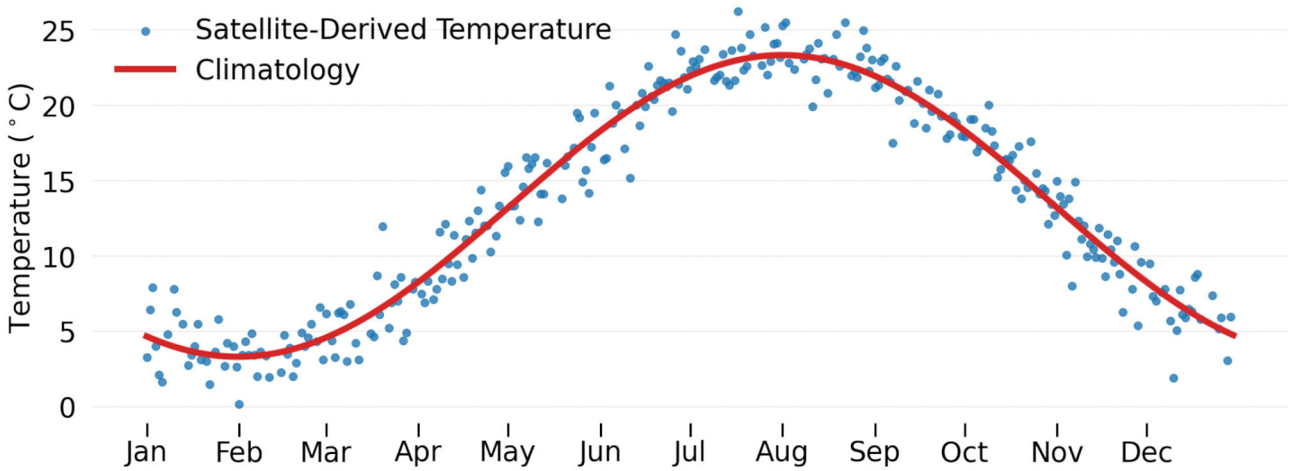

FIGURE 4 | Sample climatology for a pixel in Providence River after satellite bias correction.

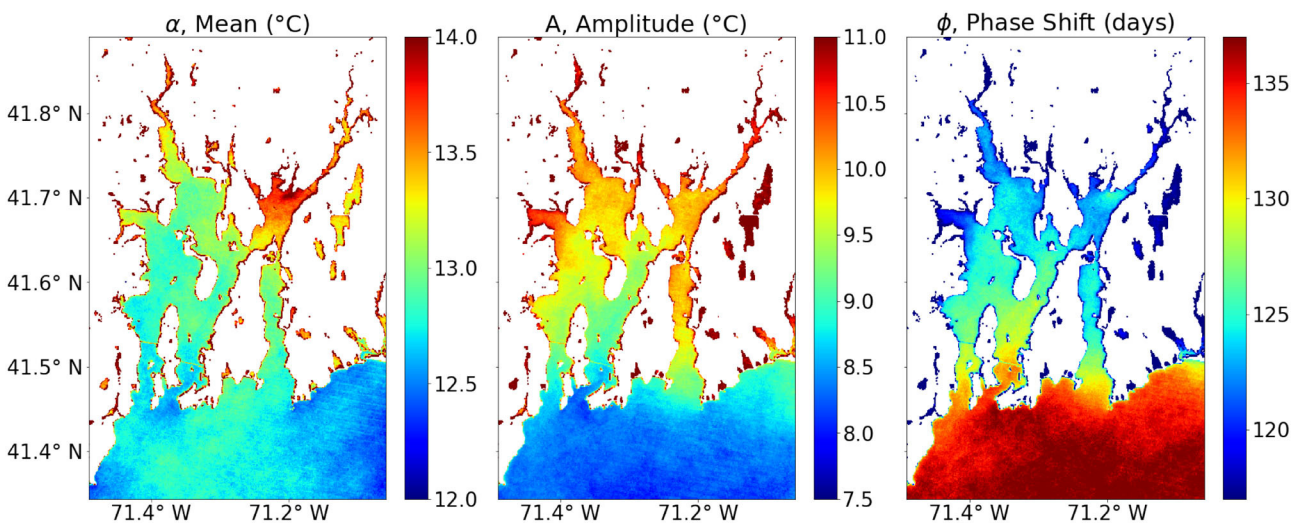

FIGURE 5 | Maps of climatology coefficients as described by Equation (1.2) calculated over 1984–2010. The climatology from the entire observation period (1984–2021) was used to seasonally detrend the data. Here the impact of the BPPS effluent is visible as an increased α term and decreased ϕ term near Brayton Point, representing greater mean temperature by 1°C or more and a delayed seasonal cycle by up to 4 days.

It should be noted that a multi-year linear trend will not affect this climatology calculation and would be present as secular terms after the climatology is removed. After the climatology was calculated for each pixel over the entire observational period, the value of the fitted climatology at the day of year of observation was subtracted to yield the anomaly used to calculate interannual trends independent of seasonal variability.

2.4. Trend Analysis

To determine the immediate impact of stopping the BPPS thermal effluent, the seasonally-corrected anomalies for Narragansett Bay are subtracted from the anomalies for Mt. Hope Bay and a region near Brayton Point. Subtracting the mean estuary anomaly from the Mt. Hope Bay and Brayton Point regions gives an estimate for how large the anomaly near the effluent was independent of larger-scale variability on the specific days of observation. Time series are split up by season and long-term averages during and after effluent release are compared to determine temperature changes in the region due to changes in power plant operation. Here, seasons were divided by month with December, January, and February representing winter; March, April, and May representing spring; June, July, and August representing summer; and September, October, and November representing autumn.

To determine multi-decade trends from the seasonally-adjusted anomalies, linear regression is conducted at each pixel, producing a map of these trends in surface temperature from

1984 to 2021. Of primary importance, this map represents the spatial complexity of the region, allowing for a comparison of the long-term trends inside Mt. Hope Bay, assumed to be cooling with reduced thermal effluent, compared to other Narragansett Bay regions, which have been known to be warming due to climatic change. Categorizing the data by month before linear interpolation yields an analysis of how these trends vary based on the seasons.

2.5. K-Means Clustering

Following previous work that conducted unsupervised clustering on Narragansett Bay temperature (Mustard et al., 1999), this work conducts K-means clustering during and after thermal effluent release (Lewis et al., 2008). Unsupervised clustering is a type of machine learning method that determines natural groupings of data based on relationships between predictors from many observations. K-means performs this clustering given k clusters by minimizing within-cluster distances. In this case, the three fitted climatology parameters (α, A, and ϕ from section 2.3), after normalization, serve as the predictors for observations at each pixel. The number of clusters, eight, was chosen by picking the smallest number of clusters that would identify the signal in Mt. Hope Bay while remaining close to the maximum inertia value—a measure of how internally coherent clusters are.

3. RESULTS

3.1. Immediate Post-Effluent Response

Clear reductions in the temperature anomaly in Mt. Hope Bay are found at the time the effluent stopped in 2011. Greater reductions in temperature are found closest to Brayton Point with plume visibility disappearing at the same time, as indicated by the plume's effects on mean temperature. **Figure 6** depicts these results using an 8-year moving average of the temperature anomaly of Mt. Hope Bay and Brayton Point from the mean temperature of Narragansett Bay by season laid over the corresponding changes in map view. The temperature anomalies in these maps are the α fitting terms as described in section 2.3 after subtracting the mean α for the estuary as a whole. The fitting terms were calculated separately for each period using the 8-year intervals shown.

The maps and time series in **Figure 6** indicate that the effluent impact was the greatest during the 1993–2000 period, became weaker leading up to when the effluent was stopped completely in 2011, and rapidly declined afterward. There is

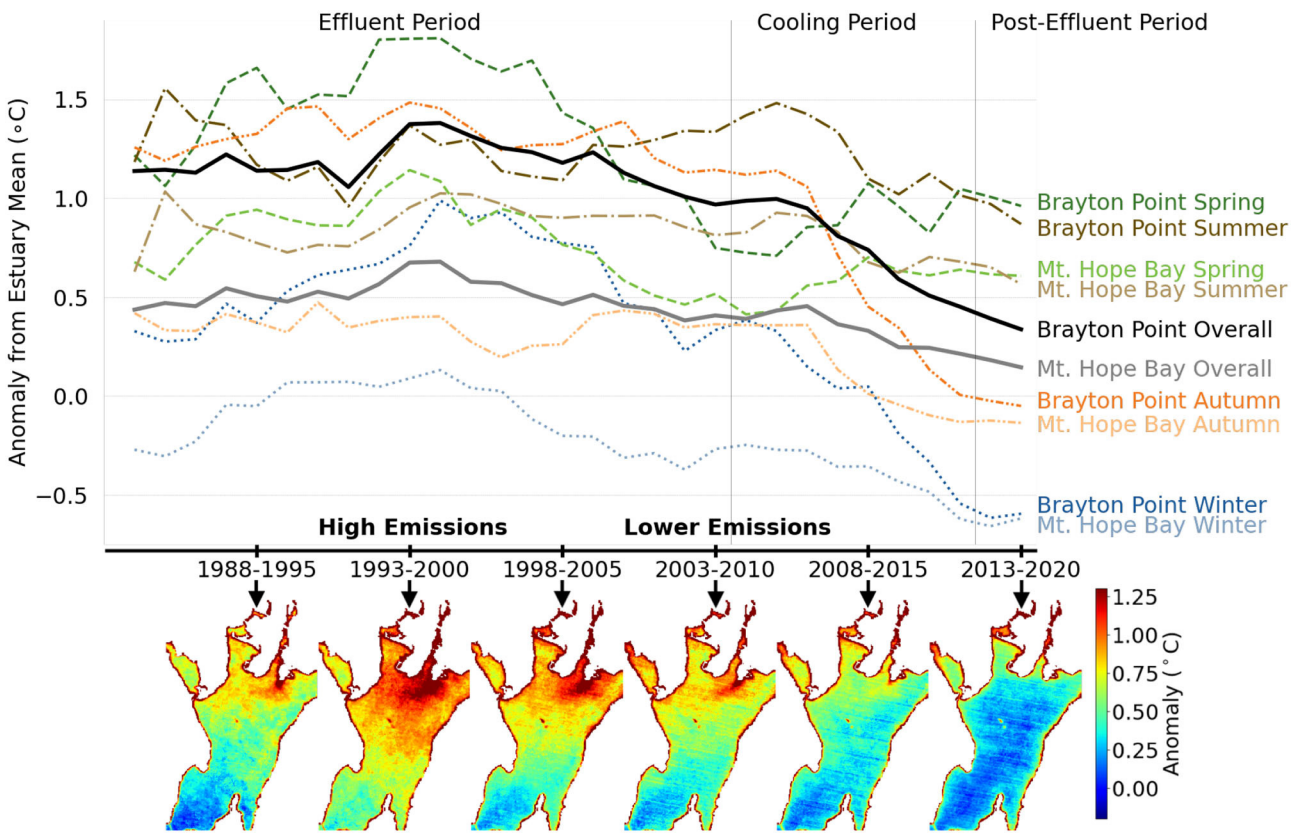

FIGURE 6 | Average Mt. Hope Bay and Brayton Point temperature anomaly minus average Narragansett anomaly for each season using an 8-year moving average. The cooling period includes data from during and after effluent release due to the moving average. Plotted below the x-axis are maps of the mean temperature anomaly in Mt. Hope Bay as determined by subtracting the mean α term from Equation (1.2) from the α values determined at each pixel for the labeled periods.

TABLE 2 | Temperature change in °C in Mt.0Hope Bay, Brayton Point, and Upper Narragansett Bay (control).

	Overall	Winter	Spring	Summer	Autumn
Mt. Hope bay high emissions	−0.53 ± 0.2	−0.70 ± 0.2	−0.54 ± 0.2	−0.38 ± 0.2	−0.54 ± 0.3
Brayton point high emissions	−1.04 ± 0.2	−1.36 ± 0.3	−0.84 ± 0.3	−0.49 ± 0.5	−1.53 ± 0.4
Mt. Hope bay lower emissions	−0.26 ± 0.1	−0.35 ± 0.2	0.10 ± 0.2	−0.25 ± 0.2	−0.49 ± 0.3
Brayton point lower emissions	−0.62 ± 0.2	−0.92 ± 0.3	0.23 ± 0.5	−0.47 ± 0.3	−1.19 ± 0.3
Control lower emissions	0.08 ± 0.2	0.14 ± 0.2	−0.03 ± 0.3	0.12 ± 0.2	0.11 ± 0.4
Control high emissions	0.07 ± 0.1	0.05 ± 0.2	0.08 ± 0.3	−0.14 ± 0.2	0.24 ± 0.3

Periods of lower effluent impact (2003–2010) and higher effluent impact (1993–2000) as determined by the difference between the mean temperature anomaly during these periods and the mean post effluent (2013–2020). Upper Narragansett Bay represents a control as no effluents are0directly released into this region.

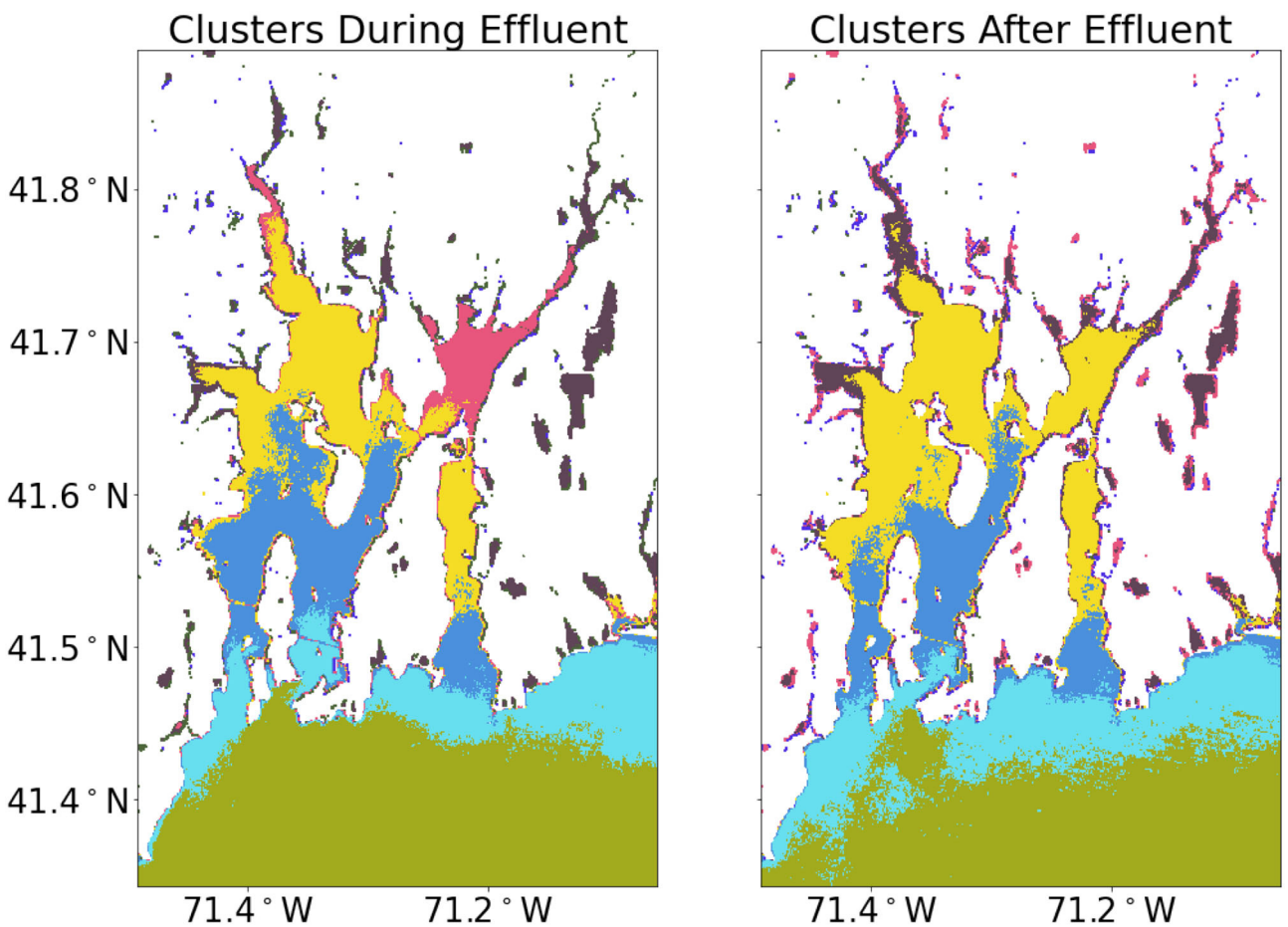

FIGURE 7 | K-means clustering on mean, amplitude, and phase shift coefficients from climatology fitting, as described by Equation (1.2), during and after the BPPS effluent.

no thermal plume in data taken after 2011. To quantify the amount of cooling for Brayton Point and Mt. Hope Bay, the mean temperature anomalies from the 2013 to 2020 period are subtracted from the 2003-2010 period, representing lower emissions, as well as from the 1993 to 2000 period, representing high emissions. Uncertainty in this metric was determined by using bootstrapping and taking the standard deviation of the resampled means. Immediate cooling in Mt. Hope Bay at the time when effluent stops totals -0.26 ± 0.1°C with the greatest cooling of -0.49 ± 0.3°C found in autumn followed by winter cooling of -0.35 ± 0.2°C. Summer cooling totaled -0.25 ± 0.2°C, and differences in spring were not statistically significant with 0.10 $\pm$ 0.2°C of warming. Close to Brayton Point, cooling was more intense for all seasons except spring with -0.62 ± 0.2°C cooling overall and a similar pattern of greatest cooling in autumn, then winter, then summer. Differences for the high emissions period

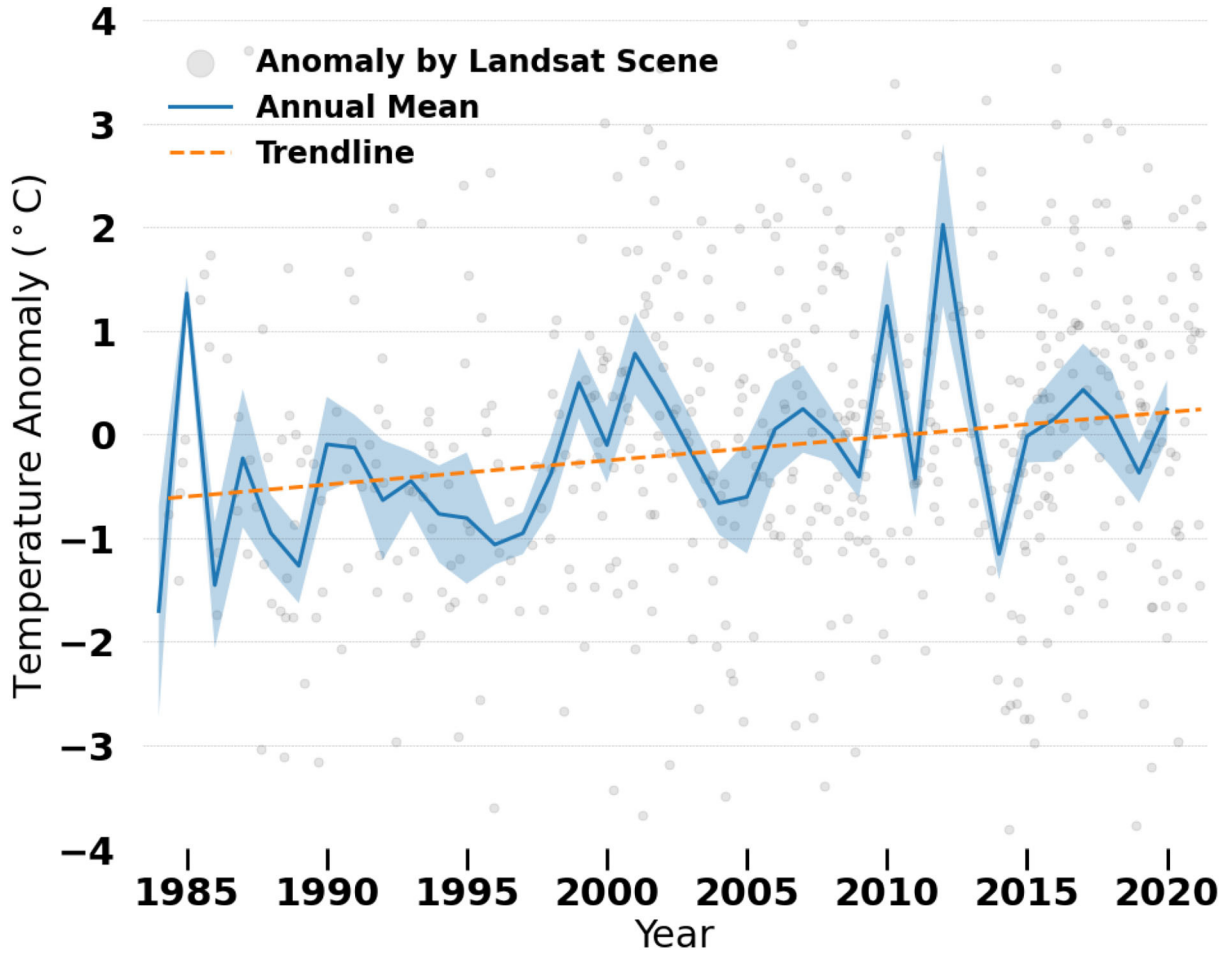

FIGURE 8 | Time series of seasonally-detrended surface temperature anomaly over Narragansett Bay with the annual mean and a linear trendline taken before averaging. The uncertainty around the annual mean represents sampling uncertainty.

are larger for all seasons with overall cooling of $-0.53 \pm 0.3°C$ in Mt. Hope Bay and $-1.04 \pm 0.2°C$ at Brayton Point. For the higher emissions period, winter cooling is the greatest in Mt. Hope Bay with spring and autumn cooling equal and summer cooling the weakest. The Brayton Point differences for the high emission period are scaled-up versions of the low emissions case for winter and autumn, but spring differences become larger than summer differences. Upper Narragansett Bay, near Warwick, serves as a control region for comparison to Mt. Hope Bay. All values in Upper Narragansett Bay have an uncertainty range that contains zero for both periods. These numeric results are tabulated in **Table 2**.

3.2. Unsupervised Clustering

K-means clustering, a form of unsupervised pattern recognition, confirms the distinct nature of the thermal effluent as shown in **Figure 7**. Clustering using eight clusters allows for a distinct grouping of the region affected by effluent in Mt. Hope Bay and a region in the upper Providence River located downstream of the Manchester St. Power Station, which releases thermal effluent to a much smaller extent than the BPPS. The upper Providence River is much shallower than Mt. Hope Bay, so it is unlikely that these two regions would naturally have similar seasonal temperature behavior. When conducting the same clustering on data without the effluent present, Mt. Hope Bay is clustered with upper Narragansett Bay regions and the Sakonnet River, regions with more comparable depths and widths for comparable exposure to winds and surface fluxes. This result confirms that the seasonal temperature behavior of Mt. Hope Bay was uniquely clustered because of the thermal effluent rather than for any unique characteristics of Mt. Hope Bay.

3.3. Climatic Warming

To investigate any long-term trends in Narragansett Bay over this period, linear regression analysis was conducted on the seasonally-adjusted anomalies described in section 2.3, depicted in **Figure 8** for the Narragansett Bay mean.

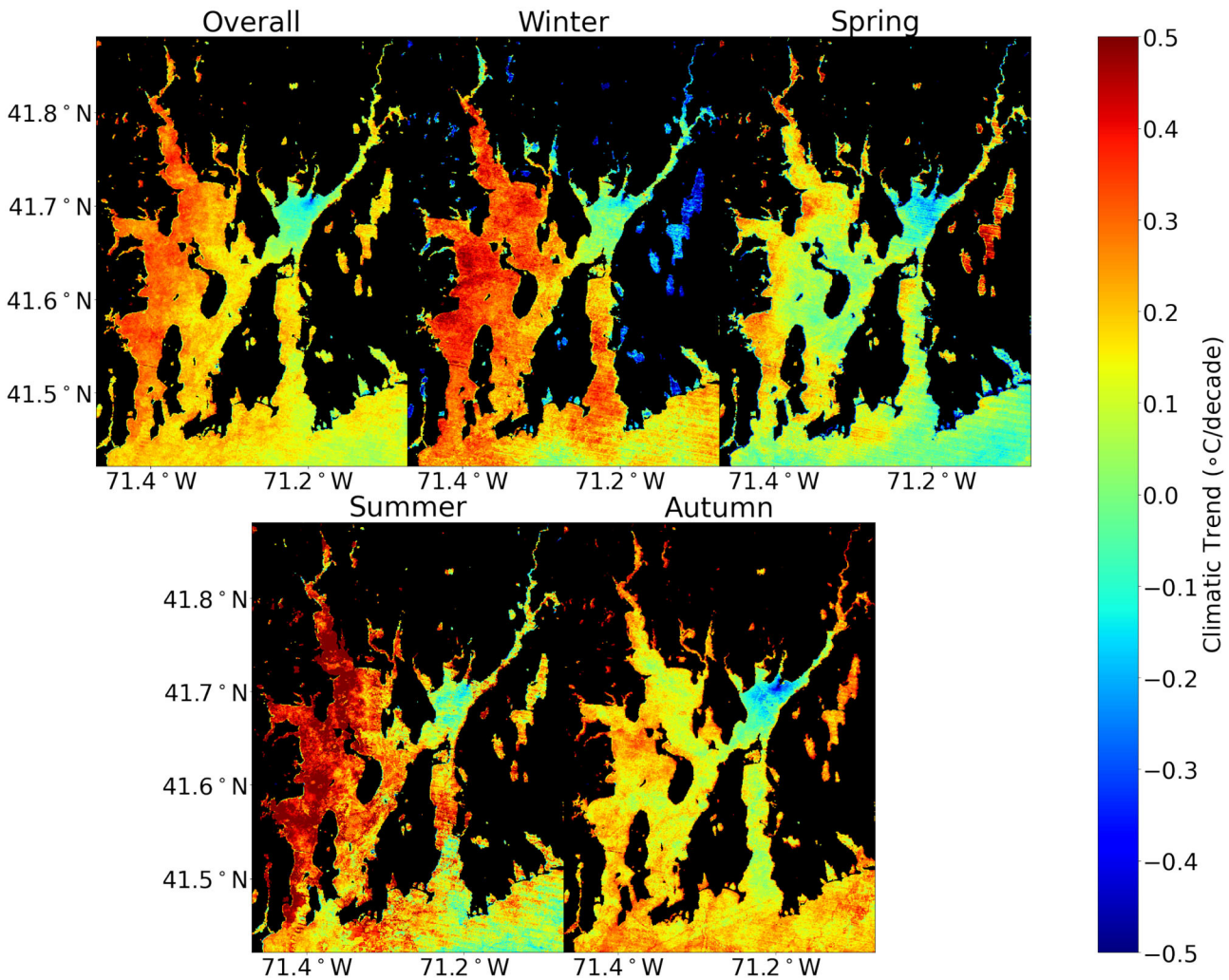

FIGURE 9 | Pixel-wise surface temperature trends for 1984–2021 using linear regression on seasonally-detrended Landsat thermal data. Data were filtered by month before interpolation to divide the trends by season.

TABLE 3 | Interannual surface temperature trends in °C/decade over the observational period for different Narragansett Bay regions over different seasons.

	Overall	Winter	Spring	Summer	Autumn
Brayton point	−0.38 ± 0.2	−0.35 ± 0.4	−0.27 ± 0.4	−0.27 ± 0.3	−0.59 ± 0.3
Mt. Hope bay	−0.02 ± 0.1	0.00 ± 0.2	−0.05 ± 0.2	0.04 ± 0.3	−0.08 ± 0.1
Narragansett bay	0.23 ± 0.1	0.30 ± 0.1	0.11 ± 0.2	0.33 ± 0.2	0.17 ± 0.1

The Narragansett Bay trends exclude Mt. Hope Bay.

Applying this linear regression method to each pixel reveals significant spatial variation in surface temperature trends, particularly between Mt. Hope Bay and the rest of Narragansett Bay (**Figure 9**). The trends are characterized by overall Narragansett Bay warming of 0.23 ± 0.1°C/decade, significant cooling of −0.38 ± 0.2°C/decade concentrated near Brayton Point, and a near-zero trend of −0.02 ± 0.1°C/decade in Mt. Hope Bay. The Narragansett Bay warming trend is statistically significant for winter, summer, and autumn but not spring. Cooling at Brayton Point is only significant when it is largest in autumn due to large uncertainties from the smaller region of interest and fewer scenes used when split up by season. The Mt. Hope Bay trends for all seasons are indistinguishable from zero when considering uncertainty. The results from this trend analysis are tabulated in **Table 3**.

To ensure interannual trends are robust against sampling uncertainty, data were resampled using bootstrapping until the mean over all resampling converged. Further, individual noise was added based on selection from a Gaussian distribution, mimicking the measurement uncertainty as determined in section 2.2. Thus, the uncertainty measurement on the reported trend represents the standard deviation of the bootstrapped means after accounting for both sampling and measurement uncertainties.

4. DISCUSSION

4.1. Post-Effluent Cooling

Recent cooling in Mt. Hope Bay with respect to the rest of Narragansett Bay corresponds to the stopping and reduction of thermal effluent release, indicating that Mt. Hope Bay had an anomalously warm temperature while effluent was being released that has since been resolved. Maximum cooling at Brayton Point reveals that the greatest heat anomaly was at the location of the BPPS (**Figure 6**), pointing to the thermal effluent as the cause of the transient heat anomaly. The greater intensity of effluent impacts during the 1993–2000 period followed by decreasing impacts until a sharp drop after 2011 indicates that effluent impacts resolved gradually at first then more rapidly at the time the cooling towers became operational and effluent stopped (2011). As a result, the immediate cooling at 2011 does not equal the full 0.8°C warm anomaly found by Mustard et al. (1999). That study was conducted when effluent impacts were greater than the 2003–2010 period (preceding tightened regulations).

Comparing the Mustard et al. (1999) estimate to the maximal impact period (1993–2000), the 0.8°C falls within the higher end of the uncertainty for winter cooling at 0.70 ± 0.2°C and autumn cooling at 0.54 ± 0.3°C. The cooling measured in this study provides a smaller central estimate for the Mt. Hope Bay heat anomaly than estimated by Mustard et al. (1999)—although in agreement including uncertainties—likely because the impacts here are averaged over 8 years, rather than anomalies over a specific time when effluent and interannual variability might contribute (**Figure 6**, upper). Though the estimate for mean cooling over Mt. Hope Bay is smaller than previous estimates, there are regions closer to Brayton Point that experienced temperature anomalies of 1–1.5°C (see **Figure 6**).

4.2. Seasonality of Impacts

Natural cycles in surface heat input from incoming radiation and in the volume of river transport are key to explaining why thermal effluent impacts are seasonally variable. Incoming radiation—including both shortwave radiation from the sun and longwave radiation from the atmosphere—is greatest during the summer and weakest during the winter, with spring and autumn having intermediate amounts. River transport also varies seasonally and is consistently greatest in the spring and winter. The ability of thermal effluent to significantly alter the temperature of Mt. Hope Bay depends on the scale of this impact with respect to these two natural heat and freshwater inputs.

Figure 10 represents the BPPS effluent impact as percent of total radiation on Mt. Hope Bay's surface and percent of upper Taunton river volume over an average seasonal cycle for a constant effluent heat and volume flux. BPPS effluent makes up a larger portion of the Mt. Hope Bay heat budget when compared to natural radiation fluxes in winter than in summer, explaining why the immediate cooling found in winter is large. Additionally, significant reductions in river fluxes in late summer and autumn explain why the low emissions BPPS impact is large (as indicated by post-effluent cooling since this period) in autumn but not spring, two seasons with similar radiation variability. Summer impacts are also regionally significant despite large total radiation because of this decreased river input and thus decreased flushing and dilution. Seasons with lower river input are able to maintain a greater heat anomaly from the effluent because a greater percentage of the river input is heated by the power station and longer flushing times mean less replacement by unheated waters.

While the above explanation is consistent with the low emission case as the BPPS impact correlates with river and solar variability, the BPPS impact tracks radiation input more strictly for the high emissions case as shown in **Figure 10**, meaning that the winter impact is strongest, the summer impact is weakest, and the spring and autumn impacts are intermediate and similar. Here, the effluent heat input has grown to a point where cooling from river flushing is too slow to reduce the heat anomaly during seasons with even the highest rates of river input. As a result, effluent impacts follow the scale of the radiation budget as the dominant cooling mechanism independent of river input.

Near Brayton Point, the seasonal impacts follow the same pattern as Mt. Hope Bay for low emissions, with autumn having the greatest impact followed by winter, summer, then spring. For high emissions, the winter and autumn impacts both scale up, the summer impact grows only slightly, and the spring impact increases to between summer and winter. In this case, the weakened effect of river flushing and dilution during high emissions is also observed as the imbalance between spring and autumn becomes smaller. The impacts at Brayton Point remain more influenced by river input than in Mt. Hope Bay for high emissions, indicating that river input played a role in distributing effluent heat from its source to the rest of Mt. Hope Bay.

4.3. A Warming Climate

While the anomalous temperature of Mt. Hope Bay from BPPS thermal effluent was significant and has resolved, Narragansett Bay warming has been large enough over the period of observation to cause a similar amount of warming due to climate change as was of concern in Mt. Hope Bay due to effluent. The 0.9 ± 0.4°C of warming from 1984 to 2021 parallels the 0.53 ± 0.2°C of cooling observed in Mt. Hope Bay such that long-term trends in Mt. Hope Bay over this period are near zero, rather than cooling. This result does not discredit the large impact of the BPPS effluent; rather, it shows that the scale of climate warming has been great enough to impact a similarly large scale of warming in Narragansett Bay as a whole

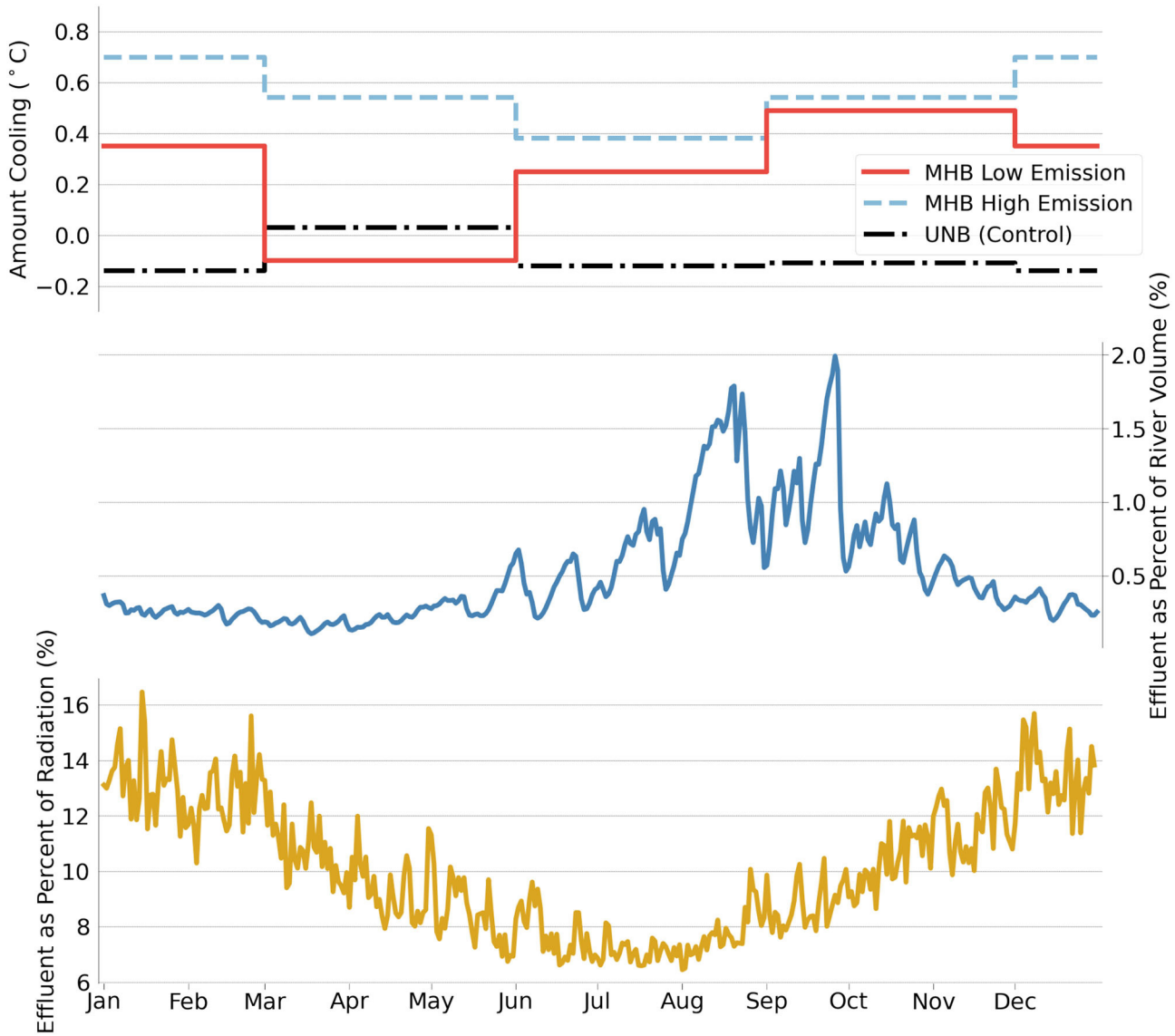

FIGURE 10 | BPPS effluent volume and heat as a percent of river volume and total longwave plus shortwave radiation, respectively, plotted below the seasonal differences in the amount of cooling observed in Mt. Hope Bay (MHB) and Upper Narragansett Bay (UNB) as recorded in **Table 2**.

to what was previously only seen in Mt. Hope Bay. Stopping thermal effluent still prevented even warmer temperatures in Mt. Hope Bay on top of climatic change. Climatic warming has not yet surpassed the effluent's effect in the most impacted region near Brayton Point as the cooling trend there remains significantly negative.

The warming trend of 0.23 ± 0.1°C/decade for the Narragansett Bay mean is on the warmer side of the long-term *in situ* and paleoceanographic estimates taken over the past century, which indicate a warming of 0.06–0.26°C/decade (Shearman and Lentz, 2010; Smith et al., 2010; Salacup et al., 2019). This difference may indicate that temperature warming is accelerating in Narragansett Bay; however, a longer-term analysis is needed to confirm this result.

Though many of the threats from climatic warming to organismal behavior and biogeochemical cycling remain the same as threats from thermal effluent, the harms from the high local intensity of thermal effluent and the entrainment of organisms during effluent processing are no longer of concern. However, climatic warming presents its own issues as there are fewer cool refugia to which aquatic organisms can migrate, and large warming offshore comes with rises in sea level (Sweet et al., 2017; Oppenheimer et al., 2019).

This paper provides an explanation of seasonal variability in thermal effluent impacts on temperate estuaries from an observational perspective as well as contextualizes Narragansett Bay's climatic warming in the context of a particularly large thermal effluent. The persistence of temperature anomalies during all seasons and explanation for their variability only

became clear in the context of this long-term, post-impact analysis. The results from this work serve as an indicator of how thermal effluent from operational power stations may impact temperate estuaries elsewhere.

DATA AVAILABILITY STATEMENT

Publicly available datasets were analyzed in this study. This data can be found here: Rhode Island Data Discovery Center (https://ridatadiscovery.org/#/) and the United States Geological Survey's Earth Explorer (https://earthexplorer.usgs.gov).

AUTHOR CONTRIBUTIONS

JB and BF-K contributed to the project design and conception, subsequent revisions of the manuscript, and approved the submitted version. JB conducted the primary data analysis as well as wrote the first draft of the manuscript. All authors contributed to the article and approved the submitted version.

FUNDING

This work was partially supported by the National Science Foundation and Brown University through the RI C-AIM program (National Science Foundation EPSCoR Award OIA-1655221) and partially by the Office of Naval Research ONR N00014-17-1-2963.

ACKNOWLEDGMENTS

Conversations with Jack Mustard and Karianne Bergen are gratefully acknowledged as having aided in selecting the scope and tools used in this project.

REFERENCES

Abdelrhman, M. (2005). Simplified modeling of flushing and residence times in 42 embayments in New England, USA, with special attention to Greenwich Bay, Rhode Island. *Estuar. Coast. Shelf Sci*. 62, 339–351. doi: 10.1016/j.ecss.2004.09.021

Conley, D., Carstensen, J., Vaquer-SunyerCarlos, R., and Duarte, C. (2009). Ecosystem thresholds with hypoxia. *Eutroph. Coast. Ecosyst*. 207, 21–29. doi: 10.1007/s10750-009-9764-2

Dayan, D., Du, X., Baris, T., Wagner, D., Crawford, D., and Oleksaik, M. (2019). Population genomics of rapid evolution in natural populations: polygenic selection in response to power station thermal effluents. *BMC Evol. Biol*. 19:61. doi: 10.1186/s12862-019-1392-5

Deacutis, C., Murray, D., Prell, W., Saarman, E., and Korhun, L. (2006). Hypoxia in the upper half of Narragansett Bay, RI, during August 2001 and 2002. *Northeastern Nat*. 13, 173–198. doi: 10.1656/1092-6194(2006)13[173:HITUHO]2.0.CO;2

DeAlteris, J., Englert, T., and Burnett, J. (2006). Trends in fish abundance in Mount Hope Bay: is the Brayton Point Power Station affecting fish stocks? *Northeastern Nat*. 13, 95–116.

Ding, H., and Elmore, A. (2015). Spatio-temporal patterns in water surface temperature from Landsat time series data in the Chesapeake Bay, U.S.A. *Remote Sens. Environ*. 168, 335–348. doi: 10.1016/j.rse.2015.07.009

Dupigny-Giroux, L., Mecray, E., Lemcke-Stampone, M., Hodgkins, G., Lentz, E., Mills, K., et al. (2018). "Northeast," in *Impacts, Risks, and Adaptation in the United States, Vol. II*, eds J. F. Knott (Washington, DC: Fourth National Climate Assessment), 669–742.

Emery, W., Baldwin, D., Schlussel, P., and Reynolds, R. (2001). Accuracy of *in situ* sea surface temperatures used to calibrate infrared satellite measurements. *J. Geophys. Res*. 106, 2387–2405. doi: 10.1029/2000JC000246

Fan, Y., and Brown, W. (2006). On the heat budget for Mount Hope Bay. *Northeastern Nat*. 13, 47–70. doi: 10.1656/1092-6194(2006)13[47:OTHBFM]2.0.CO;2

Fisher, J., and Mustard, J. (2004). High spatial resolution sea surface climatology from Landsat thermal infrared data. *Remote Sens. Environ*. 90, 293–307. doi: 10.1016/j.rse.2004.01.008

Geyer, W., and MacCready, P. (2014). The estuarine circulation. *Annu. Rev. Fluid Mech*. 46, 175–197. doi: 10.1146/annurev-fluid-010313-141302

Gibson, M. (2002). *Winter Flounder Abundance Near Brayton Point Station, Mt. Hope Bay Revisited: Separating Local From Regional Impacts Using Long Term Abundance Data*. RI Division of Fish and Wildlife Research Reference Document.

Hansen, M., Potapov, P., Moore, R., Hancher, M., Turubanova, S., Tyukavina, A., et al. (2013). High-resolution global maps of 21st-Century forest cover change. *Science* 342, 850–853. doi: 10.1126/science.1244693

Harley, C., Hughes, A., Hultgren, K., Miner, B., Sorte, C., Thornber, C., et al. (2006). The impacts of climate change in coastal marine systems. *Ecol. Lett*. 9, 228–241. doi: 10.1111/j.1461-0248.2005.00871.x

Lewis, J., Hull, P., Weinberger, K., and Saul, L. (2008). "Mapping uncharted waters: exploratory analysis, visualization, and clustering of oceanographic data," in *Seventh International Conference on Machine Learning and Applications* (San Diego, CA), 388–395. doi: 10.1109/ICMLA.2008.125

McBryan, T., Anttila, K., Healy, T., and Schulte, P. (2013). Responses to temperature and hypoxia as interacting stressors in fish: implications for adaptation to environmental change. *Integr. Compar. Biol*. 53, 648–659. doi: 10.1093/icb/ict066

Melrose, D., Oviatt, C., and Berman, M. (2007). Hypoxic events in Narragansett Bay, Rhode Island, during the summer of 2001. *Estuar. Coasts* 30, 47–53. doi: 10.1007/BF02782966

MERCINA Working Group, Pershing, A., Greene, C., Hannah, C., Sameoto, D., Head, E., et al. (2015). Oceanic response to climate in the Northwest Atlantic. *Oceanography* 14, 76–82. doi: 10.5670/oceanog.2001.25

Miller, W., and Harding, L. Jr. (2007). Climate forcing of the spring bloom in Chesapeake Bay. *Mar. Ecol. Prog. Ser*. 331, 11–22. doi: 10.3354/meps331011

Monsen, N., Cloern, J., Lucas, L., and Monismith, S. (2002). A comment on the use of flushing time, residence time, and age as transport time scales. *Limnol. Oceanogr*. 47, 1545–1553. doi: 10.4319/lo.2002.47.5.1545

Mustard, J., Carney, M., and Sen, A. (1999). The use of satellite data to quantify thermal effluent impacts. *Estuar. Coast. Shelf Sci*. 49, 509–524. doi: 10.1006/ecss.1999.0517

Mustard, J., Swanson, C., and Deacutis, C. (2001). *Narragansett Bay From Space: A Perspective for the 21st Century*. National Aeronautics and Space Administration.

Neto, A. G., Langan, J. A., and Palter, J. B. (2021). Changes in the Gulf Stream preceded rapid warming of the Northwest Atlantic Shelf. *Nat. Commun. Earth Environ*. 2:74. doi: 10.1038/s43247-021-00143-5

Oppenheimer, M., Glavovic, B. C., Hinkel, J., van de Wal, R., Magnan, A. K., Abd-Elgawad, A., et al. (2019). *IPCC Special Report on the Ocean and Cryosphere in a Changing Climate*. Intergovernmental Panel on Climate Change.

Oviatt, C., Smith, L., Krumholz, J., Coupland, C., Stoffel, H., Keller, A., et al. (2017). Managed nutrient reduction impacts on nutrient concentrations, water clarity, primary production, and hypoxia in a north temperate estuary. *Estuar. Coast. Shelf Sci*. 199, 25–34. doi: 10.1016/j.ecss.2017.09.026

Pörtner, H., Langenbuch, M., and Michaelidis, B. (2005). Synergistic effects of temperature extremes, hypoxia, and increases in co2 on marine animals: from

earth history to global change. *J. Geophys. Res*. 110. doi: 10.1029/2004JC002561

Rhode Island Department of Environmental Management (2015). *Historical Buoy Data*. Rhode Island Department of Environmental Management.

Rogers, J. (2008). *Circulation and transport in upper Narragansett Bay* (MS thesis). Graduate School of Oceanography, University of Rhode Island, Kingston, RI, United States.

Saba, V., Griffies, S., Anderson, W., Winton, M., Alexander, M., Delworth, T., et al. (2016). Enhanced warming of the Northwest Atlantic Ocean under climate change. *J. Geophys. Res*. 121, 118–132. doi: 10.1002/2015JC011346

Salacup, J., Farmer, J., Herbert, T., and Prell, W. (2019). Alkenone paleothermometry in coastal settings: evaluating the potential for highly resolved time series of sea surface temperature. *Paleoceanogr. Paleoclimatol*. 34, 164–181. doi: 10.1029/2018PA003416

Sane, A., Fox-Kemper, B., Ullman, D., Kincaid, C., and Rothstein, L. (2020). Consistent predictability of the Ocean State Ocean Model (OSOM) using information theory and flushing timescales. JGR: Oceans.

Schneider, K., and Mauser, W. (1996). Processing and accuracy of Landsat Thematic Mapper data for lake surface temperature measurement. *Int. J. Remote Sens*. 17, 2027–2041. doi: 10.1080/01431169608948757

Shearman, R., and Lentz, S. (2010). Long-term sea surface temperature variability along the U.S. east coast. *J. Phys. Oceanogr*. 40, 1004–1017. doi: 10.1175/2009JPO4300.1

Smith, L., Whitehouse, S., and Oviatt, C. (2010). Impacts of climate change on Narragansett Bay. *Northeastern Nat*. 17, 77–90. doi: 10.1656/045.017.0106

Sweet, W. V., Horton, R., Kopp, R. E., LeGrande, A. N., and Romanou, A. (2017). "Sea level rise," in *Climate Science Special Report: Fourth National Climate Assessment, Vol. I*, eds D. J. Wuebbles, D. W. Fahey, K. A. Hibbard, and T. K. Maycock (Washington, DC: U.S. Global Change Research Program), 333–363.

Torgersen, T., DeAngelo, E., and O'Donnell, J. (1997). Calculations of horizontal mixing rates using 222rn and the controls on hypoxia in western Long Island Sound, 1991. *Estuaries* 20, 328–345. doi: 10.2307/1352348

United States Environmental Protection Agency (2003). *Clean Water Act NPDES Permitting Determinations for Brayton Point Station's Thermal Discharge and Cooling Water Intake*. Somerset, MA: United States Environmental Protection Agency.

United States Geological Survey (2021). *Landsat 5, Landsat 7 and Landsat 8 Surface Reflectance Tier 1*. United States Geological Survey.

Valiela, I., McClelland, J., Hauxwell, J., Behr, P., and Foreman, K. (1997). Macroalgal blooms in shallow estuaries: controls and ecophysiological and ecosystem consequences. *Limnol. Oceanogr*. 42, 1105–1118. doi: 10.4319/lo.1997.42.5_part_2.1105

Conflict of Interest: The authors declare that the research was conducted in the absence of any commercial or financial relationships that could be construed as a potential conflict of interest.

Publisher's Note: All claims expressed in this article are solely those of the authors and do not necessarily represent those of their affiliated organizations, or those of the publisher, the editors and the reviewers. Any product that may be evaluated in this article, or claim that may be made by its manufacturer, is not guaranteed or endorsed by the publisher.

Copyright © 2021 Benoit and Fox-Kemper. This is an open-access article distributed under the terms of the Creative Commons Attribution License (CC BY). The use, distribution or reproduction in other forums is permitted, provided the original author(s) and the copyright owner(s) are credited and that the original publication in this journal is cited, in accordance with accepted academic practice. No use, distribution or reproduction is permitted which does not comply with these terms.

frontiers in Marine Science

ORIGINAL RESEARCH
published: 04 October 2021
doi: 10.3389/fmars.2021.674554

Assessing the Role of Sampling Uncertainty When Predicting Behavioral Responses of Tagged Cetaceans Exposed to Naval Sonar

Phil J. Bouchet[1,2], Catriona M. Harris[1] and Len Thomas[1,2]*

[1] Centre for Research into Ecological and Environmental Modelling, University of St Andrews, St Andrews, United Kingdom,
[2] School of Mathematics and Statistics, University of St Andrews, St Andrews, United Kingdom

OPEN ACCESS

Edited by:
Edward Urban,
Scientific Committee on Oceanic Research, United States

Reviewed by:
Stacy DeRuiter,
Calvin University, United States
J. Lawson,
Department of Fisheries and Oceans, Canada

***Correspondence:**
Phil J. Bouchet
pb282@st-andrews.ac.uk

Specialty section:
This article was submitted to Marine Ecosystem Ecology, a section of the journal Frontiers in Marine Science

Received: 01 March 2021
Accepted: 09 September 2021
Published: 04 October 2021

Citation:
Bouchet PJ, Harris CM and Thomas L (2021) Assessing the Role of Sampling Uncertainty When Predicting Behavioral Responses of Tagged Cetaceans Exposed to Naval Sonar. Front. Mar. Sci. 8:674554. doi: 10.3389/fmars.2021.674554

Concerns over cetacean mortality events coincident with maritime warfare exercises have motivated efforts to characterize the effects of anthropogenic noise on free-ranging whales and dolphins. By monitoring the movement, diving, and acoustic behaviors of individual whales before, during, and after sound exposure, behavioral response studies (BRSs) have supported significant progress in our understanding of the sensitivity of various cetacean species to high-powered naval sonar signals. However, differences in the designs and sampling capabilities of animal-borne tags typically used in BRS experiments prompt questions about the influence of data resolution in quantitative assessments of noise impacts. We conducted simulations to examine how uncertainty in the acoustic dose either measured on high-resolution multi-sensor biologging tags or modeled from position-transmitting satellite telemetry tags may affect predictions of behavioral responses in Cuvier's beaked whales (*Ziphius cavirostris*) exposed to low- and mid-frequency active sonar. We considered an array of scenarios representative of real-world BRSs and used posterior estimates of dose-response functions obtained under an established Bayesian hierarchical modeling framework to explore the consequences of different tag choices for management decision-making. Our results indicate that (1) the zone of impact from a sonar source is under-estimated in most test conditions, (2) substantial reductions in the uncertainty surrounding dose-response relationships are possible at higher sample sizes, and (3) this largely holds true irrespective of tag choice under the scenarios considered, unless positional fixes from satellite tags are consistently poor. Strategic monitoring approaches that combine both archival biologging and satellite biotelemetry are essential for characterizing complex patterns of behavioral change in cetaceans exposed to increasing levels of acoustic disturbance. We suggest ways in which BRS protocols can be optimized to curtail the effects of uncertainty.

Keywords: acoustics, dose-response, underwater noise, military sonar, beaked whales, Bayesian modelling and inference, sampling uncertainty

INTRODUCTION

Sound plays a critical role in the lives of cetaceans, with many species of whales, dolphins, and porpoises shown to be sensitive to the adverse effects of both chronic and acute exposure to anthropogenic underwater noise (Duarte et al., 2021). For instance, elevated noise levels (e.g., in areas of dense vessel traffic) can mask animal communication signals, elicit physiological stress, and/or cause displacements from preferred habitats, ultimately interfering with key life functions such as foraging, mating, nursing, or resting, with knock-on repercussions on individual fitness, energy expenditure, and survival (Erbe et al., 2018). In recognition of acoustic pollution as an emerging threat to wildlife globally, calls have been made to strengthen management and mitigation frameworks for sound-producing activities in the ocean (Chou et al., 2021). In the United States, the Marine Mammal Protection Act of 1972 (MMPA, 16 U.S.C. 1361 et seq.) regulates the take (defined as the "harassment, hunting, capture, or killing") of marine mammals by U.S.-based organizations worldwide, including areas beyond national jurisdiction (i.e., on the high seas). The U.S. Navy is legally bound to assess the potential impacts of military readiness training activities on cetaceans to meet compliance requirements under the MMPA as well as other U.S. Federal laws pertaining to protected marine taxa (e.g., the Endangered Species Act ESA 16 U.S.C.1531 et seq.) (Zirbel et al., 2011). Of particular concern are activities involving the deployment of explosives and munitions, and the use of tactical, high-powered sonar technology operating in the lower (LFAS, ∼0.1–2 kHz) and mid-frequency bands (MFAS, 3–8 kHz) (Sivle et al., 2012; Goldbogen et al., 2013; Falcone et al., 2017). LFAS and MFAS systems were developed in the 1950s for anti-submarine warfare (D'Amico and Pittenger, 2009; Bernaldo de Quirós et al., 2019), and have been implicated in a number of atypical lethal mass strandings largely involving deep-diving toothed whales from the *Ziphiidae* family (D'Amico et al., 2009; Filadelfo et al., 2009; Fernández et al., 2012; Parsons, 2017).

These events prompted a series of coordinated, collaborative, behavioral response studies (BRSs) aimed at better understanding the short-term responses of cetaceans to both simulated and real sonar sources (Southall et al., 2012, 2016; Harris et al., 2016). In many cases, BRSs entail rigorously designed Before-After Control-Impact (BACI) experimental field protocols (referred to as controlled exposure experiments, or CEEs), which allow focal animals to be monitored before, during, and after sonar transmissions using animal-mounted tags, visual follows, passive acoustics, or any combinations thereof (Southall et al., 2016; Harris et al., 2018). In some cases, silent controls (i.e., vessel approaches with sonar deployed but turned off) can provide a benchmark of baseline behavioral patterns and a test of responses to ship presence alone, in the absence of sonar activity. Additional exposure treatments are sometimes also used to contextualize the nature and magnitude of detected responses relative to other acoustic stimuli, including conspecific vocalizations, playback recordings of potential predators such as mammal-eating killer whales, or artificial tones (e.g., pseudo-random noise in the same frequency bands) (Tyack et al., 2011; Dunlop et al., 2012). The data from CEEs are complemented by other sources of information from captive settings (e.g., Houser et al., 2013) or observational studies (Falcone et al., 2017; Harris et al., 2019b; Durbach et al., 2021).

The first U.S. Navy-funded CEE was undertaken in 2007–2008 in the vicinity of the Atlantic Undersea Testing and Evaluation Center (AUTEC)'s Bahamas testing and training range (Tyack et al., 2011). Since then, numerous other studies have taken place in the Atlantic, Arctic, and Pacific oceans, as well as in the Mediterranean Sea, with a focus on a range of odontocetes and mysticetes (**Supplementary Table 1**; Southall et al., 2016). CEEs have allowed a wide spectrum of behavioral metrics to be captured under a variety of protocols and configurations (e.g., dose escalations or "ramp-ups," single vs. repeated exposures of one or multiple signal types, silent vs. full-power vessel approaches, etc.) (Southall et al., 2016; Wensveen et al., 2017), including data on animal position, body orientation, social dynamics, diving patterns, vocal activity, and swimming speeds (Harris et al., 2016). An important focus of efforts to date has been to translate these metrics into estimates of probabilities of sublethal behavioral responses, which may lead to biologically significant changes in survival or fecundity rates if elicited repeatedly (Harris et al., 2018). Detecting and characterizing such responses is difficult, however, not least because: (i) many reactions are idiosyncratic and context-dependent (DeRuiter et al., 2013; Goldbogen et al., 2013; Friedlaender et al., 2016; Gomez et al., 2016; Southall et al., 2016, 2019), making it challenging to extrapolate patterns of responsiveness across individuals, populations, and/or species (Harris et al., 2019a); (ii) success in identifying response events is a function of the amount and quality of available tag data, the duration and characteristics of the baseline period with which exposures are being compared, as well as the response detection method used; and (iii) the logistical complexities of monitoring cryptic animals that can only be approached within brief surfacing intervals limit the number of replicates available, particularly for elusive species like beaked whales (Harris et al., 2016; Hooker et al., 2019; Curtis et al., 2020).

Success in overcoming these obstacles requires the strategic integration of remote tracking technologies to maximize data collection opportunities over a range of complementary spatio-temporal scales (Tyack et al., 2011). As such, a rising number of CEEs now integrate near real-time telemetry and archival biologging (Tyack et al., 2011) by simultaneously deploying multiple types of tags on different individuals in the vicinity of planned sonar activity (e.g., Wensveen et al., 2019). Most commonly, these include multi-sensor, high-resolution, acoustic and movement tags such as Acousondes, CATS tags, or DTAGs (Johnson and Tyack, 2003) and coarser-resolution, position-transmitting satellite tags (hereafter "S-TAGs") such as those operating over the Argos system[1] (Tyack et al., 2011; Schick et al., 2019; Wensveen et al., 2019). The former combine a microprocessor with a suite of depth, temperature, hydrostatic pressure, and triaxial acceleration sensors to record fine-scale motion in three dimensions while synchronously acquiring

[1]https://www.argos-system.org/

broadband audio data with one or more built-in hydrophones. DTAGs, in particular, have revolutionized the study of cetacean behavior by offering detailed insights into activity states that could not previously be readily observed (Johnson et al., 2009). However, DTAGs were originally designed for playback experiments of short duration (<24 h), and most models are attached using non-invasive suction cups with a maximum longevity spanning a few hours to at best a couple of days (Andrews et al., 2019). Additional limitations imposed by memory capacity, battery life, and the high sampling rates required to capture sound further constrain deployment times, precluding the use of DTAGs (or other acoustic tags) for assessments of long-term baselines prior to and following noise disturbance (Schick et al., 2019). By contrast, implantable S-TAGs allow animals to be tracked over far wider spatial domains (several hundreds of km; e.g., Schorr et al., 2009) and much longer timeframes (several months; e.g., Falcone et al., 2017), though this often comes at the cost of lower resolution with respect to surface locations and individual behaviors (Nowacek et al., 2016). Importantly, most S-TAGs lack on-board acoustic recorders and sacrifice the ability to take *in situ* measurements of received sound levels, which must then be inferred indirectly from knowledge of both the acoustic transmission properties of the area of interest and the animals' position relative to the noise source at the time of exposure (von Benda-Beckmann et al., 2019). Tags transmitting via Service Argos can also suffer from substantial geo-localisation errors, which may range anywhere between 150 m and > 10 km (Nicholls et al., 2007; Irvine et al., 2020) and are likely to compromise estimates of the sound dose experienced by exposed individuals (Schick et al., 2019; von Benda-Beckmann et al., 2019). Such differences in data quality and resolution between monitoring technologies raise important questions regarding the optimisation of their use in BRSs (Harris et al., 2018). Another key challenge lies in reconciling the onerous costs and logistical demands of BRSs with the need to ensure that sonar impacts can be detected reliably (Dunlop et al., 2012), particularly as not all responses are equally identifiable on all tags. For instance, DTAGs are often used to identify cessation of foraging, interrupted dive cycles, and variations in swim kinematics, whereas S-TAGs offer better insights into patterns of horizontal avoidance, or changes in relative source-whale positions and low-resolution travel speeds. Furthermore, the number of tags available tends to be limited, as DTAGs are usually rented (ca. US $3,500 per month per device) (S. Isojunno, personal communication) and can be repeatedly used but necessitate significant labor input for deployment and recovery, whereas S-TAG prices can exceed US$ 5,000 per unit, with extra operational costs for data processing and satellite time (Thomas et al., 2012). Ethical concerns related to tag attachment may also dictate the tagging methodology used, and the ability to re-tag the same individuals or monitor different ones in the future (Hazen et al., 2012). Despite the above caveats, power analyses are seldom considered to determine the minimum sample size needed to yield conclusive results in BRSs (but see Dunlop et al., 2012; Wensveen et al., 2017).

To address this, we explored the effects of sample size and tag choice on our ability to quantify dose-response ("risk") functions from multi-tag BRS data. In the past, managers have relied on "all-or-none" step functions to estimate the proportion of a population impacted by a sound source, but this approach can grossly underestimate risk, and reduces management criteria to a single threshold that is unlikely to be adequate for meeting different regulatory needs (Tyack and Thomas, 2019). Instead, novel statistical methods have recently emerged to quantify dose-response relationships in the form of flexible probabilistic curves (Miller et al., 2014; Moretti et al., 2014). These allow (i) predictions of responses to be made for an array of doses, including at low levels of exposure, (ii) responsiveness to be contextualized, by testing hypotheses about the factors driving the type and severity of responses (e.g., auditory sensitivity, prey density, behavioral mode), and (iii) resulting insights to be translated into mitigation guidelines for specific policy scenarios, on a case-by-case basis (Moretti et al., 2014). Here, we relied on a previously published Bayesian hierarchical dose-response model (Miller et al., 2014) to simulate cetacean responses to low- and mid-frequency active sonar, and we investigated how uncertainty in our knowledge of the dose experienced by a group of animals (each carrying a DTAG or a S-TAG in different combinations) affected metrics of sonar impact, as used in management decision-making. Simulation exercises are useful tools for guiding effort allocation in tagging studies, particularly when they are designed based on real-world datasets (Sequeira et al., 2019; New et al., 2020). We drew upon existing data from the Atlantic BRS project[2] (see Schick et al., 2019) to tailor simulation inputs for scenarios involving Cuvier's beaked whales (*Ziphius cavirostris*), a species notoriously vulnerable to sonar (D'Amico et al., 2009; Filadelfo et al., 2009; Bernaldo de Quirós et al., 2019) and reported to be site-faithful, even to sonar-rich areas such as Navy training ranges (Curtis et al., 2020). Our model is not spatially explicit and does not simulate individuals traversing a landscape of disturbance. Rather, it provides a conceptual structure for linking measurements of behavioral change made at the individual level to intrinsic response thresholds for each species (**Figure 1**). We place no restrictions on the nature or magnitude of responses *per se*, as the focus of dose-response modeling will vary with research objectives and data availability. The small sample sizes typical of BRSs mean that data are often pooled before analysis (Harris et al., 2015), and numerous BRSs also rely on expert scoring to quantify the severity of behavioral responses. This is usually done based on the severity scale described in Southall et al. (2007) and modified by Miller et al. (2012), which ranges from no effect (0) to effects not likely to influence vital rates (severity of 1–3), effects that could affect vital rates (severity of 4–6), and effects that are thought likely to influence vital rates (severity of 7–9) (Curé et al., 2021). Our only assumption, therefore, is that responses are strong enough to be detected on both tags and broadly comparable, for example by being of the same type (e.g., all avoidance responses) or of similar intensity (e.g., all with a severity score > 4). Importantly, Bayesian analysis offers a natural framework for parameter estimation in complex hierarchical models that is robust to the limitations of small datasets and can provide assessments of uncertainty that are fully

[2]https://sea-inc.net/science/atlantic-brs/

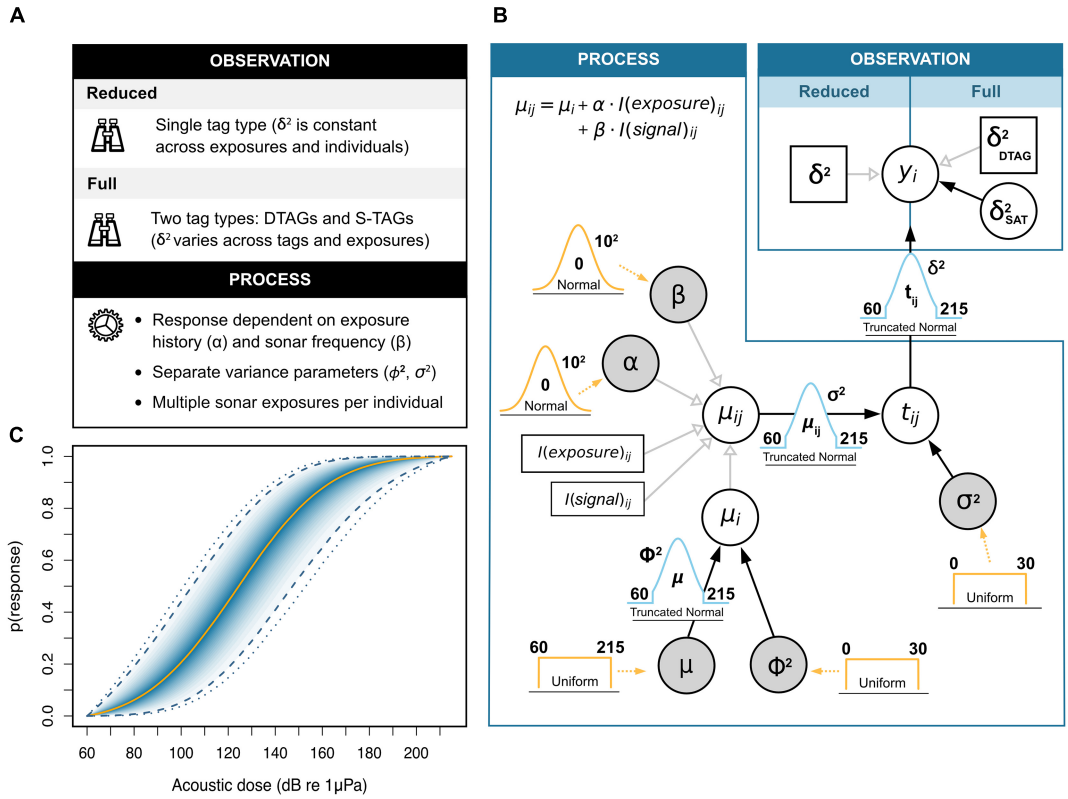

FIGURE 1 | Bayesian hierarchical dose-response model used for simulating Cuvier's beaked whale (*Ziphius cavirostris*) responses to naval sonar. **(A)** Summary of features for the observation and process model components. The treatment of sampling uncertainty (δ^2) defines variants of the original framework proposed by Miller et al. (2014). In the *reduced* model, all animals carry the same type of tag and uncertainty is treated as a constant. In the *full* model, different tags are fitted on different individuals, and the uncertainty associated with S-TAGs varies stochastically (see main text for details). **(B)** Directed acyclic graph of the model structure. The expected response threshold μ_{ij} for the *i*th whale in the *j*th exposure session is conditional on the additive effects of two contextual covariates: the animals' previous history of exposure ("exposure" with coefficient α), and the frequency band of the sonar signal (i.e., low- or mid-frequency; "signal" with coefficient β). Random variables are denoted by circles, and those monitored for posterior inference are additionally shaded in gray. Constants are represented by square boxes. Filled (black) and open (light gray) arrows indicate stochastic and deterministic relationships, respectively. Prior distributions are shown in orange, with their relevant parameters (i.e., bounds and/or mean and standard deviation) appearing in bold font. Dotted arrows indicate the parameters to which priors relate. **(C)** Example dose-response curve obtained from posterior estimates of model parameters. The curve maps the probability of behavioral response (y-axis) to the received sound level (i.e., acoustic dose, x-axis). The solid orange line denotes the posterior median, followed by the 5, 10, 15 . . . and 95% credible intervals in darker to lighter shades of blue. Dashed and dotted lines mark the 95 and 99% credible intervals, respectively.

interpretable in probabilistic terms (Antunes et al., 2014). In BRSs, this is advantageous for making appropriate predictions of responsiveness that can inform mitigation measures for naval training activities (Parsons, 2017; Harris et al., 2018).

MATERIALS AND METHODS

Dose-Response Model

Our work builds on the Bayesian hierarchical dose-response model proposed by Miller et al. (2014), which assumes that each individual whale has an inherent sensitivity threshold at which it will respond to an acoustic stimulus. This threshold is a function of: (1) the typical sensitivity of the population/species, and (2) the influence of both internal and external factors (e.g., behavioral mode, sonar frequency, distance from sonar source, etc.). Random effect terms are used to accommodate individual-level differences (i.e., between-whale variance) as well as repeated measurements of the same individuals during consecutive exposure sessions (i.e., within-whale, between-exposure variance). The full model consists of (1) a process component, which describes the underlying mechanisms conditioning the sensitivity of animals during exposure, and (2) an observation component, which links these to the observed values, measured with some degree of error (Miller et al., 2014). The former is interpreted as follows: Let t_{ij} be the true (but unknown) threshold of exposure that elicits a behavioral response (from a user-defined category, e.g., avoidance response, or response with severity score > 4) for the ith whale during the jth sonar transmission. We assume that this threshold is given by:

$$t_{ij} \sim TN\left(\mu_{ij}, \sigma^2, L, U\right) \quad (1)$$

with *TN* denoting a truncated normal distribution where μ is the location parameter (i.e., the mean of the corresponding

untruncated distribution), σ^2 the scale (i.e., the variance of the corresponding untruncated distribution), L the lower bound, and U the upper bound. Here, μ_{ij} relates to the expected response threshold of the *i*th whale during the *j*th exposure, and σ^2 relates to the within-animal, between-session variability in this threshold. Using truncation is advantageous for constraining variables within biologically sensible bounds, making sure that values align with expectations of what constitutes a plausible range of sensitivity to sound (Miller et al., 2014). We further assume that μ_{ij} hinges on the expected threshold for that individual, μ_i, and any changes arising from the animal's previous history of exposure to sonar and the frequency band of the sonar signal used, such that:

$$\mu_{ij} = \mu_i + \alpha \times I\left(\text{exposed}\right)_{ij} + \beta \times I\left(\text{MFAS}\right)_{ij} \quad (2)$$

where α is a parameter capturing the change in sensitivity from repeat exposures, and $I\left(\text{exposed}\right)_{ij}$ is an indicator to which a value of 0 is assigned during the first exposure session, and a value of 1 thereafter. Likewise, β governs the effect of MFAS relative to LFAS, with $I\left(\text{MFAS}\right)_{ij}$ taking the value 1 if MFAS is used, and 0 otherwise. Lastly, we assume that the expected threshold for each whale, μ_i, also follows a truncated normal distribution:

$$\mu_i \sim TN\left(\mu, \phi^2, L, U\right) \quad (3)$$

where μ indexes the mean threshold for all whales, ϕ^2 relates to the between-whale variability, and L and U are as above. The model also includes an observation component to capture sampling variability, which stipulates that dose measurements obtained from tags follow a truncated normal distribution centered on t_{ij}, with scale δ^2:

$$y_{ij} \sim TN\left(t_{ij}, \delta^2, L, U\right) \quad (4)$$

Dose-response curves are then computed as the cumulative distribution functions associated with the location and scale parameters of the truncated normal distribution defined in Eq. 3.

Simulation Scenarios

We adapted the above framework to formulate two complementary simulation scenarios (**Figure 1**). The first was a baseline scenario identical to Miller et al. (2014) whereby all whales carried the same type of tag and δ was treated as a constant (henceforth, "reduced model"). We tested incremental values of δ within 2.5–35 dB to emulate tag data of increasingly coarse resolution (**Table 1**). The lower bound of this range reflects the typical calibration error of DTAG hydrophones (Antunes et al., 2014), while the upper limit is consistent with maximum uncertainty estimates obtained in recent CEEs in which satellite tags were deployed (Schick et al., 2019; von Benda-Beckmann et al., 2019; Joyce et al., 2020). In a second augmented scenario, we implemented a more complex observation component that allowed for concurrent deployments of both DTAGs and S-TAGs on different individuals (henceforth, "full model"). Tags were assigned randomly to animals according to a pre-determined ratio (P_{S-TAG}), which varied from 0 to 100% (DTAG vs. S-TAG) in 20% increments. δ was kept at 2.5 dB for all DTAGs but varied for S-TAGs in order to mimic the heterogeneous quality which is characteristic of location fixes derived from conventional Argos tracking systems (Irvine et al., 2020) (see section "Accounting for Positional Uncertainty on S-TAGs" for details). We tested an array of realistic sample sizes, from a minimum of $N = 5$ to a maximum of $N = 30$ (**Supplementary Table 1**; Southall et al., 2016). Small sample sizes remain the norm in marine mammal science, as successful data collection across remote ocean habitats must comply with the many constraints imposed by logistics, safety requirements, weather conditions, and expense. Clearly, the ecological insights gleaned from single exposures on multiple tags will differ from those produced by single tags recording a sequence of multiple exposures. The latter are valuable for painting a picture of within-individual heterogeneity in behavior (e.g., Tyack et al., 2011; Sivle et al., 2015), and for learning more broadly about species' ecological requirements, patterns of habitat use, and spatial movements (Sequeira et al., 2019). However, samples of $N = 1$ do not convey information about the between-individual variance and were thus not considered here. We focused on Cuvier's beaked whales given their preponderance in sonar-associated atypical mass strandings (Bernaldo de Quirós et al., 2019), and we relied on existing datasets, published literature, and expert input to inform the selection of relevant parameter values (**Table 1**). For example, we set the location parameter indexing the mean threshold for all whales to μ = 120 dB re 1μPa, as an average of the received sound levels associated with previously reported avoidance responses for this species (136 dB re 1 μPa, Aguilar Soto et al., 2006; 98 and 127 dB re 1 μPa, DeRuiter et al., 2013). When no information was available, we turned to similar taxa such as beaked whales from the same or closely related families, or other deep-diving odontocetes. This was the case for both ϕ and σ, as we were not aware of any quantitative estimates of these parameters for *Z. cavirostris*, despite evidence of population- and individual-level differences in patterns of behavior coincident with sonar activity (e.g., Falcone et al., 2017). Here, we set ϕ = 20 dB and σ = 25 dB, respectively, based on a study of long-finned pilot whales (*Globicephala melas*) (Antunes et al., 2014). We considered that any noise stimulus below L = 60 dB re 1 μ Pa would be barely audible above ambient and therefore would not provoke a response (Schick et al., 2019), and we expected that all animals would react at or above U = 215 dB re 1 μPa. This upper bound aligns with the maximum source levels employed in BRSs to date (211–212 dB re 1 μPa, Tyack et al., 2011; 210 dB re 1μPa, DeRuiter et al., 2013; 199–214 dB re 1 μPa, Antunes et al., 2014; 210 dB re 1 μPa, Stimpert et al., 2014), though it remains markedly lower than most high-powered sonar systems in operation globally (Southall et al., 2016; Falcone et al., 2017). It also mirrors current understanding of the potential for injury at sound levels over 180 dB re 1 μPa, which underpins existing regulations surrounding sonar mitigation in areas of importance to marine mammals (U.S. Navy, 2019).

Re-sampling the same wild animals multiple times is difficult and poses numerous challenges related to interpreting order effects where sequential noise stimuli are presented over relatively short durations (Southall et al., 2016). To date, CEEs on beaked

TABLE 1 | Parameters used in simulations of Cuvier's beaked whale (*Ziphius cavirostris*) behavioral responses following exposure to mid-frequency and low-frequency active sonar.

Parameter	Definition	Values	Unit	Prior	Sources
Ns	Number of simulations	100	–	–	New et al., 2020
N	Sample size	5, 10, 20, 30	–	–	Harris et al., 2016; Southall et al., 2016; **Supplementary Table 1**
Nt	Number of consecutive exposures	2	–	–	Miller et al., 2014
δ	Sampling uncertainty (SD) in measurements or estimates of received sound levels (i.e., acoustic dose)	2.5, 5, 10, 20, 35	dB	–	Schick et al., 2019; von Benda-Beckmann et al., 2019; Joyce et al., 2020
P_{S-TAG}	Proportion of whales carrying S-TAGs	20, 40, 60, 80, 100	%	–	–
δ_{DTAG}	Sampling uncertainty (SD) in measurements of received sound levels made on DTAGs	2.5	dB	–	Antunes et al., 2014
SL	Source level of the sonar	215	dB re 1 μPa	–	Tyack et al., 2011; DeRuiter et al., 2013; Antunes et al., 2014; Stimpert et al., 2014
μ	Mean response threshold for all whales	120	dB re 1 μPa	U (60, 215)	Aguilar Soto et al., 2006; DeRuiter et al., 2013
ϕ	Between-whale variation (SD) in response threshold	20	dB	U (0, 30)	Miller et al., 2014
σ^2	Within-whale, between-exposure variation (SD) in response threshold	25	dB	U (0, 30)	Miller et al., 2014
α	Effect of exposure history on the expected response threshold for each whale	+10 (second exposure)	dB	N (0, 10)	Sivle et al., 2015
β	Effect of sonar frequency (MFAS vs. LFAS) on the expected response threshold of each whale	−10 (LFAS) and +10 (MFAS)	dB	N (0, 10)	Sivle et al., 2012, 2015, 2016; Houser et al., 2013; Miller et al., 2014
R_{ij}	Maximum realized dose for individual *i* in exposure session *j*	150–165	dB re 1μPa	–	Aguilar Soto et al., 2006; Tyack et al., 2011; Falcone et al., 2017
D	Animal density	1	Ind./km^2	–	Tyack and Thomas, 2019
Nb	Number of bins used in the calculation of the ERR	500	–	–	Tyack and Thomas, 2019

Values were chosen to reflect the range of conditions encountered in past and present BRSs and were informed by expert consultation, in keeping with the published literature (as indicated in the Sources column). Virtual animals were tagged with either digital acoustic recording tags (DTAGs) or Argos-linked satellite tags (S-TAGs), and response data were analyzed using a Bayesian hierarchical model adapted from the framework presented in Miller et al. (2014). Prior distributions are reported where relevant, including lower and upper limits for Uniform priors (U) and means and standard deviations for Normal priors (N). SD, Standard deviation.

whales have largely been limited to single exposures, and only a few BRSs overall have attempted to assess the potential for sensitisation or habituation. Despite limited statistical support for an effect of exposure history, available evidence from better-studied cetacean species points to potentially lower probabilities of response subsequent to the initial sonar transmission (Sivle et al., 2012; Houser et al., 2013; Miller et al., 2014; Sivle et al., 2015, 2016). Here, we considered two consecutive exposure sessions (the maximum reported for beaked whales, to our knowledge), and we set $\alpha = 10$ dB to simulate a higher tolerance to sound on the second exposure. In their systematic review of 370 published papers, Gomez et al. (2016) found that the type of sound source (continuous noise, pulsed sonar, seismic/explosion) was "an important variable for describing the severity of behavioral response of wild cetaceans." In addition, more recent studies indicate that some species exhibit sonar signal-specific responses (LFAS vs. MFAS) (Isojunno et al., 2018). We therefore also tested the influence of sonar signal frequency in the model. To keep the average expected threshold μ_{ij} centered with respect to this covariate, we treated it as a relative effect between individuals exposed to LFAS vs. MFAS and encoded the β parameter as an effect size, such that for $\beta = 20$ dB the corresponding coefficient values for LFAS and MFAS were set to −10 and +10 dB, respectively. LFAS has been shown to exacerbate sensitivity to sonar in a number of species (Sivle et al., 2012; Isojunno et al., 2016), yet we note that responses to low-frequency signals can be variable across taxa and strongly mediated by behavioral state (Harris et al., 2015). Lastly, BRS data often entail some degree of right-censoring, which arises when a subset of animals display no signs of behavioral disturbance across the array of doses received in any given experiment (Antunes et al., 2014). The resulting data entries are assigned missing values and must be accounted for as they hold critical information about the nature of dose-response relationships (i.e., they indicate that a response may still occur at some unknown point above the maximum realized dose, R_{ij}) (Harris et al., 2015), conditional on the definition of what constitutes a response within the context of each study. For instance, if interest lies in predicting changes in population vital rates, then responses with a severity score < 4 may be considered as "non-responses" and treated as right-censored (Southall et al., 2007; Miller et al., 2012). Similarly, models focused on avoidance responses only would include any exposures resulting in another response type (e.g., social, vocal, respiration) as right-censored data. By including right-censoring in our simulations, we can therefore accommodate for both animals that genuinely do not

respond (i.e., because their sensitivity threshold is higher than the maximum dose received), as well as animals that do not respond in a way that aligns with the focus of the dose-response modeling. To obtain right-censored observations, we generated random values of R_{ij} with equal probability within [150–165] dB re 1 μPa for each exposure. This interval is consistent with the range of minimum approach (source-whale) distances logged in previous studies (e.g., 700 m, Aguilar Soto et al., 2006; 1 km, Tyack et al., 2011; 1.9 km, Falcone et al., 2017), assuming simple spherical spreading of the acoustic signals (i.e., uniform propagation away from the source in all directions). Right-censored data points were labeled as NA and imputed using the *dinterval* distribution in software JAGS (Plummer, 2003), which ensures that the lower bound in Eq. (4) is changed to R_{ij}.

Accounting for Positional Uncertainty on Argos-Linked Satellite Tags

Most of what we know about the population ranges, diving abilities, and habitat use patterns of beaked whales comes from Argos-linked satellite tags (Schorr et al., 2009; Joyce et al., 2017; Hooker et al., 2019). The Argos system relays radio signals emitted by animal-borne transmitters to a network of remote stations on the ground for processing and distribution to users (Irvine et al., 2020). The geo-localisation of tags is achieved by determining the Doppler shift in the frequency of uplinks received by one or more polar-orbiting satellites during the course of an overhead pass, which usually lasts no more than ca. 10 min (McConnell et al., 2010). While set-up latency is negligible, the short time window available for data transfers means that Argos messages are often incomplete, corrupted, and/or subject to errors, the magnitude of which depends on latitude, animal behavior, environmental conditions, time of day, transmitter stability, and the placement of the tag on the animal's body, among other factors (Quick et al., 2019). These issues are compounded in deep-diving taxa such as *Z. cavirostris*, which engage in exceptionally long foraging dives and stay at the surface for periods of variable duration (i.e., from 2 min to over 1 h, Shearer et al., 2019; Quick et al., 2020). In practice, Argos data are therefore recorded with varying quality, even when uplinks are successful (Schick et al., 2019). Accounting for this uncertainty is critical to making fair assessments of variance in received sound levels, and thus to quantifying dose-response relationships (Schick et al., 2019). Prior to 2008, Argos position estimates were assigned one of seven location classes (LC: 3, 2, 1, 0, A, B, and Z in descending order of quality), with nominal error radii ranging from < 250 m for LC 3 to < 1,500 m for LC 0, > 10 km for the lettered classes (Nicholls et al., 2007; Irvine et al., 2020). However, these estimates are subject to substantially greater bias in the longitudinal than the latitudinal direction, such that true errors around calculated positions are better represented by 2-dimensional anisotropic ellipses rather than by 1-dimensional circles (McClintock et al., 2015). Service Argos has been supplying these ellipses with each location in recent years. Each ellipse has three components, namely its (1) semi-major axis, M, (2) semi-minor axis m, and (3) orientation, c. Taken together, these define a bivariate normal distribution of geolocation error centered on the animal's location, with larger ellipses being associated with higher positional uncertainty (McClintock et al., 2015). Published estimates of Argos error ellipses are only currently available for a small number of cetacean species, including blue (*Balaenoptera musculus*), fin (*B. physalus*), and sperm whales (*Physeter macrocephalus*) (Irvine et al., 2020). Empirical data on tagged Cuvier's beaked whales have also recently been collected as part of the Atlantic BRS (Schick et al., 2019), and we used this latter dataset as a basis for simulating appropriate levels of sampling uncertainty in S-TAGs. Specifically, we jittered the (x, y) coordinates of each simulated animal within plausible error ellipses selected at random from the BRS dataset in every exposure (**Figure 2**). This was achieved in seven steps, as follows.

- **Step 1:** Simulate response thresholds, t_{ij}, for each animal i in exposure session j.
- **Step 2:** Determine the corresponding range between whale and sonar source, under the assumption that sound spreads equally in all directions (i.e., inverse-square spherical spreading) (Tyack and Thomas, 2019). For these calculations, the absorption coefficient was set to 0.185 dB re 1μPa per km, which corresponds to the rate of absorption of an acoustic signal emitted at a nominal frequency of 3 kHz under normal sea conditions (Miller et al., 2014).
- **Step 3:** Position an animal at this range, and calculate its coordinates on the (x, y) plane relative to the source using simple trigonometry. Whale-source angles are drawn from a Uniform distribution U∼(0, 360).
- **Step 4:** Create an Argos error ellipse by randomly sampling a vector of ellipse parameters $\theta_{ij} = (M_{ij}, m_{ij}, c_{ij})$ from the Atlantic BRS dataset (Schick et al., 2019), and generate n = 10,000 candidate locations within this ellipse by sampling from the bivariate Normal distribution centered on the animal and with variance–covariance matrix defined by the values in θ_{ij}.
- **Step 5:** Compute the source-whale range for all candidate locations.
- **Step 6:** Estimate received sound levels at candidate locations using the same spherical spreading loss model as above.
- **Step 7:** Extract the standard deviation of received levels as an estimate of the sampling uncertainty associated with each S-TAG.

Model Fitting and Posterior Inference

Model fitting was performed using Markov Chain Monte Carlo (MCMC) in JAGS, interfaced via the *rjags* library in R v4.0.3 (R Core Team, 2020). Model parameters were estimated based on 10,000 posterior samples from each of three MCMC chains, taken after variable burn-in periods (**Supplementary Table 2**). Chains were assessed for convergence both visually (i.e., inspection of trace plots) and numerically (Brooks–Gelman–Rubin statistic, $\hat{R} < 1.1$) using functions from the *coda* and *bayesplot* packages. Each parameter was initialized using arbitrary starting values. Prior distributions were required on all top-level random variables in the hierarchical model (shown as

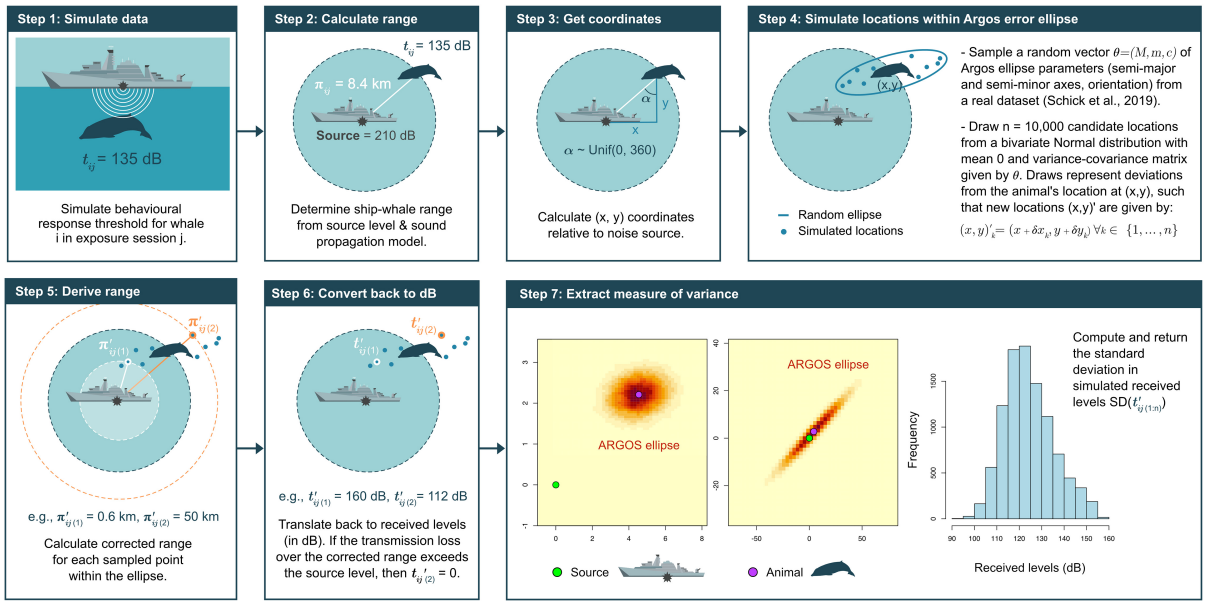

FIGURE 2 | Schematic of the approach taken to estimate sampling uncertainty on Argos-linked satellite tags (S-TAGs). Step 4 is informed by a real-world dataset on Cuvier's beaked whales (*Ziphius cavirostris*) tagged as part of the Atlantic BRS project (https://sea-inc.net/science/atlantic-brs/) (Schick et al., 2019).

gray circles in **Figure 1**), and we largely followed Miller et al. (2014) in choosing diffuse uniform priors for these. The only exceptions were the two parameters governing the respective effects of exposure history (α) and sonar frequency (β), for which normal distributions centered on zero were assumed (**Figure 1** and **Table 1**). These decisions were subjective, and it could be argued that the use of more informative priors (e.g., a low *a priori* response threshold with small variance) may have been more beneficial in the analysis of a sonar-sensitive species like *Z. cavirostris.* That said, misspecified priors have the potential to undermine inference and mislead model interpretation (McCarthy and Masters, 2005). Given the strong within- and between-individual heterogeneity in responsiveness described in previous BRSs (Harris et al., 2018), uniform priors were deemed an adequate and more precautionary alternative, and were specified so as to constrain model parameters within biologically plausible bounds (McCarthy and Masters, 2005; **Table 1**). Within each scenario, we fitted models to 100 simulated datasets for each combination of N and δ / P_{S-TAG}, running the code in parallel on multiple cores to increase execution speed. In contrast to Miller et al. (2014), we did not implement Gibbs Variable Selection (GVS), but instead assessed the ability of the models to discriminate covariate effects by examining the posterior distributions of the relevant coefficients, α and β. If the corresponding 95% credible intervals included zero, we deemed the model unable to detect an effect.

Regulatory agencies in many jurisdictions now require noise impact assessments to authorize at-sea activities involving loud sound sources which may adversely affect marine mammals (Farcas et al., 2016). The assessment process often entails the estimation of "potential zones of effect" (or alternatively, the number of animals predicted to be affected) using noise exposure criteria which define thresholds of sound at which individual- or population-level impacts can be expected (e.g., mortality, temporary or permanent hearing impairment, habitat exclusion, behavioral change) (Faulkner et al., 2018). Historically, these estimates have often been obtained from simple step functions which consider that individuals are impacted only if/when exposed above a discrete level of sound (i.e., the risk of impact increases instantaneously from 0 to 100% once that level is attained—typically, 160 dB re 1 μPa). However, this approach ignores the fact that responses do not necessarily scale with dose (Gomez et al., 2016), and overlooks the complexities of wildlife responsiveness to sound, including the large suite of contextual factors that drive the onset and intensity of behavioral responses observed to date both within and across taxonomic groups (Ellison et al., 2012). Tyack and Thomas (2019) recently proposed the effective response radius (or effective response range, ERR) as an alternative and unbiased diagnostic of impact for management applications. The ERR is derived from probabilistic dose-response curves and can be combined with information on animal density to determine the number of individuals expected to respond under given exposure conditions, making it a key metric in environmental impact assessments. Specifically, the ERR represents an "effect zone" (sensu Faulkner et al., 2018) which quantifies the distance beyond which as many animals respond as do not respond within it; it follows that the total number of animals (both those that respond and those that do not) within this range is identical to the overall number of animals responding at all distances, assuming that individuals are distributed evenly throughout the region of interest (although other spatial distributions can be readily incorporated; see Tyack and Thomas, 2019 for details). Using acoustic propagation models, the ERR can additionally be translated into an effective

received level (ERL), which yields an identical estimate of impact when used as a threshold in a step function as would be obtained from a full dose-response function (Tyack and Thomas, 2019). To explore the consequences of sampling uncertainty on decision-making, we used posterior estimates of model parameters to compute the ERR in each simulation, assuming spherical spreading loss of the acoustic signals.

To evaluate model performance, we compared the posterior distributions of parameters and derived quantity (i.e., ERR) with their "true" values, concentrating on three key diagnostics: (1) precision, expressed as the average width of posterior credible intervals; (2) accuracy, measured as the average absolute percent relative bias, defined as $100 \times \left(\frac{\text{posterior mean} - \text{true value}}{\text{true value}}\right)$; and (3) identifiability, defined as the average prior posterior overlap (PPO). The latter is useful for identifying parameter-redundant models, i.e., in which priors simply dictate posteriors and the data have little bearing on the results, if any. A guideline of 35% or greater overlap has been suggested as an indicator of weak identifiability (Gimenez et al., 2009). Lastly, we computed dose-response curves from each model in the same way as Miller et al. (2014), and created plots of the associated posterior median and credible interval lines for a range of chosen quantiles. The code used to run the analyses is publicly available at https://github.com/pjbouchet/brs_uncertainty and fully described in Bouchet et al. (2020).

RESULTS

Reduced Model

An interaction between sample size (N) and sampling error (δ) was apparent in the reduced model, with the variance surrounding dose-response curves increasing as both N declined and δ increased (**Figure 3A** and **Supplementary Figure 1**). Posterior estimates of the location parameter for the response threshold (μ) were closely aligned with their true original value under most test conditions but were subject to strong positive bias (average ± SD: 15.7 ± 1.0 dB) at the largest level of sampling error (δ = 35 dB), irrespective of sample size (**Supplementary Figure 2**). Furthermore, degrading data quality from consistently good (high N, low δ) to consistently poor (low N, high δ) incurred a ca. threefold loss in precision (average ± SD: 2.99 ± 0.46 dB) around μ. Together, these trends translated into highly uncertain assessments of responsiveness and underestimates of impact when sampling errors were magnified (**Figure 3B**). Similar patterns were observed for the scale parameter related to the within-exposure variance (σ), indicating that even as few as two repeated exposures can be useful for quantifying intra-individual variability. By contrast, the scale parameter related to between-whale variance (ϕ) was consistently more difficult to estimate, with wide credible intervals and a high prior posterior overlap under all sampling regimes (**Figure 3C** and **Supplementary Figure 2**). The model was rarely able to detect an effect of exposure history (α) (overall average ± SD: 5.7 ± 7.9% of simulation runs) but was more successful at disentangling the effect of sonar frequency (β), with credible intervals excluding zero in up to 66% of simulations runs at N = 30 and δ = 2.5 dB (overall average ± SD: 27.9 ± 20.0%). Of all model parameters, only μ was fully identifiable (PPO < 35%) in all simulations, highlighting the relevance of the information contained in simulated behavioral data for predicting the population-level thresholds of response (**Figure 3C**).

Full Model

The dose-response curves obtained from the full model were sensitive to variation in N but not P_{S-TAG}, such that sample size became the dominant driver of posterior inference when multiple tag types were used (**Figure 4A** and **Supplementary Figure 3**). Bias in estimates of μ remained low in all scenarios, even when every simulated individual carried a S-TAG (P_{S-TAG} = 100%; average ± SD: 3.67 ± 0.84 dB) (**Supplementary Figure 4**). Likewise, tag choice had a negligible influence on the precision of μ for a given sample size. By contrast, posterior credible intervals were halved when sampling effort increased from N = 5 to N = 30 whales (average ratio ± SD: 0.44 ± 0.075 dB), as was the range of plausible predictions of the ERR, which decreased from 32–114 km to 58–99 km, respectively (**Figure 4B**). On average, the model only detected an effect of exposure history in 5.5 ± 5.3% of simulations. At N = 30, the effect of sonar frequency (*beta*) was correctly detected in more than 50% of runs (overall average ± SD: 29.6 ± 20.0%). Patterns in parameter identifiability largely mirrored those observed in the reduced model (**Figure 4C**).

DISCUSSION

Over two decades of BRSs on the effects of military sonar have now been funded by the world's navies, allowing major strides in our understanding of the impacts of man-made noise on free-ranging cetaceans (Harris et al., 2016, 2018; Southall et al., 2016). While the pathways leading to physical injury and mortality are not yet fully resolved (Hooker et al., 2019), individual behavioral change has been highlighted as a pivotal symptom of sonar-related disturbance (DeRuiter et al., 2013; Southall et al., 2019). In the last 75 years, engineers and marine mammal scientists have come up with creative technological solutions to assess the behavior (e.g., spatial movements, call rates, diving patterns, group dynamics) of whales and dolphins before, during, and after sound exposure (Nowacek et al., 2016). Static passive acoustic platforms, for instance, have played a prominent role in BACI studies of shallow nearshore and shelf ecosystems, where numerous cetacean populations co-occur with human activities (e.g., Risch et al., 2012; Sarnocińska et al., 2020). Many BRSs also focus on deep-diving oceanic species in offshore habitats, where the onerous costs of running dedicated CEEs (i.e., often in excess of several US$ 100,000 for a single season) (Harris et al., 2016) provide a strong impetus for integrating multiple sampling approaches, including visual focal follows and combinations of archival biologging and near real-time biotelemetry (Berga et al., 2019; von Benda-Beckmann et al., 2019). However, commonly used animal-borne tags like DTAGs and S-TAGs capture ecological processes on fundamentally

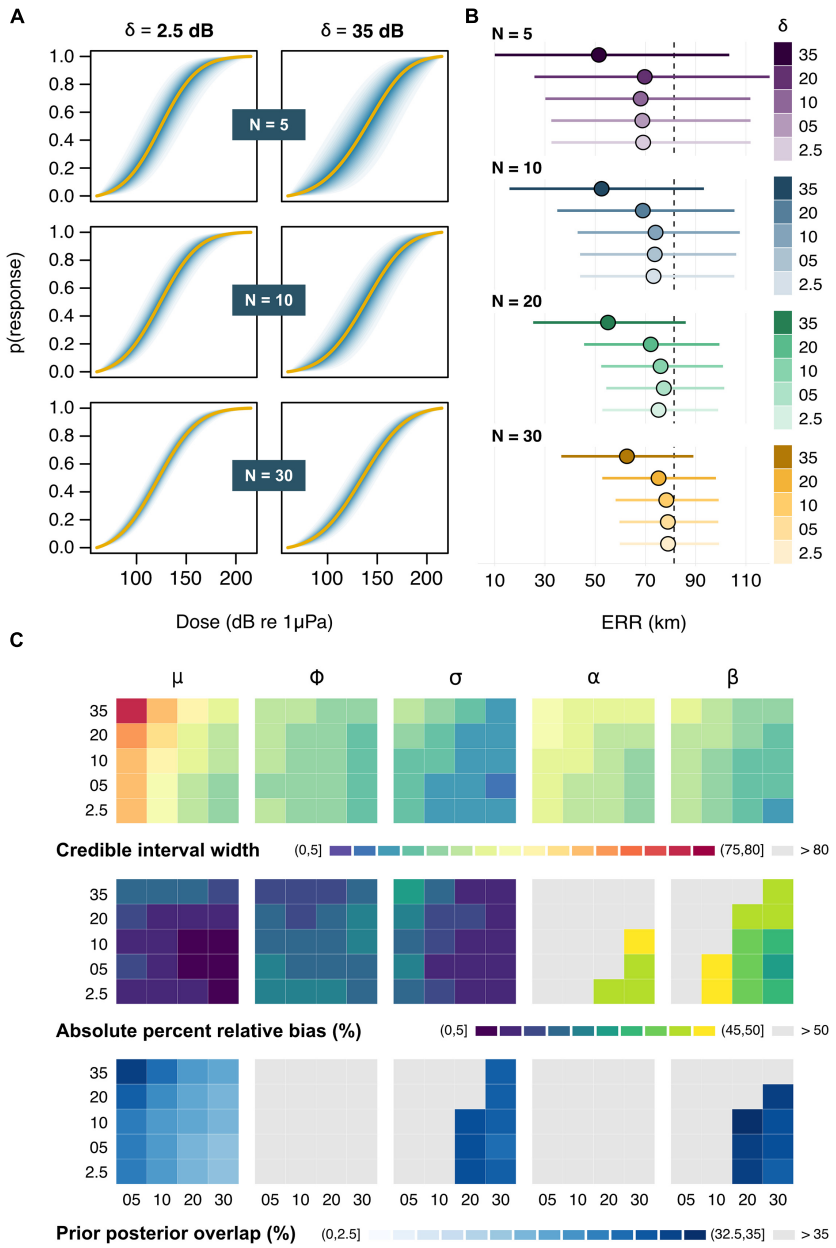

FIGURE 3 | Outputs from the reduced model. **(A)** Example dose-response curves for a subset of sample sizes (N) and sampling errors (δ). Solid lines represent the average posterior medians across Ns = 100 simulations, followed by the average 5, 10, 15 . . . and 95% credible intervals in darker to lighter shades of blue. **(B)** Posterior estimates of the effective response range (ERR). Circles and bars respectively denote the average posterior median and credible intervals for each N × δ combination. The dashed line marks the true underlying value. **(C)** Summary of patterns in the precision, accuracy, and identifiability of posterior estimates across N (across) × δ (down) combinations. Results are shown (from left to right) for the location parameter relating to the mean response threshold for all whales (μ), the scale parameters relating to the between-whale variation (*phi*) and the within-whale between-exposure variation (σ), and the two contextual covariates (α and β). Rows indicate the average posterior credible interval width (in dB) [top], absolute percent relative bias (in %) [middle], and prior posterior overlap (PPO, in %) [bottom]. PPO values above 35% indicate that parameters may be non-identifiable (2011).

different spatio-temporal scales (Hazen et al., 2012), and generate data burdened with varying levels of uncertainty. For example, estimates of received sound levels from DTAGs are typically obtained with higher precision than on S-TAGs, especially when the latter operate through the Argos system (Costa et al., 2010; Irvine et al., 2020). At present, it is unclear how sampling uncertainty from the use of different instruments propagates into metrics of risk as used in decision-making. Here, we took advantage of an existing Bayesian hierarchical model to address this question and investigate the implications of tag choice for estimating probabilistic dose-response functions (Miller et al., 2014; Tyack and Thomas, 2019).

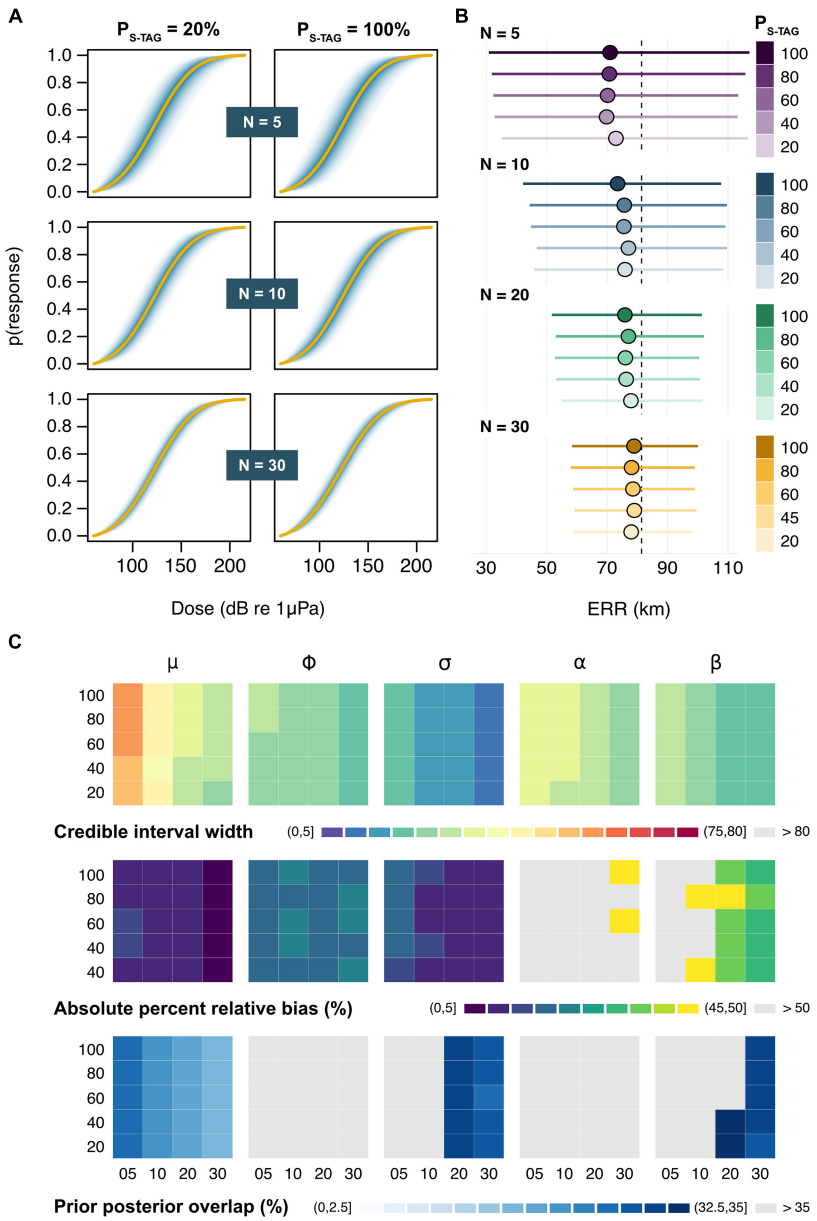

FIGURE 4 | Outputs from the full model. **(A)** Example dose-response curves for a subset of sample sizes (N) and ratios of satellite tags (P_{S-TAG}). Solid lines represent the average posterior medians across Ns = 100 simulations, followed by the average 5, 10, 15 . . . and 95% credible intervals in darker to lighter shades of blue. **(B)** Posterior estimates of the effective response range (ERR). Circles and bars respectively denote the average posterior median and credible intervals for each N × P_{S-TAG} combination. The dashed line marks the true underlying value. **(C)** Summary of patterns in the precision, accuracy, and identifiability of posterior estimates across N (across) × P_{S-TAG} (down) combinations. Results are shown (from left to right) for the location parameter relating to mean response threshold for all whales (μ), the scale parameters relating to the between-whale variation (ϕ) and the within-whale between-exposure variation (σ), and the two contextual covariates (α and β). Rows indicate the average posterior credible interval width (in dB) [top], absolute percent relative bias (in %) [middle], and prior posterior overlap (PPO, in %) [bottom]. PPO values above 35% indicate that parameters may be non-identifiable (Gimenez et al., 2009).

Our results highlight the importance of considering sample size in studies of sonar impacts on free-ranging cetaceans, and illustrate how larger datasets can deliver consistent improvements in accuracy and precision irrespective of tag choice. Obtaining reliable estimates of the location and scale parameters that relate to the mean threshold of response (μ) and its associated variance components (σ and ϕ) is essential, as it is these that define the position and steepness of the cumulative distribution function on which dose-response curves are based. As such, any biases in model parameters may undermine assessments of risk and lead to errors that can misguide decision-making. For instance, the limited information available when N is low means that posterior estimates for μ will be pulled away from the true threshold of response (here, μ = 120 dB re 1 μPa)

toward the prior mean (here, μ = 135 dB re 1μPa). If the latter exceeds the former, then impact zones from sonar transmissions will be consistently underestimated (**Figures 3**, **4**). Conversely, impact will be overestimated if the prior mean is lower than the true response threshold. When paired with adequate controls and baselines, larger datasets may also help differentiate among-individual from within-individual heterogeneity, and facilitate their separation from the proximate drivers that control reactions to sound (Cleasby et al., 2015; Dunlop et al., 2018). There is compelling evidence that many factors (other than received sound levels) affect the onset and severity of behavioral responses (Ellison et al., 2012; Gomez et al., 2016; Harris et al., 2018; Southall et al., 2019). These include (1) intrinsic traits, such as hearing sensitivity, noise tolerance, activity and motivational states at the time of exposure, age, sex, or the presence of dependent offspring, as well as (2) extrinsic elements, such as the nature of the sound (e.g., frequency band) (Isojunno et al., 2018), or the spatial relationship between emitter and receiver (e.g., motion, depth, and proximity of the sound source). Some of the most dramatic responses to underwater noise reported to date appear to have been from naïve, free-ranging individuals at very low received levels (90–120 dB re 1 Pa rms) (Finley et al., 1990), suggesting that acoustic novelty and previous history of exposure may also play a decisive role. However, efforts to appropriately assess the potential for sensitisation and habituation are complicated by the variety of timescales over which exposures may occur—from a few hours in the context of CEEs to upwards of several days or weeks during real military operations—and the lack of a standardized metric of individual experience or familiarity with sonar sounds over a range of relevant time periods (Gomez et al., 2016). Our model was rarely successful at recovering the influence of exposure history (α) in the simulations, likely because of the small effect size for this covariate relative to the overall level of variability present in the data. In the absence of appropriate empirical measurements, our choice of parameterisation for α was ultimately arbitrary, yet it points to the need to further consider statistical power in analyses of sonar effects. Modest changes in response thresholds and the behavior of individual whales associated with disturbance can have population-level consequences (e.g., through reduced energy intake, Benoit-Bird et al., 2020), but these may go undetected without adequate sample sizes.

It is important to note that the ability to tease apart the effects of contextual factors from tags that cannot directly measure sound is predicated on the assumptions made regarding acoustic transmission loss. Simple transmission loss models may not accurately predict received levels from a sonar source to a free-diving animal (Wensveen, 2012), leading to substantial uncertainties and biases in the impact assessment process (Farcas et al., 2016). This is particularly the case in oceanographically dynamic habitats and over convoluted seabed terrain, where depth-mediated changes in sound profiles can manifest throughout the water column (Siderius and Porter, 2006; Schick et al., 2019; von Benda-Beckmann et al., 2019). Accounting for fine-scale variations in sound profiles is a complicated problem to tackle which requires the development of sophisticated sound propagation models, not all of which perform well in areas different to the ones in which they were built (Siderius and Porter, 2006). Using a propagation model was outside the scope of the present study and would have undermined the applicability of our results, constraining inference to a narrow range of environmental conditions (e.g., bathymetry, ocean currents) with limited value for management. For simplicity and generality, we thus assumed that sonar pings propagated away from the source uniformly in all directions along the horizontal plane (i.e., spherical spreading). While this is clearly a simplification of the sound field, evidence suggests that it may provide a reasonable approximation of noise propagation in at least some homogeneous deep-water environments (Wensveen, 2012). Our estimates of variance in received levels at incremental distances from the source (**Supplementary Figure 5**) also align with the range of values reported in the literature, including in studies of beaked whales that did rely on sound propagation models within topographically complex shelf break habitats (Schick et al., 2019). This lends confidence that our simulation successfully captured realistic scenarios of sound exposure.

From the early days of the first DTAG deployments on single individuals, BRSs (and CEEs) have rapidly evolved into what are now fully multidisciplinary, multi-platform, operational field programs that capitalize on an array of remote sensing technologies to monitor animal behavior in complementary ways. By simulating specific sampling regimes involving several tag types, we were able to start evaluating how methodological decisions regarding tag selection may influence predictions of risk. We found that despite the occasionally high positional errors reported in previous satellite tracking studies (Tyack et al., 2011; Falcone et al., 2017; von Benda-Beckmann et al., 2019; Wensveen et al., 2019; Joyce et al., 2020), the average variability in the modeled acoustic dose experienced by whales carrying S-TAGs was sufficiently low to support the estimation of dose-response relationships (**Supplementary Figure 5**). This aligns with an expanding body of literature documenting the utility of satellite-transmitting tags for evaluating the impacts of anthropogenic sound on marine mammals (Tyack et al., 2011; Falcone et al., 2017; von Benda-Beckmann et al., 2019; Wensveen et al., 2019; Joyce et al., 2020), in complement to other tools. In our example, similar estimates of the ERR were obtained on average from a sample of N = 20 whales with DTAGs (assuming a fixed measurement error of δ = 2.5 dB) as from a sample of N = 30 whales all carrying S-TAGs (unless uplinks were consistently poor) (**Figures 3**, **4**). This type of comparative assessment is not only useful for planning future survey effort but also for framing expectations about the realm of inference that is attainable given existing datasets. A key assumption, however, is that responses are comparable and detection rates equal between tag types. This is an important caveat, as the energetic costs associated with sonar disturbance vary with the nature and strength of behavioral responses, and are a function of species' life histories and physiologies (Czapanskiy et al., 2021). For example, the relative energy expenditure of a blue whale exhibiting a "mild" foraging response has been shown to exceed that of an "extreme" flight response in Cuvier's beaked whales (Czapanskiy et al., 2021). Failure to detect weak responses, or responses of a particular type,

on instruments that deliver coarser-resolution data like S-TAGs would lead to bias in estimates of the dose-response functions and thus assessments of biological impacts. An additional issue is that the accuracy of Argos locations has been shown to be site- and species-specific, and mediated by both diving patterns and the positioning of the tag on the animal's body (Mul et al., 2019). For instance, Costa et al. (2010) and Irvine et al. (2020) provided evidence that drifts in the frequency of tag transmissions at cold temperatures may be responsible for higher levels of errors in animals undergoing deep, long-duration dives like sperm whales or northern elephant seals (*Mirounga angustirostris*)—and thus presumably beaked whales. Given the above, our estimates likely remain conservative and are strictly only relevant within the bounds of error recorded on tags deployed on *Z. cavirostris* (as part of the Atlantic BRS study), particularly as further work is required to validate our results with other species in different environments. That said, we anticipate that any disparities in performance between taxa or between instruments will quickly narrow in the near future given the enormous advances in telemetry systems that have been accomplished in recent years (e.g., higher numbers of polar-orbiting satellites, better sensitivity of satellite sensors, longer transmitter battery life, more streamlined tag shapes). Already, the accuracy of tags enabled with Fastloc-GPS surpasses conventional Argos tracking systems by several orders of magnitude (Dujon et al., 2014), leading to an exponentially rising volume of telemetry data of constantly improving quality. Similarly, much research is being directed at improving current methods for the characterisation of behavioral change,[3] and engineering efforts to enhance tag adhesion and augment the array of onboard electronics available are expected to facilitate a new generation of longer-lasting, data-rich DTAG and S-TAG attachments that can yield novel insights into not only the levels of noise required to elicit behavioral responses, but also the physiological mechanisms through which these responses may cause harm (Nowacek et al., 2013; Hooker et al., 2019). Further improvements to our modeling framework are also possible and may entail: (i) the inclusion of a formal detection process, which acknowledges that behavioral responses are harder to detect from coarser-resolution data and lead to a larger proportion of censored observations on S-TAGs relative to DTAGs, (ii) the use of dedicated sound propagation models to better represent the range of received levels which whales are likely to experience, (iii) the addition of a depth component to map received levels in three dimensions, (iv) correlated patterns of satellite uplink quality for animals fitted with S-TAGs, (iv) different model parameterisations (e.g., prior choice). We have made our code freely available to support these efforts.

CONCLUSION

Determining how cetaceans react to manmade underwater noise is vital for making informed decisions about what may constitute acceptable levels of risk to species from sound-producing activities. A significant challenge in studies of cetacean exposure to military sonar lies in teasing out pattern from noise within complex datasets gathered using instruments that are subject to varying degrees of measurement error. Very few BRSs consider how sample size and tag choice may affect statistical power (Dunlop et al., 2012; Cato et al., 2016), yet understanding how these two elements interact to shape ecological inference is essential in delivering robust estimates of uncertainty that can help managers adhere to precautionary principles in the face of many unknowns. We demonstrated that clear improvements in the accuracy and precision of parameter estimates from a Bayesian hierarchical dose-response model are possible with increased sample sizes, largely independently of tag choice (DTAG vs. S-TAG). Thus, substantial advances in our capacity to predict sonar impacts on cetaceans are likely to be made in the future as collaborative efforts to conduct multi-platform BRSs continue to persist in earnest.

[3] See https://github.com/r-glennie/CTMCdive for an example.

DATA AVAILABILITY STATEMENT

The R code used in the analyses is fully described and available on GitHub (https://github.com/pjbouchet/brs_uncertainty). The Argos data are confidential and cannot presently be made available.

AUTHOR CONTRIBUTIONS

LT designed the underlying hierarchical model. CH and LT conceived the simulation study and provided expert advice to guide parameter choice, with input from PB. PB performed the analyses, wrote the R code, and led the writing of the manuscript, with contributions from the other authors. All authors contributed to the article and approved the submitted version.

FUNDING

This work was financially supported by the US Navy Living Marine Resources Program (LMR) Contract No. N3943018C2080. Support for the Atlantic BRS project was provided by the Naval Facilities Engineering Command Atlantic under Contract No. N62470-15-D-8006, Task Order 18F4036, Issued to HDR, Inc.

ACKNOWLEDGMENTS

We are grateful to Rob Schick and the Atlantic BRS project for providing the Argos ellipse data. We thank two reviewers for their thoughtful comments on an earlier draft of the manuscript.

SUPPLEMENTARY MATERIAL

The Supplementary Material for this article can be found online at: https://www.frontiersin.org/articles/10.3389/fmars.2021.674554/full#supplementary-material

REFERENCES

Aguilar Soto, N., Johnson, M., Madsen, P. T., Tyack, P. L., Bocconcelli, A., and Fabrizio Borsani, J. (2006). Does intense ship noise disrupt foraging in deep-diving Cuvier's beaked whales (*Ziphius cavirostris*)? *Mar. Mamm. Sci.* 22, 690–699. doi: 10.1111/j.1748-7692.2006.00044.x

Andrews, R. D., Baird, R. W., Calambokidis, J., Goertz, C. E. C., Gulland, F., Heide-Jørgensen, M. P., et al. (2019). Best practice guidelines for cetacean tagging. *J. Cetacean Res* 20, 27–66.

Antunes, R., Kvadsheim, P. H., Lam, F. P. A., Tyack, P. L., Thomas, L., Wensveen, P. J., et al. (2014). High thresholds for avoidance of sonar by free-ranging long-finned pilot whales (*Globicephala melas*). *Mar. Pollut. Bull.* 83, 165–180. doi: 10.1016/j.marpolbul.2014.03.056

Benoit-Bird, K. J., Southall, B. L., Moline, M. A., Claridge, D. E., Dunn, C. A., Dolan, K. A., et al. (2020). Critical threshold identified in the functional relationship between beaked whales and their prey. *Mar. Ecol. Prog. Ser.* 654, 1–16. doi: 10.3354/meps13521

Berga, A. S., Trickey, J. S., Rice, A., Širovičė, A., Roch, M. A., Paxton, C. G., et al. (2019). Potential impact of mid-frequency active sonar on whales from passive acoustic monitoring data. *J. Acoust. Soc. Am.* 146, 2939–2939. doi: 10.1121/1.5137205

Bernaldo de Quirós, Y., Fernandez, A., Baird, R. W., Brownell, R. L. Jr., Aguilar de Soto, N., Allen, D., et al. (2019). Advances in research on the impacts of anti-submarine sonar on beaked whales. *Proc. Biol. Sci.* 286:20182533. doi: 10.1098/rspb.2018.2533

Bouchet, P. J., Harris, C. M., and Thomas, L. (2020). *Simulating Cetacean Responses to Sonar Exposure within a Bayesian Hierarchical Modelling Framework — R code Description*. St Andrews: University of St Andrews.

Cato, D. H., Dunlop, R. A., Noad, M. J., McCauley, R. D., Kniest, E., Paton, D., et al. (2016). Addressing challenges in studies of behavioral responses of whales to noise. *Adv. Exp. Med. Biol.* 875, 145–152. doi: 10.1007/978-1-4939-2981-8_17

Chou, E., Southall, B. L., Robards, M., and Rosenbaum, H. C. (2021). International policy, recommendations, actions and mitigation efforts of anthropogenic underwater noise. *Ocean Coast. Manag.* 202:105427. doi: 10.1016/j.ocecoaman.2020.105427

Cleasby, I. R., Nakagawa, S., and Schielzeth, H. (2015). Quantifying the predictability of behaviour: statistical approaches for the study of between-individual variation in the within-individual variance. *Methods Ecol. Evol.* 6, 27–37. doi: 10.1111/2041-210x.12281

Costa, D. P., Robinson, P. W., Arnould, J. P. Y., Harrison, A.-L., Simmons, S. E., Hassrick, J. L., et al. (2010). Accuracy of ARGOS locations of pinnipeds at-sea estimated using Fastloc GPS. *PLoS One* 5:e8677. doi: 10.1371/journal.pone.0008677

Curé, C., Isojunno, S., Siemensma, M. L., Wensveen, P. J., Buisson, C., Sivle, L. D., et al. (2021). Severity scoring of behavioral responses of sperm whales (*Physeter macrocephalus*) to novel continuous versus conventional pulsed active sonar. *J. Mar. Sci. Eng.* 9:444. doi: 10.3390/jmse9040444

Curtis, K. A., Falcone, E. A., Schorr, G. S., Moore, J. E., Moretti, D. J., Barlow, J., et al. (2020). Abundance, survival, and annual rate of change of Cuvier's beaked whales (*Ziphius cavirostris*) on a Navy sonar range. *Mar. Mamm. Sci.* 37, 399–419. doi: 10.1111/mms.12747

Czapanskiy, M. F., Savoca, M. S., Gough, W. T., Segre, P. S., Wisniewska, D. M., Cade, D. E., et al. (2021). Modelling short-term energetic costs of sonar disturbance to cetaceans using high-resolution foraging data. *J. Appl. Ecol.* 58, 1643–1657. doi: 10.1111/1365-2664.13903

D'Amico, A., Gisiner, R. C., Ketten, D. R., Hammock, J. A., Johnson, C., Tyack, P. L., et al. (2009). Beaked whale strandings and naval exercises. *Aquat. Mamm.* 35, 452–472. doi: 10.1578/AM.35.4.2009.452

D'Amico, A., and Pittenger, R. (2009). A brief history of active sonar. *Aquat. Mamm.* 35, 426–434. doi: 10.1578/AM.35.4.2009.426

DeRuiter, S. L., Southall, B. L., Calambokidis, J., Zimmer, W. M. X., Sadykova, D., Falcone, E. A., et al. (2013). First direct measurements of behavioural responses by Cuvier's beaked whales to mid-frequency active sonar. *Biol. Lett.* 9:20130223. doi: 10.1098/rsbl.2013.0223

Duarte, C. M., Chapuis, L., Collin, S. P., Costa, D. P., Devassy, R. P., Eguiluz, V. M., et al. (2021). The soundscape of the Anthropocene ocean. *Science* 371:eaba4658. doi: 10.1126/science.aba4658

Dujon, A. M., Lindstrom, R. T., and Hays, G. C. (2014). The accuracy of Fastloc-GPS locations and implications for animal tracking. *Methods Ecol. Evol.* 5, 1162–1169. doi: 10.1111/2041-210x.12286

Dunlop, R. A., Noad, M. J., and Cato, D. H. (2012). Behavioral-response studies: problems with statistical power. *Adv. Exp. Med. Biol.* 730, 293–297. doi: 10.1007/978-1-4419-7311-5_65

Dunlop, R. A., Noad, M. J., McCauley, R. D., Kniest, E., Slade, R., Paton, D., et al. (2018). A behavioural dose-response model for migrating humpback whales and seismic air gun noise. *Mar. Pollut. Bull.* 133, 506–516. doi: 10.1016/j.marpolbul.2018.06.009

Durbach, I., Harris, C., Martin, C., Helble, T. A., Henderson, E. E., Ierley, G., et al. (2021). Changes in the movement and calling behavior of minke whales (*Balaenoptera acutorostrata*) in response to navy training. *Front. Mar. Sci.* 8:660122. doi: 10.3389/fmars.2021.660122

Ellison, W. T., Southall, B. L., Clark, C. W., and Frankel, A. S. (2012). A new context-based approach to assess marine mammal behavioral responses to anthropogenic sounds. *Conserv. Biol.* 26, 21–28. doi: 10.1111/j.1523-1739.2011.01803.x

Erbe, C., Dunlop, R., and Dolman, S. (2018). "Effects of noise on marine mammals," in *Effects of Anthropogenic Noise on Animals*, eds H. Slabbekoorn, R. J. Dooling, A. N. Popper, and R. R. Fay (New York, NY: Springer), 277–309. doi: 10.1007/978-1-4939-8574-6_10

Falcone, E. A., Schorr, G. S., Watwood, S. L., DeRuiter, S. L., Zerbini, A. N., Andrews, R. D., et al. (2017). Diving behaviour of Cuvier's beaked whales exposed to two types of military sonar. *R. Soc. Open Sci.* 4:170629. doi: 10.1098/rsos.170629

Farcas, A., Thompson, P. M., and Merchant, N. D. (2016). Underwater noise modelling for environmental impact assessment. *Environ. Impact Assess. Rev.* 57, 114–122. doi: 10.1016/j.eiar.2015.11.012

Faulkner, R. C., Farcas, A., and Merchant, N. D. (2018). Guiding principles for assessing the impact of underwater noise. *J. Appl. Ecol.* 55, 2531–2536. doi: 10.1111/1365-2664.13161

Fernández, A., Sierra, E., Martín, V., Méndez, M., Sacchinni, S., de Quirós, Y. B., et al. (2012). Last "atypical" beaked whales mass stranding in the Canary Islands (July, 2004). *J. Mar. Sci. Res. Dev.* 2, 1–3. doi: 10.4172/2155-9910.1000107

Filadelfo, R., Mintz, J., Michlovich, E., D'Amico, A., Tyack, P. L., and Ketten, D. R. (2009). Correlating military sonar use with beaked whale mass strandings: what do the historical data show? *Aquat. Mamm.* 35, 435–444. doi: 10.1578/AM.35.4.2009.435

Finley, K. J., Miller, G. W., Davis, R. A., and Greene, C. R. (1990). Reactions of belugas, *Delphinapterus leucas*, and narwhals, *Monodon monoceros*, to ice-breaking ships in the Canadian high arctic. *Can. Bull. Fish. Aquat. Sci./Bull. Can. Sci. Halieut. Aquat.* 224, 97–117.

Friedlaender, A. S., Hazen, E. L., Goldbogen, J. A., Stimpert, A. K., Calambokidis, J., and Southall, B. L. (2016). Prey-mediated behavioral responses of feeding blue whales in controlled sound exposure experiments. *Ecol. Appl.* 26, 1075–1085. doi: 10.1002/15-0783

Gimenez, O., Morgan, B. J. T., and Brooks, S. P. (2009). "Weak identifiability in models for mark-recapture-recovery data," in *Modeling Demographic Processes in Marked Populations*, eds D. L. Thomson, E. G. Cooch, and M. J. Conroy (Boston, MA: Springer US), 1055–1067. doi: 10.1007/978-0-387-78151-8_48

Goldbogen, J. A., Southall, B. L., DeRuiter, S. L., Calambokidis, J., Friedlaender, A. S., Hazen, E. L., et al. (2013). Blue whales respond to simulated mid-frequency military sonar. *Proc. R. Soc. Lond. B Biol. Sci.* 280:20130657. doi: 10.1098/rspb.2013.0657

Gomez, C., Lawson, J. W., Wright, A. J., Buren, A. D., Tollit, D., and Lesage, V. (2016). A systematic review on the behavioural responses of wild marine mammals to noise: the disparity between science and policy. *Can. J. Zool.* 94, 801–819. doi: 10.1139/cjz-2016-0098

Harris, C. M., Martin, S. W., Martin, C., Helble, T. A., Henderson, E. E., Paxton, C. G. M., et al. (2019b). Changes in the spatial distribution of acoustically derived minke whale (*Balaenoptera acutorostrata*) tracks in response to Navy training. *Aquat. Mamm.* 45, 661–674.

Harris, C. M., Burt, M. L., Allen, A. N., Wensveen, P. J., Miller, P. J. O., and Sivle, L. D. (2019a). Foraging behavior and disruption in blue, fin, and humpback whales in relation to sonar exposure: the challenges of generalizing responsiveness in species with high individual variability. *Aquat. Mamm.* 45, 646–660. doi: 10.1578/AM.45.6.2019.646

Harris, C. M., Sadykova, D., DeRuiter, S. L., Tyack, P. L., Miller, P. J. O., Kvadsheim, P. H., et al. (2015). Dose response severity functions for acoustic disturbance in cetaceans using recurrent event survival analysis. *Ecosphere* 6:art236. doi: 10.1890/ES15-00242.1

Harris, C. M., Thomas, L., and Falcone, E. A. (2018). Marine mammals and sonar: dose-response studies, the risk-disturbance hypothesis and the role of exposure context. *J Appl. Ecol.* 55, 396–404. doi: 10.1111/1365-2664.12955

Harris, C. M., Thomas, L., Sadykova, D., DeRuiter, S. L., Tyack, P. L., Southall, B. L., et al. (2016). The challenges of analyzing behavioral response study data: an overview of the MOCHA (Multi-study OCean Acoustics Human Effects Analysis) project. *Adv. Exp. Med. Biol.* 875, 399–407. doi: 10.1007/978-1-4939-2981-8_47

Hazen, E. L., Maxwell, S. M., Bailey, H., Bograd, S. J., Hamann, M., Gaspar, P., et al. (2012). Ontogeny in marine tagging and tracking science: technologies and data gaps. *Mar. Ecol. Prog. Ser.* 457, 221–240. doi: 10.3354/meps09857

Hooker, S. K., De Soto, N. A., Baird, R. W., Carroll, E. L., Claridge, D., Feyrer, L., et al. (2019). Future directions in research on beaked whales. *Front. Mar. Sci.* 5:514. doi: 10.3389/fmars.2018.00514

Houser, D. S., Martin, S. W., and Finneran, J. J. (2013). Exposure amplitude and repetition affect bottlenose dolphin behavioral responses to simulated mid-frequency sonar signals. *J. Exp. Mar. Bio. Ecol.* 443, 123–133. doi: 10.1016/j.jembe.2013.02.043

Irvine, L. M., Winsor, M. H., Follett, T. M., Mate, B. R., and Palacios, D. M. (2020). An at-sea assessment of Argos location accuracy for three species of large whales, and the effect of deep-diving behavior on location error. *Anim. Biotelem.* 8:20. doi: 10.1186/s40317-020-00207-x

Isojunno, S., Aoki, K., Curé, C., Kvadsheim, P. H., and Miller, P. J. O. (2018). Breathing patterns indicate cost of exercise during diving and response to experimental sound exposures in long-finned pilot whales. *Front. Physiol.* 9:1462. doi: 10.3389/fphys.2018.01462

Isojunno, S., Cure, C., Kvadsheim, P. H., Lam, F.-P. A., Tyack, P. L., Wensveen, P. J., et al. (2016). Sperm whales reduce foraging effort during exposure to 1-2 kHz sonar and killer whale sounds. *Ecol. Appl.* 26, 77–93. doi: 10.1890/15-0040

Johnson, M., Aguilar de Soto, N., and Madsen, P. T. (2009). Studying the behaviour and sensory ecology of marine mammals using acoustic recording tags: a review. *Mar. Ecol. Prog. Ser.* 395, 55–73. doi: 10.3354/meps08255

Johnson, M. P., and Tyack, P. L. (2003). A digital acoustic recording tag for measuring the response of wild marine mammals to sound. *IEEE J. Ocean. Eng.* 28, 3–12. doi: 10.1109/JOE.2002.808212

Joyce, T. W., Durban, J. W., Claridge, D. E., Dunn, C. A., Fearnbach, H., Parsons, K. M., et al. (2017). Physiological, morphological, and ecological tradeoffs influence vertical habitat use of deep-diving toothed-whales in the Bahamas. *PLoS One* 12:e0185113. doi: 10.1371/journal.pone.0185113

Joyce, T. W., Durban, J. W., Claridge, D. E., Dunn, C. A., Hickmott, L. S., Fearnbach, H., et al. (2020). Behavioral responses of satellite tracked Blainville's beaked whales (*Mesoplodon densirostris*) to mid-frequency active sonar. *Mar. Mamm. Sci.* 36, 29–46. doi: 10.1111/mms.12624

McCarthy, M. A., and Masters, P. (2005). Profiting from prior information in Bayesian analyses of ecological data. *J. Appl. Ecol.* 42, 1012–1019. doi: 10.1111/j.1365-2664.2005.01101.x

McClintock, B. T., London, J. M., Cameron, M. F., and Boveng, P. L. (2015). Modelling animal movement using the Argos satellite telemetry location error ellipse. *Methods Ecol. Evol.* 6, 266–277. doi: 10.1111/2041-210X.12311

McConnell, B., Fedak, M., Hooker, S., and Patterson, T. (2010). "Telemetry," in *Marine Mammal Ecology and Conservation: A Handbook of Techniques*, eds I. L. Boyd, W. D. Bowen, and S. J. Iverson (Oxford: Oxford University Press), 222–242.

Miller, P. J. O., Antunes, R. N., Wensveen, P. J., Samarra, F. I. P., Alves, A. C., Tyack, P. L., et al. (2014). Dose-response relationships for the onset of avoidance of sonar by free-ranging killer whales. *J. Acoust. Soc. Am.* 135, 975–993. doi: 10.1121/1.4861346

Miller, P. J. O., Kvadsheim, P. H., Lam, F.-P. A., Wensveen, P. J., Antunes, R., Alves, A. C., et al. (2012). The severity of behavioral changes observed during experimental exposures of killer (*Orcinus orca*), long-finned pilot (*Globicephala melas*), and sperm (*Physeter macrocephalus*) whales to naval sonar. *Aquat. Mamm.* 38, 362–401.

Moretti, D., Thomas, L., Marques, T., Harwood, J., Dilley, A., Neales, B., et al. (2014). A risk function for behavioral disruption of Blainville's beaked whales (*Mesoplodon densirostris*) from mid-frequency active sonar. *PLoS One* 9:e85064. doi: 10.1371/journal.pone.0085064

Mul, E., Blanchet, M.-A., Biuw, M., and Rikardsen, A. (2019). Implications of tag positioning and performance on the analysis of cetacean movement. *Anim. Biotelem.* 7:11. doi: 10.1186/s40317-019-0173-7

New, L., Lusseau, D., and Harcourt, R. (2020). Dolphins and boats: when is a disturbance, disturbing? *Front. Mar. Sci.* 7:353. doi: 10.3389/fmars.2020.00353

Nicholls, D. G., Robertson, C. J. R., and Murray, M. D. (2007). Measuring accuracy and precision for CLS: argos satellite telemetry locations. *Notornis* 54, 137–157.

Nowacek, D., Bowers, M., Cannon, A., Hindell, M., Howle, L. E., Murray, M. M., et al. (2013). The next generation of multi-sensor acoustic tags: sensors, applications, and attachments. *J. Acoust. Soc. Am.* 134, 4043–4043. doi: 10.1121/1.4830757

Nowacek, D. P., Christiansen, F., Bejder, L., Goldbogen, J. A., and Friedlaender, A. S. (2016). Studying cetacean behaviour: new technological approaches and conservation applications. *Anim. Behav.* 120, 235–244. doi: 10.1016/j.anbehav.2016.07.019

Parsons, E. C. M. (2017). Impacts of Navy sonar on whales and dolphins: now beyond a smoking gun? *Front. Mar. Sci.* 4:295. doi: 10.3389/fmars.2017.00295

Plummer, M. (2003). *JAGS: A Program for Analysis of Bayesian Graphical Models Using Gibbs Sampling*. Available online at: http://citeseerx.ist.psu.edu/viewdoc/summary?doi=10.1.1.13.3406 (accessed January 4, 2021)

Quick, N. J., Cioffi, W. R., Shearer, J., and Read, A. J. (2019). Mind the gap—optimizing satellite tag settings for time series analysis of foraging dives in Cuvier's beaked whales (*Ziphius cavirostris*). *Anim. Biotelem.* 7:5. doi: 10.1186/s40317-019-0167-5

Quick, N. J., Cioffi, W. R., Shearer, J. M., Fahlman, A., and Read, A. J. (2020). Extreme diving in mammals: first estimates of behavioural aerobic dive limits in Cuvier's beaked whales. *J. Exp. Biol.* 223:jeb222109. doi: 10.1242/jeb.222109

R Core Team (2020). *R: A Language and Environment for Statistical Computing*. Vienna: R Foundation for Statistical Computing.

Risch, D., Corkeron, P. J., Ellison, W. T., and Van Parijs, S. M. (2012). Changes in humpback whale song occurrence in response to an acoustic source 200 km away. *PLoS One* 7:e29741. doi: 10.1371/journal.pone.0029741

Sarnocińska, J., Teilmann, J., Balle, J. D., van Beest, F. M., Delefosse, M., and Tougaard, J. (2020). Harbor porpoise (*Phocoena phocoena*) reaction to a 3D seismic airgun survey in the North Sea. *Front. Mar. Sci.* 6:824. doi: 10.3389/fmars.2019.00824

Schick, R. S., Bowers, M., DeRuiter, S., Friedlaender, A., Joseph, J., Margolina, T., et al. (2019). Accounting for positional uncertainty when modeling received levels for tagged cetaceans exposed to sonar. *Aquat. Mamm.* 45, 675–690. doi: 10.1578/AM.45.6.2019

Schorr, G. S., Baird, R. W., Hanson, M. B., Webster, D. L., McSweeney, D. J., and Andrews, R. D. (2009). Movements of satellite-tagged Blainville's beaked whales off the island of Hawai'i. *Endanger. Species Res.* 10, 203–213. doi: 10.3354/esr00229

Sequeira, A. M. M., Heupel, M. R., Lea, M.-A., Eguíluz, V. M., Duarte, C. M., Meekan, M. G., et al. (2019). The importance of sample size in marine megafauna tagging studies. *Ecol. Appl.* 29, e01947. doi: 10.1002/eap.1947

Shearer, J. M., Quick, N. J., Cioffi, W. R., Baird, R. W., Webster, D. L., Foley, H. J., et al. (2019). Diving behaviour of Cuvier's beaked whales (*Ziphius cavirostris*) off Cape Hatteras, North Carolina. *R. Soc. Open Sci.* 6:181728. doi: 10.1098/rsos.181728

Siderius, M., and Porter, M. B. (2006). Modeling techniques for marine-mammal risk assessment. *IEEE J. Ocean. Eng.* 31, 49–60. doi: 10.1109/JOE.2006.872211

Sivle, L. D., Kvadsheim, P. H., Curé, C., Isojunno, S., Wensveen, P. J., Lam, F.-P. A., et al. (2015). Severity of expert-identified behavioural responses of humpback whale, minke whale, and northern bottlenose whale to naval sonar. *Aquat. Mamm.* 41, 469–502. doi: 10.1578/AM.41.4.2015.469

Sivle, L. D., Kvadsheim, P. H., Fahlman, A., Lam, F. P. A., Tyack, P. L., and Miller, P. J. O. (2012). Changes in dive behavior during naval sonar exposure in killer whales, long-finned pilot whales, and sperm whales. *Front. Physiol.* 3:400. doi: 10.3389/fphys.2012.00400

Sivle, L. D., Wensveen, P. J., Kvadsheim, P. H., Lam, F.-P. A., Visser, F., Curé, C., et al. (2016). Naval sonar disrupts foraging in humpback whales. *Mar. Ecol.* 562, 211–220. doi: 10.3354/meps11969

Southall, B. L., Bowles, A. E., Ellison, W. T., Finneran, J. J., Gentry, R. L., Greene, C. R., et al. (2007). Marine mammal noise-exposure criteria: initial scientific recommendations. *Bioacoustics* 17, 273–275. doi: 10.1080/09524622.2008.9753846

Southall, B. L., DeRuiter, S. L., Friedlaender, A., Stimpert, A. K., Goldbogen, J. A., Hazen, E., et al. (2019). Behavioral responses of individual blue whales (*Balaenoptera musculus*) to mid-frequency military sonar. *J. Exp. Biol.* 222:jeb190637. doi: 10.1242/jeb.190637

Southall, B. L., Moretti, D., Abraham, B., Calambokidis, J., DeRuiter, S. L., and Tyack, P. L. (2012). Marine mammal behavioral response studies in southern California: advances in technology and experimental methods. *Mar. Technol. Soc. J.* 46, 48–59. doi: 10.4031/mtsj.46.4.1

Southall, B. L., Nowacek, D. P., Miller, P. J. O., and Tyack, P. L. (2016). Experimental field studies to measure behavioral responses of cetaceans to sonar. *Endanger. Species Res.* 31, 293–315. doi: 10.3354/esr00764

Stimpert, A. K., DeRuiter, S. L., Southall, B. L., Moretti, D. J., Falcone, E. A., Goldbogen, J. A., et al. (2014). Acoustic and foraging behavior of a Baird's beaked whale, *Berardius bairdii*, exposed to simulated sonar. *Sci. Rep.* 4:7031. doi: 10.1038/srep07031

Thomas, B., Holland, J. D., and Minot, E. O. (2012). Wildlife tracking technology options and cost considerations. *Wildl. Res.* 38, 653–663. doi: 10.1071/WR10211

Tyack, P. L., and Thomas, L. (2019). Using dose–response functions to improve calculations of the impact of anthropogenic noise. *Aquat. Conserv.* 29, 242–253. doi: 10.1002/aqc.3149

Tyack, P. L., Zimmer, W. M. X., Moretti, D., Southall, B. L., Claridge, D. E., Durban, J. W., et al. (2011). Beaked whales respond to simulated and actual navy sonar. *PLoS One* 6:e17009. doi: 10.1371/journal.pone.0017009

U.S. Navy (2019). *Final Supplemental Environmental Impact Statement for Surveillance towed Array Sensor System Low Using Frequency Active Sonar*. Philadelphia, PA: U.S. Navy.

von Benda-Beckmann, A. M., Wensveen, P. J., Prior, M., Ainslie, M. A., Hansen, R. R., Isojunno, S., et al. (2019). Predicting acoustic dose associated with marine mammal behavioural responses to sound as detected with fixed acoustic recorders and satellite tags. *J. Acoust. Soc. Am.* 145, 1401–1416. doi: 10.1121/1.5093543

Wensveen, P. (2012). *The Effects of Sound Propagation and Avoidance Behaviour on Naval Sonar Levels Received by Cetaceans*. Ph.D. thesis. St Andrews: University of St Andrews.

Wensveen, P., Isojunno, S., Hansen, R. R., von Benda-Beckmann, A. M., Kleivane, L., van IJsselmuide, S., et al. (2019). Northern bottlenose whales in a pristine environment respond strongly to close and distant navy sonar signals. *Proc. R. Soc. Lond. B Biol. Sci.* 286, 20182592. doi: 10.1098/rspb.2018.2592

Wensveen, P. J., Kvadsheim, P. H., Lam, F.-P. A., von Benda-Beckmann, A. M., Sivle, L. D., Visser, F., et al. (2017). Lack of behavioural responses of humpback whales (*Megaptera novaeangliae*) indicate limited effectiveness of sonar mitigation. *J. Exp. Biol.* 220, 4150–4161. doi: 10.1242/jeb.161232

Zirbel, K., Balint, P., and Parsons, E. C. M. (2011). Navy sonar, cetaceans and the US Supreme Court: a review of cetacean mitigation and litigation in the US. *Mar. Pollut. Bull.* 63, 40–48. doi: 10.1016/j.marpolbul.2011.03.018

Conflict of Interest: The authors declare that the research was conducted in the absence of any commercial or financial relationships that could be construed as a potential conflict of interest.

Publisher's Note: All claims expressed in this article are solely those of the authors and do not necessarily represent those of their affiliated organizations, or those of the publisher, the editors and the reviewers. Any product that may be evaluated in this article, or claim that may be made by its manufacturer, is not guaranteed or endorsed by the publisher.

Copyright © 2021 Bouchet, Harris and Thomas. This is an open-access article distributed under the terms of the Creative Commons Attribution License (CC BY). The use, distribution or reproduction in other forums is permitted, provided the original author(s) and the copyright owner(s) are credited and that the original publication in this journal is cited, in accordance with accepted academic practice. No use, distribution or reproduction is permitted which does not comply with these terms.

Advantages of publishing in Frontiers

OPEN ACCESS
Articles are free to read for greatest visibility and readership

FAST PUBLICATION
Around 90 days from submission to decision

HIGH QUALITY PEER-REVIEW
Rigorous, collaborative, and constructive peer-review

TRANSPARENT PEER-REVIEW
Editors and reviewers acknowledged by name on published articles

Frontiers
Avenue du Tribunal-Fédéral 34
1005 Lausanne | Switzerland

Visit us: www.frontiersin.org
Contact us: frontiersin.org/about/contact

REPRODUCIBILITY OF RESEARCH
Support open data and methods to enhance research reproducibility

DIGITAL PUBLISHING
Articles designed for optimal readership across devices

FOLLOW US
@frontiersin

IMPACT METRICS
Advanced article metrics track visibility across digital media

EXTENSIVE PROMOTION
Marketing and promotion of impactful research

LOOP RESEARCH NETWORK
Our network increases your article's readership